mgr farm. Joanna Krajewska

Badania aktywności przeciwdrobnoustrojowej nowych związków z grupy pochodnych boraheterocyklicznych i kwasów aryloboronowych

Rozprawa na stopień doktora nauk medycznych i nauk o zdrowiu w dyscyplinie nauki farmaceutyczne

Promotor: dr hab. Agnieszka E. Laudy

Zakład Mikrobiologii Farmaceutycznej i Bioanalizy

Obrona rozprawy doktorskiej przed Radą Dyscypliny Nauk Farmaceutycznych Warszawskiego Uniwersytetu Medycznego

Warszawa 2023

Źródła finansowania

Badania były finansowane w ramach projektu Narodowego Centrum Nauki OPUS 16 (UMO-2018/31/B/ST5/00210), pt. „*Poszukiwanie korelacji struktura – aktywność przeciwdrobnoustrojowa wybranych grup związków boraheterocyklicznych*”, realizowanego przez konsorcjum Politechnika Warszawska – Warszawski Uniwersytet Medyczny w latach 2019-2024 oraz częściowo przez Fundację Rozwoju Diagnostyki i Terapii w Warszawie (REGON: 006220910, NIP:5262173856, KRS: 0000195643).

Badania przeprowadzono z wykorzystaniem infrastruktury Centrum Badań Przedklinicznych i Technologii (CePT) Warszawskiego Uniwersytetu Medycznego, sfinansowanej przez Unię Europejską za pośrednictwem Europejskiego Funduszu Rozwoju Regionalnego w ramach Programu Operacyjnego „Innowacyjna Gospodarka” na lata 2007-2013.

Pragnę serdecznie podziękować:

Pani dr hab. Agnieszce E. Laudy, **Promotor niniejszej pracy**

- za ogromne wsparcie i zaangażowanie na każdym etapie mojego naukowego rozwoju, za zarażanie pasją do nauki, dzielenie się wiedzą, motywowanie do działania, zagrzewanie do walki z przeciwnościami, za nieustającą wiarę w sukces i w sens podejmowanych wysiłków, a także za ogromną życzliwość, cierpliwość i profesjonalizm. *Summa summarum:* za bycie wspaniałym przewodnikiem po świecie mikrobiologii oraz szeroko pojętej nauki.

Panu prof. dr hab. Stefanowi Tyskiemu

- za wsparcie merytoryczne, poświęcony czas, bezinteresowne zaangażowanie oraz cenne uwagi.

Panu prof. dr hab. inż. Sergiuszowi Lulińskiemu oraz całemu Zespołowi Pana Profesora z Katedry Chemii Fizycznej Politechniki Warszawskiej

- za życzliwość, profesjonalizm i wspaniałą współpracę przy realizacji grantu OPUS 16. W sposób szczególny pragnę natomiast podziękować **mgr inż. Krzysztofowi Nowickiemu** - za jego ogromną serdeczność, zaangażowanie, uczynność, bezinteresowność oraz zaraźliwy entuzjazm.

Wszystkim moim Koleżankom z Zakładu Mikrobiologii Farmaceutycznej i Bioanalizy WUM

- za stworzenie sympatycznej atmosfery w miejscu pracy. **Mgr Karolinie Stępień** oraz **mgr Adriannie Dydze** dziękuję również za spory pakiet cennych wskazówek, ułatwiających codzienne życie w laboratorium.

Moim Rodzicom i Rodzeństwu

- za pełne wsparcia zainteresowanie, wierne kibicowanie i liryczną dokumentację postępów.

I wreszcie*, last but not least,* mojemu Mężowi Kamilowi

- za emanowanie optymizmem i gorący doping, za wiarę w moje możliwości i w sens tego co robię, za szczere zainteresowanie tematem i chęć zrozumienia mikroorganizmów, za inspirujące dyskusje i wspólne świętowanie sukcesów oraz za cierpliwe rozganianie moich wątpliwości o każdej porze dnia i nocy.

Dorobek naukowy

I. Wykaz publikacji stanowiących pracę doktorską

Prace przeglądowe

P1. **Krajewska J**, Laudy AE. The European Medicines Agency approved the new antibacterial drugs – response to the 2017 WHO report on the global problem of multi-drug resistance. *Postępy Mikrobiologii – Advancements of Microbiology* **2021**, 60:249-264, doi: 10.21307/pm-2021.60.4.20.

IF_{2021} = 1,106 **$MEiN_{2021}$ = 20**

Prace oryginalne

O1. Pacholak P, **Krajewska J**, Wińska P, Dunikowska J, Gogowska U, Mierzejewska J, Durka K, Woźniak K, Laudy AE, Luliński S. Development of structurally extended benzosiloxaboroles – synthesis and *in vitro* biological evaluation. *RSC Advances* **2021**, 11:25104-25121, doi: 10.1039/d1ra04127d.

IF_{2021} = 4,036 **$MEiN_{2021}$ = 100**

O2. **Krajewska J**, Nowicki K, Durka K, Marek-Urban PH, Wińska P, Stępniewski T, Woźniak K, Laudy AE, Luliński S. Oxazoline scaffold in synthesis of benzosiloxaboroles and related ring-expanded heterocycles: diverse reactivity, structural peculiarities and antimicrobial activity. *RSC Advances* **2022**, 12:23099-23117, doi: 10.1039/d2ra03910a.

IF_{2022} = 3,9 **$MEiN_{2022}$ = 100**

O3. **Krajewska J**, Tyski S, Laudy AE. Mutant prevention concentration, frequency of spontaneous mutant selection, and mutant selection window - a new approach to the *in vitro* determination of the antimicrobial potency of compounds. *Antimicrobial Agents and Chemotherapy* **2023**, 67(5):e0137322
doi: 10.1128/aac.01373-22.

IF_{2022}= 4,9 **$MEiN_{2022}$ = 140**

O4. **Krajewska J**, Chyży P, Durka K, Wińska P, Krzyśko KA, Luliński S, Laudy AE. Aromatic diboronic acids as effective KPC/AmpC inhibitors. *Molecules* **2023**, 28:7362, doi: 10.3390/molecules28217362

IF_{2022} = 4,6 **$MEiN_{2022}$ = 140**

Sumaryczny IF: 18,542 Sumaryczny MEiN: 500

II. Publikacje niewchodzące w cykl rozprawy doktorskiej

Prace oryginalne

NO1. Laudy AE, Mrowka A, **Krajewska J**, Tyski S. The influence of efflux pump inhibitors on the activity of non-antibiotic NSAIDS against Gram-negative rods. *PLoS One* **2016**, 11:e0147131. doi: 10.1371/journal.pone.0147131
IF_{2016} = 2,806 $MEiN_{2016}$ = 35

III. Abstrakty z konferencji naukowych

Konferencje międzynarodowe

AM1. World Microbe Forum. Online worldwilde, 20-24 VI 2021.
Krajewska J, Nowicki K, Luliński S, Tyski S, Laudy AE.
The influence of halogen substituents on the activity of bis(siloxaboroles) against *Staphylococcus* and *Enterococcus* strains - **e-plakat.**

AM2. XXVI EFMC International Symposium on Medicinal Chemistry. Virtual Event, 28 VIII – 2 IX 2021.
Nowicki K, **Krajewska J,** Pacholak P, Wińska P, Laudy AE, Luliński S.
Bis(oxaboroles) and bis(siloxaboroles) as potent antimicrobial agents - **e-plakat.**

AM3. IUMS Congress. The Online Edition, 20-22 VII 2022.
Krajewska J, Luliński S, Tyski S, Laudy AE.
The antimicrobial activity of new oxazoline-substituted benzosiloxaboroles and their derivatives - **e-plakat.**

AM4. 2nd Edition of International Conference and Expo on Clinical Microbiology. Włochy, Rzym, 22-23 VI 2023.
Krajewska J, Tyski S, Durka K, Luliński S, Laudy AE.
New phenylenediboronic acid derivatives – direct antibacterial and beta-lactamase inhibitory activity – **plakat**.

Konferencje krajowe

AK1. Druga Wirtualna Konferencja Naukowa Kampusu Ochota. 20-21 IX 2021.
Nowicki K, **Krajewska J,** Wińska P, Durka K, Laudy AE, Luliński S. Funkcjonalizowane benzosiloksaborole – synteza, charakterystyka i zastosowania w chemii medycznej - **e-plakat**.

AK2. VI Pomorskie Spotkania z Mikrobiologią. Gdańsk/online, 24-25 VI 2021.
Krajewska J, Tyski S, Luliński S, Laudy AE.
Nowe podejście do wyznaczania wartości minimalnego stężenia substancji zapobiegającej selekcji opornych mutantów (MPC). Postępy Mikrobiologii 60, Supl. 1, s. 30-31 - **e-plakat**.

AK3. XXIX Ogólnopolski Zjazd Polskiego Towarzystwa Mikrobiologów, Warszawa, 15-17 IX 2022.
Krajewska J, Laudy AE. Wieloetapowa metoda otrzymywania inokulum bakterii o gęstości $\geq 10^{11}$ CFU/ml. Materiały zjazdowe: sesja 4, streszczenie nr 0284 – **e-plakat**.

AK4. XXIX Ogólnopolski Zjazd Polskiego Towarzystwa Mikrobiologów, Warszawa, 15-17 IX 2022.
Krajewska J, Luliński S, Laudy AE. Nowe parametry wyznaczania zakresu stężeń, w którym może dochodzić do selekcji lekoopornych mutantów, tzw. mutant selection window (MSW) – istotny etap badań przedklinicznych. Materiały zjazdowe, sesja 4, streszczenie nr 0029 – **doniesienie ustne (autor prezentujący)**.

IV. Udział w projektach badawczych

PB1. Doktorant-stypendysta przy realizacji grantu Narodowego Centrum Nauki OPUS16 (UMO-2018/31/B/ST5/00210), pt. „Poszukiwanie korelacji struktura – aktywność przeciwdrobnoustrojowa wybranych grup związków boraheterocyklicznych", realizowanego przez konsorcjum Politechnika Warszawska–Warszawski Uniwersytet Medyczny w latach 2019-2024.

V. Aktywność w towarzystwach naukowych

TN1. Polskie Towarzystwo Mikrobiologów – członek zwyczajny od X 2019 roku, zaangażowany w organizację XXIX Ogólnopolskiego Zjazdu Polskiego Towarzystwa Mikrobiologów w Warszawie w 2022 roku.

Spis treści

1. Wykaz stosowanych skrótów 9
2. Streszczenie w języku polskim 11
3. Streszczenie w języku angielskim 14
4. Wstęp 17
   4.1. Selekcja antybiotykoopornych mutantów bakteryjnych 21
   4.2. Konieczność poszukiwania nowych leków przeciwdrobnoustrojowych 25
   4.3. Bor i jego związki w medycynie 30
   4.4. Podsumowanie części teoretycznej 45
5. Założenia i cele pracy 47
6. Omówienie wyników i dyskusja 49
   6.1. Badania bezpośredniej aktywności przeciwdrobnoustrojowej 49
   6.2. Udział pomp MDR w usuwaniu nowych związków z komórek bakterii Gram-ujemnych 55
   6.3. Zdolność nowych związków boroorganicznych do inhibicji β-laktamaz bakterii Gram-ujemnych 55
   6.4. Analiza zależności między strukturą a siłą synergistycznego oddziaływania nowych kwasów aryloboronowych z β-laktamami 61
   6.5. Opracowanie nowej metodyki wyznaczania górnej granicy MSW 62
7. Kopie opublikowanych prac 66
   7.1. Publikacja P1 66
   7.2. Publikacja O1 82
   7.3. Publikacja O2 106
   7.4. Publikacja O3 131
   7.5. Publikacja O4 145
8. Podsumowanie 184
9. Wnioski 190
10. Bibliografia 192
11. Opinie Komisji Bioetycznej 210
12. Oświadczenia współautorów publikacji 212

1. Wykaz stosowanych skrótów

ACP	białko nośnikowe grup acylowych (ang. *acyl carrier protein*)
cAmpC	chromosomalnie kodowany enzym typu AmpC (ang. *chromosomally encoded AmpC enzyme*)
pAmpC	plazmidowo kodowany enzym typu AmpC (ang. *plasmid-encoded AmpC enzyme*)
BATSI	kwas boronowy - inhibitor stanu przejściowego (ang. *boronic acid transition state inhibitors*)
BLI	inhibitor β-laktamaz (ang. β-*lactamse inhibitor*)
CDT	krążkowy test kombinowany (ang. *combination disc test*)
CFU	jednostka tworząca kolonię (ang. *colony forming unit*)
CHDL	karbapenemazy z klasy D (ang. *carbapenem-hydrolyzing class D β-lactamases*)
CLSI	Instytut Norm Klinicznych i Laboratoryjnych (ang. *Clinical and Laboratory Standards Institute*)
CRAB	*Acinetobacter baumannii* oporny na karbapenemy (ang. *carbapenem-resistant A. baumannii*)
CRE	*Enterobacterales* oporne na karbapenemy (ang. *carbapenem-resistant Enterobacterales*)
CRPA	*Pseudomonas aeruginosa* oporny na karbapenemy (ang. *carbapenem-resistant P. aeruginosa*)
EMA	Europejska Agencja Leków (ang. *European Medicines Agency*)
ESBL	β-laktamazy o rozszerzonym spektrum substratowym (ang. *extended-spectrum β-lactamases*)
EUCAST	Europejski Komitet ds. Oznaczania Lekowrażliwości (ang. *European Committee on Antimicrobial Susceptibility Testing*)
FDA	Agencja Żywności i Leków (ang. *Food and Drug Administration*)
FICI	indeks częściowego stężenia hamującego (ang. *fractional inhibitory concentration index*)
FSMS	częstość selekcji spontanicznych mutantów (ang. *frequency of spontaneus mutant selection*)
KPC	karbapenemaza typu KPC (ang. *Klebsiella pneumoniae carbapenemase*)
LeuRS	syntetaza leucylo-tRNA (ang. *leucyl-tRNA synthetase*)
MBC	minimalne stężenie bakteriobójcze (ang. *minimal bactericidal concentration*)
MDR	wielolekooporny (ang. *multidrug-resistant*)
MFC	minimalne stężenie grzybobójcze (ang. *minimal fungicidal concentration*)
MIC	minimalne stężenie hamujące wzrost (ang. *minimal inhibitory concentration*)
MPC	minimalne stężenie zapobiegające selekcji opornych mutantów (ang. *mutant prevention concentration*)
MPC-D	minimalne stężenie zapobiegające selekcji mutantów dominujących (ang. *dominant mutant prevention concentration*)
MPC-F	minimalne stężenie zapobiegające selekcji mutantów o obniżonej sprawności (ang. *inferior mutant prevention concentration*)

MRSA	*Staphylococcus aureus* oporny na metycylinę (ang. *methicillin-resistant S. aureus*)
MSC	minimalne stężenie selekcyjne (ang. *minimal selective concentration*)
MSSA	*S. aureus* wrażliwy na metycylinę (ang. *methicillin-sensitive S. aureus*)
MSW	okno selekcji mutantów (ang. *mutant prevention concentration*)
MSW-D	okno selekcji mutantów dominujących (ang. *dominant mutant prevention concentration*)
MSW-F	okno selekcji mutantów o obniżonej sprawności (ang. *inferior mutant prevention concentration*)
NDM	metalo-β-laktamaza typu NDM (ang. *New Delhi metallo-β-lactamase*)
OBORT	pułapkowanie tRNA oksaborolem (ang. *oxaborole tRNA-trapping*)
PAβN	L-fenyloalanino-L-arginino-β-naftylamid
PBA	kwas fenyloboronowy (ang. *phenylboronic acid*)
PDR	oporny na wszystkie leki (ang. *pandrug-resistant*)
VIM	metalo-β-laktamaza typu VIM (ang. *Verona integron-encoded metallo-β-lactamase*)
VISA	*S. aureus* o obniżonej wrażliwości na wankomycynę (ang. *vancomycin-intermediate S. aureus*)
VRE	enterokoki oporne na wankomycynę (ang. *vancomycin-resistant enterococci*)
VRSA	*S. aureus* oporny na wankomycynę (ang. *vancomycin-resistant S. aureus*)
WHO	Światowa Organizacja Zdrowia (ang. *World Health Organization*)
XDR	o rozszerzonej oporności (ang. extensively drug-resisnat)

2. Streszczenie w języku polskim

Słowa kluczowe: antybiotykooporność, benzosiloksaborole, kwasy aryloboronowe, aktywność przeciwdrobnoustrojowa, inhibitory β-laktamaz, selekcja opornych mutantów, MPC, MSW

Narastająca wielolekooporność wśród szczepów drobnoustrojów sprawiła, że w lecznictwie pilnie potrzebne są kolejne, oryginalne leki aktywne wobec patogenów, głównie wobec tzw. patogenów priorytetowych, dla których dostępnych jest niepokojąco mało opcji terapeutycznych. W opinii WHO, liczba takich leków wprowadzonych w ostatnich latach do obrotu oraz aktualnie przechodzących badania kliniczne jest niewystarczająca. Jednocześnie, w badaniach przedklinicznych znajduje się wiele substancji o obiecującej aktywności wobec bakterii i grzybów. Brakuje jednak parametrów *in vitro* pozwalających na tym etapie precyzyjnie przewidzieć zakres stężeń, w którym może dochodzić do selekcji opornych mutantów w warunkach *in vivo* (ang. *mutant selection window* – MSW). Wartość MPC (ang. *mutant prevention concentration*) wyznaczająca górną granicę MSW często przekracza próg toksyczności leków, a także charakteryzuje się niedostateczną powtarzalnością *in vitro* oraz słabą odtwarzalnością *in vivo*. Utrudnia to wskazywanie do dalszych etapów prac badawczo-rozwojowych związków o najmniejszym potencjale selekcjonowania oporności szczepów bakteryjnych *in vivo* oraz opracowanie nowych, ograniczających narastanie oporności schematów dawkowania.

Celami niniejszej pracy było: (**I**) poszukiwanie wśród nowych pochodnych boraheterocyklicznych i kwasów aryloboronowych substancji aktywnych wobec bakterii i grzybów drożdżopodobnych oraz (**II**) opracowanie nowego podejścia do oceny potencjału selekcjonowania oporności wśród szczepów bakteryjnych przez związki przeciwbakteryjne, możliwego do zastosowania na wczesnym etapie przedklinicznych badań *in vitro*.

Realizując **cel I** prowadzono szerokie badania mikrobiologiczne 44 benzosiloksaboroli oraz 33 kwasów aryloboronowych, głównie di- oraz triboronowych. W pracy zbadano: (**A**) ich bezpośrednią aktywność wobec bakterii i grzybów drożdżopodobnych (wyznaczając wartości MIC, MBC i MFC dla szczepów wzorcowych i klinicznych); (**B**) udział błonowych pomp MDR (ang. *multidrug-resistant*) bakterii Gram-ujemnych w aktywnym usuwaniu związków z komórki (wyznaczając wartości MIC w obecności inhibitora pomp), (**C**) zdolność związków do inhibicji

β-laktamaz (krążkowymi testami kombinowanymi, wyznaczając wartości MIC β-laktamów w obecności badanych związków dla szczepów KPC-, AmpC- oraz VIM-dodatnich, oraz potwierdzając cel molekularny metodami mikrobiologicznymi i biochemicznymi) oraz (**D**) zależność struktura – siła synergistycznego oddziaływania kwasów aryloboronowych z β-laktamami (wyznaczając metodą szachownicy wartości FICI i określając rodzaj interakcji, a także przeprowadzając analizę statystyczną).

W pracy stwierdzono wysoką aktywność przeciwgronkowcową, 18 benzosiloksaboroli benzenosulfonianowych i sulfonamidowych (wartości MIC 0,39-6,25 mg/l) oraz wysoką aktywność przeciwenterokokową 3 benzosiloksaboroli benzenosulfonianowych (wartości MIC 6,25 mg/l). Wykazano zdolność do inhibicji β-laktamaz typu KPC/AmpC 25 związków w wysokich stężeniach (30-300 μg/krążek), a 17 kwasów aryloboronowych także w niskich stężeniach (4–16 mg/l). Kwas *orto*-fenylenodiboronowy najefektywniej przywracał wrażliwość na karbapenemy szczepom *Escherichia coli* i *Klebsiella pneumoniae* KPC-dodatnim (powodując nawet 64-krotne redukcje wartości MIC karbapenemów) oraz umiarkowanie zwiększał aktywność ceftazydymu wobec szczepów *E. coli* i *Pseudomonas aeruginosa* AmpC-dodatnich, nie przywracając wrażliwości tym szczepom. Kwasy *para*-fenylenodiboronowe przywracały wrażliwość na karbapenemy szczepom KPC-dodatnim i na ceftazydym szczepom AmpC-dodatnim, natomiast kwasy *meta*-fenylenodiboronowe przywracały wrażliwość na ceftazydym szczepowi *E. coli* CMY-2-dadatniemu. Badania z wykorzystaniem całych komórek oraz wyizolowanych białek całkowitych transformanta *E. coli* DH5α niosącego gen $bla_{\text{KPC-3}}$ potwierdziły, że enzymy typu KPC są punktem uchwytu kwasów *orto*- i *para*- ale nie *meta*-fenyleonodiboronowych. Przeprowadzona analiza statystyczna wykazała, że obecność dwóch grup boronowych w pozycji *orto* istotnie nasila synergię kwasów fenylenodiboronowych z karbapenemami (p=0,0001) ale osłabia ich synergię z ceftazydymem (p=0,04). Z kolei obecność fluoru w cząsteczce osłabia synergię tych kwasów z karbapenemami (p=0,036) ale nasila synergię z ceftazydymem (p=0,005). Nie wykryto natomiast istotnego udziału błonowych pomp MDR w aktywnym usuwaniu badanych związków z komórek bakteryjnych.

Realizując **cel II** opracowano: (**A**) nowe parametry *in vitro* do wyznaczania górnej granicy zakresu MSW, tj. parametr MPC-D (odnoszący się do tzw. dominujących mutantów o wysokim potencjale selekcjonowania także *in vivo*) oraz parametr MPC-F (odnoszący się do mutantów o obniżonej sprawności), (**B**) nową metodę rozcieńczeń w bulionie do wyznaczania wartości MPC-D i MPC-F oraz (**C**) nową, wielostopniową metodę otrzymywania inokulum bakteryjnego o wysokiej gęstości ($>10^{11}$ CFU/ml),

zwiększającego precyzję wyznaczania zaproponowanych parametrów. Nowością pracy jest także powiązanie wartości klasycznego MPC z częstością selekcji opornych mutantów w metodzie rozcieńczeń w agarze, co ma miejsce w opracowanej metodyce wyznaczania wartości nowego parametru MPC-D. Badania prowadzono na szczepie *S. aureus* ATCC 29213 dla 3 związków będących przedstawicielami różnych grup o działaniu przeciwbakteryjnym, tj. cyprofloksacyny, linezolidu i benzosiloksaborolu No37. Metodą rozcieńczeń w agarze wyznaczono wartości MPC i MPC-D, a metodą rozcieńczeń w bulionie wartości MPC-D i MPC-F. Wyjściowe inokula bakterii, uzyskane nową metodą miały gęstości 5–7,5x10^{11} CFU/ml, co jest kluczowe przy wyznaczaniu parametrów MPC. W przypadku linezolidu i benzosiloksaborolu No37 wszystkie wyznaczone parametry miały taką samą wartość. W przypadku cyprofloksacyny uzyskano wynik: MPC-D<MPC-F<MPC. Jej wartości MPC-D wyznaczone obiema metodami były porównywalne. W pracy wykazano zatem, iż: (I) MPC-D może być w przypadku niektórych związków przeciwbakteryjnych niższe niż MPC, przez co bardziej akceptowalne klinicznie jako podstawa schematów dawkowania, (II) powiązanie wartości MPC-D z częstością selekcji opornych mutantów jest kluczowe dla zwiększenia powtarzalności *in vitro* parametru MPC-D w porównaniu do parametru MPC oraz (III) zaproponowana metoda rozcieńczeń w bulionie pozwala na zróżnicowanie mutantów powstających *in vitro* na mutanty dominujące oraz mutanty o obniżonej sprawności, przez co parametr MPC-D ma szansę być lepiej odtwarzalny *in vivo* w porównaniu do parametru MPC.

Uzyskane w pracy wyniki aktywności przeciwdrobnoustrojowej badanych związków boroorganicznych w połączeniu z brakiem ich cytotoksyczności pozwalają stwierdzić, że (**I**) benzosiloksaborole benzenosulfonianowe i sulfonamidowowe mogą być postrzegane jako potencjalne źródło nowych leków aktywnych wobec priorytetowych ziarenkowców Gram-dodatnich oraz (**II**) kwasy fenylenodiboronowe są interesującymi strukturami wyjściowymi do syntezy nowych inhibitorów β-laktamaz typu KPC/AmpC. Wykazano także, iż wartości zaproponowanego parametru MPC-D mogą być niższe, bardziej powtarzalne *in vitro* i lepiej odtwarzalne *in vivo* niż wartości MPC, co może usprawnić badania przedkliniczne kandydatów na nowe leki przeciwdrobnoustrojowe oraz ułatwić opracowanie nowych, ograniczających narastanie oporności schematów dawkowania.

3. Streszczenie w języku angielskim

Studies on the antimicrobial activity of new compounds from the group of boraheterocyclic derivatives and arylboronic acids.

Key words: antimicrobial resistance, boraheterocycles, arylboronic acids, antimicrobial activity, resistant mutants selection, MPC, MSW

The growing multidrug resistance among microbial strains has led to the urgent need for new, original drugs active against pathogens, primarily against so-called priority pathogens, for which alarmingly few therapeutic options are left. According to the WHO, the number of such drugs marketed in recent years and currently under clinical trials is insufficient. Simultaneously, there are abundant compounds with promising activity against bacteria and fungi in preclinical trials. However, *in vitro* parameters that can predict at this stage the concentration range in which resistant mutants would likely be selected under *in vivo* conditions (so-called mutant selection window - MSW) are lacking. The mutant prevention concentration (MPC) value marking the upper boundary of the MSW frequently exceeds the drug toxicity threshold, is insufficiently repeatable *in vitro*, and can not always be reproduced *in vivo*. This impedes choosing the compound with the lowest potential to select resistance of bacterial strains *in vivo* for further drug development and the establishment of novel, resistance-restricting dosing regimens.

The aims of this thesis were: (**I**) to search for substances active against bacteria and yeasts among new boraheterocyclic derivatives and arylboronic acids, and (**II**) to develop a new approach to assess the potential of compounds to select resistance among bacterial strains, possible to implement at the early stage of *in vitro* preclinical research.

To realize aim **I**, extensive microbiological research was conducted on 44 benzosiloxaboroles and 33 arylboronic acids, mainly di- and triboronic acids. It was evaluated: (**A**) their direct activity against bacteria and yeasts (by the MIC, MBC, and MFC determination for reference and clinical strains); (**B**) the contribution of MDR efflux pumps of Gram-negative bacteria in the active removal of compounds from bacterial cells (by determining the MIC value in the presence of an efflux pumps inhibitor), (**C**) compounds' ability to inhibit β-lactamases (by phenotypic combination disc tests, determining β-lactams' MICs in the presence of tested compounds for KPC-, AmpC- and VIM-positive strains, and confirming the molecular target in microbiological and

biochemical assays), and (**D**) the correlation: structure – strength of the synergy between arylboronic acids and β-lactams (by determining the FICI values and the type of the interaction in the checkerboard as well as by performing statistical analysis).

High antistaphylococcal activity, also against clinical strains of methicillin-resistant *Staphylococcus aureus* (MRSA) was found for 18 benzenesulfonate and sulfonamide benzosiloxaboroles (MICs 0.39-6.25 mg/L), whereas high antienterococcal activity for 3 benzenesulfonate benzosiloxaboroles (MICs 6.25 mg/L). The ability to inhibit KPC/AmpC β-lactamases at high concentrations (30-300 μg/disc) was demonstrated for 25 arylboronic acids and at low concentrations (4-16 mg/L) for 17 arylboronic acids. *ortho*-Phenylenediboronic acid most effectively restored the sensitivity to carbapenems of *Escherichia coli* and *Klebsiella pneumoniae* KPC-positive strains (up to 64-fold MIC reductions) and moderately increased ceftazidime activity against *E. coli* and *Pseudomonas aeruginosa* AmpC-positive strains, without restoring the sensitivity of these strains. *para*-Phenylenediboronic acids restored the susceptibility to carbapenems of KPC-positive strains and the susceptibility to ceftazidime of AmpC-positive strains, whereas *meta*-phenylenediboronic acids restored ceftazidime activity against *E. coli* CMY-2-positive. Studies with the whole cells and total proteins extract of the *E. coli* DH5α transformant carrying the $bla_{\text{KPC-3}}$ gene confirmed that KPC-type enzymes are indeed molecular targets for *ortho*- and *para*-, but not for *meta*-phenylenediboronic acids. The statistical analysis revealed that the presence of two boronic groups in the *ortho* position significantly increases the synergy of phenylenediboronic acids with carbapenems (p=0.0001) but weakens their synergy with ceftazidime (p=0.04). In turn, fluorine in the molecule weakens the synergy of these acids with carbapenems (p=0.036) but increases their synergy with ceftazidime (p=0.005). Also, no significant contribution of MDR efflux pumps in their active removal from bacterial cells was detected.

To realize aim **II** it was developed: (**A**) new *in vitro* parameters marking the upper boundary of the MSW, *i.e.*, parameter MPC-D (related to the so-called dominant mutants with high selection potential *in vivo*) and parameter MPC-F (related to mutants with impaired fitness), (**B**) a new broth-dilution method for determining MPC-Ds and MPC-Fs, and (**C**) a new, multi-stage method for obtaining a high-density bacterial inoculum (>10^{11} CFU/mL), which increases the precision of determining the proposed parameters. Another novelty of the work is linking the classical MPC value with the frequency of resistant mutant selection in the agar-dilution method, which takes place in the developed

methodology for determining the value of the new MPC-D parameter. The research was conducted on the *S. aureus* ATCC 29213 strain for three compounds representing different groups of antimicrobials, i.e., ciprofloxacin, linezolid, and benzosiloxaborole No37. MPC and MPC-D values were determined by the agar-dilution method, while MPC-D and MPC-F values were determined by the broth-dilution method. The initial bacterial inocula obtained by the new method had densities of 5–7.5x10^{11} CFU/ml, which is crucial when determining the MPCs parameters. All determined parameters had the same value in the linezolid and benzosiloxaborole No37 case. In the case of ciprofloxacin, the result was as follows: MPC-D<MPC-F<MPC. Its MPC-Ds determined by both methods were comparable. Therefore, the study showed that (**I**) MPC-D may be lower than MPC for some antibacterials, making it more clinically acceptable as a basis for dosage regimens, (**II**) determining the MPC-D value based on the frequency of spontaneous mutant selection is crucial to increase its *in vitro* repeatability compared to the MPC, and (**III**) the proposed broth dilution method allows for the differentiation of mutants generated *in vitro* into dominant mutants and mutants with impaired fitness, which makes likely that the MPC-D would be better reproducible *in vivo* compared to the MPC.

The obtained results of the antimicrobial activity of the tested organoboron compounds, combined with their lack of cytotoxicity, allow to conclude that (**I**) benzenesulfonate and sulfonamide benzosiloxaboroles can be considered a potential source of new drugs active against priority Gram-positive cocci and (**II**) phenylenediboronic acids are interesting scaffolds for the future development of novel KPC/AmpC β-lactamases inhibitors. It has also been shown that the proposed MPC-D parameter may be lower, better repeatable *in vitro,* and likely better reproducible *in vivo* than the MPC parameter, which may improve preclinical testing of candidates for new antimicrobial drugs and facilitate the development of novel, resistance-restricting dosing regimens.

4. Wstęp

Wprowadzenie do lecznictwa skutecznych i bezpiecznych leków przeciwdrobnoustrojowych jest uznawane za jeden z kamieni milowych w rozwoju współczesnej medycyny [1]. Dzięki nim, niegdyś zagrażające życiu infekcje stały się łatwo wyleczalnymi chorobami, drastycznie spadła śmiertelność okołoporodowa, możliwe stało się również bezpieczne przeprowadzanie poważnych interwencji medycznych [1-3]. Większość znanych dziś klas leków przeciwdrobnoustrojowych wprowadzono jeszcze przed końcem lat 60. XX wieku (Rycina 1). Do stosowania ogólnego u ludzi dostępne są leki pochodzenia naturalnego, tj. antybiotyki (12 klas leków przeciwbakteryjnych i 2 klasy leków przeciwgrzybiczych) oraz leki syntetyczne, których struktury nie mają swojego pierwowzoru w naturze, tzw. chemioterapeutyki (6 klas leków przeciwbakteryjnych i 3 klasy leków przeciwgrzybiczych) [3]. W ostatnich dekadach znacznie maleje skuteczność znanych antybiotyków i chemioterapeutyków w leczeniu zakażeń. Oszacowano, że w samym tylko 2019 roku infekcje bakteryjne były powiązane z ok. 4,95 mln zgonów globalnie i były bezpośrednią przyczyną 1,27 mln zgonów [4]. Liczbę zgonów z powodu infekcji grzybiczych określa się natomiast na ponad 2 mln rocznie [5]. Szacuje się, że bez podjęcia zdecydowanych działań do 2050 roku z powodu infekcji umierać będzie 10 milionów ludzi rocznie [6]. Pojawiają się nawet głosy, że ludzkość stoi u progu ery post-antybiotykowej [7,8].

Przyczyną takiego stanu rzeczy jest narastająca oporność drobnoustrojów. W praktyce klinicznej szczep uważa się za oporny na dany antybiotyk, jeśli minimalne stężenie tego antybiotyku hamujące jego wzrost *in vitro* (ang. *minimal inhibitory concentration* – MIC) jest wyższe niż stężenie możliwe do osiągnięcia *in vivo* (we krwi lub w tkankach pacjenta) [9]. W warunkach laboratoryjnych wartość MIC antybiotyku wyznacza się, gdy jego działaniu poddanych zostanie 10^4 CFU (ang. *colony forming unit* – jednostka tworząca kolonie) [10,11]. Szczepy klasyfikuje się jako wrażliwe, wrażliwe – zwiększona ekspozycja (dawniej określane jako średnio wrażliwe lub o obniżonej wrażliwości) oraz oporne na podstawie ustalonych, granicznych wartości MIC, tzw. punktów odcięcia (ang. *breakpoints*) [12-15].

Pewne gatunki, rodzaje lub całe grupy bakterii i grzybów cechuje oporność naturalna (nazywana również wrodzoną) na niektóre grupy środków przeciwdrobnoustrojowych [12-15]. Bakterie i grzyby mają także zdolność do nabywania oporności [16]. Wrażliwe komórki typu dzikiego danego szczepu mogą nabywać geny oporności (czyli geny warunkujące oporność) od komórek innego szczepu tego gatunku,

a nawet innego gatunku lub rodzaju, w drodze tzw. horyzontalnego transferu genów. Tą drogą często przekazywane są np. geny kodujące enzymy dezaktywujące antybiotyki [17]. Geny oporności mogą także powstawać w komórkach typu dzikiego *de novo* dzięki mutacjom, tj. zmianom w sekwencji nukleotydowej DNA będących następstwem spontanicznych błędów podczas procesu jego replikacji. Spontaniczne mutacje pojawiają się ze średnią częstością 1 na $10^{10} - 10^{9}$ nukleotydów na generację [18-20]. Do fenotypowego ujawnienia się oporności niekiedy wystarczające jest pojawienie się pojedynczej mutacji punktowej (tzw. oporność jednostopniowa), czasami natomiast konieczna jest akumulacja kilku mutacji w DNA (tzw. oporność wielostopniowa) [21,22]. Dzięki mutacjom nabywana jest często oporność związana z modyfikacją miejsca docelowego antybiotyku (tzw. punktu uchwytu), zmniejszeniem przepuszczalności błony zewnętrznej czy też ze zmianami w systemach regulatorowych prowadzącymi do nadekspresji operonów kodujących pompy błonowe odpowiedzialne za aktywne usuwanie antybiotyku z komórki (tzw. zjawisko z ang. *efflux*) [18,19]. Powstające w drodze horyzontalnego transferu genów lub mutacji komórki o zmienionym genotypie i zmniejszonej wrażliwości na dany antybiotyk w porównaniu do komórki macierzystej określa się mianem antybiotykoopornych mutantów [18,19].

W efekcie tych zjawisk, oporne szczepy bakterii izolowano od pacjentów niemal równolegle z wprowadzeniem do lecznictwa każdej nowej grupy antybiotyków (Rycina 1). Zjawisko narastania oporności zaobserwowano także u grzybów np. wśród szczepów z rodzaju *Candida*. Z biegiem lat zaczęły również pojawiać się wielolekooporne (ang. *multidrug-resistant* – MDR) szczepy drobnoustrojów, tj. oporne na co najmniej jeden związek w trzech różnych grupach, z wyłączeniem grup, na które są one naturalnie oporne oraz szczepy o rozszerzonej oporności (ang. *extensively drug-resisnat* – XDR), zachowujące wrażliwość tylko na antybiotyki z jednej lub dwóch grup [23,24]. Najgroźniejszą aktualnie grupę stanowią natomiast szczepy oporne na wszystkie znane leki przeciwdrobnoustrojowe (ang. *pandrug-resistant* – PDR) [23,24]. Dekady powszechnego stosowania antybiotyków w medycynie, weterynarii, hodowli zwierząt oraz w rolnictwie znacznie zwiększyły częstość powstawania antybiotykoopornych mutantów – obecność antybiotyku w środowisku nasila bowiem horyzontalny transfer genów [17,25] oraz zwiększa częstość powstawania mutacji [26]. Wiadomo jednak, że jedynie niewielki odsetek pojawiających się antybiotykoopornych mutantów ma zdolność do zdominowania populacji komórek danego szczepu i do rozprzestrzeniania się [16].

Rycina 1. Kalendarium wprowadzania do lecznictwa klas leków przeciwdrobnoustrojowych do stosowania ogólnego (z wyłączeniem leków przeciwprątkowych) oraz pojawiania się pierwszych szczepów opornych i wybranych fenotypów oporności drobnoustrojów. Opracowano na podstawie: [27-45].

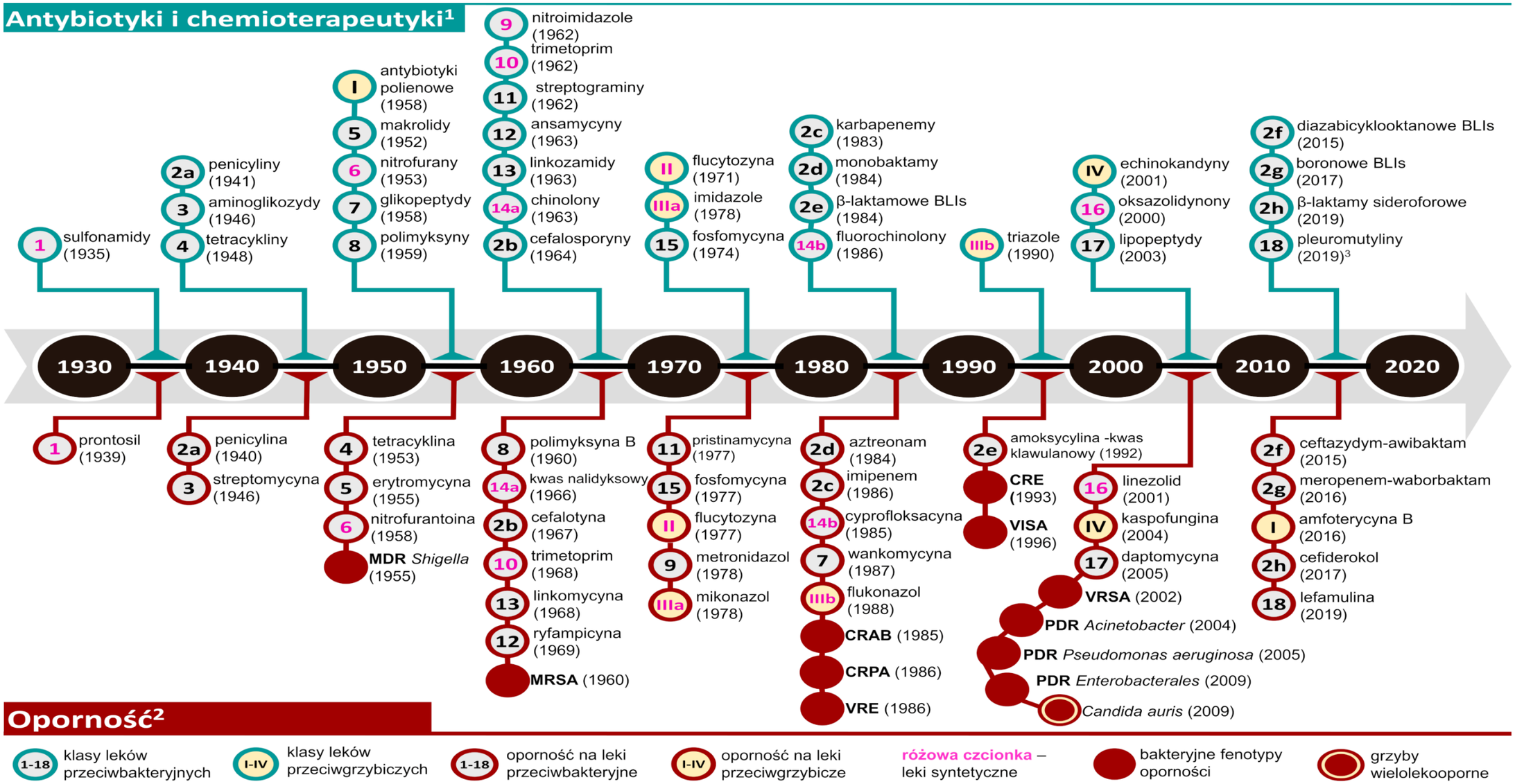

[1] Podano datę pierwszego wprowadzenia na rynek europejski lub amerykański pierwszego leku z danej klasy do stosowania ogólnego u ludzi.
[2] Podano nazwę leku i rok, w którym pierwszy raz opisano oporność drobnoustrojów na lek z danej klasy.
[3] Podano rok zarejestrowania pleuromutylin do stosowania ogólnego u ludzi – leki z tej grupy były wcześniej zarejestrowane do stosowania miejscowego.
BLIs – inhibitory β-laktamaz (ang. *β-lactamses inhibitors*); **MDR** – wielolekooporny (ang. *multidrug-resistant*); **MRSA** – *Staphylococcus aure*us oporny na metycylinę (ang. *methicillin-resistant S. aureus*); **CRAB**–*Acinetobacter baumannii* oporna na karbapenemy (ang. *carbapenem-resistant A. baumannii*); **CRPA** – *Pseudomonas aeruginosa* oporny na karbapenemy (ang. *carbapenem-resistant P. aeruginosa*); **VRE**–enterokoki oporne na wankomycynę (ang. *vancomycin-resistant enterococci*); **CRE**–*Enterobacterales* oporne na karbapenemy (ang. *carbapenem-resistant Enterobacterales*), **VISA** – *S. aureus* o obniżonej wrażliwości na wankomycynę (ang. *vancomycin-intermediate S. aureus*); **VRSA** – *S. aureus* oporny na wankomycynę (ang. *vancomycin-resistant S. aureus*); **PDR** – oporny na wszystkie znane leki (ang. *pandrug-resistant*).

4.1. Selekcja antybiotykoopornych mutantów bakteryjnych

Zdolność komórek nowo powstałego, antybiotykoopornego mutanta do zdominowania populacji i następnie do rozprzestrzeniania się jest uzależniona zarówno od ponoszonych przez niego tzw. kosztów sprawnościowych nabycia oporności (ang. *fitness costs of resistance*) jak i od warunków zewnętrznych, tj. przede wszystkim od stężenia antybiotyku w środowisku oraz od aktywności układu immunologicznego gospodarza [18,46-48]. Koszty sprawnościowe nabycia oporności, rozumiane jako spowolnienie tempa podziałów komórkowych w porównaniu do komórek wrażliwych, to częsta sytuacja, niezależnie od mechanizmu powstania mutanta. Replikacja, transkrypcja i translacja nowych genów, nabytych drogą transferu horyzontalnego wymaga od komórki bakteryjnej dodatkowych nakładów energii i zasobów, może również zakłócać pewne własne funkcje komórkowe. Z kolei oporność mutacyjna polegająca np. na modyfikacji miejsca docelowego leku oznacza zmianę struktury białka zaangażowanego w ważny proces metaboliczny bakterii, co może niekorzystnie wpłynąć na funkcjonowanie komórek [18,48]. W przypadku braku antybiotyku w środowisku lub gdy jego stężenie nie przekracza wartości MIC komórek typu dzikiego, powstałe komórki antybiotykoopornych mutantów o obniżonej sprawności zazwyczaj nie są w stanie skutecznie konkurować z komórkami dzikimi o zasoby pokarmowe środowiska i w większości przypadków zanikają – nie są wykrywane w badanej ponownie populacji komórek danego szczepu [49,50]. Wyjątkiem jest sytuacja, gdy nabycie oporności nie wiąże się z żadnymi kosztami sprawnościowymi (komórki antybiotykoopornych mutantów mogą wówczas utrzymywać się w populacji nawet po ustaniu presji antybiotykowej) lub gdy subinhibitorowe stężenia antybiotyku w niewielkim stopniu spowalniają tempo podziałów komórek typu dzikiego, dając przewagę antybiotykoopornym mutantom [47,51]. Komórki mutantów mogą wówczas stopniowo zwiększać swoją liczebność w ogólnej populacji komórek i ustanowić antybiotykooporną subpopulację, a z czasem nawet zniwelować koszty sprawnościowe dzięki pojawieniu się dodatkowych mutacji kompensacyjnych [47,51]. Zakres stężeń w którym dochodzi do takiej sytuacji nazwano subinhibitorowym oknem selekcyjnym (ang. *sub-MIC selective window*). Jego górną granicę stanowi wartość MIC komórek typu dzikiego, a dolną granicę wyznacza wartość tzw. minimalnego stężenia selekcyjnego (ang. *minimal selective concentration* – MSC), przy którym tempo podziałów komórkowych mutantów i komórek typu dzikiego zrównuje się [47,51]. Wartość MSC jest specyficzna dla każdej

kombinacji antybiotyk-szczep, niekiedy jest także ekstremalnie niska, nawet rzędu 1/230 wartości MIC. Do ekspozycji drobnoustrojów na takie stężenia antybiotyku może zatem dochodzić często, zarówno w środowisku jak i w trakcie antybiotykoterapii, np. wskutek stosowania zbyt niskich dawek, niewłaściwego przyjmowania leku przez pacjenta lub słabej penetracji antybiotyku do określonych tkanek i narządów [47,51-55]. W efekcie tych zjawisk, raz powstałe antybiotykooporne mutanty są trudne do eradykacji. Ich subpopulacje mogą być obecne w populacji komórek odpowiedzialnych za wywoływanie infekcji, pozostając niewykrywalne podczas wyznaczania wartości MIC szczepu. Antybiotykooporne mutanty mogą jednak szybko zdominować populację po jej ponownej ekspozycji na antybiotyk, zwłaszcza gdy jego stężenia przekroczą wartość MIC komórek typu dzikiego [56,57].

Obecność w środowisku antybiotyku w stężeniu przekraczającym wartość MIC komórek typu dzikiego, ale nie wystarczającym do zahamowania wzrostu antybiotykoopornych mutantów powoduje natomiast, że komórki mutantów mogą się selektywnie rozmnażać, pomimo niekiedy znacznych kosztów sprawnościowych. Taki zakres stężeń antybiotyku nazwano oknem selekcji mutantów (ang. *mutant selection window* – MSW). Jago dolną granicę stanowi wartość MIC komórek typu dzikiego, a górną tzw. stężenie zapobiegające selekcji mutantów (ang. *mutant prevention concentration* – MPC) [46,58,59]. Zgodnie z oryginalną definicją zaproponowaną w pracy Dong i wsp. z 1999 roku, MPC to najmniejsze stężenie antybiotyku całkowicie hamujące wzrost bakterii, gdy jego działaniu poddanych zostanie co najmniej 10^{10} CFU [58]. Tak duża gęstość populacji zapewnia wysokie prawdopodobieństwo obecności w niej spontanicznych mutantów (częstość ich powstawania wynosi zwykle $10^{-6} – 10^{-8}$), jest to również liczebność populacji typowa dla wielu miejsc infekcji [21,58]. Do wyznaczania wartości MPC, Dong i wsp. [58] zaproponowali metodę rozcieńczeń antybiotyku w agarze. Autorzy podkreślili także, iż uzyskana w ten sposób wartość jest ściśle uzależniona od liczby CFU poddanych badaniu, istotne jest zatem dodanie odpowiedniego subskryptu przy podawaniu wyniku, np. $MPC_{10^{10}}$, jeśli w badaniu zastosowano 10^{10} CFU [58]. Rozmnażanie się antybiotykoopornych drobnoustrojów przy stężeniach powyżej wartości MPC wymagałaby jednoczesnego powstania dwóch mutacji, co jest zjawiskiem niezwykle rzadkim [46,58]. Autorzy teorii okna selekcji mutantów podkreślili także, iż jest to zakres stężeń, w którym mogą selektywnie zwiększać swoją liczebność zarówno spontaniczne mutanty powstające w trakcie antybiotykoterapii jak i te obecne w wyjściowej populacji przed jej ekspozycją na

antybiotyk [46,60]. Wartość MPC jest więc tak naprawdę najmniejszym stężeniem hamującym wzrost najbardziej opornego mutanta w populacji, niezależnie od czasu i sposobu jego powstania [46,60].

Zauważono, że gdy schematy dawkowania eksponowały bakterie na stężenia antybiotyku z zakresu MSW, szczepy oporne pojawiały się w stosunkowo krótkim czasie od jego wprowadzenia do lecznictwa [46,59]. Z kolei w przypadku antybiotyków, których stężenia w trakcie terapii przekraczały wartości MPC, szczepy oporne w warunkach klinicznych izolowano rzadko [61,62]. Istnienie okna selekcji mutantów potwierdzono także w modelach dynamicznych *in vitro*, polegających na prowadzeniu hodowli bakteryjnej w cyrkulującym bulionie z dodatkiem antybiotyku [63-67]. W większości przypadków dochodziło do selekcji antybiotykoopornych mutantów, gdy stężenia oscylowały w zakresie MSW wyznaczonym *in vitro* [58]. Podobna sytuacja miała miejsca w trakcie doświadczeń ze zwierzętami, co dowiodło, że dla wielu kombinacji antybiotyk-szczep okno selekcji mutantów istnieje także *in vivo* [68-72]. Uzyskane wyniki potwierdziły wyjściowe hipotezy [46,59,60,73], zgodnie z którymi dawkowanie w sposób zapewniający utrzymywanie stężenia antybiotyków w trakcie terapii powyżej wartości MPC dla danego szczepu powinno znacznie ograniczyć narastanie oporności wśród bakterii, przyczyniając się tym samym do wydłużenia okresu skuteczności klinicznej antybiotyków. Znane już antybiotyki, o bardzo szerokich zakresach MSW dla danych szczepów bakteryjnych powinny natomiast być stosowane tylko w terapii skojarzonej, wyłącznie z antybiotykiem o innym mechanizmie działania. W trakcie terapii skojarzonej utrzymywanie stężeń obu antybiotyków w powyżej ich indywidualnych wartości MPC powoduje, iż rozmnażanie się antybiotykoopornych mutantów byłoby możliwe jedynie w przypadku posiadania co najmniej dwóch mutacji (tj. warunkujących oporność na jeden i drugi antybiotyk) [46,59]. Zauważono również, że antybiotyki z tej samej grupy, o znacznym stopniu podobieństwa strukturalnego i porównywalnych wartościach MIC, mogą różnić się istotnie pod względem szerokości okien selekcji lekoopornych mutantów [58,59,61,62,74-76]. Ważne jest zatem wyznaczanie parametru MPC już na etapie wczesnych badań przedklinicznych kandydatów na nowe leki przeciwbakteryjne, w celu wskazania do dalszych prac związków nie tylko o niskich wartościach MIC, ale również o jak najwęższych zakresach MSW. Takie związki w najmniejszym stopniu stymulowałyby narastanie oporności wśród szczepów bakteryjnych w trakcie ich stosowania w lecznictwie.

Mimo udowodnienia, że aktualnie obowiązujące, oparte na wartościach MIC schematy dawkowania antybiotyków sprzyjają narastaniu oporności wśród bakterii i skracają okres przydatności klinicznej antybiotyków [46,59,60,73], z kilku powodów są stosowane do dziś. Po pierwsze, zwiększenie dawek tak, by utrzymywać stężenie antybiotyków w trakcie terapii powyżej wartości MPC nie zawsze jest osiągalne, ze względu na możliwe działania niepożądane antybiotyku [46,73]. Po drugie, zwiększanie dawek leków nie zawsze jest zasadne – aktualnie obowiązujące schematy dawkowania zapewniają sukces terapeutyczny u większości pacjentów przy najmniejszym możliwym nasileniu efektów niepożądanych antybiotyków [46,73]. Po trzecie, wiadomo, że komórki lekoopornych mutantów mogą być pod kontrolą układu immunologicznego gospodarza, jeżeli tylko ich liczba utrzymuje się na niskim poziomie [46,73]. Za bezpieczne dla powodzenia antybiotykoterapii przyjmuje się często te stężenia antybiotyków, dla których częstość selekcji opornych mutantów *in vitro* wynosi $1x10^{-8}$ lub mniej (tj. nie więcej niż 1 mutant selekcjonowany jest spośród 10^8 wrażliwych komórek) [46,77,78]. Sytuacja wygląda jednak odmiennie u pacjentów z immunosupresją (np. po transplantacjach, czy zakażonych wirusem HIV), których liczba nieustannie rośnie. Selekcjonujące się w tej grupie chorych oporne mutanty mogą być przyczyną niepowodzenia terapeutycznego lub nawrotu infekcji. Może również dojść do kolonizacji takich pacjentów przez lekooporne mutanty bakteryjne, a następnie do rozprzestrzenienia się lekoopornych mutantów na innych pacjentów [46,79].

Wyznaczanie wartości MPC za pomocą obecnie stosowanej metody rozcieńczeń w agarze [58] jest także pracochłonne oraz implikuje kilka problemów technicznych. Jednym z nich jest konieczność uzyskania inokulum o wysokiej gęstości, najlepiej przekraczającej 10^{11} CFU/ml. Przy obecnie stosowanej metodzie jego przygotowywania, polegającej na jednostopniowym zagęszczaniu hodowli płynnej, rzadko uzyskiwano tak gęste zawiesiny [58,74,80], częściej osiągając gęstość rzędu 10^{10} CFU/ml [64,66,67,72,81-83] lub tylko 10^9 CFU/ml [84,85]. Uzyskanie zawiesiny o mniejszej gęstości, zważywszy na konieczność poddania ekspozycji na każde stężenie antybiotyku minimum 10^{10} CFU, wymaga przygotowania dużej liczby płytek agarowych z każdym stężeniem badanego antybiotyku. Zwiększa to czasochłonność i pracochłonność wyznaczania wartości MPC, utrudniając jego wyznaczanie w warunkach laboratoriów szpitalnych. Z tych samych powodów, wyznaczenie wartości MPC jest problematyczne także na etapie badań przedklinicznych kandydatów na nowe leki przeciwbakteryjne, gdzie liczba badanych substancji jest duża, a ich dostępność często znacznie ograniczona.

Wreszcie, wykorzystanie MPC jako podstawy do opracowania nowych schematów dawkowania utrudnia również fakt, że wartość ta nie cechuje się pożądaną powtarzalnością. Gdy oznaczenie wartości MPC pięciu antybiotyków z różnych klas dla jednego szczepu *Staphylococcus epidermidis* powtórzono 20 razy w obrębie tego samego laboratorium, wyniki różniły się znacznie w przypadku każdego z badanych antybiotyków [83]. Stanowi to wyraźny kontrast z dobrze powtarzalnymi wartościami MIC [83]. Ponadto, granice MSW wyznaczone *in vitro* nie zawsze pokrywają się z granicami obserwowanymi później *in vivo* – jak chociażby w przypadku fosfomycyny, dla której okno selekcji opornych mutantów *Escherichia coli* i *Staphylococcus aureus* okazało się istnieć wyłącznie *in vitro* [86,87]. Wciąż aktualny pozostaje zatem apel Światowej Organizacji Zdrowia (ang. *World Health Organization* – WHO) o konieczności poszukiwania nowych, ograniczających narastanie oporności schematów dawkowania, zawarty w raporcie pt. „Globalna strategia WHO dotycząca ograniczania oporności na środki przeciwdrobnoustrojowe" (ang. *WHO Global strategy for containment of antimicrobial resistance*") z 2001 roku [57]. Są one niezbędne do maksymalnego wydłużenia okresu skuteczności klinicznej znanych oraz nowych antybiotyków. We wspomnianym raporcie zarekomendowano również podjęcie szeregu dodatkowych działań, ukierunkowanych na zmniejszenie presji antybiotykowej, takich jak racjonalizacja stosowania antybiotyków w medycynie i weterynarii (stosowanie zgodne ze wskazaniami, właściwe dawkowanie, monitorowanie zużycia antybiotyków), ograniczenie ich wykorzystywania w rolnictwie i hodowli zwierząt oraz ograniczanie szerzenia się chorób zakaźnych [57]. Zalecenia te były potem wielokrotnie powtarzane na forum międzynarodowym [8,88-90]. Zważywszy jednak na fakt, że raz powstałe antybiotykooporne mutanty są trudne a niekiedy wręcz niemożliwe do wyeliminowania, od samego początku podkreślono, że realizacja w/w zaleceń może jedynie spowolnić nieuchronny proces narastania oporności drobnoustrojów i stopniowej utraty skuteczności antybiotyków. Istnieje zatem także konieczność poszukiwania wciąż nowych związków przeciwdrobnoustrojowych [8,88-90].

4.2. Konieczność poszukiwania nowych leków przeciwdrobnoustrojowych

Mimo ponawianych apeli [8,88-90], wciąż nie udało się przerwać trwającego od lat 70. XX wieku impasu we wprowadzaniu na rynek nowych klas antybiotyków (Rycina 1) [8,57]. Przyczyną takiego stanu rzeczy są przede wszystkim wysokie koszty opracowania i zarejestrowania oryginalnego antybiotyku połączone z ograniczeniami narzucanymi

w jego stosowaniu oraz wysokim ryzykiem utraty klinicznej skuteczności nawet przed zwróceniem się poniesionych nakładów finansowych [8,57]. Powszechnie uważa się, że należy pilnie zwiększyć fundusze przeznaczane na poszukiwania nowych leków przeciwdrobnoustrojowych i zachęcać do podejmowania prac badawczo-rozwojowych w tej dziedzinie. Aby ukierunkować te prace na najbardziej pilne potrzeby, w 2017 roku opublikowana została lista tzw. bakteryjnych patogenów priorytetowych WHO (ang. *WHO priority pathogens*) [91], a w 2022 roku pojawiła się analogiczna lista najgroźniejszych, chorobotwórczych grzybów [92]. Znalazły się na nich drobnoustroje, dla których liczba dostępnych opcji terapeutycznych jest niepokojąco ograniczona, a zatem poszukiwanie nowych, aktywnych wobec nich leków jest szczególnie pilne. W obu dokumentach patogeny zostały przypisane do trzech kategorii: o krytycznym, wysokim lub średnim priorytecie. Ich pełną listę przedstawiono w Tabeli 1. Zgodnie z rekomendacjami WHO, poza aktywnością wobec patogenów priorytetowych, nowo opracowywane leki powinny być również innowacyjne, tj. mieć nową strukturę (nowa klasa chemiczna), nowy punkt uchwytu, nowy mechanizm działania lub dla których nie istnieje znana oporność krzyżowa [93]. Innowacyjność leków została uznana za czynnik istotnie zwiększający szanse na ich długi okres przydatności klinicznej.

Szeroko zakrojone działania na rzecz zintensyfikowania prac badawczo-rozwojowych nad nowymi lekami przeciwdrobnoustrojowymi nie przyniosły jak dotąd zadowalających efektów. W latach 2018-2020 Europejska Agencja Leków (ang. *European Medicines Agency* – EMA) dopuściła zaledwie sześć oryginalnych, szerokospektralnych preparatów, aktywnych wobec bakteryjnych patogenów priorytetowych: dwie kombinacje β-laktamów z inhibitorami β-laktamaz (imipenem/relebaktam – Recarbrio® oraz meropenem/waborbaktam – Vaborem®), pierwszy antybiotyk sideroforowy (cefiderokol – Fetroja®), nowy fluorochinolon (delafloksacynę – Quofenix®), nową tetracyklinę (erawacyklinę – Xerava®) i pierwszą pleuromutylinę do stosowania ogólnego (lefamulinę – Xenleta®). Ich właściwości dokładnie scharakteryzowano w przeglądowej **Publikacji P1** [94], wchodzącej w skład cyklu publikacji stanowiących niniejszą rozprawę doktorską. W tym samym czasie amerykańska Agencja Żywności i Leków (ang. *Food and Drug Administration* – FDA) zarejestrowała dodatkowo jeszcze jedną tetracyklinę (omadacyklinę – Nuzyra®) i aminoglikozyd nowej generacji (plazomycynę – Zemdri®) [38].

Tabela 1. Szczepy chorobotwórczych bakterii i grzybów o krytycznym, wysokim i średnim priorytecie wg WHO [91,92].

Bakterie	**Grzyby**
priorytet krytyczny	
• *Acinetobacter baumannii* oporne na karbapenemy; • *Pseudomonas aeruginosa* oporne na karbapenemy; • *Enterobacterales* oporne na karbapenemy; • *Enterobacterales* oporne na cefalosporyny III generacji; • *Mycobacterium tuberculosis;*	• *Cryptococcus neoformans* • *Candida auris* • *Aspergillus fumigatus* • *Candida albicans*
priorytet wysoki	
• *Staphylococcus aureus* oporne na metycylinę; • *Staphylococcus aureus* oporne na wankomycynę; • *Enterococcus faecium* oporne na wankomycynę; • *Helicobacter pylori* oporne na klarytromycynę; • *Campylobacter* spp. oporne na fluorochinolony; • *Salmonella* spp. oporne na fluorochinolony; • *Neisseria gonorrhoeae* oporne na fluorochinolony i cefalosporyny III generacji	• *Nakaseomyces glabrata* (*Candida glabrata*) • *Histoplasma* spp. • eumycetoma causative agents • *Mucorales* • *Fusarium* spp. • *Candida tropicalis* • *Candida parapsilosis*
priorytet średni	
• *Streptococcus pneumoniae* niewrażliwe na penicylinę • *Haemophilus influenzae* oporne na ampicylinę • *Shigella* spp. oporne na fluorochinolony	• *Scedosporium* spp. • *Lomentospora prolificans* • *Coccidioides* spp. • *Pichia kudriavzeveii* (*Candida krusei*) • *Cryptococcus gattii* • *Talaromyces marneffei* • *Pneumocystis jirovecii* • *Paracoccidioides* spp.

Następny, oryginalny lek przeciwbakteryjny pojawił się dopiero w maju bieżącego roku na rynku amerykańskim, kiedy to FDA zarejestrowała kolejną kombinację β-laktamu z inhibitorem β-laktamaz: sulbaktam/durlobaktam pod nazwą Xacduro® [95]. Spośród w/w dziewięciu oryginalnych leków tylko jeden (cefiderokol) wykazuje istotną aktywność wobec wszystkich patogenów krytycznych. Kolejne cztery leki (meropenem/waborbaktam, imipenem/relebaktam, erawacyklina oraz plazomycyna) są aktywne tylko wobec szczepów *Enterobacterales* opornych na karbapenemy (ang. *carbapenem-resistant Enterobacterales* – CRE*),* natomiast sulbaktam/durlobaktam tylko wobec szczepów *A. baumannii* opornych na karbapenemy (ang. *carbapenem-resistant A. baumannii* – CRAB). Pozostałe trzy leki (delafloksacyna, lefamulina i omadacyklina) wykazują aktywność wobec patogenów o wysokim priorytecie, tj. enterokoków opornych na wankomycynę (ang. *vancomycin-resistant enterococci* – VRE) i szczepów *S. aureus* opornych na metycylinę (ang. *methicillin-resistant S. aureus* – MRSA) [38]. Kryteria innowacyjności WHO spełniają: meropenem/waborbaktam (nowa klasa chemiczna, prawdopodobnie także brak oporności krzyżowej), lefamulina (nowa klasa chemiczna do stosowania ogólnego) oraz prawdopodobnie cefiderokol (brak oporności krzyżowej) [94]. Najnowszym oryginalnym lekiem przeciwgrzybiczym do stosowania ogólnego na rynku amerykańskim jest rezafungina (Rezzayo®) – nowa echinokandyna, zarejestrowana w marcu 2023 do leczenia inwazyjnych kandydoz [96]. Rezafungina nie uzyskała jeszcze rejestracji na rynku europejskim, na którym ostatnim dopuszczonym, oryginalnym lekiem przeciwgrzybiczym do stosowania ogólnego pozostaje izawukonazol (Cresemba®) – przedstawiciel azoli, zarejestrowany zarówno przez EMA jak i FDA w 2015 roku do leczenia inwazyjnej aspergilozy oraz mukormykozy u pacjentów, u których leczenie amfoterycyną B nie jest wskazane [97,98].

Przeprowadzona ostatnio przez WHO analiza leków przeciwbakteryjnych przechodzących aktualnie badania kliniczne wykazała, że nie odpowiadają one w pełni na najpilniejsze potrzeby [38]. W 2021 roku w badaniach klinicznych znajdowało się łącznie 45 nowych leków przeciwbakteryjnych. Spośród nich 12 wykazywało aktywność wobec *M. tuberculosis*, a kolejnych 27 wobec innych patogenów priorytetowych, z czego aż 13 stanowiły nowe kombinacje β-laktamów z inhibitorami β-laktamaz. Spośród 27 leków aktywnych wobec patogenów priorytetowych tylko 6 spełniało co najmniej jedno kryterium innowacyjności, z czego zaledwie dwa były aktywne wobec patogenów o krytycznym priorytecie. Zdaniem WHO, podstawowym problemem jest zbyt niska innowacyjność leków przeciwbakteryjnych w badaniach klinicznych oraz

niewystarczająca liczba leków aktywnych wobec patogenów o krytycznym priorytecie [38]. W badaniach klinicznych znajduje się ponadto 8 nowych leków przeciwgrzybiczych do stosowania ogólnego. Wśród nich 3 związki to nowi przedstawiciele znanych grup, tj. dwa azole i jeden antybiotyk polienowy. Pozostałe 5 związków to leki innowacyjne – jeden jest przedstawicielem nowej grupy triterpenoidów (o tym samym co echinokandyny mechanizmie działania, zrejestrowany już w 2019 roku do leczenia grzybicy pochwy), natomiast kolejne 4 związki wykazują innowacyjny mechanizm działania [99-101].

W badaniach przedklinicznych w 2021 roku znajdowało się łącznie 217 związków o właściwościach przeciwbakteryjnych, z których 69 wykazywało aktywność wobec opornych na karbapenemy szczepów *P. aeruginosa* (ang. *carbapenem-resistant P. aeruginosa* – CRPA), 50 wobec szczepów CRAB, a 60 wobec szczepów CRE. Aż 95 związków wykazywało selektywną aktywność wobec określonych drobnoustrojów, w tym 21 związków wobec *P. aeruginosa*, 8 wobec *A. baumannii*, 15 wobec *Enterobacterales*, 19 wobec *S. aureus* i 20 wobec *M. tuberculosis.* Zwrócono również uwagę na stosunkowo wysoki poziom innowacyjności leków przeciwbakteryjnych w badaniach przedklinicznych [38]. Ostatnio opisano również wiele innowacyjnych pod względem struktury substancji przeciwgrzybiczych oraz wytypowano kilku kandydatów na nowe leki przeciwgrzybicze spośród substancji zarejestrowanych już z innymi wskazaniami, m. in. przeciwnowotworowy tamoxifen, przeciwdepresyjna sertralina oraz celekoksyb z grupy niesteroidowych leków przeciwzapalnych [100]. Dodatkowo, udało się wskazać nowe punkty uchwytu dla leków przeciwgrzybiczych, takie jak hemobiosynteza oraz synteza sfingolipidów. Jest to szczególnie cenne, zważywszy na znaczne podobieństwo komórek eukariotycznych grzybów do komórek ludzkich, utrudniające opracowanie skutecznego leku o niskim poziomie toksyczności dla człowieka [100].

Mimo tak dużej liczby nowych, innowacyjnych substancji o aktywności przeciwdrobnoustrojowej w badaniach przedklinicznych, liczba nowo zarejestrowanych leków oraz leków w badaniach klinicznych jest wciąż niewystarczająca. Istnieje zatem potrzeba przyspieszenia opracowywania nowych, przede wszystkim innowacyjnych, kandydatów na leki. W ostatnich latach duże zainteresowanie jako źródło takich substancji wzbudzają związki boroorganiczne.

4.3. Bor i jego związki w medycynie

Bor to pierwiastek z grupy metaloidów, szeroko rozpowszechniony w naturze. Dla bakterii, grzybów i roślin jest niezbędnym mikroelementem. Jego rola w organizmach zwierzęcych nie jest w pełni poznana, aczkolwiek został on sklasyfikowany przez WHO jako pierwiastek „prawdopodobnie niezbędny" dla człowieka. Uważa się, że jest istotny dla prawidłowego przebiegu gospodarki wapniowej czy metabolizmu hormonów steroidowych [102,103]. Jako pierwiastek chemiczny bor prezentuje szereg ciekawych właściwości. Pusty orbital *p* powoduje, że jest on silnym kwasem Lewisa oraz elektrofilem, zdolnym do tworzenia wiązań koordynacyjnych z nukleofilami, takimi jak grupy hydroksylowe i aminowe obecne w białkach, węglowodanach i kwasach nukleinowych. Powstanie takiego wiązania pociąga za sobą zmianę hybrydyzacji atomu boru z sp^2 na sp^3 oraz konwersję płaskiej, trójkątnej struktury obojętnej do tetraedrycznej struktury anionowej. W przypadku wielu jego związków jest to możliwe także w warunkach fizjologicznego pH. Stwarza to szerokie możliwości ich zastosowania w medycynie, m. in. do inhibicji różnych enzymów. Obecność boru w cząsteczce związku odpowiada za jego interakcję z miejscem aktywnym enzymu, natomiast siłę i selektywność jej wiązania z cząsteczkami docelowymi można modulować, wprowadzając odpowiednie modyfikacje strukturalne [104,105]. Związki boru obecne są w medycynie od lat. Antyseptyczne właściwości prostego kwasu borowego zaczęto wykorzystywać już w XIX wieku i do dziś jest to zarówno popularny konserwant oraz składnik antyseptycznych preparatów do stosowania zewnętrznego [105,106]. Mimo to, związki boru przez wiele lat były pomijane jako źródło substancji leczniczych do stosowania ogólnego ze względu na domniemaną toksyczność tego pierwiastka. Ostatecznie jednak wykazano, że bor nie jest toksyczny *per se*, a toksyczność niektórych jego związków wynika z ich indywidualnej struktury i mechanizmu działania [104,105].

Brak toksyczności oraz opisane powyżej, interesujące właściwości boru sprawiły, że jego związki, przede wszystkim te boroorganiczne (tj. zawierające wiązanie bor-węgiel), to w chwili obecnej niezwykle liczna grupa, w której intensywnie poszukuje się nowych substancji o aktywności biologicznej. Wśród badanych pochodnych można wyróżnić związki niecykliczne (alifatyczne i aromatyczne kwasy boronowe oraz ich estry i hemiestry) jak również związki boraheterocykliczne (zawierające w pierścieniu poza borem i węglem także inny atom, np. tlen, azot czy krzem), np. cykliczne estry i hemiestry kwasów boronowych (nazywane czasem cyklicznymi kwasami boronowymi), benzoksaborole, benzosiloksaborole, diazaboryny, oksadiazaborole i oksazaborolidyny

(Rycina 2) [104-107]. Wśród związków boraheterocyklicznych największą i najintensywniej badaną grupę stanowią benzoksaborole – cykliczne hemiestry kwasu 2-(hydroksymetylo)fenyloboronowego, których cząsteczka składa się z pierścienia benzenowego skondensowanego z pięcioczłonowym pierścieniem oksaborolu [108]. Ich strukturalnymi analogami są benzosiloksaborole, zawierające atom krzemu w miejscu jednego atomu węgla w pierścieniu oksaborolu [109,110]. W odróżnieniu od niecyklicznych kwasów boronowych wiązanie bor-węgiel w pierścieniu oksaborolu jest mniej podatne na hydrolizę. Dodatkowo, benzoksaborole charakteryzują się znacznie niższą kwasowością niż kwasy boronowe, co przekłada się na ich lepszą rozpuszczalność w wodzie przy fizjologicznym pH oraz łatwiejsze tworzenie wiązań z biologicznymi nukleofilami, a co za tym idzie na większą aktywność terapeutyczną. Dalsze obniżenie kwasowości benzoksaboroli można uzyskać między innymi poprzez wprowadzenie atomu krzemu do pierścienia oksaborolu [111,112].

Rycina 2. Grupy związków boroorganicznych, których przedstawiciele wykazują aktywność przeciwbakteryjną lub przeciwgrzybiczą.

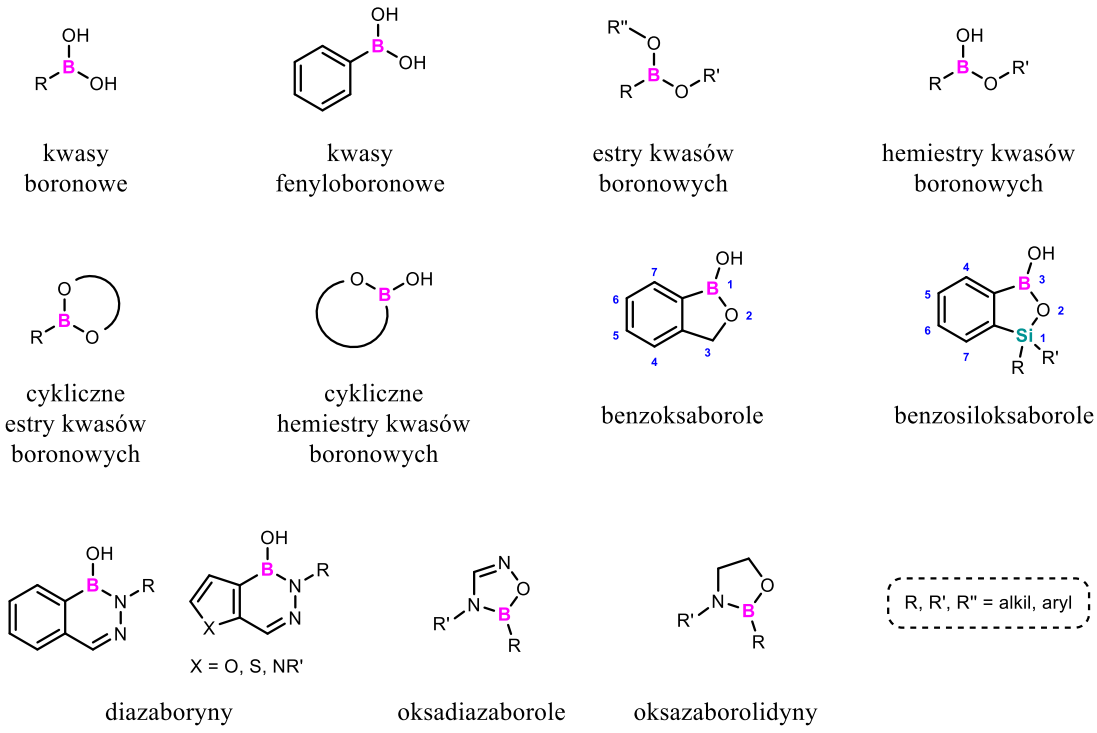

Wśród dotąd otrzymanych związków boroorganicznych uzyskano liczne pochodne o działaniu m. in. przeciwnowotworowym, przeciwzapalnym, przeciwbakteryjnym, przeciwgrzybiczym, przeciwwirusowym i przeciwpasożytniczym [104-107]. Pierwszym

borooganicznym lekiem był bortezomib (Velcade®) – dipeptydowy kwas boronowy, zarejestrowany w 2003 przez FDA, a w 2004 roku przez EMA do leczenia szpiczaka mnogiego i chłoniaka z komórek płaszcza [107,113]. Kolejny lek z tej samej grupy i o tym samym wskazaniu (iksazomib) został zarejestrowany przez FDA w 2015, a przez EMA w 2016 roku pod nazwą Ninlaro® [107,113]. W następnych latach FDA zarejestrowała również pierwsze benzoksaborole do stosowania miejscowego – w 2014 roku tawaborol (Kerydin®) do leczenia grzybicy paznokci, a w 2017 crisaborol (Eucrisa®) do leczenia atopowego zapalenia skóry [104]. Pierwszym boroorganicznym związkiem przeciwbakteryjnym zarejestrowanym jako lek do stosowania ogólnego u ludzi był natomiast opisany w przeglądowej **Publikacji P1** waborbaktam (w kombinacji z meropenemem) [94]. Sukces tawaborolu i waborbaktamu w połączeniu z innowacyjnością struktury związków boroorganicznych jako leków przeciwdrobnoustrojowych sprawiły, że ich właściwości przeciwgrzybicze i przeciwbakteryjne są w ostatnich latach intensywnie badane, a wśród uzyskanych pochodnych znajdują się zarówno związki o wysokiej aktywności bezpośredniej wobec grzybów i bakterii (także szczepów priorytetowych wg WHO) jak i związki zdolne do inhibicji bakteryjnych β-lakatamaz. Najbardziej obiecujące właściwości przeciwdrobnoustrojowe wykazano jak dotąd dla kwasów boronowych, benzoksaboroli i benzosiloksaboroli [104,107].

4.3.1. Boroorganiczne inhibitory β-laktamaz

Znanym sposobem przywracania skuteczności antybiotyków β-laktamowych wobec bakterii wytwarzających inaktywujące je enzymy (β-laktamazy) jest ich podawanie razem z odpowiednim inhibitorem β-laktamaz (ang. *β-lactamses inhibitor* – BLI). Pierwsze tego typu związki, tj. kwas klawulanowy, sulbaktam, tazobaktam, oparte na szkielecie β-laktamowym, pojawiły się na rynku już w latach 80. i 90. XX wieku [37]. Nie wykazują one jednak aktywności wobec najistotniejszych obecnie β-laktamaz, tj. karbapenemaz. Wytwarzanie karbapenemaz jest jedną z głównych przyczyn oporności patogenów krytycznych wg WHO [32]. Najistotniejsze klinicznie karbapenemazy pałeczek Gram-ujemnych należą, zgodnie z klasyfikacją Amblera [114], do klasy A (przede wszystkim enzymy typu KPC – ang. *Klebsiella pneumoniae carbapenemase*, spośród których najbardziej rozpowszechnione na świecie są warianty KPC-2 i KPC-3), klasy B (tzw. metalo-β-laktamazy, np. z rodzin NDM – ang. *New Delhi metallo-β-lactamase* oraz VIM – ang. *Verona integron-encoded metallo-β-lactamase*) i klasy

D (enzymy z grupy CHDL – ang. *carbapenem-hydrolyzing class D β-lactamases*, o zachowanej aktywności oksacylinaz z rodziny OXA) [32]. Rzadsze są karbapenemazy z klasy C, jak np. enzym ADC-68 u *A. baumannii* [115,116]. Dużym problemem klinicznym jest także oporność bakterii o krytycznym priorytecie na cefalosporyny III generacji, co związane jest z wytwarzaniem należących do klasy A β-laktamaz o rozszerzonym spektrum substratowym (ang. *extended-spectrum β-lactamases*–ESBL), np. typu CTX-M lub z nadprodukcją cefalosporynaz z klasy C (enzymów AmpC), zarówno chromosomalnych (cAmpC) jak i kodowanych plazmidowo (pAmpC, np. enzymu CMY-2) [117,118]. Dopiero w ostatnich latach wprowadzono do lecznictwa kilka nowych, nie-β-laktamazowych inhibitorów diazabicyklooktanowych (awibaktam, relebaktam oraz durlobaktam) i boroorganicznych (waborbaktam), których spektrum obejmuje także niektóre karbapenemazy z klasy A, w tym enzymy typu KPC [94,119] oraz z klasy D [95]. Jednakże enzymy z klasy B są wciąż poza spektrum inhibitorów dopuszczonych do stosowania w lecznictwie [38,119].

Odwracalne hamowanie penicylinazy *Bacillus cereus* przez kwas borowy, fenyloboronowy (ang. *phenylboronic acid* – PBA) oraz *meta*-aminofenyloboronowy opisano już w latach 70. XX wieku [120]. Dwa ostatnie kwasy są wciąż wykorzystywane w rekomendowanych przez Europejski Komitet ds. Oznaczania Lekowrażliwości (ang. *European Committee on Antimicrobial Susceptibility Testing* – EUCAST) fenotypowych metodach wykrywania szczepów pałeczek Gram-ujemnych wytwarzających enzymy typu KPC [121]. Kwasy boronowe nazywane są często inhibitorami stanu przejściowego (ang. *boronic acid transition state inhibitors*–BATSIs), ponieważ atom boru naśladując karbonylowy atom węgla pierścienia β-laktamowego tworzy tetrahedralny addukt z seryną w centrum katalitycznym β-laktamaz, przypominający stan przejściowy w reakcji hydrolitycznej. W efekcie związki te działają jako kompetycyjne, odwracalne inhibitory β-laktamaz serynowych [122,123]. W ostatnich latach prace badawczo-rozwojowe koncentrowały się przede wszystkim na syntezie kwasów boronowych o bardziej rozbudowanej strukturze, zapewniającej większą selektywność wobec bakteryjnych β-laktamaz oraz niższą toksyczność – otrzymano wiele pochodnych (zarówno niecyklicznych jak i cyklicznych) o obiecującej aktywności [113,123]. Ponadto opisano również boroorganiczne inhibitory β-laktamaz z grupy benzoksaboroli [124-126] oraz benzosiloksaboroli [110].

4.3.1.1. Cykliczne kwasy boronowe jako inhibitory β-laktamaz

Pierwszym wprowadzonym do lecznictwa inhibitorem β-laktamaz z grupy tzw. cyklicznych kwasów boronowych jest opisany w przeglądowej **Publikacji P1** waborbaktam, tj. kwas 2-[(3R,6S)-2-hydroksy-3-[(2-tiofen-2-ylacetyl)amino] oksaborinan-6-yl]octowy (Rycina 3) [94,127]. Jest to monocykliczny inhibitor enzymów z klasy A (enzymów ESBL z rodzin CTX-M, TEM i SHV, karbapenemaz typu KPC i SME) oraz klasy C (enzymów AmpC), ale bez aktywności inhibicyjnej wobec β-laktamaz z klasy B (np. z rodzin NDM, VIM) oraz D (np. OXA-48). Nie wykazuje on także bezpośredniej aktywności przeciwbakteryjnej w stężeniach terapeutycznych [94]. Stwierdzono, że waborbaktam skutecznie zwiększa aktywność meropenemu wobec szczepów CRE (z wyłączeniem szczepów produkujących metalo-β-laktamazy) ale nie wobec szczepów CRPA, CRAB czy *Stenotrophomonas maltophilia* [94]. Oporność na meropenem/waborbaktam jest zwykle związana z wytwarzaniem metalo-β-laktamaz, zaburzeniem wnikania waborbaktamu do komórki (mutacje w genach kodujących białka poryn takich jak OmpK35, OmpK36), lub nadprodukcją enzymów typu KPC, związanej ze zwiększeniem liczby kopii genów bla_{KPC} w genomie bakteryjnym. Jak dotąd, nie opisano przypadku oporności szczepu wynikającej jedynie z mutacji w genach bla_{KPC} [94,128]. Kombinacja meropenem/waborbaktam do stosowania dożylnego została zarejestrowana przez FDA 29 VIII 2017 roku (Vabomere®) [129], a przez EMA 20 XI 2018 roku (Vaborem®) [130]. Wskazania tych leków obejmują leczenie powikłanych zakażeń układu moczowego (w tym odmiedniczkowego zapalenia nerek), powikłanych zakażeń w obrębie jamy brzusznej, szpitalnych zapaleń płuc (także respiratorowych zapaleń płuc) oraz zakażeń wywołanych tlenowymi drobnoustrojami Gram-ujemnymi u pacjentów dorosłych, z ograniczonymi możliwościami leczenia [131]. Ze względu na narastający problem zakażeń szczepami wytwarzającymi metalo-β-laktamazy podjęto również próby skojarzenia meropenemu/waborbaktamu z aztreonamem – monobaktamem rozkładanym przez szereg enzymów z klasy A, C oraz D (tzw. serynowych β-laktamaz), ale opornym na działanie metalo-β-laktamaz. Taka trójskładnikowa kombinacja wykazuje wysoką skuteczność *in vitro* wobec wielolekoopornych szczepów *K. pneumoniae* oraz *E. coli* wytwarzających zarówno enzymy typu NDM jak i enzymy typu ESBL lub KPC [94]. Istnieją również doniesienia o klinicznych sukcesach terapeutycznych wynikających ze stosowania takiej kombinacji w leczeniu zakażeń wywołanych szczepami produkującymi metalo-β-laktamazy, opornymi na kombinację ceftazydym/awibaktam [132,133].

Badania kliniczne przechodzą aktualnie trzy kolejne boroorganiczne inhibitory β-laktamaz oparte na farmakoforze cyklicznego kwasu boronowego (Rycina 3). Są to [38,134,135]:

- taniborbaktam (wcześniej nazywany VNRX-5133) – aktualnie w fazie 3, testowany w kombinacji z cefepimem do podawania dożylnego w powikłanych zakażeniach dróg moczowych;
- ledaborbaktam (wcześniej VNRX-5236) – aktualnie w fazie 1, testowany w kombinacji z ceftibutenem do podawania doustnego w leczeniu powikłanych zakażeń dróg moczowych;
- kseruborbaktam (wcześniej QPX7728) – aktualnie w fazie 1, testowany w kombinacji z β-laktamem QPX2014 do podawania dożylnego oraz w kombinacji z β-laktamem QPX2015 do podawania dożylnego oraz doustnego.

Rycina 3. Boroorganiczne leki o aktywności inhibitorów β-laktamaz.

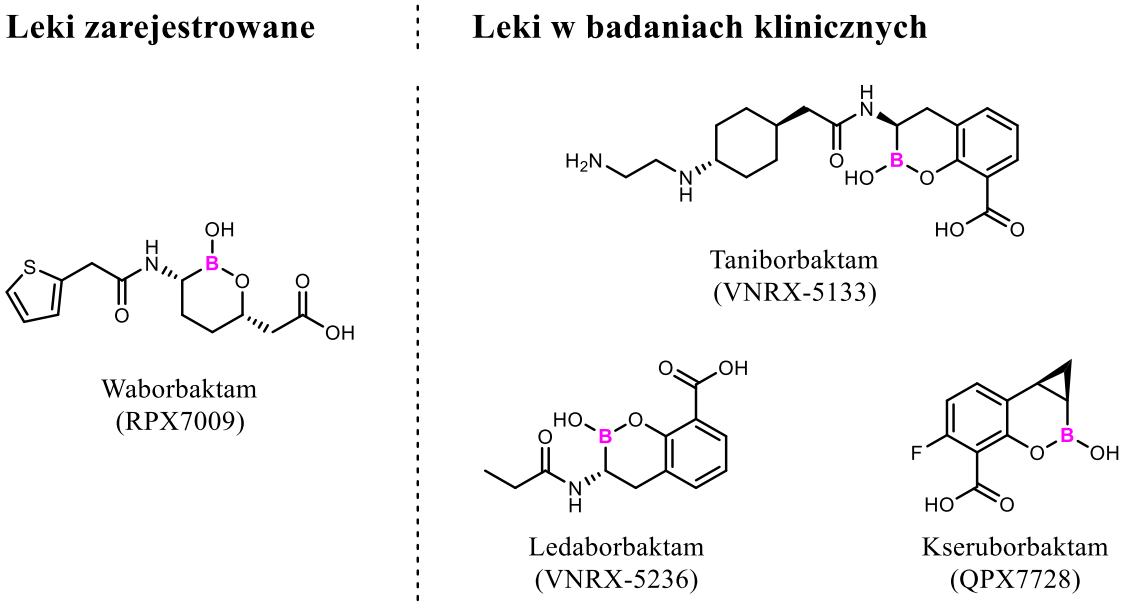

W porównaniu do waborbaktamu, taniborbaktam jest inhibitorem bicyklicznym, o znacznie szerszym spektrum substratowym, obejmującym zarówno serynowe β-laktamazy z klasy A (ESBL z rodzin SHV i CTX-M oraz karbapenemazy KPC-2 i KPC-3), z klasy C (AmpC) oraz D (z grupy OXA-48), jak i metalo-β-laktamazy (z rodzin NDM, VIM, z wyłączeniem IMP). Taniborbaktam przywraca wrażliwość na cefepim zarówno szczepom CRE jak i CRPA [136-138]. Zmniejszoną wrażliwość na

kombinację cefepim/taniborbaktam stwierdzano u szczepów produkujących enzymy IMP, ze zmienionym białkiem PBP3, ze zmianami w strukturze poryn błony zewnętrznej (OmpK35, OmpK36) oraz z nadprodukcją pompy błonowej AcrAB [136,137]. Ostatnio wykazano jednak, że taniborbaktam nie hamuje aktywności enzymu NDM-9, różniącego się od enzymu NDM-1 zaledwie jednym aminokwasem [139]. Znaczne rozpowszechnienie szczepów wytwarzających NDM-9 [140], w połączeniu ze stwierdzonym niedawno rozpowszechnieniem heterooporności na cefepim/taniborbaktam wśród szczepów CRE wytwarzających metalo-β-laktamazy [141] grożą skróceniem okresu klinicznej skuteczności tego inhibitora wobec szczepów wytwarzających metalo-β-lakatamazy.

Ledaborbaktam jest bicyklicznym inhibitorem enzymów typu ESBL (np. z rodzin CTX-M oraz SHV), cefalosporynaz z klasy C (np. P99 oraz CMY-2) oraz karbapenemaz z klasy A (typu KPC) i D (z grupy OXA-48). Nie jest jednak inhibitorem enzymów z klasy B, jak również nie wykazuje bezpośredniej aktywności przeciwbakteryjnej [134,142-144]. Skutecznie przywraca wrażliwość na ceftibuten wytwarzającym powyższe enzymy szczepom z rzędu *Enterobacterales*, a jego niewątpliwą zaletą jest możliwość podawania *per os* (w postaci proleku – etzadroksylu ledaborbaktamu, wcześniej nazywanego VNRX-7145). Stwarza to możliwości leczenia zakażeń wywołanych opornymi szczepami *Enterobacterales* bez konieczności hospitalizacji [134,142]. Częstość selekcji spontanicznych mutantów *in vitro* na stężeniach odpowiadających 4xMIC ceftibutenu w obecności 4 mg/l ledaborbaktamu jest niska ($<10^{-10}$) [143], wciąż jednak brakuje szczegółowych danych dotyczących ewentualnych mechanizmów niespecyficznej oporności na ceftibuten/ledaborbaktam [134].

Najszersze spektrum aktywności spośród inhibitorów boroorganicznych wykazuje jak dotąd kseruborbaktam – także reprezentant inhibitorów bicyklicznych [127,135]. Hamuje on aktywność serynowych enzymów typu ESBL z klasy A (z rodzin CTX-M, SHV, TEM, VEB oraz PER), karbapenemaz z klasy A (z rodzin KPC, SME, NMCA oraz enzymów GES-20, VCC-1 i BKC-1), enzymów z klasy C (zarówno plazmidowych z rodzin CMY, FOX, MIR oraz DHA, jak i chromosomalnie kodowanych z rodzin PDC i ADC), oraz karbapenemaz z klasy D (z grupy OXA-48 u *Enterobacterales* oraz enzymów CHDL z rodzin OXA-23, OXA-24, OXA-72 oraz OXA-58 u *A. baumannii*). Ponadto, w jego spektrum działania jako inhibitora wchodzą metalo-β-laktamazy typu NDM, VIM, IMP oraz GIM, jak również enzym CcrA1 [145,146]. Kseruborbaktam przywracał wrażliwość na meropenem, cefepim, aztreonam szczepom CRE, na

meropenem szczepom CRAB oraz na meropenem, cefepim, ceftolozan i piperacylinę szczepom CRPA [145]. Rozważana jest zatem możliwość jego dopuszczenia do obrotu jako samodzielnego leku, do stosowania w terapii skojarzonej z różnymi β-lakatamami [145]. W przeciwieństwie do innych boroorganicznych inhibitorów β-laktamaz, kseruborbaktam wykazuje także umiarkowaną aktywność bezpośrednią wobec szczepów *Enterobacterales* (wartości MIC rzędu 16−32 mg/l) oraz *A. baumannii* (wartości MIC rzędu 16−64 mg/l), co jest wynikiem jego wiązania się z białkami PBP. W rezultacie kseruborbaktam działa synergistycznie z karbapenemami także wobec szczepów niewytwarzających karbapenemaz [135]. Wykazano również, że niespecyficzne mechanizmy oporności (takie jak zmniejszenie przepuszczalności błony zewnętrznej czy zwiększenie aktywnego usuwania z komórek bakteryjnych przez pompy błonowe) mają niewielki wpływ na aktywność kseruborbaktamu [147]. Poza wymienionymi powyżej związkami, wiele innych, cyklicznych inhibitorów boroorganicznych znajduje się aktualnie w różnych fazach badań przedklinicznych [123,148-151].

4.3.1.2. Niecykliczne kwasy boronowe jako inhibitory β-laktamaz

Bogatym źródłem substancji o aktywności inhibitorów β-laktamaz są także niecykliczne kwasy boronowe, zarówno alifatyczne jak i aromatyczne. Wśród nich uzyskano pochodne zdolne do hamowania aktywności enzymów z klasy A, np. PC1 [152], TEM-1 [152,153] oraz z rodzin SHV [154], GES [155], KPC [154-158] i CTX-M [122,153,158,159], jak również enzymów z klasy C, tj. cAmpC [152,153,155,158-164]. Ostatnio otrzymano także pochodne o aktywności inhibitora enzymów klasy D, tj. z rodzin OXA-24 [158,164,165] oraz OXA-48 [166], a nawet klasy B, tj. z rodzin VIM [158,166] i NDM [158,166]. Niektóre związki charakteryzowały się szerokim spektrum hamowanych β-laktamaz, obejmującym zarówno enzymy klasy A jak i enzymy klasy C [153,158] lub klasy C oraz D [164]. Opisano nawet cząsteczki kwasów boronowych zdolne do hamowania enzymów należących do wszystkich czterech klas wg Amblera, włącznie z enzymami z klasy B np. VIM-2 i NDM-1 [166]. Wiele z tych związków było w stanie także zwiększać aktywność antybiotyków wobec bakterii wytwarzających określone β-laktamazy, w tym także wobec bakterii Gram-ujemnych, np. *E. coli* [154,155,157,158,163], *K. pneumoniae* [154,158], *A. baumannii* [158,163], *P. aeruginosa* [155,158]. Niestety, niektóre pochodne kwasów boronowych, zwłaszcza o rozbudowanej strukturze mimo dużego powinowactwa do β-laktamaz *in vitro*, nie były jednak w stanie zwiększać aktywności antybiotyków β-laktamowych wobec bakterii Gram-ujemnych, co

przypuszczalnie wynikało z niemożliwości ich wnikania do wnętrza komórek bakteryjnych. Błona zewnętrzna występująca u pałeczek Gram-ujemnych jest bowiem barierą, która chroni je przed wieloma antybiotykami, będąc częstą przyczyną braku skuteczności związków przeciwbakteryjnych [152,161,164-166].

Mimo tak dużego zainteresowania kwasami boronowymi jako potencjalnymi inhibitorami β-laktamaz, prowadzone dotąd badania koncentrowały się na otrzymywaniu kolejnych pochodnych kwasu boronowego lub fenyloboronowego. Tymczasem interesującą grupą związków boroorganicznych są także kwasy di- oraz triboronowe, które dzięki obecności dodatkowych grup boronowych charakteryzują się zmniejszoną lipofilowością oraz kwasowością w porównaniu do związków monoboronowych. Aromatyczne kwasy di- oraz triboronowe są od dawna stosowane w syntezie organicznej [167,168], jednak dane o ich aktywności biologicznej są szczątkowe [169]. Jest to również grupa dotąd pomijana w pracach badawczo-rozwojowych nad nowymi lekami przeciwdrobnoustrojowymi.

4.3.1.3. Benzoksaborole oraz benzosiloksaborole jako inhibitory β-laktamaz

Boroorganiczne inhibitory β-laktamaz o strukturze benzoksaboroli [124,125] oraz benzosiloksaboroli [110] znajdują się aktualnie w fazie badań przedklinicznych. Jak dotąd wykazano, że wiele C6-heterofenylenoksy podstawionych benzoksaboroli w testach enzymatycznych hamuje aktywność enzymów z klasy A (CTX-M-9a oraz TEM-1), jak również z klasy C (cAmpC oraz CMY-2), a najbardziej aktywne z nich już w stężeniu 8 mg/l przywracały wrażliwość na ceftazydym szczepowi *Enterobacter cloacae* cAmpC-dodatniemu oraz *E. coli* CMY-2-dodatniemu [125]. Dalsze modyfikacje strukturalne doprowadziły do otrzymania innych, 6-fenylenoksy podstawionych pochodnych, które w testach enzymatycznych poza enzymami z klasy A (TEM-1, CTX-M-15 oraz karbapenemazy KPC-2) i z klasy C (P99 czy cAmpC), hamowały także aktywność karbapenemazy OXA-24 z klasy D. Najbardziej aktywny był 6-tiadiazoloksy podstawiony benzoksaborol, który już w stężeniu 4 mg/l zwiększał aktywność cefepimu wobec klinicznych szczepów *E. coli* i *K. pneumoniae* wytwarzających różne β-laktamazy, w tym KPC-2 [124]. Ostatnio otrzymano natomiast 3-fenylenobenzoksaborole o szerokim spektrum inhibicji, obejmującym w testach enzymatycznych zarówno enzymy serynowe (m. in. KPC-2) jak i metalo-β-laktamazę NDM-1. Najbardziej aktywny inhibitor zwiększał także aktywność meropenemu wobec szczepów *E. coli* KPC-2-dodatnich [126].

Spośród benzosiloksaboroli największą aktywność wykazywała jak dotąd pochodna zawierająca grupę $B(OH)_2$ w pozycji 6. Związek ten już w stężeniu 16 mg/l powodował znaczącą (tj. minimum 4-krotną) redukcję wartości MIC meropenemu u szczepów *E. coli* i *K. pneumoniae* wytwarzających enzymy KPC-2 oraz KPC-3, jak również ceftazydymu u szczepów wytwarzających cAmpC (*P. aeruginosa*) i CMY-2 (*E. coli* i *K. pneumoniae*). Dokowanie molekularne potwierdziło, że jego forma dianionowa tworzy silne wiązania z enzymem KPC-2 [110]. Analogiczne benzosiloksaborole zawierające grupę $B(OH)_2$ w pozycji 5 lub 7 nie były natomiast aktywne [110]. Umiarkowaną aktywność inhibitorów enzymu CMY-2 wykazywały również benzosiloksaborole podstawione atomami fluoru w pozycji 6 i 7, oraz dwa związki o unikatowej strukturze, zawierające dodatkowy pierścień oksaborolu skondensowany z pierścieniem benzenowym benzosiloksaborolu. Pochodne te, dodane w ilości 300 μg na krążek z 30 μg ceftazydymu znacząco powiększały strefę zahamowania wzrostu szczepu *E. coli* CMY-2-dodatniego w porównaniu do krążka z samym antybiotykiem [110].

4.3.2. Boroorganiczne związki o bezpośredniej aktywności przeciwdrobnoustrojowej

Związki boroorganiczne są także bogatym źródłem substancji o bezpośredniej aktywności przeciwbakteryjnej oraz przeciwgrzybiczej. Najwięcej związków o wysokiej bezpośredniej aktywności przeciwdrobnoustrojowej uzyskano w grupie benzoksaboroli oraz benzosiloksaboroli. Spośród innych związków boroorganicznych najwięcej doniesień dotyczyło potencjału przeciwdrobnoustrojowego niektórych kwasów boronowych i diazaboryn, rzadko oksadiazaboroli czy oksazaborolidyn [104,107].

4.3.2.1. Mechanizmy bezpośredniego działania przeciwdrobnoustrojowego związków boroorganicznych

Najczęściej opisywanym mechanizmem działania przeciwdrobnoustrojowego związków boroorganicznych jest hamowanie syntezy białek poprzez blokownie aktywności syntetazy leucylo-tRNA (ang. *leucyl-tRNA synthetase* - LeuRS) – enzymu odpowiedzialnego za przyłączanie leucyny do tRNA, należącego do grupy 20 syntetaz aminoacylo-tRNA, specyficznych dla każdego z 20 aminokwasów [170]. Uchodzą one za dobry cel terapeutyczny dla nowych leków przeciwdrobnoustrojowych, przede wszystkim ze względu na znaczne różnice między enzymami występującymi u ssaków,

a ich odpowiednikami u bakterii i grzybów [170]. Przykładem antybiotyku o takim mechanizmie działania jest mupirocyna, będąca inhibitorem syntetazy izoleucylo-tRNA. Lek ten nie jest jednak zarejestrowany do stosowania ogólnego ze względu na swój profil farmakokinetyczny [170]. Po raz pierwszy hamowanie aktywności LeuRS opisano dla benzoksaboroli, które tworzą stabilne „spiroaddukty" z kompleksem LeuRS-tRNA, uniemożliwiając tRNA zarówno opuszczenie tego kompleksu jak i przemieszczenie się do centrum aktywnego enzymu. Ten specyficzny mechanizm inhibicji LeuRS nazwano pułapkowaniem tRNA oksaborolem (ang. *oxaborole tRNA-trapping* - OBORT) [171]. Leki przeciwdrobnoustrojowe hamujące LeuRS spełniają kryteria innowacyjności wg WHO (nowy mechanizm działania) [38]. Rzadziej opisywane są inne niż LeuRS punkty uchwytu benzoksaboroli o bezpośrednim działaniu przeciwdrobnoustrojowym, takie jak: (I) dehydrogenaza NADH u *M. tuberculosis* w przypadku 7-fenylobenzoksaboroli [172], (II) zaangażowana w syntezę kwasów tłuszczowych reduktaza enoilo-ACP (ang. *acyl carrier protein*– białko nośnikowe grup acylowych) u *E. coli* w przypadku 6-benzyloksybenzoksaboroli [173], oraz (III) anhydrazy węglanowe u *Vibrio cholerae* w przypadku benzoksaboroli podstawionych mocznikiem lub tiomocznikiem w pozycji 6 [174]. Inhibitorami reduktazy enoilo-ACP są także niektóre diazaboryny [105,107]. Niewiele wiadomo jak dotąd o molekularnych mechanizmach działania innych grup związków boroorganicznych o bezpośredniej aktywności przeciwdrobnoustrojowej.

4.3.2.2. Benzoksaborole i benzosiloksaborole o bezpośrednim działaniu przeciwdrobnoustrojowym

Jedynym zarejestrowanym już lekiem boroorganicznym o bezpośredniej aktywności przeciwdrobnoustrojowej jest w chwili obecnej tawaborol (wcześniej o nazwie AN2690), tj. 5-fluoro-1,3-dihydro-1-hydroksy-2,1-benzoksaborol (Rycina 4). Jego 5% roztwór do stosowania miejscowego (Kerydin®) został dopuszczony w 2014 roku przez FDA do leczenie grzybicy płytki paznokcia wywoływanej przez dermatofity *Trichophyton rubru*m i *Trichophyton mentagrophytes* [175]. Zasadniczą trudnością w opracowywaniu leków skutecznych w tym schorzeniu jest konieczność ich przeniknięcia do płytki paznokcia. Tawaborol, z uwagi na swoje niewielkie rozmiary, bardzo dobrze przenika do tego kompartmentu, osiągając zarówno w płytce jak i łożysku paznokcia stężenia przekraczające wartości minimalnych stężeń grzybobójczych (ang. *minimal fungicidal concentration* – MFC) [175]. W warunkach *in vitro* tawaborol wykazuje szerokie spektrum aktywności – w stężeniach 0,25−2 mg/l hamuje wzrost

szczepów *Candida* spp., *Malassezia* spp., *Microsporum* spp., *Trichophyton* spp., *Crypococcus neoformans* oraz *A. fumigatus*. Zakres wartości MIC dla klinicznych izolatów *T. rubrum* i *T. mentagrophytes* wynosił 1−32 mg/l, a wartości MFC wynosiły 2−>32 mg/l [175,176]. Wykazuje on również umiarkowaną aktywność wobec bakterii Gram-dodatnich (zakres wartości MIC 12,5–200 mg/l), Gram-ujemnych pałeczek niefermentujących (zakres wartości MIC 6,25–400 mg/l) oraz pałeczek z rzędu *Enterobacterales* (zakres wartości MIC 6.25–100 mg/l) [175,177]. Mechanizm działania tawaborolu polega na hamowaniu aktywności LeuRS [171]. Oporność na tawaborol powstaje w następstwie mutacji w genie kodującym LeuRS ale jak dotąd nie wiązała się ona z opornością krzyżową na inne leki przeciwgrzybicze. Częstość selekcji spontanicznych, jednostopniowych mutantów *T. rubrum* przy stężeniu 4xMIC tawaborolu kształtowała się na poziomie ok. 10^{-8} [178]. Wykazano, że do selekcji opornych na tawaborol mutantów może dochodzić także w stężeniach subinhibitorowych (0,5xMIC). Zważywszy jednak na osiągane w trakcie terapii wysokie stężenia w miejscu infekcji oraz brak oporności krzyżowej uznano, że tawaborol może być z powodzeniem stosowany w leczeniu grzybicy paznokci [178]. Ostatnio wykazano również synergistyczne oddziaływanie tawaborolu z aminoglikozydami wobec szczepów *E. coli* [179]. Zważywszy na niską toksyczność tawaborolu po podaniu ogólnym, może on być rozważany jako kandydat do zastosowania w systemowej, skojarzonej terapii przeciwbakteryjnej [179].

Rycina 4. Boroorganiczne leki o bezpośredniej aktywności przeciwbakteryjnej lub przeciwgrzybiczej.

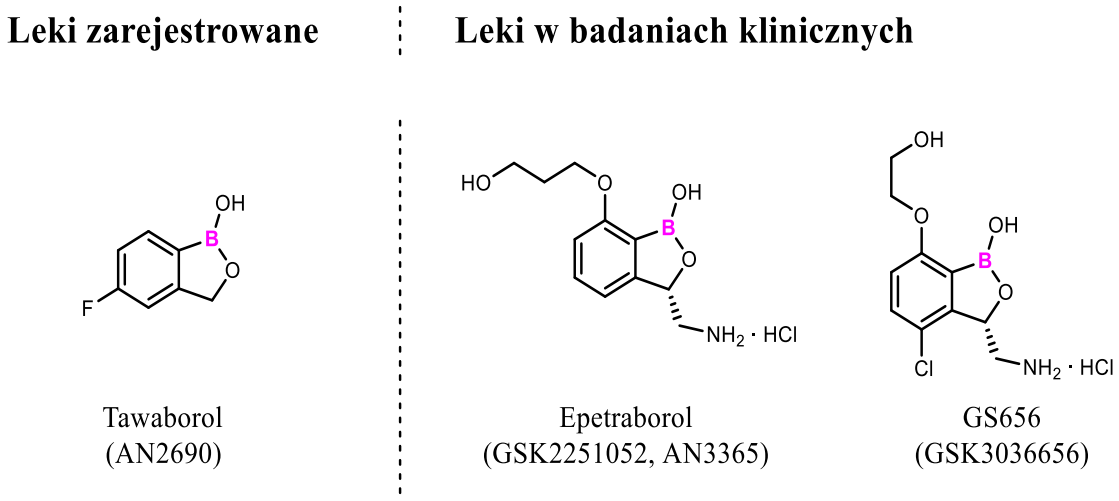

Tawaborol (AN2690)

Epetraborol (GSK2251052, AN3365)

GS656 (GSK3036656)

W chwili obecnej w fazie badań klinicznych znajdują się dwa boroorganiczne związki (benzoksaborole) o bezpośredniej aktywności przeciwdrobnoustrojowej, a ściślej przeciwprątkowej – GSK3036656 (nazywany także GSK656) [180,181] oraz epetraborol (wcześniej GSK2251052 oraz AN3365) [182,183]. Ich struktury przedstawiono na Rycinie 4. Obydwa związki są inhibitorami LeuRS o wysokiej aktywności zarówno wobec prątków gruźliczych (*M. tuberculosis*) jak i niegruźliczego prątka *Mycobacterium abscessus* – wewnątrzkomórkowego patogenu o wysokim poziomie naturalnej oporności na znane antybiotyki, wywołującego groźne infekcje u pacjentów z mukowiscydozą [180-183]. GSK656 jest aktualnie testowany w fazie 2 badań klinicznych jako lek przeciwgruźliczy [180,181]. Z kolei epetraborol, z racji większej aktywności wobec *M. abscessus* niż *M. tuberculosis,* jest testowany (aktualnie w fazie 3) jako lek na choroby wywoływane przez prątki niegruźlicze [182,183]. Ostatnio wykazano również synergistyczne wobec *M. abscessus* działanie epetraborolu z norwaliną (niebiałkowym aminokwasem), która nie tylko zmniejsza częstość selekcji opornych mutantów *in vitro,* ale także nasila działanie epetraborolu *in vivo*. Wykazano, że zmieniona LeuRS mutantów opornych na epetraborol wykorzystuje norwalinę zamiast leucyny do syntezy białek, co jest dla tych mutantów toksyczne [184]. Ponadto aktywność przeciwprątkową na etapie badań przedklinicznych wykazuje wiele innych benzoksaboroli [172,185,186].

Epetraborol był już wcześniej testowany w badaniach klinicznych jako lek przeciwbakteryjny do stosowania ogólnego w powikłanych zakażeniach dróg moczowych oraz powikłanych zakażeniach wewnątrzbrzusznych [187,188]. W warunkach *in vitro* jest on wysoce skuteczny wobec szczepów *Enterobacterales* (także KPC-dodatnich), *P. aeruginosa* (także opornych na karbapenemy), *A. baumannii* oraz *S. maltophilia* [188]. Badania kliniczne zostały jednak przerwane na etapie fazy 2 ze względu na gwałtowne narastanie oporności – już drugiego dnia leczenia izolaty *E. coli* pobrane od czterech pacjentów wykazywały minimum 32-krotny wzrost wartości MIC epetraborolu. Wykazano, że powstały one w wyniku mutacji w genie kodującym LeuRS. Tak krótki czas od rozpoczęcia terapii do zdominowania populacji szczepu wyjściowego przez komórki lekoopornych mutantów był zaskakujący, bowiem u szczepów izolowanych od pacjentów nie stwierdzono zwiększonej częstości selekcji jednostopniowych mutantów w porównaniu do szczepów badanych wcześniej *in vitro* [187]. Dopiero ostatnio wykazano, że uzyskiwane *in vivo* stężenia epetraborolu oscylują w zakresie MSW [189]. Przypadek epetraborolu dobitnie podkreślił konieczność udoskonalenia metod przedklinicznych badań *in vitro* oceniających potencjał do

selekcjonowania oporności przez nowe związki, tak by lepiej przewidywały selekcję oporności *in vivo* [187].

Mimo tego niepowodzenia, benzoksaborole są w dalszym ciągu przedmiotem licznych, przedklinicznych prac badawczo-rozwojowych nad nowymi lekami przeciwdrobnoustrojowymi. Przechodzi je m. in. analog epetraborolu –DS86760016, także będący inhibitorem LeuRS [189]. Wykazuje on wysoką aktywność wobec szerokiej gamy wielolekoopornych bakterii Gram-ujemnych – wartości MIC dla szczepów *Enterobacterales, P. aeruginosa* i *S. maltophilia* kształtują się na poziomie 0,25−2 mg/l. Związek ten nie hamuje wzrostu szczepów *A. baumannii, Bacteroides* spp. ani bakterii Gram-dodatnich [189,190]. Częstość selekcji opornych na niego mutantów na stężeniu 4xMIC była porównywalna do epetraborolu (rzędu 10^{-8} do 10^{-6} dla szczepów *P. aeruginosa, E. coli* i *K. pneumoniae*), podobnie jak wartości MPC obu związków dla szczepów *E. coli* i *K. pneumoniae*. Natomiast wartości MPC benzoksaborolu DS86760016 dla *P. aeruginosa* były co najmniej 8-krotnie niższe niż w przypadku epetraborolu [189]. Właściwości farmakokinetyczne DS86760016 pozwalają jednak na uzyskanie *in vivo* stężeń powyżej wartości MPC w trakcie terapii – w efekcie nie izolowano opornych mutantów *E. coli* ani *P. aeruginosa* od myszy leczonych DS86760016. Uważa się zatem, że DS86760016 w znacznie mniejszym stopniu predysponuje do szybkiego narastania oporności w warunkach klinicznych [189]. Ostatnio wykazano także obiecującą aktywność tego związku *in vitro* wobec *M. abscessus* [191]. W badaniach przedklinicznych znajduje się ponadto wiele innych benzoksaboroli o obiecującej, bezpośredniej aktywności wobec bakterii takich jak *E. coli* [173], *V. cholerae* [174], *S. pneumoniae* [192,193], *S. aureus* (także MRSA) [194] oraz wobec grzybów [195].

Wśród niedawno opisanych benzosiloksaboroli uzyskano z kolei pochodne o obiecującej aktywności przeciwgrzybiczej. Dla szczepów *Candida* spp. wartości MIC pochodnych podstawionych fluorem przy pierścieniu benzenowym wynosiły 0,78−200 mg/l [109,110], a pochodnych podstawionych chlorem mieściły się w granicach 3,12−25 mg/l [110]. Wiele benzosiloksaboroli wykazywało także bezpośrednią aktywność wobec bakterii Gram-dodatnich, zarówno z rodzaju *Staphylococcus* (zakres wartości MIC 6,25−200 mg/l) jak i *Enterococcus* (zakres wartości MIC 25−>400 mg/l). Pochodne chlorowe były bardziej aktywne niż fluorowe wobec bakterii Gram-dodatnich. Największą aktywność wykazywały jednak benzosiloksaborole o unikatowej strukturze, zawierające dodatkowy pierścień oksaborolu skondensowany z pierścieniem

benzenowym benzosiloksaborolu. Hamowały one wzrost szczepów *S. aureus* i *S. epidermidis* już w stężeniach 3,12−6,25 mg/l [110]. Jednocześnie związki te nie wykazywały istotnej aktywności przeciw bakteriom Gram-ujemnym, prawdopodobnie bowiem są substratami dla pomp błonowych tych pałeczek [110].

4.3.2.3. Kwasy boronowe i inne związki boroorganiczne o bezpośredniej aktywności przeciwdrobnoustrojowej

Kwasy boronowe mogą również wykazywać bezpośrednie działanie przeciwdrobnoustrojowe. Ostatnio opisano bis(indolilo)metanową pochodną kwasu boronowego o wysokiej aktywności wobec szczepu MRSA (MIC 3,91 mg/l). Dokowanie molekularne wykazało, że jego prawdopodobny mechanizm działania może być związany z hamowaniem aktywności LeuRS, aczkolwiek działanie bakteriobójcze tego związku sugeruje istnienie także dodatkowego mechanizmu działania. Możliwe, że związek ten oddziałuje na ścianę komórkową bakterii Gram-dodatnich, wykazywał bowiem powinowactwo do warstwy peptydoglikanu [196]. Rzadziej opisywane są kwasy fenyloboronowe o bezpośrednim działaniu przeciwdrobnoustrojowym, jak np. kwasy (trifluorometoksy)fenyloboronowe o niskiej aktywności wobec *E. coli* i *B. cereus* (zakres wartości MIC 125–>500 mg/l) [197] oraz kwas 5-trifluorometylo-2-formylofenyloboronowy o umiarkowanej aktywności wobec *B. cereus* (MIC 8 mg/l) i niskiej wobec *E. coli* (MIC 125 mg/l), *Aspergillus niger* (MIC 32 mg/l) oraz *C. albicans* (MIC 50 mg/l) [198]. Dokowanie molekularne wykazało, że prawdopodobny mechanizm działania tych związków również polega na hamowaniu aktywności LeuRS [197,198].

Kwasy boronowe mogą także działać jako inhibitory błonowych pomp MDR. Wykazano, że kwasy 6-(fenyleno)alkoksypirydyno-3-boronowe hamują aktywność pompy NorA u *S. aureus* [199,200]. Pompa ta jest odpowiedzialna m. in. za usuwanie z komórki bakteryjnej fluorochinolonów, a nadekspresja genu *norA* wśród szczepów MRSA jest częsta. Szczepy o takim mechanizmie oporności na fluorochinolony stanowią istotny problem kliniczny. W obecności niektórych kwasów 6-(fenyleno)-alkoksypirydyno-3-boronowych w stężeniu 16 mg/l wartości MIC cyprofloksacyny oraz norfloksacyny szczepów MRSA ulegały 4-8-krotnej redukcji. Jednocześnie związki te nie wykazywały bezpośredniej aktywności wobec badanych szczepów. Wykazano, że dla uzyskania aktywności inhibitora błonowych pomp NorA u tych związków niezbędna jest obecność boru oraz podstawnika w pozycji *para* w stosunku do grupy $B(OH)_2$ [199,200].

Spośród innych grup związków boroorganicznych bezpośrednią aktywność przeciwdrobnoustrojową wykazują m. in. diazaboryny [105,107]. Niektóre z nich hamują wzrost szczepów *E. coli* (wartości MIC 2−16 mg/l), *Mycobacterium smegmatis* (MIC najbardziej aktywnej pochodnej 4 mg/l) oraz *M. tuberculosis* (MIC 4 mg/l dla najbardziej aktywnego związku). Mechanizm działania tych związków wynika z hamowania reduktazy enoilo-ACP [105,107]. Opisano także kilka związków z grupy oksadiazaboroli aktywnych wobec szczepów *C. albicans* (zakres wartości MIC 0,08−0,75 μM) i *S. aureus* (MIC 0,06 μM dla najbardziej aktywnej pochodnej) oraz z grupy oksazaborolidyn hamujących wzrost szczepów *Streptococcus mutans* (zakres wartości MIC 0,53−6,75 μM) także w formie biofilmu [107].

4.4. Podsumowanie części teoretycznej

Narastanie oporności drobnoustrojów na antybiotyki i chemioterapeutyki jest naturalnym procesem, nierozerwalnie związanym z ich powszechnym stosowaniem oraz w większości przypadków nieodwracalnym. Utrata klinicznej skuteczności znanych leków przeciwdrobnoustrojowych jest zatem nieuchronna. Narastaniu oporności sprzyja powszechne i często niewłaściwe stosowanie antybiotyków oraz chemioterapeutyków w lecznictwie, aktualnie obowiązujące schematy dawkowania oraz ich wykorzystywanie w hodowli zwierząt i w rolnictwie. Poza działaniami mającymi na celu spowolnienie tego procesu (np. racjonalizacja antybiotykoterapii oraz ograniczenia w pozamedycznym stosowaniu antybiotyków), niezbędne jest także opracowywanie i wprowadzenie do lecznictwa wciąż nowych leków przeciwdrobnoustrojowych lub substancji przywracających skuteczność tych już znanych (np. przez łączne stosowanie z nowymi inhibitorami β-laktamaz). Liczba nowych leków tego typu w badaniach klinicznych oraz wprowadzonych do obrotu w ostatnich latach jest wciąż wysoce niewystarczająca. Szczególnie niepokojąca jest niewielka liczba leków skutecznych wobec patogenów priorytetowych oraz leków innowacyjnych. W badaniach przedklinicznych znajduje się natomiast ogromna liczba związków o obiecującym potencjale przeciwdrobnoustrojowym, także tych spełniających kryteria innowacyjności WHO, jak chociażby opisane powyżej związki boraheterocykliczne i kwasy boronowe. Jednym z największych wyzwań tego etapu badań pozostaje jednak wskazanie najlepszego kandydata do dalszych prac badawczo-rozwojowych spośród wielu pochodnych o podobnej strukturze i porównywalnej aktywności. Powinien to być związek nie tylko

wysoce aktywny, lecz również w jak najmniejszym stopniu generujący narastanie oporności w trakcie jego stosowania w lecznictwie. Metody wyznaczania parametrów *in vitro* charakteryzujących bezpośrednią aktywność przeciwdrobnoustrojową nowych związków, takich jak wartości MIC czy minimalne stężenie bakteriobójcze (ang. *minimal bactericidal concentration* – MBC) oraz MFC są dobrze wystandaryzowane i rutynowo stosowane. Te dobrze wystandaryzowane parametry nie są jednak bezpośrednio powiązane z narastaniem oporności drobnoustrojów. Wyzwaniem pozostaje zatem prawidłowe wyznaczenie w warunkach *in vitro* zakresu stężeń badanych związków, w których może dochodzić do selekcji opornych mutantów *in vivo* tj. okna selekcji opornych mutantów – parametru MSW. W chwili obecnej za górną granicę MSW przyjmuje się wartość MPC wyznaczaną metodą rozcieńczeń w agarze. Metoda ta implikuje jednak szereg trudności technicznych, uzyskiwane wartości MPC charakteryzują się niedostateczną powtarzalnością, a zakresy MSW wyznaczone *in vitro* nie zawsze są tożsame z zakresami obserwowanymi później *in vivo*. Nie udało się również wykorzystać parametru MPC jako podstawy do opracowania nowego, ograniczającego narastanie oporności schematu dawkowania antybiotyków. Istnieje więc pilna potrzeba zwiększenia precyzji metod *in vitro* określających potencjał kandydatów na leki przeciwdrobnoustrojowe do selekcjonowania oporności, jak również opracowania charakteryzujących go parametrów *in vitro* i metod ich wyznaczania.

5. Założenia i cele pracy

Głównymi celami niniejszej pracy było:

I. poszukiwanie wśród nowych pochodnych boraheterocyklicznych i kwasów aryloboronowych substancji przeciwdrobnoustrojowych, aktywnych wobec wielolekoopornych szczepów bakterii i grzybów drożdżopodobnych, a w konsekwencji wytypowanie nowych, potencjalnych kandydatów na leki lub interesujących struktur wyjściowych do syntezy nowych pochodnych o potencjalnie wysokiej aktywności przeciwdrobnoustrojowej;

II. opracowanie nowego podejścia do oceny potencjału selekcjonowania oporności, wśród szczepów bakteryjnych przez związki przeciwdrobnoustrojowe, możliwego do zastosowania na wczesnym etapie przedklinicznych badań *in vitro* (także nowych związków zawierających bor), w celu wskazania do dalszych prac związku wysoce aktywnego i również w jak najmniejszym stopniu generującego narastanie oporności w trakcie jego stosowania w lecznictwie.

Cele główne były realizowane poprzez cele szczegółowe:

1) Dokonanie przeglądu piśmiennictwa i analizy:
   a. oryginalnych leków przeciwbakteryjnych zarejestrowanych po publikacji listy patogenów priorytetowych WHO w celu ukierunkowania prac eksperymentalnych na najistotniejsze potrzeby;
   b. właściwości przeciwdrobnoustrojowych znanych związków boraheterocyklicznych i kwasów boronowych, w celu ustalenia możliwych kierunków i mechanizmów działania nowych związków z tych grup oraz zaprojektowania części eksperymentalnej pracy umożliwiającej ich zbadanie.
2) Przeprowadzenie szerokich badań mikrobiologicznych nowo otrzymanych związków boraheterocyklicznych i kwasów aryloboronowych, obejmujących:
   a. oznaczenie bezpośredniej aktywności przeciwbakteryjnej i przeciwgrzybiczej wobec szczepów wzorcowych z gatunków istotnych klinicznie, także priorytetowych wg WHO;
      - dla nowych związków o aktywności porównywalnej z substancjami czynnymi znanych leków przeciwdrobnoustrojowych oznaczenie także

aktywności wobec szczepów klinicznych, o zdefiniowanych mechanizmach oporności;

b. badania udziału pomp błonowych w aktywnym usuwaniu nowych związków z komórek bakteryjnych;
c. badanie zdolności nowych związków do inhibicji najistotniejszych klinicznie β-laktamaz (karbapenemaz, cefalosporynaz, enzymów typu ESBL) wytwarzanych przez pałeczki Gram-ujemne;
d. badania dodatkowe dla wybranych związków o najwyższej aktywności przeciwdrobnoustrojowej (np. poszukiwanie synergistycznego oddziaływania ze znanymi antybiotykami).

3) opracowanie nowej metodyki wyznaczania górnej granicy okna selekcji opornych mutantów, w oparciu o zaproponowane w niniejszej pracy doktorskiej nowe parametry, uwzględniające częstość selekcji opornych mutantów oraz ich potencjał do dominowania w populacji.

6. Omówienie wyników i dyskusja

W niniejszej pracy poszukiwano nowych substancji przeciwdrobnoustrojowych wśród 77 nowych związków, w tym 44 benzosiloksaboroli i pokrewnych heterocykli o rozszerzonym pierścieniu (**Publikacje O1** i **O2**) oraz 33 kwasów aryloboronowych, głównie fenyloboronowych (29 związków) (**Publikacja O4**). Opracowano również metodę wyznaczania górnej granicy okna selekcji opornych mutantów *in vitro* wykorzystującą rozcieńczenia związku w podłożu płynnym, w oparciu o nowe parametry uwzględniające potencjał selekcjonowanych mutantów do dominowania w populacji oraz częstość ich selekcji – **Publikacja O3**.

Badania były prowadzone w ramach projektu Narodowego Centrum Nauki OPUS16 UMO-2018/31/B/ST5/00210 pt. „Poszukiwanie korelacji struktura-aktywność przeciwdrobnoustrojowa wybranych grup związków boraheterocyklicznych", realizowanego przez konsorcjum Politechnika Warszawska (PW) – Warszawski Uniwersytet Medyczny (WUM), w latach 2019-2024. Syntezy i analizy chemiczne nowych związków były prowadzone przez zespół Pana Prof. dr hab. inż. Sergiusza Lulińskiego z PW, a analizy mikrobiologiczne przeprowadzano w ramach niniejszej pracy doktorskiej pod kierunkiem dr hab. Agnieszki E. Laudy w Zakładzie Mikrobiologii Farmaceutycznej i Bioanalizy WUM. Zgodnie z założeniami w/w projektu w pierwszym etapie do badań mikrobiologicznych otrzymywano związki, które stanowiły podstawową strukturę danej grupy oraz ewentualnie jej nieliczne pochodne. Na podstawie uzyskiwanych wyników aktywności mikrobiologicznej i ich analizy, podejmowane były decyzje o kierunkach dalszych syntez. W ten sposób otrzymywane, nowe pochodne poddawane były badaniom mikrobiologicznym. Uzyskane wyniki zostały zawarte w cyklu **Publikacji O1, O2** oraz **O4**. W tej części rozprawy doktorskiej przedstawiono sumaryczną analizę aktywności przeciwdrobnoustrojowej wszystkich uzyskanych związków z badanych grup.

6.1. Badania bezpośredniej aktywności przeciwdrobnoustrojowej

Podstawowymi badaniami wykonywanymi w części eksperymentalnej było określenie bezpośredniej aktywności przeciwdrobnoustrojowej nowych benzosiloksaboroli i kwasów aryloboronowych wobec szczepów wzorcowych. Do badań włączono szczepy z gatunków o krytycznym i wysokim priorytecie wg WHO [91,92], jak również inne gatunki potencjalnie chorobotwórcze dla człowieka. Łącznie wykorzystano 24 szczepy wzorcowe:

- 6 szczepów bakterii Gram-dodatnich: metycylinowrażliwy *S. aureus* (ang. *methicillin-sensitive S. aureus* – MSSA) ATCC 6538P, metycylinooporny *S. aureus* subsp. *aureus* (MRSA) ATCC 43300, *S. epidermidis* ATCC 12228, *Enterococcus faecalis* ATCC 29212, *E. faecium* ATCC 6057, *Bacillus subtilis* ATCC 6633;
- 5 szczepów bakterii Gram-ujemnych z rzędu *Enterobacterales***:** *E. coli* ATCC 25922, *K. pneumoniae* ATCC 13883, *Proteus mirabilis* ATCC 12453, *Enterobacter cloacae* DSM 6234, *Serratia marcescens* ATCC 13880;
- 6 szczepów Gram-ujemnych pałeczek niefermentujących: *P. aeruginosa* ATCC 27853, *A. baumannii* ATCC 19606, *S. maltophilia* ATCC 13637, *S. maltophilia* ATCC 12714 (oprócz **Publikacji O4**), *Burkholderia cepacia* ATCC 25416, *Bordetella bronchiseptica* ATCC 4617;
- 7 szczepów grzybów drożdżopodnych: *C. albicans* ATCC 90028, *C. parapsilosis* ATCC 22019, *C. tropicalis* IBA 171, *C. tropicalis* (Castellani) Berkhout ATCC 750, *Candida guilliermondii* IBA 155, *C. krusei* ATCC 6258, oraz dodatkowo niepatogenny *Saccharomyces cerevisiae* ATCC 9763.

Dla wszystkich badanych związków wykonywano oznaczenie bezpośredniej aktywności wobec bakterii oraz grzybów metodą krążkowo-dyfuzyjną według zaleceń EUCAST [201] oraz amerykańskiego Instytutu Norm Klinicznych i Laboratoryjnych (ang. *Clinical and Laboratory Standards Institute* - CLSI [202], a następnie wyznaczając wartości MIC, MBC i MFC według wytycznych EUCAST [11], CLSI [10,14,203] oraz zgodnie z metodologią opisaną w pracy Cantón i wsp. [204]. Wyjątkiem były związki, które nawet przy niskich stężeniach ulegały wytrąceniu w środowisku badania określającego wartości MIC. Dla tych związków możliwe było jedynie wykonanie oznaczenia aktywności metodą krążkowo-dyfuzyjną.

Dla wszystkich powyższych szczepów wzorcowych określono średnicę strefy zahamowania wzrostu wokół krążków zawierających 400 μg badanych związków. Oznaczenia wykonano dla wszystkich 77 badanych związków (**Publikacje O1**, **O2** i **O4**). Następnie, dla tych samych szczepów (z wyjątkiem *B. subtilis,* ze względu na problem z uzyskaniem jednorodnej zawiesiny) wyznaczano aktywność związków metodą mikrorozcieńczeń w bulionie, wartości MIC oraz MBC/MFC, w zakresie stężeń

0,39−400 mg/l. W przypadku niektórych związków, ulegających wytrąceniu w wyższych stężeniach w środowisku badania, oznaczenie wartości MIC prowadzono w węższym, możliwym do uzyskania zakresie tj. 0,39−200 mg/l, 0,39−100 mg/l lub 0,39−50 mg/l. Na tym etapie zbadano bezpośrednią aktywność przeciwbakteryjną 68 związków rozpuszczalnych w podłożu Mueller-Hinton II bulion, w tym 36 benzosiloksaboroli (**Publikacje O1** i **O2**) i 32 kwasów aryloboronowych (**Publikacja O4**). Bezpośrednią aktywność przeciwgrzybiczą zbadano dla 75 związków rozpuszczalnych w podłożu RPMI, w tym 43 benzosiloksaboroli (**Publikacje O1** i **O2**) i 32 kwasów aryloboronowych (**Publikacja O4**). Dla wyselekcjonowanych związków o wysokiej aktywności wobec szczepów wzorcowych, wykonano dodatkowo oznaczenia aktywności wobec szczepów klinicznych. W pracy wykorzystano pięć szczepów klinicznych *S. aureus* MRSA o następujących numerach: NMI 664K, NMI 1576K, NMI 1712K, NMI 1991K oraz NMI 2541K. Szczepy te pochodziły z kolekcji Zakładu Mikrobiologii Farmaceutycznej i Bioanalizy WUM.

6.1.1. Aktywność wobec bakterii Gram-dodatnich

W badaniach aktywności nowych związków wobec bakterii Gram-dodatnich (zarówno szczepów wzorcowych jaki i klinicznych) jako antybiotyk referencyjny stosowano linezolid – przedstawiciela jednej z nowszych grup leków przeciwbakteryjnych (oksazolidynonów), wykorzystywanego w leczeniu zakażeń wielolekoopornymi ziarenkowcami, w tym także szczepami MRSA i wankomycyno-opornymi enterokokami (tj. szczepami VRE) [205,206]. Wartości MIC linezolidu dla badanych szczepów wzorcowych wynosiły: 1 mg/l dla szczepu *S. aureus* ATCC 6538P MSSA i szczepu *S. epidermidis* ATCC 12228 oraz 2 mg/l dla szczepu *S. aureus* ATCC 43300 MRSA i obu enterokoków. Wykazano, że większość badanych związków jest aktywna wobec ziarenkowców Gram-dodatnich w badanym zakresie stężeń – wartości MIC dla co najmniej 3 z 5 badanych szczepów wzorcowych oznaczono dla 28 z 36 rozpuszczalnych benzosiloksaboroli oraz dla 26 z 32 kwasów aryloboronowych. Wysoką aktywność wobec wzorcowych szczepów MSSA i MRSA wykazywało 18 benzosiloksaboroli, w tym: 16 pochodnych benzenosulfonianowych (zakres wartości MIC 0,39–3,12 mg/l – Publikacja **O1**) oraz 2 pochodne sulfonamidowe (zakres wartości MIC 3,12– 6,25 mg/l – Publikacja **O2**). W publikacji **O2** oznaczono także aktywność benzosiloksaboroli sulfonamidowych wobec pięciu klinicznych szczepów MRSA. Wartości MIC tych benzosiloksaboroli mieściły się zakresie 3,12–6,25 mg/l, a wartości

MIC linezolidu wynosiły 1 mg/l. Tym samym uzyskane wyniki potwierdziły wysoką aktywność benzosiloksaboroli sulfonamidowych także wobec klinicznych szczepów MRSA. Wśród 16 benzosiloksaboroli benzenosulfonianowych o wysokiej aktywności przeciwgronkowcowej 3 pochodne wykazywały dodatkowo wysoką aktywność przeciwenterokową (MIC 6,25 mg/l – **Publikacja O1**). Kolejnych 10 z 36 rozpuszczalnych benzosiloksaboroli wykazywało skuteczność od umiarkowanej po niską wobec gronkowców (zakres wartości MIC 12,5–400 mg/l) oraz enterokoków (zakres wartości MIC 50–>400 mg/l) (**Publikacje O1** i **O2**). Wśród 32 badanych kwasów aryloboronowych (**Publikacja O4**) najbardziej aktywne były kwas 2-merkapto-fenyloboronowy (wartości MIC zarówno dla gronkowców jak i enterokoków w zakresie 12,5–25 mg/l) oraz kwas 2-fluoro-5-trifluorometylo-1,3-fenylenodiboronowy (zakres wartości MIC dla gronkowców 0,78–12,5 mg/l, a dla enterokoków 50–100 mg/l). Kolejne 24 kwasy aryloboronowe wykazywały aktywność od umiarkowanej po niską (zakres wartości MIC 25–>400 mg/l) w zależności od szczepu, a 4 kwasy boronowe niską lub brak aktywności (zakres wartości MIC 200–>400 mg/l).

Analiza uzyskanych w niniejszej pracy wyników aktywności przeciwbakteryjnej 44 nowo otrzymanych benzosiloksaboroli pozwoliła na wyciągnięcie ważnych wniosków dotyczących korelacji struktura-aktywność tej grupy związków. Choć aktywność wobec bakterii Gram-dodatnich jest w niej powszechna, do uzyskania wysokiej aktywności kluczowe znaczenie okazała się mieć obecność ugrupowania benzenosulfonianowego (**Publikacja O1**) lub benzenosulfonamidowego (**Publikacja O2**). Wykazano również, że siła działania pochodnych benzenosulfonianowych jest największa w przypadku: (I) obecności atomu chloru lub grupy trifluorometylowej w pozycji *para*, (II) obecności obu tych podstawników lub tylko chloru w pozycji *para* i *meta* lub (III) obecności trzech grup metylowych w pozycji 2, 4 i 6. Wartości MIC takich pochodnych były mniejsze niż linezolidu dla szczepów *S. aureus* (0,39–0,78 mg/l dla MSSA oraz 0,39–1,56 mg/l dla MRSA). Pochodne te wykazywały również wysoką aktywność przeciwenterokokową (MIC 6,25 mg/l). Pochodne niepodstawione lub mające inny podstawnik w tym miejscu (tj. fluor, brom, jod, jedną grupę metylową, nitrową, metoksylową, acetylową lub *tert*-butylową) wykazywały aktywność wobec szczepów *S. aureus* porównywalną lub mniejszą niż linezolid (zakres wartości MIC 1,56–3,12 mg/l) oraz umiarkowaną wobec enterokoków (wartości MIC 12,5–50 mg/l) (**Publikacja O1**). Umiarkowaną aktywność stwierdzono także dla benzosiloksaboroli funkcjonalizowanych grupami benzoiloksylowymi i pirydyn-2-oksylowymi (**Publikacja O1**). Z kolei związki

boraheterocykliczne o rozszerzonym pierścieniu nie wykazywały aktywności przeciwbakteryjnej (**Publikacja O2**).

W trakcie wyznaczania wartości MBC dla szczepów *S. aureus* w przypadku 15 benzosiloksaboroli (**Publikacje O1** i **O2**) zaobserwowano występowanie tzw. efektu Eagle'a, inaczej wzrostu paradoksalnego [207]. Konsekwencją tego było wyznaczenie dla tych związków dwóch wartości MBC. Zgodnie z definicją, wartość MBC to najniższe stężenie związku zabijające przynajmniej 99,9% komórek bakteryjnych [203]. W przypadku badanych związków, pierwsza wartość MBC była równa 2−4xMIC. Natomiast na kilku kolejnych, wyższych stężeniach przeżywalność bakterii była paradoksalnie większa (powyżej progu MBC), po czym ponownie spadała do wartości progowej, w zależności od związku przy stężeniach rzędu 16−256xMIC (druga wartość MBC). Molekularne podstawy oraz kliniczne implikacje wzrostu paradoksalnego nie zostały jak dotąd w pełni poznane, chociaż jest to zjawisko stosunkowo często obserwowane *in vitro* [207]. Istnieją jednak doniesienia, że niższe dawki leków wykazujących efekt Eagle'a były skuteczniejsze w leczeniu zakażeń u zwierząt niż dawki wyższe [207].

Niezbędnym elementem badań nad poszukiwaniem nowych związków przeciwdrobnoustrojowych jest wykazanie, iż związki te nie mają aktywności cytotoksycznej wobec komórek ludzkich. Dla wszystkich przebadanych w niniejszej pracy doktorskiej związków oznaczenie cytototoksyczności wobec ludzkich fibroblastów MRC-5 wykonała Pani dr hab. Patrycja Wińska z Katedry Biotechnologii Środków Leczniczych i Kosmetyków Politechniki Warszawskiej. Wykazany przez Nią brak toksyczności tych związków w stężeniach odpowiadających wyznaczonym w niniejszej pracy doktorskiej wartościom MIC (**Publikacje O1**, **O2** i **O4**) jest kolejnym argumentem potwierdzającym ich potencjał jako źródła nowych leków. Mając na uwadze powyższe oraz uzyskaną w badaniach eksperymentalnych wysoką aktywność przeciwbakteryjną, po dokonanej analizie wytypowano 4 związki do dalszych prac *in silico*. Na podstawie dokonanego przeglądu literaturowego wskazano syntetazę leucylo-tRNA jako potencjalny cel molekularny dla wykazanej bezpośredniej aktywności badanych związków [170,171]. Dokowania molekularne do tego enzymu zostały wykonane przez Pana mgr inż. Krzysztofa Nowickiego z Zakładu Chemii Fizycznej Politechniki Warszawskiej oraz Pana dr Tomasza Stępniewskiego z GPCR Drug Discovery Lab Hospital del Mar Medical Research Institute w Barcelonie. Uzyskane wyniki

potwierdziły, że związki te faktycznie mogą tworzyć stabilne addukty z enzymem LeuRS i wiązać się do jej miejsca aktywnego (**Publikacja O2**).

Wyniki powyższych badań interdyscyplinarnych, tj. wykazana w niniejszej pracy doktorskiej wysoka aktywność przeciwgronkowcowa zsyntezowanych na Politechnice Warszawskiej nowych benzosiloksaboroli w połączeniu z brakiem ich toksyczności w stężeniach hamujących wzrost drobnoustrojów, sprawiają, że związki te mogą być brane pod uwagę jako potencjalni kandydaci na nowe leki przeciwbakteryjne, będące najprawdopodobniej inhibitorami syntetazy leucylo-tRNA.

6.1.2. Aktywność wobec bakterii Gram-ujemnych

W niniejszej pracy wykazano, iż zarówno otrzymane benzosiloksaborole jak i kwasy ayloboronowe nie wykazują istotnej aktywności bezpośredniej wobec bakterii Gram-ujemnych. Wśród 36 badanych benzosiloksaboroli dominował brak aktywności w badanym zakresie stężeń (**Publikacje O1** i **O2**). Tylko 13 pochodnych wykazywało niską aktywność (zakres wartości MIC 50−400 mg/l) wobec szczepów wzorcowych *S. maltophilia* lub *B. bronchiseptica* (**Publikacja O1**). Natomiast wśród 32 badanych kwasów aryloboronowych dominowała niska aktywność – wartości MIC 19 pochodnych wahały się od 50 do >400 mg/l w zależności od szczepu, natomiast brak aktywności w badanym zakresie stężeń wobec większości szczepów stwierdzono w przypadku 11 pochodnych (**Publikacja O4**).

6.1.3. Aktywność przeciwgrzybicza

Zaobserwowana w pracy aktywność przeciwgrzybicza otrzymanych związków była zazwyczaj umiarkowana lub niska (**Publikacje O1**, **O2** i **O4**). Wyjątkowo, kwas 4-trifluorometylo-1,2-fenylenodiboronowy wykazywał wysoką aktywność wobec większości badanych szczepów *Candida* spp. (zakres wartości MIC 3,12–12,5 mg/l) i umiarkowaną wobec *C. krusei* (MIC 25 mg/l) (**Publikacja O4**). Wśród 43 zbadanych benzosiloksaboroli najniższe wartości MIC uzyskano w przypadku 4 pochodnych benzoiloksylowych dla *C. tropicalis* oraz *C. krusei* (3,12−12,5 mg/l). Wśród nich najbardziej aktywna była pochodna zawierająca grupę metylową w pozycji *para* pierścienia fenylowego podstawnika (**Publikacja O1**). Umiarkowaną aktywność przeciwgrzybiczą wykazywały ponadto 3 *orto* podstawione kwasy fenyloboronowe oraz kwas 2,5-dibromo-1,4-fenylenodiboronowy (zakres wartości MIC 6,25–50 mg/l). Kolejnych 17 kwasów aryloboronowych wykazywało niską aktywność przeciwgrzybiczą

(zakres wartości MIC 50–>400 mg/l) (**Publikacja O4**). Spośród benzosiloksaboroli aktywność od umiarkowanej do niskiej wobec *Candida* spp. (zakres wartości MIC 12,5−>400 mg/l) wykazywało 27 związków (**Publikacja O1**). Brak aktywności w badanym zakresie stężeń wykazano dla 7 kwasów fenylenodiboronowych, 2 kwasów fenylenotriboronowych i kwasu pirydynodiboronowego (**Publikacja O4**), jak również dla 8 benzosiloksaboroli funkcjonalizowanych grupami opartymi na rdzeniu oksazolinowym i 4 pokrewnych im związków o poszerzonym pierścieniu (**Publikacja O2**).

6.2. Udział pomp MDR w usuwaniu nowych związków z komórek bakterii Gram-ujemnych

Zważywszy na fakt, iż brak aktywności wielu antybiotyków oraz leków z grupy *non-antibiotics* wobec bakterii Gram-ujemnych jest często związany z ich aktywnym usuwaniem z komórki przez pompy błonowe [208-210], dla wszystkich rozpuszczalnych związków oznaczono także ich wartości MIC w obecności inhibitora tych pomp: L-fenyloalanino-L-arginino-β-naftylamidu (PAβN) [211,212]. W celu uniknięcie wpływu PAβN na destabilizację osłon komórkowych zastosowano go w stężeniu 20 mg/l, a oznaczenie wykonywano na podłożu z dodatkiem 1mM $MgSO_4$ [213-215]. Oznaczenie wartości MIC wykonano metodą mikrorozcieńczeń w bulionie, zgodnie z zaleceniami CLSI [10]. Wykazano, że zjawisko aktywnego usuwania związków przez błonowe pompy ma niewielki wpływ na aktywność badanych związków wobec pałeczek Gram-ujemnych. Znaczące spadki wartości MIC (tj. min. 4-krotne) w obecności inhibitora PAβN, w stosunku do wartości MIC oznaczonych przy braku inhibitora w podłożu, stwierdzono dla zaledwie 5 benzosiloksaboroli (**Publikacja O1**) oraz 3 kwasów aryloboronowych (**Publikacja O4**) wobec pojedynczych szczepów. W przypadku pozostałych związków uzyskane wyniki wskazują, że związki te nie są substratami dla błonowych pomp MDR i potwierdzają ich brak bezpośredniej aktywności wobec bakterii Gram-ujemnych.

6.3. Zdolność nowych związków boroorganicznych do inhibicji β-laktamaz bakterii Gram-ujemnych

Biorąc pod uwagę, iż: (I) niedawno dopuszczony do stosowania w lecznictwie inhibitor β-laktamaz (ang. *β-lactamase inhibitor* – BLI) tj. waborbaktam jest przedstawicielem nowej grupy związków – cyklicznych kwasów boronowych, (II) badnia kliniczne przechodzą trzy kolejne inhibitory z grupy bicyklicznych kwasów boronowych oraz (III) dane z piśmiennictwa wskazują, że aktywność BLI wykazują również

niecykliczne kwasy boronowe [122,152-166], benzoksaborole [124,125] i benzosiloksaborole [110], w niniejszej pracy poszukiwano związków o aktywności BLI wśród wszystkich 77 nowo otrzymanych związków boroorganicznych, w tym 44 benzosiloksaboroli oraz 33 kwasów aryloboronowych.

6.3.1. Badania przesiewowe

W pierwszym etapie badań poszukiwano związków zdolnych do inhibicji enzymów typu KPC, cAmpC, pAmpC i ESBL w wysokich stężeniach, przy użyciu następujących, fenotypowych krążkowych testów kombinowanych (ang. *combination disc tests* – CDTs), wykonywanych zgodnie z metodyką opisaną w **Publikacji O4**:

- CDT-KPC – z wykorzystaniem rekomendowanego szczepu *K. pneumoniae* ATCC BAA-1705 KPC-2-dodatniego, krążków z samym meropenemem, krążków z meropenemem i PBA (jako referencyjnym inhibitorem enzymów KPC-2) oraz krążków z meropenemem i badanymi związkami;
- CDT-AmpC – z wykorzystaniem dwóch klinicznych izolatów: *P. aeruginosa* MUW 700 cAmpC-dodatniego oraz *E. coli* 77 CMY-2-dodatniego, krążków z samym ceftazydymem, krążków z ceftazydymem i PBA (jako referencyjnym inhibitorem enzymów AmpC) oraz krążków z ceftazydymem i badanymi związkami;
- CDT-ESBL EUCAST – z wykorzystaniem rekomendowanego szczepu *K. pneumoniae* ATCC 700603 ESBL-dodatniego, krążków z samym ceftazydymem, krążków z ceftazydymem i kwasem klawulanowym (jako referencyjnym inhibitorem enzymów typu ESBL) oraz krążków z ceftazydymem i badanymi związkami.

Otrzymane związki testowano w najwyższym stężeniu (300, 100 lub 30 μg/krążek), w którym nie wykazywały one bezpośredniej aktywności wobec szczepów wykorzystywanych na tym etapie, co oznaczono przed przystąpieniem do eksperymentu za pomocą metody krążkowo-dyfuzyjnej. Uznawano, że aktywność BLI wykazują te związki, których dodanie na krążek z antybiotykiem powoduje powiększenie strefy zahamowania wzrostu co najmniej takie samo jak dodanie na taki sam krążek odpowiedniego inhibitora referencyjnego.

Stwierdzono, że żaden z 44 badanych benzosiloksaboroli nie wykazuje aktywności BLI w żadnym z przeprowadzonych testów przesiewowych. Aktywność taką stwierdzono natomiast dla 25 z 33 badanych kwasów aryloboronowych – uzyskane dla nich wyniki przedstawiono w **Publikacji O4**. Spośród badanych kwasów aryloboronowych 12 związków znacząco zwiększało średnicę strefy zahamowania wzrostu zarówno

szczepu wytwarzającego KPC-2 jak i obu szczepów wytwarzających cefalosporynazy. Były to kwasy *orto*-, *meta*- i *para*-fenylenodiboronowe, 6 ich pochodnych podstawionych fluorem, kwas fenyleno-1,2,4-triboronowy, kwas 2,5-difluorofenyloboronowy oraz kwas tiofeno-2,5-diboronowy. Kolejnych 12 pochodnych wykazywało taką aktywność wyłącznie wobec szczepów wytwarzających cefalosporynazy (były to kwasy fenylenodiboronowe podstawione fluorem, bromem, CF_3 lub OMe oraz kwasy fenyleno-1,3,5-triboronowy i tiofeno-2,3,5-triboronowy). Natomiast kwas 2-merkaptofenylo-boronowy powiększał jedynie średnicę strefy zahamowania wzrostu szczepu wytwarzającego KPC-2. Żaden z badanych kwasów boronowych nie powiększał średnicy strefy zahamowania wzrostu szczepu ESBL-dodatniego.

6.3.2. Związki wykazujące aktywność BLI w niskich stężeniach

Do kolejnego etapu badań wybrano 25 kwasów aryloboronowych wykazujących aktywność BLI w co najmniej jednym teście przesiewowym. Wśród nich poszukiwano związków aktywnych w stężeniach porównywalnych ze stężeniami, w których stosowane są najnowsze inhibitory β-laktamaz (waborbaktam, relebaktam oraz awibaktam) [12]. W tym celu, w obecności 25 w/w związków w stężeniach 16, 8 i 4 mg/l wyznaczono wartości MIC następujących antybiotyków β-laktamowych:

- meropenemu dla dwóch szczepów KPC-2-dodatnich (*K. pneumoniae* ATCC BAA-1705 oraz klinicznego szczepu *E. coli* 76), jednego szczepu KPC-3-dodatniego (kliniczny szczep *K. pneumoniae* 81) oraz jednego szczepu KPC-3/CTX-M-3-dodatniego (kliniczny szczep *K. pneumoniae* 83);
- meropenemu dla szczepu klinicznego *P. aeruginosa* 1204 VIM-dodatniego;
- ceftazydymu dla klinicznego szczepu *P. aeruginosa* MUW 700 cAmpC-dodatniego oraz klinicznego szczepu *E. coli* 77 CMY-2-dodatniego.

Co najmniej 4-krotna redukcja wartości MIC antybiotyku w obecności badanego związku uznawana była za znaczącą i traktowana jako wskaźnik jego aktywności jako BLI. Analizowano również, czy otrzymane związki przywracają wrażliwość w/w szczepów na te antybiotyki, tj. czy powodują redukcję wartości MIC antybiotyku do odpowiedniego punktu odcięcia wg EUCAST [12]. Zważywszy na fakt, iż jednym z celów pracy była ocena wpływu obecności w cząsteczce dodatkowej grupy boronowej na aktywność BLI związku jako inhibitor referencyjny zastosowano PBA. Uzyskane wyniki przedstawiono w **Publikacji O4**. Stwierdzono, że 17 z 25 badanych związków wykazuje

aktywność BLI w niskich stężeniach wobec szczepów KPC- lub AmpC-dodatnich. Co ważne, poza niepodstawionymi kwasami boronowymi aktywne były wyłącznie ich fluorowe pochodne. Żaden z badanych związków nie powodował natomiast zmian wartości MIC meropenemu u szczepu VIM-dodatniego.

Aktywność BLI wobec obu szczepów AmpC-dodatnich wykazano dla 16 związków. Największe redukcje wartości MIC ceftazydymu uzyskano w przypadku 5 kwasów *para*-fenylenodiboronowych oraz kwasu 2,5-difluorofenyloboronowego (nawet 32/16/8-krotne odpowiednio przy 16/8/4 mg/l), nieznacznie mniejsze w przypadku 4 kwasów *meta*-fenylenodiboronowych (maksymalnie 16/8/4-krotne odpowiednio przy 16/8/4 mg/l). W/w 10 związków wykazywało wyższą niż PBA aktywność wobec szczepu *E. coli* CMY-2-dodatniego, wszystkie także przywróciły jego wrażliwość na ceftazydym (uzyskano redukcję wartości MIC do poziomu ≤2 mg/l – punkt odcięcia dla ceftazydymu w obecności 4 mg/l awibaktamu u *Enterobacterales* [12]). Natomiast wobec szczepu *P. aeruginosa* cAmpC-dodatniego aktywność tych 10 związków była mniejsza niż aktywność PBA oraz jedynie dwa spośród nich (kwas *para*-fenylenodiboronowy oraz 2,5-difluorofenyloboronowy) przywróciły jego wrażliwość na ceftazydym (punkt odcięcia dla ceftazydymu-awibaktamu również równy 2 mg/l [12]). Pozostałe aktywne wobec szczepów AmpC-dodatnich związki, tj. 2 kwasy tiofenoboronowe, 2 kwasy *orto*-fenyloenodiboronowe oraz kwas fenyleno-1,2,4-triboronowy powodowały maksymalnie 8/4/2-krotne redukcje wartości MIC ceftazydymu odpowiednio przy stężeniach 16/8/4 mg/l i nie przywracały wrażliwości na tę cefalosporynę żadnemu z badanych szczepów AmpC-dodatnich.

Dla szczepów wytwarzających enzymy typu KPC znaczące redukcje wartości MIC meropenemu uzyskano w obecności 7 związków: 4 kwasów *para*-fenylenodiboronowych, 2 kwasów *orto*-fenylenodiboronowych oraz kwasu 2,5-difluorofenyloboronowego. W kolejnym etapie badań w obecności tych związków w stężeniach 16, 8 i 4 mg/l wyznaczono dodatkowo wartości MIC imipenemu oraz ertapenemu dla tych samych szczepów KPC-dodatnich. Wykazano, że powodują one porównywalne redukcje wartości MIC każdego z badanych karbapenemów. Największą aktywność (i większą niż PBA wobec wszystkich szczepów) wykazał kwas *orto*-fenylenodiboronowy, który w stężeniach 16/8/4 mg/l redukował wartości MIC karbapenemów odpowiednio nawet 64/16/8-krotnie. Przywrócił on wrażliwość na meropenem wszystkim czterem badanym szczepom (osiągnięto redukcje wartości MIC do poziomu ≤8 mg/l – punkt odcięcia dla meropenemu w obecności 8 mg/l waborbaktamu

u *Enterobacterales* [12]), a na imipenem 3 z 4 badanych szczepów (osiągnięto redukcje wartości MIC do poziomu ≤ 2 mg/l - punkt odcięcia dla imipenemu w obecności 4 mg/l relebaktamu u *Enterobacterales* [12]). Aktywność porównywalną lub większą niż PBA wykazywały również kwasy *para*-fenylenodiboronowy oraz 2,5-difluoro-fenyloboronowy (maksymalnie 16/8/2-krotne redukcje wartości MIC odpowiednio przy ich stężeniach 16/8/4 mg/l). Kwas *para*-fenylenodiboronowy przywrócił wrażliwość na meropenem wszystkim czterem badanym szczepom, a kwas 2,5-difluorofenyloboronowy 3 z 4 szczepów. Obydwa związki przywróciły także wrażliwość na imipenem 2 z 4 szczepów (wyłącznie KPC-3-dodatnim). Fluorowe pochodne kwasów *para*- i *orto*-fenylenodiboronowego powodowały mniejsze redukcje wartości MIC karbapenemów niż odpowiednie kwasy wyjściowe. Żaden z 7 związków o aktywności BLI wobec szczepów KPC-dodatnich nie przywracał im wrażliwości na ertapenem (nie osiągnięto redukcji wartości MIC do poziomu ≤0,5 mg/l - punkt odcięcia dla ertapenemu stosowanego samodzielnie u szczepów *Enterobacterales* [12]), aczkolwiek kwasy *para*- i *orto*-fenylenodiboronowe redukowały wartości MIC ertapenemu odpowiednio nawet 8- i 16-krotnie bardziej niż PBA wobec wszystkich szczepów.

6.3.3. Potwierdzenie celu molekularnego badanych kwasów fenylenodiboronowych

Mając na uwadze (I) wysoką skuteczność niepodstawionych kwasów *orto*- i *para*-fenylenodiboronowych w przywracaniu wrażliwości na karbapenemy szczepów KPC-dodatnich oraz (II) brak takiej aktywności kwasu *meta*-fenylenodiboronowego, do dalszych prac wytypowano trzy najbardziej reprezentatywne pochodne, tj. niepodstawione kwasy *orto*-, *meta*- i *para*-fenylenodiboronowe. Celem kolejnych badań było wykazanie, że punktem uchwytu w/w związków są faktycznie enzymy typu KPC. Zważywszy na fakt, iż redukcje wartości MIC karbapenemów w obecności badanych związków były 2-4-krotnie większe u szczepów wytwarzających enzymy KPC-3 niż KPC-2, wykorzystano wrażliwy na meropenem szczep *E. coli* DH5α (MIC 0,016 mg/l) oraz jego transformanta – szczep *E. coli* 82 TR(pl 81) niosący plazmid z genem $bla_{\text{KPC-3}}$ (MIC meropenemu 2 mg/l). Transformant pochodził z kolekcji Zakładu Mikrobiologii Farmaceutycznej i Bioanalizy WUM. Potwierdzenie celu molekularnego w/w związków przebiegało trzyetapowo i zostało opisane w **Publikacji O4**.

W pierwszym etapie oznaczono wartości MIC meropenemu szczepu *E. coli* DH5α i jego transformanta w obecności 16, 8 i 4 mg/l badanych kwasów fenylenodiboronowych oraz PBA. Zgodnie z oczekiwaniami, żaden z badanych związków nie spowodował

zmiany wartości MIC meropenemu u *E. coli* DH5α, co wykluczyło aktywność bezpośrednią nowych związków wobec szczepu macierzystego. Znaczące redukcje wartości MIC meropenemu uzyskano natomiast dla jego transformanta w obecności kwasów *orto*- i *para*-fenylenodiboronowych oraz PBA w stężeniach 16/8/4 mg/l (odpowiednio 32/16/4-krotne, 16/8/4-krotne oraz 8/8/4-krotne). Kwas *meta*-fenylenodiboronowy redukował natomiast wartości MIC meropenemu tego szczepu maksymalnie 2-krotnie. Potwierdzono tym samym zdolność kwasów *orto*- i *para*-fenylenodiboronowych do zwiększania aktywności karbapenemów wobec szczepów wytwarzających enzym KPC-3 i brak takiej aktywności kwasu *meta*-fenylenodiboronowego.

W drugim etapie wykonano oznaczenia biochemiczne aktywności badanych związków wobec wyizolowanych białek całkowitych transformanta *E. coli* 82 TR(pl 81), przeprowadzając test hydrolizy nitrocefiny. W teście tym hydroliza pierścienia β-laktamowego nitrocefiny przez β-laktamazę powoduje zmianę zabarwienia roztworu z żółtego na różowy, co wyraża się wzrostem absorbancji. W niniejszej pracy mierzono spektrofotometrycznie absorbancję roztworu nitrocefiny w obecności wyizolowanych białek całkowitych transformanta *E. coli* 82 TR(pl 81) zarówno przy braku jak i w obecności badanych związków i PBA w stężeniach 16, 8 i 4 mg/l. Wzrost absorbancji przy nieobecności badanych związków i PBA potwierdził aktywność enzymu KPC-3 w uzyskanym ekstrakcie białkowym (kontrola pozytywna). Z kolei redukcje absorbancji w porównaniu do kontroli pozytywnej uzyskane w obecności PBA oraz kwasów *orto*-, *para*- i *meta*-fenylenodiboronowych (odpowiednio o 53/44/42/29% przy stężeniu 16 mg/l oraz o 43/35/35/18% przy stężeniu 8 mg/l) potwierdziły, że badane związki są faktycznie inhibitorami enzymu KPC-3.

W trzecim etapie dla kwasów *orto*-, *meta*- i *para*-fenylenoodiboronowych zostały przeprowadzone badania *in silico*, wykonane przez Panią dr Krystianę A. Krzyśko z Zakładu Biofizyki Uniwersytetu Warszawskiego oraz Pana mgr Piotra Chyżego z Centrum Nowych Technologii Uniwersytetu Warszawskiego. Przeprowadzone przez Nich symulacje metodami opartymi na mechanice kwantowej/ mechanice molekularnej (ang. *quantum mechanics/molecular mechanics* – QM/MM) potwierdziły, że kwas *orto*-fenylenodiboronowy jest najlepszym spośród badanych związków BLI, najczęściej i najszybciej osiągającym konfigurację pozwalającą na przeprowadzenie addycji nukleofilowej w sprzyjających warunkach (centralny punkt hamowania niekompetycyjnego).

Wykazana w niniejszej pracy wysoka aktywność kwasów fenylenodiboronowych jako inhibitorów enzymów typu KPC/AmpC w połączeniu z ich brakiem cytotoksyczności w aktywnym zakresie stężeń (wykazanym przez Panią dr hab. Patrycję Wińską z Katedry Biotechnologii Środków Leczniczych i Kosmetyków Politechniki Warszawskiej) oraz cytotoksycznością PBA w tym samym zakresie stężeń pozwala stwierdzić, że pomijane dotąd w projektowaniu leków kwasy fenylenodiboronowe mogą być postrzegane jako lepsze niż PBA struktury wyjściowe do syntezy nowych, innowacyjnych inhibitorów β-laktamaz bakterii Gram-ujemnych, zwłaszcza enzymów typu KPC.

6.4. Analiza zależności między strukturą a siłą synergistycznego oddziaływania nowych kwasów aryloboronowych z β-laktamami

Zważywszy na szczątkowe jak dotąd dane o aktywności biologicznej kwasów di- oraz triboronowych [169], mimo ich powszechnego stosowania w syntezie organicznej [167,168], jednym z celów niniejszej pracy była także ocena wpływu obecności dodatkowych grup boronowych w cząsteczce na zdolność związku do hamowania bakteryjnych β-laktamaz. W niniejszej pracy przeprowadzono analizę korelacji struktura – siła synergistycznego oddziaływania z β-laktamami nowych, aromatycznych kwasów mono-, di- oraz triboronowych (**Publikacja O4**). Do badań wytypowano 17 pochodnych, które we wcześniejszym etapie wykazały aktywność BLI w niskich stężeniach wobec szczepów KPC- lub AmpC-dodatnich. W pierwszym etapie, posługując się metodą szachownicy wyznaczono wartości indeksu częściowego stężenia hamującego (ang. *fractional inhibitory concentration index* – FICI) dla kombinacji:

- 16 kwasów boronowych i PBA z ceftazydymem wobec dwóch szczepów AmpC-dodatnich (łącznie wyznaczono 34 wartości FICI);
- 7 kwasów boronowych i PBA trzeba karbapenemami wobec 4 szczepów KPC-dodatnich (łącznie wyznaczono 96 wartości FICI).

Wartości FICI w niniejszej pracy obliczono korzystając z poniższego wzoru [216]:

FICI = [(MIC antybiotyku w kombinacji) / (MIC antibiotyku)] + [(MIC związku w kombinacji) / (MIC związku)]

Następnie, wychodząc z założenia, że im niższa wartość FICI tym silniejsze synergistyczne oddziaływanie, przeprowadzono analizę statystyczną, w celu określenia

czy badane grupy związków (zgodnie z klasyfikacją strukturalną) różnią się istotnie pod względem uzyskiwanych wartości FICI dla ich kombinacji z β-laktamami. Ze względu na wykazany testem Shapiro−Wilka brak rozkładu normalnego zastosowano test nieparametryczny Kruskala−Wallisa. Analiza *post-hoc* została przeprowadzona przy użyciu testu wielokrotnych porównań (test Dunna). Poziom istotności ustalono na $p<0,05$. Stosując powyższe metody wykazano, że:

- synergia otrzymanych kwasów fenyleonodiboronowych z karbapenemami jest istotnie silniejsza wobec szczepów KPC-3- niż wobec szczepów KPC-2-dodatnich ($p=0,046$);
- synergia kwasów *orto*-fenylenodiboronowych z karbapenemami jest istotnie silniejsza niż synergia kwasów *para*-fenylenodiboronowych i fenyloboronowych (w obu przypadkach $p=0,0001$);
- synergia kwasów *orto*-fenylenodiboronowych z ceftazydymem wobec szczepów AmpC-dodatnich jest istotnie słabsza niż synergia kwasów *meta*-fenylenodiboronowych ($p=0,04$) oraz fenyloboronowych ($p=0,008$);
- obecność fluoru w cząsteczce osłabia synergistyczne oddziaływanie kwasów fenylenodiboronowych z karbapenemami wobec szczepów KPC-dodatnich ($p=0,036$) ale nasila synergistyczne oddziaływanie z ceftazydymem wobec szczepu CMY-2-dodatniego ($p=0,005$).

W pracy wykazano zatem, iż wprowadzenie do cząsteczki kwasu fenyloboronowego dodatkowej grupy boronowej w pozycji *orto* istotnie zwiększa siłę synergistycznego oddziaływania z karbapenemami choć osłabia synergię z ceftazydymem. Z kolei obecność fluoru w cząsteczce kwasów aryloboronowych osłabia synergię z karbapenemami, ale nasila synergię z ceftazydymem.

6.5. Opracowanie nowej metodyki wyznaczania górnej granicy MSW

Istotnym elementem badań przedklinicznych nowych związków przeciwdrobnoustrojowych jest prawidłowe wyznaczenie w warunkach *in vitro* ich zakresu stężeń, w których może dochodzić do selekcji lekoopornych mutantów *in vivo* (tzw. parametru MSW) [46,59]. Jego dolną granicę stanowi wartość MIC komórek wrażliwych typu dzikiego a górną wartość MPC, tj. najmniejszego stężenia antybiotyku całkowicie hamującego wzrost drobnoustrojów, gdy jego działaniu poddanych zostanie co najmniej 10^{10} CFU [58]. Wiadomo, że stężenia antybiotyków utrzymujące się w trakcie terapii w zakresie MSW mogą być przyczyną niepowodzeń terapeutycznych oraz

sprzyjają selekcji szczepów opornych [187], a pochodne o porównywalnej aktywności i podobnej strukturze mogą znacznie różnić się pod względem zakresu MSW [46,59,189]. Do dalszych prac badawczo-rozwojowych należy więc typować związki nie tylko o wysokiej aktywności, ale także takie, dla których będzie możliwe osiągnięcie *in vivo* stężeń powyżej wartości MPC, tj. w najmniejszym stopniu generujące szybkie narastanie oporności szczepów bakteryjnych w trakcie stosowania związku w lecznictwie. Mając jednak na uwadze, iż: (I) wartości MPC wyznaczane aktualnie *in vitro* metodą rozcieńczeń w agarze charakteryzują się niedostateczną powtarzalnością [83], (II) zakresy MSW wyznaczone aktualnie *in vitro* nie zawsze są tożsame z zakresami obserwowanymi później *in vivo* [86,87], (III) istnieje konieczność opracowania nowych, ograniczających narastanie oporności schematów dawkowania antybiotyków [8,57] oraz (IV) jak dotąd nie udało się wykorzystać parametru MPC jako podstawy takiego schematu dawkowania, w niniejszej pracy doktorskiej, w **Publikacji O3** zaproponowano nowe podejście do wyznaczania potencjału selekcjonowania oporności przez związki przeciwdrobnoustrojowe.

Opracowano nowe parametry *in vitro* charakteryzujące ten potencjał: minimalne stężenie zapobiegające selekcji mutantów dominujących (ang. *dominant mutant prevention concentration*–MPC-D), okno selekcji mutantów dominujących (ang. *dominant mutant selection window* – MSW-D), minimalne stężenie zapobiegające selekcji mutantów o obniżonej sprawności (ang. *inferior mutant prevention concentration*–MPC-F) oraz okno selekcji mutantów o obniżonej sprawności (ang. *inferior mutant selection window*–MSW-F). Wartości MPC-D oraz MSW-D odnoszą się do lekoopornych mutantów selekcjonowanych z dużą częstością, bez znaczących zmian w sprawności w porównaniu do komórek typu dzikiego, co do których istnieje wysokie prawdopodobieństwo, że będą one w stanie ustanowić oporną populację *in vivo*. Zaproponowano by w metodzie rozcieńczeń w agarze wartość MPC-D wyznaczać jako najmniejsze stężenie związku przeciwdrobnoustrojowego, dla którego częstość selekcji lekoopornych mutantów *in vitro* (ang. *frequency of spontaneus mutant selection* – FSMS) wynosi $<10^{-10}$. Uznano, że mutanty powstające z mniejszą częstością niż 10^{-10} będą w minimalnym stopniu przyczyniały by się do selekcji szczepów opornych, bowiem lekooporne mutanty mogą być kontrolowane przez układ immunologiczny większości pacjentów jeżeli tylko ich liczba utrzymuje się na niskim poziomie. Za bezpieczne dla powodzenia antybiotykoterapii przyjmuje się często już te stężenia antybiotyków, dla których częstość selekcji opornych mutantów w warunkach *in vitro* wynosi $1x10^{-8}$ lub

mniej [46,77,78]. Mutanty powstające z mniejszą częstością niż 10^{-10} nie zawsze mogą być również wykryte w trakcie badań *in vitro*. Powiązanie wartości MPC-D z wartością FSMS jest zatem kluczowe dla zwiększenia powtarzalności oznaczania parametru MPC-D w porównaniu do oryginalnej wartości MPC.

Aby jednak lepiej i szybciej ocenić czy lekooporne mutanty selekcjonowane *in vitro* nie są znacząco mniej sprawne niż komórki typu dzikiego, zaproponowano wyznaczanie wartości MPC-D metodą rozcieńczeń związku w bulionie. W tej metodzie wartość MPC-D zdefiniowano jako najniższe stężenie leku, które uniemożliwia lekoopornym mutantom selekcjonowanych spośród 10^{10} CFU ustanowienie opornej populacji o gęstości co najmniej 10 CFU/ml w trakcie 24h inkubacji w podłożu płynnym ze związkiem (tj. mutanty nie są w stanie zdominować populacji o tak wysokiej gęstości). Z kolei parametry MPC-F/MSW-F odnoszą się do lekoopornych mutantów, u których nabycie lekooporności spowodowało jednocześnie znaczne osłabienie sprawności. Mutanty te mogą powstać *in vitro,* ale zważywszy na ich brak zdolności do dominowania w populacji, jest mało prawdopodobne by były selekcjonowane *in vivo*.

Ponadto, mając na uwadze fakt, iż do precyzyjnego wyznaczenia górnej granicy MSW kluczowe znaczenie ma otrzymanie zawiesiny komórek bakterii o wysokiej gęstości, tj. min. 10^{10} CFU/ml [58], a analiza piśmiennictwa wykazała, że tylko w kilku publikacjach udało się otrzymać do doświadczeń tak gęste zawiesiny komórek [58,74,80], w niniejszej pracy doktorskiej opracowano nową metodę otrzymywania inokulum o wysokiej gęstości (>10^{11} CFU/ml), polegającą na wielostopniowym zagęszczaniu hodowli płynnej.

W **Publikacji O3** wyznaczono potencjał selekcjonowania oporności przy użyciu powyższej, nowej metodyki i dokonano porównania z klasyczną metodą wyznaczania MPC. Wyznaczono wartości MPC-D/MSW-D oraz MPC/MSW cyprofloksacyny, linezolidu i nowego benzosiloksaborolu No37 dla szczepu *S. aureus* ATCC 29213 metodą rozcieńczeń w agarze. Nowością pracy jest także powiązanie wartości klasycznego MPC z częstością selekcji opornych mutantów w metodzie rozcieńczeń w agarze co ma miejsce w opracowanej metodyce wyznaczania wartości nowego parametru MPC-D. Ponadto wyznaczono wartości MPC-D/MSW-D i MPC-F/MSW-F tych związków przeciwbakteryjnych dla tego samego szczepu nową metodą rozcieńczeń w bulionie. Badany zakres stężeń każdego związku przeciwbakteryjnego w obu metodach wynosił 1−32xMIC, a badaniu na każdym stężeniu poddawano 10^{10} CFU. Dzięki zastosowaniu nowej metody wielostopniowego zagęszczania hodowli płynnej bakterii

w trakcie dwóch powtórzeń doświadczenia uzyskano wyjściowe inokula o gęstości $7{,}5x10^{11}$ CFU/ml oraz $5x10^{11}$ CFU/ml. Niezależnie od zastosowanej metody, zakresy wszystkich okien selekcji mutantów ($MSW_{10^{10}}$, $MSW\text{-}D_{10^{10}}$, $MSW\text{-}F_{10^{10}}$) opornych na linezolid i benzosiloksaborol No37 były identyczne i wynosiły odpowiednio 1−2xMIC oraz 1−32xMIC. Zupełnie inne wyniki uzyskano w przypadku cyprofloksacyny, dla której najwęższy zakres miało $MSW\text{-}D_{10^{10}}$ w metodzie rozcieńczeń w bulionie (1−8xMIC) oraz $MSW\text{-}D_{10^{10}}$ w metodzie rozcieńczeń w agarze (1−16xMIC). Zakres $MSW\text{-}F_{10^{10}}$ wynosił natomiast 1−32xMIC a zakres oryginalnego $MSW_{10^{10}}$ aż 1−>32xMIC. Jednakże częstość selekcji cyprofloksacyno-opornych mutantów na stężeniu 32xMIC była ekstremalnie niska i wynosiła $4{,}5x10^{-11}$. Zatem wartość MPC cyprofloksacyny uzyskana w niniejszej pracy nie byłaby odtwarzalna w przypadku poddaniu badaniu populacji mniejszej niż $2{,}2x10^{10}$ CFU, mimo iż byłaby to populacja wystarczająca do wyznaczenia wyniku $MPC_{10^{10}}$.

W **Publikacji O3** wykazano zatem, że wartości MPC-D w przypadku niektórych związków przeciwbakteryjnych są niższe niż wartości MPC, przez co mogą okazać się bardziej akceptowalne klinicznie jako podstawa schematów dawkowania leków. Wykazano również, że wyznaczane metodą rozcieńczeń w agarze wartości MPC-D mogą być bardziej powtarzalne i odtwarzalne niż wartości MPC. W pracy zaproponowano ponadto wyznaczanie zakresu MSW za pomocą nowej metody rozcieńczeń w bulionie, w której dodatkowy etap 24-godzinnej inkubacji wyjściowej populacji w podłożu ze związkiem pozwala zróżnicować dominujące mutanty od mutantów o obniżonej sprawności. Zakresy MSW-D wyznaczane tą metodą powinny lepiej korelować z zakresami MSW obserwowanymi później w badaniach *in vivo*. W badaniach przedklinicznych zaproponowane w niniejszej pracy nowe podejście do oceny potencjału selekcjonowania oporności przez związki przeciwdrobnoustrojowe zwiększy szansę na wytypowanie do dalszych prac *in vitro* i *in vivo* związku i jego zakresu stężeń w najmniejszym stopniu sprzyjających narastaniu oporności w czasie jego stosowania w lecznictwie. W dalszej perspektywie, może ono przyczynić się do opracowania ograniczających narastanie oporności schematów dawkowania.

7. Kopie opublikowanych prac

7.1. Publikacja P1

POSTĘPY MIKROBIOLOGII – ADVANCEMENTS OF MICROBIOLOGY
2021, 60, 4, 249–264
DOI: 10.21307/PM-2021.60.4.20

THE EUROPEAN MEDICINES AGENCY APPROVED THE NEW ANTIBACTERIAL DRUGS – RESPONSE TO THE 2017 WHO REPORT ON THE GLOBAL PROBLEM OF MULTI-DRUG RESISTANCE

Joanna Krajewska, Agnieszka Ewa Laudy*

Department of Pharmaceutical Microbiology, Medical University of Warsaw

Received in July, accepted in September 2021

Abstract: The growing problem of antimicrobial resistance has been classified by the World Health Organization (WHO) as one of the top ten threats to mankind. In a special report published in 2017, the WHO presented a list of microorganisms for which the search for new therapeutic options is a priority. The highest (critical) priority was given to the search for new antibiotics active against carbapenem-resistant strains of *Acinetobacter baumannii* and *Pseudomonas aeruginosa* as well as against carbapenem- and third-generation-cephalosporin-resistant *Enterobacterales* strains (so-called critical priority pathogens). Whereas the second (high) priority was given among others to the search for new antibiotics active against methicillin- and vancomycin-resistant strains of *Staphylococcus aureus* (MRSA and VRSA) and vancomycin-resistant strains of *Enterococcus faecium* (VRE). Since the publication of the WHO report the European Medicines Agency has approved 6 novel, broad-spectrum antibiotics, from 6 different groups, addressing the priority pathogens to a different extent. Two of them are new combinations of carbapenems with non-β-lactam inhibitors of β-lactamases (active also against carbapenemases), belonging to two novel groups of inhibitors: diazabicyclooctanes (relebactam, combined with imipenem) and boronates (vaborbactam, combined with meropenem). The third new drug is a siderophore cephalosporin (cefiderocol) with an innovative mechanism of penetration into the bacterial cell. The next two antibiotics are the new fluoroquinolone (delafloxacin) and the new tetracycline (eravacycline), designed and synthesized to be more active than older members of these groups. The last innovative antibiotic is lefamulin – the first pleuromutilin approved for systemic use in humans. New approvals have expanded the number of available therapeutic options in the treatment of complicated urinary tract infections (meropenem/vaborbactam, cefiderocol), complicated intra-abdominal infections (meropenem/vaborbactam, eravacycline), nosocomial pneumonia (meropenem/vaborbactam, imipenem/relebactam), acute bacterial skin and skin structure infections (delafloxacin) and community-acquired pneumonia (lefamulin).

1. Introduction 2. Boronate β-lactamases inhibitors 3. Diazabicyclooctane β-lactamases inhibitors 4. Siderophore cephalosporins 5. New fluoroquinolones 6. New tetracyclines 7. Pleuromutilins 8. Summary

Keywords: delafloxacin, eravacycline, β-lactamases inhibitors, siderophores, vaborbactam

1. Introduction

According to the World Health Organization (WHO), the growing drug resistance of microorganisms is one of the top ten threats to humanity. In 2017, the WHO published a special report containing a list of pathogens for which the search for new therapeutic options is a priority, due to the increasingly limited range of antibiotics that can be used to treat infections caused by them [121]. Twelve pathogens were entered on the list, divided into 3 categories according to the urgency of searching for new therapeutic options active against them. The first group of pathogens with the highest critical priority included carbapenem-resistant Gram-negative bacilli. Carbapenem-resistant *Acinetobacter baumannii* (CRAB) strains were considered to be the most dangerous, followed by carbapenem-resistant *Pseudomonas aeruginosa* strains CRPA) and, in third place, carbapenem-resistant *Enterobacterales* (CRE). This group also includes *Enterobacterales* strains resistant to third-generation cephalosporins, as well as *Mycobacterium tuberculosis* and other acid-fast mycobacteria. Whereas, multidrug-resistant strains of Gram-positive cocci have been classified by the WHO into the second group of pathogens with a high priority of search for new drugs against them. This group includes *Staphylococcus aureus* strains resistant to methicillin (methicillin-resistant *S. aureus* – MRSA) and vancomycin (vancomycin-resistant *S. aureus* – VRSA); vancomycin-resistant *Enterococcus faecium*, as well as clarithromycin-resistant *Helicobacter pylori*; *Campylobacter* spp., and *Salmonella* spp. resistant to fluoroquinolones; and *Neisseria gonorrhoeae* resistant to fluoroquinolones and third-generation cephalosporins [121].

The most important problem among the critical priority pathogens is their resistance to carbapenems,

* Corresponding author: Agnieszka E. Laudy, Dept. Pharmaceutical Microbiology, Faculty of Pharmacy, Medical University of Warsaw, Center for Preclinical Research and Technology (CEPT), Banacha 1 b Str., 02-097 Warsaw, Poland, e-mail: alaudy@wp.pl

associated with the production of hydrolyzing them enzymes (carbapenemases), or with non-specific mechanisms such as decreasing the outer membrane permeability and overexpression of genes encoding efflux pumps [26, 37, 60]. According to Ambler classification [4], carbapenemases occurring among the strains of Gram-negative bacilli belong mainly to classes A, B and D. So far, only a few class C carbapenemases have been described, e.g., the enzyme ADC-68 in *A. baumannii*. Among the class A enzymes, the KPC plasmid carbapenemases (*Klebsiella pneumoniae* carbapenemase), mainly the variants KPC-2 and KPC-3, are of the highest clinical significance [37]. They are widespread in *Enterobacterales* strains, primarily in *K. pneumoniae* strains and increasingly in *E. coli* strains. The ability to produce them has also been demonstrated in Gram-negative strains of non-fermenting bacilli, i.e., *P. aeruginosa*, and recently in *A. baumannii*. The genes encoding them are located in transposons in large conjugative plasmids, which creates the possibility of their easy horizontal transfer. In the therapy of infections caused by KPC-positive strains only colistin, tigecycline and sometimes aminoglycosides can be administered. The strains producing carbapenemases of the family GES (Guiana extended-spectrum β-lactamase) are of much lower clinical importance. It is relatively rare for GES enzymes to be detected in both *P. aeruginosa* strains and in the bacilli of *Enterobacterales*, and the genes encoding them are most often located in class 1 integrons [37].

Out of the class B enzymes of the Ambler classification system (metallo-β-lactamases – MBL) [37], the enzymes of the NDM (New Delhi metallo-β-lactamase) family occur the most frequently in Gram-negative bacilli strains worldwide. Originally, enzymes of MBL type posed a therapeutic problem mainly in *P. aeruginosa* strains. The predominant enzymes in Europe, also in Poland, were the ones from the VIM (Verona integrated-encoded metallo-β-lactamase) family, and in the Far East, IMP (imipenemase) enzymes. The first case of the production of the NDM-1 enzyme in *Enterobacterales* was described in 2009, and in the following years the ability to produce NDM enzymes became widely spread, mainly in *K. pneumoniae*, *E. coli*, *P. aeruginosa* and other bacilli. A wide substrate range of MBL enzymes (they hydrolize all β-lactams except monobactams) in combination with the easy horizontal transfer of the genes encoding them (located in plasmids, integrons or transposons) and the lack of an inhibitor that can be utilized in therapy (they are inhibited, among others, by EDTA) make these enzymes a significant clinical problem. It is considered that the greatest threat are NDM-positive strains , whose genomes also contain genes encoding other β-lactamases (AmpC, OXA-48, VIM, KPC) and genes determining resistance to other antibiotics (aminoglycosides and fluoroquinolones). The strains producing MBL enzymes usually remain sensitive to colistin, tigecycline and fosfomycin [37].

D class carbapenemases, according to the Ambler classification system, are oxacillinases of the OXA family, the substrate range of which has been expanded, giving them the capability of hydrolysing also carbapenems. The greatest clinical importance is possessed by the enzymes of the CHDL group (carbapenem-hydrolysing class D β-lactamases) and OXA-48 β-lactamase. CHDL enzymes are the dominant mechanism responsible for carbapenem resistance in *A. baumannii* strains [79, 102]. In *A. baumannii* strains, in addition to the naturally occurring chromosomal OXA-51-like enzyme, also OXA-23-like and OXA-24-like CHDL carbapenemases are most commonly detected. In turn, the carbapenemase of OXA-48 is commonly found in the bacilli of the order *Enterobacterales*. The hydrolytic activity of class D carbapenemases towards carbapenems and cephalosporins is lower compared to MBL and KPC-type enzymes. However, the presence of insertion sequences (IS*Aba*) preceding the bla_{CHDL} genes significantly increases the resistance of *A. baumannii* strains to carbapenems. *A. baumannii* CRAB strains, owing to the variety of other resistance mechanisms simultaneously occurring in them, are considered to be among the most dangerous pathogens, against which WHO recommends priority search for new therapeutic options.

Resistance to carbapenems has also been described among *Enterobacterales* strains as well as Gram-negative non-fermenting bacilli which do not produce carbapenemases. The cause of the insensitivity of the strains to carbapenems may lie in the reduction of the outer membrane permeability, due to a reduction in the abundance or changes in the conformation of the porins through which carbapenems penetrate into the cell, the so-called influx mechanism [26]. The reduced abundance or absence of OprD porins was the first reported mechanism of the resistance of *P. aeruginosa* to imipenem. This mechanism of resistance to carbapenems has also been described in *K. pneumoniae* strains (associated with OmpK35 and OmpK36 porins), *E. coli* (associated with OmpC and OmpF porins) and in *A. baumannii* (primarily CarO). Active removal of antibiotics from bacterial cells by the efflux pump systems, the so-called efflux mechanism plays an important role – in CRE strains, RND family pumps are the most important (e.g., AcrAB-TolC systems in *E. coli* as well as in *K. pneumoniae*) in CRPA strains, the MexAB-OprM and MexXY systems and the AdeABC system in CRAB strains [60]. It is often found that the resistance of Gram-negative bacilli to carbapenems includes simultaneous participation of two or three mechanisms, such as production of two different carbapenemases

and/or disruption of antibiotic penetration into cells and/or active removal of drugs with the participation of efflux pump systems.

Among the pathogens from the second group according to WHO classification, the high priority kind, resistance of staphylococcal strains to methicillin and glycopeptides and resistance of enterococci to glycopeptides are the dominant problems [121]. The resistance to methicillin in staphylococci is linked to the presence of the *mecA* gene or its homologues, i.e., *mecB, mecC* or *mecD*, which determine the synthesis of the altered PBP-2a protein, having no affinity for β-lactam antibiotics (except for ceftaroline and ceftobiprole) [28]. The *mec* genes are located within a large mobile DNA fragment, i.e., SCC*mec* (staphylococcal cassette chromosome *mec*). In addition to being resistant to β-lactam, MRSA strains also typically exhibit resistance to aminoglycosides, fluoroquinolones, macrolides and lincosamins. On the other hand, they often remain sensitive to ceftaroline, ceftobiprole, linezolid, tigecycline, daptomycin, dalbavancin and rifampicin. Following the emergence of methicillin-resistant staphylococci, vancomycin became the drug of choice for the treatment of infections caused by them. Soon, however, strains with reduced susceptibility to this antibiotic (vancomycin intermediate-resistant *Staphylococcus aureus* – VISA), and (less frequently) vancomycin resistant strains appeared (vancomycin resistant *Staphylococcus aureus* – VRSA) [28]. The reasons for the reduced sensitivity of the VISA phenotype to vancomycin are not yet fully understood. Most likely, it is related to a change in the cell wall structure and a decrease in its permeability to vancomycin. In turn, the complete resistance to vancomycin, a VRSA phenotype, is conditioned by the presence of an operon containing the *vanA* gene. It has been demonstrated that this operon was located in the Tn1546 transposon, derived from the enterococcal conjugative plasmid. The resistance to vancomycin was first observed in enterococci. Among the VRE (vancomycin-resistant enterococci) strains responsible for hospital infections, *E. faecium* isolates display resistance to vancomycin significantly more often than *E. faeca*lis [95]. The *vanA* gene, as well as other previously detected *van* genes (*vanB*, *vanC*, *vanD*, *vanE*, *vanG*, *vanL*, *vanM*, *vanN*), which determine resistance or reduced sensitivity of enterococci to vancomycin, are the ones responsible for the synthesis of the altered D-alanyl-D-alanine peptide fragment in the cell wall precursor, forming the D-alanyl-D-lactate or D-alanyl-D-serine. Thus, the target site of glycopeptide action changes, which is expressed through different levels of isolate resistance. In addition to VRE and MRSA strains, also the strains simultaneously resistant to linezolid are isolated, which may pose a serious clinical problem. The resistance of priority pathogens to fluoroquinolones results mainly from mutations in the genes encoding topoisomerase II, i.e., gyrase (in the *gyrA* genes) and topoisomerase IV (in the genes *parC* in *E. coli* and *grlA* in staphylococci), which results in the synthesis of altered subunits of these enzymes, with reduced affinity for fluoroquinolones [42]. Additionally, fluoroquinolones are substrates for many MDR pumps in priority pathogens, e.g., AdeABC in *A. baumannii*, MexAB-OprM in *P. aeruginosa*, AcrAB-TolC in *Enterobacterales*, NorA in *S. aureus*, CmeABC in *Campylobacter* spp. or NorM in *N. gonorrhoeae* [42].

Since the publication of the 2017 WHO report sounding alarm on the issue of searching for new effective drugs against dangerous pathogens, six new antibiotics from six different groups, addressing WHO priorities to various degree have been approved on the European market by the European Medicines Agency (EMA). Two of them are a new combination of carbapenems with non-β-lactam inhibitors of β-lactamases (also active against carbapenemases), from two new groups: diazabicyclooctane inhibitors (relebactam, combined with imipenem) and boronate ones (vaborbactam, combined with meropenem). The success of approving after many years new β-lactamase inhibitors from two unused before chemical groups resulted in extending the scope of the search for new inhibitors [12, 19, 39]. In turn, the search for new ways to overcome the barrier posed by the outer membrane of Gram-negative bacteria, resulted in the market authorisation of cefiderocol – siderophore cephalosporin. The use of siderophores in drug design is a novel approach to the concept of modern medication [80, 119]. Both the new combination of carbapenems with β-lactamase inhibitors and cefiderocol are active towards critical WHO pathogens to a varying degree. The next two original antibiotics comprise a novel fluoroquinolone (delafloxacin) and a new tetracycline (eravacycline), the molecules of which were designed and synthesized in order to increase efficacy and minimize the susceptibility to bacterial resistance mechanisms, typical of the older representatives of these groups. Both antibiotics are active against many WHO high priority pathogens. The last of the new antibiotics is lefamulin, the first representative of the pleuromutilin group registered for systemic use in humans. A distinctive feature of this group of antibiotics is its unique structure (meeting the WHO innovation criteria), rare occurrence of resistance and activity against pathogens of high priority according to the WHO. In turn, the strains of Gram-negative bacilli, i.e., *P. aeruginosa*, *A. baumannii* and *Enterobacterales* are naturally resistant to lefamulin. This article provides a review of new, wide-spectrum antibiotics active against the WHO priority pathogens, authorized for use in the European Union since 2018 (Figure 1).

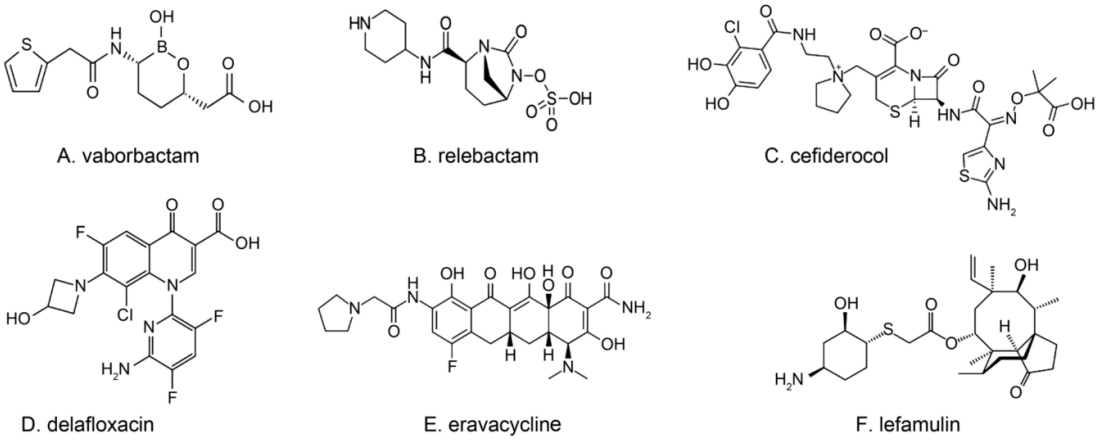

Figure 1. Structures of new antimicrobial compounds

Compounds are active against priority pathogens according to WHO, approved in the European Union since 2018: A) vaborbactam – a boron inhibitor of β-lactamases (combined with meropenem); B) relebactam – a diazabicyclooctane β-lactamase inhibitor (in combination with imipenem / cilastatin); C) cefiderocol – siderophore cephalosporin; D) delafloxacin – the fourth generation fluoroquinolones; E) eravacycline – the first fully synthetic tetracycline; F) lefamulin – the first pleuromutilin for systemic use in humans.

2. Boronate inhibitors of β-lactamases

Boronate β-lactamase inhibitors are a relatively new class of compounds with cyclic boronic acid as a pharmacophore. Vaborbactam (previously RPX7009) was dicovered under a program aimed at developing an inhibitor of serine β-lactamases, especially of the KPC type [39]. It is a monocyclic, reversible competitive inhibitor of class A enzymes according to the Ambler system (CTX-M, KPC, BKC, FRI, SME, TEM, SHV) and class C (AmpC) with which it creates covalent bonds between the boronate moiety and the catalytic serine centre. The inhibition of KPC by vaborbactam does not trigger its inactivation and is characterized by extremely slow reversibility. At the same time, vaborbactam is not active against class B enzymes (e.g., NDM, VIM) and class D (e.g., OXA-48), does not inhibit human serine enzymes and does not exhibit direct antimicrobial activity in therapeutic concentrations [15, 39, 111]. *In vitro* research has demonstrated that vaborbactam reduces the MIC values of carbapenems more vigorously than of the other β-lactams, hence the meropenem-vaborbactam combination was selected for further research [66].

In trials conducted on clinical isolates of Gram-negative strains of (*E. coli, Enterobacter* spp., *K. pneumoniae*, *A. baumannii* and *P. aeruginosa*), it was confirmed that vaborbactam increases the activity of meropenem against carbapenem-resistant strains of *Enterobacterales* but not against *P. aeruginosa* and *A. baumannii* strains [59, 97]. In large-scale surveillance programmes, the overall percentage of meropenem/vaborbactam among *Enterobacterales* was 99.3% and was higher than for meropenem (96.9%). In contrast, among *Enterobacterales* resistant to carbapenem, vaborbactam restored meropenem activity in 73.9% of the strains, and among the strains producing KPC in as much as 99.5%. Vaborbactam did not restore sensitivity to meropenem in strains producing metallo-β-lactamases and OXA-48 enzymes [88] as well as in the strains of *A. baumannii*, *P. aeruginosa* and *Stenotrophomonas maltophilia* [14]. Similar results were obtained by analysing the sensitivity of the collection of clinical *E. coli* strains resistant to carbapenems isolated around the world, in which the overall proportion of meropenem/vaborbactam-sensitive strains was 66% and was only lower than the percentage of strains sensitive to tigecycline (100%) and amikacin (74%). Sensitivity was greater among the strains of Latin American origin (88%) and lower among strains isolated in Europe (75%) and Asia (51%) [52]. Also, in the study by Zhou et al. [129], it was concluded that the proportion of *K. pneumoniae* strains with increased MIC values of meropenem and vaborbactam in China is higher than in other geographical areas, possibly due to the dissemination in this area of strains with defects in both major porins (OmpK35 and OmpK36) involved in the entry of carbapenems into a bacterial cell.

The growing problem of infections caused by the strains producing metallo-β-lactamases (and therefore resistant to all β-lactams, except aztreonam), combined with the absence of an effective inhibitor of these enzymes, has also resulted in attempts to combined meropenem/vaborbactam with aztreonam – a monobactam resistant to carbapenemases but destroyed by a number of serine enzymes. So far, *in vitro* research has demonstrated that meropenem/vaborbactam acts synergistically with aztreonam against multidrug-

resistant *K. pneumoniae* and *E. coli* strains producing both NDM-type enzymes and serine β-lactamases [11, 70]. However, the effectiveness of this combination requires further research.

The hitherto observed resistance of strains to meropenem/vaborbactam was most likely associated with the production of metallo-β-lactamases [15], mutations in genes encoding porins (OmpK35, OmpK36) [24, 66, 108] responsible for drug influx and/or overexpression of AcrAB-TolC pump systems [15] involved in the efflux mechanism, less often resistance was associated with an overproduction of KPC, associated with an increase in the number of bla_{KPC} gene copies [108]. So far, no case of resistance associated with a mutation in the bla_{KPC} genes has been described.

In clinical trials it was demonstrated that meropenem/vaborbactam (administered 2 g/2 g every 8 h) is non-inferior to piperacillin/tazobactam (4 g/0.5 g every 8 h) in patients with complicated urinary tract infection (cUTI) [55]. The results of the latest clinical trial (TANGO II) further indicate that meropenem-vaborbactam is superior to the best available therapy (BAT) in patients with a confirmed or suspected infection with *Enterobacterales* resistant to carbapenems and with multiple comorbidities such as renal failure, immunodeficiency, or prior antibiotic therapy [9, 10]. Increased cure rate, decreased mortality, and lower nephrotoxicity were observed in the patients group treated with meropenem/vaborbactam [9].

A preparation containing meropenem with vaborbactam powder for concentrate for solution for infusion (1 g/1 g) under the trade name of Vaborem has been approved on the European market since 20.11.2018 [20]. Its therapeutic indications include the treatment of complicated urinary tract infections (including pyelonephritis), complicated intra-abdominal infections, nosocomial pneumonia (including ventilator-associated pneumonia) and infections caused by Gram-negative aerobic organisms in adult patients with limited treatment options.

3. Diazabicyclooctane inhibitors of β-lactamases

Relebactam (formerly MK-7655) is the second, after avibactam, non-β-lactam inhibitor of β-lactamases from the group of diazabicyclooctane derivatives, approved for treatment [20]. Relebactam is structurally similar to avibactam, however, it contains an additional piperidine ring which ensures a positive charge at physiological pH for the molecule, crucial for reducing its susceptibility to active removal by pump systems in the phenomenon of efflux. Biochemical analyses have demonstrated that relebactam is an inhibitor of class A (of KPC type) and class C enzymes (AmpC type, e.g., AmpC *Pseudomonas*-derived cephalosporinase-3, PDC-3) and in addition (similarly to imipenem), it is not a substrate for the MDR pump systems in *P. aeruginosa* [7, 12, 124]. The lack of susceptibility of the imipenem/relebactam combination to being removed from bacterial cells by the *P. aeruginosa* MDR pump systems and the activity of relebactam against AmpC enzymes resulted in this combination being selected for further research. *In vitro* research has confirmed that relebactam actually increases the activity of imipenem against *Enterobacterales* strains, whose carbapenem resistance was associated with the production of KPC enzymes or in which the production of AmpC or ESBL β-lactamases was observed combined with the reduced permeability of the outer membrane (mutations in OmpK36). As was also observed in the *P. aeruginosa* OprD-deficient strains and (at higher concentrations of the drug) against *P. aeruginosa* MDR strains. Similarly to vaborbactam, relebactam is not an inhibitor of metallo-β-lactamases (NDM, IMP, VIM) or class D enzymes (OXA), neither does it display direct antibacterial activity [36, 40, 63]. The synergistic interaction of imipenem/relebactam with amikacin and colistin against imipenem-resistant *P. aeruginosa* strains has also been described under *in vitro* conditions [6].

In many large surveillance studies, the susceptibility to imipenem/relebactam of clinical strains isolated from patients with lower respiratory tract infections, urinary tracts infections and intra-abdominal infections has been tested [53, 54, 64, 65]. It has been demonstrated that in the presence of relebactam, imipenem concentrations able to prevent the growth of most clinical *Enterobacterales* strains (including carbapenem-resistant strains) were reduced, although the MIC values of imipenem for *Serratia marcescens* strains are usually higher than for other species. The percentage of imipenem/relebactam-sensitive strains of *E. coli, Klebsiella* spp., *Citrobacter* spp., and *Enterobacter* spp. reached over 95%. However, among *S. marcescens* the percentage of susceptible strains was lower. Imipenem/relebactam is also effective against *P. aeruginosa* strains (the percentage of susceptible strains reaching over 90%), with the exception of strains producing β-lactamases of class B or D. Among the strains resistant to carbapenems, 42–66% of *Enterobacterales* strains and 74–78% of *P. aeruginosa* strains remain sensitive to imipenem/relebactam. Relebactam, however, does not increase the activity of imipenem against *Acinetobacter* spp. [53, 54, 64, 65, 115].

The observed resistance of Gram-negative bacilli to imipenem/relebactam stems mainly from the production of metalloenzymes. In *P. aeruginosa* strains, it may also be due to the ability to produce class A carbapenemases from the GES family and overexpression of genes encoding PDC enzymes in combination with the loss of

the OprD porin proteins [65, 124]. In *Enterobacterales*, in turn, resistance may be caused by the production of oxacillinases with carbapenemase activity, e.g., OXA-48, as well as mutations in the genes encoding porin proteins and a decrease in the abundance of these porins (OmpK35, OmpK36, OmpC and OmpF), thereby limiting imipenem/relebactam penetration into bacterial cells [30, 51].

Clinical studies have demonstrated that imipenem (administered at a dose of 500 mg every 6 hours) in combination with relebactam (125 mg or 250 mg every 6 hours) is a well-tolerated treatment and is non-inferior than imipenem used alone in the group of patients with complicated intra-abdominal infections and complicated urinary tract infections [67, 101]. Imipenem/relebactam was also characterized by comparable efficacy and lower nephrotoxicity than the use of imipenem and colistin in the combination therapy of infections caused by imipenem-resistant Gram-negative bacilli [78]. On the basis of the obtained results, a preparation containing imipenem/cilastatin (where cilastatin is an inhibitor of dehydrogenase I, a kidney enzyme which inactivates imipenem) with relebactam (Recarbrio 500 mg/500 mg + 250 mg, powder for solution for infusion) was approved by EMA on 13.02.2020 for the treatment of nosocomial pneumonia (also associated with mechanical ventilation) and in the treatment of Gram-negative bacterial infections in adults with limited therapeutic options [20].

4. Siderophore cephalosporins

Cefiderocol is a representative of a new group of antibiotics – siderophore cephalosporins [80]. Siderophores are a structurally diverse group of small molecules (150–2000 Da) with chelating properties and high iron affinity [119]. Iron is an essential element for the functioning of many enzymes, and therefore also for microorganisms. However, its acquisition by bacteria is hampered due to the low solubility of iron at physiological pH under aerobic conditions, in which easily bioavailable Fe (II) ions are oxidized to Fe (III), causing the formation of insoluble ferric oxyhydroxides. In addition, host defence mechanisms cause further reduction in iron accessibility at the infection site due to the secretion of their own iron-binding proteins, such as lipocalin 2, also called siderocalin, or neutrophil gelatinase associated lipocalin (NGAL). In order to obtain the sufficient amount of iron, the bacteria produce and secrete siderophores into the extracellular environment, whose task is to bind its ions and transport them inside the cell. More than 500 different siderophores have been identified so far. Characteristic structural elements in their molecules are iron chelating functional groups (hydroxamates, catechols, carboxylates, phenolate moieties or combinations thereof) attached to a linear or cyclic scaffold forming a hexadentate structure. After binding an iron ion, the resulting complex (ferrisiderophore) is absorbed in the mode of active transport. In Gram-negative bacteria, the entire complex crosses both the outer and inner membranes, and the bounded iron is released in the cytoplasm. Alternatively, iron may be released in the periplasmic space [119].

The first attempts to use siderophores to transport antibiotics inside the cell were made already in the 1970s. In the 20th century, this strategy was called the "trojan horse approach" [80]. Cefiderocol (formerly S-649266, GSK2696266) is the first antibiotic of this type introduced into healthcare. It is used in the form of cefiderocol sulphate tosylate. It is a catechol siderophore cephalosporin, which was selected from other derivatives of a similar structure, in the course of a program aimed at finding a new antibiotic active against carbapenem-resistant strains [5]. Cefiderocol has a structural similarity to cefepime, such as the presence of a pyrrolidinium group on the C-3 side chain, increasing antimicrobial activity and stability against β-lactamases, and a carboxypropanoxyimino group on the C-7 side chain, which improves the transport of cefiderocol across the outer membrane. Additionally, cefiderocol also has a chlorocatechol group at the end of the C-3 side chain, which is responsible for siderophoric activity [96].

The principal mechanism of action of cefiderocol is the inhibition of cell wall synthesis by binding to PBPs (mainly PBP-3). Cefiderocol, after binding iron, reaches the periplasmic space through active transport, in which, inter alia, CirA and Fiu transporters in *E. coli* and PiuA in *P. aeruginosa* are involved. This transport mechanism eliminates the problem of resistance associated with reducing the number of porins in the outer membrane or the overexpression of the MDR pumps, which are responsible for the phenomenon of efflux [96]. Furthermore, a cefiderocol molecule is resistant to a wide range of β-lactamases, both serine (KPC-3, OXA-23, AmpC) and metallo-β-lactamases (IMP-1, VIM-2) [46, 47]. However, this resistance may arise due to mutations within the genes encoding either PBPs, or a protein related to the regulation of iron ion uptake or siderophores transport protein, as well as the production of β-lactamases capable of hydrolysing cefiderocol (NDM, PER type) and overexpression of native bacterial siderophores [58, 69, 96].

Cefiderocol is highly active against a broad spectrum of Gram-negative bacteria, both representatives of *Enterobacterales* (*Enterobacter* spp., *Klebsiella* spp., *Proteus* spp., *S. marcescens*, *Shigella flexneri*, *Salmonella* spp., *Yersinia* spp.) as well as non-fermenting bacilli

(*Acinetobacter* spp., *Pseudomonas* spp., *Burkholderia* spp., *S. maltophilia*) and *Vibrio* spp. [48]. However, it displays no activity against aerobic Gram-positive bacteria (*Staphylococcus* spp., *Enterococcus* spp.) as well as anaerobic bacteria. Cefiderocol is also active against strains producing various β-lactamases, such as the KPC, VIM, NDM and OXA-48 types in *Enterobacterales*, or the VIM, IMP, NDM and GES types in *P. aeruginosa* or CHDL enzymes from the OXA-23, OXA-24/40 and OXA-58 groups in *A. baumannii* [48]. The sensitivity of the clinical strains of *Enterobacterales* and non-fermenting bacilli has been analysed in several international surveillance studies [27, 35, 106]. So far, the percentages of cefiderocol-sensitive strains isolated from patients suffering from, e.g., nosocomial pneumonia, bloodstream infection, complicated intra-abdominal infections and complicated urinary tract infections are at a level > 95%, irrespective of the geographic region. A lower percentage was observed only in the case of *K. pneumoniae* strains (88%).

In clinical studies it has been demonstrated that cefiderocol (administered 2 g every 8 hours) is non-inferior to imipenem (1 g every 8 hours) in the treatment of complicated urinary tract infections (cUTI) (APEKS-cUTI study) [89], and non-inferior to meropenem (2 g every 8 hours) in the treatment of nosocomial pneumonia (also linked to mechanical ventilation) (APEKS-NP) [122]. It has also been demonstrated that cefiderocol has similar clinical and microbiological efficacy in the treatment of critically ill patients infected with carbapenem-resistant Gram-negative bacilli, compared to the best available therapy (BAT), although in the group treated with cefiderocol, higher mortality has also been reported, mainly in patients with infections caused by *Acinetobacter* spp. [8]. Cefiderocol was approved by EMA on 23.04.2020 under the name of Fetcroja 1 g, powder for concentrate for solution for infusion. Its current therapeutic indications include the treatment of infections caused by aerobic Gram-negative bacteria in adults, with limited therapeutic options [20].

5. New fluoroquinolones

Delafloxacin (formerly WQ-3034, ABT-492) is a new 4 th generation fluoroquinolone and the first anionic compound in this group [57, 112]. Its molecule is distinguished primarily by the absence of the basic group in the C7 position (which ensures acidic properties), the presence of chlorine in the C8 position, which serves as an electron-withdrawing group on the aromatic ring (which increases the polarity of the compound and improves its activity and stability) and the presence of a voluminous heteroaromatic substituent in the N1 position, whereby the surface area of delafloxacin is much larger than that of other fluoroquinolones. As a result, delafloxacin exists in an anionic form at neutral pH and in a neutral form in an acidic medium. This contributes to its increased activity under low pH conditions, while the activity of other fluoroquinolones decreases as the pH drops.

The mechanism of action of delafloxacin, like all fluoroquinolones, consists in inhibiting gyrase and topoisomerase IV [81]. However, it has been shown to act with comparable potency on both of these topoisomerases in both *E. coli* and *S. aureus*. Whereas the remaining fluoroquinolones are more active against topoisomerase IV in Gram-positive bacteria and against gyrase in Gram-negative bacteria. The inhibition of gyrase activity is a more effective way of inhibiting DNA replication due to the involvement of this enzyme at an earlier stage (removal of positive supercoils before the replication forks) than in the case of topoisomerase IV, which operates behind the replication forks (DNA decatenation and chromosomal separation). Thus, the stronger interaction of delafloxacin with gyrase in Gram-positive bacteria (in comparison to the remaining fluoroquinolones) contributes to the increased activity of this new fluoroquinolone against these bacteria.

Additionally, the similar affinity to both topoisomerases suggested that delafloxacin, compared to other fluoroquinolones, should predispose strains to developing resistance to a lesser degree due to the necessity to create mutations simultaneously in both genes encoding these topoisomerases. *In vitro* studies have demonstrated a lower potential for the selection of resistant, spontaneous mutants of *S. aureus* MRSA strains than in the case of other fluoroquinolones [92]. The mutant prevention concentration (MPC) values of delafloxacin were 8 to 32 times lower than the MPC values of moxifloxacin, levofloxacin and ciprofloxacin, and additionally, in the obtained mutants, compared to the parent strain, a decrease in viability was observed. The sensitivity analysis of the strains isolated from patients treated with delafloxacin during clinical examinations confirmed that delafloxacin retained high activity also against the strains with mutations in quinolone resistance-determining regions (QRDR) [72]. Delafloxacin MIC values were not significantly increased (i.e., MIC > 0.5 mg/l) until there were simultaneous double mutations in both *gyrA* and *parC* genes.

As anticipated, in *in vitro* studies, delafloxacin demonstrated more significant activity than trovafloxacin, levofloxacin and ciprofloxacin against sensitive and quinolone-resistant strains of Gram-positive bacteria *(Staphylococcus* spp., *Enterococcus* spp., *Streptococcus* spp., *Listeria monocytogenes*), fastidious Gram-negative bacteria (*H. influenzae, Moraxella catarrhalis*, *N. gonorrhoeae, Legionella pneumophila*) and *H. pylori*. Its

effectiveness against *Enterobacterales* and *P. aeruginosa* strains was comparable with other fluoroquinolones, and its effectiveness against *Chlamydia* spp. was comparable with trovafloxacin and higher than levofloxacin [3, 29, 81]. Under *in vitro* conditions, delafloxacin is also effective against *Mycoplasma pneumoniae, Mycoplasma fermentans, Mycoplasma hominis* and *Ureaplasma* spp. [113]. It also shows activity against the biofilm formed by *S. aureus* MSSA and MRSA, with the ability to penetrate into its interior reaching 52% (depending on the proportion of polysaccharides in the matrix) and increased effectiveness against biofilms of lower pH [100]. It has been demonstrated that delafloxacin usually has a bactericidal effect against *Streptococcus pneumoniae*, *H. influenzae* and *M. catarrhalis* strains [34].

The high activity of delafloxacin against staphylococci (also MRSA) and streptococci, the strains most often causing acute bacterial skin and skin structure infections (ABSSSI), combined with its high activity in the acidic environment (typical for the skin), directed further research on the application of delafloxacin to this disease. The recently published results of the surveillance studies of the sensitivity of 11,866 strains isolated over the years 2014–2019 in the USA and Europe from patients with ABSSSI confirmed the high activity of delafloxacin [99]. The most frequently isolated strains were *S. aureus* MSSA (~ 30.6%), *E. coli* (11%), *Streptococcus* spp. (10%) and *S. aureus* MRSA (7.2%). The susceptibility to this antibiotic was confirmed for 98.7% of MSSA strains, 98.4% of *Streptococcus* spp. strains, 58% of *E. coli* strains and 65.6% of MRSA strains.

In clinical trials, delafloxacin turned out to be a drug with linear pharmacokinetics, minimal accumulation and was well-tolerated – gastrointestinal side effects were observed only at single oral doses > 1200 mg or multiple doses > 800 mg [44]. An oral dose of 450 mg and an intravenous dose of 300 mg proved to have comparable effects, providing an option of changing the route of administration during the therapy [43].

In randomized clinical trials in patients with complicated infections of the skin and subcutaneous tissue (abscesses and wound infections after surgery, trauma, burns and bites) intravenous delafloxacin (300 mg twice daily) was as effective as tigecycline (50 mg twice daily) [83], vancomycin with aztreonam (15 mg/kg + 2 g twice daily) [91] and linezolid (600 mg twice daily) [56] and more effective than vancomycin (15 mg/kg of body mass twice daily) [56]. Efficacy not worse than that of vancomycin with aztreonam has also been demonstrated for delafloxacin with the dosage pattern of 300 mg intravenously (twice daily) for 2 days and then 450 mg orally [82]. The same dosage pattern for delafloxacin was non-inferior than moxifloxacin (400 mg intravenously followed by 400 mg orally once daily) in the treatment of community-acquired bacterial pneumonia (CABP), also pneumonia caused by atypical pathogens (*M. pneumoniae, Chlamydia pneumoniae*, *L. pneumophila*) [45]. Delafloxacin showed at least 16-fold greater activity than moxifloxacin against Gram-positive bacteria and fastidious Gram-negative bacilli, and also retained activity against resistant strains, e.g., *S. pneumoniae* MDR, *Haemophilus* spp. producing β-lactamases and macrolide-resistant strains, as well as *S. aureus* MRSA and fluoroquinolone-resistant strains [71, 73].

However, a single 900 mg dose of delafloxacin turned out to be an ineffective form of treating uncomplicated gonorrhoea – many treatments for *N. gonorrhoeae* infections with MIC values below 0.008 mg/l were unsuccessful, indicating the need to modify the dosing regimen [41].

In the European Union, delafloxacin was approved on 16.12.2019 for the treatment of acute bacterial skin and skin structure infections (ABSSSI) and community acquired pneumonia (CABP) in adults, when the application of other antibacterial agents commonly recommended for the initial treatment of these infections is considered to be inappropriate. Both the oral (450 mg tablets) and intravenous (300 mg) forms were registered under the trade name Quofenix [20].

6. New tetracyclines

Tetracyclines are natural or semi-synthetic compounds with amphoteric properties, containing four fused carbocyclic rings (including an aromatic one) in their molecule [31]. Their mechanism of action consists in inhibiting protein synthesis by binding to the 30S ribosome subunit. All compounds from this group are characterized by a broad spectrum of activity, both against Gram-positive and Gram-negative bacteria, mycoplasmas, chlamydia, rickettsiae and some protozoa. The differences between individual representatives concern the pharmacokinetic properties and potency. The first tetracycline antibiotics (produced by various species of actinomycetes – *Streptomyces*) were introduced into medicine at the turn of the 1940s and 1950s. Unfortunately, their intensive use in medicine led to the rapid emergence and spread of resistance associated with the presence of *tet* genes, encoding membrane pump proteins involved in the phenomenon of the so-called efflux (e.g., *tet*(A), *tet*(B), *tet*(K), *tet*(L) genes), ribosome protective proteins (e.g., *tet*(M), *tet*(O), *tet*(P), *tet*(S)) or tetracycline-inactivating enzymes, i.e., the *tet*(X) gene.

However, the growing drug resistance of microorganisms to antibiotics from other groups contributed to the renewed interest in tetracyclines. Determining the structure of the tetracycline-30S ribosome co-crystal demonstrated that the binding to the ribosome does not involve only the region around the C5-C9 carbon

atoms [13]. Therefore, attempts were made to introduce structural modifications at C7 and C9 atoms, which resulted in the market launch of semi-synthetic tetracyclines (minocycline, tigecycline, omadacycline). The new tetracyclines are characterized by increased antibacterial activity and lower susceptibility to bacterial resistance mechanisms [31]. However, the number of the chemical modifications of natural tetracyclines and thus the possibility of obtaining new, semi-synthetic derivatives is limited. It was only the *de novo* synthesis of subsequent compounds containing the tetracycline skeleton that significantly increased the number of new compounds from this group [107].

Eravacycline (formerly TP-434) is the first fully synthetic tetracycline introduced into medicine [20]. Its molecule is characterized by the presence of fluorine at the C7 carbon atom and the pyrrolidinoacetamido group at the C9 carbon of the tetracycline core and is also active against tetracycline-resistant strains with the *tet*(M) and *tet*(Q) genes (responsible for blocking the tetracycline binding site to the ribosome) and the genes *tet*(A), *tet*(B) and *tet*(K) (responsible for the synthesis of membrane proteins of MDR pumps) [33, 123]. The spectrum of eravacycline activity includes strains of *S. aureus* (also linezolid resistant MRSA and MRSA), *Streptococcus* spp., *Enterococcus* spp. (also VRE), *E. coli, K. pneumoniae*, *Klebsiella oxytoca*, *Enterobacter cloacae*, *Enterobacter aerogenes*, *Citrobacter freundii*, *Morganella morganii*, *Proteus mirabilis*, *Proteus vulgaris*, *Providencia stuartii*, *S. marcescens*, *Salmonella* spp., *Shigella* spp., *A. baumannii*, *Acinetobacter lwoffii*, *S. maltophilia, Legionella pneumophila*, *H. influenzae*, *M. catarrhalis*, *N. gonorrhoeae*, *Bacteroides fragilis*, *Bacteroides vulgatus, Bacteroides thetaiotaomicron, Bacteroides ovatus, Prevotella* spp., *Clostridioides difficile,* and *Clostridium perfringens.* Eravacycline maintains its effectiveness also against strains resistant to fluoroquinolones, aminoglycosides, third-generation cephalosporins, carbapenems, polymyxins and MDR strains, and its effectiveness is usually 2–4 times higher than or equal to tigecycline, both against Gram-positive and Gram-negative bacteria [1, 23, 50, 62, 103, 110, 125, 127]. It has also been shown that under *in vitro* conditions eravacycline acts synergistically with colistin against *A. baumannii* strains, also against strains resistant to carbapenems and colistin [84]. Nevertheless, the strains of *P. aeruginosa* and *Burkholderia cenocepacia* are resistant to eravacycline [110].

Moreover, it has been demonstrated that eravacycline is effective against the biofilm of the uropathogenic *E. coli* strain to a degree comparable to that of gentamicin and levofloxacin, and to a greater degree than in the case of colistin and meropenem [32]. However, eravacycline has not been shown to be effective against the biofilm formed by *S. aureus* strains isolated from periprosthetic-joint infections [130].

Recently published results of large surveillance studies have confirmed the high effectiveness of eravacycline against a wide spectrum of clinical strains [76, 77]. The percentage shares of susceptible strains were respectively: 97.6% for *S. aureus* (95.5% for MRSA and 99.8% for MSSA), 84.6% for *S. epidermidis*, 89.9% for *S. haemolyticus*, 99.4% for *E. faecalis* (98.3% for VR strains, 99.5% for VS), 97.7% for *E. faecium* (96.1% for VR strains and 98.9% for VS) and 92.6% for *Enterobacterales* (82% for MDR strains). In turn, for *A. baumannii* strains for which no MIC breakpoints have been defined, the MIC_{50}/MIC_{90} values reached 0.5 mg/l and 1 mg/l, respectively (for MDR strains the MIC_{90} reached 2 mg/l).

However, the clinical effectiveness of eravacycline may be threatened in the future by the increasing resistance arising from the antibiotic-removal mechanism (efflux), enzymatic degradation of this antibiotic and modification of its binding site in the ribosome. So far, it has been demonstrated that in *S. aureus* (both MRSA and MSSA), *E. faecalis* and *S. agalactiae* strains, the MIC values of eravacycline (similar to tigecyclines) showed significant decreases in the presence of MDR pump inhibitors such as carbonyl cyanide 3-chlorophenylhydrazone (CCCP) and L-phenylalanine-L-arginine-β-naphthylamide (PAβN) [61, 118, 127]. Additionally, research describes clinical strains of *A. baumannii* resistant to eravacycline with overexpression of the AdeABC pump system [98], *K. pneumoniae* with overexpression of OqxAB and MacAB-TolC pumps [128] as well as *K. pneumoniae* PDR (pan-drug resistant) strains isolated from farm animals in China with the expression of a new RND efflux pump, of the MexCD-OprJ type, called TMexCD1-TOprJ1, responsible for the resistance, among others to all tetracycline antibiotics [68]. Since the genes encoding it are located in the plasmid, their spread among zoonotic strains of *K. pneumoniae* may pose a serious clinical threat in the future. Another, equally important threat to the effectiveness of applying eravacycline in therapy is the spread of *tet*(X) genes located in plasmids and transposons. Several variants of these genes have recently been described in China in *A. baumannii* strains (environmental and clinical) [16, 116] and in *Enterobacterales* strains isolated from the stool samples of healthy adults in Singapore [18]. They are also widespread among *E. coli* strains isolated from animals (pigs, chickens, migratory birds) and soil [17, 109], and recently the presence of these genes has also been confirmed in *Proteus* sp. isolated from retail pork [38]. Resistance to eravacycline may also result from mutations in the genes encoding the proteins of the 30S ribosome subunit, as already described in *S. aureus* and *S. agalactiae* strains [61, 117].

Clinical studies have shown that when it comes to the treatment of complicated intra-abdominal

infections, eravacycline (administered 1 mg/kg every 12 hours) is well tolerated and safe, as well as non-inferior to meropenem (administered 1 g every 8 hours) and non-inferior to ertapenem (1 g every 24 hours) [104, 105]. Based on the results obtained, eravacycline was approved by the EMA for use against this nosological unit on 20.09.2018 and registered under the trade name Xerava 50 mg, powder for concentrate for solution for infusion [20].

7. Pleuromutilins

Lefamulin is a new antibiotic from the group of pleuromutilins – derivatives of naturally occurring pleuromutilin, isolated in the 1950s from the fungus *Pleurotus mutilus* (presently, *Clitophilus scyphoides*) [86]. The first semi-synthetic derivatives of pleuromutilin (tiamulin and valnemulin) were approved for veterinary use in 1979 and 1999, respectively. However, these drugs were used only in the treatment of pulmonary and intestinal infections in animals but not in the production of food of animal origin as growth promoters or for enhancement of feed efficiency (unlike, among others, tetracyclines, streptogramins or sulphonamides). This may explain the low prevalence of bacterial resistance to pleuromutilins. Retapamulin was the first antibiotic of this class approved for human use, but it was only available as an ointment for topical application for a short-term treatment of superficial skin infections (impetigo, minor lacerations, abrasions, or sutured wounds). Lefamulin (formerly BC-3781) is the second pleuromutilin approved for human use, but the first to be approved for systemic use, both in the intravenous and oral forms [86].

Chemically, pleuromutilins are diterpenoids containing in their molecule a 14-carbon tricyclic scaffold (essential for antimicrobial activity) and a glycolic ester moiety forming a side chain at the C14 position, various modifications of which correspond, among others, to different pharmacodynamic properties of derivatives [126]. The mechanism of action of this group of antibiotics consists in inhibiting protein synthesis by binding to the 50S ribosome subunit at the peptidyl transferase centre (PTC), in the middle of the domain V of the 23S rRNA molecule. A tricyclic core that forms hydrogen bonds with the nucleotides in the pocket near the A-site of the ribosome is responsible for the attachment of pleuromutilins to the ribosome, while the side chain at position C14 extendes towards the P-site, hindering the movement of the 3' tRNA end towards the P site. A lefamulin molecule features a stronger bond to the ribosome than other pleuromutilins due to the presence of the 2-(4-amino-2-hydroxycyclohexyl) sulfanylacetate side chain at the C14 position, the amino group of which allows the formation of another hydrogen bond. Additionally, the presence of hydroxyl and primary amine groups in this chain increases the solubility of lefamulin in water [21].

Under *in vitro* conditions, lefamulin is effective against most Gram-positive cocci (*S. aureus* MSSA and MRSA, *S. epidermidis*, vancomycin-resistant *E. faecium*, *S. pneumoniae* (also resistant to penicillin, macrolides and MDR strains), *S. pyogenes, S. agalactiae, Streptococcus* spp. groups C and G), and some Gram-negative bacteria (*H. influenzae, Haemophilus parainfluenzae, L. pneumophila, M. catarrhalis, N. gonorrhoeae*) and atypical pathogens (*M. pneumoniae, Ch. pneumoniae*). However, it is not active against Gram-negative non-fermenting bacilli and *Enterobacterales* [49, 74, 85, 93, 94, 114].

Surveillance studies have confirmed that lefamulin is exceedingly active against pathogens causing community-acquired pneumonia, isolated from patients worldwide (SENTRY Antimicrobial Surveillance Program) [85, 87]. The overall percentage share of strains with the MIC values for lefamulin below 1 mg/l (breakpoint for *S. pneumoniae*) was 99.2%, including 100% for *S. pneumoniae* and *M. catarrhalis* strains, 99.8% for *S. aureus*, 93.8% for *H. influenzae* and 88.1% for *E. faecium*. Simultaneously, no cross-resistance was detected between lefamulin and β-lactams, fluoroquinolones and macrolides.

Resistance to lefamulin in the strains of usually sensitive bacterial species may be a result of mutations in the V domain 23S rRNA, e.g., due to the nucleotide methylation at position 2503 influenced by Cfr methyltransferase [75]. The Cfr enzyme provides cross resistance to oxazolidinones, lincosamides, phenicols and streptogramins. Furthermore, the acquisition of resistance may result from mutations in the genes encoding the ribosomal protein L3 (*rplC*) and L4 (*rplD*), which modifies the structure of PTC and disturbs lefamulin attachment to it. It has been demonstrated that the resistance may also be related to the protection of the lefamulin target binding site by membrane pump proteins of the ABC-F subfamily encoded by the *vga*(A), *vga*(B), *vga*(E) and *Isa*(E) genes. ABC-F proteins may induce cross-resistance to lincosamides and streptogramins A [75]. It has also been demonstrated that the inactivation of the MtrCDE pump (but not MacAB and NorM) in *N. gonorrhoeae* reduces significantly (at least 4-fold) the MIC values of lefamulin [49].

In clinical trials it has been demonstrated that lefamulin (administered 150 mg intravenously every 12 hours for 3 days, followed by 600 mg orally every 12 hours) is non-inferior as moxifloxacin (400 mg administered intravenously every 24 hours for 3 days, followed by 400 mg orally every 24 hours) in the treatment of community-acquired pneumonia [22]. Comparable results were obtained when lefamulin and moxifloxacin were

administered orally exclusively [2]. At the same time, in the treatment of acute bacterial skin and skin structure infections caused by Gram-positive pathogens, in the group of patients treated with lefamulin (100 or 150 mg intravenously every 12 hours), the percentage of clinical successes was comparable to the group of patients treated with vancomycin (1 g intravenously every 12 hours) [90]. Currently, the intravenous (150 mg injections every 12 hours) and oral (600 mg tablets) forms of lefamulin, under the trade name Xenleta, were approved for use on 27.07.2020 only in the treatment of community-acquired pneumonia in adults [20].

8. Summary

Six new, broad-spectrum antibacterial drugs have been registered on the European market since 2018, which are, according to WHO, active against the strains classified as pathogens with a critical and high priority need of search for new drugs. Two of them are new combinations of β-lactams with non-β-lactam inhibitors of β-lactamases (meropenem with vaborbactam and imipenem/cilastatin with relebactam), one is a representative of a new group of siderophore antibiotics (cefiderocol), the next two are new derivatives of known groups of antibiotics: fluoroquinolones (delafloxacin) and tetracyclines (eravacycline). Moreover, EMA approved lefamulin as the last of the new drugs in July 2020, i.e., the first representative of a new group of drugs – pleuromutilin, intended for systemic use in humans. Lefamulin, unlike the aforementioned new drugs, is not active against Gram-negative non-fermenting bacilli and *Enterobacterales*, which are naturally resistant to it. According to the criteria adopted by the WHO, two of the 6 new antibacterial drugs (delafloxacin and lefamulin) were registered as effective against high priority pathogens (vancomycin-resistant enterococci, MRSA), and the remaining four (meropenem/vaborbactam, imipenem/cilastatin/relebactam, eravacycline and cefiderocol) as active against critical pathogens (carbapenem-resistant *Enterobacterales*), while only one (cefiderocol) displays high effectiveness also against carbapenem-resistant strains of *P. aeruginosa* and *A. baumannii*. The WHO innovation criterion is fully met only by meropenem/vaborbactam (in the new chemical class category) and partially by lefamulin, with the reservation that the representatives of this group (pleuromutilins) have already been used in veterinary medicine and for topical treatment in humans. On the other hand, the innovation criterion in the category of the lack of cross-resistance is potentially met by meropenem/vaborbactam and cefiderocol.

Two of the approved drugs are available in both intravenous and oral formulations (delafloxacin and lefamulin). Owing to new registrations, there has been an increase in the number of therapeutic options in the treatment of complicated urinary tract infections (meropenem/vaborbactam, cefiderocol), complicated intra-abdominal infections (meropenem/vaborbactam, eravacycline), nosocomial pneumonia, including those associated with mechanical ventilation (meropenem/vaborbactam, cilastatin/relebactam), acute bacterial skin and skin structure infections (delafloxacin) and community-acquired pneumonia (lefamulin). According to the recent WHO report on new antibiotics, the number of new therapeutic options available for the treatment of infections caused by high and critical priority pathogens, as well as PDR (pan-drug resistant) and XDR (extensively drug resistant) pathogens is still insufficient [120]. Recently, however, a case of therapeutic success has been reported in the treatment of *Achromobacter* sp. PDR infection in a 10-year-old female patient with cystic fibrosis after applying the combination of cefiderocol, meropenem with vaborbactam and phage therapy (Ax2CJ45ϕ2). The treatment was well tolerated and led to the eradication of *Achromobacter* sp. [25]. It is thus possible that, owing to the combination therapy, the new antibiotics will also prove effective against PDR and XDR pathogens, which will enhance the prospects of their application in healthcare.

Acknowledgments

The article was created with the support of the Berlin-Chemie company.

References

1. Abdallah M., Olafisoye O., Cortes C., Urban C., Landman D., Quale J.: Activity of eravacycline against *Enterobacteriaceae* and *Acinetobacter baumannii*, including multidrug-resistant isolates, from New York City. *Antimicrob. Agents Chemother.* **59**, 1802–1805 (2015)
2. Alexander E., Schranz J., et al.: Oral lefamulin vs moxifloxacin for early clinical response among adults with community-acquired bacterial pneumonia: the LEAP 2 randomized clinical trial. *Jama*, **322**, 1661–1671 (2019)
3. Almer L.S., Hoffrage J.B., Keller E.L., Flamm R.K., Shortridge V.D.: *In vitro* and bactericidal activities of ABT-492, a novel fluoroquinolone, against Gram-positive and Gram-negative organisms. *Antimicrob. Agents Chemother.* **48**, 2771–2777 (2004)
4. Ambler R.P.: The structure of β-lactamases. *Philos. Trans. R. Soc. Lond. B Biol. Sci.* **289**, 321–331 (1980)
5. Aoki T., Yamano Y., et al.: Cefiderocol (S-649266), a new siderophore cephalosporin exhibiting potent activities against *Pseudomonas aeruginosa* and other Gram-negative pathogens including multi-drug resistant bacteria: structure activity relationship. *Eur. J. Med. Chem.* **155**, 847–868 (2018)

6. Asempa T.E., Nicolau D.P., Kuti J.L.: *In vitro* activity of imipenem-relebactam alone or in combination with amikacin or colistin against *Pseudomonas aeruginosa*. *Antimicrob. Agents Chemother.* **63**, DOI: 10.1128/aac.00997-19 (2019)
7. Barnes M.D., Bethel C.R., Alsop J., Becka S.A., Rutter J.D., Papp-Wallace K.M., Bonomo R.A.: Inactivation of the *Pseudomonas*-derived cephalosporinase-3 (PDC-3) by relebactam. *Antimicrob. Agents Chemother.* **62**, DOI: 1 0.1128/aac.02406-17 (2018)
8. Bassetti M., Nagata T.D., et al.: Efficacy and safety of cefiderocol or best available therapy for the treatment of serious infections caused by carbapenem-resistant Gram-negative bacteria (CREDIBLE-CR): a randomised, open-label, multicentre, pathogen-focused, descriptive, phase 3 trial. *Lancet Infect. Dis.* **21**, 226–240 (2021)
9. Bassetti M., Giacobbe D.R., Patel N., Tillotson G., Massey J.: Efficacy and safety of meropenem-vaborbactam *versus* best available therapy for the treatment of carbapenem-resistant *Enterobacteriaceae* infections in patients without prior antimicrobial failure: a post hoc analysis. *Adv. Ther.* **36**, 1771–1777 (2019)
10. Bhowmick T.: Clinical outcomes of patient subgroups in the TANGO II study. *Infect. Dis. Ther.* **10**, 35–46 (2021)
11. Biagi M., Wu T., Lee M., Patel S., Butler D., Wenzler E.: Searching for the optimal treatment for metallo- and serine-β-lactamase producing *Enterobacteriaceae*: aztreonam in combination with ceftazidime-avibactam or meropenem-vaborbactam. *Antimicrob. Agents Chemother.* **63**, DOI: 10.1128/aac.01426-19 (2019)
12. Blizzard T.A., Hammond M.L., et al.: Discovery of MK-7655, a β-lactamase inhibitor for combination with Primaxin®. *Bioorg. Med. Chem. Lett.* **24**, 780–785 (2014)
13. Brodersen D.E., Clemons W.M., Jr., Carter A.P., Morgan-Warren R.J., Wimberly B.T., Ramakrishnan V.: The structural basis for the action of the antibiotics tetracycline, pactamycin, and hygromycin B on the 30S ribosomal subunit. *Cell*, **103**, 1143–1154 (2000)
14. Castanheira M., Huband M.D., Mendes R.E., Flamm R.K.: Meropenem-vaborbactam tested against contemporary Gram-negative isolates collected worldwide during 2014, including carbapenem-resistant, KPC-producing, multidrug-resistant, and extensively drug-resistant *Enterobacteriaceae*. *Antimicrob. Agents Chemother.* **61**, e00567-17 (2017)
15. Castanheira M., Rhomberg P.R., Flamm R.K., Jones R.N.: Effect of the β-lactamase inhibitor vaborbactam combined with meropenem against serine carbapenemase-producing *Enterobacteriaceae*. *Antimicrob. Agents Chemother.* **60**, 5454–5458 (2016)
16. Chen C., Liu Y.H., et al.: Genetic diversity and characteristics of high-level tigecycline resistance Tet(X) in *Acinetobacter* species. *Genome Med.* **12,** DOI:10.1186/s13073-020-00807-5 (2020)
17. Chen C., Sun J., et al.: Emergence of mobile tigecycline resistance mechanism in *Escherichia coli* strains from migratory birds in China. *Emerg. Microbes Infect.* **8**, 1219–1222 (2019)
18. Ding Y., Saw W.Y., Tan L.W.L., Moong D.K.N., Nagarajan N., Teo Y.Y., Seedorf H.: Emergence of tigecycline- and eravacycline-resistant Tet(X4)-producing *Enterobacteriaceae* in the gut microbiota of healthy Singaporeans. *J. Antimicrob. Chemother.* **75,** 3480–3484 (2020)
19. Durka K., Laudy A.E., Charzewski Ł., Urban M., Stępień K., Tyski S., Krzyśko K.A., Luliński S.: Antimicrobial and KPC/AmpC inhibitory activity of functionalized benzosiloxaboroles. *Eur. J. Med. Chem.* **171**, 11–24 (2019)
20. European Medicines Agency: Medicines. https://www.ema.europa.eu/en/medicines/field_ema_web_categories%253Aname_field/Human (16.07.2021)
21. Eyal Z., Matzov D., Krupkin M., Paukner S., Riedl R., Rozenberg H., Zimmerman E., Bashan A., Yonath A.: A novel pleuromutilin antibacterial compound, its binding mode and selectivity mechanism. *Sci. Rep.* **6**, DOI:10.1038/srep39004 (2016)
22. File T.M., Gasink L.B., et al.: Efficacy and safety of intravenous-to-oral lefamulin, a pleuromutilin antibiotic, for the treatment of community-acquired bacterial pneumonia: the phase III lefamulin evaluation against pneumonia (LEAP 1) trial. *Clin. Infect. Dis.* **69**, 1856–1867 (2019)
23. Fyfe C., LeBlanc G., Close B., Nordmann P., Dumas J., Grossman T.H.: Eravacycline is active against bacterial isolates expressing the polymyxin resistance gene *mcr-1*. *Antimicrob. Agents Chemother.* **60**, 6989–6990 (2016)
24. Gaibani P., Lombardo D., Bussini L., Bovo F., Munari B., Giannella M., Bartoletti M., Viale P., Lazzarotto T., Ambretti S.: Epidemiology of meropenem/vaborbactam resistance in KPC-producing *Klebsiella pneumoniae* causing bloodstream infections in northern Italy, 2018. *Antibiotics*, **10**, DOI:10.3390/antibiotics10050536 (2021)
25. Gainey A.B., Burch A.K., Brownstein M.J., Brown D.E., Fackler J., Horne B., Biswas B., Bivens B.N., Malagon F., Daniels R.: Combining bacteriophages with cefiderocol and meropenem/vaborbactam to treat a pan-drug resistant *Achromobacter* species infection in a pediatric cystic fibrosis patient. *Pediatr. Pulmonol.* **55**, 2990–2994 (2020)
26. Ghai I., Ghai S.: Exploring bacterial outer membrane barrier to combat bad bugs. *Infect. Drug Resist.* **10**, 261–273 (2017)
27. Giacobbe D.R., Ciacco E., Girmenia C., Pea F., Rossolini G.M., Sotgiu G., Tascini C., Tumbarello M., Viale P., Bassetti M.: Evaluating cefiderocol in the treatment of multidrug-resistant Gram-negative bacilli: a review of the emerging data. *Infect. Drug Resist.* **13,** 4697–4711 (2020)
28. Giulieri S.G., Tong S.Y.C., Williamson D.A.: Using genomics to understand methicillin- and vancomycin-resistant *Staphylococcus aureus* infections. *Microb. Genom.* **6**, DOI: 10.1099/mgen.0.000324 (2020)
29. Goldstein E.J., Citron D.M., Merriam C.V., Warren Y.A., Tyrrell K.L., Fernandez H.T.: *In vitro* activities of ABT-492, a new fluoroquinolone, against 155 aerobic and 171 anaerobic pathogens isolated from antral sinus puncture specimens from patients with sinusitis. *Antimicrob. Agents Chemother.* **47**, 3008–3011 (2003)
30. Gomez-Simmonds A., Stump S., Giddins M.J., Annavajhala M.K., Uhlemann A.C.: Clonal background, resistance gene profile, and porin gene mutations modulate *in vitro* susceptibility to imipenem-relebactam in diverse *Enterobacteriaceae*. *Antimicrob. Agents Chemother.* **62**, DOI:10.1128/aac.00573-18 (2018)
31. Grossman T.H.: Tetracycline antibiotics and resistance. *Cold Spring Harb. Perspect. Med.* **6**, DOI:10.1101/cshperspect.a025387 (2016)
32. Grossman T.H., O'Brien W., Kerstein K.O., Sutcliffe J.A.: Eravacycline (TP-434) is active *in vitro* against biofilms formed by uropathogenic *Escherichia coli*. *Antimicrob. Agents Chemother.* **59**, 2446–2449 (2015)
33. Grossman T.H., Starosta A.L., Fyfe C., O'Brien W., Rothstein D.M., Mikolajka A., Wilson D.N., Sutcliffe J.A.: Target- and resistance-based mechanistic studies with TP-434, a novel fluorocycline antibiotic. *Antimicrob. Agents Chemother.* **56**, 2559–2564 (2012)
34. Gunderson S.M., Hayes R.A., Quinn J.P., Danziger L.H.: *In vitro* pharmacodynamic activities of ABT-492, a novel quinolone, compared to those of levofloxacin against *Streptococcus pneumoniae, Haemophilus influenzae*, and *Moraxella catarrhalis*. *Antimicrob. Agents Chemother.* **48**, 203–208 (2004)
35. Hackel M.A., Tsuji M., Yamano Y., Echols R., Karlowsky J.A., Sahm D.F.: *In vitro* activity of the siderophore cephalosporin, cefiderocol, against carbapenem-nonsusceptible and multidrug-resistant isolates of Gram-negative bacilli collected worldwide in 2014 to 2016. *Antimicrob. Agents Chemother.* **62**, DOI:10.1128/aac.01968-17 (2018)

36. Haidar G., Clancy C.J., Chen L., Samanta P., Shields R.K., Kreiswirth B.N., Nguyen M.H.: Identifying spectra of activity and therapeutic niches for ceftazidime-avibactam and imipenem-relebactam against carbapenem-resistant *Enterobacteriaceae*. *Antimicrob. Agents Chemother.* **61**, DOI:10.1128/aac.00642-17 (2017)
37. Hammoudi Halat D., Ayoub Moubareck C.: The current burden of carbapenemases: review of significant properties and dissemination among Gram-negative bacteria. *Antibiotics*, **9**, DOI:10.3390/antibiotics9040186 (2020)
38. He D., Wang L., Zhao S., Liu L., Liu J., Hu G., Pan Y.: A novel tigecycline resistance gene, tet(X6), on an SXT/R391 integrative and conjugative element in a *Proteus genomospecies* 6 isolate of retail meat origin. *J. Antimicrob. Chemother.* **75**, 1159–1164 (2020)
39. Hecker S.J., Dudley M.N., et al.: Discovery of a cyclic boronic acid β-lactamase inhibitor (RPX7009) with utility vs class A serine carbapenemases. *J. Med. Chem.* **58**, 3682–3692 (2015)
40. Hirsch E.B., Ledesma K.R., Chang K.T., Schwartz M.S., Motyl M.R., Tam V.H.: *In vitro* activity of MK-7655, a novel β-lactamase inhibitor, in combination with imipenem against carbapenem-resistant Gram-negative bacteria. *Antimicrob. Agents Chemother.* **56**, 3753–3757 (2012)
41. Hook E.W., 3rd, Golden M.R., Taylor S.N., Henry E., Tseng C., Workowski K.A., Swerdlow J., Nenninger A., Cammarata S.: Efficacy and safety of single-dose oral delafloxacin compared with intramuscular ceftriaxone for uncomplicated gonorrhea treatment: an open-label, noninferiority, phase 3, multicenter, randomized study. *Sex. Transm. Dis.* **46**, 279–286 (2019)
42. Hooper D.C., Jacoby G.A.: Topoisomerase inhibitors: fluoroquinolone mechanisms of action and resistance. *Cold Spring Harb. Perspect. Med.* **6**, DOI:10.1101/cshperspect.a025320 (2016)
43. Hoover R., Hunt T., Benedict M., Paulson S.K., Lawrence L., Cammarata S., Sun E.: Safety, tolerability, and pharmacokinetic properties of intravenous delafloxacin after single and multiple doses in healthy volunteers. *Clin. Ther.* **38**, 53–65 (2016)
44. Hoover R., Hunt T., Benedict M., Paulson S.K., Lawrence L., Cammarata S., Sun E.: Single and multiple ascending-dose studies of oral delafloxacin: effects of food, sex, and age. *Clin. Ther.* **38**, 39–52 (2016)
45. Horcajada J.P., Salata R.A., Álvarez-Sala R., Nitu F.M., Lawrence L., Quintas M., Cheng C.Y., Cammarata S.: A phase 3 study to compare delafloxacin with moxifloxacin for the treatment of adults with community-acquired bacterial pneumonia (DEFINE-CABP). *Open Forum Infect. Dis.* **7**, DOI:10.1093/ofid/ofz514 (2020)
46. Ito-Horiyama T., Ishii Y., Ito A., Sato T., Nakamura R., Fukuhara N., Tsuji M., Yamano Y., Yamaguchi K., Tateda K.: Stability of novel siderophore cephalosporin S-649266 against clinically relevant carbapenemases. *Antimicrob. Agents Chemother.* **60**, 4384–4386 (2016)
47. Ito A., Nishikawa T., Ota M., Ito-Horiyama T., Ishibashi N., Sato T., Tsuji M., Yamano Y.: Stability and low induction propensity of cefiderocol against chromosomal AmpC β-lactamases of *Pseudomonas aeruginosa* and *Enterobacter cloacae*. *J. Antimicrob. Chemother.* **73**, 3049–3052 (2018)
48. Ito A., Yamano Y., et al.: *In vitro* antibacterial properties of cefiderocol, a novel siderophore cephalosporin, against Gram-negative bacteria. *Antimicrob. Agents Chemother.* **62**, DOI:10.1128/aac.01454-17 (2018)
49. Jacobsson S., Paukner S., Golparian D., Jensen J.S., Unemo M.: *In vitro* activity of the novel pleuromutilin lefamulin (BC-3781) and effect of efflux pump inactivation on multidrug-resistant and extensively drug-resistant *Neisseria gonorrhoeae*. *Antimicrob. Agents Chemother.* **61**, DOI:10.1128/aac.01497-17 (2017)
50. Johnson J.R., Porter S.B., Johnston B.D., Thuras P.: Activity of eravacycline against *Escherichia coli* clinical isolates collected from U.S. veterans in 2011 in relation to coresistance phenotype and sequence Type 131 genotype. *Antimicrob. Agents Chemother.* **60**, 1888–1891 (2015)
51. Johnston B.D., Thuras P., Porter S.B., Anacker M., VonBank B., Vagnone P.S., Witwer M., Castanheira M., Johnson J.R.: Activity of imipenem-relebactam against carbapenem-resistant *Escherichia coli* isolates from the United States in relation to clonal background, resistance genes, coresistance, and region. *Antimicrob. Agents Chemother.* **64**, DOI:10.1128/aac.02408-19 (2020)
52. Johnston B.D., Thuras P., Porter S.B., Castanheira M., Johnson J.R.: Activity of meropenem/vaborbactam against international carbapenem-resistant *Escherichia coli* isolates in relation to clonal background, resistance genes, resistance to comparators and region. *J. Glob. Antimicrob. Resist.* **24**, 190–197 (2021)
53. Karlowsky J.A., Lob S.H., Kazmierczak K.M., Hawser S.P., Magnet S., Young K., Motyl M.R., Sahm D.F.: *In vitro* activity of imipenem/relebactam against Gram-negative ESKAPE pathogens isolated in 17 European countries: 2015 SMART surveillance programme. *J. Antimicrob. Chemother.* **73**, 1872–1879 (2018)
54. Karlowsky J.A., Lob S.H., Kazmierczak K.M., Young K., Motyl M.R., Sahm D.F.: *In vitro* activity of imipenem/relebactam and key β-lactam agents against Gram-negative bacilli isolated from lower respiratory tract infection samples of intensive care unit patients – SMART Surveillance United States 2015–2017. *Int. J. Antimicrob. Agents*, **55**, DOI:10.1016/j.ijantimicag.2019.10.022 (2020)
55. Kaye K.S., Giamarellos-Bourboulis E.J., et al.: Effect of meropenem-vaborbactam vs piperacillin-tazobactam on clinical cure or improvement and microbial eradication in complicated urinary tract infection: the TANGO I randomized clinical trial. *Jama*, **319**, 788–799 (2018)
56. Kingsley J., Mehra P., Lawrence L.E., Henry E., Duffy E., Cammarata S.K., Pullman J.: A randomized, double-blind, phase 2 study to evaluate subjective and objective outcomes in patients with acute bacterial skin and skin structure infections treated with delafloxacin, linezolid or vancomycin. *J. Antimicrob. Chemother.* **71**, 821–829 (2016)
57. Kocsis B., Domokos J., Szabo D.: Chemical structure and pharmacokinetics of novel quinolone agents represented by avarofloxacin, delafloxacin, finafloxacin, zabofloxacin and nemonoxacin. *Ann. Clin. Microbiol. Antimicrob.* **15**, DOI:10.1186/s12941-016-0150-4 (2016)
58. Kohira N., Hackel M.A., Ishioka Y., Kuroiwa M., Sahm D.F., Sato T., Maki H., Yamano Y.: Reduced susceptibility mechanism to cefiderocol, a siderophore cephalosporin, among clinical isolates from a global surveillance programme (SIDERO-WT-2014). *J. Glob. Antimicrob. Resist.* **22**, 738–741 (2020)
59. Lapuebla A., Abdallah M., Olafisoye O., Cortes C., Urban C., Quale J., Landman D.: Activity of meropenem combined with RPX7009, a novel β-lactamase inhibitor, against Gram-negative clinical isolates in New York City. *Antimicrob. Agents Chemother.* **59,** 4856–4860 (2015)
60. Laudy A.E.: MDR efflux pumps – the mechanism of Gram--negative rods resistance to antibiotics. *Post. Mikrobiol.* **47**, 415–422 (2008)
61. Li P., Wei Y., Li G., Cheng H., Xu Z., Yu Z., Deng Q., Shi Y.: Comparison of antimicrobial efficacy of eravacycline and tigecycline against clinical isolates of *Streptococcus agalactiae* in China: *In vitro* activity, heteroresistance, and cross-resistance. *Microb. Pathog.* **149**, DOI:10.1016/j.micpath.2020.104502 (2020)
62. Livermore D.M., Mushtaq S., Warner M., Woodford N.: *In vitro* activity of eravacycline against carbapenem-resistant *Enterobacteriaceae* and *Acinetobacter baumannii*. *Antimicrob. Agents Chemother.* **60**, 3840–3844 (2016)

63. Livermore D.M., Warner M., Mushtaq S.: Activity of MK-7655 combined with imipenem against *Enterobacteriaceae* and *Pseudomonas aeruginosa*. *J. Antimicrob. Chemother.* **68**, 2286–2290 (2013)
64. Lob S.H., Hackel M.A., Kazmierczak K.M., Young K., Motyl M.R., Karlowsky J.A., Sahm D.F.: *In vitro* activity of imipenem-relebactam against Gram-negative ESKAPE pathogens isolated by clinical laboratories in the United States in 2015 (Results from the SMART Global Surveillance Program). *Antimicrob. Agents Chemother.* **61**, DOI:10.1128/aac.02209-16 (2017)
65. Lob S.H., Karlowsky J.A., Young K., Motyl M.R., Hawser S., Kothari N.D., Sahm D.F.: *In vitro* activity of imipenem-relebactam against resistant phenotypes of *Enterobacteriaceae* and *Pseudomonas aeruginosa* isolated from intraabdominal and urinary tract infection samples – SMART Surveillance Europe 2015–2017. *J. Med. Microbiol.* **69**, 207–217 (2020)
66. Lomovskaya O., Sun D., Rubio-Aparicio D., Nelson K., Tsivkovski R., Griffith D.C., Dudley M.N.: Vaborbactam: spectrum of β-lactamase inhibition and impact of resistance mechanisms on activity in *Enterobacteriaceae*. *Antimicrob. Agents Chemother.* **61**, DOI:10.1128/aac.01443-17 (2017)
67. Lucasti C., Paschke A., et al.: Phase 2, dose-ranging study of relebactam with imipenem-cilastatin in subjects with complicated intra-abdominal infection. *Antimicrob. Agents Chemother.* **60**, 6234–6243 (2016)
68. Lv L., Liu J.H., et al.: Emergence of a plasmid-encoded resistance-nodulation-division efflux pump conferring resistance to multiple drugs, including tigecycline, in *Klebsiella pneumoniae*. *mBio*, **11**, DOI:10.1128/mBio.02930-19 (2020)
69. Malik S., Kaminski M., Landman D., Quale J.: Cefiderocol resistance in *Acinetobacter baumannii*: roles of β-lactamases, siderophore receptors, and penicillin binding protein 3. *Antimicrob. Agents Chemother.* **64,** DOI:10.1128/aac.01221-20 (2020)
70. Maraki S., Mavromanolaki V.E., Moraitis P., Stafylaki D., Kasimati A., Magkafouraki E., Scoulica E.: Ceftazidime-avibactam, meropenen-vaborbactam, and imipenem-relebactam in combination with aztreonam against multidrug-resistant, metallo-β-lactamase-producing *Klebsiella pneumoniae*. *Eur. J. Clin. Microbiol. Infect. Dis.* DOI:10.1007/s10096-021-04197-3 (2021)
71. McCurdy S., Keedy K., Lawrence L., Nenninger A., Sheets A., Quintas M., Cammarata S.: Efficacy of delafloxacin versus moxifloxacin against bacterial respiratory pathogens in adults with community-acquired bacterial pneumonia (CABP): microbiology results from the delafloxacin phase 3 CABP trial. *Antimicrob. Agents Chemother.* **64**, DOI:10.1128/aac.01949-19 (2020)
72. McCurdy S., Lawrence L., Quintas M., Woosley L., Flamm R., Tseng C., Cammarata S.: *In vitro* activity of delafloxacin and microbiological response against fluoroquinolone-susceptible and nonsusceptible *Staphylococcus aureus* isolates from two phase 3 studies of acute bacterial skin and skin structure infections. *Antimicrob. Agents Chemother.* **61**, DOI:10.1128/aac.00772-17 (2017)
73. McCurdy S., Nenninger A., Sheets A., Keedy K., Lawrence L., Quintas M., Cammarata S.: Efficacy of delafloxacin versus moxifloxacin against atypical bacterial respiratory pathogens in adults with community-acquired bacterial pneumonia (CABP): data from the delafloxacin phase 3 CABP trial. *Int. J. Infect. Dis.* **97**, 374–379 (2020)
74. Mendes R.E., Farrell D.J., Flamm R.K., Talbot G.H., Ivezic-Schoenfeld Z., Paukner S., Sader H.S.: *In vitro* activity of lefamulin tested against *Streptococcus pneumoniae* with defined serotypes, including multidrug-resistant isolates causing lower respiratory tract infections in the United States. *Antimicrob. Agents Chemother.* **60**, 4407–4411 (2016)
75. Mendes R.E., Paukner S., Doyle T.B., Gelone S.P., Flamm R.K., Sader H.S.: Low prevalence of Gram-positive isolates showing elevated lefamulin MIC. Results during the SENTRY Surveillance Program for 2015–2016 and characterization of resistance mechanisms. *Antimicrob. Agents Chemother.* **63**, DOI:10.1128/aac.02158-18 (2019)
76. Morrissey I., Hawser S., Lob S.H., Karlowsky J.A., Bassetti M., Corey G.R., Olesky M., Newman J., Fyfe C.: *In vitro* activity of eravacycline against Gram-positive bacteria isolated in clinical laboratories worldwide from 2013 to 2017. *Antimicrob. Agents Chemother.* **64**, DOI: 10.1128/aac.01715-19 (2020)
77. Morrissey I., Olesky M., Hawser S., Lob S.H., Karlowsky J.A., Corey G.R., Bassetti M., Fyfe C.: *In vitro* activity of eravacycline against Gram-negative bacilli isolated in clinical laboratories worldwide from 2013 to 2017. *Antimicrob. Agents Chemother.* **64**, DOI: 10.1128/aac.01699-19 (2020)
78. Motsch J., Paschke A., et al.: RESTORE-IMI 1: a multicenter, randomized, double-blind trial comparing efficacy and safety of imipenem/relebactam vs colistin plus imipenem in patients with imipenem-nonsusceptible bacterial infections. *Clin. Infect. Dis.* **70**, 1799–1808 (2020)
79. Namysłowska A., Laudy A.E., Tyski S.: *Acinetobacter baumannii* mechanisms of resistance to antibacterial agents. *Post. Mikrobiol.* **54**, 392–406 (2015)
80. Negash K.H., Norris J.K.S., Hodgkinson J.T.: Siderophore-antibiotic conjugate design: new drugs for bad bugs? *Molecules*, **24**, DOI:10.3390/molecules24183314 (2019)
81. Nilius A.M., Shen L.L., Hensey-Rudloff D., Almer L.S., Beyer J.M., Balli D.J., Cai Y., Flamm R.K.: *In vitro* antibacterial potency and spectrum of ABT-492, a new fluoroquinolone. *Antimicrob. Agents Chemother.* **47**, 3260–3269 (2003)
82. O'Riordan W., McManus A., Teras J., Poromanski I., Cruz-Saldariagga M., Quintas M., Lawrence L., Liang S., Cammarata S.: A comparison of the efficacy and safety of intravenous followed by oral delafloxacin with vancomycin plus aztreonam for the treatment of acute bacterial skin and skin structure snfections: a phase 3, multinational, souble-blind, randomized study. *Clin. Infect. Dis.* **67**, 657–666 (2018)
83. O'Riordan W., Mehra P., Manos P., Kingsley J., Lawrence L., Cammarata S.: A randomized phase 2 study comparing two doses of delafloxacin with tigecycline in adults with complicated skin and skin-structure infections. *Int. J. Infect. Dis.* **30**, 67–73 (2015)
84. Ozger H.S., Cuhadar T., Yildiz S.S., Demirbas Gulmez Z., Dizbay M., Guzel Tunccan O., Kalkanci A., Simsek H., Unaldi O.: *In vitro* activity of eravacycline in combination with colistin against carbapenem-resistant *A. baumannii* isolates. *J. Antibiot.* **72**, 600–604 (2019)
85. Paukner S., Gelone S.P., Arends S.J.R., Flamm R.K., Sader H.S.: Antibacterial activity of lefamulin against pathogens most commonly causing community-acquired bacterial pneumonia: SENTRY Antimicrobial Surveillance Program (2015–2016). *Antimicrob. Agents Chemother.* **63**, DOI:10.1128/aac.02161-18 (2019)
86. Paukner S., Riedl R.: Pleuromutilins: potent drugs for resistant bugs-mode of action and resistance. *Cold Spring Harb. Perspect. Med.* **7**, DOI:10.1101/cshperspect.a027110 (2017)
87. Paukner S., Sader H.S., Ivezic-Schoenfeld Z., Jones R.N.: Antimicrobial activity of the pleuromutilin antibiotic BC-3781 against bacterial pathogens isolated in the SENTRY antimicrobial surveillance program in 2010. *Antimicrob. Agents Chemother.* **57**, 4489–4495 (2013)
88. Pfaller M.A., Huband M.D., Mendes R.E., Flamm R.K., Castanheira M.: *In vitro* activity of meropenem/vaborbactam and characterisation of carbapenem resistance mechanisms among carbapenem-resistant *Enterobacteriaceae* from the 2015

meropenem/vaborbactam surveillance programme. *Int. J. Antimicrob. Agents,* **52**, 144–150 (2018)
89. Portsmouth S., van Veenhuyzen D., Echols R., Machida M., Ferreira J.C.A., Ariyasu M., Tenke P., Nagata T.D.: Cefiderocol versus imipenem-cilastatin for the treatment of complicated urinary tract infections caused by Gram-negative uropathogens: a phase 2, randomised, double-blind, non-inferiority trial. *Lancet Infect. Dis.* **18**, 1319–1328 (2018)
90. Prince W.T., Ivezic-Schoenfeld Z., Lell C., Tack K.J., Novak R., Obermayr F., Talbot G.H.: Phase II clinical study of BC-3781, a pleuromutilin antibiotic, in treatment of patients with acute bacterial skin and skin structure infections. *Antimicrob. Agents Chemother.* **57**, 2087–2094 (2013)
91. Pullman J., Gardovskis J., Farley B., Sun E., Quintas M., Lawrence L., Ling R., Cammarata S.: Efficacy and safety of delafloxacin compared with vancomycin plus aztreonam for acute bacterial skin and skin structure infections: a phase 3, double-blind, randomized study. *J. Antimicrob. Chemother.* **72**, 3471–3480 (2017)
92. Remy J.M., Tow-Keogh C.A., McConnell T.S., Dalton J.M., Devito J.A.: Activity of delafloxacin against methicillin-resistant *Staphylococcus aureus*: resistance selection and characterization. *J. Antimicrob. Chemother.* **67**, 2814–2820 (2012)
93. Sader H.S., Biedenbach D.J., Paukner S., Ivezic-Schoenfeld Z., Jones R.N.: Antimicrobial activity of the investigational pleuromutilin compound BC-3781 tested against Gram-positive organisms commonly associated with acute bacterial skin and skin structure infections. *Antimicrob. Agents Chemother.* **56**, 1619–1623 (2012)
94. Sader H.S., Paukner S., Ivezic-Schoenfeld Z., Biedenbach D.J., Schmitz F.J., Jones R.N.: Antimicrobial activity of the novel pleuromutilin antibiotic BC-3781 against organisms responsible for community-acquired respiratory tract infections (CARTIs). *J. Antimicrob. Chemother.* **67**, 1170–1175 (2012)
95. Sadowy E.: Mobile genetic elements beyond the VanB-resistance dissemination among hospital-associated *enterococci* and other Gram-positive bacteria. *Plasmid*, **114**, DOI:10.1016/j.plasmid.2021.102558 (2021)
96. Sato T., Yamawaki K.: Cefiderocol: discovery, chemistry, and in vivo profiles of a novel siderophore cephalosporin. *Clin. Infect. Dis.* **69**, 538–543 (2019)
97. Savov E., Trifonova A., Kovachka K., Kjosseva E., Strateva T.: Antimicrobial *in vitro* activities of ceftazidime-avibactam, meropenem-vaborbactam and plazomicin against multidrug-resistant *Acinetobacter baumannii* and *Pseudomonas aeruginosa* – a pilot Bulgarian study. *Infect. Dis.* **51**, 870–873 (2019)
98. Shi Y., Hua X., Xu Q., Yang Y., Zhang L., He J., Mu X., Hu L., Leptihn S., Yu Y.: Mechanism of eravacycline resistance in *Acinetobacter baumannii* mediated by a deletion mutation in the sensor kinase adeS, leading to elevated expression of the efflux pump AdeABC. *Infect. Genet. Evol.* **80**, DOI:10.1016/j.meegid.2020.104185 (2020)
99. Shortridge D., Pfaller M.A., Streit J.M., Flamm R.K.: Update on the activity of delafloxacin against acute bacterial skin and skin-structure infection isolates from European hospitals (2014–2019). *J. Glob. Antimicrob. Resist.* **23**, 278–283 (2020)
100. Siala W., Mingeot-Leclercq M.P., Tulkens P.M., Hallin M., Denis O., Van Bambeke F.: Comparison of the antibiotic activities of daptomycin, vancomycin, and the investigational fluoroquinolone delafloxacin against biofilms from *Staphylococcus aureus* clinical isolates. *Antimicrob. Agents Chemother.* **58**, 6385–6397 (2014)
101. Sims M., Mariyanovski V., McLeroth P., Akers W., Lee Y.C., Brown M.L., Du J., Pedley A., Kartsonis N.A., Paschke A.: Prospective, randomized, double-blind, phase 2 dose-ranging study comparing efficacy and safety of imipenem/cilastatin plus relebactam with imipenem/cilastatin alone in patients with complicated urinary tract infections. *J. Antimicrob. Chemother.* **72**, 2616–2626 (2017)
102. Słoczyńska A., Wand M.E., Tyski S., Laudy A.E.: Analysis of bla_{CHDL} genes and insertion sequences related to carbapenem resistance in *Acinetobacter baumannii* clinical strains isolated in Warsaw, Poland. *Int. J. Mol. Sci.* **22**, DOI:10.3390/ijms22052486 (2021)
103. Snydman D.R., McDermott L.A., Jacobus N.V., Kerstein K., Grossman T.H., Sutcliffe J.A.: Evaluation of the *in vitro* activity of eravacycline against a broad spectrum of recent clinical anaerobic isolates. *Antimicrob. Agents Chemother.* **62**, DOI: 10.1128/aac.02206-17 (2018)
104. Solomkin J.S., Gardovskis J., Lawrence K., Montravers P., Sway A., Evans D., Tsai L.: IGNITE4: results of a phase 3, randomized, multicenter, prospective trial of eravacycline vs meropenem in the treatment of complicated intraabdominal infections. *Clin. Infect. Dis.* **69**, 921–929 (2019)
105. Solomkin J.S., Ramesh M.K., Cesnauskas G., Novikovs N., Stefanova P., Sutcliffe J.A., Walpole S.M., Horn P.T.: Phase 2, randomized, double-blind study of the efficacy and safety of two dose regimens of eravacycline versus ertapenem for adult community-acquired complicated intra-abdominal infections. *Antimicrob. Agents Chemother.* **58**, 1847–1854 (2014)
106. Stracquadanio S., Torti E., Longshaw C., Henriksen A.S., Stefani S.: *In vitro* activity of cefiderocol and comparators against isolates of Gram-negative pathogens from a range of infection sources: SIDERO-WT-2014-2018 studies in Italy. *J. Glob. Antimicrob. Resist.* **25,** 390–398 (2021)
107. Sun C., Wang Q., Brubaker J.D., Wright P.M., Lerner C.D., Noson K., Charest M., Siegel D.R., Wang Y.M., Myers A.G.: A robust platform for the synthesis of new tetracycline antibiotics. *J. Am. Chem. Soc.* **130**, 17913–17927 (2008)
108. Sun D., Rubio-Aparicio D., Nelson K., Dudley M.N., Lomovskaya O.: Meropenem-vaborbactam resistance selection, resistance prevention, and molecular mechanisms in mutants of KPC-producing *Klebsiella pneumoniae*. *Antimicrob. Agents Chemother.* **61**, DOI:10.1128/aac.01694-17 (2017)
109. Sun J., Liu Y.H., et al.: Plasmid-encoded *tet*(X) genes that confer high-level tigecycline resistance in *Escherichia coli*. *Nat. Microbiol.* **4,** 1457–1464 (2019)
110. Sutcliffe J.A., O'Brien W., Fyfe C., Grossman T.H.: Antibacterial activity of eravacycline (TP-434), a novel fluorocycline, against hospital and community pathogens. *Antimicrob. Agents Chemother.* **57,** 5548–5558 (2013)
111. Tsivkovski R., Lomovskaya O.: Biochemical activity of vaborbactam. *Antimicrob. Agents Chemother.* **64**, DOI: 10.1128/aac.01935-19 (2020)
112. Tulkens P.M., Van Bambeke F., Zinner S.H.: Profile of a novel anionic fluoroquinolone-delafloxacin. *Clin. Infect. Dis.* **68**, 213–222 (2019)
113. Waites K.B., Crabb D.M., Duffy L.B.: Comparative in vitro susceptibilities and bactericidal activities of investigational fluoroquinolone ABT-492 and other antimicrobial agents against human mycoplasmas and ureaplasmas. *Antimicrob. Agents Chemother.* **47**, 3973–3975 (2003)
114. Waites K.B., Crabb D.M., Duffy L.B., Jensen J.S., Liu Y., Paukner S.: *In vitro* activities of lefamulin and other antimicrobial agents against macrolide-susceptible and macrolide-resistant *Mycoplasma pneumoniae* from the United States, Europe, and China. *Antimicrob. Agents Chemother.* **61**, DOI: 10.1128/aac.02008-16 (2017)
115. Walkty A., Karlowsky J.A., Baxter M.R., Adam H.J., Golden A., Lagace-Wiens P., Zhanel G.G.: *In vitro* activity of imipenem-relebactam against various resistance phenotypes/genotypes

of *Enterobacterales* and *Pseudomonas aeruginosa* isolated from patients across Canada as part of the CANWARD study, 2016–2019. *Diag. Microbiol. Infect. Dis.* **101**, DOI:10.1016/j.diagmicrobio.2021.115418 (2021)

116. Wang L., Walsh T.R., et al.: Novel plasmid-mediated tet(X5) gene conferring resistance to tigecycline, eravacycline, and omadacycline in a clinical *Acinetobacter baumannii* isolate. *Antimicrob. Agents Chemother.* **64**, DOI:10.1128/aac.01326-19 (2019)
117. Wang Z., Lin Z., Bai B., Xu G., Li P., Yu Z., Deng Q., Shang Y., Zheng J.: Eravacycline susceptibility was impacted by genetic mutation of 30S ribosome subunits, and branched-chain amino acid transport system II carrier protein, Na/Pi cotransporter family protein in *Staphylococcus aureus*. *BMC Microbiol.* **20**, DOI:10.1186/s12866-020-01869-6 (2020)
118. Wen Z., Shang Y., Xu G., Pu Z., Lin Z., Bai B., Chen Z., Zheng J., Deng Q., Yu Z.: Mechanism of eravacycline resistance in clinical *Enterococcus faecalis* isolates from China. *Front. Microbiol.* **11**, DOI:10.3389/fmicb.2020.00916 (2020)
119. Wilson B.R., Bogdan A.R., Miyazawa M., Hashimoto K., Tsuji Y.: Siderophores in iron metabolism: from mechanism to therapy potential. *Trends Mol. Med.* **22**, 1077–1090 (2016)
120. World Health Organization: 2020 antibacterial agents in clinical and preclinical development: an overview and analysis. http://apps.who.int/iris/handle/10665/340694 (16.07.2021)
121. World Health Organization: Prioritization of pathogens to guide discovery, research and development of new antibiotics for drug-resistant bacterial infections, including tuberculosis. https://apps.who.int/iris/handle/10665/311820 (16.07.2021)
122. Wunderink R.G., Nagata T.D., et al.: Cefiderocol versus high-dose, extended-infusion meropenem for the treatment of Gram-negative nosocomial pneumonia (APEKS-NP): a randomised, double-blind, phase 3, non-inferiority trial. *Lancet Infect. Dis.* **21**, 213–225 (2021)
123. Xiao X.Y., Sutcliffe J.A., et al.: Fluorocyclines. 7-fluoro-9-pyrrolidinoacetamido-6-demethyl-6-deoxytetracycline: a potent, broad spectrum antibacterial agent. *J. Med. Chem.* **55**, 597–605 (2012)
124. Young K., Motyl M.R., et al.: *In vitro* studies evaluating the activity of imipenem in combination with relebactam against *Pseudomonas aeruginosa*. *BMC Microbiol.* **19**, DOI:10.1186/s12866-019-1522-7 (2019)
125. Zhanel G.G., Baxter M.R., Adam H.J., Sutcliffe J., Karlowsky J.A.: *In vitro* activity of eravacycline against 2213 Gram-negative and 2424 Gram-positive bacterial pathogens isolated in Canadian hospital laboratories: CANWARD surveillance study 2014–2015. *Diag. Microbiol. Infect. Dis.* **91**, 55–62 (2018)
126. Zhanel G.G., Karlowsky J.A., et al.: Lefamulin: a novel oral and intravenous pleuromutilin for the treatment of community-acquired bacterial pneumonia. *Drugs*, **81**, 233–256 (2021)
127. Zhang F., Yu Z.J., et al.: Eravacycline activity against clinical *S. aureus* isolates from China: *in vitro* activity, MLST profiles and heteroresistance. *BMC Microbiol.* **18**, DOI:10.1186/s12866-018-1349-7 (2018)
128. Zheng J.X., Lin Z.W., Sun X., Lin W.H., Chen Z., Wu Y., Qi G.B., Deng Q.W., Qu D., Yu Z.J.: Overexpression of OqxAB and MacAB efflux pumps contributes to eravacycline resistance and heteroresistance in clinical isolates of *Klebsiella pneumoniae*. *Emerg. Microbes Infect.* **7**, DOI:10.1038/s41426-018-0141-y (2018)
129. Zhou M., Yang Q., Lomovskaya O., Sun D., Kudinha T., Xu Z., Zhang G., Chen X., Xu Y.: *In vitro* activity of meropenem combined with vaborbactam against KPC-producing *Enterobacteriaceae* in China. *Antimicrob. Chemother.* **73**, 2789–2796 (2018)
130. Zhuchenko G., Schmidt-Malan S., Patel R.: Planktonic and biofilm activity of eravacycline against *Staphylococci* isolated from periprosthetic joint infections. *Antimicrob. Agents Chemother.* **64**, DOI:10.1128/aac.01304-20 (2020)

7.2. Publikacja O1

RSC Advances

PAPER

View Article Online
View Journal | View Issue

Cite this: *RSC Adv.*, 2021, **11**, 25104

Development of structurally extended benzosiloxaboroles – synthesis and *in vitro* biological evaluation†

P. Pacholak,[ab] J. Krajewska,[c] P. Wińska,[a] J. Dunikowska,[a] U. Gogowska,[a] J. Mierzejewska,[a] K. Durka,[a] K. Woźniak,[b] A. E. Laudy*[c] and S. Luliński*[a]

The synthesis of potassium 6-hydroxy-7-chloro-1,1-dimethyl-3,3-difluorobenzo-1,2,3-siloxaborolate **5b** from readily available 4-bromo-2-chlorophenol was developed. This compound proved useful in various derivatizations resulting in a wide range of *O*-functionalized benzosiloxaboroles. Reactions of **5b** with selected substituted benzoyl chlorides gave rise to a series of respective derivatives with 6-benzoate side groups attached to the benzosiloxaborole core. Furthermore, treatment of **5b** with substituted benzenesufonyl chlorides afforded several benzosiloxaboroles bearing functionalized benzenesulfonate moieties at the 6 position. The synthesis of related chloropyridine-2-yloxy substituted benzosiloxaboroles was accomplished by a standard approach involving silylation/boronation of appropriate heterodiaryl ethers. Investigation of biological activity of obtained compounds revealed that some benzoate and most benzenesulfonate derivatives exhibit high activity against Gram-positive cocci such as methicillin-sensitive *Staphylococcus aureus* ATCC 6538P as well as methicillin-resistant *S. aureus* ATCC 43300 with the MIC values in the range of 0.39–3.12 mg L^{-1}. Some benzenesulfonate derivatives showed also potent activity against *Enterococcus faecalis* ATCC 29212 and *E. faecium* ATCC 6057 with MIC = 6.25 mg L^{-1}. Importantly, for the most promising cocci-active benzenesulfonate derivatives the obtained MIC values were far below the cytotoxicity limit determined with respect to human normal lung fibroblasts (MRC-5). For those derivatives, the obtained IC_{50} values were higher than 12.3 mg L^{-1}. The results of antimicrobial activity and cytotoxicity indicate that the tested compounds can be considered as potential antibacterial agents.

Received 27th May 2021
Accepted 9th July 2021

DOI: 10.1039/d1ra04127d

rsc.li/rsc-advances

1. Introduction

Recently, organoboron compounds have attracted increased attention as a subject of studies in the area of medicinal chemistry.[1–3] Numerous compounds were found to exhibit biological activity, mostly as anti-cancer, anti-inflammatory and anti-microbial agents. From the structural point of view, selected classes of organoboranes seem to be especially suitable for such applications. These include boron-rich cluster compounds, *i.e.*, carborane derivatives considered for the use in Boron Neutron Capture Therapy.[4] There are also numerous examples of biologically active boronated peptide derivatives.[5–7] Currently, arylboronic acids are highly popular synthetic reagents which found also applications in other fields, *e.g.*, as potent receptors of saccharides and other diols with a special emphasis on nucleosides and catechol derivatives.[8] Their antimicrobial activity was recognized in the 1930's.[9] Benzoxaboroles are a specific class of cyclic arylboronic hemiesters which were obtained the 1950's.[10,11] However, they became highly popular only 50 years later when their potent antimicrobial activity was discovered.[12] Extensive studies resulted in the preparation of numerous derivatives which were further evaluated from the point of view of medicinal chemistry.[13–15] Those efforts have already met with success as two benzoxaboroles including antifungal agent Tavaborole **I** (trade name Kerydin) (Fig. 1), and anti-inflammatory Crisaborole II (trade name Eucrisa) (Fig. 1), were approved by FDA for the clinical use.[16] The mechanism of action of benzoxaboroles relies on their physicochemical specifity based on enhanced electron-deficient character of the boron atom. In fact, benzoxaboroles are stronger Lewis acids than the corresponding arylboronic acids.[17] In general, the boron centre plays the key role in the binding to the biological targets through formation of strong covalent bonds. However, the binding can be substantially enhanced by additional interactions occurring with participation of various functional

[a]*Faculty of Chemistry, Warsaw University of Technology, Noakowskiego 3, 00-664 Warsaw, Poland. E-mail: sergiusz.lulinski@pw.edu.pl*
[b]*University of Warsaw, Faculty of Chemistry, Pasteura 1, 02-093 Warsaw, Poland*
[c]*Department of Pharmaceutical Microbiology, Medical University of Warsaw, Oczki 3, 02-007 Warsaw, Poland. E-mail: alaudy@wp.pl*

† Electronic supplementary information (ESI) available. CCDC 2068345–2068349, 2069477 and 2077619. For ESI and crystallographic data in CIF or other electronic format see DOI: 10.1039/d1ra04127d

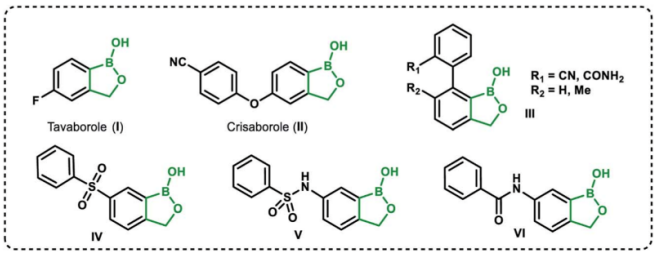

Fig. 1 Examples of biologically active benzoxaboroles.

groups or larger structural fragments. Thus, a specific activity can be achieved by proper structural design, therefore intensive efforts resulted in elaboration of synthetic protocols for the preparation of thousands of functionalized benzoxaboroles.[15] For example, 7-(cyanophenyl) benzoxaboroles **III** (Fig. 1) showed antituberculosis potency[18] whereas 3-aminomethyl derivatives were active against Gram-negative bacteria.[19] In another work, the series of compounds bearing substituted phenyl groups connected to benzoxaborole core at the 6 position through various linkages (Fig. 1) were prepared and tested as potential antitrypanosomal agents.[20] It was demonstrated that compounds with sulfone **IV**, sulfonamide **V** and amide **VI** linkages were most promising, and therefore it was concluded that their improved activity is connected to enhanced hydrogen-bond-acceptor character of these linkage groups.

Based on the concept of bioisosterism,[21] we decided to prepare some benzoxaborole congeners. Thus, we developed synthetic routes to pyridoxaboroles[22] where the benzene rings replaced with the pyridine one. However, we have put our major efforts to benzosiloxaboroles[23,24] where the silicon atom serves as the bioisostere of the carbon atom in the oxaborole ring. Despite the close analogy resulting from the location of carbon and silicon in the same group of periodic table, the chemical properties of those elements are quite different. From the point of view of biological activity it is important to note that Lewis acidity of the boron atom is increased when comparing benzosiloxaboroles to benzoxaboroles which may be attributed to increased π-acceptor ability of silicon *vs.* saturated carbon atom.[25] In addition, one can expect that lipophilicity will be increased when the methylene group is replaced with the larger $SiMe_2$ fragment. As a consequence, antimicrobial activity of respective benzoxa- and benzosiloxaboroles is different. We have already succeeded in preparation and comprehensive characterization of various functionalized benzosiloxaboroles **VII** (Fig. 2). It was found that simple fluorinated benzosiloxaboroles are potent antifungal agents whereas other diboron derivatives **VIII–IX** were identified as inhibitors of KPC-2 β-lactamase.[26] We have also observed that replacement of fluorines with chlorines at 6 and 7 positions was beneficial for antibacterial activity. Therefore, we decided to check whether introduction of larger substituents adjacent to chlorine will further enhance antibacterial potency. To some extent, this concept was inspired by the fact that diverse biological activity of benzoxaboroles is observed or improved due to attachment of various pendant aryl substituents as demonstrated by examples shown in Fig. 1. Thus, in this work we report new family of structurally expanded benzosiloxaboroles with a special focus on derivatives with arylsulfonate side groups which showed the most promising antibacterial activity, especially towards various strains of *Staphylococcus aureus*. Clinical strains of methicillin-resistant *S. aureus* have been a serious problem in both hospital and open treatment for many years. *S. aureus* MRSA strains are resistant to almost all β-lactams and often resistant to antibiotics of other classes. Recently, an increase in the number of isolates resistant to one of the newer group of antibiotics, *i.e.*, glycopeptides, has been observed.[27] Therefore, it is necessary to search for new groups of compounds active against these bacteria, preferably with a new mechanism of action.

2. Results and discussion

2.1. Synthesis

The general synthetic approach to final targeted benzosiloxaboroles started with inexpensive 4-bromo-2-halophenols **1a–1b**

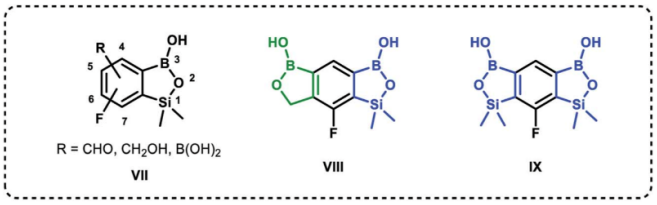

Fig. 2 Examples of functionalized benzosiloxaboroles.[26] Position numbering scheme is additionally provided for the general structure VII (note that it is different between benzoxa- and benzosiloxaboroles).

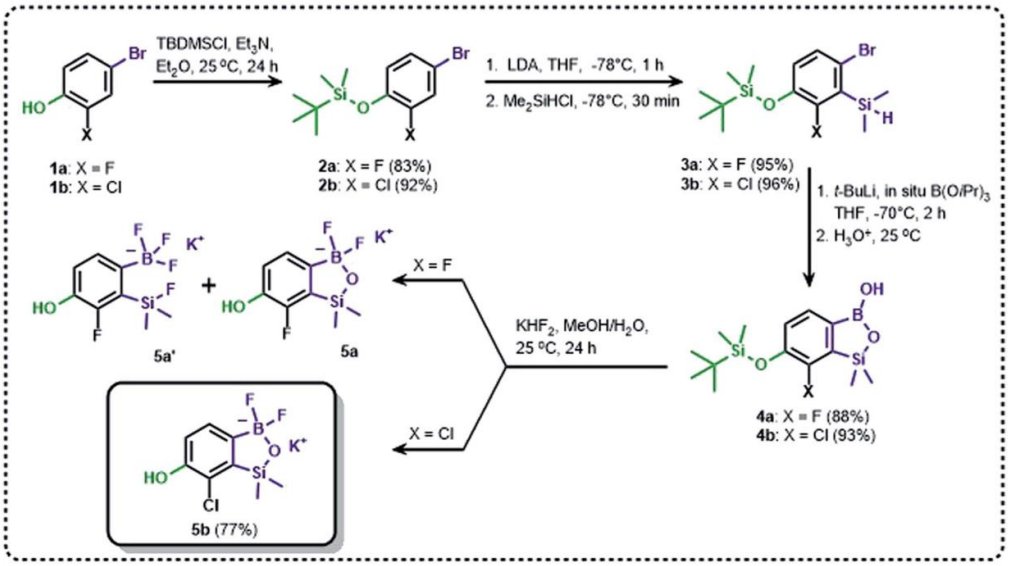

Scheme 1 Synthesis of hydroxy-substituted benzosiloxa(difluoro)borolates **5a–5b**.

(Scheme 1). The hydroxyl groups were protected with chloro(*tert*-butyl)dimethylsilane (TBDMSCl) and the resulting silyl ethers **2a–2b** were subjected to deprotonation with LDA in THF at −78 °C followed by trapping of corresponding aryllithium intermediates with $Me_2Si(H)Cl$ in accordance with a general protocol reported by us previously.[23] The reactions occurred regioselectively at the position between two halogens in accordance with a strong cumulated *ortho*-acidifying effect of those two substituents.[28,29] The functionalized arylsilanes **3a–3b** were converted to respective benzosiloxaboroles **4a–4b** after some optimization of reaction conditions. Thus, the most effective approach involved Br/Li exchange with *t*-BuLi in THF at −78 °C followed by immediate trapping with $B(OiPr)_3$ present in a reaction mixture ("*in situ* quench" technique[30]). The hydrolysis effected with water resulted in cleavage of Si–H bond which occurs rapidly under alkaline conditions due to *ortho*-assistance of the anionic boronate group.[31] The benzosiloxaboroles **4a–4b** bearing silyloxy groups at the 6-position have been obtained in good yields as white solids soluble in common organic solvents (Scheme 1). In a subsequent step, **4a–4b** were subjected to deprotection of OTBDMS groups with KHF_2 in $MeOH/H_2O$. Unfortunately, in the case of **4a**, the reaction resulted in a mixture of potassium salts of benzosiloxaborolate and aryltrifluoroborate anions **5a**, **5a′**, respectively; the latter product formed due to subsequent cleavage of siloxaborole ring in **5a**. The attempts to isolate the desired product **5a** in a pure form were unsuccessful. In contrast, the salt **5b** was formed selectively as it was not prone to subsequent ring opening. It was isolated as a non-stoichiometric DMF solvate as this solvent was used for the final extraction of **5b** from a crude product containing substantial amounts of inorganic fluoride salts. The solvent could not be quantitatively removed even by prolonged heating under reduced pressure (10^{-3} mbar). However, the presence of DMF does not disturb subsequent derivatization of **5b** as it was also carried out using this solvent.

The presence of free hydroxyl group in **5b** was utilized in various derivatization reactions through initial generation of anionic phenolate species. Various bases including K_2CO_3/acetone, NaOH/EtOH and DIPEA (Hünig's base)/THF were tested but they proved ineffective which can be attributed to the poor solubility or degradation of **5b** under such conditions. Finally, the use of sodium hydride in anhydrous DMF gave satisfactory results allowing for clean and effective deprotonation of the 6-OH group. Subsequent nucleophilic substitution reactions with MeI, Et_2NCOCl, benzoyl, and benzenesulfonyl chlorides as electrophilic partners proceeded smoothly under mild conditions (temperature range of 0–25 °C) giving rise to a series of functionalized benzosiloxaboroles **6**, **7**, **8a–8g**, and **9a–9r**, respectively (Scheme 2). In addition, we attempted to use the mixture **5a**/**5a′** using the protocol developed for derivatization of **5b** but the results were not satisfactory as we were unable to isolate 7-fluoro analogues of aforementioned products.

We have also used dichloropyridines **10a–10b** as electrophiles in order to attach the pyridine ring through the ether linkage. Unfortunately, the reactions did not proceed under conditions described above whereas at higher temperatures a tarry mixture was obtained indicating that degradation of starting materials occurred during heating. Thus, we have changed the reactions sequence leading to targeted products **13a–13b** (Scheme 3). In the first step, **10a–10b** were subjected to

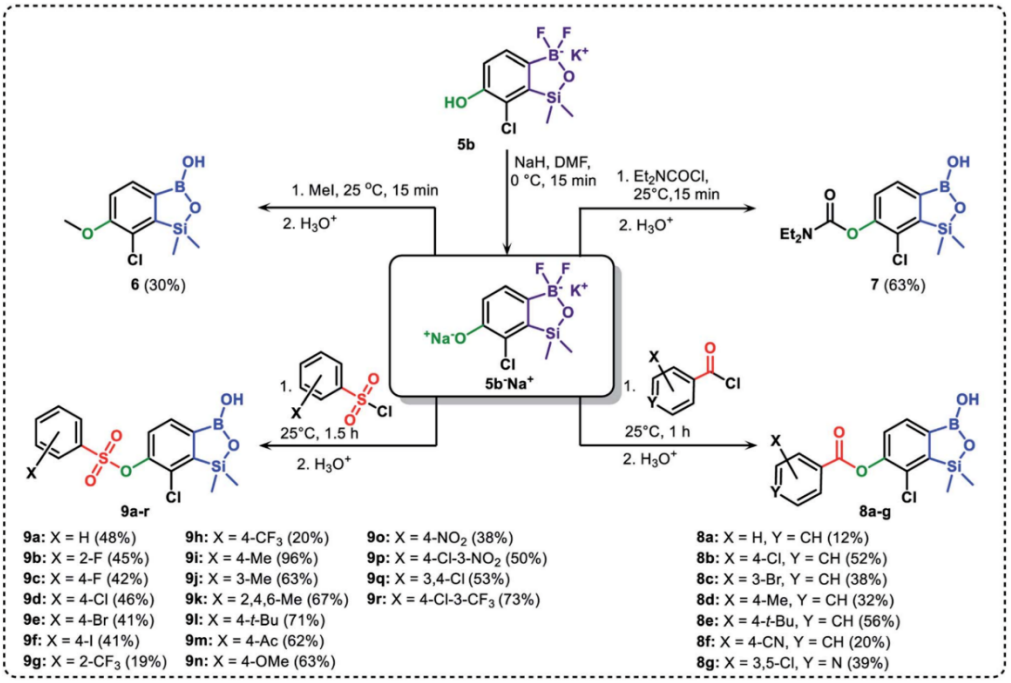

Scheme 2 Synthesis of functionalized benzosiloxaboroles **6**, **7**, **8a–8g**, **9a–9r**.

S_N2Ar reactions with the phenolate anion generated from **1b** using NaOH/DMSO at 100 °C.[32] The obtained halogenated phenoxypyridines **11a–11b** were converted to respective dimethylsilyl derivatives **12a–12b** followed by final transformation to benzosiloxaboroles **13a–13b**; both steps were carried out using a protocol described for preparation of **4a–4b** from **2a–2b**.

2.2. Compound characterization

All final benzosiloxaboroles were obtained and fully characterized by multinuclear NMR spectroscopy and HRMS analysis. The ^{11}B NMR spectrum of the salt **5b** in DMSO-d_6 showed a broadened resonance at 5.5 ppm consistent with the presence of tetracoordinate boron atom whereas the respective ^{19}F NMR

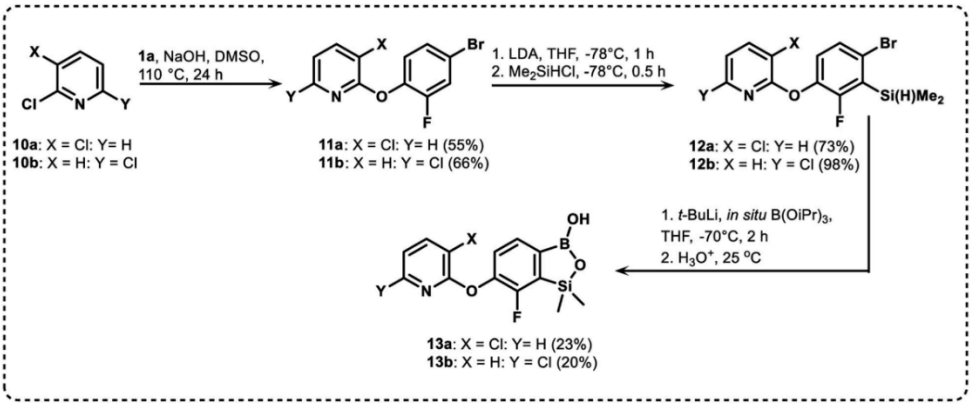

Scheme 3 Synthesis of chloropyridin-2-yloxy substituted benzosiloxaboroles **13a–13b**.

Table 1 Acidity (pK_a values) of some obtained benzosiloxaboroles[a]

	4b	8a	8b	9a	9b	9c	9d	9k	9n	9o	13a
pK_a	7.6	6.6	6.4	5.6	5.6	5.4	5.4	6.1	6.0	5.8	6.7

[a] Determined by potentiometric titration with 0.05 M NaOH in MeOH/H_2O (2 : 1).

spectrum showed a signal at −133.60 ppm indicating the attachment of fluorides. In addition, X-ray diffraction analysis of the salt **5b** confirmed the tetrahedral arrangement of the boron atom (Fig. 3b) whereas the geometry of the entire boracyclic ring in the benzosiloxaborolate anion is slightly different than that in neutral benzosiloxaboroles,[23] mainly due to elongation of the B–O distance. The structural formulation of selected benzosiloxaboroles **4b**, **6**, **8a**, **9a**, **9h** and **13a** was also confirmed by single-crystal X-ray diffraction analyses (Fig. 3a and c–g). The metric features of five-membered boracyclic rings in all studied structures are similar to those found previously in analogous compounds (Table S3, see ESI†).[23] In most cases, the molecules tend to form centrosymmetric dimers due to formation of intermolecular hydrogen bonds between BOH groups (Fig. S84, ESI†). Exceptionally, in the case of **13b**, the dimer is formed by O–H···N hydrogen bonds between B(OH) hydroxyl group and pyridine nitrogen atom (Fig. S85, ESI†). Furthermore, the acidity (pK_a values) of selected derivatives was determined by potentiometric titration with 0.05 M aq. NaOH in water/methanol solution (1 : 2). The results (see Table 1) indicate that the benzenesulfonate derivatives (**9a**, **9c**, **9k**, **9o**) exhibit the highest acidity in the studied series (pK_a in the range 5.4–6.1) which depends to some extent on the structure of the pendant aryl substituent. This is in agreement with the strong electron-withdrawing effect of the benzenesulfonate group. The benzoate derivatives are slightly weaker acids (pK_a in the range 6.4–6.6) whereas acidity of **4b** (pK_a = 7.6) is decreased due to strong electron-donating character of TBDMSO group. Overall, the obtained pK_a values indicate that the most of studied compounds tend strongly to exist as corresponding anions under standard physiological conditions (pH = 7.4), which should enhance their solubility.

2.3. Antibacterial activity

It has been shown recently, that sulfonamide-substituted benzoxaboroles have high activity against *S. aureus* including methicillin-resistant *S. aureus* ATCC BAA-1762 strain.[33] The MIC

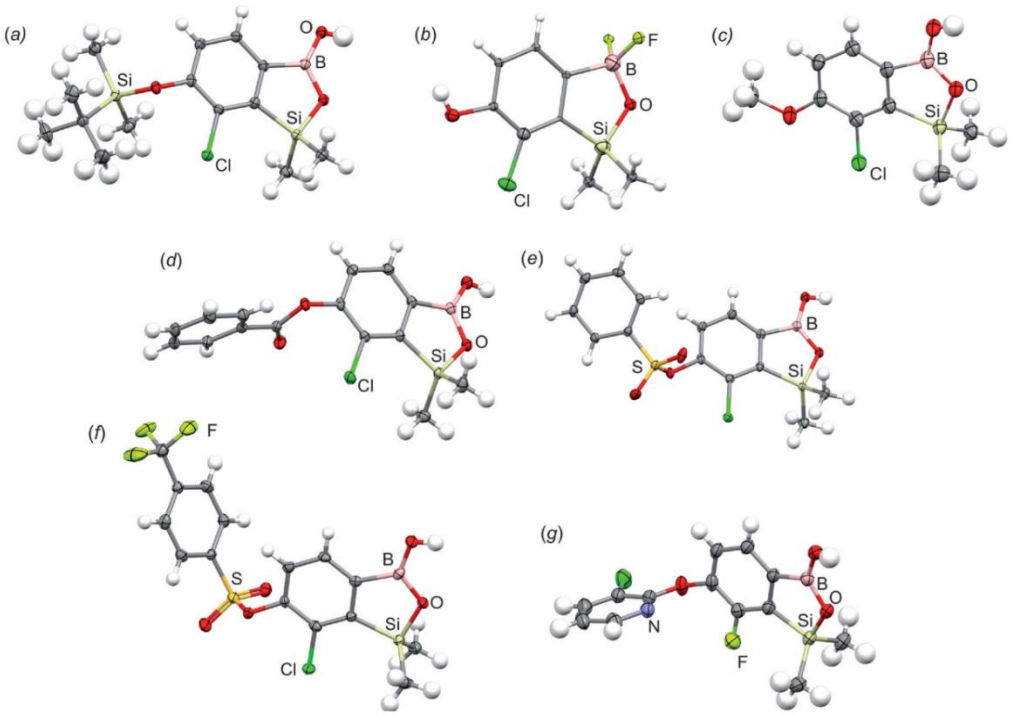

Fig. 3 Molecular structures of (a) **4b**, (b) **5b**, (c) **6**, (d) **8a**, (e) **9a**, (f) **9h** and (g) **13a**. Thermal motions given as ADPs at the 50% probability level. In the case of the potassium salt **5b** only the organoboron anion is presented.

values from 0.4 to 6.25 mg L^{-1} were obtained for the most active compounds. Besides, we have previously presented the antibacterial activity, also against Gram-positive cocci, of the several benzosiloxaboroles.[26] In this study we have investigated antimicrobial activity of the following groups of the newly synthesized benzosiloxaboroles: Group I (TBDMSO derivatives **4a–4b**), Group II (benzoyloxy derivatives **8a–8g**), Group III (benzenesulfonyloxy **9a–9r**) and Group IV (chloropyridin-2-yloxy derivatives **13a–13b**). All obtained data for the new derivatives of benzosiloxaboroles and the reference agents are presented in the ESI in Tables S4–S6†. In general, the compounds from the Group III (**9a–9r**) showed the highest antibacterial activity towards cocci of the *Staphylococcus* genus, especially *S. aureus*. It is worth to underline, that study was carried out with methicillin-sensitive *S. aureus* ATCC 6538P and methicillin-resistant *S. aureus* ATCC 43300. 14 out of 16 well soluble compounds from the Group III showed the high activity against methicillin-sensitive as well as methicillin-resistant *S. aureus* strains, with the MIC values in the range of 0.39–3.12 mg L^{-1} (Table 2, for full data set see Table S4†).

Interestingly, compounds **9k**, **9q** and **9r** showed relatively high activity also against other Gram-positive cocci such as *Enterococcus faecalis* ATCC 29212 and *E. faecium* ATCC 6057, with the MIC value of 6.25 mg L^{-1} (Tables 2 and S4†). The activity of new groups of compounds against *Enterococcus* sp. is rarely observed. It is worth emphasizing that *E. faecalis* and *E. faecium* used in our research belong to two species of the genus *Enterococcus* responsible for frequent human infections, including nosocomial infections.[34] Compounds from the remaining three groups (**4a–4b**, **8a–8g** and **13a–13b**) showed lower activity against Gram-positive bacteria as the MIC range was 12.5–400 mg L^{-1} whilst diameters of the growth inhibition zones ranged from 18–24 mm (Tables 2 and S4†). Thus, the substitution of benzosiloxaboroles with benzenesulfonate substituents is necessary to achieve high activity against staphylococci and enterococci. In this study, linezolid – one of the relatively new group of antibacterial drugs belonging to the oxazolidinones, was used as the reference substance. The indications for linezolid treatment are infections caused by multi-drug resistant cocci including both methicillin-resistant staphylococci and glycopeptide-resistant enterococci strains.[27,34] We have found that five compounds from the Group III were more active than linezolid against MSSA and MRSA strains. The obtained MIC range of these compounds (**9d**, **9h**, **9k**, **9q** and **9r**) was 0.39–0.78 mg L^{-1} for the MSSA strain (linezolid: MIC = 1 mg L^{-1}) and 0.39–1.56 mg L^{-1} for the MRSA strain (linezolid: MIC = 2 mg L^{-1}) (Table 2). The high activity of these compounds is due to the presence of chloro or trifluoromethyl groups at the *para* position or two such groups at the *meta* and *para* positions of the benzenesulfonate substituent. Also the presence of three methyl groups at the 2,4,6 positions of the benzenesulfonate substituent results in the high activity of **9k**.

Table 2 The MIC values of selected new compounds against standard Gram-positive strains[a]

	MIC [mg L^{-1}]				
Compound	*S. aureus* ATCC 6538P MSSA	*S. aureus* ATCC 43300 MRSA	*S. epidermidis* ATCC 12228	*E. faecalis* ATCC 29212	*E. faecium* ATCC 6057
6	50	50	50	200	50
7	12.5	12.5	50	200	200
8a	12.5	25	25	50	50
8f	12.5	12.5	12.5	50	50
8g	100	100	100	400	400
9a	**1.56**	**1.56**	12.5	50	50
9b	**3.12**	**3.12**	12.5	50	50
9c	**3.12**	**3.12**	12.5	50	50
9d	**0.78**	**1.56**	**3.12**	12.5	12.5
9e	**1.56**	**1.56**	6.25	12.5	25
9g	**1.56**	**1.56**	6.25	25	25
9h	**0.39**	**1.56**	**3.12**	25	25
9i	**1.56**	**1.56**	6.25	25	25
9j	**1.56**	**1.56**	6.25	25	25
9k	**0.78**	**1.56**	**3.12**	6.25	6.25
9m	**3.12**	**3.12**	6.25	50	25
9n	**1.56**	**1.56**	12.5	50	50
9o	**1.56**	**3.12**	**0.78**	50	12.5
9p	**3.12**	**3.12**	**3.12**	25	25
9q	**0.78**	**0.78**	**3.12**	6.25	6.25
9r	**0.39**	**0.39**	**3.12**	6.25	6.25
13a	25	25	25	100	50
13b	25	50	25	50	50
LIN[b]	1	2	1	2	2

[a] The highest activity indicated by the low MIC values (≤3.12 mg L^{-1}) is shown in boldface. [b] LIN, linezolid was used as a reference agent active against Gram-positive bacteria.

Contrary to staphylococci, no potency of the obtained sulfonate-substituted benzosiloxaboroles comparable to linezolid was observed against enterococci. In the case of nine derivatives of the parent compound **9a**, the activity against *E. faecalis* and *E. faecium* increased from 2- to 8-fold indicative of positive effect of substituents at the benzenesulfonate scaffold. The analysis of the relationship between the activity and the structure of the tested compounds revealed that the presence of two Cl (**9q**) or Cl and CF_3 groups (**9r**) as well as the presence of three Me groups (**9k**) is necessary to achieve the highest activity against enterococci. However, the activity of these compounds was still 3-fold weaker than that of linezolid.

Examining the antibacterial activity of new compounds, the minimum bactericidal concentration (MBC) can be determined after establishing the MIC value. For most compounds of Groups I, II and IV, the MBC values were high $\geq$ 200 mg L^{-1}. Interestingly, in the case of the tested compounds from Group III, a paradoxical growth effect was observed during the determination of bactericidal activity. This so-called Eagle effect has previously been reported for several antibiotics, such as some β-lactams, glycopeptides, aminoglycosides, quinolones and polymyxins.[35] This phenomenon was first published for *S. aureus.*[36] According to the EUCAST and CLSI definitions, the MBC value is the lowest concentration of a agent that kills 99.9% of bacteria.[37,38] For 11 out of 16 well soluble compounds (**9a**, **9c**, **9d**, **9g**, **9i**, **9j**, **9m**, **9n**, **9p–9r**) the two MBC values for both *S. aureus* strains were observed (Table S4†). Following the CLSI guidelines,[38] the results were read as the low MBC values in range 0.78–12.5 mg L^{-1} for *S. aureus* MSSA and 1.56–25 mg L^{-1} for *S. aureus* MRSA. However unusually, on the plates with samples taken from the wells containing progressively increasing the agent concentrations (from 2- to 4-fold over the first MBC values), a significant increase in the number of growing colonies, as a paradoxical growth effect, was observed. Finally the second MBC value (in the range 25–400 mg L^{-1}) was obtained. So far, the mechanisms causing paradoxical bacterial growth with increasing concentrations of antibiotics are not fully elucidated. However, there have also been several *in vivo* studies in animal models to support the occurrence of the Eagle effect.[35] In addition, two case reports of the Eagle effect observation during the treatment of human bacterial infections have been described. The reduction in the doses of antibiotics resulted in therapeutic success and correlated with a reduction of the bacteria survived in the bloodstream.[35]

Overall, all the studied groups of the newly synthesized benzosiloxaboroles showed no significant activity against Gram-negative rods (Table S5†). Only a few compounds from the Group II and III of benzosiloxaboroles derivatives showed weak activity against *Stenotrophomonas maltophilia* strains (MICs 200–400 mg L^{-1}) and *Bordetella bronchiseptica* (MICs 50–400 mg L^{-1}). As in our previous publications, we have investigated the contribution of efflux pumps to the resistance of Gram-negative bacilli to the new synthesized compounds.[23,26] We used the well-known RND efflux pump inhibitor, Phe-Arg-β-naphthylamide (PAβN).[39,40] It inhibits the activity of efflux systems found in all Gram-negative rods, like *Escherichia coli, Klebsiella pneumoniae, Enterobacter* sp., *Proteus mirabilis*, *Pseudomonas aeruginosa, S. maltophilia* and *Acinetobacter baumannii.*[39–43] According to the recent publications, we have used lower concentration of PAβN, *i.e.*, 20 mg L^{-1} because the destabilization of bacterial cell covers was observed at higher concentration of this inhibitor.[44–46] In order to minimize the influence of PAβN on cell covers, the tests were conducted also in the presence of 1 mM $MgSO_4$.[44] Only in the case of six compounds, we showed a significant (4-fold) decrease in the MIC value of the studied compound in the presence of PAβN. These results confirm the lack of activity of the tested benzosiloxaborole derivatives against Gram-negative rods.

2.4. Antifungal activity

Inspired by our previous report about high activity of few benzosiloxaborole derivatives against yeast-like fungi, *Candida tropicalis* and *C. guilliermondii*,[23,26] we have investigated the activity of the newly synthesized benzosiloxaboroles against 5 species of *Candida* and *Saccharomyces cerevisiae* ATCC 9763. For all but one compounds, the antifungal activity determination was performed using the disk diffusion method as well as by an evaluation of the MIC and MFC values. The results of antifungal activity of the newly synthesized benzosiloxaboroles agents are presented in the ESI (Table S6†). The collection strains of *Candida* species which most commonly cause infections in humans were selected for the study. In most cases, they are responsible for opportunistic infections. However, they can cause also nosocomial infections, including severe infections, and cause death, mainly of immunocompromised patients.[47,48] Compounds from the Group II demonstrated the highest activity against all tested *Candida* species, especially against *C. krusei* and *C. tropicalis*. The presence of methyl group at the *para* position of the phenyl ring (compound **8d**) led to 2–4-fold

Table 3 The viability of human normal lung fibroblasts, MRC-5 after 72 h treatment with the tested compounds. Linezolid was used as a reference. The concentration (IC_{50}) that causes a response half way between the maximal (top) response and the maximally inhibited (bottom) response was calculated using MTT-based assay data and an equation $Y = \text{bottom} + (\text{top} - \text{bottom})/(1 + 10^{((\log IC_{50} - X) \times \text{HillSlope})})$

Compound	IC_{50} [mg L^{-1}]	Compound	IC_{50} [mg L^{-1}]
9a	>50	**5b**	>50
9c	49.13 ± 8.93	**7**	32.04 ± 3.76
9d	24.96 ± 3.37	**8a**	>50
9e	24.12 ± 9.82	**8b**	21.67 ± 2.72
9f	25.89 ± 2.00	**8d**	13.31 ± 3.09
9g	>50	**8e**	14.30 ± 1.96
9h	21.95 ± 2.24	**8f**	>50
9i	24.85 ± 4.23	**8g**	>50
9j	25.00 ± 4.74	**13a**	40.46 ± 2.70
9k	15.64 ± 3.47	**13b**	30.91 ± 2.31
9m	27.52 ± 3.61	Linezolid	>50
9n	29.43 ± 5.76		
9o	25.74 ± 3.56		
9p	3.19 ± 1.07		
9q	16.83 ± 3.89		
9r	12.30 ± 4.51		

increase in the activity against all tested *Candida* strains. The lowest MIC values 3.12–6.25 mg L^{-1} were observed for two strains of *C. tropicalis*. Other studied benzosiloxaboroles showed relatively high activity only against *S. cerevisiae*, a species that is not clinically significant.

2.5. Cytotoxic activity

To evaluate the cytotoxic effect of the tested compounds, MTT-based assay was performed. Human normal lung fibroblasts MRC-5 were treated with the newly synthesized compounds at the concentrations range of 0.78 to 50 mg L^{-1} for 72 h. IC_{50} values describing half inhibitory concentrations of each tested compound were calculated and summarized in Table 3. The representative plots demonstrating sigmoidal dose response curves for the tested compounds were shown in the ESI (Fig. S86–S91†). The obtained IC_{50} values for compounds **9a–9r**, **8a–8g**, **13a–13b** are in the range of 3.19 to above 50 mg L^{-1}, with the lowest value for the 4-chloro-3-nitrobenzenesulfonate derivative **9p**, and the highest values for compounds **9a**, **9g**, **5b**, **8f** and **8g**.

3. Conclusions

In conclusion, simple (MeO) and more structurally extended moieties (Et_2NCO_2, $ArCO_2$, $ArSO_3$, Py-2-O) were successfully installed onto the benzosiloxaborole scaffold using modular approaches based in most cases on the functionalization of the newly obtained potassium 6-hydroxy-7-chloro-1,1-dimethyl-3,3-difluorobenzo-1,2,3-siloxaborolate **5b**. It seems that the elaborated protocols can be directly adapted for the synthesis of other benzosiloxaboroles with various substitution patterns. Comprehensive characterization of antimicrobial activity of obtained compounds was performed. Most importantly, selected derivatives showed high activity against Gram-positive cocci from *Staphylococcus* and *Enterococcus* genera with the MIC values for as low as 0.39–0.78 mg L^{-1} and 6.25 mg L^{-1} respectively. SAR analysis comprising derivatives bearing $ArCO_2$, $ArSO_3$, Py-2-O moieties clearly indicates that the presence of $–SO_2–O–$ linker between two aromatic units is essential for achieving high antibacterial potency as the MIC values (determined for *S. aureus*) for benzenesulfonate derivatives (Group III) were typically in the range of 0.39–3.12 mg L^{-1}. In contrast, compounds from the Group II and IV were significantly less active as the corresponding MIC values were equal to 12.5 mg L^{-1} at best. It should be stressed that the cytotoxicity tests performed for human lung fibroblasts revealed that the IC_{50} values are much higher than MIC values for the majority of analyzed compounds. Importantly, for the most promising cocci-active benzenesulfonate derivatives (except for **9p** agent), the obtained MIC values were not cytotoxic towards human normal lung fibroblasts (MRC-5) with IC_{50} values exceeding 12.3 mg L^{-1}. To summarize, benzenesulfonate substituted benzosiloxaboroles can be considered as potential candidates for the treatment of infections caused by Gram-positive bacterial pathogens and therefore, extended studies on the topic by our research group are currently in progress.

4. Experimental section

4.1. General comments

Solvents used for reactions were dried by heating to reflux with sodium/benzophenone and distilled under argon. Starting materials including halogenated phenols (*tert*-butyl)dimethylsilyl chloride (TBDMSCl), alkyllithiums, diisopropylamine, trialkyl borates, chlorodimethylsilane as well as other reagents were used as received without further purification. In the ^{13}C NMR spectra the resonances of boron-bound carbon atoms were not observed in most cases as a result of their broadening by a quadrupolar boron nucleus. ^{1}H, and ^{13}C NMR chemical shifts are given relative to TMS using residual solvent resonances. For signal assignments purposes in selected ^{1}H NMR data, Ar^B, Ar^C, Ar^S stand for boronated benzene, benzoate and benzenesulfonyl fragments, respectively. ^{11}B and ^{19}F NMR chemical shifts are given relative to $BF_3 \cdot Et_2O$ and $CFCl_3$, respectively. Crystallographic Information Files (CIFs) have been deposited with the Cambridge Crystallographic Data Centre as supplementary publications no. 2068345 (**4b**), 2068347 (**5b**), 2069477 (**6**), 2068346 (**8a**), 2068348 (**9a**), 2077619 (**9h**) and 2068349 (**13a**). Relevant crystallographic data is provided in Table S1†.

4.2. Synthesis

4.2.1 (2a) 4-Bromo-2-fluoro-1-(*tert*-butyldimethylsilyloxy) benzene. 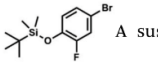 A suspension of NaH in mineral oil (60%, 6.30 g, 157 mmol, 3.0 eq.) under argon atmosphere was washed twice with anhydrous hexane (20 mL) and anhydrous THF (20 mL) was added. The mixture was stirred for 10 min and cooled to 0 °C and solution of 4-bromo-2-fluorophenol (10.0 g, 53.0 mmol, 1.0 eq.) in anhydrous THF (50 mL) was added for 20 min. After *ca.* 15 min stirring in 0 °C it was warmed to room temperature and solution of TBDMSCl (8.4 g, 55.0 mmol, 1.1 eq.) in Et_2O (30 mL) was added to the white suspension for 10 min. It was stirred for another 2 h at room temperature, then it was evaporated to dryness under reduced pressure and the residue was subjected to a simple distillation under reduced pressure. The product was obtained as a yellow liquid, bp 70 °C/5 10^{-3} mbar. Yield 13.4 g (83%). ^{1}H NMR (400 MHz, $CDCl_3$) δ 7.22 (dd, J = 10.1, 2.4 Hz, 1H, Ar), 7.12 (ddd, J = 8.6, 2.4, 1.5 Hz, 1H, Ar), 6.80 (t, J = 8.7 Hz, 1H, Ar), 1.01 (s, 9H, *t*-Bu), 0.20 (d, J = 1.2 Hz, 6H, $SiMe_2$) ppm. ^{13}C NMR (101 MHz, $CDCl_3$) δ 154.20 (d, J = 249.2 Hz), 142.8 (d, J = 12.4 Hz), 127.4 (d, J = 3.9 Hz), 123.4 (d, J = 2.5 Hz), 119.9 (d, J = 22.1 Hz), 112.8 (d, J = 8.2 Hz), 25.5, 18.3, −4.7 (d, J = 1.8 Hz) ppm. Anal. calcd for $C_{12}H_{18}BrFOSi$ (305.26): C 47.22, H 5.94; found C 47.27, H 5.88.

4.2.2 (2b) 4-Bromo-2-chloro-1-(*tert*-butyldimethylsilyloxy) benzene. 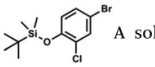 A solution of 4-bromo-2-chlorophenol (51.86 g, 0.250 mol, 1.0 eq.), TBDMSCl (41.45 g, 0.275 mol, 1.1 eq.) and Et_3N (52.3 mL, 0.375 mol, 1.5 eq.) in Et_2O (300 mL) was stirred under argon atmosphere for 24 h at room temperature. Obtained white suspension was evaporated to dryness under

reduced pressure. The residue was triturated with heptane (400 mL) followed by filtration under reduced pressure. The yellow filtrate was evaporated under reduced pressure and the residue was subjected to a fractional distillation under reduced pressure. The product was obtained as a yellow liquid, bp 106–115 °C/5 10^{-3} mbar. Yield 74.3 g (92%). ^{1}H NMR (400 MHz, $CDCl_3$) δ 7.48 (d, J = 2.5 Hz, 1H, Ar), 7.23 (dd, J = 8.7, 2.5 Hz, 1H, Ar), 6.76 (d, J = 8.6 Hz, 1H, Ar), 1.03 (s, 9H, *t*-Bu), 0.22 (s, 6H, $SiMe_2$) ppm. ^{13}C NMR (101 MHz, $CDCl_3$) δ 151.1, 132.8, 130.6, 126.9, 122.0, 113.4, 25.8, 18.4, −4.2 ppm. Anal. calcd for $C_{12}H_{18}BrClOSi$ (321.71): C 44.80, H 5.64; found C 44.69, H 5.53.

4.2.3 (3a) 4-Bromo-2-fluoro-3-(dimethylsilyl)-1-(*tert*-butyldimethylsilyloxy)benzene. 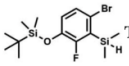 This compound was obtained using the protocol described for **3b** using **2a** (12.2 g, 40.0 mmol, 1.0 eq.), *n*-BuLi (11 M, 4 mL, 44.0 mmol, 1.1 eq.), iPr$_2$NH (6.2 mL, 44.0 mmol, 1.1 eq.) and Me_2SiHCl (4.8 mL, 44.0 mmol, 1.1 eq.) as the starting materials. It was obtained as a white powder. bp 95–100 °C. Yield 13.7 g (95%). ^{1}H NMR (300 MHz, $CDCl_3$) δ 7.19 (dd, J = 8.5, 1.4 Hz, 1H, Ar), 6.79 (dd, J = 9.2, 8.5 Hz, 1H, Ar), 4.79–4.73 (m, 1H, SiH), 1.01 (d, J = 0.5 Hz, 9H, *t*-Bu), 0.46 (dd, J = 3.9, 1.8 Hz, 6H, Si(H)$\underline{Me}_2$), 0.20 (d, J = 1.1 Hz, 6H, Si(*t*-Bu)$\underline{Me}_2$) ppm. ^{13}C NMR (101 MHz, $CDCl_3$) δ 158.50 (d, J = 243.5 Hz), 142.50 (d, J = 16.6 Hz), 129.0 (d, J = 3.7 Hz), 126.5 (d, J = 30.0 Hz), 124.4 (d, J = 3.0 Hz), 120.30 (d, J = 10.9 Hz), 25.6, 18.4, −3.1 (d, J = 4.3 Hz), −4.7 (d, J = 1.9 Hz) ppm. ^{19}F NMR (282 MHz, $CDCl_3$) δ −114.09 (t, J = 7.1 Hz) ppm. Anal. calcd for $C_{14}H_{24}BrFOSi_2$ (363.42): C 46.27, H 6.66; found C 46.12, H 6.58.

4.2.4 (3b) 4-Bromo-2-chloro-3-(dimethylsilyl)-1-(*tert*-butyldimethylsiloxy)benzene. 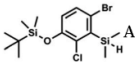 A solution of **2b** (74.30 g, 231.00 mmol, 1.0 eq.) in Et_2O (70 mL) was added dropwise at −75 °C for 15 min to a stirred solution of LDA, freshly prepared from diisopropylamine (35.6 mL, 254.1 mmol, 1.1 eq.) and *n*-BuLi (2.5 M, 101.64 mL, 254.10 mmol, 1.1 eq.) in THF (400 mL). The solution turned lucid yellow. After *ca.* 1.25 h stirring at −75 °C chlorodimethylsilane (30.8 mL, 277.2 mmol, 1.2 eq.) was added slowly for 15 min and the formation of thick slurry was observed. It was stirred for another 15 min at −75 °C, then it was allowed to warm to room temperature. The obtained white suspension was evaporated to dryness under reduced pressure. The residue was triturated with heptane (200 mL) followed by filtration. The yellow filtrate was evaporated under reduced pressure and the residue was subjected to a simple distillation under reduced pressure. The product was obtained as a yellow liquid, bp 125–130 °C (5 10^{-3} mbar). Yield 84.3 g (96%). ^{1}H NMR (400 MHz, $CDCl_3$) δ 7.31 (d, J = 8.6 Hz, 1H, Ar), 6.73 (d, J = 8.5 Hz, 1H, Ar), 5.02 (sept, J = 3.9 Hz, 1H, SiH), 1.02 (s, 9H, *t*-Bu), 0.49 (d, J = 4.0 Hz, 6H, Si(H)$\underline{Me}_2$), 0.22 (s, 6H, Si(*t*-Bu)$\underline{Me}_2$) ppm. ^{13}C NMR (101 MHz, $CDCl_3$) δ 150.7, 138.8, 133.3, 132.2, 122.4, 121.4, 25.6, 18.3, −2.6, −4.4 ppm. Anal. calcd for $C_{14}H_{24}BrClOSi_2$ (379.87): C 44.27, H 6.37; found C 44.19, H 6.32.

4.2.5 (4a) 6-(*tert*-Butyldimethylsilyloxy)-7-fluoro-1,1-dimethyl-3-hydroxybenzo-1,2,3-siloxaborole. 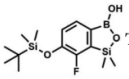 This compound was obtained using the protocol described for **4b** using **3a** (12.1 g, 33.0 mmol, 1.0 eq.), *t*-BuLi (1.7 M, 39 mL, 66.0 mmol, 2.0 eq.) and B(OiPr)$_3$ (14.0 mL, 50.0 mmol, 1.5 eq.) as the starting materials. It was obtained as a white powder. mp 84 °C. Yield 9.5 g (88%). ^{1}H NMR (300 MHz, $CDCl_3$) δ 7.43 (dd, J = 7.7, 0.6 Hz, 1H, Ar), 7.01 (t, J = 7.8 Hz, 1H, Ar), 1.01 (s, 9H, *t*-Bu), 0.48 (s, 6H, $OSiMe_2$), 0.22 (d, J = 1.0 Hz, 6H, Si (*t*-Bu)$\underline{Me}_2$) ppm. ^{13}C NMR (101 MHz, $CDCl_3$) δ 155.4 (d, J = 243.4 Hz), 145.4 (d, J = 14.9 Hz), 136.2 (d, J = 28.5 Hz), 128.5 (d, J = 3.1 Hz), 125.0 (d, J = 1.4 Hz), 25.5, 18.3, −0.7, −4.7 (d, J = 1.9 Hz). ^{11}B NMR (96 MHz, $CDCl_3$) δ 30.5 ppm. ^{19}F NMR (282 MHz, $CDCl_3$) δ −123.40 (d, J = 7.9 Hz) ppm. HRMS (ESI, positive ion mode): calcd for $C_{14}H_{25}BFO_3Si_2^+$ $[MH]^+$ 327.1414; found 327.1416.

4.2.6 (4b) 6-(*tert*-Butyldimethylsilyloxy)-7-chloro-1,1-dimethyl-3-hydroxybenzo-1,2,3-siloxaborole. 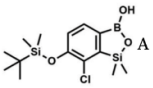 A solution of *t*-BuLi (1.9 M, 150 mL, 285.0 mmol, 2.1 eq.) was added dropwise at −75 °C for 30 min to a stirred solution of **3b** (51.55 g, 135.71 mmol, 1.0 eq.) and B(OiPr)$_3$ (27.7 mL, 162.9 mmol, 1.2 eq.) in anhydrous THF (400 mL) under argon atmosphere. After *ca.* 30 min stirring at −75 °C a thick slurry was formed. It was stirred for another 1.5 h at −75 °C and warmed to −10 °C, quenched with water and stirred at room temperature until evolution of H_2 ceased. 1.5 M aq. H_2SO_4 was dropped to reach the pH = 2–3. Et_2O (150 mL) and brine (50 mL) were added. The aqueous phase was separated followed by extraction with Et_2O (2 × 100 mL). The extracts were added to the organic phase and dried with anhydrous $MgSO_4$. Then it was concentrated under reduced pressure. An oily residue was mixed with water and hexane resulting in the formation of a white slurry. The white solid was filtered, washed several times with water and dried *in vacuo*, to give the product, mp 84–85 °C. Yield 43.3 g (93%). ^{1}H NMR (400 MHz, $CDCl_3$) δ 7.56 (d, J = 7.8 Hz, 1H, Ar), 6.96 (d, J = 7.8 Hz, 1H, Ar), 1.04 (s, 9H, *t*-Bu), 0.49 (s, 6H, $OSiMe_2$), 0.26 (s, 6H, Si (*t*-Bu)$\underline{Me}_2$) ppm. ^{13}C NMR (101 MHz, $CDCl_3$) δ 153.7, 151.9, 131.1, 128.2, 122.7, 25.7, 18.4, −1.4, −4.2 ppm. HRMS (ESI, positive ion mode): calcd for $C_{14}H_{25}BClO_3Si_2^+$ $[MH]^+$ 343.1118; found 343.1119.

4.2.7 (5b) Potassium 7-chloro-6-hydroxy-3,3-difluorobenzo-1,2,3-siloxaborolate. 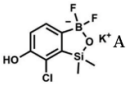 A solution of KHF_2 in water (5 M, 115 mL, 574 mmol, 6.7 eq.) was added to a stirred solution of **4b** (29.3 g, 85.5 mmol, e. 1.0) in MeOH (200 mL) in a sealed polypropylene beaker. After 24 h of stirring at room temperature it was concentrated under reduced pressure and obtained residue was suspended in DMF. It was filtered and concentrated under reduced pressure. The obtained white solid was dried *in vacuo* at 70 °C, mp 248–249 °C. Yield 19.0 g (77%). ^{1}H NMR (400

MHz, DMSO-d_6) δ 9.29 (s, 1H, OH), 6.97 (d, J = 7.5 Hz, 1H, Ar), 6.75 (d, J = 7.5 Hz, 1H, Ar), 0.15 (s, 6H, $SiMe_2$) ppm. ^{13}C NMR (101 MHz, DMSO-d_6) δ 162.3, 150.0, 146.3, 127.7 (t, J = 3.0 Hz), 121.3, 117.4, 1.0 ppm. ^{19}F NMR (376 MHz, DMSO-d_6) δ −133.65 ppm. ^{11}B NMR (96 MHz, DMSO) δ 5.8 ppm. HRMS (ESI, negative ion mode): calcd for $C_8H_9BClF_2O_2Si^-$ $[M - K]^-$ 249.0127; found 249.0125.

4.2.8 (6) 7-Chloro-6-methoxy-1,1-dimethyl-3-hydroxybenzo-1,2,3-siloxaborole. 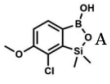 A suspension of NaH in mineral oil (60%, 0.30 g, 7.50 mmol, 2.1 eq.) under argon atmosphere was washed with anhydrous hexane (5 mL) twice and anhydrous DMF (10 mL) was added and stirred for 10 min. Then it was cooled to 0 °C and **5b** (1.00 g, 3.50 mmol, 1.0 eq.) was added. After *ca.* 30 min stirring in 0 °C, iodomethane (0.45 mL, 7.00 mmol, 2.0 eq.) was added to the white suspension. It was stirred for 1.0 h at room temperature and concentrated by a simple distillation under reduced pressure. The solid residue was treated with 1.5 M aq. H_2SO_4 to reach the pH = 2–3. The obtained white solid was filtered and washed with water (5 mL) and hexane (2 × 5 mL) and dried to give the product, mp 84–85 °C. Yield 0.25 g (30%). ^{1}H NMR (400 MHz, $CDCl_3$) δ 7.68 (d, J = 8.0 Hz, 1H, Ar), 7.02 (d, J = 8.0 Hz, 1H, Ar), 3.94 (s, 3H, OMe), 0.50 (s, 6H, $SiMe_2$) ppm. ^{13}C NMR (101 MHz, $CDCl_3$) δ 156.9, 151.5, 131.6, 125.1, 114.2, 56.3, −1.3 ppm. HRMS (ESI, positive ion mode): calcd for $C_9H_{13}BClO_3Si^+$ $[MH]^+$ 243.0410; found 243.0412.

4.2.9 (7) 7-Chloro-6-(*N*,*N*-diethylcarbamoyloxy)-1,1-dimethyl-3-hydroxybenzo-1,2,3-siloxaborole. 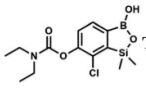 This compound was obtained using the protocol described for **6** using suspension of NaH in mineral oil (60%, 0.14 g, 3.50 mmol, 2.0 eq.), **5b** (0.5 g, 1.7 mmol, 1.0 eq.) and *N*,*N*-diethylcarbamoyl chloride (0.44 mL, 3.5 mmol, 2.1 eq.) as the starting materials. It was obtained as a white powder, mp 115–117 °C. Yield 0.35 g (63%). ^{1}H NMR (300 MHz, $CDCl_3$) δ 7.66 (d, J = 7.8 Hz, 1H, Ar), 7.29 (d, J = 7.8 Hz, 1H, Ar), 5.21 (s, 1H, OH), 3.52 (q, J = 7.0 Hz, 2H, CH_2), 3.43 (q, J = 7.0 Hz, 2H, CH_2), 1.33 (t, J = 7.0 Hz, 3H, Me), 1.25 (t, J = 7.0 Hz, 3H, Me), 0.49 (s, 6H, $SiMe_2$) ppm. ^{13}C NMR (101 MHz, $CDCl_3$) δ 153.1, 151.7, 149.4, 130.9, 126.2, 42.47, 42.1, 14.1, 13.3, −1.4 ppm. ^{11}B NMR (96 MHz, $CDCl_3$) δ 31.4 ppm. HRMS (ESI, positive ion mode): calcd for $C_{13}H_{20}BClNO_4Si^+$ $[MH]^+$ 328.0938; found 328.0940.

4.2.10 (8a) 7-Chloro-6-benzoyloxy-1,1-dimethyl-3-hydroxybenzo-1,2,3-siloxaborole. 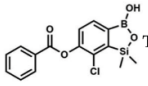 This compound was obtained using the protocol described for **6** using suspension of NaH in mineral oil (60%, 0.10 g, 2.50 mmol, 1.8 eq.), **5b** (0.5 g, 1.7 mmol, 1.0 eq.) and benzoyl chloride (0.24 mL, 2.0 mmol, 1.2 eq.) as the starting materials. It was obtained as a white powder. mp 150–152 °C. Yield 0.07 g (12%). ^{1}H NMR (400 MHz, $CDCl_3$) δ 8.24 (d, J = 7.8 Hz, 2H, Ar^C), 7.75 (d, J = 7.7 Hz, 1H, Ar^B), 7.67 (t, J = 7.5 Hz, 1H, Ar^C), 7.54 (t, J = 7.6 Hz, 2H, Ar^C), 7.36 (d, J = 7.5 Hz, 1H, Ar^B), 0.52 (s, 6H, $SiMe_2$) ppm. ^{13}C NMR (101 MHz, $CDCl_3$) δ 164.4, 151.9, 149.2, 134.1, 131.3, 130.5, 130.3, 129.8, 128.8, 128.6, 126.1, −1.2 ppm. HRMS (ESI, positive ion mode): calcd for $C_{15}H_{15}BClO_4Si^+$ $[MH]^+$ 333.0516; found 333.0518.

4.2.11 (8b) 7-Chloro-6-(4′-chlorobenzoyloxy)-1,1-dimethyl-3-hydroxybenzo-1,2,3-siloxaborole. 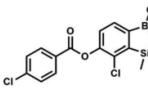 This compound was obtained using the protocol described for **8d** using suspension of NaH in mineral oil (60%, 0.14 g, 3.50 mmol, 2.0 eq.), **5b** (0.5 g, 1.70 mmol, 1.0 eq.) and 4-chlorobenzoyl chloride (0.22 mL, 1.70 mmol, 1.0 eq.) as the starting materials. It was obtained as a white powder. mp 161–164 °C. Yield 0.32 g (52%). ^{1}H NMR (400 MHz, $CDCl_3$) δ 8.18 (d, J = 8.5 Hz, 2H, Ar^C), 7.76 (d, J = 7.7 Hz, 1H, Ar^B), 7.52 (d, J = 8.5 Hz, 2H, Ar^C), 7.36 (d, J = 7.7 Hz, 1H, Ar^B), 5.48 (s, 1H, OH), 0.53 (s, 6H, $SiMe_2$). ^{13}C NMR (101 MHz, $CDCl_3$) δ 163.4, 152.0, 148.8, 140.6, 131.7, 131.2, 129.5, 129.1, 127.2, 125.8, −1.4 ppm. HRMS (ESI, positive ion mode): calcd for $C_{15}H_{14}BCl_2O_4Si^+$ $[MH]^+$ 367.0126; found 367.0126.

4.2.12 (8c) 7-Chloro-6-(3′-bromobenzoyloxy)-1,1-dimethyl-3-hydroxybenzo-1,2,3-siloxaborole. 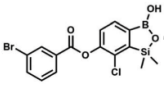 This compound was obtained using the protocol described for **8d** using suspension of NaH in mineral oil (60%, 0.14 g, 3.50 mmol, 2.0 eq.), **5b** (0.5 g, 1.70 mmol, 1.0 eq.) and 3-bromobenzoyl chloride (0.24 mL, 1.70 mmol, 1.0 eq.) as the starting materials. It was obtained as a white powder. Yield 0.25 g (38%). ^{1}H NMR (400 MHz, $CDCl_3$) δ 8.38 (s, 1H, Ar^C), 8.17 (d, J = 7.8 Hz, 1H, Ar^C), 7.80 (d, J = 7.8 Hz, 1H, Ar^C), 7.75 (d, J = 7.7 Hz, 1H, Ar^B), 7.42 (t, J = 7.9 Hz, 1H, Ar^C), 7.35 (d, J = 7.7 Hz, 1H, Ar^B), 4.86 (s, 1H), 0.52 (s, 6H, $SiMe_2$) ppm. ^{13}C NMR (101 MHz, $CDCl_3$) δ 162.9, 152.3, 148.7, 136.9, 133.3, 131.1, 130.7, 130.2, 129.5, 128.9, 125.7, 122.7, −1.4 ppm. HRMS (ESI, positive ion mode): calcd for $C_{15}H_{14}BBrClO_4Si^+$ $[MH]^+$ 410.9621; found 410.9621.

4.2.13 (8d) 7-Chloro-6-(4′-methylbenzoyloxy)-1,1-dimethyl-3-hydroxybenzo-1,2,3-siloxaborole. 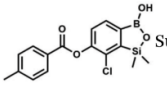 Suspension of NaH in mineral oil (60%, 0.14 g, 3.50 mmol, 2.0 eq.) under argon atmosphere was washed with anhydrous hexane (5 mL) twice and anhydrous DMF (10 mL) was added and stirred for 10 min. Then it was cooled to 0 °C and **5b** (0.5 g, 1.70 mmol, 1.0 eq.) was added. After *ca.* 30 min stirring in 0 °C, 4-toluoyl chloride (0.22 mL, 1.70 mmol, 1.0 eq.) was added to the white suspension. It was stirred for another 1.0 h at room temperature, then concentrated by a simple distillation under reduced pressure. The solid residue was treated with 1.5 M aq. H_2SO_4 to reach the pH = 2–3. The obtained white solid was filtered and washed with water (2 × 5 mL) and hexane (2 × 5 mL). Aqueous $NaHCO_3$ (5 wt% in water, 2 mL) was added and the suspension was stirred for *ca.* 30 min. The white solid product was filtered and washed with water (2 ×

2 mL). The product was dried *in vacuo*, mp 140–145 °C. Yield 0.19 g (32%). ^{1}H NMR (400 MHz, $CDCl_3$) δ 8.14 (d, J = 8.1 Hz, 2H, Ar^C), 7.75 (d, J = 7.7 Hz, 1H, Ar^B), 7.38–7.32 (m, 3H, Ar^C + Ar^B), 5.35 (s, 1H, OH), 2.47 (s, 3H, Me), 0.53 (s, 6H, $SiMe_2$) ppm. ^{13}C NMR (101 MHz, $CDCl_3$) δ 164.3, 151.9, 149.1, 131.1, 130.5, 130.2, 129.7, 129.4, 129.2, 126.01, 125.99, 21.8, −1.4 ppm. HRMS (ESI, positive ion mode): calcd for $C_{16}H_{17}BClO_4Si^+$ $[MH]^+$ 347.0672; found 347.0674.

4.2.14 (8e) 7-Chloro-6-[4′-(*tert*-butyl)benzoyloxy]-1,1-dimethyl-3-hydroxybenzo-1,2,3-siloxaborole.

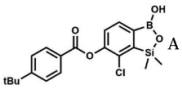

A suspension of NaH in mineral oil (60%, 0.14 g, 3.50 mmol, 2.0 eq.) under argon atmosphere was washed twice with anhydrous hexane (5 mL) and anhydrous DMF (10 mL) was added. The mixture was stirred for 10 min, cooled to 0 °C and **5b** (0.50 g, 1.70 mmol, 1.0 eq.) was added. After *ca.* 30 min stirring in 0 °C, 4-*tert*-butylbenzoyl chloride (0.34 mL, 1.70 mmol, 1.0 eq.) was added to the white suspension. It was stirred for another 1.0 h at room temperature, and concentrated by a simple distillation under reduced pressure. The solid residue was treated with 1.5 M aq. H_2SO_4 to reach the pH = 2–3. Et_2O (15 mL) and brine (10 mL) were added, and the aqueous phase was separated followed by the extraction with Et_2O (2 × 10 mL). The extracts were added to the organic phase and dried with anhydrous $MgSO_4$. Then it was concentrated under reduced pressure. The solid was filtered and washed with water (2 × 5 mL) and hexane (2 × 5 mL). Aqueous $NaHCO_3$ (5 wt%, 2 mL) was added and the suspension was stirred for *ca.* 30 min. The white solid was filtered, washed with water (2 × 2 mL) and dried *in vacuo*. Yield 0.36 g (56%). ^{1}H NMR (400 MHz, $CDCl_3$) δ 8.18 (d, J = 8.8 Hz, 2H, Ar^C), 7.76 (d, J = 7.7 Hz, 1H, Ar^B), 7.56 (d, J = 8.9 Hz, 2H, Ar^C), 7.35 (d, J = 7.7 Hz, 1H, Ar^B), 5.46 (s, 1H, OH), 1.38 (s, 9H, *t*-Bu), 0.53 (s, 6H, $SiMe_2$) ppm. ^{13}C NMR (101 MHz, $CDCl_3$) δ 164.2, 157.8, 151.9, 149.1, 131.1, 130.3, 129.7, 127.0, 126.0, 125.9, 125.7, 125.2, 35.3, 31.1, −1.4 ppm. HRMS (ESI, positive ion mode): calcd for $C_{19}H_{23}BClO_4Si^+$ $[MH]^+$: 389.1142; found 389.1142.

4.2.15 (8f) 7-Chloro-6-(4′-cyanobenzoyloxy)-1,1-dimethyl-3-hydroxybenzo-1,2,3-siloxaborole.

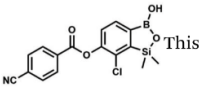

This compound was obtained using the protocol described for **8d** using suspension of NaH in mineral oil (60%, 0.14 g, 3.50 mmol, 2.0 eq.), **5b** (0.50 g, 1.70 mmol, 1.0 eq.) and 4-cyanobenzoyl chloride (0.28 g, 1.70 mmol, 1.0 eq.) as the starting materials. It was obtained as a white powder. mp 160–165 °C. Yield 0.12 g (20%). ^{1}H NMR (400 MHz, $CDCl_3$) δ 8.35 (d, J = 8.0 Hz, 2H, Ar^C), 7.85 (d, J = 8.0 Hz, 2H, Ar^C), 7.77 (d, J = 7.8 Hz, 1H, Ar^B), 7.36 (d, J = 7.7 Hz, 1H, Ar^B), 4.96 (s, 1H, *OH*), 0.52 (s, 6H, $SiMe_2$) ppm. ^{13}C NMR (101 MHz, $CDCl_3$) δ 162.7, 152.4, 148.5, 132.6, 132.5, 131.2, 130.8, 129.3, 127.7, 125.5, 117.7, 117.3, −1.4 ppm. HRMS (ESI, negative ion mode) calcd for $C_{16}H_{12}BClNO_4Si^-$ $[M - H]^-$ 356.0323; found 356.0321.

4.2.16 (8g) 7-Chloro-6-(2′,6′-dichloroisonicotinoyl)-1,1-dimethyl-3-hydroxybenzo-1,2,3-siloxaborole.

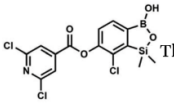

This compound was obtained using the protocol described for **6** using suspension of NaH in mineral oil (60%, 0.10 g, 2.50 mmol, 1.8 eq.), **5b** (0.4 g, 1.4 mmol, 1.0 eq.) and 2,6-dichloroisonicotinoyl chloride (0.23 mL, 1.7 mmol, 1.2 eq.) as the starting materials. It was obtained as a white powder, mp 113–114 °C. Yield 0.22 g (39%). ^{1}H NMR (400 MHz, acetone-d_6) δ 7.89 (s, 2H, Py), 7.60 (d, J = 7.8 Hz, 1H, Ar^B), 7.08 (d, J = 7.8 Hz, 1H, Ar^B), 0.43 (s, 6H, $SiMe_2$) ppm. ^{13}C NMR (101 MHz, acetone-d_6) δ 163.5, 155.2, 151.3, 144.3, 131.8, 123.3, 119.2, −1.8 ppm. HRMS (ESI, positive ion mode): calcd for $C_{14}H_{12}BCl_3NO_4Si^+$ $[MH]^+$ 401.9689; found 401.9689.

4.2.17 (9a) 7-Chloro-6-phenylsulfonyloxy-1,1-dimethyl-3-hydroxybenzo-1,2,3-siloxaborole.

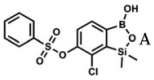

A suspension of NaH in mineral oil (60%, 0.10 g, 2.48 mmol, 2.5 eq.) under argon atmosphere was washed with anhydrous hexane (5 mL) twice and anhydrous DMF (10 mL) was added and stirred for 10 min. Then it was cooled to 0 °C and **5b** (0.5 g, 1.7 mmol, 1.0 eq.) was added. After *ca.* 30 min stirring in 0 °C, benzenesulfonyl chloride (0.24 mL, 2.0 mmol, 1.2 eq.) was added to the white suspension. It was stirred for another 1.5 h at room temperature, then it was concentrated by a simple distillation under reduced pressure and was quenched with water (5 mL) and then with 1.5 M aq. H_2SO_4 to reach the pH = 2–3. Et_2O (15 mL) and brine (10 mL) were added, then the aqueous phase was separated followed by the extraction with Et_2O (2 × 10 mL). The extracts were added to the organic phase and dried under anhydrous $MgSO_4$. Then it was concentrated under reduced pressure. Hexane (5 mL) and acetone (0.5 mL) were added to obtained oily residue and the mixture was stirred for 24 h. Then, precipitated white solid was filtered and washed with hexane (2 × 2 mL). The product was dried *in vacuo*, mp 150–152 °C. Yield 0.28 g (48%). ^{1}H NMR (400 MHz, $CDCl_3$) δ 7.93–7.89 (m, 2H, Ar^S), 7.72–7.69 (m, 1H, Ar^S), 7.66 (d, J = 7.8 Hz, 1H, ArB), 7.56–7.51 (m, 2H, Ar^S), 7.36 (d, J = 7.8 Hz, 1H, ArB), 0.44 (s, 6H, $SiMe_2$) ppm. ^{13}C NMR (101 MHz, $CDCl_3$) δ 152.7, 147.3, 135.8, 134.6, 131.2, 130.3, 129.8, 129.3, 128.8, 126.2, −1.4 ppm. ^{11}B NMR (96 MHz, $CDCl_3$) δ 30.6 ppm. HRMS (ESI, negative ion mode): calcd for $C_{14}H_{14}BClO_5SSi^-$ $[M - H]^-$ 367.0040; found 367.0039.

4.2.18 (9b) 7-Chloro-6-(2′-fluorophenylsulfonyloxy)-1,1-dimethyl-3-hydroxybenzo-1,2,3-siloxaborole.

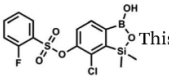

This compound was obtained using the protocol described for **9a** using suspension of NaH in mineral oil (60%, 0.14 g, 3.5 mmol, 2.0 eq.), **5b** (0.51 g, 1.8 mmol, 1.0 eq.) and 2-fluorobenzenesulfonyl chloride (0.23 mL, 1.7 mmol, 1.0 eq.) as the starting materials. It was obtained as a white powder,

mp 158–161 °C. Yield 0.30 g (45%). ^{1}H NMR (400 MHz, $CDCl_3$) δ 7.92–7.82 (m, 1H, Ar^S), 7.75–7.71 (m, 1H, Ar^S), 7.67 (d, J = 7.9 Hz, 1H, Ar^B), 7.36 (d, J = 7.9 Hz, 1H, Ar^S), 7.30 (d, J = 7.9 Hz, 1H, Ar^B), 7.28–7.26 (m, 1H, Ar^S), 0.45 (s, 6H, $SiMe_2$) ppm. ^{13}C NMR (101 MHz, $CDCl_3$) δ 159.7 (d, J = 261.3 Hz), 152.6, 147.1, 137.0 (d, J = 8.6 Hz), 131.4, 131.2 (d, J = 6.8 Hz), 129.9, 126.0, 124.4 (d, J = 4.1 Hz), 124.2 (d, J = 13.7 Hz), 117.6 (d, J = 20.9 Hz), 114.0, −1.6 ppm. ^{19}F NMR (376 MHz, $CDCl_3$) δ −100.52 (m) ppm. HRMS (ESI, negative ion mode): calcd $C_{14}H_{13}BClFO_5SSi^-$ for $[M - H]^-$ 384.9946; found 384.9949.

4.2.19 (9c) 7-Chloro-6-(4′-fluorophenylsulfonyloxy)-1,1-dimethyl-3-hydroxybenzo-1,2,3-siloxaborole.

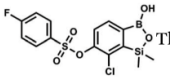

This compound was obtained using the protocol described for **9a** using suspension of NaH in mineral oil (60%, 0.14 g, 3.5 mmol, 2.0 eq.), **5b** (0.51 g, 1.8 mmol, 1.0 eq.) and 4-fluorobenzenesulfonyl chloride (0.36 g, 1.8 mmol, 1.0 eq.) as the starting materials. It was obtained as a white powder, mp 142–144 °C. Yield 0.40 g (42%). ^{1}H NMR (400 MHz, $CDCl_3$) δ 7.95–7.90 (m, 2H, Ar^S), 7.69 (d, J = 7.9 Hz, 1H, Ar^B), 7.40 (d, J = 7.9 Hz, 1H, Ar^B), 7.24–7.18 (m, 2H, Ar^S), 5.44 (s, 1H, OH), 0.45 (s, 6H, $SiMe_2$) ppm. ^{13}C NMR (101 MHz, $CDCl_3$) δ 166.4 (d, J = 257.9 Hz), 152.7, 147.2, 132.1 (d, J = 1.6 Hz), 131.7 (d, J = 9.8 Hz), 131.7, 131.4, 130.1, 126.3, 116.7 (d, J = 22.9 Hz), −1.4 ppm. ^{19}F NMR (376 MHz, $CDCl_3$) δ −101.53 to −101.67 (m) ppm. HRMS (ESI, negative ion mode): calcd for $C_{14}H_{13}BClFO_5SSi^-$ $[M - H]^-$ 384.9946; found 384.9949.

4.2.20 (9d) 7-Chloro-6-(4′-chlorophenylsulfonyloxy)-1,1-dimethyl-3-hydroxybenzo-1,2,3-siloxaborole.

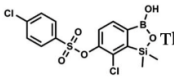

This compound was obtained using the protocol described for **9a** using suspension of NaH in mineral oil (60%, 0.20 g, 4.96 mmol, 2.0 eq.), **5b** (0.72 g, 2.48 mmol, 1.0 eq.) and 4-chlorobenzenesulfonyl chloride (0.52 g, 2.48 mmol, 1.0 eq.) as the starting materials. It was obtained as a white powder. mp 121–123 °C. Yield 0.46 g (46%). ^{1}H NMR (400 MHz, $CDCl_3$) δ 7.84 (d, J = 8.7 Hz, 2H, Ar^S), 7.69 (d, J = 7.8 Hz, 1H, Ar^B), 7.51 (d, J = 8.7 Hz, 2H, Ar^S), 7.38 (d, J = 7.8 Hz, 1H, Ar^B), 5.47 (s, 1H, OH), 0.45 (s, 6H, $SiMe_2$) ppm. ^{13}C NMR (101 MHz, $CDCl_3$) δ 152.7, 147.0, 141.4, 134.0, 131.2, 130.1, 130.0, 129.5, 126.0, −1.6 ppm. HRMS (ESI): calcd for $C_{14}H_{13}BCl_2O_5SSi$ $[M - H]^-$ 400.9650; found 400.9652.

4.2.21 (9e) 7-Chloro-6-(4′-bromophenylsulfonyloxy)-1,1-dimethyl-3-hydroxybenzo-1,2,3-siloxaborole.

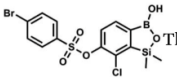

This compound was obtained using the protocol described for **9a** using suspension of NaH in mineral oil (60%, 0.20 g, 4.96 mmol, 2.0 eq.), **5b** (0.72 g, 2.48 mmol, 1.0 eq.) and 4-bromobenzenesulfonyl chloride (0.64 g, 2.48 mmol, 1.0 eq.) as the starting materials. It was obtained as a white powder, mp 108–111 °C. Yield 0.45 g (41%). ^{1}H NMR (400 MHz, $CDCl_3$) δ 7.74–7.72 (m, 2H, Ar^S), 7.69–7.66 (m, 3H, Ar^S + Ar^B), 7.38 (d, J = 7.8 Hz, 1H, Ar^B), 0.45 (s, 6H, $SiMe_2$) ppm. ^{13}C NMR (101 MHz, $CDCl_3$) δ 152.6, 147.0, 134.6, 132.5, 131.3, 130.1, 130.0, 127.8, 126.0, −1.6 ppm. HRMS (ESI): calcd for $C_{14}H_{13}BBrClO_5SSi$ $[M - H]^-$ 444.9145; found 444.9147.

4.2.22 (9f) 7-Chloro-6-(4′-iodophenylsulfonyloxy)-1,1-dimethyl-3-hydroxybenzo-1,2,3-siloxaborole.

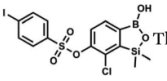

This compound was obtained using the protocol described for **9a** using suspension of NaH in mineral oil (60%, 0.20 g, 4.96 mmol, 2.0 eq.), **5b** (0.72 g, 2.48 mmol, 1.0 eq.) and 4-iodobenzenesulfonyl chloride (0.74 g, 2.48 mmol, 1.0 eq.) as the starting materials. It was obtained as a white powder, mp 112–116 °C. Yield 0.50 g (41%). ^{1}H NMR (400 MHz, $CDCl_3$) δ 7.90 (d, J = 8.7 Hz, 2H), 7.67 (d, J = 7.8 Hz, 1H), 7.59 (d, J = 8.7 Hz, 2H), 7.37 (d, J = 7.8 Hz, 1H), 0.44 (s, 6H, $SiMe_2$) ppm. ^{13}C NMR (101 MHz, $CDCl_3$) δ 152.7, 147.0, 138.5, 135.2, 131.2, 130.0, 129.8, 126.0, 102.6, −1.6 ppm. HRMS (ESI): calcd for $C_{14}H_{13}BClIO_5SSi^-$ $[M - H]^-$ 492.9006; found 492.9010.

4.2.23 (9g) 7-Chloro-6-[2′-(trifluoromethyl)phenylsulfonyloxy]-1,1-dimethyl-3-hydroxybenzo-1,2,3-siloxaborole.

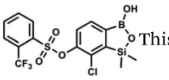

This compound was obtained using the protocol described for **9a** using suspension of NaH in mineral oil (60%, 0.14 g, 3.5 mmol, 2.0 eq.), **5b** (0.50 g, 1.8 mmol, 1.0 eq.) and 2-(trifluoromethyl)benzenesulfonyl chloride (0.26 mL, 1.7 mmol, 1.0 eq.) as the starting materials. It was obtained as a white powder, mp 160–162 °C. Yield 0.14 g (19%). ^{1}H NMR (400 MHz, $CDCl_3$) δ 8.13 (d, J = 7.3 Hz, 1H, Ar^S), 8.00 (d, J = 7.2 Hz, 1H, Ar^S), 7.84 (t, J = 7.7 Hz, 1H, Ar^S), 7.72 (t, J = 7.2 Hz, 1H, Ar^S), 7.66 (d, J = 7.9 Hz, 1H, Ar^B), 7.29 (d, J = 7.9 Hz, 1H, Ar^B), 5.26 (s, 1H, OH), 0.45 (s, 6H, $SiMe_2$) ppm. ^{13}C NMR (101 MHz, $CDCl_3$) δ 152.8, 147.2, 134.7, 134.5, 132.4, 132.2, 131.1, 129.9, 129.5 (q, J = 34.1 Hz), 128.8 (q, J = 6.1 Hz), 127.7, 126.2, 122.3 (q, J = 273 Hz), −1.6 ppm. ^{19}F NMR (376 MHz, $CDCl_3$) δ −58.11 ppm. HRMS (ESI, negative ion mode): calcd for $C_{15}H_{13}BClF_3O_5SSi^-$ $[M - H]^-$ 434.9914; found 434.9915.

4.2.24 (9h) 7-Chloro-6-[4′-(trifluoromethyl)phenylsulfonyloxy]-1,1-dimethyl-3-hydroxybenzo-1,2,3-siloxaborole.

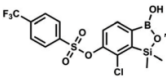

This compound was obtained using the protocol described for **9a** using suspension of NaH in mineral oil (60%, 0.14 g, 3.5 mmol, 2.0 eq.), **5b** (0.51 g, 1.8 mmol, 1.0 eq.) and 4-(trifluoromethyl)benzenesulfonyl chloride (0.43 g, 1.8 mmol, 1.0 eq.) as the starting materials. It was obtained as a white powder. Yield 0.15 g (20%). ^{1}H NMR (400 MHz, $CDCl_3$) δ 8.04 (dt, J = 8.2, 0.7 Hz, 1H, Ar^S), 7.80 (dt, J = 8.2, 0.7 Hz, 2H, Ar^S), 7.70 (d, J = 7.8 Hz, 1H, Ar^B), 7.42 (d, J = 7.9 Hz, 1H, Ar^B), 5.18 (s, 1H, OH), 0.43 (s, 6H, $SiMe_2$) ppm. ^{13}C NMR (101 MHz, $CDCl_3$) δ 152.9, 146.8, 139.1, 136.1 (q, J = 33.2 Hz), 131.3, 129.2, 126.2 (q, J = 3.8 Hz), 126.0, 125.7 (q, J = 271.7 Hz), −1.7 ppm. ^{19}F NMR (376 MHz, $CDCl_3$) δ −63.3 ppm. HRMS (ESI, negative ion mode): calcd for $C_{15}H_{13}BClF_3O_5SSi^-$ $[M - H]^-$ 434.9914; found 434.9913.

4.2.25 (9i) 7-Chloro-6-(4′-methylphenylsulfonyloxy)-1,1-dimethyl-3-hydroxybenzo-1,2,3-siloxaborole.

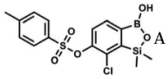

A suspension of NaH in mineral oil (60%, 0.20 g, 4.96 mmol, 2.0 eq.) under argon atmosphere was washed with anhydrous hexane (5 mL) twice and anhydrous DMF (10 mL) was added and stirred for 10 min. Then it was cooled to 0 °C and **5b** (0.72 g, 2.48 mmol, 1.0 eq.) was added. After *ca.* 30 min stirring in 0 °C, tosyl chloride (0.47 g, 2.48 mmol, 1.0 eq.) was added to the white suspension. It was stirred for another 1.5 h at room temperature, then it was concentrated by a simple distillation under reduced pressure and was quenched with water (5 mL) and then with 1.5 M aq. H_2SO_4 to reach the pH = 2–3. Et_2O (15 mL) and brine (10 mL) were added, then the aqueous phase was separated followed by the extraction with Et_2O (2 × 10 mL). The extracts were added to the organic phase and dried under anhydrous $MgSO_4$. Then it was concentrated under reduced pressure. 5% $NaHCO_3/H_2O$ (10 mL) was added to obtained oily residue and was stirred for 15 min pending the precipitation of white solid. It was filtered, washed with 1.5 M H_2SO_4 (10 mL) and washed several times with water. The product was dried *in vacuo*, mp 109–122 °C. Yield 0.98 g (96%). ^{1}H NMR (400 MHz, $CDCl_3$) δ 7.78 (d, J = 8.4 Hz, 1H, Ar^S), 7.64 (d, J = 7.8 Hz, 1H, Ar^B), 7.35–7.30 (m, 3H, Ar^S + Ar^B), 5.18 (s, 1H, OH), 2.45 (s, 3H, Me), 0.43 (s, 6H, $SiMe_2$) ppm. ^{13}C NMR (101 MHz, $CDCl_3$) δ 152.6, 147.2, 145.7, 132.6, 131.0, 130.2, 130.0, 129.7, 128.7, 128.5, 125.9, 21.7, −1.6 ppm. HRMS (ESI, negative ion mode): calcd for $C_{15}H_{16}BClO_5SSi^-$ $[M - H]^-$ 381.0197; found 381.0200.

4.2.26 (9j) 7-Chloro-6-(3′-methylphenylsulfonyloxy)-1,1-dimethyl-3-hydroxybenzo-1,2,3-siloxaborole.

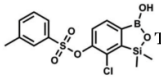

This compound was obtained using the protocol described for **9i** using suspension of NaH in mineral oil (60%, 0.20 g, 4.96 mmol, 2.0 eq.), **5b** (0.72 g, 2.48 mmol, 1.0 eq.) and 3-methylbenzenesulfonyl chloride (0.47 g, 2.48 mmol, 1.0 eq.) as the starting materials. It was obtained as a white powder, mp 116–120 °C. Yield 0.60 g (63%). ^{1}H NMR (400 MHz, $CDCl_3$) δ 7.76–7.62 (m, 3H, Ar^S + Ar^B), 7.55–7.46 (m, 1H, Ar^S), 7.41 (t, J = 7.7 Hz, 1H, Ar^S), 7.34 (d, J = 7.8 Hz, 1H, Ar^B), 2.42 (s, 3H, Me), 0.45 (s, 6H, $SiMe_2$). ^{13}C NMR (101 MHz, $CDCl_3$) δ 152.7, 147.4, 139.7, 135.6, 135.4, 131.2, 130.3, 129.1, 129.0, 126.2, 125.9, 21.4, −1.4 ppm. HRMS (ESI, negative ion mode): calcd for $C_{15}H_{16}BClO_5SSi^-$ $[M - H]^-$ 381.0197; found 381.0198.

4.2.27 (9k) 7-Chloro-6-[2′,4′,4′-trimethylphenylsulfonyloxy]-1,1-dimethyl-3-hydroxybenzo-1,2,3-siloxaborole.

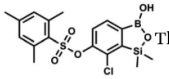

This compound was obtained using the protocol described for **9i** using suspension of NaH in mineral oil (60%, 0.20 g, 4.96 mmol, 2.0 eq.), **5b** (0.72 g, 2.48 mmol, 1.0 eq.) and 2,4,6-trimethylbenzenesulfonyl chloride (0.54 g, 2.48 mmol, 1.0 eq.) as the starting materials. It was obtained as a white powder, mp 162–169 °C. Yield 0.68 g (67%). ^{1}H NMR (400 MHz, $CDCl_3$) δ 7.59 (d, J = 7.8 Hz, 1H, Ar^B), 7.12 (d, J = 7.8 Hz, 1H, Ar^B), 7.00 (s, 2H, Ar^S), 2.61 (s, 6H, *o*-Me), 2.34 (s, 3H, *p*-Me), 0.47 (s, 6H, $SiMe_2$) ppm. ^{13}C NMR (101 MHz, $CDCl_3$) δ 152.6, 147.4, 144.1, 140.5, 131.8, 131.4, 130.9, 130.3, 125.5, 22.3, 21.1, −1.5 ppm. HRMS (ESI, negative ion mode): calcd for $C_{17}H_{20}BClO_5SSi^-$ $[M - H]^-$ 409.0510; found 409.0513.

4.2.28 (9l) 7-Chloro-6-[4′-(*tert*-butyl)phenylsulfonyloxy]-1,1-dimethyl-3-hydroxybenzo-1,2,3-siloxaborole.

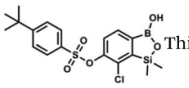

This compound was obtained using the protocol described for **9a** using suspension of NaH in mineral oil (60%, 0.20 g, 4.96 mmol, 2.0 eq.), **5b** (0.72 g, 2.48 mmol, 1.0 eq.) and 4-*tert*-butylbenzenesulfonyl chloride (0.58 g, 2.48 mmol, 1.0 eq.) as the starting materials. It was obtained as a white powder, mp 122–124 °C. Yield 0.75 g (71%). ^{1}H NMR (400 MHz, $CDCl_3$) δ 7.81–7.77 (m, 2H, Ar^S), 7.67 (d, J = 7.8 Hz, 1H, Ar^B), 7.53–7.50 (m, 2H, Ar^S), 7.40 (d, J = 7.8 Hz, 1H, Ar^B), 1.34 (s, 9H, *t*-Bu), 0.43 (s, 6H, $SiMe_2$) ppm. ^{13}C NMR (101 MHz, $CDCl_3$) δ 158.8, 152.5, 147.2, 132.3, 131.1, 130.3, 128.6, 126.2, 126.1, 35.4, 31.0, −1.6 ppm. HRMS (ESI, negative ion mode): calcd for $C_{18}H_{22}BClO_5SSi^-$ $[M - H]^-$ 423.0666; found 423.0670.

4.2.29 (9m) 7-Chloro-6-(4′-acetylphenylsulfonyloxy)-1,1-dimethyl-3-hydroxybenzo-1,2,3-siloxaborole.

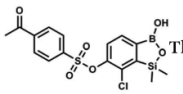

This compound was obtained using the protocol described for **9a** using suspension of NaH in mineral oil (60%, 0.20 g, 4.96 mmol, 2.0 eq.), **5b** (0.72 g, 2.48 mmol, 1.0 eq.) and 4-acetylbenzenesulfonyl chloride (0.53 g, 2.48 mmol, 1.0 eq.) as the starting materials. It was obtained as a white powder, mp 113–115 °C. Yield 0.63 g (62%). ^{1}H NMR (400 MHz, $CDCl_3$) δ 8.09 (d, J = 8.2 Hz, 2H, Ar^S), 8.01 (d, J = 8.1 Hz, 2H, Ar^S), 7.68 (d, J = 7.8 Hz, 1H, Ar^B), 7.37 (d, J = 7.9 Hz, 1H, Ar^B), 2.67 (s, 3H, MeCO), 0.43 (s, 6H, $SiMe_2$) ppm. ^{13}C NMR (101 MHz, $CDCl_3$) δ 196.6, 152.8, 147.0, 141.3, 139.4, 131.2, 129.9, 129.0, 129.0, 126.0, 26.9, −1.6 ppm. HRMS (ESI, negative ion mode): calcd for $C_{16}H_{16}BClO_6SSi^-$ $[M - H]^-$ 409.0146; found 409.0146.

4.2.30 (9n) 7-Chloro-6-(4′-methoxyphenylsulfonyloxy)-1,1-dimethyl-3-hydroxybenzo-1,2,3-siloxaborole.

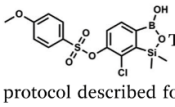

This compound was obtained using the protocol described for **9a** using suspension of NaH in mineral oil (60%, 0.20 g, 4.96 mmol, 2.0 eq.), **5b** (0.72 g, 2.48 mmol, 1.0 eq.) and 4-methoxybenzenesulfonyl chloride (0.53 g, 2.48 mmol, 1.0 eq.) as the starting materials. It was obtained as a white powder, mp 120–124 °C. Yield 0.62 g (63%). ^{1}H NMR (400 MHz, $CDCl_3$) δ 7.84–7.79 (m, 2H, Ar^S), 7.65 (d, J = 7.8 Hz, 1H, Ar^S), 7.36 (d, J = 7.9 Hz, 1H, Ar^B), 7.00–6.95 (m, 2H, Ar^S), 3.89 (s, 3H, OMe), 0.44 (s, 6H, $SiMe_2$). ^{13}C NMR (101 MHz, $CDCl_3$) δ 164.4, 152.6, 147.3, 131.0, 131.0, 127.0, 126.1, 55.8, −1.6 ppm. HRMS (ESI, negative ion mode): calcd for $C_{15}H_{16}BClO_6SSi$ $[M - H]^-$ 397.0146; found 397.0146.

4.2.31 (9o) 7-Chloro-6-(4′-nitrophenylsulfonyloxy)-1,1-dimethyl-3-hydroxybenzo-1,2,3-siloxaborole.

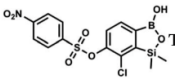

This compound was obtained using the protocol described for **9a** using suspension of NaH in mineral oil (60%, 0.20 g, 4.96 mmol, 2.0 eq.), **5b** (0.72 g, 2.48 mmol, 1.0 eq.) and 4-nitrobenzenesulfonyl chloride (0.55 g, 2.48 mmol, 1.0 eq.) as the starting materials. It was obtained as a white powder, mp 146–148 °C. Yield 0.39 g (38%). ^{1}H NMR (400 MHz, $CDCl_3$) δ 8.39 (d, J = 8.8 Hz, 2H, Ar^S), 8.12 (d, J = 8.9 Hz, 2H, Ar^S), 7.72 (d, J = 7.8 Hz, 1H, Ar^B), 7.42 (d, J = 7.9 Hz, 1H, Ar^B), 5.68 (s, 1H, OH), 0.44 (s, 6H, $SiMe_2$) ppm. ^{13}C NMR (101 MHz, $CDCl_3$) δ 152.9, 151.2, 146.7, 141.3, 131.5, 130.0, 129.6, 126.0, 124.3, 118.6, −1.6 ppm. HRMS (ESI, negative ion mode): calcd for $C_{14}H_{13}BClNO_7SSi$ $[M - H]^-$ 411.9891; found 411.9894.

4.2.32 (9p) 7-Chloro-6-(4′-chloro-3′-nitrophenylsulfonyloxy)-1,1-dimethyl-3-hydroxybenzo-1,2,3-siloxaborole.

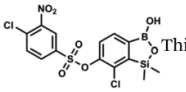

This compound was obtained using the protocol described for **9a** using suspension of NaH in mineral oil (60%, 0.20 g, 4.96 mmol, 2.0 eq.), **5b** (0.72 g, 2.48 mmol, 1.0 eq.) and 4-chloro-3-nitrobenzenesulfonyl chloride (0.63 g, 2.48 mmol, 1.0 eq.) as the starting materials. It was obtained as a white powder, mp 96–98 °C. Yield 0.55 g (50%). ^{1}H NMR (400 MHz, DMSO-d_6) δ 8.57 (dd, J = 2.0, 0.6 Hz, 1H, Ar^S), 8.11–8.05 (m, 2H, Ar^S), 7.21 (d, J = 7.7 Hz, 1H, Ar^B), 7.00 (d, J = 7.6 Hz, 1H, Ar^B), 0.13 (s, 6H, $SiMe_2$) ppm. ^{13}C NMR (101 MHz, DMSO-d_6) δ 148.6, 148.2, 142.5, 135.3, 133.9, 133.2, 132.4, 128.9, 127.7, 126.0, 124.0, 1.0 ppm. HRMS (ESI, negative ion mode): calcd for $C_{14}H_{12}BCl_2NO_7SSi$ $[M - H]^-$ 445.9501; found 445.9502.

4.2.33 (9q) 7-Chloro-6-(3′,4′-dichlorophenylsulfonyloxy)-1,1-dimethyl-3-hydroxybenzo-1,2,3-siloxaborole.

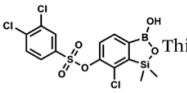

This compound was obtained using the protocol described for **9i** using suspension of NaH in mineral oil (60%, 0.20 g, 4.96 mmol, 2.0 eq.), **5b** (0.72 g, 2.48 mmol, 1.0 eq.) and 3,4-dichlorobenzenesulfonyl chloride (0.61 g, 2.48 mmol, 1.0 eq.) as the starting materials. It was obtained as a white powder, mp 95–100 °C. Yield 0.58 g (53%). ^{1}H NMR (400 MHz, $CDCl_3$) δ 7.96 (d, J = 2.2 Hz, 1H, Ar^S), 7.75–7.69 (m, 2H, Ar^S + Ar^B), 7.62 (d, J = 8.5 Hz, 1H, Ar^S), 7.40 (d, J = 7.8 Hz, 1H, Ar^B), 5.58 (s, 1H, OH), 0.46 (s, 6H, $SiMe_2$). ^{13}C NMR (101 MHz, $CDCl_3$) δ 152.8, 146.8, 139.7, 135.2, 134.0, 131.4, 131.2, 130.4, 129.8, 127.5, 126.1, 121.8, −1.6 ppm. HRMS (ESI, negative ion mode): calcd for $C_{14}H_{12}BCl_3O_5SSi$ $[M - H]^-$ 434.9261; found 434.9261.

4.2.34 (9r) 7-Chloro-6-[4′-chloro-3′-(trifluoromethyl)phenylsulfonyloxy]-1,1-dimethyl-3-hydroxybenzo-1,2,3-siloxaborole.

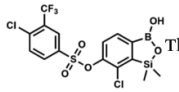

This compound was obtained using the protocol described for **9i** using suspension of NaH in mineral oil (60%, 0.20 g, 4.96 mmol, 2.0 eq.), **5b** (0.72 g, 2.48 mmol, 1.0 eq.) and 4-chloro-3-(trifluoromethyl)-benzenesulfonyl chloride (0.53 g, 2.48 mmol, 1.0 eq.) as the starting materials. It was obtained as a white powder, mp 124–126 °C. Yield 0.85 g (73%). ^{1}H NMR (400 MHz, $CDCl_3$) δ 8.18 (d, J = 2.1 Hz, 1H, Ar^S), 8.04–8.00 (m, 1H, Ar^S), 7.74–7.68 (m, 2H, Ar^S + Ar^B), 7.45 (d, J = 7.9 Hz, 1H, Ar^B), 5.09 (s, 1H, OH), 0.44 (s, 6H, $SiMe_2$) ppm. ^{13}C NMR (101 MHz, $CDCl_3$) δ 153.0, 146.7, 139.4, 134.7, 132.7, 132.6 (q, J = 14.6 Hz), 129.8 (q, J = 32.8 Hz), 129.5, 128.00 (q, J = 5.4 Hz), 124.6 (q, J = 274.3 Hz), −1.7 ppm. ^{19}F NMR (376 MHz, chloroform-d) δ −63.22 ppm. HRMS (ESI, negative ion mode): calcd for $C_{15}H_{12}BCl_2F_3O_5SSi$ $[M - H]^-$ 468.9524; found 468.9525.

4.2.35 (11a) 2-(4-Bromo-2-fluorophenoxy)-3-chloropyridine.

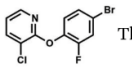

This compound was obtained using the protocol described below for **11b** using 4-bromo-2-fluorophenol (12 ml, 110 mmol, 1.1 eq.), NaOH (4.40 g, 110 mmol, 1.1 eq.) and 2,3-dichloropyridine (14.80 g, 100 mmol, 1.0 eq.) as the starting materials. However, the temperature was maintained at 150 °C during the reaction. The product was obtained as a yellow solid. mp 71–73 °C. Yield 16.6 g (55%). ^{1}H NMR (400 MHz, $CDCl_3$) δ 7.98 (dd, J = 4.9, 1.7 Hz, 1H, Py), 7.77 (dd, J = 7.7, 1.7 Hz, 1H, Py), 7.37 (dd, J = 9.6, 2.3 Hz, 1H, Ar), 7.33 (ddd, J = 8.6, 2.3, 1.3 Hz, 1H, Ar), 7.15 (dd, J = 8.5, 8.1 Hz, 1H, Ar), 6.99 (dd, J = 7.7, 4.9 Hz, 1H, Py) ppm. ^{13}C NMR (101 MHz, $CDCl_3$) δ 158.0, 154.7 (d, J = 254.1 Hz), 145.1, 140.1 (d, J = 12.2 Hz), 139.6, 128.0 (d, J = 3.8 Hz), 125.4 (d, J = 1.6 Hz), 120.6 (d, J = 21.4 Hz), 119.9, 118.47 (d, J = 2.3 Hz), 118.4 ppm. ^{19}F NMR (376 MHz, $CDCl_3$) δ −123.69 to −124.40 (m) ppm. Anal. calcd for $C_{11}H_6BrClFNO$ (302.53): C 43.67, H 2.00, N 4.63; found C 43.57, H 1.93, N 4.60.

4.2.36 (11b) 2-(4-Bromo-2-fluorophenoxy)-6-chloropyridine.

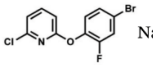

NaOH (4.40 g, 110 mmol, 1.1 eq.) was dissolved in DMSO (100 mL) in 80 °C and obtained solution was cooled to 50 °C. 4-Bromo-2-fluorophenol (12 ml, 110 mmol, 1.1 eq.) and 2,6-dichloropyridine (14.8 g, 100 mmol, 1.0 eq.) was added to the stirred solution of NaOH in DMSO in 50 °C. It was heated in 110 °C for 24 h, then it was cooled to the room temperature and AcOEt (20 mL) was added and stirred for *ca.* 20 min. It was filtered and concentrated to dryness under reduced pressure. Obtained solid was washed with water (100 mL) and it was filtered under reduce pressure. Then Et_2O (70 mL) was added and obtained suspension was filtered under reduce pressure. The filtrate was concentrated to dryness and obtained solid residue was crystallized in heptane. The light brown solid was filtered and washed several times with cold heptane. The product was dried *in vacuo*, mp 69–72 °C. Yield 20.1 g (66%). ^{1}H NMR (400 MHz, $CDCl_3$) δ 7.65 (dd, J = 8.1, 7.6 Hz, 1H, Py), 7.36 (dd, J = 9.7, 2.3 Hz, 1H, Ar), 7.30 (ddd, J = 8.6, 2.3, 1.4 Hz, 1H, Ar), 7.14–7.10 (m, 1H, Ar), 7.05 (dd, J = 7.6, 0.6 Hz, 1H, Py), 6.89 (dd, J = 8.1, 0.7 Hz, 1H, Py) ppm. ^{13}C NMR (101 MHz, $CDCl_3$) δ 161.89, 154.65 (d, J = 254.0 Hz), 148.9, 141.7, 140.0 (d, J = 11.9 Hz), 128.0 (d, J = 3.8 Hz), 125.1 (d, J =

1.8 Hz), 120.6 (d, J = 21.4 Hz), 119.1, 118.1 (d, J = 8.3 Hz), 109.0 ppm. ^{19}F NMR (376 MHz, $CDCl_3$) δ −124.50 to −124.76 (m) ppm. Anal. calcd for $C_{11}H_6BrClFNO$ (302.53): C 43.67, H 2.00, N 4.63; found C 43.53, H 1.92, N 4.58.

4.2.37 (12a) 2-[4-Bromo-3-(dimethylsilyl)-2-fluorophenoxy]-3-chloropyridine. 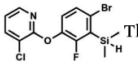 This compound was obtained using the protocol described for **3b** using **11a** (1.01 g, 3.3 mmol, 1.0 eq.), *n*-BuLi (1.6 M, 2.3 mL, 3.7 mmol, 1.1 eq.), *i*Pr_2NH (0.6 mL, 4.3 mmol, 1.3 eq.) and Me_2SiHCl (0.5 mL, 4.5 mmol, 1.4 eq.) as the starting materials. It was obtained as a yellow oil. Yield 0.87 g (73%). ^{1}H NMR (300 MHz, $CDCl_3$) δ 8.02 (dd, J = 4.9, 1.7 Hz, 1H, Py), 7.79 (dd, J = 7.7, 1.7 Hz, 1H, Py), 7.43 (dd, J = 8.5, 1.4 Hz, 1H, Ar), 7.16 (t, J = 8.5 Hz, 1H, Ar), 7.02 (dd, J = 7.7, 4.9 Hz, 1H, Py), 4.79–4.74 (m, 1H, SiH), 0.48 (dd, J = 3.9, 1.8 Hz, 6H, $SiMe_2$) ppm. ^{13}C NMR (101 MHz, $CDCl_3$) δ 158.6 (d, J = 248.4 Hz), 158.0, 145.0, 139.7 (d, J = 16.7 Hz), 139.4, 129.4 (d, J = 3.5 Hz), 127.4 (d, J = 29.4 Hz), 126.3 (d, J = 2.2 Hz), 125.8 (d, J = 10.8 Hz), 119.7, −3.2 (d, J = 4.3 Hz) ppm. ^{19}F NMR (282 MHz, $CDCl_3$) δ −110.72 to −110.80 (m) ppm. Anal. calcd for $C_{13}H_{12}BrClFNOSi$ (360.68): C 43.29, H 3.35, N 3.88; found C 43.13, H 3.28, N 3.87.

4.2.38 (12b) 2-[4-Bromo-3-(dimethylsilyl)-2-fluorophenoxy]-6-chloropyridine. 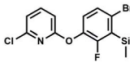 This compound was obtained using the protocol described for **3b** using **11b** (3.03 g, 10.0 mmol, 1.0 eq.), *n*-BuLi (8 M, 1.1 mL, 9.0 mmol, 0.9 eq.), *i*Pr_2NH (1.7 mL, 12.0 mmol, 1.2 eq.) and Me_2SiHCl (1.4 mL, 13.0 mmol, 1.3 eq.) as the starting materials. It was obtained as a yellow oil. Yield 3.53 g (98%). ^{1}H NMR (400 MHz, $CDCl_3$) δ 7.65 (dd, J = 8.4, 7.6 Hz, 1H, Py), 7.37 (dd, J = 8.6, 1.4 Hz, 1H, Ar), 7.11 (t, J = 8.5 Hz, 1H, Ar), 7.04 (dd, J = 7.6, 0.7 Hz, 1H, Py), 6.86 (dd, J = 8.1, 0.7 Hz, 1H, Py), 4.79–4.71 (m, 1H, SiH), 0.46 (dd, J = 4.0, 1.8 Hz, 6H, $SiMe_2$) ppm. ^{13}C NMR (101 MHz, $CDCl_3$) δ 161.8, 158.5 (d, J = 248.0 Hz), 148.8, 141.5, 139.5 (d, J = 16.4 Hz), 129.3 (d, J = 3.8 Hz), 127.4 (d, J = 29.6 Hz), 125.9 (d, J = 2.3 Hz), 125.5 (d, J = 11.0 Hz), 120.5 (d, J = 21.4 Hz), 118.8, −3.3 (d, J = 4.2 Hz) ppm. ^{19}F NMR (376 MHz, $CDCl_3$) δ −109.94 to −111.02 (m) ppm. Anal. calcd for $C_{13}H_{12}BrClFNOSi$ (360.68): C 43.29, H 3.35, N 3.88; found C 43.22, H 3.22, N 3.85.

4.2.39 (13a) 7-Fluoro-6-(3-chloropyridin-2-oxy)-1,1-dimethyl-3-hydroxybenzo-1,2,3-siloxaborole.

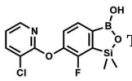 This compound was obtained using the protocol described for **4b** using **12a** (0.87 g, 2.4 mmol, 1.0 eq.), *t*-BuLi (1.9 M, 3.0 mL, 5.7 mmol, 2.4 eq.) and B(O*i*Pr)$_3$ (2.9 mL, 13.0 mmol, 5.4 eq.) as the starting materials. However, the temperature was maintained below −90 °C during the reactions. It was obtained as a yellow powder, mp 134–141 °C. Yield 0.18 g (23%). ^{1}H NMR (400 MHz, $CDCl_3$) δ 8.01 (dd, J = 4.8, 1.7 Hz, 1H, Py), 7.78 (dd, J = 7.6, 1.7 Hz, 1H, Py), 7.63 (d, J = 7.7 Hz, 1H, Ar^B), 7.36 (t, J = 7.5 Hz, 1H, Ar^B), 6.99 (dd, J = 7.7, 4.9 Hz, 1H, Py), 0.50 (s, 6H, $SiMe_2$) ppm. ^{13}C NMR (101 MHz, $CDCl_3$) δ 158.5, 155.9 (d, J = 248.5 Hz), 145.3, 142.7 (d, J = 14.9 Hz), 139.5, 137.2 (d, J = 28.2 Hz), 128.7 (d, J = 3.4 Hz), 126.7, 119.8, 118.7, −0.5. ^{19}F NMR (376 MHz, $CDCl_3$) δ −119.78 (d, J = 7.4 Hz) ppm. HRMS (ESI, negative ion mode): calcd for $C_{13}H_{11}BClFNO_3Si^-$ $[M - H]^-$ 322.0279; found 322.0282.

4.2.40 (13b) 7-Fluoro-6-(6-chloropyridin-2-oxy)-1,1-dimethyl-3-hydroxybenzo-1,2,3-siloxaborole.

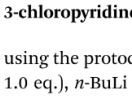 This compound was obtained using the protocol described for **4b** using **12b** (3.53 g, 9.8 mmol, 1.0 eq.), *t*-BuLi (1.9 M, 11 mL, 21.0 mmol, 2.1 eq.) and B(O*i*Pr)$_3$ (3.4 mL, 15.0 mmol, 1.5 eq.) as the starting materials. It was obtained as a pale brown solid, mp 94–104 °C. Yield 0.41 g (20%). ^{1}H NMR (400 MHz, DMSO-d_6) δ 9.35 (s, 1H, OH), 7.94 (t, J = 8.0 Hz, 1H, Py), 7.70 (d, J = 7.7 Hz, 1H, Ar^B), 7.43 (t, J = 7.6 Hz, 1H, Ar^B), 7.28 (dd, J = 7.7, 0.6 Hz, 1H, Py), 7.14 (dd, J = 8.1, 0.6 Hz, 1H, Py), 0.43 (s, 6H, $SiMe_2$) ppm. ^{13}C NMR (101 MHz, DMSO-d_6) δ 162.1, 155.5 (d, J = 246.2 Hz), 147.8, 143.80, 141.9 (d, J = 14.9 Hz), 137.0 (d, J = 28.3 Hz), 129.5 (d, J = 3.2 Hz), 126.8, 119.7, 110.1, −0.2 ppm. ^{19}F NMR (376 MHz, DMSO-d_6) δ −120.86 (d, J = 7.6 Hz) ppm. HRMS (ESI, negative ion mode): calcd for $C_{13}H_{11}BClFNO_3Si^-$ $[M - H]^-$ 322.0279; found 322.0281.

4.3. Antimicrobial activity

4.3.1 Bacterial and fungal strains and their growth conditions. The following standard strains to determine the direct antimicrobial activity were used in the study: (1) Gram-positive cocci: *Staphylococcus aureus* ATCC 6538P MSSA, *S. aureus* subsp. *aureus* ATCC 43300 MRSA, *S. epidermidis* ATCC 12228, *Enterococcus faecalis* ATCC 29212, *E. faecium* ATCC 6057, *Bacillus subtilis* ATCC 6633; (2) Gram-negative bacteria from *Enterobacteriales* order: *Escherichia coli* ATCC 25922, *Klebsiella pneumoniae* ATCC 13883, *Proteus mirabilis* ATCC 12453, *Enterobacter cloacae* DSM 6234, *Serratia marcescens* ATCC 13880; (3) Gram-negative non-fermentative rods: *Pseudomonas aeruginosa* ATCC 27853, *Acinetobacter baumannii* ATCC 19606, *Stenotrophomonas maltophilia* ATCC 12714, *S. maltophilia* ATCC 13637, *Burkholderia cepacia* ATCC 25416, *Bordetella bronchiseptica* ATCC 4617; (4) yeasts: *Candida albicans* ATCC 90028, *C. parapsilosis* ATCC 22019, *C. tropicalis* IBA 171, *C. tropicalis* (Castellani) Berkhout ATCC 750, *C. guilliermondii* IBA 155, *C. krusei* ATCC 6258 and *Saccharomyces cerevisiae* ATCC 9763.

All strains were stored at −80 °C. Prior to testing, each bacterial strain was subcultured twice on tryptic soy agar TSA (bioMerieux) medium and yeast strains on Sabouraud dextrose agar (bioMerieux) for 24–48 h at 30 °C to ensure viability.

4.3.2 Determination of antimicrobial activity. Direct antimicrobial activity against yeast, Gram-positive and Gram-negative bacterial strains was examined by the disc-diffusion test and the MIC determination assays according to the EUCAST[49,50] and CLSI[51–53] recommendations. Additionally, in the study of antimicrobial activity of new benzosiloxaboroles three following reference agents were used: fluconazole (in the case of fungi), linezolid (for Gram-positive bacteria) and nitrofurantoin (for Gram-negative rods). The MIC value of fluconazole was tested by Etest method.[54,55] Determination of MIC/MBC

values of linezolid and nitrofurantoin was done using the CLSI methods,[38,53] however, its concentration range was compatible with Etest. The solutions of all tested benzosiloxaboroles were prepared in DMSO (Sigma). The disc-diffusion test was determined on Mueller–Hinton II agar medium (MHA) (Becton Dickinson) for bacteria and on MHA supplemented with 2% glucose and 0.5 mg L^{-1} methylene blue dye (Sigma) (MHA + GMB medium) for yeasts. The MIC determination was performed in Mueller–Hinton II broth medium (MHB) (Becton Dickinson) for bacteria and in RPMI 1640 broth medium (Sigma) with 2% glucose (Sigma) for yeasts. Results of antimicrobial activity were evaluated after incubation at 35 °C for 18 h (bacteria) and 24 h (yeasts). Determination of bactericidal (MBC) and fungicidal (MFC) activity was performed according to the CLSI recommendations.[38,56]

4.3.3 Determination of the MICs of agents in the presence of PAβN. To determine the ability of the Gram-negative bacterial strains to remove newly synthesis compounds by MDR efflux pumps, the MIC values of studied agents, with or without the pump inhibitor, PAβN (20 mg L^{-1}) (Sigma) were evaluated.[45] The MIC determination was performed in MHB with 1 mM $MgSO_4$ (Sigma), using 2-fold serial dilutions, according to the CLSI guidelines[53] in order to compare these two assays. The presence of 1 mM $MgSO_4$ stabilizes the outer membrane.[44] At least a 4-fold decrease in the MIC value after the addition of PAβN was considered significant.[42,43]

4.4. Cytotoxicity studies

4.4.1 Culture method. MRC-5 pd30 human fibroblasts were cultured in MEME, Minimum Essential Medium Eagle (Sigma-Aldrich) supplemented with 10% fetal bovine serum (Sigma-Aldrich), 2 mM L-glutamine, antibiotics (100 U mL^{-1} penicillin, 100 μg mL^{-1} streptomycin, Sigma-Aldrich) and 1% non-essential amino-acids (Sigma-Aldrich). Cells were grown in 75 cm^2 cell culture flasks (Sarstedt), in a humidified atmosphere of CO_2/air (5/95%) at 37 °C.

4.4.2 MTT-based viability assay. Stock solutions of the tested compounds were prepared in DMSO, so the final concentration of vehicle was 0.5% in each case. For the cytotoxicity studies 2-fold serial dilutions were prepared in the proper medium containing 0.5% DMSO. All the experiments were performed in exponentially growing cultures. Before the treatment MRC-5 cells were trypsinized in 0.25% trypsin–EDTA solution (Sigma-Aldrich) and seeded into 96-well microplates (Sarstedt) at a density of 6×10^3 cells per well. Cells were treated with the tested compounds or DMSO (0.5%) at the appropriate concentrations 18 h after plating. After 72 h incubation with the compounds, the supernatants were discarded, and subsequently MTT stock solution (Sigma-Aldrich) was added to each well to the final concentration of 1 mg mL^{-1}. After 1 h incubation at 37 °C, water-insoluble dark blue formazan crystals were dissolved in DMSO (100 μL) (37 °C/10 min incubation). Optical densities were measured at 570 nm using BioTek microplate reader. All measurements were carried out in three replicates and the results expressed as a percent of viable cells *versus* control cells.

Author contributions

Conceptualization: S. L.; A. E. L., funding acquisition: S. L.; investigation: P. P., J. K., P. W., J. D., U. G., J. M., K. D., K. W., project administration: S. L.; supervision: S. L., A. E. L., visualization: P. P., J. K., P. W., writing – original draft – P. P., J. K., P. W., S. L., A. E. L. writing – review & editing – P. P., S. L., A. E. L.

Conflicts of interest

There are no conflicts to declare.

Acknowledgements

This work was supported by the National Science Centre (Poland) within the framework of the project DEC-UMO-2018/31/B/ST5/00210. Work implemented as a part of Operational Project Knowledge Education Development 2014–2020 cofinanced by European Social Fund (the TRIBIOCHEM interdisciplinary PhD programme (P. P)). We also acknowledge the support by the Warsaw University of Technology.

References

1 S. J. Baker, C. Z. Ding, T. Akama, Y.-K. Zhang, V. Hernandez and Y. Xia, *Future Med. Chem.*, 2009, **1**, 1275–1288.
2 B. C. Das, P. Thapa, R. Karki, C. Schinke, S. Das, S. Kambhampati, S. K. Banerjee, P. Van Veldhuizen, A. Verma, L. M. Weiss and T. Evans, *Future Med. Chem.*, 2013, **5**, 653–676.
3 G. F. S. Fernandes, W. A. Denny and J. L. Dos Santos, *Eur. J. Med. Chem.*, 2019, **179**, 791–804.
4 R. F. Barth, Mg. H Vicente, O. K. Harling, W. Kiger, K. J. Riley, P. J. Binns, F. M. Wagner, M. Suzuki, T. Aihara, I. Kato and S. Kawabata, *Radiat. Oncol.*, 2012, **7**, 146.
5 P. F. Bross, R. Kane, A. T. Farrell, S. Abraham, K. Benson, M. E. Brower, S. Bradley, J. V. Gobburu, A. Goheer, S.-L. Lee, J. Leighton, C. Y. Liang, R. T. Lostritto, W. D. McGuinn, D. E. Morse, A. Rahman, L. A. Rosario, S. L. Verbois, G. Williams, Y.-C. Wang and R. Pazdur, *Clin. Cancer Res.*, 2004, **10**, 3954–3964.
6 S. Touchet, F. Carreaux, B. Carboni, A. Bouillon and J.-L. Boucher, *Chem. Soc. Rev.*, 2011, **40**, 3895–3914.
7 D. B. Diaz and A. K. Yudin, *Nat. Chem.*, 2017, **9**, 731–742.
8 *Boronic Acids: Preparation and Applications in Organic Synthesis, Medicine and Materials, 2 Volume Set*, ed. D. G. Hall, Completely Revised Edition, Wiley, 2nd edn, 2011.
9 F. R. Bean and J. R. Johnson, *J. Am. Chem. Soc.*, 1932, **54**, 4415–4425.
10 K. Torssell, *Ark. Kemi.*, 1957, **10**, 507–511.
11 H. R. Snyder, A. J. Reedy and Wm. J. Lennarz, *J. Am. Chem. Soc.*, 1958, **80**, 835–838.
12 S. J. Baker, Y.-K. Zhang, T. Akama, A. Lau, H. Zhou, V. Hernandez, W. Mao, M. R. K. Alley, V. Sanders and J. J. Plattner, *J. Med. Chem.*, 2006, **49**, 4447–4450.
13 J. Zhang, M. Zhu, Y. Lin and H. Zhou, *Sci. China Chem.*, 2013, **56**, 1372–1381.

14 C. T. Liu, J. W. Tomsho and S. J. Benkovic, *Bioorg. Med. Chem.*, 2014, **22**, 4462–4473.
15 A. Adamczyk-Woźniak, K. M. Borys and A. Sporzyński, *Chem. Rev.*, 2015, **115**, 5224–5247.
16 A. Nocentini, C. T. Supuran and J.-Y. Winum, Benzoxaborole compounds for therapeutic uses: a patent review (2010-2018), *Expert Opin. Ther. Pat.*, 2018, **28**, 493–504.
17 J. W. Tomsho, A. Pal, D. G. Hall and S. J. Benkovic, *ACS Med. Chem. Lett.*, 2011, **3**, 48–52.
18 A. Korkegian, T. O'Malley, Y. Xia, Y. Zhou, D. S. Carter, B. Sunde, L. Flint, D. Thompson, T. R. Ioerger, J. Sacchettini, M. R. K. Alley and T. Parish, *Tuberculosis*, 2018, **108**, 96–98.
19 V. Hernandez, T. Crépin, A. Palencia, S. Cusack, T. Akama, S. J. Baker, W. Bu, L. Feng, Y. R. Freund, L. Liu, M. Meewan, M. Mohan, W. Mao, F. L. Rock, H. Sexton, A. Sheoran, Y. Zhang, Y.-K. Zhang, Y. Zhou, J. A. Nieman, M. R. Anugula, E. M. Keramane, K. Savariraj, D. S. Reddy, R. Sharma, R. Subedi, R. Singh, A. O'Leary, N. L. Simon, P. L. D. Marsh, S. Mushtaq, M. Warner, D. M. Livermore, M. R. K. Alley and J. J. Plattner, *Antimicrob. Agents Chemother.*, 2013, **57**, 1394–1403.
20 D. Ding, Y. Zhao, Q. Meng, D. Xie, B. Nare, D. Chen, C. J. Bacchi, N. Yarlett, Y.-K. Zhang, V. Hernandez, Y. Xia, Y. Freund, M. Abdulla, K.-H. Ang, J. Ratnam, J. H. McKerrow, R. T. Jacobs, H. Zhou and J. J. Plattner, *ACS Med. Chem. Lett.*, 2010, **1**, 165–169.
21 G. A. Showell and J. S. Mills, *Drug Discov. Today*, 2003, **8**, 551–556.
22 I. Steciuk, K. Durka, K. Gontarczyk, M. Dąbrowski, S. Luliński and K. Woźniak, *Dalton Trans.*, 2015, **44**, 16534–16546.
23 A. Brzozowska, P. Ćwik, K. Durka, T. Kliś, A. E. Laudy, S. Luliński, J. Serwatowski, S. Tyski, M. Urban and W. Wróblewski, *Organometallics*, 2015, **34**, 2924–2932.
24 M. Czub, K. Durka, S. Luliński, J. Łosiewicz, J. Serwatowski, M. Urban and K. Woźniak, *Eur. J. Org. Chem.*, 2017, 818–826.
25 Y. S. Kochergin, Y. Noda, R. Kulkarni, K. Škodáková, J. Tarábek, J. Schmidt and M. J. Bojdys, *Macromolecules*, 2019, **52**, 7696–7703.
26 K. Durka, A. E. Laudy, Ł. Charzewski, M. Urban, K. Stępień, S. Tyski, K. A. Krzyśko and S. Luliński, *Eur. J. Med. Chem.*, 2019, **171**, 11–24.
27 Y. Guo, G. Song, M. Sun, J. Wang and Y. Wang, *Front. Cell. Infect. Microbiol.*, 2020, **10**, 107.
28 J. Moyroud, J.-L. Guesnet, B. Bennetau and J. Mortier, *Tetrahedron Lett.*, 1995, **36**, 881–884.
29 F. Mongin and M. Schlosser, *Tetrahedron Lett.*, 1996, **37**, 6551–6554.
30 W. Li, D. P. Nelson, M. S. Jensen, R. S. Hoerner, R. Cai, R. D. Larsen and P. J. Reider, *J. Org. Chem.*, 2002, 5394–5397.
31 K. Durka, M. Urban, M. Czub, M. Dąbrowski, P. Tomaszewski and S. Luliński, *Dalton Trans.*, 2018, **47**, 3705–3716.
32 Q. Liu, Z. Lu, W. Ren, K. Shen, Y. Wang and Q. Xu, *Chin. J. Chem.*, 2013, **31**, 764–772.
33 Y. Si, S. Basak, Y. Li, J. Merino, J. N. Iuliano, S. G. Walker and P. J. Tonge, *ACS Infect. Dis.*, 2019, **5**, 1231–1238.
34 T. O'Driscoll and C. W. Crank, *Infect. Drug Resist.*, 2015, **8**, 217–230.
35 A. Prasetyoputri, A. M. Jarrad, M. A. Cooper and M. A. T. Blaskovich, *Trends Microbiol.*, 2019, **27**, 339–354.
36 H. Eagle and A. D. Musselman, *J. Exp. Med.*, 1948, **88**, 99–131.
37 European Committee on Antimicrobial Susceptibility Testing (EUCAST) Definitive Dokument E.Def. 1.2, Terminology relating to methods for the determination of susceptibility of bacteria to antimicrobial agents, *Clin. Microbiol. Infect.*, 2000, **6**, 503–508.
38 Clinical and Laboratory Standards Institute (CLSI), *Methods for determining bactericidal activity of antimicrobial agents, Approved Guideline, Document M26-A*, CLSI, 940 West Valley Road, Wayne, Pennsylvania, USA, 1999.
39 T. J. Opperman and S. T. Nguyen, *Front. Microbiol.*, 2015, **6**, 421.
40 B. Zechini and I. Versace, *Recent Pat. Anti-Infect. Drug Discovery*, 2009, **4**, 37–50.
41 A. E. Laudy, P. Osińska, A. Namysłowska, O. Zając and S. Tyski, *PLoS One*, 2015, **10**, e0119997.
42 A. E. Laudy, A. Mrowka, J. Krajewska and S. Tyski, *PLoS One*, 2016, **11**, e0147131.
43 A. E. Laudy, E. Kulińska and S. Tyski, *Molecules*, 2017, **22**, 114.
44 R. P. Lamers, J. F. Cavallari and L. L. Burrows, *PLoS One*, 2013, **8**, e60666.
45 R. Misra, K. D. Morrison, H. J. Cho and T. Khuu, *J. Bacteriol.*, 2015, **197**, 2479–2488.
46 S. Schuster, J. A. Bohnert, M. Vavra, J. W. Rossen and W. V. Kern, *Molecules*, 2019, **24**, 470.
47 M. A. Pfaller and D. J. Diekema, *Clin. Microbiol. Rev.*, 2007, **20**, 133–163.
48 J. Gong, M. Xiao, H. Wang, T. Kudinha, Y. Wang, F. Zhao, W. Wu, L. He, Y.-C. Xu and J. Zhang, *Front. Microbiol.*, 2018, **9**, 2717.
49 European Committee on Antimicrobial Susceptibility Testing (EUCAST), *Method for the determination of broth dilution MIC of antifungal agents for yeasts Document E.DEF 7.3.2*, 2020, http://www.eucast.org/.
50 European Committee on Antimicrobial Susceptibility Testing (EUCAST), *Disk diffusion method for antimicrobial susceptibility testing, Document Version 9.0*, 2021, http://www.eucast.org/.
51 Clinical and Laboratory Standards Institute (CLSI), *Method for antifungal disk diffusion susceptibility testing of yeasts, Document M44-A2*, CLSI, 940 West Valley Road, Wayne, Pennsylvania, USA, 2nd edn, 2009.
52 Clinical and Laboratory Standards Institute (CLSI), *Reference method for broth dilution antifungal susceptibility testing of yeasts, Document M27A3*, CLSI, 940 West Valley Road, Wayne, Pennsylvania, USA, 3rd edn, 2008.
53 Clinical and Laboratory Standards Institute (CLSI), *Methods for dilution antimicrobial susceptibility tests for bacteria that grow aerobically, Approved Standard, Document M07-A9*,

CLSI, 940 West Valley Road, Wayne, Pennsylvania, USA, 9th edn, 2012.
54 ETEST Application Guide, *BioMerieux*. http://www.biomerieux-usa.com/clinical/etest.
55 ETEST for Antifungal Susceptibility Testing – Research Gate, *AB BIODISK*. https://www.researchgate.net/fungal/Etest.pdf.
56 E. Cantón, J. Pemán, A. Viudes, G. Quindós, M. Gobernado and A. Espinel-Ingroff, *Diagn. Microbiol. Infect. Dis.*, 2003, **45**, 203–206.

Electronic Supplementary Material (ESI) for RSC Advances.

Supporting Information

Development of structurally extended benzosiloxaboroles – synthesis and *in vitro* biological evaluation

P. Pacholak,[a,b] J. Krajewska,[c] P. Wińska,[a] J. Dunikowska,[a] U. Gogowska,[a] J. Mierzejewska,[a] K. Durka,[a] K. Woźniak,[b] A. E. Laudy**,[c] S. Luliński*[a]

[a] *Faculty of Chemistry, Warsaw University of Technology, Noakowskiego 3, 00-664 Warsaw, Poland*

[b]*University of Warsaw, Faculty of Chemistry, Warsaw, Poland, Pasteura 1, 02-093*

[c]*Department of Pharmaceutical Microbiology, Medical University of Warsaw, Oczki 3, 02-007 Warsaw, Poland*

*Corresponding author responsible for chemical research.
Email address: sergiusz.lulinski@pw.edu.pl (S. Luliński).
**Corresponding author responsible for microbiological research.
Email address: alaudy@wp.pl (A. E. Laudy).

Keywords: benzosiloxaboroles, antifungal activity, antibacterial activity, molecular docking, efflux pump, Eagle effect

Table of content

1. NMR spectra 2
2. Single-crystal X-ray diffraction analysis 43
3. Antimicrobial activity. 46
4. Cytotoxic activity 50
5. References 53

3. Antimicrobial activity.

Table S4. The antibacterial activity of tested agents against standard Gram-positive strains.

Agent tested	MIC in mg/L [MBC in mg/L][a] (Diameter of inhibition zone in mm)					
	S. aureus **ATCC 6538P MSSA**	***S. aureus*** **ATCC 43300 MRSA**	***S. epidermidis*** **ATCC 12228**	***E. faecalis*** **ATCC 29212**	***E. faecium*** **ATCC 6057**	***B. subtilis*** **ATCC 6633[b]**
4a	NT (24)	NT (23)	NT (36)	NT (17)	NT (20)	NT (30)
4b	NT (21)	NT (21)	NT (29)	NT (15)	NT (16)	NT (26)
6	50 (24)	50 (24)	50 (26)	200 (14)	50 (17)	NT (27)
7	12.5 (22)	12.5 (22)	50 (26)	200 (14)	200 (15)	NT (30)
8a	12.5 (22)	25 [50] (22)	25 [200] (27)	50 [100] (16)	50 [200] (18)	NT (26)
8b	NT (19)	NT (18)	NT (24)	NT (16)	NT (17)	NT (23)
8c	NT (18)	NT (15)	NT (23)	NT (16)	NT (17)	NT (21)
8d	NT (23)	NT (24)	NT (24)	NT (17)	NT (19)	NT (24)
8e	NT (15)	NT (14)	NT (18)	NT (14)	NT (13)	NT (17)
8f[c]	12.5 [200] (20)	12.5 [100] (21)	12.5 [200] (19)	50 (-)	50 (12)	NT (15)
8g	100 (16)	100 (16)	100 (23)	400 (-)	400 (-)	NT (15)
9a	**1.56** [*6,25/200*][g](28)	**1.56** [*25/200*] (27)	12.5 [200] (24)	50 [400] (17)	50 (15)	NT (29)
9b	**3.12** [200] (26)	**3.12** [*12,5/200*](25)	12.5 [400] (18)	50 (-)	50 (-)	NT (16)
9c	**3.12** [*6.25/200*] (26)	**3.12** [*12,5/200*] (27)	12.5 [200] (27)	50 [400] (17)	50 (16)	NT (27)
9d[c]	**0.78** [*3.12/50*] (27)	**1,56** [*6,25/200*] (22)	**3.12** [50] (25)	12.5 [200] (16)	12.5 (15)	NT (28)
9e[d]	**1,56** [50] (26)	**1,56** [*6,25/50*] (25)	6.25 [100] (25)	12.5 [100] (17)	25 (14)	NT (26)
9f	NT (24)	NT (23)	NT (25)	NT (14)	NT (14)	NT (23)
9g[c]	**1.56** [*3.12/100*] (27)	**1,56** [*6,25/100*] (20)	6.25 [100] (26)	25 (16)	25 (17)	NT (24)
9h[d]	**0.39** [50] (28)	**1,56** [50] (26)	**3.12** [50] (22)	25 [100] (17)	25 (17)	NT (26)
9i[c]	**1.56** [*3,12/100*] (23)	**1,56** [*12,5/200*] (26)	6.25 (22)	25 (17)	25 (17)	NT (24)
9j	**1.56** [*3,12/100*] (28)	**1,56** [*12,5/200*] (25)	6.25 [200] (25)	25 [200] (17)	25 [200] (16)	NT (24)
9k[e]	**0.78** [50] (23)	**1.56** [50] (23)	**3.12** (22)	6.25 (16)	6.25 (16)	NT (21)
9l	NT (21)	NT (20)	NT (22)	NT (16)	NT (15)	NT (20)
9m	**3.12** [*6.25/200*] (18)	**3.12** [*12,5/200*] (26)	6.25 [400] (24)	50 (15)	25 (14)	NT (26)
9n	**1.56** [*6.25/400*] (29)	**1,56** [*12,5/400*] (26)	12.5 (22)	50 (16)	50 (15)	NT (29)
9o	**1.56** [50] (26)	**3,12** [50] (25)	**0.78** [50] (28)	50 (16)	12.5 (19)	NT (27)
9p	**3.12** [*12.5/50*] (23)	**3.12** [*6.25/50*] (24)	**3.12** [12.5] (22)	25 [400] (17)	25 (20)	NT (24)
9q[e]	**0.78** [*1.56/25*] (25)	**0.78** [*3.12/25*] (25)	**3.12** (25)	6.25 [50] (18)	6.25 [50] (20)	NT (24)
9r[e]	**0.39** [*0,78/25*] (25)	**0.39** [*1.56/25*] (27)	**3.12** (25)	6.25 [50] (19)	6.25 [50] (18)	NT (25)
13a	25 [200] (22)	25 [200] (22)	25 [400] (23)	100 (13)	50 (14)	NT (27)
13b[c]	25 [200] (20)	50 (22)	25 (22)	50 (15)	50 (15)	NT (24)
LIN[f]	1 [>128] (25)	2 [>128] (25)	1 [>128] (26)	2 [>128] (15)	2 [>128] (14)	NT (30)

The highest activity against Gram-positive bacteria indicated by the low MIC values (≤3.12 mg/L) is shown in boldface.

(-): The inhibition zone was not observed in the disc-diffusion method. The diameter of paper discs was 9 mm. NT: not tested. The MIC determination could not be performed, because tested substance dissolved in DMSO precipitated after implementation into the MHB (Mueller-Hinton II broth) medium.

[a] Only the MBC values ≤400 mg/L are presented.

[b] The growth type of *B. subtilis* in the MHB medium prevented reading the MIC values of tested substances.

[c] The MIC and MBC values of the substance were determined up to 200 mg/L. In the table, only the MBC values ≤200 mg/L are presented. The tested substance dissolved in DMSO precipitated after implementation into the MHB medium at a concentration above 200 mg/L.

[d] The MIC and MBC values of the substance were determined up to 100 mg/L. In the table, only the MBC values ≤100 mg/L are presented. The tested substance dissolved in DMSO precipitated after implementation into the MHB medium at a concentration above 100 mg/L.

[e] The MIC and MBC values of the substance were determined up to 50 mg/L. In the table, only the MBC values ≤50 mg/L are presented. The tested substance dissolved in DMSO precipitated after implementation into the MHB medium at a concentration above 50 mg/L.

[f] LIN, linezolid was used as a reference agent active against Gram-positive bacteria. The diameter of commercial disc containing 0.03 mg of linezolid was 6 mm; the MIC of linezolid was determined according to the CLSI recommendations. [4]

[g] The Eagle effect was observed during the determination of the MBC value of same tested agents against *S. aureus* strains. [5] The Eagle effect is shown in italic face.

Table S5. The antibacterial activity of tested agents against standard Gram-negative strains.

	MIC in mg/L [MBC in mg/L][a] / x-fold reduction of MIC in the presence of PAßN[b] (Diameter of inhibition zone in mm)										
Agent tested	***E. coli* ATCC 25922**	***K. pneumonia* ATCC 13883**	***P. mirabilis* ATCC 12453**	***E. cloacae* DSM 6234**	***S. marcescens* ATCC 13880**	***P. aeruginosa* ATCC 27853**	***S. maltophilia* ATCC 13637**	***S. maltophilia* ATCC 12714**	***A. baumannii* ATCC 19606**	***B. cepacia* ATCC 25416[c]**	***B.bronchiseptica* ATCC 4617[c]**
4a	NT (-)	NT (-)	NT (-)	NT (-)	NT (-)	NT (-)	NT (-)	NT (-)	NT (-)	NT (-)	NT (-)
4b	NT (-)	NT (-)	NT (-)	NT (-)	NT (-)	NT (-)	NT (-)	NT (-)	NT (-)	NT (-)	NT (-)
6	>400/**4** (-)	>400/2 (-)	>400 (-)	>400/2 (-)	>400 (-)	>400 (-)	400 [400]/2 (-)	400 [400]/2 (-)	>400/2 (-)	>400 (-)	>400 (-)
7	>400 (-)	>400 (-)	>400 (-)	>400 (-)	>400 (-)	>400 (-)	>400 (-)	400 (-)	>400 (-)	>400 (-)	>400 (-)
8a	>400 (-)	>400 (-)	>400 (-)	>400 (-)	>400 (-)	>400 (-)	400/2 (-)	200/2 (-)	>400/**4** (-)	>400 (-)	200 (-)
8b	NT (-)	NT (-)	NT (-)	NT (-)	NT (-)	NT (-)	NT (-)	NT (-)	NT (-)	NT (-)	NT (-)
8c	NT (-)	NT (-)	NT (-)	NT (-)	NT (-)	NT (-)	NT (-)	NT (-)	NT (-)	NT (-)	NT (-)
8d	NT (-)	NT (-)	NT (-)	NT (-)	NT (-)	NT (-)	NT (-)	NT (-)	NT (-)	NT (-)	NT (-)
8e	NT (-)	NT (-)	NT (-)	NT (-)	NT (-)	NT (-)	NT (-)	NT (-)	NT (-)	NT (-)	NT (-)
8f[d]	>200 (-)	>200 (-)	>200 (-)	>200 (-)	>200 (-)	>200 (-)	>200 (-)	>200 (-)	>200 (-)	>200 (-)	>200 (-)
8g	>400 (-)	>400/**4** (-)	>400 (-)	>400 (-)	>400 (-)	>400 (-)	400/2 (-)	400 (-)	>400 (-)	>400 (-)	400 (-)
9a	>400 (-)	>400 (-)	>400 (-)	>400 (-)	>400 (-)	>400 (-)	>400 (-)	400 (-)	>400 (-)	>400 (-)	400 (-)
9b	>400 (-)	>400 (-)	>400 (-)	>400 (-)	>400 (-)	>400 (-)	>400 (-)	>400 (-)	>400 (-)	>400 (-)	>400 (-)
9c	>400 (-)	>400 (-)	>400 (-)	>400 (-)	>400 (-)	>400 (-)	>400 (-)	400 (-)	>400 (-)	>400(-)	400 (-)
9d[d]	>200 (-)	>200 (-)	>200 (-)	>200 (-)	>200 (-)	>200 (-)	>200 (-)	>200 (-)	>200 (-)	>200 (-)	200 (-)
9e[e]	>100 (-)	>100 (-)	>100 (-)	>100 (-)	>100 (-)	>100 (-)	>100 (-)	>100 (-)	>100 (-)	>100 (-)	>100 (-)
9f	NT (-)	NT (-)	NT (-)	NT (-)	NT (-)	NT (-)	NT (-)	NT (-)	NT (-)	NT (-)	NT (-)
9g[d]	>200 (-)	>200 (-)	>200 (-)	>200 (-)	>200 (-)	>200 (-)	>200 (-)	200 (-)	>200 (-)	>200 (-)	>200 (-)
9h	>400 (-)	>400 (-)	>400 (-)	>400 (-)	>400 (-)	>400 (-)	>400 (12)	400 (-)	>400 (-)	>400 (-)	400 (-)
9i[d]	>200 (-)	>200 (-)	>200 (-)	>200 (-)	>200 (-)	>200 (-)	>200 (-)	>200 (-)	>200 (-)	>200 (-)	100 (-)
9j	>200 (-)	>200 (-)	>200 (-)	>200 (-)	>200 (-)	>200 (-)	>200 (-)	>200 (-)	>200 (-)	>200 (-)	100 (-)
9k[f]	>50 (-)	>50 (-)	>50 (-)	>50 (-)	>50 (-)	>50 (-)	>50 (-)	>50 (-)	>50 (-)	>50 (-)	>50 (-)
9l	NT (-)	NT (-)	NT (-)	NT (-)	NT (-)	NT (-)	NT (-)	NT (-)	NT (-)	NT (-)	NT (-)
9m	>400 (-)	>400 (-)	>400 (-)	>400 (-)	>400 (-)	>400 (-)	>400 (-)	>400 (-)	>400 (-)	>400 (-)	>400 (-)
9n	>400 (-)	>400 (-)	>400 (-)	>400 (-)	>400 (-)	>400 (-)	>400 (-)	>400 (-)	>400 (-)	>400 (-)	>400 (-)
9o[d]	>200 (-)	>200 (-)	>200 (-)	>200 (-)	>200 (-)	>200 (-)	>200 (-)	>200 (-)	>200 (-)	>200 (-)	>200 (-)
9p	>400 (-)	>400 (-)	>400 (-)	>400 (-)	>400 (-)	>400 (-)	>400 (-)	>400 (-)	>400 (-)	>400 (-)	100 (-)
9q[f]	>50/2 (-)	>50 (-)	>50 (-)	>50 (-)	>50 (-)	>50 (-)	>50 (-)	>50 (-)	>50 (-)	>50 (-)	50 (-)
9r[f]	>50/**4** (-)	>50 (-)	>50 (-)	>50 (-)	>50 (-)	>50 (-)	>50 (-)	>50 (-)	>50 (-)	>50 (-)	50 (-)
13a	>400 (-)	>400 (-)	>400 (-)	>400 (-)	>400 (-)	>400 (-)	>400/**4** (-)	>400/**4** (-)	>400 (-)	>400 (-)	>400 (-)

13b[d]	>200 (-)	>200 (-)	>200 (-)	>200 (-)	>200 (-)	>200 (-)	>200 (-)	>200 (-)	>200 (-)	>200 (-)	>200 (-)
Nf[f]	8 [8] (24)	32 [32] (23)	128 [>128] (9)	32 [32] (17)	128 [>128] (12)	>128 [>128] (-)	128 [>128] (-)	128 [>128] (-)	64 [128] (9)	32 [32] (12)	64 [128] (-)

PAβN , efflux pump inhibitor. The significant decreases (at least a 4-fold) in the MIC values of tested compounds after the addition of PAβN are shown in boldface. The test was performed in the MHB medium supplemented with 1 mM $MgSO_4$.

(-): The inhibition zone was not observed in the disc-diffusion method. The diameter of paper discs was 9 mm.

NT: not tested. The MIC determination could not be performed, because tested substance dissolved in DMSO precipitated after implementation into the MHB (Mueller-Hinton II broth) medium.

[a] Only the MBC values ≤400 mg/L are presented.

[b] In the table, only at least a 2-fold decrease in the MIC values of tested compounds after the addition of PAβN are presented.

[c] The growth of *B. cepacia* ATCC 25416 and *B. bronchiseptica* ATCC 4617 strains was inhibited in the MHB medium supplemented with 1 mM $MgSO_4$ and 20 mg/L PAβN.

[d] The MIC and MBC values of the substance were determined up to 200 mg/L. In the table, only the MBC values ≤200 mg/L are presented. The tested substance dissolved in DMSO precipitated after implementation into the MHB medium at a concentration above 200 mg/L.

[e] The MIC and MBC values of the substance were determined up to 100 mg/L. In the table, only the MBC values ≤100 mg/L are presented. The tested substance dissolved in DMSO precipitated after implementation into the MHB medium at a concentration above 100 mg/L.

[f] The MIC and MBC values of the substance were determined up to 50 mg/L. In the table, only the MBC values ≤50 mg/L are presented. The tested substance dissolved in DMSO precipitated after implementation into the MHB medium at a concentration above 50 mg/L.

[g] Nf, nitrofurantoin was used as a reference agent active against Gram-negative bacteria. The diameter of commercial disc containing 0.3 mg of nitrofurantoin was 6 mm; the MIC of nitrofurantoin was determined according to the CLSI recommendations. [4]

Table S6. The antifungal activity of tested agents against yeasts strains.

	MIC in mg/L [MFC in mg/L][a] (Diameter of inhibition zone in mm)						
Agent tested	***C. albicans* ATCC 90028**	***C. parapsilosis* ATCC 22019**	***C. tropicalis* IBA 171**	***C. tropicalis* ATCC 750**	***C. guilliermondii* IBA 155**	***C. krusei* ATCC 6258**	***S. cerevisiae* ATCC 9763**
4a	>400 (-)	>400 (-)	>400 (-)	>400 (-)	>400 (-)	>400 (-)	>400 (-)
4b	NT (-)	NT (12)	NT (11)	NT (-)	NT (19)	NT (-)	NT (-)
6	100 (21)	100 (18)	100 [400] (21)	200 (16)	50 [400] (30)	100 (15)	**3.12** [200] (37)
7	50 (20)	400 (-)	400 (-)	>400 (-)	200 (12)	200 (22)	**0.78** [6.25] (38)
8a	200 (-)	100 (-)	**12.5** [100] (13)	25 (15)	100 (14)	50 (-)	**0.39** [50] (26)
8b[b]	50 (-)	**12.5** (-)	**12.5** (14)	50 (13)	50 (14)	**12.5** (13)	**3.12** (20)
8c[b]	50 (-)	25 (-)	25 [50] (-)	>50 (-)	>50 (-)	**12.5** (-)	**12.5** [25] (16)
8d[b]	50 (-)	25 (12)	**3.12** (17)	**6.25** (17)	50 (-)	**12.5** (13)	**0.19** [12.5] (31)
8e[b]	>50 (-)	>50 (-)	**12.5** (-)	>50 (-)	>50 (-)	**12.5** (-)	>50 (-)
8f	100 (-)	100 (-)	200 (-)	100 (-)	50 (-)	100 (-)	50 [100] (-)
8g	>400 (-)	>400 (-)	>400 (-)	>400 (-)	>400 (-)	>400 (-)	>400 (-)
9a	>400 (-)	>400 (-)	400 (-)	400 (-)	>400 (-)	100 (-)	**0.78** [25] (22)
9b	>400 (-)	>400 (-)	400 (-)	400 (-)	400 (-)	200 (-)	**0.39** [50] (22)
9c	400 (-)	200 (-)	200 [400] (-)	400 (-)	100 (-)	50 (20)	50 [50] (21)
9d	200 (-)	100 (-)	50 [100] (-)	100 [200] (-)	25 (-)	25 [400] (17)	**12.5** [50] (20)
9e	200 (-)	100 (-)	50 [200] (-)	200 (-)	400 (-)	25 [200] (16)	**12.5** [25] (-)
9f[b]	>50 (18)	>50 (-)	>50 (-)	>50 (-)	>50 (-)	**12.5** (13)	**6.25** [25] (20)
9g	>400 (-)	>400 (-)	>400 (-)	400 (-)	>400 (-)	100 (-)	**12.5** [25] (23)
9h	200 (-)	400 (-)	100 (-)	400 (-)	>400 (-)	25 (13)	25 [50] (-)
9i	400 (-)	>400 (-)	100 (-)	400 (-)	200 (-)	100 (16)	**6.25** [50] (30)
9j	400 [400] (-)	400 (-)	100 [400] (-)	400 (-)	200 (-)	100 (-)	**1.56** [25] (34)
9k[c]	>100 (-)	>100 (-)	>100 (-)	>100 (-)	>100 (-)	50 (-)	25 [100] (15)
9l[b]	>50 (-)	>50 (-)	>50 (-)	>50 (-)	>50 (-)	>50 (-)	**0.19** [12.5] (20)
9m	>400 (-)	>400 (-)	>400 (-)	>400 (-)	>400 (-)	200 (-)	100 [100] (21)
9n	400 (-)	400 (-)	200 (-)	400 (-)	400 (-)	100 (15)	25 [50] (20)
9o	400 (-)	200 (-)	100 [400] (-)	200 (-)	>400 (-)	50 [400] (19)	50 [100] (18)
9p	100 (26)	100 (-)	50 (-)	100 (-)	>400 (-)	25 [400] (15)	25 [50] (-)
9q[c]	>100 (-)	>100 (-)	50 (-)	100 (-)	>100 (-)	25 (15)	**12.5** [50] (20)
9r[c]	>100 (-)	>100 (-)	100 (-)	>100 (-)	>100 (-)	>100 (-)	25 [50] (13)
13a	50 (-)	100 (-)	25 (16)	200 (-)	50 (-)	100 (18)	100 (16)
13b	100 (22)	200 (-)	25 (21)	100 (15)	200 (-)	100 (15)	**1.56** [50] (34)
Fl[d]	**1** (43)	**2** (32)	**0.38** (39)	**0.38** (40)	**0.75** (40)	64[e] (16)	16[f] (12)

The highest activity against yeasts indicated by the low MIC values (≤12.5 mg/L) is shown in boldface.

(-): The inhibition zone was not observed in the disc-diffusion method. The diameter of paper discs was 9 mm. NT: not tested. The MIC determination could not be performed, because tested substance dissolved in DMSO precipitated after implementation into the RPMI medium.

[a] Only the MFC values ≤400 mg/L are presented.

[b] The MIC and MFC values of the substance were determined up to 50 mg/L. In the table, only the MFC values ≤50 mg/L are presented. The tested substance dissolved in DMSO precipitated after implementation into the RPMI medium at a concentration above 50 mg/L.

[c] The MIC and MFC values of the substance were determined up to 100 mg/L. In the table, only the MFC values ≤100 mg/L are presented. The tested substance dissolved in DMSO precipitated after implementation into the RPMI medium at a concentration above 100 mg/L.

[d]FL, fluconazole was used as a reference antifungal agent; the diameter of commercial disc containing 0.025 mg of fluconazole was 6 mm; the MIC value of fluconazole was determined by the Etest method. [6]

[e] The ellipse was visible pointing the MIC value 64 mg/L, however, with macro-colonies up to concentration ≥256 mg/L. In accordance with the recommendations for Etest method, the MIC value of fluconazole against *C. krusei* can be also interpreted as ≥256 mg/L. [6,7] *C. krusei* is intrinsically resistant to fluconazole.

[f] The ellipse was visible pointing the MIC value 16 mg/L, with colonies up to concentration ≥256 mg/L. There are no recommendations for Etest method interpretation of the MIC value of fluconazole against *S. cerevisiae*. The obtained MIC 16 mg/L is in line with the published results. [8]

5. References

1 *CrysAlis Pro Software*, Oxford Diffraction Ltd, Oxford, U.K., 2010.
2 G. M. Sheldrick, *Acta Crystallogr. A*, 2008, **64**, 112–122.
3 G. M. Sheldrick, *Acta Crystallogr. Sect. C Struct. Chem.*, 2015, **71**, 3–8.
4 Clinical and Laboratory Standards Institute (CLSI), Methods for dilution antimicrobial susceptibility tests for bacteria that grow aerobically, Approved Standard, Document M07-A9, 9th ed., CLSI, 940 West Valley Road, Wayne, Pennsylvania, USA
5 A. Prasetyoputri, A. M. Jarrad, M. A. Cooper and M. A. T. Blaskovich, *Trends Microbiol.*, 2019, **27**, 339–354.
6 ETEST Application guide, BioMerieux. http://www.biomerieux-usa.com/clinical/etest
7 ETEST for antifungal susceptibility testing – research gate, AB BIODISK. https://www.researchgate.net/...fungal.../Etest.pdf,
8 M. A. Pfaller, M. Bale, B. Buschelman, M. Lancaster, A. Espinel-Ingroff, J. H. Rex and M. G. Rinaldi, *J. Clin. Microbiol.*, 1994, **32**, 1650–1653.

Kompletne *Supplementary Materials* do Publikacji O1 dostępne są pod adresem:

https://www.rsc.org/suppdata/d1/ra/d1ra04127d/d1ra04127d1.pdf

7.3. Publikacja O2

RSC Advances

PAPER

View Article Online
View Journal | View Issue

Cite this: *RSC Adv.*, 2022, **12**, 23099

Oxazoline scaffold in synthesis of benzosiloxaboroles and related ring-expanded heterocycles: diverse reactivity, structural peculiarities and antimicrobial activity†

Joanna Krajewska, [a] Krzysztof Nowicki, [b] Krzysztof Durka, [b] Paulina H. Marek-Urban, [b] Patrycja Wińska, [b] Tomasz Stępniewski, [c] Krzysztof Woźniak, [d] Agnieszka E. Laudy *[a] and Sergiusz Luliński *[b]

Two isomeric benzosiloxaborole derivatives **3a** and **5a** bearing fluorine and 4,4-dimethyl-2-oxazolin-2-yl substituents attached to the aromatic rings were obtained. Both compounds were prone to hydrolytic cleavage of the oxazoline ring after initial protonation or methylation of the nitrogen atom. The derivative **3c** featuring *N*-methylammoniumalkyl ester functionality was successfully subjected to *N*-sulfonylation and *N*-acylation reactions to give respective derivatives which demonstrates its potential for modular synthesis of structurally extended benzosiloxaboroles. Compound **5c** bearing *N*-ammoniumalkyl ester underwent conversion to a unique macrocyclic dimer due to siloxaborole ring opening. Furthermore, an unexpected 4-electron reduction of the oxazoline ring occurred during an attempted synthesis of **5a**. The reaction gave rise to an unprecedented 7-membered heterocyclic system **4a** comprising a relatively stable B–O–B–O–Si linkage and stabilized by an intramolecular N–B coordination. It could be cleaved to derivative **4c** bearing BOH and $SiMe_2OH$ groups which acts as a pseudo-diol as demonstrated by formation of an adduct with Tavaborole. Apart from the multinuclear NMR spectroscopy characterization, crystal structures of the obtained products were determined in many cases by X-ray diffraction. Investigation of biological activity of the obtained compounds revealed that derivatives **3e** and **3f** with pendant *N*-methyl arylsulfonamide groups exhibit high activity against Gram-positive cocci such as methicillin-sensitive *Staphylococcus aureus* ATCC 6538P, methicillin-resistant *S. aureus* (MRSA) ATCC 43300 as well as the MRSA clinical strains, with MIC values in the range of 3.12–6.25 mg L^{-1}. These two compounds also showed activity against *Enterococcus faecalis* ATCC 29212 and *Enterococcus faecium* ATCC 6057 (with MICs of 25–50 mg L^{-1}). The results of the antimicrobial activity and cytotoxicity studies indicate that **3e** and **3f** can be considered as potential antibacterial agents, especially against *S. aureus* MRSA.

Received 24th June 2022
Accepted 7th August 2022

DOI: 10.1039/d2ra03910a

rsc.li/rsc-advances

Introduction

Benzoxaboroles constitute one of the most extensively studied groups of boron heterocycles which contain an endocyclic B–O linkage providing high thermodynamic stabilization.[1–3] Recently, various heterocyclic organoboron compounds have attracted strong interest due to their promising properties associated with improved stability and Lewis acidity compared to analogous acyclic organoboranes.[4] Thus, they are predestined for applications in medicine as they are hydrolytically stable and resistant to oxidation in air. Benzosiloxaboroles can be regarded as silicon bioisosteres of benzoxaboroles and show analogous physicochemical and biological properties. Indeed, available data indicate that selected benzosiloxaboroles are potent antimicrobial agents. For example, simple halogenated derivatives show strong antifungal activity whilst more extended systems, especially compounds with pendant arylsulfonate $ArSO_3$ substituents were recognized as effective antibacterials, especially towards Gram-positive cocci such as *Staphylococcus aureus* (including methicillin-resistant *S. aureus*

[a]*Department of Pharmaceutical Microbiology, Medical University of Warsaw, Banacha 1 b, 02-097, Warsaw, Poland. E-mail: alaudy@wp.pl*

[b]*Warsaw University of Technology, Faculty of Chemistry, Noakowskiego 3, 00-664 Warsaw, Poland. E-mail: sergiusz.lulinski@pw.edu.pl*

[c]*GPCR Drug Discovery Lab, Research Programme on Biomedical Informatics (GRIB), Hospital del Mar Medical Research Institute (IMIM) – Department of Experimental and Health Sciences of Pompeu Fabra University (UPF), Carrer del Dr Aiguader, 88, 08003 Barcelona, Spain*

[d]*University of Warsaw, Faculty of Chemistry, Pasteura 1, 02-093 Warsaw, Poland*

† Electronic supplementary information (ESI) available. CCDC 2166283–2166291. For ESI and crystallographic data in CIF or other electronic format see https://doi.org/10.1039/d2ra03910a

strains, MRSA), *Staphylococcus epidermidis*, and *Enterococcus faecalis*.[5] In addition, a few benzosiloxaboroles were identified as effective inhibitors of KPC-2 β-lactamase responsible for resistance among clinical strains of Gram-negative rods *e.g. Klebsiella pneumoniae* towards β-lactam antibiotics, including carbapenems.[6] Other applications of benzosiloxaboroles involved chemometric differential sensing of selected sugars.[7] On the other hand, oxazolines and closely related oxazole heterocycles are useful synthons in medicinal chemistry.[8–12] Examples of boronated aryl oxazolines are rare. The synthesis of *ortho*-boronated 2-phenyl-4,4-dimethyloxazoline was reported in 1986 but it was only reported as an intermediate prone to rapid hydrolysis resulting in a 2-carboxamidophenyl boronic acid derivative.[13] However, three isomeric boronated 2-phenyl-4,4-dimethyloxazolines were successfully isolated in 2009 and used with varying success for Suzuki cross-coupling reactions.[14] Since it is known that the biological properties of benzosiloxaboroles (and benzoxaboroles) are strongly tuned by pendant structurally diverse functional groups, we embarked on the preparation and characterization of compounds comprising 4,4-dimethyl-2-oxazoline rings attached to the benzosiloxaborole scaffold. It is worth noting here that the chemistry of arylboronic derivatives bearing nitrogen-based functionalities is diverse and offers many synthetic possibilities; various systems were also tested as potential antimicrobial agents.[15–18] Since oxazolines have potential for subsequent transformations *via* ring cleavage, we also exploited this possibility in our work which gave rise to novel heterocyclic systems including derivative **4a** featuring an unprecedented 7-membered ring comprising a BOBOSi linkage. The obtained new derivatives were comprehensively characterized including by single crystal X-ray diffraction analyses. In addition, comprehensive screening of antimicrobial activity was performed in order to complement the assessment of the structure–activity relationships of benzosiloxaboroles.

Results and discussion

Synthesis and structural characterization

The synthesis of oxazoline precursors **1b** and **2b** was performed using one of the general methods (Scheme 1).[19–21] It involved conversion of 4-bromo-2-fluorobenzoic acids **1** and **2** to corresponding hydroxyamides **1a** and **2a** which involved treatment with $SOCl_2$ to give benzoyl chlorides followed by addition of 2 equiv. of 2-amino-2-methylpropan-1-ol. The intermediate amides were subjected to dehydrative cyclization using $SOCl_2$ in excess resulting in 2-aryl-4,4-dimethyl-2-oxazolines **1b** and **2b** in good yields (*ca.* 70%). In the next step, the lithiation of **1b** and **2b** occurred regioselectively at the position between fluorine and bromine using LDA/THF at −78 °C. It should be noted that the oxazoline substituent is generally recognized to act as strong *ortho*-directing group in aromatic lithiation which also provides significant thermodynamic stabilization for resulting aryllithiums.[22] However, we were pleased to find that in both studied cases the cumulated *ortho*-acidifying effect of halogens seems to prevail strongly as subsequent trapping with $Me_2Si(H)Cl$ afforded respective products **1c** and **2c**. However, it is important to control the stoichiometry as in the case of **2b** where the formation of a disilylated byproduct was observed.

The conversion of **1c** to oxazoline-substituted benzosiloxaborole **3a** was performed using a general protocol described by us previously[5] which involves the use of *t*-BuLi/Et_2O at low temperature (<−90 °C) followed by trapping of aryllithium intermediates with $B(OMe)_3$ (Scheme 2). After warming the mixture to *ca.* 0 °C, hydrolysis was initially carried out by addition of aq. NaOH which facilitates a cleavage of Si–H bonds. Subsequent neutralization with dilute aq. HCl resulted in precipitation of **3a** which was isolated as a white solid; the process should be performed under precise pH control in order to avoid oxazoline protonation. The structure of compound **3a** was confirmed by multinuclear (^1H, ^{13}C, ^{11}B, ^{19}F and ^{29}Si) NMR spectroscopy. ^{11}B NMR spectrum of **3a** shows a resonance at 30.0 ppm typical of boronic acid derivatives with trigonal planar boron atom which means that there is no tendency to self-aggregation resulting from plausible formation of N–B dative bonds.[23] ^{29}Si NMR chemical shift of 19.61 ppm is in agreement with the values reported previously for other benzosiloxaboroles.[24,25] In addition, single crystal X-ray diffraction revealed that geometric parameters of benzosiloxaborole core in **3a** are very similar to those found previously in other derivatives whilst the oxazoline ring is twisted with respect to aromatic ring by 47.3(2)° (Fig. 1). It is worth noting that discrete molecules do not produce centrosymmetric dimeric motifs due to H-bonding interactions of boronic groups which are characteristic for most boronic acids[26] and their cyclic analogues including

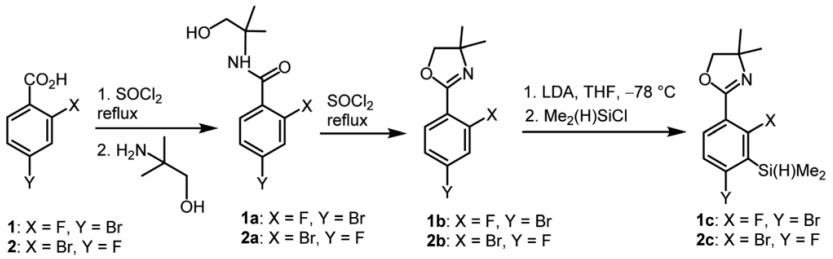

Scheme 1 Synthesis of benzosiloxaborole precursors **1c** and **2c**.

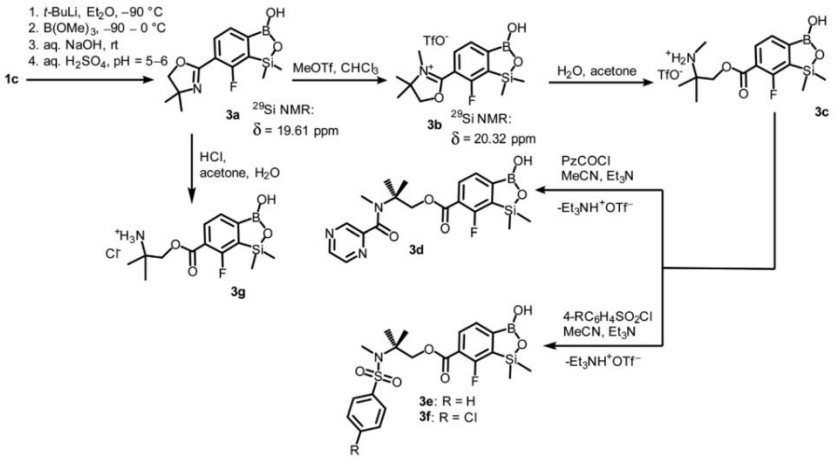

Scheme 2 Synthesis of benzosiloxaborole **3a** and its transformation to derivatives **3b–3g**.

benzoxa- and benzosiloxaboroles.[27] In contrast, the molecules are assembled by means of OH···N hydrogen bonds ($d_{O\cdots N}$ = 2.752(2) Å, $d_{H\cdots N}$ = 1.89(2) Å, $\alpha_{O-H\cdots N}$ = 169(2)°) to form infinite chains as a primary supramolecular motif (Fig. S1, ESI†).

Compound **3a** was subjected to a subsequent functionalization involving hydrolytic opening of the oxazoline ring. The process is typically initiated by alkylation or protonation of the nitrogen atom which facilitates the nucleophilic attack owing to

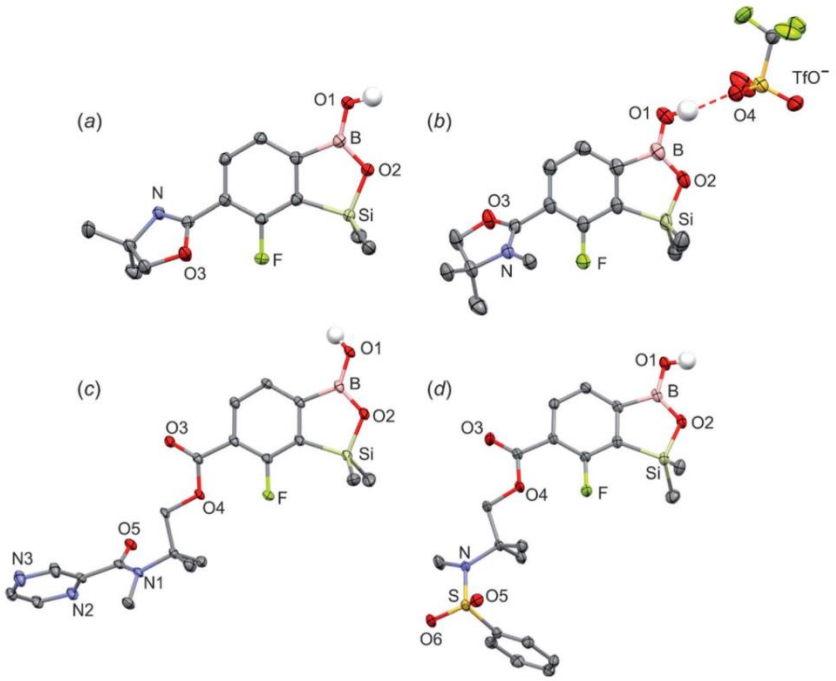

Fig. 1 The molecular structures of (a) **3a**, (b) **3b**, (c) **3d**, (d) **3e**. Thermal motions given as ADPs at the 50% probability level. C–H hydrogen atoms were omitted for clarity. HB interaction between $3b^+$ and TfO^- is marked as red dashed line.

generation of positive charge on the oxazoline ring. Thus, we treated **3a** with excess of MeOTf in chloroform which resulted in rapid precipitation of the ionic species **3b** in the form of white relatively non-hygroscopic solid which can be handled under ambient conditions. This enabled full characterization by multinuclear NMR spectroscopy and X-ray diffraction (molecular structure is shown in Fig. 1b). The comparison of ^{11}B and ^{29}Si NMR data of **3a** *vs.* **3b** shows that they are essentially unaffected by introduction of charge to the pendant oxazoline framework. The geometric parameters of the benzosiloxaborole cation of **3b** and its precursor **3a** are also very similar, although the oxazoline ring in crystal structure **3b** is inversely twisted around C–C bond with respect to **3a** molecule. The formation of hydrogen-bonded chain motif is hampered as B–OH group is arranged in HB interaction with TfO^- anion ($d_{O\cdots N} = 2.827(3)$ Å, $d_{H\cdots N} = 2.03(2)$ Å, $\alpha_{O\text{–}H\cdots N} = 160(4)^\circ$). Upon addition of water to the acetone solution of **3b**, the cleavage of the imine bond in oxazoline ring occurs readily at room temperature affording cleanly derivative **3c** which comprises ester functionality decorated with *N*-methylammonium end group. It should be noted that oxazoline ring opening occurs frequently with the formation of a respective amide functionality.[28,29] However, seminal mechanistic studies by Deslongchamps *et al.*[30,31] confirmed by further examples[32,33] showed that hydrolysis of oxazoline ring results in a respective aminoester. However, it is often prone to rapid intramolecular *N*-acylation yielding a final hydroxyamide product.[34,35] The latter reaction can be suppressed by the protonation of the nitrogen atom in the aminoester intermediate. Compound **3c** was subjected to subsequent derivatizations. Inspired by the potential of pyrazineamide motif in medicinal chemistry,[36–40] we have obtained compound **3d** by *N*-acylation of **3c** with pyrazinoyl chloride. Furthermore we have also considered the importance of sulfonamides and converted **3c** to benzosiloxaboroles **3e** and **3f**. The molecular structures of **3d** and **3e** were additionally confirmed by single crystal X-ray diffraction (Fig. 1c and d). In addition, we performed direct hydrolysis of **3a** in a mixture of acetone and 2 M aq. HCl. This resulted in the ionic product **3g** which is a close analogue of **3c**. However, subsequent acylation and sulfonylation of **3g** gave unsatisfactory results due to formation of mixtures of products which may be ascribed to a higher reactivity of NH_2 *versus* NHMe group.

When the protocol elaborated for synthesis **3a** was used for preparation of its regioisomer **5a** from **2c**, a mixture of products was obtained. Subsequent workup resulted in the isolation of an unexpected product **4a** (Scheme 3). The molecular structure of **4a** was unambiguously determined by single crystal X-ray diffraction (Fig. 2a) and represents the first example of a seven-membered ring system comprising B–O–B–O–Si linkage. It crystallizes as a racemic mixture in centrosymmetric $P2_1/c$ space group. The geometric parameters of **4a** including the B–O and Si–O bond distances are similar to those found in related systems such as boroxines and borosiloxane derivatives. The rather wide B–O–Si bond angle of 137.9(1)° is also characteristic for borosiloxane derivatives.[25] The ring features a quasi-boat conformation which implies steric non-equivalence of Si-bound methyl groups manifested by the shortest H···F contact of 2.691(2) Å for one of them *vs.* 2.907(2) Å for the second one. One of boron atoms covalently bound to aromatic carbon and two oxygen atoms is four-coordinate due to existence of another dative bond with amine nitrogen which is relatively short (1.650(2) Å) considering a family of related arylboronic azaesters.[41] The presence of B–N coordination bond is consistent with the presence of two boron-centered five-membered chelate rings. The ^{1}H NMR spectrum of **4a** is rather complicated which reflects the lack of symmetry owing to presence of the centre of chirality at the tetrahedral boron atom (Fig. 3a). As a result, multiplets of diastereotopic protons of both methylene groups as well as two separate singlets of methyl groups attached to the oxazoline ring are observed.

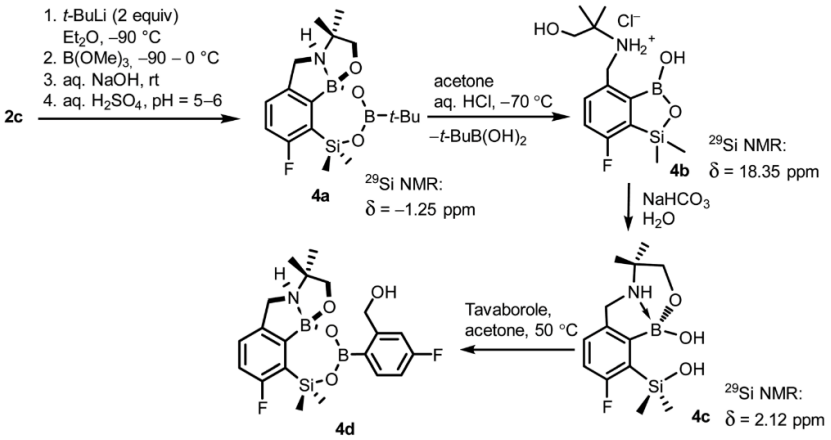

Scheme 3 Synthesis of **4a–4d** including general reaction conditions.

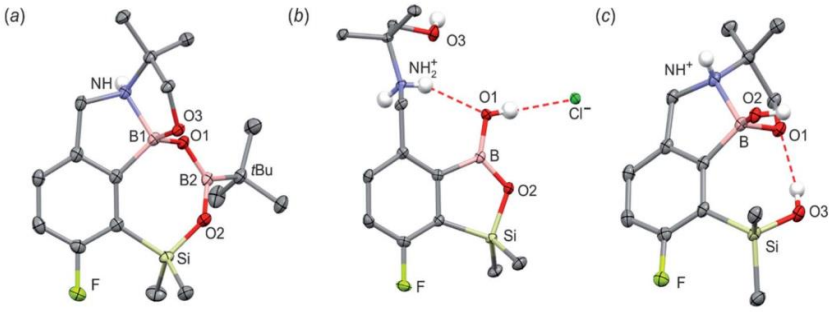

Fig. 2 The molecular structures of (a) **4a**, (b) **4b** and (c) **4c**. Thermal motions given as ADPs at the 50% probability level. C–H hydrogen atoms were omitted for clarity. HB in **4b** ($d_{N\cdots O1} = 2.961(2)$ Å, $d_{H\cdots O1} = 2.26(2)$ Å, $\alpha_{N-H\cdots O1} = 140(2)°$; $d_{O1\cdots Cl} = 3.074(1)$ Å, $d_{H\cdots Cl} = 2.24(2)$ Å, $\alpha_{O1-H\cdots Cl} = 172(2)°$) and **4c** ($d_{O3\cdots O1} = 2.826(1)$ Å, $d_{H\cdots O1} = 2.00(2)$ Å, $\alpha_{O3-H\cdots O1} = 165(2)°$) are marked as red dashed line.

Interestingly, one of Si-bound methyl group resonances is not a singlet but a doublet which can be explained by effective through-space coupling (J_{HF} = 2.8 Hz) with adjacent fluorine atom. A similar situation is observed in the ^{13}C NMR spectrum which shows a doublet at 2.0 ppm (J_{CF} = 4.0 Hz) and a singlet at 1.8 ppm. This is in line with a closer contact between one of those methyl groups and F atom observed in the molecular structure determined by X-ray crystallography. ^{11}B NMR spectrum of **4** shows two signals at 32.6 and 12.7 ppm (Fig. 3b); the latter value confirms the tetrahedral coordination of one of the boron atoms and is in the range characteristic for related arylboronic azaesters. ^{29}Si NMR chemical shift of **4a** is −1.2 ppm consistent with significantly higher shielding of silicon atom (by *ca.* 20 ppm) relative to benzosiloxaboroles. This can be explained by the release of strain at the silicon atom which is generated in five-membered heterocyclic ring of benzosiloxaboroles due to compression of Si–O–B bond angle by *ca.* 20° compared to the value observed in **4a.** In addition, it is worth noting that addition of a drop of CF_3SO_3D/D_2O to the solution of **4a** in DMSO-d_6 resulted in a strong simplification of the ^1H NMR spectrum which can be generally explained by the collapse of chirality caused by protonation of NH group with concomitant formation of the trigonal planar boron centre. However, neutralization of the solution results in regeneration of **4a** which suggests that the covalently bound scaffold of the molecule is relatively stable.

The formation of **4a** must involve 4-electron reduction of oxazoline ring. It is plausible that the process is preceded by hydride/methoxide interconversion between silicon and boron atoms in the intermediate ate complex which occurs during heating to ambient temperature. Such a process was observed previously and seems to be responsible for activation of Si–H

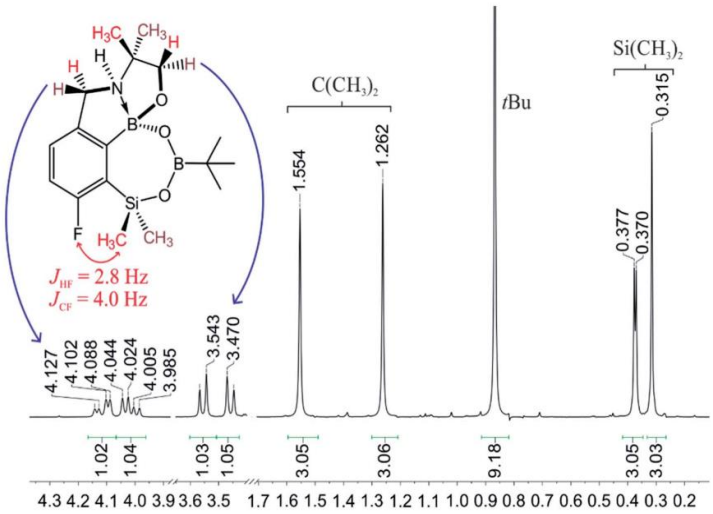

Fig. 3 The fragment of ^1H NMR spectrum of **4a** showing the signals of diastereotopic protons.

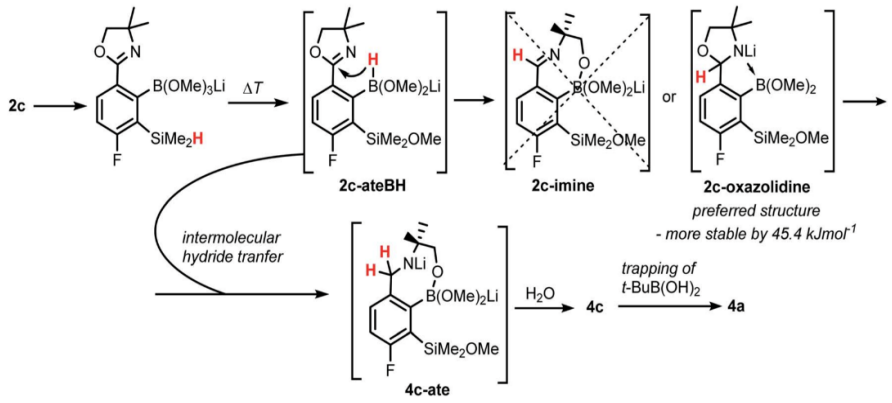

Scheme 4 Proposed mechanism of the formation of **4a** showing consecutive boron mediated hydride transfer steps from silicon to carbon atom.

bond in aryldimethylsilanes with anionic trialkoxyborate group at the *ortho* position.[42] The resulting borohydride species **2c-ateBH** undergoes an intramolecular hydride transfer to the oxazoline C2 atom. The process is somewhat related to the intramolecular hydrosilylation of cyano group to imine which was effected with Si–H bond activated by adjacent $B(OMe)_3^-$ group.[25] We considered two structures of a plausible intermediate: the first one **2c-imine** would result from expansion of the oxazoline ring initiated by the cleavage of the C–O bond. However, DFT calculations (with Me_2O molecules added to fill the coordination sphere of lithium) indicate that the reduction of the C=N bond in **2c-ateBH** leading to **2c-oxazolidine** is strongly favourable (Scheme 4). However, the efficient formation of **4a** implies that the subsequent intermolecular reduction of an intermediate (presumably **2c-oxazolidine**) with the unreacted **2c-ateBH** is strongly favourable. In other words, it seems that the initial two-electron reduction of oxazoline is the rate-limiting step which is followed by rapid conversion of an intermediate product to the benzylamine species **4c-ate**. It should be stressed that the hydride transfer to oxazoline is effective owing to its intramolecular character as an analogous process was not observed during synthesis of **3a**. The subsequent formation of **4a** comprising unprecedented 7-membered ring with B–O–B–O–Si linkage presumably occurs through a trapping of an intermediate **4c** possessing two hydroxyl groups attached to boron and silicon atoms. Such a diol-like species would combine with the molecule of *tert*-butylboronic acid which is generated from the reaction of excess of *t*-BuLi with $B(OMe)_3$. Thus, the proposed explanation is based on the known tendency of boronic acids to form cyclic esters with various dihydroxyl compounds. In addition, the structure seems to be stabilized owing to the presence of dative N–B bond and also, a hydrophobic effect of bulky *tert*-butyl group. As a result, the reverse hydrolysis process seems to be disfavored. For some analogy, cyclic boronic esters with more lipophilic diols such as pinacol are much more stable towards hydrolysis than esters with ethylene glycol. However, heating of acidic solution of **4a** in acetone/H_2O resulted in degradation 7-membered heterocycle and formation of a benzosiloxaborole framework **4b** with pendant *N*-(1-hydroxy-2-methylprop-2-yl)aminomethyl arm isolated as a hydrochloride salt. The structure of this product was confirmed by multinuclear NMR spectroscopy and single-crystal X-ray diffraction studies (Fig. 2b). Structural analysis shows that the combination of intermolecular hydrogen bond interactions involving BOH, NH_2^+ and Cl^- gives rise to infinite molecular chains (Fig. S5, ESI†) further assembled through $CH_2OH\cdots Cl^-$ HB interactions. Subsequent neutralization of **4b** with aq. $NaHCO_3$ led to the cleavage of siloxaborole ring which clearly results from preferred formation of **4c** featuring an 8-membered heterocyclic ring stabilized by an intramolecular N–B coordination ($d_{B\text{–}N} = 1.667(2)$ Å), while Si–OH group acts as a donor of intramolecular hydrogen bond interaction ($d_{O3\cdots O1} = 2.826(1)$ Å, $d_{H\cdots O1} = 2.00(2)$ Å, $\alpha_{O3\text{–}H\cdots O1} = 165(2)^\circ$, Fig. 2c). Overall, the process is analogous to chelation of boronic derivatives with various ethanolamine and diethanolamine derivatives which is well documented and used for protection of boron atom against nucleophilic attack.[43,44] The DFT calculations confirm the higher stability of **4c** over other hypothetical tautomeric structure comprising siloxaborole ring and pendant *N*-(1-hydroxy-2-methylprop-2-yl)aminomethyl arm ($\Delta G^\circ = 34.2$ kJ mol^{-1}), **4b′**, *i.e.*, the neutral form of **4b** (Fig. S10, ESI†). In addition, the dehydration of the Si–OH and B–OH group is thermodynamically disfavored ($\Delta G^\circ = 47.0$ kJ mol^{-1}) as it would generate considerable strain between both boracyclic rings. Notably, compound **4c** does not undergo dehydrative condensation of BOH and $SiMe_2OH$ which would give rise to a dimeric species as observed for a related derivative.[25] In contrast, it acts as a diol-like species and effectively traps Tavaborole to give a system **4d** comprising again the 7-membered boracylic ring (Scheme 3). Theoretical calculations show that **4c** is able to bind both aliphatic and aromatic boronic acids as well as catechol (see Scheme S1, ESI†).

In order to obtain compound **5a**, the synthetic protocol elaborated for **3a** was modified. Most importantly, the

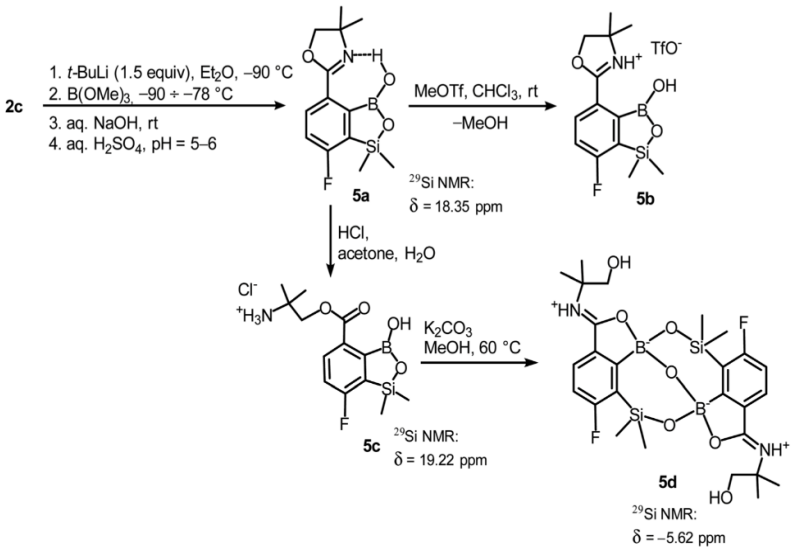

Scheme 5 Synthesis of benzosiloxaborole **5a** and its conversion to derivatives **5b–5d**.

hydrolysis of the intermediate ate complex was carried out at the low temperature (−70 °C) which prevented its transformations initiated by activation of the Si–H bond. Moreover, the amount of *t*-BuLi was reduced from 2 to 1.5 equiv. which was still sufficient to perform Br–Li exchange quantitatively. Overall, the introduced changes allowed to finally obtain **5a** in satisfactory yield (*ca.* 60%) (Scheme 5). Notably, in the ^{1}H NMR spectrum of **5a** the broad signal of BOH proton is strongly deshielded (13.5 ppm) which points to the formation of a strong intramolecular H-bond with the nitrogen atom of the oxazoline ring. **5a** is a much weaker acid ($pK_a = 9.5$ in H_2O/MeOH, 1 : 1) compared to other benzosiloxaboroles.[6] It should be noted that the acidity of the isomeric compound **3a** is relatively high; the pK_a of 5.8 falls within the range characteristic for various benzosiloxaboroles bearing the formyl group instead of 4,4-dimethyloxazolin-2-yl substituent which would indicate that both substituents exert a similar acidifying effect on the boron atom. The low acidity of **5a** can be ascribed to the destabilization of the anionic $B(OH)_2O^-$ group by the adjacent bulky oxazoline ring. Moreover, the neutral form of **5a** gains additional stabilization owing to the strong intramolecular hydrogen bond. Accordingly, the theoretical calculations performed at M062X/6-311++G(d,p) level of theory confirms the higher stability of **5a** with respect to its **3a** isomer (ΔG° = 35.3 kJ mol^{-1}). This trend is also preserved for the pair of corresponding anions **5a-OH**$^-$ and **3a-OH**$^-$, although the free enthalpy difference is smaller ($\Delta G^\circ = 15.3$ kJ mol^{-1}). Finally, the DFT calculations of the standard free enthalpy of OH^- binding to boron centres ΔG_{OH}° are in line with acidity levels of both isomers as the ΔG_{OH}° value for **3a** is more negative than for **5a** (−115.4 *vs.* −99.0 kJ mol^{-1}).

Unlike the case of **3a**, the methylation of oxazoline ring in **5a** with MeOTf failed resulting in the isolation of the stable salt **5b** with protonated nitrogen atom. Presumably, methylation of oxygen atom of B–OH group is preferred in this case as its nucleophilic character is enhanced due to participation in the aforementioned OH···N hydrogen bond. The BOMe moiety in a resulting cationic species is readily hydrolyzed to regenerate BOH group. The structure **5b** was confirmed by single crystal X-ray diffraction showing the formation of ion-pair through B–OH···$^-$OTf hydrogen bond ($d_{O1\cdots O4}$ = 2.661(3) Å, $d_{H\cdots O4}$ = 1.87(2) Å, $\alpha_{O1-H\cdots O4} = 155(2)^\circ$) as it was observed in case of **3b**, and intramolecular hydrogen bond interaction between NH proton and B(OH) group acting as donor and acceptor of HB (Fig. 4a), respectively ($d_{N\cdots O1}$ = 2.638(5) Å, $d_{H\cdots O1}$ = 1.81(2) Å, $\alpha_{N-H\cdots O1} = 155(2)^\circ$). The facile hydrolytic cleavage of the oxazoline ring in **5a** was accomplished by the addition of aq. HCl in acetone giving rise to the ammonium salt **5c**, *i.e.*, the analogue of **3g**. Unfortunately, subsequent derivatizations with sulfonamide or carboxamide end groups were not effective due to low selectivity. In contrast, **5c** underwent a clean intramolecular aminolysis of ester group to give the hydroxyamide derivative **5d**. Single crystal X-ray diffraction revealed a unique dimeric structure formed by means of two covalent B–O–Si linkages (the bond angles of 131.3(1)° and 134.2(1)°, Fig. 4b). Thus, the central part of the molecule comprises two seven-membered rings fused through the B–O–B linkage with bond angle of 113.5(1)°. The structure is additionally stabilized by strong dative O–B bonds (d_{O-B} = 1.597–1.602 Å) owing to the intramolecular coordination with amide groups. The tetrahedral character of the boron atoms is retained in solution as confirmed by ^{10}B NMR chemical shift of 9.9 ppm. It is also worth noting that the signal in the ^{29}Si NMR spectrum of **5d** is strongly shifted upfield ($\delta = -5.62$ ppm) relative to that recorded for **5c** ($\delta = 19.22$ ppm) which clearly reflects the release of ring strain characteristic for the latter compound.

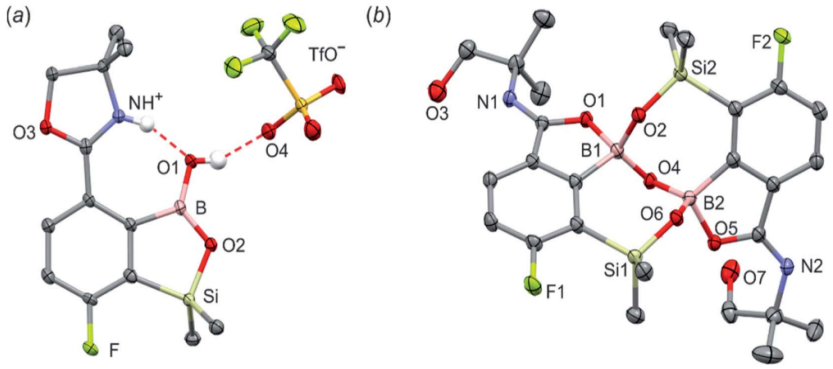

Fig. 4 The molecular structures of **5b** (a) and **5d** (b). Thermal motions given as ADPs at the 50% probability level. C–H hydrogen atoms were omitted for clarity. HBs are marked as red dashed lines.

Antimicrobial activity

As a part of our ongoing studies on the antimicrobial potential of benzosiloxaboroles and related heterocycles we performed comprehensive screening of activity of obtained compounds towards selected bacteria and fungi strains. The obtained results (Tables S5–S7, ESI†) indicate that the most of tested compounds were moderately active against Gram-positive bacteria including *Staphylococcus aureus* and *Staphylococcus epidermidis*. The only exception were the compounds **3e** and **3f** that showed high activity against Gram-positive cocci such as methicillin-sensitive *S. aureus* (MSSA) ATCC 6538P, methicillin-resistant *S. aureus* (MRSA) ATCC 43300 as well as the MRSA clinical strains, with the minimal inhibitory concentration (MIC) values in the range of 3.12–6.25 mg L^{-1} (Tables 1 and 2). Moreover, it has been observed that both compounds were potentially active also against *E. faecalis* ATCC 29212 and *Enterococcus faecium* ATCC 6057 (MICs range 25–50 mg L^{-1}) (Table 1). Structure–activity relationships for **3d–3f** shows that the sulfonamide moiety is mainly responsible for biological activity whilst the additional substitution of the pendant aryl ring with chlorine (**3f**) did not significantly increase the antimicrobial activity. The MIC values of **3e** and **3f** were from 16- to 32-fold lower than the MICs of compound **3d** for all *S. aureus* strains. Recently, we demonstrated high activity of arylsulfonate derivatives of benzosiloxaboroles against Gram-positive cocci including MRSA ATCC 43300 (MICs in the range of 0.39–6.25 mg L^{-1}) and *Enterococcus* spp. (MICs range 6.25–50 mg L^{-1}).[5] As the reference substance for the determination of the activity against Gram-positive cocci we used linezolid (LIN) which belongs to the relatively new group of antibacterial drugs – oxazolidinones. It is used for treatment of severe infections caused by multi-drug resistant cocci including MRSA strains.[45] The most promising compounds **3e** and **3f**, showed 3- to 6-fold less activity than LIN against MRSA. It should be emphasized that, according to the CLSI recommendation from 2022, the cut-off points for the MIC values determining the susceptibility of clinical *S. aureus* strains to LIN are ≤4 mg L^{-1} for susceptible strains and ≥8 mg L^{-1} for resistant ones.[46] Thus, the new compounds **3e** and **3f** show promising activity against *S. aureus* strains, including MRSA.

Furthermore, examining the antibacterial activity of new compounds also the minimal bactericidal concentration (MBC)

Table 1 The antibacterial activity of agents **3a** and **3d–3f** against standard Gram-positive strains[a]

	MIC[b] [MBC], mg L^{-1} (diameter of inhibition zone in mm)					
Agent tested	*S. aureus* ATCC 6538P MSSA	*S. aureus* ATCC 43300 MRSA	*S. epidermidis* ATCC 12228	*E. faecalis* ATCC 29212	*E. faecium* ATCC 6057	*B. subtilis* ATCC 6633[c]
3a	50 [100] (21)	50 (21)	50 [200] (18)	>400 (—)	>400 (—)	NT (20)
3d	200 [400] (15)	200 [400] (14)	400 (—)	>400 (—)	200 (—)	NT (13)
3e	**6.25** (28)	**6.25** (26)	12.5 (19)	50 (—)	25 (—)	NT (20)
3f	**3.12** [400] (25)	**6.25** (22)	12.5 (16)	25 (13)	25 (15)	NT (22)
LIN[d]	1 [>128] (25)	2 [>128] (25)	1 [>128] (26)	2 [>128] (15)	2 [>128] (14)	NT (30)

[a] The highest activity against Gram-positive bacteria indicated by the low MIC values (≤6.25 mg L^{-1}) is shown in boldface. (—): the inhibition zone was not observed in the disc-diffusion method. The diameter of paper discs was 9 mm. [b] Only the MBC values ≤400 mg L^{-1} are presented. [c] The growth type of *B. subtilis* in the MHB medium prevented reading the MIC values of tested substances. [d] Linezolid (LIN) was used as a reference agent active against Gram-positive bacteria. The diameter of commercial disc containing 0.03 mg of LIN was 6 mm; the MIC of linezolid was determined according to the CLSI recommendations.[47]

Table 2 The antibacterial activity of agents **3a** and **3d–3f** against methicillin-resistant *S. aureus* clinical strains[a]

	MIC[b] [MBC], mg L^{-1}				
	NMI 664K	NMI 1576K	NMI 1712K	NMI 1991K	NMI 2541K
3a	100	100	100	100	100
3d	200	100 [200]	200 [200]	200	100 [400]
3e	**6.25** [*6.25/>400*][c]	**6.25** [*6.25/>400*]	**6.25** [*25/>400*]	**6.25**	**6.25** [*25/>400*]
3f	**6.25**	**3.12** [*6.25/400*]	**6.25** [*12.5/400*]	**6.25**	**6.25**
LIN[d]	1 [>128]	1 [>128]	1 [>128]	1 [>128]	1 [>128]

[a] The highest activity against Gram-positive bacteria indicated by the low MIC values (≤6.25 mg L^{-1}) is shown in boldface. (—): The inhibition zone was not observed in the disc-diffusion method. The diameter of paper discs was 9 mm. [b] Only the MBC values ≤400 mg L^{-1} are presented. [c] The Eagle effect was observed during the determination of the MBC value of same tested agents against *S. aureus* strains.[48] The Eagle effect is shown in italic face. [d] Linezolid (LIN) was used as a reference agent active against Gram-positive bacteria. The diameter of commercial disc containing 0.03 mg of LIN was 6 mm; the MIC of LIN was determined according to the CLSI recommendations.[47]

was determined. In the case of **3e** and **3f**, a paradoxical growth effect, *i.e.*, the two MBC values, was observed for *S. aureus* clinical strains (Table 2). This paradoxical re-increase in the number of observed colonies during the determination of bactericidal activity is called Eagle effect and has been previously reported for several antibiotics.[48] Some previously reported arylsulfonate-substituted benzosiloxaboroles also showed exhibit this Eagle effect.[5] The first lowest MBC values of **3e** and **3f** compounds determined according to CLSI recommendations were 6.25–25 mg L^{-1}. However, on the plates with samples taken from the wells containing progressively increasing the agent concentrations (from 2- to 4-fold over the first MBC values), a significant increase in the number of growing colonies, as a paradoxical growth effect, was observed. Finally the second MBC value (≥400 mg L^{-1}) was revealed. So far, the causes of the Eagle effect have not yet been fully elucidated in *in vivo* studies in an animal models.[48] However, there have been reports of therapeutic cases in which a reduction in antibiotic doses resulted in a reduction of bacteria in bloodstream and, consequently, curing patients.[48]

In general, no activity was observed against the Gram-negative rods and yeasts, the MIC values were above the solubility limit of tested compounds (≥400 mg L^{-1}, Tables S6 and S7, ESI†). Exceptionally, compound **4d** demonstrated the activity against yeasts *Candida* spp. (the MIC value ranges were 3.12–12.5 mg L^{-1}) and against Gram-negative bacteria from *Enterobacterales* as well as from Gram-negative non-fermentative rods (MICs 25–100 mg L^{-1}). Compound **4d** can be regarded as a conjugate of the pseudo-diol **4c** and the well-known Tavaborole. Food and Drug Administration (FDA) approved in 2014 Tavaborole (trade name *Kerydin*) for the treatment of onychomycosis – a fungal infection of the nail and nail bed.[2] In this study, we also observed the activity of Tavaborole against Gram-positive cocci (MICs 12.5–200 mg L^{-1}) and non-fermentative Gram-negative rods (MICs 6.25–400 mg L^{-1}) and from the order of *Enterobacterales* (MICs 6.25–100 mg L^{-1}). Data concerning the following strains: *S. aureus* MSSA, MRSA, *S. epidermidis*, *E. faecalis*, *E. faecium*, *Escherichia coli* and *Pseudomonas aeruginosa*, are in agreement with data presented for Tavaborole in FDA document.[49] Unfortunately, inspection of antimicrobial activity data for **4c**, **4d** and Tavaborole (Table S8, ESI†) points to a decrease in activity of **4d** against all tested strains of bacteria and yeast compared to Tavaborole which is consistent with the lack of any synergistic effect which might potentially result from combination of two organoboron building blocks.

In the case of Gram-negative rods, one of the most likely causes of resistance to new compounds as well as to the active substances of the drugs used is their active removal through membrane pump systems.[5,6,24,50] The multidrug (MDR) efflux pumps are widespread in Gram-negative rods. The biggest problem is the resistance–nodulation–division (RND) efflux systems which have a wide substrate range.[51] To assess the role of efflux systems in resistance of Gram-negative rods to new compounds the RND efflux pump inhibitor, phenylalanine–arginine β-naphthylamide (PAβN), was used.[52] No significant (at least 4-fold) decrease in the MIC values of the new benzosiloxaborole derivatives tested in the presence of the inhibitor PAβN was observed (Table S6, ESI†). The obtained results firmly confirm the lack of activity of the new compounds against Gram-negative rods.

In addition, cytotoxicity studies were conducted for compounds **3d–3f** as well as their precursor **3b**. We tested viability of MRC-5 pd30 human fibroblasts after 72 h treatment with the compounds used in the concentration range of 0.78–50 mg L^{-1}. The most cytotoxic compound, *i.e.*, **3f** reduced viability of cells more than 80%, whereas the least cytotoxic compounds, *i.e.*, **3b** and **3d** decreased cell viability by about 30% at the highest concentration (for details, see Table S9, ESI†). Moreover, the compounds **3e** and **3f** were not cytotoxic at the concentration close to their MICs for *S. aureus*, *i.e.*, 3.12–6.25 mg L^{-1}.

Structural insights into the antibacterial activity of benzosiloxaboroles

Although promising antibacterial activity results have been obtained for compounds **3e** and **3f**, the mechanism of their action on the bacteria remains unclear. However, there are more and more reports indicating that molecular target for the benzoxaboroles is leucyl-tRNA synthetase (LeuRS) and the inhibition of this enzyme is based on the oxaborole tRNA-trapping mechanism so-called OBORT mechanism.[53–57] This

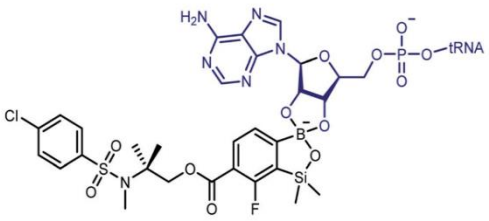

Scheme 6 Chemical structure of the covalent adduct between oxaborole and the terminal AMP of tRNA on the example of benzosiloxaborole **3f**.

mechanism presupposes the formation of a stable $tRNA^{Leu}$–oxaborole adduct in which the boron atom forms two covalent bonds with the 2′- and 3′-oxygen atoms of the ribose of the terminal 3′ tRNA adenosine in the LeuRS editing site (Scheme 6). It leads to trapping of the enzyme-bound $tRNA^{Leu}$ and thus to the prevention of catalytic turnover of leucine and consequently inhibition of protein synthesis.[58–60] Considering the similarity of benzosiloxaboroles and benzoxaboroles it is tempting to speculate that both compound families share their antibacterial mechanism. In support of this hypothesis, investigated benzosiloxaboroles display rather bacteriostatic than bactericidal character which is in line with the characteristics of the OBORT mechanism. Following this assumption, we modelled the AMP covalent adducts of **3a**, **3d**–**3f**, with the putative molecular target, to try and identify properties of the ligand–target complex, that could help us better understand the differences in bacteriostatic activity.

We modelled the *S. aureus* MRSA leucyl-tRNA synthetase (*Sa*LeuRS) structure based on the crystal structure of the *T. thermopilus* LeuRS (*Tt*LeuRS) with an adduct of AMP and a closely related antibacterial benzoxaborole locked in the editing site (PDB code: 2V0C).[60] The sequence of the modelled protein was derived from NCBI GenBank[61,62] (sequence similarity to template 68.7%). Each ligand was studied as an AMP adduct in order to mimic a terminus of the trapped tRNA which is a common practice for molecular modelling studies concerning the OBORT mechanism.[54,63,64] Afterwards, the AMP adducts of each of the studied compounds were placed in the enzyme editing site, using coordinates of the crystallized ligand. The resulting complexes were then minimized, using the internal protocol available in MOE.[65] The obtained complexes allow us to appreciate how in all adducts, the AMP moiety is stabilized by multiple polar interactions with the protein, *i.e.*, T247, Y331, R345, K408 (Fig. 5a–d). Interestingly when

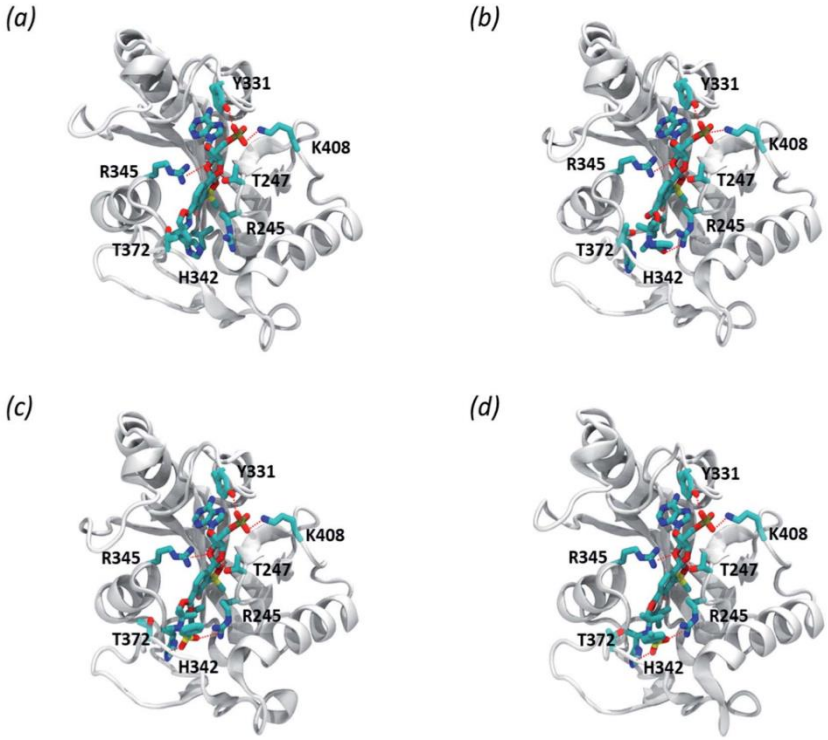

Fig. 5 Predicted complexes of benzosiloxaboroles **3a** (a), **3d** (b), **3e** (c), and **3f** (d) bound to LeuRS in complex with *S. aureus* MRSA leucyl-tRNA synthetase. Residues contacting the compound are depicted in licorice, polar interactions are depicted as red lines.

comparing compounds **3a** and **3d** we can appreciate, that within the longer compound the carbonyl group is able to form polar interactions with R245. This additional interaction does not appear to impact the biological activity of this compound, as both compounds **3a** and **3d** have similar antibacterial potency. In contrast, both compounds **3e** and **3f**, apart from forming polar interactions with R245, also interact with H342 which is due to presence of a sulfonamide group in their structure. Presumably, an increased number of polar bonds formed by **3e** and **3f** contributes to the stability of their complexes with LeuRS resulting in higher anti-bacterial activity.

Conclusions

In conclusion, two isomeric fluorinated benzosiloxaboroles **3a** and **5a** bearing pendant oxazoline rings were successfully obtained. The synthesis of compound **5a** needs careful temperature control after boronation step as a specific merry-go-round intramolecular hydride transfer from silicon through boron to oxazoline C2 atom occurs at higher temperatures eventually leading to a unique structure **4a** being the first example of a 7-membered heterocycle with Si–O–B–O–B linkage. It can be readily converted to benzosiloxaborole **4b** by simple treatment with dilute aq. HCl. Under the same conditions, the opening of oxazoline ring in **3a** and **5a** results in derivatives **3b** and **5b**, respectively. They comprise carboxylic alkyl ester group with attached terminal ammonium functionality. Interestingly, **3a** and **5a** showed different reactivity towards methyl triflate which is clearly affected by position of oxazoline ring with respect to boronic functionality. Thus, *N*-methylation of **3a** occurs cleanly to give the salt **3c** which is in contrast with net protonation of **5a**. The *N*-methyloxazolinium cation in **3c** undergoes readily hydrolytic ring opening which results in compound **3d**. Its synthetic utility was demonstrated by *N*-sulfonylation and *N*-acylation to give structurally expanded benzosiloxaboroles **3e–3g**. Antimicrobial activity of all new obtained benzosiloxaborole has been investigated in order to gain deeper insight into structure–property relationships for this group of organoboron heterocycles. Compounds **3e** and **3f** demonstrate relatively high antibacterial activity which shows that the presence of arylsulfonamide motif attached to the benzosiloxaborole core was beneficial. Overall, obtained oxazoline-substituted benzosiloxaboroles and products of their transformations seem to be good candidates for various transformations including conjugation with selected biomolecules which may give rise to novel systems with diverse and potent bioactivity. Further studies in this area will be carried out in our group and the results will be presented in due course.

Experimental section

General comments

Solvents used for reactions were dried by heating to reflux with sodium/benzophenone and distilled under argon. Starting materials and other reagents including thionyl chloride, alkyllithiums, diisopropylamine, trimethyl borate, chlorodimethylsilane, were used as received without further purification. In the ^{13}C NMR spectra the resonances of boron-bound carbon atoms were not observed in most cases as a result of their broadening by a quadrupolar boron nucleus. ^{1}H, and ^{13}C NMR chemical shifts are given relative to TMS using residual solvent resonances. ^{11}B and ^{19}F NMR chemical shifts are given relative to $BF_3 \cdot Et_2O$ and $CFCl_3$, respectively.

Synthesis

***N*-[2-(1-Hydroxy-2-methyl)propyl]-2-fluoro-4-bromobenzamide (1a).** A mixture of 2-fluoro-4-bromobenzoic acid **1** (25.0 g, 0.114 mol) and thionyl chloride (45.0 g, 28 mL, 0.378 mol) was refluxed under an argon atmosphere for 8 h. The excess of $SOCl_2$ was removed under reduced pressure to leave crude 2-fluoro-4-bromobenzoyl chloride as a colorless liquid. It was dissolved in dry CH_2Cl_2 (100 mL); the solution was cooled in an ice bath followed by a dropwise addition a solution of 2-amino-2-methyl-1-propanol (19.5 g, 0.219 mol) in CH_2Cl_2 (100 mL) during 30 min. A white precipitate was formed immediately and the obtained slurry was stirred at ambient temperature for 2 h. It was filtered and washed with CH_2Cl_2 (2 × 50 mL). The combined solutions were washed with water (2 × 100 mL) and dried with anhydrous $MgSO_4$. The solvent was evaporated under reduced pressure to give **1a** (28.4 g, 86%) as a colorless viscous oil. ^{1}H NMR (400 MHz, $CDCl_3$) δ 7.87 (t, J = 8.5 Hz, 1H), 7.38 (ddd, J = 8.5, 1.8, 0.4 Hz, 1H), 7.28 (dd, J = 11.3, 1.8 Hz, 1H), 6.77 (d, J = 13.5 Hz, 1H), 4.44 (s, 1H), 3.65 (s, 2H), 1.39 (s, 6H) ppm. ^{13}C NMR (101 MHz, $CDCl_3$) δ 162.9 (d, J = 3.7 Hz), 160.0 (d, J = 251.0 Hz), 133.1 (d, J = 2.6 Hz), 128.5 (d, J = 3.4 Hz), 126.5 (d, J = 10.5 Hz), 120.7 (d, J = 11.5 Hz), 119.7 (d, J = 28.2 Hz), 70.3, 56.8, 24.6 ppm. ^{19}F NMR (376 MHz, $CDCl_3$) δ −110.99 (ddd, J = 13.6, 11.3, 8.6 Hz) ppm. Anal. calcd for $C_{11}H_{13}BrFNO_2$ (290.13): C, 45.54; H, 4.52; N, 4.83. Found: C, 45.42; H, 4.40; N, 4.80.

2-(2′-Fluoro-4′-bromophenyl)-4,4-dimethyl-2-oxazoline (1b). Thionyl chloride (33.0 g, 0.277 mol) was added to the neat **1a** (28.0 g, 0.097 mol) at 0 °C. The yellow solution was formed in an exothermic reaction; it was stirred at ambient temperature for 6 h. It was diluted with Et_2O (300 mL) and the resulting slurry was stirred for 1 h at 0 °C. It was filtered and the collected white solid was washed with cold Et_2O (50 mL) and dissolved in water (200 mL). The obtained clear colorless solution was neutralized by dropwise addition of aqueous 20% NaOH (150 mL) at 0 °C, with stirring. The product was extracted with Et_2O (2 × 100 mL) and the organic phase was dried over anhydrous $MgSO_4$. The solvent was removed under reduced pressure and the liquid residue was subjected to distillation under reduced pressure, to give pure **1b** as a colorless viscous oil (b.p. 95–98 °C, *ca.* 1 mbar) which crystallizes on standing to give a white solid, m.p. 38–40 °C. Yield 22.3 g (85%). ^{1}H NMR (400 MHz, $CDCl_3$) δ 7.71 (dd, J = 8.6, 7.8 Hz, 1H), 7.31–7.29 (m, 1H), 7.28–7.27 (m, 1H), 4.05 (s, 2H), 1.35 (s, 6H) ppm. ^{13}C NMR (101 MHz, $CDCl_3$) δ 160.8 (d, J = 262.5 Hz), 158.3 (d, J = 5.5 Hz), 132.2 (d, J = 2.6 Hz), 127.4 (d, J = 3.8 Hz), 125.8 (d, J = 9.2 Hz), 120.3 (d, J = 25.2 Hz), 115.6 (d, J = 10.7 Hz), 78.9, 68.0, 28.4 ppm. ^{19}F NMR (376 MHz, $CDCl_3$) δ −106.66 (dd, J = 9.9, 7.7 Hz) ppm. Anal. calcd for $C_{11}H_{11}BrFNO$ (272.12): C, 48.55; H, 4.07; N, 5.15. Found: C, 48.52; H, 4.03; N, 5.14.

2-(2′-Fluoro-3′-dimethylsilyl-4′-bromophenyl)-4,4-dimethyl-2-oxazoline (1c). A solution of **1b** (10.9 g, 40.0 mmol) in THF (30 mL) was added dropwise at −75 °C to a stirred solution of LDA, freshly prepared from diisopropylamine (4.55 g, 45.0 mmol) and *n*BuLi (1.6 M, 27.5 mL, 44.0 mmol) in THF (80 mL). After *ca.* 30 min stirring at −78 °C chlorodimethylsilane (4.70 g, 50 mmol) was added slowly and the mixture was stirred for 30 min at −75 °C. It was allowed to warm to room temperature. The resulting almost clear colorless solution was concentrated under reduced pressure. The residue was triturated with heptane (20 mL) and the obtained suspension was filtered in order to remove the solid byproduct LiCl. The filtrate was concentrated and finally subjected to high vacuum (105–110 °C, *ca.* 1 mbar) to give **1c** as a pale yellow oil. Yield 11.5 g (87%). ^{1}H NMR (400 MHz, $CDCl_3$) δ 7.72–7.67 (m, 1H), 7.38 (dd, J = 8.3, 0.5 Hz, 1H), 4.83–4.75 (m, 1H), 4.08 (s, 2H), 1.39 (s, 6H), 0.46 (dd, J = 3.9, 1.9 Hz, 6H) ppm. ^{13}C NMR (101 MHz, $CDCl_3$) δ 165.00 (d, J = 256.5 Hz), 158.5 (d, J = 6.0 Hz), 133.6 (d, J = 12.2 Hz), 133.3 (d, J = 3.3 Hz), 129.0 (d, J = 3.6 Hz), 127.4 (d, J = 33.6 Hz), 115.3 (d, J = 15.6 Hz), 78.8, 68.1, 28.4, −3.1 (d, J = 4.3 Hz) ppm. ^{19}F NMR (376 MHz, $CDCl_3$) δ −91.47 (dddt, J = 7.3, 5.5, 3.8, 1.9 Hz) ppm. Anal. calcd for $C_{13}H_{17}BrFNOSi$ (330.27): C, 47.28; H, 5.19; N, 4.24. Found: C, 47.22; H, 5.11; N, 4.20.

***N*-[2-(1-Hydroxy-2-methyl)propyl]-2-bromo-4-fluorobenzamide (2a).** The synthesis was performed as described for **1a** using 2-bromo-4-fluorobenzoic acid (20.0 g, 0.091 mol) and thionyl chloride (36.0 g, 22.5 mL, 0.302 mol). The product was obtained as a white solid, m.p. 97–99 °C. Yield (24.7 g, 93%). ^{1}H NMR (400 MHz, $CDCl_3$) δ 7.48 (dd, J = 8.6, 5.9 Hz, 1H), 7.30 (dd, J = 8.2, 2.5 Hz, 1H), 7.05 (ddd, J = 8.6, 7.8, 2.5 Hz, 1H), 6.30 (s, 1H), 4.39 (broad, 1H), 3.63 (s, 2H), 1.39 (s, 6H) ppm. ^{13}C NMR (101 MHz, $CDCl_3$) δ 167.6, 163.0 (d, J = 254.8 Hz), 134.4 (d, J = 3.7 Hz), 131.1 (d, J = 8.8 Hz), 120.7 (d, J = 24.8 Hz), 119.9 (d, J = 9.5 Hz), 115.12 (d, J = 21.4 Hz), 70.3, 57.3, 24.5 ppm. ^{19}F NMR (376 MHz, $CDCl_3$) δ 108.11 (td, J = 8.0, 6.0 Hz) ppm. Anal. calcd for $C_{11}H_{13}BrFNO_2$ (290.13): C, 45.54; H, 4.52; N, 4.83. Found: C, 45.47; H, 4.43; N, 4.77.

2-(2′-Bromo-4′-fluoro)-4,4-dimethyl-2-oxazoline (2b). The synthesis was performed as described for **1b** starting with **2a** (24.0 g, 0.083 mol). The product was obtained as a colorless oil (b.p. 94–96 °C, *ca.* 1 mbar). Yield (20.5 g, 91%). ^{1}H NMR (400 MHz, $CDCl_3$) δ 7.62 (dd, J = 8.7, 6.0 Hz, 1H), 7.31 (dd, J = 8.3, 2.5 Hz, 1H), 7.00 (ddd, J = 8.7, 7.9, 2.5 Hz, 1H), 4.07 (s, 2H), 1.35 (s, 6H) ppm. ^{13}C NMR (101 MHz, $CDCl_3$) δ 164.5, 161.4 (d, J = 98.9 Hz), 132.8 (d, J = 9.1 Hz), 126.6 (d, J = 3.5 Hz), 122.6 (d, J = 9.6 Hz), 121.1 (d, J = 24.5 Hz), 114.5 (d, J = 21.3 Hz), 79.4, 68.2, 28.3 ppm. ^{19}F NMR (376 MHz, $CDCl_3$) δ −107.95 (td, J = 7.9, 6.0 Hz) ppm. Anal. calcd for $C_{11}H_{11}BrFNO$ (272.12): C, 48.55; H, 4.07; N, 5.15. Found: C, 48.43; H, 4.00; N, 5.11.

2-(2′-Bromo-3′-dimethylsilyl-4′-fluorophenyl)-4,4-dimethyl-2-oxazoline (2c). The synthesis was performed as described for **1c** starting with **2b** (10.9 g, 40 mmol). The product **2c** was obtained as a colorless viscous oil (b.p. 108–112 °C, *ca.* 1 mbar). Yield 11.1 g (84%). ^{1}H NMR (400 MHz, $CDCl_3$) δ 7.51 (dd, J = 8.5, 6.1 Hz, 1H), 6.97 (t, J = 8.3 Hz, 1H), 4.76 (dhept, J = 5.7, 3.9 Hz, 1H), 4.10 (s, 2H), 1.38 (s, 6H), 0.43 (dd, J = 3.9, 1.9 Hz, 6H) ppm. ^{13}C NMR (101 MHz, $CDCl_3$) δ 167.6 (d, J = 249.4 Hz), 161.9, 133.6 (d, J = 10.2 Hz), 130.0 (d, J = 12.6 Hz), 128.0 (d, J = 3.5 Hz), 127.81 (d, J = 31.6 Hz), 114.1 (d, J = 27.8 Hz), 79.5, 68.2, 28.2, −3.0 (d, J = 4.6 Hz) ppm. ^{19}F NMR (376 MHz, $CDCl_3$) δ −92.24 to −92.17 (m) ppm. Anal. calcd for $C_{13}H_{17}BrFNOSi$ (330.27): C, 47.28; H, 5.19; N, 4.24. Found: C, 47.20; H, 5.07; N, 4.22.

6-(4,4-Dimethyl-2-oxazolin-2-yl)-7-fluoro-1,1-dimethyl-3-hydroxybenzo[1,2,3]siloxaborole (3a). A solution of **1c** (9.9 g, 30 mmol) in Et_2O (30 mL) was added dropwise to a solution of *t*-BuLi (1.9 M in pentane, 31.5 mL, 60 mmol) in Et_2O (50 mL) at −90 °C. After 30 min of stirring at −95 °C, $B(OMe)_3$ (6.6 mL, 60 mmol) was added slowly to the orange mixture at −90 °C. The resulting suspension was warmed slowly to *ca.* 0 °C, quenched with 1 M aq. NaOH (40 mL) and stirred at room temperature until evolution of H_2 ceased. The two-phase mixture was concentrated under reduced pressure in order to remove solvents and other volatile organic components. The residual aqueous alkaline solution was transferred to a separatory funnel and washed with Et_2O (30 mL) and hexane (30 mL). Then it was placed in a beaker, cooled in an ice bath and carefully neutralized by a slow dropwise addition with 1 M aq. H_2SO_4 (to reach the pH = 5–6). The precipitated voluminous white solid was filtered and washed several times with distilled water. Then it was resuspended in hexane (30 mL), stirred for 30 min and filtered. Finally, the product was dried *in vacuo* to give **3a** as a white powder, m.p. 132–134 °C. Yield 6.68 g (76%). ^{1}H NMR (400 MHz, $CDCl_3$) δ 7.93 (t, J = 7.2 Hz, 1H), 7.58 (dd, J = 7.5, 1.6 Hz, 1H), 6.62 (broad, 1H), 4.12 (s, 2H), 1.41 (s, 6H), 0.46 (s, 6H) ppm. ^{13}C NMR (101 MHz, $CDCl_3$) δ 162.7 (d, J = 255.9 Hz), 159.3 (d, J = 5.9 Hz), 136.7 (d, J = 32.4 Hz), 133.8, 127.4 (d, J = 3.6 Hz), 117.7 (d, J = 13.4 Hz), 79.0, 68.1, 28.5, −0.7 ppm. ^{19}F NMR (376 MHz, $CDCl_3$) δ −100.43 to −100.45 (m) ppm. ^{10}B NMR (54 MHz, acetone-d_6) δ 30.0 ppm. ^{29}Si NMR (99.3 MHz, acetone-d_6) δ 19.61 ppm. Anal. calcd for $C_{13}H_{17}BFNO_3Si$ (293.18): C, 53.26; H, 5.84; N, 4.78. Found: C, 53.12; H, 5.80; N, 4.75. HRMS (ESI, negative ion mode) calcd for $C_{13}H_{16}BFNO_3Si^-$ $[M - H]^-$: 292.0982; found: 292.0984. HRMS (ESI, positive ion mode) calcd for $C_{13}H_{18}BFNO_3Si^+$ $[M + H]^+$: 294.1128; found: 294.1125.

6-(3,4,4-Trimethyl-2-oxazolinium-2-yl)-7-fluoro-1,1-dimethyl-3-hydroxybenzo[1,2,3]siloxaborole trifluoromethanesulfonate (3b). Methyl trifluoromethanesulfonate (3.1 g, 18.9 mmol) was added dropwise to a stirred solution of **3a** (2.05 g, 7.0 mmol) in $CHCl_3$ (10 mL). The temperature increased to *ca.* 50 °C during a few minutes indicating the progress of the reaction. Subsequently, a gradual precipitation of a white solid was observed. The suspension was stirred overnight at ambient temperature. Then it was cooled to *ca.* −20 °C and filtered under argon. The solid was washed with cold $CHCl_3$ (10 mL) and dried under reduced pressure, to give **3b**, m.p. 200–202 °C. Yield 2.65 g (83%). ^{1}H NMR (400 MHz, acetone-d_6) δ 8.07 (dd, J = 7.5, 6.4 Hz, 1H), 7.92 (dd, J = 7.5, 1.9 Hz, 1H), 5.17 (s, 2H), 3.52 (d, J = 2.3 Hz, 3H), 1.83 (s, 6H), 0.51 (s, 6H) ppm. ^{13}C NMR (101 MHz, acetone-d_6) δ 169.8 (d, J = 2.0 Hz), 162.1 (d, J = 255.3 Hz), 154.2 (broad), 137.7 (d, J = 31.2 Hz), 135.0, 129.0 (d, J = 3.2 Hz), 122.2 (d, J = 321.4 Hz), 111.6 (d, J = 16.0 Hz), 83.6, 70.0, 31.3 (d, J = 5.3 Hz), 23.9, −0.9 ppm. ^{19}F NMR (376 MHz, acetone-d_6) δ −78.93,

−100.22 (dp, J = 6.8, 2.3 Hz) ppm. ^{10}B NMR (54 MHz, acetone-d_6) δ 30.1 ppm. ^{29}Si NMR (99.3 MHz, acetone-d_6) δ 20.32 ppm.

6-[2-Methyl-2-(*N*-methylammonium)propoxycarbonyl]-7-fluoro-1,1-dimethyl-3-hydroxybenzo[1,2,3]siloxaborole trifluoromethanesulfonate (3c). Compound **3b** (2.7 g, 7 mmol) was dissolved in acetone (20 mL) and water (2 mL, 0.1 mol) was added. The mixture was stirred for 2 h at ambient temperature. Acetone was evaporated under reduced pressure and the residue was dried under high vacuum. DCM (20 mL) was added and the suspension was filtered to give **3c** as a white solid, m.p. 161–164 °C. Yield (2.25 g, 80%). ^{1}H NMR (400 MHz, DMSO-d_6) δ 8.55 (q, J = 5.4 Hz, 2H), 8.13 (t, J = 7.4 Hz, 1H), 7.76 (dd, J = 7.4, 1.5 Hz, 1H), 4.38 (s, 2H), 2.58 (t, J = 5.4 Hz, 3H), 1.35 (s, 6H), 0.44 (s, 6H) ppm. ^{13}C NMR (101 MHz, DMSO-d_6) δ 163.1 (d, J = 4.4 Hz), 162.6 (d, J = 257.3 Hz), 150.5 (broad), 136.5 (d, J = 32.5 Hz), 134.6, 127.7 (d, J = 3.5 Hz), 120.7 (q, J = 322.2 Hz), 118.7 (d, J = 12.1 Hz), 67.0, 57.4, 26.7, 20.3, −0.7 ppm. ^{19}F NMR (376 MHz, DMSO-d_6) δ −77.79, −101.52 (d, J = 7.4 Hz) ppm. Anal. calcd for $C_{15}H_{22}BF_4NO_7SSi$ (475.29): C, 37.91; H, 4.67; N, 2.95; S, 6.75. Found: C, 37.79; H, 4.62; N, 2.85; S, 6.67. HRMS (ESI, positive ion mode) calcd for $C_{13}H_{22}BFNO_3Si^+$ [M − OTf]$^+$: 326.1390; found: 326.1387.

6-[2-Methyl-2-(*N*-methylpyrazinamido)propoxycarbonyl]-7-fluoro-1,1-dimethyl-3-hydroxybenzo[1,2,3]siloxaborole (3d). To a solution of **3c** (293 mg, 1.0 mmol) in MeCN (5 mL) Et_3N (0.45 mL, 3.5 mmol) and pyrazinoyl chloride[66] (170 mg, 1.2 mmol) were added. The mixture was heated at 60 °C for 3 h. Then it was evaporated to leave the violet residue. It was dissolved in acetone (5 mL) and water (5 mL) was added. The mixture was concentrated to remove acetone and a white suspension was obtained. The product was isolated as a white powder, m.p. 129–131 °C. Yield 255 mg (59%). ^{1}H NMR (400 MHz, $CDCl_3$) δ 8.83 (d, J = 1.6 Hz, 1H), 8.60 (d, J = 2.5 Hz, 1H), 8.54 (dd, J = 2.5, 1.5 Hz, 1H), 8.09–8.02 (m, 1H), 7.62 (dd, J = 7.4, 1.6 Hz, 1H), 5.09 (s, 1H), 4.83 (s, 2H), 3.03 (s, 3H), 1.65 (s, 6H), 0.49 (s, 6H) ppm. ^{13}C NMR (101 MHz, $CDCl_3$) δ 168.5, 164.7 (d, J = 4.0 Hz), 163.3 (d, J = 257.9 Hz), 151.5, 149.0 (br), 145.0, 144.7, 143.1, 137.2 (d, J = 33.2 Hz), 134.9, 127.5 (d, J = 3.4 Hz), 119.8 (d, J = 12.9 Hz), 69.6, 59.4, 35.5, 24.1, −0.6 ppm. ^{19}F NMR (376 MHz, $CDCl_3$) δ −100.75 ppm. Anal. calcd for $C_{19}H_{23}BFN_3O_5Si$ (431.30): C, 52.91; H, 5.38; N, 9.74. Found: C, 52.87; H, 5.33; N, 9.67. HRMS (ESI, negative ion mode) calcd for $C_{19}H_{22}BFN_3O_5Si^-$ [M − H]$^-$: 430.1411; found: 430.1412.

6-[2-Methyl-2-(*N*-methylphenylsufonamido) propoxycarbonyl]-7-fluoro-1,1-dimethyl-3-hydroxybenzo[1,2,3] siloxaborole (3e). To a solution of **2b** (190 mg, 0.40 mmol) in MeCN (2 mL) Et_3N (0.15 mL, 1.0 mmol) and $PhSO_2Cl$ (88 mg, 0.5 mmol) were added. The mixture was heated at 60 °C for 3 h. Then it was evaporated to leave the viscous colorless residue. It was dissolved in acetone (5 mL) and water (5 mL) was added. The mixture was concentrated to remove acetone and a white suspension was obtained. The solid product **3** was collected by filtration, washed with water (2 × 1 mL) and dried, m.p. 130–132 °C. Yield 140 mg (75%). ^{1}H NMR (400 MHz, $CDCl_3$) δ 7.92 (t, J = 7.1 Hz, 1H), 7.85–7.81 (m, 2H), 7.60 (dd, J = 7.4, 1.6 Hz, 1H), 7.39 (tt, J = 8.8, 6.2 Hz, 3H), 5.05 (s, 1H), 4.52 (s, 2H), 3.05 (s, 3H), 1.50 (s, 8H), 0.51 (s, 6H) ppm. ^{13}C NMR (101 MHz, $CDCl_3$) δ 164.4 (d, J = 4.5 Hz), 163.4 (d, J = 258.6 Hz), 142.6, 137.2 (d, J = 32.9 Hz), 134.9, 132.2, 128.9, 127.4 (d, J = 3.7 Hz), 127.0, 119.7 (d, J = 12.9 Hz), 71.1, 60.5, 33.2, 25.3, −0.6 ppm. ^{19}F NMR (376 MHz, $CDCl_3$) δ −100.52 (dd, J = 7.4, 1.6 Hz) ppm. Anal. calcd for $C_{20}H_{25}BFNO_6SSi$ (465.37): C, 51.62; H, 5.41; N, 3.01; S, 6.89. Found: C, 51.40; H, 5.34; N, 2.97; S, 6.67. HRMS (ESI, negative ion mode) calcd for $C_{20}H_{24}BFNO_6Si^-$ [M − H]$^-$: 464.1176; found: 464.1177.

6-{2-Methyl-2-[*N*-methyl-(4-chlorophenyl)sulfonamido] propoxycarbonyl}-7-fluoro-1,1-dimethyl-3-hydroxybenzo[1,2,3] siloxaborole (3f). The synthesis was performed as described for **3d** using 4-chlorophenylsulfonyl chloride. Yield 125 mg (63%). ^{1}H NMR (400 MHz, $CDCl_3$) δ 7.91 (dd, J = 7.5, 6.8 Hz, 1H), 7.75 (d, J = 8.9 Hz, 1H), 7.61 (dd, J = 7.4, 1.7 Hz, 1H), 7.31 (d, J = 8.8 Hz, 1H), 4.85 (s, 1H), 4.51 (s, 2H), 3.04 (s, 3H), 1.51 (s, 6H), 0.51 (s, 6H) ppm. ^{13}C NMR (101 MHz, $CDCl_3$) δ 164.4 (d, J = 4.1 Hz), 163.3 (d, J = 258.3 Hz), 145.6, 141.1, 138.6, 137.3 (d, J = 32.8 Hz), 134.8, 129.2, 128.4, 127.5 (d, J = 3.7 Hz), 119.5 (d, J = 12.8 Hz), 71.0, 60.7, 33.3, 25.4, −0.6 ppm. ^{19}F NMR (376 MHz, $CDCl_3$) δ −100.54 (dd, J = 6.8, 1.3 Hz) ppm. Anal. calcd for $C_{20}H_{24}BClFNO_6SSi$ (499.82) C, 48.06; H, 4.84; N, 2.80; S, 6.41. Found: C, 47.88; H, 4.79; N, 2.70; S, 6.23. HRMS (ESI, negative ion mode) calcd for $C_{20}H_{23}BClFNO_6Si^-$ [M − H]$^-$: 498.0786; found: 498.0794.

6-[2-Methyl-2-ammoniumpropoxycarbonyl]-7-fluoro-1,1-dimethyl-3-hydroxybenzo[1,2,3]siloxaborole chloride (3g). Compound **3a** (293 mg, 1.0 mmol) was dissolved in acetone (5 mL) followed by addition of 2 M aq. HCl (0.7 mL). The mixture was stirred for 30 min and concentrated under reduced pressure. The residue was triturated with Et_2O (5 mL) and the obtained suspension was filtered. The solid was washed with Et_2O (5 mL) and dried to give the product as a white powder, m.p. 220–224 °C. Yield 310 mg (89%). ^{1}H NMR (400 MHz, DMSO-d_6) δ 8.40 (s, 3H), 8.20 (t, J = 7.3 Hz, 1H), 7.78 (dd, J = 7.5, 1.6 Hz, 1H), 4.31 (s, 2H), 1.36 (s, 6H), 0.44 (s, 6H) ppm. ^{13}C NMR (101 MHz, DMSO-d_6) δ 163.1 (d, J = 4.2 Hz), 162.6 (d, J = 256.0 Hz), 150.3 (broad), 136.3 (d, J = 32.3 Hz), 134.6, 127.7 (d, J = 3.7 Hz), 118.6 (d, J = 11.9 Hz), 68.8, 52.8, 22.5, −0.7 ppm. ^{19}F NMR (376 MHz, DMSO-d_6) δ −96.95 (d, J = 7.1 Hz) ppm. HRMS (ESI, positive ion mode) calcd for $C_{13}H_{20}BFNO_4Si^+$ [M − Cl]$^+$: 312.1233; found: 312.1227.

10-(*tert*-Butyl)-7-fluoro-3,3,8,8-tetramethyl-2,3-dihydro-4*H*,8*H*-1,9,11-trioxa-3*a*-aza-8-sila-10,11*a*,l4-diborabenzo[*ij*] cyclopenta[*c*]azulene (4a). A solution of **2c** (9.9 g, 30 mmol) in Et_2O (30 mL) was added dropwise to a solution of *t*-BuLi (1.9 M in pentane, 23.5 mL, 45 mmol) in Et_2O (40 mL) at −90 °C. After 30 min of stirring at −95 °C, $B(OMe)_3$ (6.6 mL, 60 mmol) was added slowly to the orange mixture at −90 °C. The resulting suspension was warmed slowly to *ca.* 0 °C, quenched with 1 M aq. NaOH (40 mL) and stirred at room temperature until evolution of H_2 ceased. The two-phase mixture was concentrated under reduced pressure in order to remove solvents and other volatile organic components. The residual aqueous alkaline suspension was cooled in an ice bath and carefully neutralized by a slow dropwise addition with 1 M aq. H_2SO_4 (to reach the pH = 5–6). It was filtered and washed several times with distilled water, hexane (3 × 30 mL) and dried. The crude

solid product was mixed with chloroform (50 mL), stirred for 30 min and filtered. The filter cake was washed with chloroform (2 × 20 mL). Combined chloroform solution concentrated under reduced pressure; the residue was mixed with hexane (20 mL) and obtained suspension was filtered, to give **4** as a white powder, m.p. 247–250 °C. Yield 2.92 g (54%). ^{1}H NMR (400 MHz, DMSO-d_6) δ 7.13 (dd, J = 8.3, 5.1 Hz, 1H), 6.85 (t, J = 8.6 Hz, 1H), 6.72 (t, J = 6.8 Hz, 1H), 4.09 (dd, J = 15.8, 5.8 Hz, 1H), 3.99 (dd, J = 15.8, 8.0 Hz, 1H), 3.53 (d, J = 9.4 Hz, 1H), 3.44 (d, J = 9.4 Hz, 1H), 1.53 (s, 3H), 1.24 (s, 3H), 0.85 (s, 9H), 0.35 (d, J = 2.8 Hz, 3H), 0.29 (s, 3H) ppm. ^{13}C NMR (101 MHz, DMSO-d_6) δ 165.1 (d, J = 238.1 Hz), 155.6, 136.8 (d, J = 1.8 Hz), 125.4 (d, J = 8.1 Hz), 124.6 (d, J = 27.2 Hz), 113.0 (d, J = 27.4 Hz), 73.1, 60.7, 47.5, 27.9, 25.3, 20.7, 2.0 (d, J = 4.0 Hz), 1.8 ppm. ^{19}F NMR (376 MHz, DMSO-d_6) δ −106.06 to −106.11 (m) ppm. ^{10}B NMR (54 MHz, DMSO-d_6) δ 32.6, 12.7 ppm. ^{29}Si NMR (99.3 MHz, DMSO-d_6) δ −1.25 ppm. ^{1}H NMR (400 MHz, DMSO-d_6 + TfOD/D_2O) δ 7.60 (dd, J = 8.3, 5.1 Hz, 1H), 7.26 (dd, J = 8.3, 6.9 Hz, 1H), 4.31 (s, 2H), 3.48 (s, 2H), 1.29 (s, 6H), 0.83 (s, 8H), 0.41 (s, 6H) ppm. ^{19}F NMR (376 MHz, DMSO-d_6 + TfOD/D_2O) δ −104.26 (t, J = 5.6 Hz) ppm. Anal. calcd for $C_{17}H_{28}B_2FNO_3Si$ (363.12): C, 56.23; H, 7.77; N, 3.86. Found: C, 56.04; H, 7.62; N, 3.81. HRMS (ESI, negative ion mode) calcd for $C_{17}H_{27}B_2FNO_3Si^-$ [M − H]$^-$: 362.1936; found: 362.1943. HRMS (ESI, positive ion mode) calcd for $C_{17}H_{29}B_2FNO_3Si^+$ [M + H]$^+$: 364.2081; found: 364.2077.

***N*-((7-Fluoro-3-hydroxy-1,1-dimethyl-1,3-dihydrobenzo[*c*][1,2,5]oxasilaborol-4-yl)methyl)-1-hydroxy-2-methylpropan-2-aminium chloride (4b).** Compound **4a** (0.55 g, 1.5 mmol) was suspended in acetone (5 mL) followed by the addition of 2 M aq. HCl (2 mL). The mixture was stirred for 2 h at 60 °C and the resulting solution was cooled and concentrated under reduced pressure. The residue was triturated with Et_2O (5 mL) and the obtained suspension was filtered. The solid was washed with Et_2O (5 mL) and dried to give the product as a white powder, m.p. 234–238 °C (decomp.). Yield 390 mg (78%). ^{1}H NMR (500 MHz, DMSO-d_6) δ 9.60 (s, 1H), 8.68 (s, 2H), 7.78 (dd, J = 8.4, 5.0 Hz, 1H), 7.26 (t, J = 7.6 Hz, 1H), 4.39–4.33 (m, 2H), 3.54 (s, 2H), 1.32 (s, 6H), 0.43 (s, 6H) ppm. ^{13}C NMR (101 MHz, DMSO-d_6) δ 164.3 (d, J = 244.0 Hz), 145.6, 136.5 (d, J = 6.8 Hz), 134.5 (d, J = 31.9 Hz), 133.0 (d, J = 2.9 Hz), 116.6 (d, J = 24.4 Hz), 65.1, 60.3, 42.3 (d, J = 2.4 Hz), 20.6, −0.6 ppm. ^{19}F NMR (376 MHz, DMSO-d_6) δ −104.47 (t, J = 6.1 Hz) ppm. ^{10}B NMR (54 MHz, DMSO-d_6) δ 29.0 ppm. ^{29}Si NMR (99 MHz, DMSO-d_6) δ 18.33 ppm. HRMS (ESI, positive ion mode) calcd for $C_{13}H_{22}BFNO_3Si^+$ [M − Cl]$^+$: 298.1441; found: 298.1437.

8-Fluoro-9-(hydroxydimethylsilyl)-3,3-dimethyl-2,3,5-trihydro-10λ4-benzo[3,4][1,2]azaborolo[2,1-*b*][1,3,2]oxazaborol-10-ol (4c). Compound **4b** (333 mg, 1.0 mmol) was treated with the solution of $NaHCO_3$ (125 mg, 1.5 mmol) in water (3 mL). The obtained suspension was stirred for 1 h and filtered. The solid was washed with cold water (2 × 2 mL) and dried to give the product as a white powder, m.p. 153–156 °C. Yield 223 mg (75%). ^{1}H NMR (400 MHz, DMSO-d_6) δ 7.08 (dd, J = 8.2, 5.1 Hz, 1H), 6.81 (dd, J = 9.3, 8.2 Hz, 1H), 6.14 (t, J = 6.0 Hz, 1H), 4.45 (s, 1H), 3.99 (d, J = 5.3 Hz, 2H), 3.44 (d, J = 9.3 Hz, 1H), 3.11 (d, J = 9.3 Hz, 1H), 1.36 (s, 3H), 1.07 (s, 3H), 0.28 (d, J = 2.8 Hz, 3H), 0.25 (d, J = 1.7 Hz, 3H) ppm. ^{13}C NMR (101 MHz, DMSO-d_6) δ 165.6 (d, J = 236.5 Hz), 137.7 (d, J = 1.7 Hz), 126.4 (d, J = 26.6 Hz), 124.6 (d, J = 8.5 Hz), 113.0 (d, J = 28.5 Hz), 72.5, 60.1, 46.8, 25.8, 20.6, 2.73 (d, J = 4.6 Hz), 2.69 (d, J = 2.8 Hz) ppm. ^{10}B NMR (54 MHz, DMSO-d_6) δ 12.7 ppm. ^{19}F NMR (376 MHz, DMSO-d_6) δ −104.36 ppm. ^{29}Si NMR (99 MHz, DMSO-d_6) δ 2.12 ppm. Anal. calcd for $C_{13}H_{21}BFNO_3Si$ (297.20): C, 52.54; H, 7.12; N, 4.71. Found: C, 52.31; H, 6.80; N, 4.65. HRMS (ESI, positive ion mode) calcd for $C_{13}H_{22}BFNO_3Si^+$ [M + H]$^+$: 298.1441; found: 298.1436.

(5-Fluoro-2-(7-fluoro-3,3,8,8-tetramethyl-2,3-dihydro-4*H*,8*H*-1,9,11-trioxa-3*a*-aza-8-sila-10,11*a*λ^4-diborabenzo[*ij*]cyclopenta[*c*]azulen-10-yl)phenyl)methanol (4d). A mixture of **4c** (75 mg, 0.25 mmol) and Tavaborole (38 mg, 0.25 mmol) in acetone (2 mL) was heated at 50 °C for *ca.* 10 min. The resulting solution was concentrated and the residue was triturated with DCM (1 mL) followed by addition of hexane (2 mL). The obtained suspension was cooled and filtered to give **4d** as a white solid. Yield 71 mg (66%). ^{1}H NMR (400 MHz, DMSO-d_6) ^{1}H NMR (400 MHz, acetone-d_6) δ 7.77 (dd, J = 8.1, 5.7 Hz, 1H), 7.19 (ddt, J = 9.4, 1.6, 0.8 Hz, 1H), 7.14–7.06 (m, 2H), 6.79 (dd, J = 9.2, 8.3 Hz, 1H), 5.02 (s, 2H), 4.22–4.17 (m, 2H), 3.56 (d, J = 9.3 Hz, 1H), 3.22 (d, J = 9.3 Hz, 1H), 1.47 (s, 3H), 1.18 (s, 3H), 0.31 (d, J = 2.3 Hz, 3H), 0.29 (d, J = 2.3 Hz, 3H) ppm. ^{19}F NMR (376 MHz, acetone-d_6) δ −105.21, −111.89 (td, J = 9.4, 5.7 Hz) ppm. ^{1}H and ^{19}F NMR spectra show additional signals which may indicate some instability of **4d** in solution, therefore ^{13}C NMR analysis was not performed. The formation of **4d** was confirmed by mass spectrometry. HRMS (ESI, positive ion mode) calcd for $C_{20}H_{26}B_2F_2NO_4Si^+$ [M + H]$^+$: 432.1780; found: 432.1783.

4-(4,4-Dimethyl-2-oxazolin-2-yl)-7-fluoro-1,1-dimethyl-3-hydroxybenzo[1,2,3]siloxaborole (5a). A solution of **2c** (9.9 g, 30 mmol) in Et_2O (30 mL) was added dropwise to a solution of *t*-BuLi (1.9 M in pentane, 23.5 mL, 45 mmol) in Et_2O (40 mL) at −90 °C. After 30 min of stirring at −95 °C, $B(OMe)_3$ (5.5 mL, 50 mmol) was added slowly to the orange mixture at −90 °C. The resulting suspension was allowed to warm slowly to *ca.* −70 °C, quenched with 1 M aq. NaOH (40 mL) and stirred at room temperature until evolution of H_2 ceased. A two-phase mixture was concentrated under reduced pressure in order to remove solvents and other volatile organic components. A residual aqueous alkaline suspension was cooled in an ice bath and carefully neutralized by a slow dropwise addition with 1 M aq. H_2SO_4 (to reach the pH = 5–6). It was filtered and washed several times with water. The crude solid product was mixed with hexane (70 mL), stirred for 30 min and filtered; the filter cake was washed with hexane (2 × 30 mL). Combined hexane solution was dried with $MgSO_4$ and evaporated to dryness, to give **5a** as a white powder, m.p. 67–69 °C. Yield 6.2 g (71%). ^{1}H NMR (400 MHz, $CDCl_3$) δ 12.81 (broad s, 1H), 8.02 (dd, J = 8.6, 5.4 Hz, 1H), 7.10 (dd, J = 8.6, 6.3 Hz, 1H), 4.16 (s, 2H), 1.43 (s, 6H), 0.47 (s, 6H) ppm. ^{13}C NMR (101 MHz, $CDCl_3$) δ 166.6 (d, J = 250.8 Hz), 163.6, 146.2, 137.6 (d, J = 33.3 Hz), 134.8 (d, J = 7.5 Hz), 126.8 (d, J = 3.1 Hz), 116.4 (d, J = 24.9 Hz), 79.0, 67.3, 28.4, −0.7 ppm. ^{19}F NMR (376 MHz, $CDCl_3$) δ −98.86 (dd, J = 6.3, 5.4 Hz) ppm. ^{10}B NMR (54 MHz, acetone-d_6) δ 30.1 ppm. ^{29}Si NMR (99.3 MHz, acetone-d_6) δ 18.35 ppm. Anal. calcd for $C_{13}H_{17}BFNO_3Si$ (293.18): C, 53.26; H, 5.84; N, 4.78. Found: C, 53.22; H,

5.70; N, 4.68. HRMS (ESI, negative ion mode) calcd for $C_{13}H_{16}BFNO_3Si^-$ $[M-H]^-$: 292.0982; found: 292.0985.

4-(4,4-Dimethyl-2-oxazolin-2-yl)-7-fluoro-1,1-dimethyl-3-hydroxybenzo[1,2,3]siloxaborole trifluoromethanesulfonate (5b). The synthesis was performed as described as described for **3b** starting with **5a** (1.46 g, 5.00 mmol). The product **5b** was obtained as a white powder, m.p. 206–209 °C. Yield 1.37 g (62%). ^{1}H NMR (400 MHz, acetone-d_6) δ 13.16 (s, 1H), 8.37 (dd, J = 8.7, 5.2 Hz, 1H), 7.54 (dd, J = 8.7, 6.4 Hz, 1H), 5.10 (s, 2H), 1.78 (s, 6H), 0.53 (s, 6H) ppm. ^{13}C NMR (101 MHz, acetone-d_6) δ 171.2, 169.4 (d, J = 255.5 Hz), 139.8 (d, J = 34.7 Hz), 138.5 (d, J = 9.2 Hz), 122.1 (q, J = 321.2 Hz), 121.5, 118.7 (d, J = 25.6 Hz), 84.2, 65.1, 26.6, −1.2 ppm. ^{19}F NMR (376 MHz, acetone-d_6) δ −78.98 (s, OTf^-), −93.52 (s) ppm. Anal. calcd for $C_{14}H_{18}BF_4NO_6SiS$ (443.25): C, 37.94; H, 4.09; N, 3.16; S, 7.23. Found: C, 37.66; H, 3.98; N, 3.12; S, 7.11.

4-[2-Methyl-2-ammoniumpropoxycarbonyl]-7-fluoro-1,1-dimethyl-3-hydroxybenzo[1,2,3]siloxaborole chloride (5c). The synthesis was performed as described for **3g** using **5a** (0.59 g, 2.0 mmol) as a starting material. The product was isolated as a white powder, m.p. 221–224 °C. Yield 0.66 g (95%). ^{1}H NMR (400 MHz, DMSO-d_6) δ 9.43 (s, 1H), 8.50 (dd, J = 8.6, 4.9 Hz, 4H), 7.46–7.39 (m, 2H), 4.36 (s, 2H), 1.38 (s, 6H), 0.44 (s, 6H) ppm. ^{13}C NMR (101 MHz, DMSO-d_6) δ 168.4, 166.8 (d, J = 250.7 Hz), 147.0, 137.5 (d, J = 7.9 Hz), 136.7 (d, J = 33.0 Hz), 129.4 (d, J = 3.2 Hz), 116.9 (d, J = 24.9 Hz), 69.7 (d, J = 2.1 Hz), 52.7, 22.4, −0.8 ppm. ^{19}F NMR (376 MHz, DMSO-d_6) δ −97.02 ppm. ^{10}B NMR (54 MHz, DMSO-d_6) δ 30.0 ppm. ^{29}Si NMR (99 MHz, DMSO-d_6) δ 19.22 ppm. HRMS (ESI, positive ion mode) calcd for $C_{13}H_{20}BFNO_4Si^+$ $[M-Cl]^+$: 312.1233; found: 312.1227.

5,12-Difluoro-2,9-bis((1-hydroxy-2-methylpropan-2-yl)iminio)-6,6,13,13-tetramethyl-2*H*,6*H*,9*H*,13*H*-1,7,8,14,15-pentaoxa-6,13-disila-7*a*,14*a*-dibora-7*a*,14*a*-methanocyclodeca[1,2,3-*cd*:6,7,8-*c*′*d*′]diindene-7*a*,14*a*-diuide (5d). Compound **5c** (347 mg, 1.0 mmol) was dissolved in methanol (10 mL) followed by the addition of K_2CO_3 (276 mg, 2 mmol). The mixture was stirred for 12 h at 70 °C and cooled. 2 M aq. HCl (3 mL) was added and mixture was concentrated. The obtained suspension was filtered; the solid was washed with water (2 × 5 mL) and dried to give the product as a white solid, m.p. 219–222 °C. Yield 274 mg (91%). ^{1}H NMR (400 MHz, DMSO-d_6) δ 10.27 (s, 1H), 8.52 (dd, J = 8.6, 4.7 Hz, 1H), 7.17 (t, J = 8.5 Hz, 1H), 3.59 (d, J = 11.2 Hz, 1H), 3.56 (d, J = 11.2 Hz, 1H), 1.41 (s, 3H), 1.39 (s, 3H), 0.32 (s, 3H), 0.24 (s, 3H) ppm. ^{13}C NMR (101 MHz, DMSO-d_6) δ 172.0, 169.5 (d, J = 249.9 Hz), 165.6, 129.0 (d, J = 11.3 Hz), 127.1, 126.3 (d, J = 30.7 Hz), 114.7 (d, J = 28.0 Hz), 66.6, 59.4 (d, J = 2.1 Hz), 23.1, 22.9, 1.83, 1.80 ppm. ^{10}B NMR (54 MHz, DMSO-d_6) δ 9.9 ppm. ^{19}F NMR (376 MHz, DMSO-d_6) δ −95.38 ppm. ^{29}Si NMR (99 MHz, DMSO-d_6) δ −5.62 ppm. Anal. calcd. for $C_{26}H_{36}B_2F_2N_2O_7Si_2$ (604.36): C, 51.67; H, 6.00; N, 4.64. Found: C, 51.43; H, 5.92; N, 4.64. HRMS (ESI, negative ion mode) calcd for $C_{26}H_{35}B_2F_2N_2O_7Si_2^-$ $[M-H]^-$: 603.2142; found: 603.2158. HRMS (ESI, positive ion mode) calcd for $C_{26}H_{37}B_2F_2N_2O_7Si_2^+$ $[M+H]^+$: 605.2288; found: 605.2279.

Single crystal X-ray diffraction. Single crystals of all studied systems were prepared by slow solvent evaporation at room temperature from corresponding concentrated $CHCl_3$ solutions. Obtained crystals were measured on SuperNova diffractometer equipped with Atlas detector (Cu-K_α radiation, λ = 1.54184 Å). In all the cases a selected crystal was maintained at low temperature (T = 100 K) with the use of Oxford Cryosystems nitrogen gas-flow device. The crystal structures were established in a conventional way *via* X-ray data refinement employing the Independent Atom Model (IAM). Data reduction and analysis were carried out with the *CrysAlisPro* suites of programs.[67] All structures were solved by direct methods using *SHELXS-97* (ref. 68) and refined using *SHELXL-2016*.[69] The refinement was based on F^2 for all reflections except those with highly negative values of F^2. Weighted R factors (wR) and all goodness-of-fit (GooF) values are based on F^2. Conventional R factors are based on F with F set to zero for negative F^2. The $F_o^2 > 2\sigma(F_o^2)$ criterion was used only for calculating R factors and is not relevant to the choice of reflections for the refinement. All non-hydrogen atoms were refined anisotropically. All carbon-bound hydrogen atoms were placed in calculated positions. The positions of O–H hydrogen atoms were derived from difference electron density maps. The O–H distances were fixed to 0.87 Å with standard deviation of 0.01 Å. All-important crystallographic data including measurement, reduction, structure solution and refinement details are included in Tables S1–S3 (ESI†) or in the associated CIF files. Deposition numbers 2166283 (**3a**), 2166284 (**3b**), 2166285 (**3d**), 2166286 (**3e**), 2166287 (**4a**), 2166288 (**4c**), 2166289 (**5b**), 2166290 (**5c**), 2166291 (**5d**) contain the supplementary crystallographic data for this paper. Additional information on measured crystal structures including packing description, parameters of hydrogen-bond interactions and other relevant parameters can be found in the ESI.†

Theoretical calculations. Theoretical calculations were performed using *Gaussian16* program.[70] Molecules were optimized using M062X[71] method with 6-311++G(d,p) basis set.[72] The starting geometries were adopted from corresponding crystal structures or manually modified in the *GaussView*[73] programme, if crystal data was not available. Following geometry optimization, the vibrational frequencies were calculated and the results showed that optimized structures are stable geometric structures (no imaginary frequencies, Table S4, ESI†). Symmetry constraints were not applied in optimization processes. The standard Gibbs free energies (ΔG°) were obtained from the frequency calculations with the temperature set to 298 K. To take into account the experimental conditions all calculations were performed in the presence of the solvent field with the polarizable continuum model (PCM) using the CPCM polarizable conductor calculation model.[74] The standard Gibbs free energies for the complexation of hydroxyl group (ΔG_{OH}°) in **3a** and **5a** were determined for the process $A + OH^- = AOH^-$.

Antimicrobial activity

Bacterial and fungal strains and their growth conditions. To determine the direct antimicrobial activity the standard and clinical strains were used. The following standard strains were tested: (1) Gram-positive cocci: methicillin-sensitive *Staphylococcus aureus* ATCC 6538P (MSSA), methicillin-resistant *S.*

aureus subsp. *aureus* ATCC 43300 (MRSA), *S. epidermidis* ATCC 12228, *Enterococcus faecalis* ATCC 29212, *E. faecium* ATCC 6057, *Bacillus subtilis* ATCC 6633; (2) Gram-negative bacteria from *Enterobacteriales* order: *Escherichia coli* ATCC 25922, *Klebsiella pneumoniae* ATCC 13883, *Proteus mirabilis* ATCC 12453, *Enterobacter cloacae* DSM 6234, *Serratia marcescens* ATCC 13880; (3) Gram-negative non-fermentative rods: *Pseudomonas aeruginosa* ATCC 27853, *Acinetobacter baumannii* ATCC 19606, *Stenotrophomonas maltophilia* ATCC 12714, *S. maltophilia* ATCC 13637, *Burkholderia cepacia* ATCC 25416, *Bordetella bronchiseptica* ATCC 4617; (4) yeasts: *Candida albicans* ATCC 90028, *C. parapsilosis* ATCC 22019, *C. tropicalis* IBA 171, *C. tropicalis* (Castellani) Berkhout ATCC 750, *C. guilliermondii* IBA 155, *C. krusei* ATCC 6258 and *Saccharomyces cerevisiae* ATCC 9763. Moreover, the study was carried out on 5 clinical strains of methicillin-resistant *S. aureus* No. NMI 664K, NMI 1576K, NMI 1712K, NMI 1991K and NMI 2541K. All strains were stored at −80 °C. Prior to testing, each bacterial strain was subcultured twice on tryptic soy agar TSA (bioMerieux) medium and yeast strains on Sabouraud dextrose agar (bioMerieux) for 24–48 h at 30 °C to ensure viability.

Determination of antimicrobial activity. Direct antimicrobial activity against yeast, Gram-positive and Gram-negative bacterial strains was examined as previously described[5] by the disc-diffusion test and the MIC determination assays according to the EUCAST[75,76] and CLSI[47,77,78] recommendations. Determination of bactericidal (MBC) and fungicidal (MFC) activity was performed according to the CLSI recommendations.[79,80] The following reference agents were used: fluconazole (in the case of fungi), linezolid (for Gram-positive bacteria) and nitrofurantoin (for Gram-negative rods). The tested compounds were dissolved in DMSO.

Determination of the MICs of compounds in the presence of PAβN. To investigate the contribution of the MDR efflux pumps to the resistance of Gram-negative rods to the new synthesized compounds, the MIC values of studied agents with or without the pump inhibitor PAβN (20 mg L^{-1}) (Sigma) were determined.[81] The MIC determination was performed in Mueller–Hinton II broth medium (MHB) (Becton Dickinson) using 2-fold serial dilutions of tested agents, according to the CLSI guidelines.[47] In order to minimize the influence of PAβN on destabilization of bacterial cell covers, the tests were conducted in the presence of 1 mM $MgSO_4$ (Sigma).[82] At least a 4-fold decrease in the MIC value after the addition of PAβN was considered significant.[83,84]

Cytotoxicity studies. MRC-5 pd30 human fibroblasts (ECACC) were cultured in MEME, Minimum Essential Medium Eagle (Merck) supplemented with 10% fetal bovine serum (Merck), 2 mM L-glutamine, antibiotics (100 U mL^{-1} penicillin, 100 mg L^{-1} streptomycin, Merck) and 1% non-essential amino-acids (Merck). Cells were grown in 75 cm^2 cell culture flasks (Sarstedt), in a humidified atmosphere of CO_2/air (5/95%) at 37 °C. MTT-based viability assay was conducted as described previously.[5] Optical densities were measured at 570 nm using BioTek microplate reader. All measurements were carried out in three replicates and the results expressed as a percent of viable cells *versus* control cells.

Structural insights into the antibacterial activity of benzosiloxaboroles. Homology modelling of the *S. aureus* MRSA leucyl-tRNA synthetase (*Sa*LeuRS) editing domain has been done based on the structure of the *T. thermopilus* LeuRS (*Tt*LeuRS) (PDB code: 2V0C). Studied molecules were placed based on the ligand coordinates obtained from the crystal structure. The resulting complexes were then minimized (Amber10:EHT forcefield). All steps were carried out in MOE.[65] Images were rendered using VMD.[85]

Conflicts of interest

There are no conflicts of interest to declare.

Acknowledgements

This research was financially supported by National Science Centre (Poland) in the framework of the project UMO-2018/31/B/ST5/00210. Work implemented as a part of Operational Project Knowledge Education Development 2014–2020 co-financed by the European Social Fund (the TRIBIOCHEM interdisciplinary PhD programme for P.H.M.-U.). The authors thank Wroclaw Centre for Networking and Supercomputing (http://www.wcss.pl), grant no. 285, for providing computer facilities (*Gaussian16*). The molecular docking studies were performed under the Project HPC-EUROPA3 (INFRAIA-2016-1-730897), with the support of the EC Research Innovation Action under the H2020 Programme; in particular, the authors gratefully acknowledge the support by Hospital del Mar Medical Research Institute (IMIM), Pompeu Fabra University (Barcelona, Spain) and the computer resources and technical support provided by Barcelona Supercomputing Center (BSC); the authors thank Dr Jana Selent for her assistance in this matter. The work was supported by the Warsaw University of Technology.

References

1 A. Adamczyk-Woźniak, K. M. Borys and A. Sporzyński, *Chem. Rev.*, 2015, **115**, 5224–5247.
2 A. Nocentini, C. T. Supuran and J.-Y. Winum, *Expert Opin. Ther. Pat.*, 2018, **28**, 493–504.
3 F. Yang, M. Zhu, J. Zhang and H. Zhou, *MedChemComm*, 2018, **9**, 201–211.
4 K. Nowicki, P. Pacholak and S. Luliński, *Molecules*, 2021, **26**, 5464.
5 P. Pacholak, J. Krajewska, P. Wińska, J. Dunikowska, U. Gogowska, J. Mierzejewska, K. Durka, K. Woźniak, A. E. Laudy and S. Luliński, *RSC Adv.*, 2021, **11**, 25104–25121.
6 K. Durka, A. E. Laudy, Ł. Charzewski, M. Urban, K. Stępień, S. Tyski, K. A. Krzyśko and S. Luliński, *Eur. J. Med. Chem.*, 2019, **171**, 11–24.
7 P. Ćwik, P. Ciosek-Skibińska, M. Zabadaj, S. Luliński, K. Durka and W. Wróblewski, *Sensors*, 2020, **20**, 3540.
8 A. Ahmad, A. Ahmad, R. Sudhakar, H. Varshney, N. Subbarao, S. Ansari, A. Rauf and A. U. Khan, *J. Biomol. Struct. Dyn.*, 2017, **35**, 3412–3431.

9 M. Schmidt, L. K. Bast, F. Lanfer, L. Richter, E. Hennes, R. Seymen, C. Krumm and J. C. Tiller, *Bioconjugate Chem.*, 2017, **28**, 2440–2451.
10 S. Kakkar and B. Narasimhan, *BMC Chem.*, 2019, **13**, 16.
11 M. Zhou, Y. Qian, J. Xie, W. Zhang, W. Jiang, X. Xiao, S. Chen, C. Dai, Z. Cong, Z. Ji, N. Shao, L. Liu, Y. Wu and R. Liu, *Angew. Chem.*, 2020, **132**, 6474–6481.
12 M. Zhou, W. Jiang, J. Xie, W. Zhang, Z. Ji, J. Zou, Z. Cong, X. Xiao, J. Gu and R. Liu, *ChemMedChem*, 2021, **16**, 309–315.
13 J. Altman, H. Böhnke, A. Steigel and G. Wulff, *J. Organomet. Chem.*, 1986, **309**, 241–246.
14 S. Ghosh, A. S. Kumar, G. N. Mehta, R. Soundararajan and S. Sen, *J. Chem. Res.*, 2009, 205–207.
15 J. M. Blacquiere, O. Sicora, C. M. Vogels, M. Čuperlović-Culf, A. Decken, R. J. Ouellette and S. A. Westcott, *Can. J. Chem.*, 2005, **83**, 2052–2059.
16 J. W. Hicks, C. B. Kyle, C. M. Vogels, S. L. Wheaton, F. J. Baerlocher, A. Decken and S. A. Westcott, *Chem. Biodiversity*, 2008, **5**, 2415–2422.
17 J. Yang, B. J. Johnson, A. A. Letourneau, C. M. Vogels, A. Decken, F. J. Baerlocher and S. A. Westcott, *Aust. J. Chem.*, 2015, **68**, 366–372.
18 D. Zhu, C. D. Hunter, S. R. Baird, B. R. Davis, A. Bos, S. J. Geier, C. M. Vogels, A. Decken, C. A. Gray and S. A. Westcott, *Heteroat. Chem.*, 2017, e21405.
19 A. I. Meyers, D. L. Temple, D. Haidukewych and E. D. Mihelich, *J. Org. Chem.*, 1974, **39**, 2787–2793.
20 G. J. Summers, R. B. Maseko and C. A. Summers, *Polym. Int.*, 2014, **63**, 1785–1796.
21 M. S. Shchepinov, R. Chalk and E. M. Southern, *Tetrahedron*, 2000, **56**, 2713–2724.
22 R. R. Fraser, M. Bresse and T. S. Mansour, *J. Am. Chem. Soc.*, 1983, **105**, 7790–7791.
23 I. Steciuk, K. Durka, K. Gontarczyk, M. Dąbrowski, S. Luliński and K. Woźniak, *Dalton Trans.*, 2015, **44**, 16534–16546.
24 A. Brzozowska, P. Ćwik, K. Durka, T. Kliś, A. E. Laudy, S. Luliński, J. Serwatowski, S. Tyski, M. Urban and W. Wróblewski, *Organometallics*, 2015, **34**, 2924–2932.
25 M. Czub, K. Durka, S. Luliński, J. Łosiewicz, J. Serwatowski, M. Urban and K. Woźniak, *Eur. J. Org. Chem.*, 2017, 818–826.
26 *Boronic Acids: Preparation and Applications in Organic Synthesis, Medicine and Materials*, ed. D. G. Hall, Wiley-VCH Verlag GmbH & Co. KGaA, Weinheim, Germany, 2011.
27 A. Adamczyk-Woźniak, M. K. Cyrański, M. Jakubczyk, P. Klimentowska, A. Koll, J. Kołodziejczak, G. Pojmaj, A. Żubrowska, G. Z. Żukowska and A. Sporzyński, *J. Phys. Chem. A*, 2010, **114**, 2324–2330.
28 W. Chen, M. Liu, H.-J. Li and Y.-C. Wu, *Org. Chem. Front.*, 2021, **8**, 584–590.
29 Z. Wrzeszcz and R. Siedlecka, *Catalysts*, 2021, **11**, 444.
30 P. Deslongchamps, *Tetrahedron*, 1975, **31**, 2463–2490.
31 P. Deslongchamps, P. Dube, C. Lebreux, D. R. Patterson and R. J. Tallefer, *Can. J. Chem.*, 1975, **53**, 2791–2806.
32 M. N. Holerca and V. Percec, *Eur. J. Org. Chem.*, 2000, 2257–2263.
33 R. A. Gossage, H. A. Jenkins and J. W. Quail, *J. Chem. Crystallogr.*, 2010, **40**, 272–277.
34 R. B. Martin and A. Parcell, *J. Am. Chem. Soc.*, 1961, **83**, 4835–4838.
35 P. Rota, P. La Rocca, F. Cirillo, M. Piccoli, P. Allevi and L. Anastasia, *RSC Adv.*, 2020, **10**, 162–165.
36 W. Shi, X. Zhang, X. Jiang, H. Yuan, J. S. Lee, C. E. Barry, H. Wang, W. Zhang and Y. Zhang, *Science*, 2011, **333**, 1630–1632.
37 M. Dolezal, P. Cmedlova, L. Palek, J. Vinsova, J. Kunes, V. Buchta, J. Jampilek and K. Kralova, *Eur. J. Med. Chem.*, 2008, **43**, 1105–1113.
38 S. C. Ngo, O. Zimhony, W. J. Chung, H. Sayahi, W. R. Jacobs and J. T. Welch, *Antimicrob. Agents Chemother.*, 2007, **51**, 2430–2435.
39 J. Zitko, B. Servusová, A. Janoutová, P. Paterová, J. Mandíková, V. Garaj, M. Vejsová, J. Marek and M. Doležal, *Bioorg. Med. Chem.*, 2015, **23**, 174–183.
40 P. Gopal, J. P. Sarathy, M. Yee, P. Ragunathan, J. Shin, S. Bhushan, J. Zhu, T. Akopian, O. Kandror, T. K. Lim, M. Gengenbacher, Q. Lin, E. J. Rubin, G. Grüber and T. Dick, *Nat. Commun.*, 2020, **11**, 1661.
41 K. Durka, R. Kamiński, S. Luliński, J. Serwatowski and K. Woźniak, *Phys. Chem. Chem. Phys.*, 2010, **12**, 13126–13136.
42 K. Durka, M. Urban, M. Czub, M. Dąbrowski, P. Tomaszewski and S. Luliński, *Dalton Trans.*, 2018, **47**, 3705–3716.
43 K. Durka, P. Kurach, S. Luliński and J. Serwatowski, *Eur. J. Org. Chem.*, 2009, 4325–4332.
44 K. Durka, M. Urban, M. Dąbrowski, P. Jankowski, T. Kliś and S. Luliński, *ACS Omega*, 2019, **4**, 2482–2492.
45 Y. Guo, G. Song, M. Sun, J. Wang and Y. Wang, *Front. Cell. Infect. Microbiol.*, 2020, **10**, 107.
46 J. S. Lewis II, M. P. Weinstein, A. M. Bobenchik, S. Campeau, S. K. Cullen, M. F. Galas, H. Gold, R. M. Humphries, T. J. Kirn Jr, B. Limbago, A. Matherns, T. Mazzulli, S. Richter, M. Satlin, A. Schuetz, S. Sharp and P. Simner, *Performance Standards for Antimicrobial Susceptibility Testing, Document CLSI supplement M100*, Clinical and Laboratory Standards Institute (CLSI), West Valley Road, Wayne, Pennsylvania, USA, 32nd edn, 2022.
47 F. R. Cockerill III, M. A. Wikler, J. Alder, M. N. Dudley, G. M. Eliopoulos, M. J. Ferraro, D. J. Hardy, D. W. Hecht, J. A. Hindler, J. B. Patel, M. Powell, J. M. Swenson, R. B. Thomson Jr, M. M. Traczewski, J. D. Turnidge, M. P. Weinstein and B. L. Zimmer, *Methods for dilution antimicrobial susceptibility tests for bacteria that grow aerobically, Approved Standard, Document M07-A9*, Clinical and Laboratory Standards Institute (CLSI), 940 West Valley Road, Wayne, Pennsylvania, USA, 9th edn, 2012.
48 A. Prasetyoputri, A. M. Jarrad, M. A. Cooper and M. A. T. Blaskovich, *Trends Microbiol.*, 2019, **27**, 339–354.
49 FDA Document, **https://www.accessdata.fda.gov/drugsatfda_docs/nda/2014/204427Orig1s000TOC.cfm**.
50 A. E. Laudy, *Pol. J. Microbiol.*, 2018, **67**, 129–135.
51 H. Nikaido and J. M. Pages, *FEMS Microbiol. Rev.*, 2012, **36**, 340–363.

52 T. J. Opperman and S. T. Nguyen, *Front. Microbiol.*, 2015, **6**, 421.
53 V. Hernandez, T. Crépin, A. Palencia, S. Cusack, T. Akama, S. J. Baker, W. Bu, L. Feng, Y. R. Freund, L. Liu, M. Meewan, M. Mohan, W. Mao, F. L. Rock, H. Sexton, A. Sheoran, Y. Zhang, Y.-K. Zhang, Y. Zhou, J. A. Nieman, M. R. Anugula, E. M. Keramane, K. Savariraj, D. S. Reddy, R. Sharma, R. Subedi, R. Singh, A. O'Leary, N. L. Simon, P. L. De Marsh, S. Mushtaq, M. Warner, D. M. Livermore, M. R. K. Alley and J. J. Plattner, *Antimicrob. Agents Chemother.*, 2013, **57**, 1394–1403.
54 Q.-H. Hu, R.-J. Liu, Z.-P. Fang, J. Zhang, Y.-Y. Ding, M. Tan, M. Wang, W. Pan, H.-C. Zhou and E.-D. Wang, *Sci. Rep.*, 2013, **3**, 2475.
55 A. Palencia, X. Li, W. Bu, W. Choi, C. Z. Ding, E. E. Easom, L. Feng, V. Hernandez, P. Houston, L. Liu, M. Meewan, M. Mohan, F. L. Rock, H. Sexton, S. Zhang, Y. Zhou, B. Wan, Y. Wang, S. G. Franzblau, L. Woolhiser, V. Gruppo, A. J. Lenaerts, T. O'Malley, T. Parish, C. B. Cooper, M. G. Waters, Z. Ma, T. R. Ioerger, J. C. Sacchettini, J. Rullas, I. Angulo-Barturen, E. Pérez-Herrán, A. Mendoza, D. Barros, S. Cusack, J. J. Plattner and M. R. K. Alley, *Antimicrob. Agents Chemother.*, 2016, **60**, 6271–6280.
56 X. Li, V. Hernandez, F. L. Rock, W. Choi, Y. S. L. Mak, M. Mohan, W. Mao, Y. Zhou, E. E. Easom, J. J. Plattner, W. Zou, E. Pérez-Herrán, I. Giordano, A. Mendoza-Losana, C. Alemparte, J. Rullas, I. Angulo-Barturen, S. Crouch, F. Ortega, D. Barros and M. R. K. Alley, *J. Med. Chem.*, 2017, **60**, 8011–8026.
57 Y. Si, S. Basak, Y. Li, J. Merino, J. N. Iuliano, S. G. Walker and P. J. Tonge, *ACS Infect. Dis.*, 2019, **5**, 1231–1238.
58 S. J. Baker, J. W. Tomsho and S. J. Benkovic, *Chem. Soc. Rev.*, 2011, **40**, 4279–4285.
59 H. Zhao, A. Palencia, E. Seiradake, Z. Ghaemi, S. Cusack, Z. Luthey-Schulten and S. Martinis, *ACS Chem. Biol.*, 2015, **10**, 2277–2285.
60 F. L. Rock, W. Mao, A. Yaremchuk, M. Tukalo, T. Crépin, H. Zhou, Y.-K. Zhang, V. Hernandez, T. Akama, S. J. Baker, J. J. Plattner, L. Shapiro, S. A. Martinis, S. J. Benkovic, S. Cusack and M. R. K. Alley, *Science*, 2007, **316**, 1759–1761.
61 E. Von Dach, S. M. Diene, C. Fankhauser, J. Schrenzel, S. Harbarth and P. François, *J. Infect. Dis.*, 2016, **213**, 1370–1379.
62 *Staphylococcus aureus* strain MRSA_S24 MRSA_S24_contig005, whole genome shotgun sequence; available from: **https://www.ncbi.nlm.nih.gov/nuccore/NZ_LFVO01000005.1**, accessed March 1, 2022.
63 D. Ding, Q. Meng, G. Gao, Y. Zhao, Q. Wang, B. Nare, R. Jacobs, F. Rock, M. R. K. Alley, J. J. Plattner, G. Chen, D. Li and H. Zhou, *J. Med. Chem.*, 2011, **54**, 1276–1287.
64 A. Adamczyk-Woźniak, M. Tarkowska, Z. Lazar, E. Kaczorowska, I. D. Madura, A. M. Dąbrowska, J. Lipok and D. Wieczorek, *Bioorg. Chem.*, 2022, **119**, 105560.
65 S. M. Diene, E. von Dach, C. Fankhauser, J. Schrenzel, S. Harbarth, and P. Francois, *Molecular Operating Environment (MOE)*, 2020.09 Chemical Computing Group ULC, 1010 Sherbooke St. West, Suite #910, Montreal, QC, Canada, H3A 2R7, 2022.
66 M. de L. F. Bispo, R. S. B. Gonçalves, C. H. da S. Lima, L. N. de F. Cardoso, M. C. S. Lourenço and M. V. N. de Souza, *J. Heterocycl. Chem.*, 2012, **49**, 1317–1322.
67 Rigaku Oxford Diffraction, *Crysalis Pro v. 1.171.38.46*, 2018.
68 G. M. Sheldrick, *Acta Crystallogr.*, 2008, **A64**, 112–122.
69 G. M. Sheldrick, *Acta Crystallogr.*, 2015, **C71**, 3–8.
70 M. J. Frisch, G. W. Trucks, H. B. Schlegel, G. E. Scuseria, M. A. Robb, J. R. Cheeseman, G. Scalmani, V. Barone, G. A. Petersson, H. Nakatsuji, X. Li, M. Caricato, A. V. Marenich, J. Bloino, B. G. Janesko, R. Gomperts, B. Mennucci, H. P. Hratchian, J. V. Ortiz, A. F. Izmaylov, J. L. Sonnenberg, D. Williams-Young, F. Ding, F. Lipparini, F. Egidi, J. Goings, B. Peng, A. Petrone, T. Henderson, D. Ranasinghe, V. G. Zakrzewski, J. Gao, N. Rega, G. Zheng, W. Liang, M. Hada, M. Ehara, K. Toyota, R. Fukuda, J. Hasegawa, M. Ishida, T. Nakajima, Y. Honda, O. Kitao, H. Nakai, T. Vreven, K. Throssell, J. A. Montgomery, Jr., J. E. Peralta, F. Ogliaro, M. J. Bearpark, J. J. Heyd, E. N. Brothers, K. N. Kudin, V. N. Staroverov, T. A. Keith, R. Kobayashi, J. Normand, K. Raghavachari, A. P. Rendell, J. C. Burant, S. S. Iyengar, J. Tomasi, M. Cossi, J. M. Millam, M. Klene, C. Adamo, R. Cammi, J. W. Ochterski, R. L. Martin, K. Morokuma, O. Farkas, J. B. Foresman, and D. J. Fox, *Gaussian 16, Revision C.01*, Gaussian, Inc., Wallingford CT, 2016.
71 Y. Zhao and D. G. Truhlar, *Theor. Chem. Acc.*, 2008, **120**, 215–241.
72 C. Lee, W. Yang and R. G. Parr, *Phys. Rev. B*, 1988, **37**, 785–789.
73 R. Dennington, T. A. Keith, and J. M. Millam, *GaussView, Version 6.1*, Semichem Inc., Shawnee Mission, KS, 2016.
74 J. Tomasi, B. Mennucci and R. Cammi, *Chem. Rev.*, 2005, **105**, 2999–3094.
75 European Committee on Antimicrobial Susceptibility Testing (EUCAST), *Method for the determination of broth dilution MIC of antifungal agents for yeasts Document E.DEF 7.3.2*, 2020, **http://www.eucast.org/**.
76 European Committee on Antimicrobial Susceptibility Testing (EUCAST), *Disk diffusion method for antimicrobial susceptibility testing, Document Version 9.0*, 2021, **http://www.eucast.org/**.
77 J. H. Rex, M. A. Ghannoum, B. D. Alexander, D. Andes, S. D. Brown, D. J. Diekema, A. Espinel-Ingroff, C. L. Fowler, E. M. Johnson, C. Knapp, M. R. Motyl, L. Ostrosky-Zeichner, M. A. Pfaller, D. J. Sheehan and T. J. Walsh, *Method for antifungal disk diffusion susceptibility testing of yeasts, Document M44-A2*, Clinical and Laboratory Standards Institute (CLSI), 940 West Valley Road, Wayne, Pennsylvania, USA, 2nd edn, 2009.
78 J. H. Rex, B. D. Alexander, D. Andes, B. Arthington-Skaggs, S. D. Brown, V. Chaturvedi, M. A. Ghannoum, A. Espinel-Ingroff, C. Knapp, L. Ostrosky-Zeichnerm, M. A. Pfaller, D. J. Sheehan and T. J. Walsh, *Reference method for broth dilution antifungal susceptibility testing of yeasts, Document M27A3*, Clinical and Laboratory Standards Institute (CLSI),

940 West Valley Road, Wayne, Pennsylvania, USA, 3rd edn, 2008.
79 A. L. Barry, W. A. Craig, H. Nadler, L. Barth Reller, C. C. Sanders and J. M. Swenson, *Methods for determining bactericidal activity of antimicrobial agents, Approved Guideline, Document M26-A*, Clinical and Laboratory Standards Institute (CLSI), 940 West Valley Road, Wayne, Pennsylvania, USA, 1999.
80 E. Cantón, J. Pemán, A. Viudes, G. Quindós, M. Gobernado and A. Espinel-Ingroff, *Diagn. Microbiol. Infect. Dis.*, 2003, **45**, 203–206.
81 R. Misra, K. D. Morrison, H. J. Cho and T. Khuu, *J. Bacteriol.*, 2015, **197**, 2479–2488.
82 R. P. Lamers, J. F. Cavallari and L. L. Burrows, *PLoS One*, 2013, **8**, e60666.
83 A. E. Laudy, A. Mrowka, J. Krajewska and S. Tyski, *PLoS One*, 2016, **11**, e0147131.
84 A. E. Laudy, E. Kulińska and S. Tyski, *Molecules*, 2017, **22**, 114.
85 W. Humphrey, A. Dalke and K. Schulten, VMD: Visual Molecular Dynamics, *J. Mol. Graphics*, 1996, **14**, 33–38.

Electronic Supplementary Material (ESI) for RSC Advances.

Oxazoline scaffold in synthesis of benzosiloxaboroles and related ring-expanded heterocycles: diverse reactivity and structural peculiarities and antimicrobial activity

Joanna Krajewska,[a] Krzysztof Nowicki,[b] Krzysztof Durka,[b] Paulina H. Marek-Urban,[b] Patrycja Wińska,[b] Tomasz Stępniewski,[c] Krzysztof Woźniak,[d] Agnieszka E. Laudy,[a,*] Sergiusz Luliński[b,*]

[a]*Department of Pharmaceutical Microbiology, Medical University of Warsaw, Oczki 3, 02-007, Warsaw, Poland*

[b]*Warsaw University of Technology, Faculty of Chemistry, Noakowskiego 3, 00-664 Warsaw, Poland*

[c]*GPCR Drug Discovery Lab, Research Programme on Biomedical Informatics (GRIB), Hospital del Mar Medical Research Institute (IMIM) – Department of Experimental and Health Sciences of Pompeu Fabra University (UPF), Carrer del Dr. Aiguader, 88, 08003 Barcelona, Spain*

[d]*University of Warsaw, Faculty of Chemistry, Pasteura 1, 02-093 Warsaw, Poland*

Supporting Information

List of contents

1. **Single-crystal X-ray diffraction……..…….…..S2**
2. **Theoretical calculations..……..…..S8**
3. **Antimicrobial activity……..…….…....S11**
4. **NMR spectra……..…..……..S16**

3. Antimicrobial activity.

Table S5. The antibacterial activity of tested agents against standard Gram-positive strains.

	MIC in mg/L [MBC in mg/L][a] (Diameter of inhibition zone in mm)					
Agent tested	***S. aureus* ATCC 6538P**	***S. aureus* ATCC 43300 MRSA**	***S. epidermidis* ATCC 12228**	***E. faecalis* ATCC 29212**	***E. faecium* ATCC 6057**	***B. subtilis* ATCC 6633[b]**
3a	50 [100] (21)	50 (21)	50 [200] (18)	>400 (-)	>400 (-)	NT (20)
3b	>400 (-)	>400 (-)	>400 (-)	>400 (-)	>400 (-)	NT (-)
3d	200 [400] (15)	200 [400] (14)	400 (-)	>400 (-)	200 (-)	NT (13)
3e	**6.25** (28)	**6.25** (26)	12.5 (19)	50 (-)	25 (-)	NT (20)
3f	**3.12** [400] (25)	**6.25** [400] (22)	12.5 (16)	25 (13)	25 (15)	NT (22)
3g	>400 (-)	>400 (-)	>400 (-)	>400 (-)	>400 (-)	NT (-)
4a	>200 (-)	>200 (-)	>200 (-)	>200 (-)	>200 (-)	NT (-)
4b	>400 (-)	>400 (-)	>400 (-)	>400 (-)	>400 (-)	NT (-)
4c	>100 (-)	>100 (-)	>100 (-)	>100 (-)	>100 (-)	NT (-)
4d	50 (19)	100 (19)	50 (28)	400 (-)	>400 (-)	NT (26)
5a	>400 (-)	>400 (-)	>400 (-)	>400 (-)	>400 (-)	NT (-)
5c	>400 (-)	>400 (-)	>400 (-)	>400 (-)	>400 (-)	NT (-)
5d	>400 (-)	>400 (-)	>400 (-)	>400 (-)	>400 (-)	NT (-)
LIN[c]	1 [>128] (25)	2 [>128] (25)	1 [>128] (26)	2 [>128] (15)	2 [>128] (14)	NT (30)

The highest activity against Gram-positive bacteria indicated by the low MIC values (≤6.25 mg/L) is shown in boldface.

(-): The inhibition zone was not observed in the disc-diffusion method. The diameter of the paper discs was 9 mm.

[a] Only the MBC values ≤400 mg/L (for **3a–3g**, **4b**, **4d**, **5a**, **5c** and **5d**), ≤200 mg/L (for **4a**) and ≤100 mg/L (for **4c**) are presented. The tested substance **4a** and **4c** dissolved in DMSO precipitated after implementation into the MHB medium at a concentration above 200 mg/L for **4a** and above 100 mg/L for **4c**.

[b] The growth type of *B. subtilis* in the MHB medium prevented reading the MIC values of tested substances.

[c] LIN, linezolid was used as a reference agent active against Gram-positive bacteria. The diameter of commercial disc containing 0.03 mg of linezolid was 6 mm; the MIC of linezolid was determined according to the CLSI recommendations.[1]

Table S6. The antibacterial activity of tested agents against standard Gram-negative strains.

Agent tested	MIC in mg/L [MBC in mg/L][a] / x-fold reduction of MIC in the presence of PAβN[b] (Diameter of inhibition zone in mm)										
	E. coli **ATCC 25922**	***K. pneumonia*** **ATCC 13883**	***P. mirabilis*** **ATCC 12453**	***E. cloacae*** **DSM 6234**	***S. marcescens*** **ATCC 13880**	***P. aeruginosa*** **ATCC 27853**	***S. maltophilia*** **ATCC 13637**	***S. maltophilia*** **ATCC 12714**	***A. baumannii*** **ATCC 19606**	***B. cepacia*** **ATCC 25416[c]**	***B. bronchiseptica*** **ATCC 4617[c]**
3a	>400 (-)	>400 (-)	>400 (-)	>400 (-)	>400 (-)	>400 (-)	>400 (-)	>400 (-)	>400 (-)	>400 (-)	>400 (-)
3b	>400 (-)	>400 (-)	>400 (-)	>400 (-)	>400 (-)	>400 (-)	>400 (-)	>400 (-)	>400 (-)	>400 (-)	>400 (-)
3d	>400 (-)	>400 (-)	>400 (-)	>400 (-)	>400 (-)	>400 (-)	>400 (-)	>400 (-)	>400 (-)	>400 (-)	>400 (-)
3e	>400 (-)	>400 (-)	>400 (-)	>400 (-)	>400 (-)	>400 (-)	>400 (-)	>400 (-)	>400 (-)	>400 (-)	>400 (-)
3f	>400 (-)	>400 (-)	>400 (-)	>400 (-)	>400 (-)	>400 (-)	>400 (-)	>400 (-)	>400 (-)	>400 (-)	>400 (-)
3g	>400 (-)	>400 (-)	>400 (-)	>400 (-)	>400 (-)	>400 (-)	>400 (-)	>400 (-)	>400 (-)	>400 (-)	>400 (-)
4a	>200 (-)	>200 (-)	>200 (-)	>200 (-)	>200 (-)	>200 (-)	>200 (-)	>200 (-)	>200 (-)	>200 (-)	>200 (-)
4b	>400 (-)	>400 (-)	>400 (-)	>400 (-)	>400 (-)	>400 (-)	>400 (-)	>400 (-)	>400 (-)	>400 (-)	>400 (-)
4c	>100 / 2 (-)	>100 (-)	>100 (-)	>100 (-)	>100 (-)	>100 (-)	>100 (-)	>100 (-)	>100 (-)	>100 (-)	>100 (-)
4d	25 (32)	100 (20)	100 (26)	50 (29)	50 (29)	>400 (-)	200 (20)	100 (25)	>400 (-)	>400 (-)	50 (32)
5a	>400 (-)	>400 (-)	>400 (-)	>400 (-)	>400 (-)	>400 (-)	>400 (-)	>400 (-)	>400 (-)	>400 (-)	>400 (-)
5c	>400 (-)	>400 (-)	>400 (-)	>400 (-)	>400 (-)	>400 (-)	>400 (-)	>400 (-)	>400 (-)	>400 (-)	>400 (-)
5d	>400 /2 (-)	>400 (-)	>400 (-)	>400 (-)	>400 (-)	>400 (-)	>400 (-)	>400 (-)	>400 (-)	>400 (-)	>400 (-)
Nf[d]	8 [8] (24)	32 [32] (23)	128 [>128] (9)	32 [32] (17)	128 [>128] (12)	>128 [>128] (-)	128 [>128] (-)	128 [>128] (-)	64 [128] (9)	32 [32] (12)	64 [128] (-)

PaβN: efflux pump inhibitor. (-): The inhibition zone was not observed in the disc-diffusion method. The diameter of the paper discs was 9 mm.

[a] Only the MBC values ≤400 mg/L (for **3a–3g**, **4b**, **4d**, **5a**, **5c** and **5d**), ≤200 mg/L (for **4a**) and ≤100 mg/L (for **4c**) are presented. The tested substance **4a** and **4c** dissolved in DMSO precipitated after implementation into the MHB medium at a concentration above 200 mg/L for **4a** and above 100 mg/L for **4c**.

[b] In the table, only at least a 2-fold decrease in the MIC values of tested compounds after the addition of PAβN is presented.

[c] The growth of *B. cepacia* ATCC 25416 and *B. bronchiseptica* ATCC 4617 strains was inhibited in the MHB medium supplemented with 1 mM $MgSO_4$ and 20 mg/L PAβN.

[d] Nf, nitrofurantoin was used as a reference agent active against Gram-negative bacteria. The diameter of commercial disc containing 0.3 mg of nitrofurantoin was 6 mm; the MIC of nitrofurantoin was determined according to the CLSI recommendations.[1]

Table S7. The antifungal activity of tested agents against yeasts strains.

Agent tested	MIC in mg/L [MFC in mg/L][a] (Diameter of inhibition zone in mm)						
	C. albicans **ATCC 90028**	***C. parapsilosis*** **ATCC 22019**	***C. tropicalis*** **IBA 171**	***C. tropicalis*** **ATCC 750**	***C. guilliermondii*** **IBA 155**	***C. krusei*** **ATCC 6258**	***S. cerevisiae*** **ATCC 9763**
3a	>400 (-)	>400 (-)	>400 (-)	>400 (-)	>400 (-)	>400 (-)	50 (18)
3b	>400 (-)	>400 (-)	>400 (-)	>400 (-)	>400 (-)	>400 (-)	>400 (-)
3d	>400 (-)	>400 (-)	>400 (-)	>400 (-)	>400 (-)	>400 (-)	>400 (-)
3e	>400 (-)	>400 (-)	>400 (-)	>400 (-)	>400 (-)	>400 (-)	>400 (-)
3f	>400 (-)	>400 (-)	>400 (-)	>400 (-)	>400 (-)	>400 (-)	400 (16)
3g	>400 (-)	>400 (-)	>400 (-)	>400 (-)	>400 (-)	>400 (-)	>400 (-)
4a	>200 (-)	>200 (-)	>200 (-)	>200 (-)	>200 (-)	>200 (-)	>200 (-)
4b	>400 (-)	>400 (-)	>400 (-)	>400 (-)	>400 (-)	>400 (-)	>400 (-)
4c	>100 (-)	>100 (-)	>100 (-)	>100 (-)	>100 (-)	>100 (-)	>100 (-)
4d	3.12 (41)	6.25 (37)	3.12 (33)	3.12 (40)	3.12 (40)	12.5 (25)	0.78 [100] (51)
5a	>400 (-)	>400 (-)	>400 (-)	>400 (-)	>400 (-)	>400 (-)	>400 (-)
5c	>400 (-)	>400 (-)	>400 (-)	>400 (-)	>400 (-)	>400 (-)	>400 (-)
5d	>400 (-)	>400 (-)	>400 (-)	>400 (-)	>400 (-)	>400 (-)	>400 (-)
Fl[b]	1 (43)	2 (32)	0.38 (39)	0.38 (40)	0.75 (40)	64[c] (16)	16[d] (12)

(-): The inhibition zone was not observed in the disc-diffusion method. The diameter of paper discs was 9 mm.

[a] Only the MFC values ≤400 mg/L (for **3a–3g**, **4b**, **4d**, **5a**, **5c** and **5d**), ≤200 mg/L (for **4a**) and ≤100 mg/L (for **4c**) are presented. The tested substance **4a** and **4c** dissolved in DMSO precipitated after implementation into the RPMI medium at a concentration above 200 mg/L for **4a** and above 100 mg/L for **4c**. Only the MFC values ≤400 mg/L are presented.

[b] Fl, fluconazole was used as a reference antifungal agent; the diameter of a commercial disc containing 0.025 mg of fluconazole was 6 mm; the MIC value of fluconazole was determined by the Etest method.[2]

[c] The ellipse was visible pointing the MIC value 64 mg/L, however, with macro-colonies up to concentration ≥256 mg/L. In accordance with the recommendations for Etest method, the MIC value of fluconazole against *C. krusei* can be also interpreted as ≥256 mg/L.[2,3] *C. krusei* is intrinsically resistant to fluconazole.

[d] The ellipse was visible pointing the MIC value 16 mg/L, with colonies up to concentration ≥256 mg/L. There are no recommendations for Etest method interpretation of the MIC value of fluconazole against *S. cerevisiae*. The obtained MIC 16 mg/L is in line with the published results.[4]

Table S8. Comparison of activity of **4c**, **4d**, and Tavaborole against standard strains of bacteria and yeasts.

	MIC in mg/L [MBC/MFC in mg/L][a]/ x-fold reduction of MIC In the presence of PAβN[b] (Diameter of inhibition zone in mm)		
Strain	**4c**	**4d**	**Tavaborole**
***S. aureus* ATCC 6538P**	>100 (-)	50 (19)	25 (20)
***S. aureus* ATCC 43300 MRSA**	>100 (-)	100 (19)	50 (35)
***S. epidermidis* ATCC 12228**	>100 (-)	50 (28)	12.5 [400] (40)
***E. faecalis* ATCC 29212**	>100 (-)	400 (-)	100 (20)
***E. faecium* ATCC 6057**	>100 (-)	>400 (-)	200 (-)
***B. subtilis* ATCC 6633[c]**	NT (-)	NT (26)	NT (35)
***E. coli* ATCC 25922**	>100/2 (-)	25 (32)	6.25 (37)
***K. pneumoniae* ATCC 13883**	>100 (-)	100 (20)	12.5 (33)
***P. mirabilis* ATCC 12453**	>100 (-)	100 (26)	100 (22)
***E. cloacae* DSM 6234**	>100 (-)	50 (29)	12.5 (29)
***S. marcescens* ATCC 13880**	>100 (-)	50 (29)	25 (36)
***P. aeruginosa* ATCC 27853**	>100 (-)	>400 (-)	400 (13)
***S. maltophilia* ATCC 13637**	>100 (-)	200 (20)	100 (19)
***S. maltophilia* ATCC 12714**	>100 (-)	100 (25)	100 (19)
***A. baumannii* ATCC 19606**	>100 (-)	>400 (-)	6.25 (30)
***B. cepacia* ATCC 25416[d]**	>100 (-)	>400 (-)	400 (14)
***B. bronchiseptica* ATCC 4617[d]**	>100 (-)	50 (32)	12.5 (32)
***C. albicans* ATCC 90028**	>100 (-)	3.12 (41)	0.78 (63)
***C. parapsilosis* ATCC 22019**	>100 (-)	6.25 (37)	1.56 (59)
***C. tropicalis* IBA 171**	>100 (-)	3.12 (33)	1.56 (48)
***C. tropicalis* ATCC 750**	>100 (-)	3.12 (40)	1.56 (60)
***C. guilliermondii* IBA 155**	>100 (-)	3.12 (40)	1.56 (64)
***C. krusei* ATCC 6258**	>100 (-)	12.5 (25)	3.12 (45)
***S. cerevisiae* ATCC 9763**	>100 (-)	0.78 [100] (51)	0.39 (74)

PAβN, efflux pump inhibitor. (-) The inhibition zone was not observed in the disc-diffusion method. The diameter of paper discs was 9 mm.

[a] Only the MBC/MFC values ≤400 mg/L (for **4d** and Tavaborole) and ≤100 mg/L (for **4c**) are presented. The tested substance **4c** dissolved in DMSO precipitated after implementation into the MHB and RPMI medium at a concentration above 100 mg/L. [b] The growth type of *B. subtilis* in the MHB medium prevented reading the MIC values of tested substances. [c] In the table, only at least a 2-fold decrease in the MIC values of tested compounds after the addition of PAβN are presented. [d] The growth of *B. cepacia* ATCC 25416 and *B. bronchiseptica* ATCC 4617 strains was inhibited in the MHB medium supplemented with 1 mM $MgSO_4$ and 20 mg/L PAβN.

References

1. Clinical and Laboratory Standards Institute (CLSI), Methods for dilution antimicrobial susceptibility tests for bacteria that grow aerobically, Approved Standard, Document M07-A9, 9th ed., CLSI, 940 West Valley Road, Wayne, PA, USA, 2012.
2. ETEST Application guide, BioMerieux. http://www.biomerieux-usa.com/clinical/etest.
3. ETEST for antifungal susceptibility testing – research gate, AB BIODISK. https://www.researchgate.net/...fungal.../Etest.pdf
4. M. A. Pfaller, M. Bale, B. Buschelman, M. Lancaster, A. Espinel-Ingroff, J. H. Rex and M. G. Rinaldi., *J. Clin. Microbiol*., 1994, **32**, 1650–1653.

Kompletne *Supplementary Materials* do Publikacji O2 dostępne są pod adresem:

https://www.rsc.org/suppdata/d2/ra/d2ra03910a/d2ra03910a5.pdf

7.4. Publikacja O3

AMERICAN SOCIETY FOR MICROBIOLOGY | Antimicrobial Agents and Chemotherapy®

ANALYTICAL PROCEDURES

Mutant Prevention Concentration, Frequency of Spontaneous Mutant Selection, and Mutant Selection Window—a New Approach to the *In Vitro* Determination of the Antimicrobial Potency of Compounds

Joanna Krajewska,[a] Stefan Tyski,[b] Agnieszka E. Laudy[a]

[a]Department of Pharmaceutical Microbiology and Bioanalysis, Medical University of Warsaw, Warsaw, Poland
[b]Department of Antibiotics and Microbiology, National Medicines Institute, Warsaw, Poland

ABSTRACT The analysis of antimicrobial activity is usually MIC- and minimal bactericidal concentration (MBC)-focused, though also crucial are resistance-related parameters, e.g., the frequency of spontaneous mutant selection (FSMS), the mutant prevention concentration (MPC), and the mutant selection window (MSW). *In vitro*-determined MPCs, however, are sometimes variable, poorly repeatable, and not always reproducible *in vivo*. We propose a new approach to the *in vitro* determination of MSWs, along with novel parameters: MPC-D, MSW-D (for dominant mutants, i.e., selected with a high frequency, without a fitness loss), and MPC-F, MSW-F (for inferior mutants, i.e., with an impaired fitness). We also propose a new method for preparing the high-density inoculum ($>10^{11}$ CFU/mL). In this study, the MPC and MPC-D (limited by FSMS of $<10^{-10}$) of ciprofloxacin, linezolid, and novel benzosiloxaborole (No37) were determined for *Staphylococcus aureus* ATCC 29213 using the standard agar method, while the MPC-D and MPC-F were determined by the novel broth method. Regardless of the method, $MSWs_{10}^{10}$ of linezolid and No37 were the same. However, $MSWs_{10}^{10}$ of ciprofloxacin in the broth method was narrower than in the agar method. In the broth method, the 24-h incubation of $\sim10^{10}$ CFU in a drug-containing broth differentiates the mutants that can dominate the cell population from those that can only be selected under exposure. We consider MPC-Ds in the agar method to be less variable and more repeatable than MPCs. Meanwhile, the broth method may decrease discrepancies between *in vitro* and *in vivo* MSWs. The proposed approaches may help establish MPC-D-related resistance-restricting therapies.

KEYWORDS MPC, MSW, FSMS, MPC-D, MSW-D, MPC-F, MSW-F, antibiotic resistance, antimicrobial activity, antimicrobial agents

In vitro parameters describing the antimicrobial potency of compounds are important concerning the increasing antimicrobial resistance. They apply to the search for both new combination therapies (known antibiotics that would show a synergistic effect) and structurally new compounds. Based on these parameters, the best new drug candidate is selected, while many other compounds are eliminated from further studies. Currently, despite tremendous efforts and an abundance of compounds in preclinical trials, the number of new antibiotics on the market is still insufficient (1 to 4). Thus, refining old or introducing new *in vitro* parameters (especially those that can predict the emergence and the expansion of resistant mutants) is an approach aimed at improving the preclinical screening for novel antimicrobials and, consequently, facilitating the development of novel therapies.

Currently, the most common parameters determined in preliminary studies concerning the activity of newly developed compounds against microorganisms are the

Address correspondence to Agnieszka E. Laudy, alaudy@wp.pl.

The authors declare no conflict of interest.

Received 14 October 2022
Returned for modification 7 November 2022
Accepted 26 February 2023
Published 6 April 2023

MIC values and the minimal bactericidal/fungicidal concentration (MBC/MFC) values (5 to 8). However, an extremely important stage of preclinical research is also to determine the resistance-related parameters like the frequency of spontaneous mutant selection (FSMS) and the so-called mutant prevention concentration (MPC) values (9 to 12). These are necessary for subsequent *in vivo* studies to determine the dose of the new compound as a drug in animal models. It is known that resistant cells can be selected at a high frequency in the population of bacteria living in the presence of an antibiotic in a concentration ranging from the MIC value to slightly above the MIC value (9, 10). In the natural environment, e.g., in a human host, a single-step mutation often occurs in bacterial cells. If the frequency of spontaneous mutations is very low, the host's immune system will likely be able to combat the emerging bacterial mutants (10). Zhao et al., in their reviews on the restriction of fluoroquinolone-resistant mutant selection in *Staphylococcus aureus* and *Mycobacterium bovis* cell population, indicated that mutants arising at a low FSMS value of 1×10^{-6} to 1×10^{-8} could be controlled by the host organism (10, 11). Similarly, Sun et al. used a frequency of $<1 \times 10^{-8}$ as a threshold for reduced mutant selection in *in vitro* analysis assessing the activity of the meropenem–vaborbactam combination against *Klebsiella pneumoniae* strains producing the *Klebsiella pneumoniae* carbapenemase (KPC)-type enzymes (13). Moreover, mutants with a significant fitness cost of acquired resistance (with the decreased growth rate) also cannot establish a resistant population *in vivo* and can be easily outcompeted by sensitive bacteria in a nonantibiotic environment (14, 15). On the other hand, in preclinical *in vitro* studies of new compounds, the concept of MPC was introduced as a value relating to the prevention of the emergence of resistant mutants' growth. The concept and definition of MPC were proposed by Dong et al. in 1999 (9). According to this first definition, the MPC is estimated by determining the minimal antibiotic concentration that allows no mutant to be obtained when a large number of bacterial cells ($>10^{10}$) are applied to agar plates containing the antibiotic. Thus, the MPC value is sufficient to block the growth of single-step mutants (9 to 11). More importantly, Dong et al. underlined that the MPC value depends on the number of cells used in the study (9). Consequently, a subscript indicating the number of cells used in the test should be added to the MPC (e.g., $MPC_{10}{}^{10}$ indicates that 10^{10} cells were applied to the plates). The acquired antibiotic resistance of the obtained mutants was checked by their regrowth on the new agar plates with the same concentration of antibiotic (9).

The selective proliferation of resistant mutants (also called mutants enrichment) is considered to occur only in the presence of an antibiotic in the concentration range from the MIC value for a wide-type strain up to the MPC value that inhibits the growth of single-step resistant mutants. This interval of the antibiotic concentrations was named the mutant selection window (MSW) (10). However, it is also known that mutants may arise in sub-MIC concentrations of antibiotics (16 to 19), though their recovery drops off sharply then (20), as the growth of sensitive wide-type cells is not inhibited (10). The basis for determining the currently used drug doses are the MIC values and the standardized cutoff points defining the susceptibility or resistance of the tested strains, according to the European Committee on Antimicrobial Susceptibility Testing (EUCAST) (21) and the Clinical and Laboratory Standards Institute (CLSI) documents (22). The MPC/MIC ratio ranges from 4 to >32, depending on the antibiotic and the tested strain (9, 23 to 27). It seems that such a sizeable x-fold increase in drug dose is not always necessary (20, 28) and not always feasible, due to a higher risk of side effects, with little benefit to the patient (10), especially since MIC-based doses are generally high enough to clear the infection with the lowest possible toxicity (10). On the other hand, the problem may occur with immunocompromised patients who may experience therapeutic failure due to the generation of resistant mutants, as emphasized by Zhao and Drlica (10). Another problem is the scale of the mutant selection in a public health context. When the bulk of therapies put antibiotic concentrations within the MSW, the abundance of selected mutants and their spread will accelerate the loss of its activity (10). Therefore, the question may still be raised about what concentrations should be used to achieve therapeutic success, minimize toxicity for the patients and, at the same time, not generate a selection of bacterial mutants to preserve the effectiveness of antibiotics.

In this article, we propose a new approach to *in vitro* determination of the resistance potential of antibacterial compounds. To date, no MPC-based, resistance-restricting dosing scheme is in use. Moreover, Gianvecchio et al. have recently reported poor repeatability and reproducibility of MPC results for some strain-drug combinations (29), while others observed some discrepancies between the ranges of *in vitro*- and *in vivo*-determined MSWs (30, 31). We assume that this is related to the frequency of mutant selection. Mutants selected extremely rarely may not always be detectable in the agar-dilution method. Another problem is the mutants' fitness, which is not assessed during the MPC determination. Considering the above, we propose the following new resistance-related parameters characterizing the *in vitro*-determined antimicrobial potency of compounds: a dominant mutant prevention concentration (MPC-D), an inferior mutant prevention concentration (MPC-F), a dominant mutant selection window (MSW-D), and an inferior mutant selection window (MSW-F). MPC-D and MSW-D refer to mutants selected with a high frequency, without a resistance-associated fitness loss, which we named the dominant mutants. We assume they are likely to establish a resistant population *in vivo* and should be considered relevant in the public health context. MPC-D is the lowest drug concentration that blocks the selection of dominant mutants. In the agar-dilution method, we defined MPC-D as the lowest drug concentration with the FSMS $<10^{-10}$, considering mutants selected less often are hardly detectable and of less significance due to their rarity. However, to quickly predict whether mutants selected *in vitro* are not significantly inferior to sensitive cells due to the fitness costs of the resistance, we proposed a new broth-dilution method for their selection. In this method, we defined MPC-D as the lowest drug concentration that, after the 24 h of incubation, prevents mutants selected among 10^{10} CFU from establishing a resistant population of at least 10 CFU/mL in the drug-supplemented broth culture (i.e., mutants are not able to dominate the population). In turn, MPC-F and MSW-F refer to mutants with impaired fitness that can be selected *in vitro* in concentrations above the MPC-D but cannot dominate the population in the broth culture. We named them the inferior mutants, whereas MPC-F was defined as the lowest drug concentration that blocks their selection. We consider mutants unable to dominate in the broth culture unlikely to appear in subsequent *in vivo* studies. The assumptions of our work were based on the original definition of MPC. However, we believe that the ability of mutants to dominate the cell population, rather than mutant selection, is the most important point to consider in the further steps of both *in vivo* animal studies and clinical trials.

RESULTS

Susceptibility testing and the high-density inoculum. The MIC values for the parent strain of *Staphylococcus aureus* ATCC 29213 were as follows: 0.25 mg/L for ciprofloxacin, 2 mg/L for linezolid, and 3.12 mg/L for novel benzosiloxaborole No37.

The assumed high-density inoculum ($>10^{11}$ CFU/mL) was obtained by a 6-stage progressive culture concentration by centrifugation. Obtained densities for the two repetitions of the experiment were 7.5×10^{11} CFU/mL and 5×10^{11} CFU/mL.

Frequency of spontaneous mutant selection (FSMS). The single-step spontaneous mutant selection was performed on A-series plates (mutant selection by the agar-dilution method [AM]), which were visually assessed after incubation. Four types of growth were observed on the plates, depending on the tested antimicrobial compound and its concentration (Table 1).

In the case of ciprofloxacin, the dense bacterial lawn was detected at concentrations up to 0.5 mg/L (2×MIC), the colony lawn with uncountable colonies at the concentration of 1 mg/L (4×MIC), and countable colonies were detected at every higher concentration. All obtained colonies were recovered on agar medium in the agar mutant recovery test (aMRTest). Therefore, colony numbers at concentrations up to 1 mg/L (4×MIC) were classified as uncountable, and the FSMS values were classified as being above the upper detection limit ($>3 \times 10^{-8}$). Colonies at the 2-, 4-, and 8-mg/L concentrations were counted (mean values are presented in Table 1), and the FSMS values were calculated as 5.5×10^{-9}, 6×10^{-11}, and 4.5×10^{-11}, respectively (means from two repetitions).

Visual screening of the linezolid A-series plates only revealed a dense, noncolony lawn, slightly thinner on the three highest concentrations tested. Such a result made

TABLE 1 Agent-resistant mutant selection and their ability to regrow on the same concentration of the antibacterial compound

	Agent concentration		Agar-dilution method: MPC and MPC-D determination[b]			Broth-dilution method: MPC-D determination[b]			Broth-dilution method: MPC-F determination[b]	
				aMRTests' results (hours to mutants' regrowth)[b]			bMRTests' results (hours to mutants' regrowth)[b]			bMRTests' results (hours to mutants' regrowth)[b]
Agent tested[a]	mg/L	x-fold MIC	Visual mutants' growth on A-series plates[c]	Agar medium	FSMS[b]	Visual mutants' growth on B-series plates[c]	Broth medium	Agar medium	Visual mutants' growth on C-series plates[c]	Broth medium	Agar medium
CIP	0.25	1	L	+(24)	$>3 \times 10^{-8}$	L	+(24)	+(24)	L	+(24)	+(24)
	0.5	2	L	+(24)	$>3 \times 10^{-8}$	CL	+(24)	+(24)	CL	+(24)	+(24)
	1	4	CL	+(24)	$>3 \times 10^{-8}$	65	+(24)	+(24)	CL	+(24)	+(24)
	2	8	330	+(24)	$5{,}5 \times 10^{-9}$	NL	−(72)	−(72)	25	+(24)	+(24)
	4	16	4	+(24)	6×10^{-11}	NL	−(72)	−(72)	1	+(24)	+(24)
	8	32	3	+(24)	$4{,}5 \times 10^{-11}$	NL	−(72)	−(72)	NL	−(72)	−(72)
LIN	2	1	L	+(24)	$>3 \times 10^{-8}$	L	+(24)	+(24)	L	+(24)	+(24)
	4	2	L	−(72)	$<2 \times 10^{-11}$	SL	−(72)	−(72)	L	−(72)	−(72)
	8	4	L	−(72)	$<2 \times 10^{-11}$	NL	−(72)	−(72)	NL	−(72)	−(72)
	16	8	SL	−(72)	$<2 \times 10^{-11}$	NL	−(72)	−(72)	NL	−(72)	−(72)
	32	16	SL	−(72)	$<2 \times 10^{-11}$	NL	−(72)	−(72)	NL	−(72)	−(72)
	64	32	SL	−(72)	$<2 \times 10^{-11}$	NL	−(72)	−(72)	NL	−(72)	−(72)
No37	3.12	1	L	+(24)	$>3 \times 10^{-8}$	L	+(24)	+(24)	L	+(24)	+(24)
	6.24	2	L	+(24)	$>3 \times 10^{-8}$	L	+(24)	+(24)	L	+(24)	+(24)
	12.5	4	L	+(24)	$>3 \times 10^{-8}$	CL	+(24)	+(24)	L	+(24)	+(24)
	25	8	L	+(48)	$>3 \times 10^{-8}$	CL	+(48)	+(48)	L	+(48)	+(48)
	50	16	L	+(48)	$>3 \times 10^{-8}$	CL	+(48)	+(72)	L	+(48)	+(72)
	100	32	L	−(72)	$<2 \times 10^{-11}$	NL	−(72)	−(72)	CL	−(72)	−(72)

[a]CIP, ciprofloxacin; LIN, linezolid; No37, novel benzosiloxaborole compound No37.
[b]MPC, mutant prevention concentration; MPC-D, dominant mutant prevention concentration; MPC-F, inferior mutant prevention concentration; FSMS, frequency of spontaneous mutant selection; aMRTests, agar mutants recovery tests; bMRTests, broth mutants recovery tests.
[c]L, dense lawn; SL, semi-lawn (less dense, no colonies visible); CL, colony lawn (uncountable colonies); NL, no lawn (visually clear plate).

colony counting impossible. In the aMRTest, however, mutant growth was only confirmed for the concentration equal to 2 mg/L (1×MIC), although no visual difference in the density of the plate lawns was observed for concentrations up to 4×MIC. Based on the aMRTest results, the FSMS for 2 mg/L (1×MIC) was established as being above the upper detection limit ($>3 \times 10^{-8}$). In contrast, those for concentrations of 4 mg/L and above (≥2×MIC) were considered as being below the lower limit of detection ($<2 \times 10^{-11}$).

The aMRTest was also required to determine the FSMS values for different concentrations of compound No37, as only a dense, noncolony lawn was observed on all A-series plates, regardless of the concentration. The aMRTest revealed that mutants were present on all plates except those with the highest concentration tested (100 mg/L, 32×MIC); however, the regrowth of mutants selected at No37 concentrations of 25 mg/L (8×MIC) and 50 mg/L (16×MIC) was impaired. At 8×MIC and 16×MIC, mutants needed 48 h to recover on agar. Based on the aMRTest results, the FSMS for concentrations equal to and below 50 mg/L (≤16×MIC) were calculated as being above the upper detection limit ($>3 \times 10^{-8}$). In comparison, those for the concentration of 100 mg/L (32×MIC) were considered being below the lower limit of detection ($<2 \times 10^{-11}$).

Reduced mutant selection ($<10^{-8}$) was obtained for concentrations ≥8×MIC for ciprofloxacin, ≥2×MIC for linezolid, and ≥32×MIC for compound No37.

Mutant prevention concentration (MPC) value and dominant mutant prevention concentration (MPC-D) parameter, determined by the agar-dilution method (AM). The visual mutants' growth on A-series plates, the mutants' ability to regrow in the aMRTest, and the cutoff points for both the MPC and MPC-D parameters are presented in Table 1, while the MPC_{10}[10], $MPC\text{-}D_{10}$[10], selection index (SI), and dominant selection index (SI-D) values for the tested agents are shown in Table 2.

TABLE 2 Activity of tested agents, expressed as MPC and SI values

Methods	Parameters of activity[a]	Agents[b]		
		CIP	LIN	No37
Susceptibility test	MIC [mg/L]	0.25	2	3.12
Agar dilution	MPC_{10}^{10} [mg/L]	>8	4	100
	SI	>32	2	32
	$MPC\text{-}D_{10}^{10}$ [mg/L]	4	4	100
	SI-D	16	2	32
Broth dilution	$MPC\text{-}D_{10}^{10}$ [mg/L]	2	4	100
	SI-D	8	2	32
	$MPC\text{-}F_{10}^{10}$ [mg/L]	8	4	100
	SI-F	32	2	32

[a]MPC, mutant prevention concentration; SI, selection index; MPC-D, dominant mutant prevention concentration; SI-D, dominant selection index; MPC-F, inferior mutant prevention concentration; SI-F, inferior selection index.
[b]CIP, ciprofloxacin; LIN, linezolid; No37, novel benzosiloxaborole compound No37.

In the case of ciprofloxacin, as mutants were also detected at the highest tested concentration of 8 mg/L (32×MIC), the MPC_{10}^{10} value was estimated as being above 8 mg/L (>32×MIC). However, we consider mutants selected with extremely rare frequency ($<1 \times 10^{-10}$) unlikely to appear later *in vivo* often enough to be clinically significant (thus, they are not dominant mutants). Consequently, 4 mg/L (16×MIC) was designated the $MPC\text{-}D_{10}^{10}$ of ciprofloxacin, as it was the lowest concentration with the FSMS value below 1×10^{-10}.

On the contrary, when linezolid and compound No37 were tested, a visual assessment of mutant presence on the plates was impossible: only a gradually fading lawn was observed on all A-series plates with linezolid, while a dense lawn was present on all plates for compound No37, including the highest tested concentration. The aMRTest revealed mutants capable of regrowth in the presence of the tested agent and allowed the MPC_{10}^{10} values to be determined as 4 mg/L (2×MIC) for linezolid and 100 mg/L (32×MIC) for compound No37. Because a sharp decrease in the FSMS values (from $>3 \times 10^{-8}$ to $<2 \times 10^{-11}$) was shown between 1×MIC (2 mg/L) and 2×MIC (4 mg/L) for linezolid and between 50 mg/L (16×MIC) and 100 mg/L (32×MIC) for compound No37, the concentrations of 4 mg/L of linezolid and 100 mg/L of compound No37 were designated the $MPC\text{-}D_{10}^{10}$.

The MPC_{10}^{10} values determined for two of the three compounds tested, linezolid and compound No37, were equal to the $MPC\text{-}D_{10}^{10}$ values, while the MPC_{10}^{10} of ciprofloxacin was at least 2 times higher than the $MPC\text{-}D_{10}^{10}$ value associated with its FSMS.

Overall, linezolid had the smallest selection indices in the AM: its SI (MPC/MIC ratio) and SI-D (MPC-D/MIC ratio) were equal to 2.

Dominant mutant prevention concentration (MPC-D) and inferior mutant prevention concentration (MPC-F) parameters, determined by the broth-dilution method (BM). The visual mutants' growth on B-series plates (inoculated with the aliquots from the liquid culture after 24 h of incubation) and C-series plates (inoculated with the concentrated content of the liquid culture after 24 h of incubation), results of the broth mutant recovery test (bMRTest), and the cutoff points for both MPC-D and MPC-F parameters are presented in Table 1, while the $MPC\text{-}D_{10}^{10}$, $MPC\text{-}F_{10}^{10}$, SI-D, and inferior selection index (SI-F) values for tested agents are shown in Table 2.

In the case of ciprofloxacin on B-series plates, a dense lawn was observed at 0.25 mg/L (1×MIC), an uncountable colony lawn at 0.5 mg/L (2×MIC), and 65 colonies were detected at 1 mg/L (4×MIC). No visual growth was observed on plates with 2, 4, and 8 mg/L of ciprofloxacin (8 to 32×MIC). The regrowth ability of the obtained resistant mutants in the presence of an antibiotic was confirmed by the bMRTest. Thus, the concentration of 2 mg/L (8×MIC) was designated the $MPC\text{-}D_{10}^{10}$ value. On ciprofloxacin C-series plates, a dense lawn was observed at 0.25 mg/L (1×MIC), an uncountable colony lawn at 0.5 to 1 mg/L (2 to 4×MIC), 25 colonies at 2 mg/L (8×MIC), and 1 colony at 4 mg/L (16×MIC). No colony was obtained on the plate with 8 mg/L (32×MIC) of

ciprofloxacin, which is why this concentration was designated the MPC-F_{10}^{10} for ciprofloxacin.

On B- and C-series linezolid plates, a dense lawn was observed at 2 mg/L (1×MIC), while at 4 mg/L (2×MIC) a thicker lawn, a semi-lawn, and a dense lawn, respectively. In the bMRTest, however, the bacterial lawn obtained at 4 mg/L was not able to recover in broth medium with the same linezolid concentration, which is why the MPC-D_{10}^{10} and MPC-F_{10}^{10} values were determined as 4 mg/L.

On B-series plates with compound No37, a dense lawn was visible up to 6.25 mg/L (2×MIC), while a colony lawn from 12.5 to 50 mg/L (4 to 16×MIC). No visual growth was observed at the concentration of 100 mg/L (32×MIC). The bMRTest confirmed obtained resistant mutants' ability to regrow in the same antibiotic concentrations. Thus, the concentration of 100 mg/L (32×MIC) was designated the MPC-D_{10}^{10} value. In contrast, on C-series plates, the colony lawn visible at 100 mg/L failed the bMRTest. As a result, the MPC-F_{10}^{10} value was also designated 100 mg/L.

The MPC-D_{10}^{10} values determined for two of the three compounds tested, linezolid and compound No37, were equal to the MPC-F_{10}^{10} values, while the MPC-F_{10}^{10} of ciprofloxacin was 4 times higher than the MPC-D_{10}^{10} value.

Overall, in the broth-dilution method, linezolid had the smallest SI-D and SI-F (both equal to 2), followed by ciprofloxacin (SI-D = 8, SI-F = 32) and compound No37 (both equal to 32).

Mutant selection window (MSW), dominant mutant selection window (MSW-D), and inferior mutant selection window (MSW-F) ranges. The ranges of MSW, MPC-D, and MSW-F are presented in Fig. 1.

Overall, linezolid had the narrowest ranges of MSWs, MSW-Ds, and MSW-Fs. Regardless of the method, all of the above-mentioned parameters ranged between 1 and 2×MIC. Also, for compound No37, the MSW, MSW-Ds, and MSW-F had the same range of 1 to 32×MIC. In the case of ciprofloxacin, the narrowest range had the MSW-D_{10}^{10} determined in the BM (1 to 8×MIC), while the MSW-D_{10}^{10} determined in the AM was broader, ranging up to 4 mg/L (16×MIC), and the MSW-F_{10}^{10} ranged up to 8 mg/L (32×MIC). The upper limit of the MSW_{10}^{10} for ciprofloxacin was above the highest tested concentration of 8 mg/L (>32×MIC).

DISCUSSION

Since the introduction of the mutant selection window hypothesis in 2001 (10), MPC values have been determined for a large number of isolates according to the initially proposed agar-dilution method (9). Generally, there is no correlation between MPC and MIC (32). Moreover, currently used doses were proven to put many drug concentrations inside the mutant selection window during therapy (11). However, for new fluoroquinolones, achieving serum concentrations above the MPC was possible with existing dosing schemes (33, 34). For compounds whose serum level cannot exceed the MPC (e.g., due to toxicity concerns), combination therapy was proved to restrict the mutant selection, as then, two concurrent mutations are needed for resistance (10, 11, 35). Finally, it was established that derivatives within the same group of antibacterial compounds might differ significantly in the mutant selection window size for particular strains (9, 11, 33, 34, 36 to 38). Consequently, preferential use of the derivatives with narrow selection windows may prolong the life span of the whole class of antibiotics (10). Though generally successful, the broad validation of the mutant selection window hypothesis provides some evidence that *in vitro*-determined MSW ranges do not always fit *in vivo* boundaries (30, 31). Also, concerns about the repeatability of the MPC values have been recently raised (29). This article presents the concept of new resistance-related parameters that differentiate mutants selected *in vitro* into dominant mutants (relevant in the public health context) and inferior mutants (unlikely to appear *in vivo* due to impaired fitness). We suggest the *in vitro*-determined MSW-D (the concentration range where dominant mutants are selected, limited by the MPC-D) should be avoided when adjusting doses *in vivo*, rather than the original MSW, which refers to all mutants selected *in vitro*. Moreover, this article

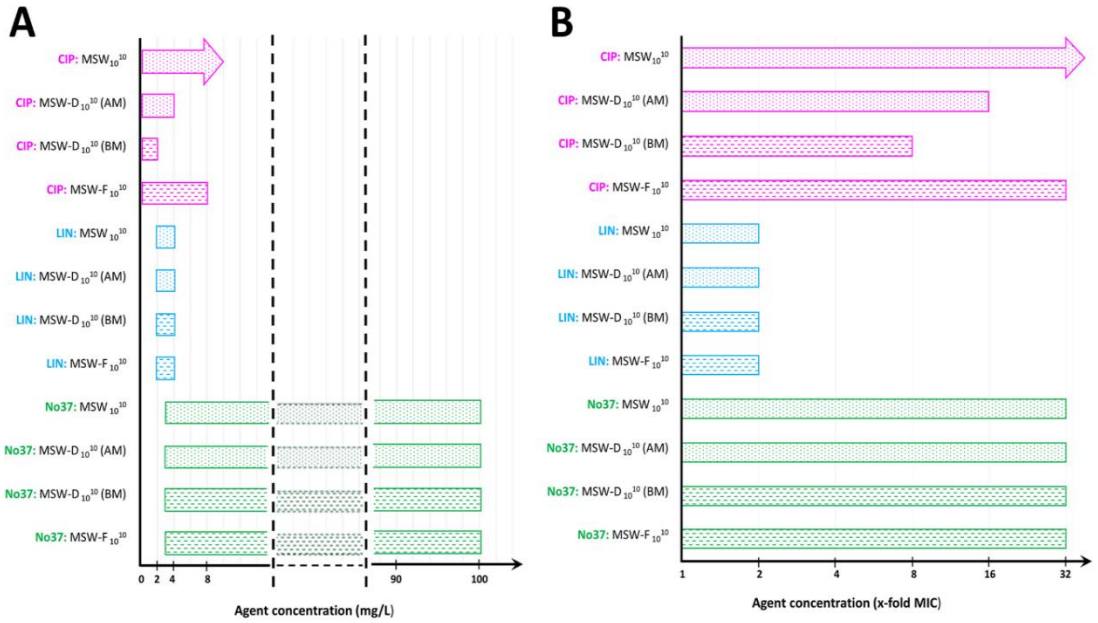

FIG 1 Scheme presenting the MSW_{10}^{10} ranges. Agents' concentrations expressed in mg/L (A) or as x-fold MIC (B). CIP, ciprofloxacin; LIN, linezolid; No37, novel benzosiloxaborole compound No37; MSW, mutant selection window; MSW-D, dominant mutant selection window; MSW-F, inferior mutant selection window; AM, agar-dilution method; BM, broth-dilution method; pink color, MSWs of CIP; blue color, MSWs of LIN; green color, MSWs of No37; dotted pattern, MSWs determined by the agar-dilution method; striped pattern, MSWs determined by the broth-dilution method; arrows indicate the MSW's upper boundary was above the highest concentration tested.

shows that MPC-D can be lower than MPC. Thus, it should be more clinically useful due to the lower risk of side effects.

In this article, the MICs, MPCs, and SIs (MPC/MIC ratios) of ciprofloxacin, linezolid, and novel benzosiloxaborole No37 were determined for *S. aureus* ATCC 29213 by the initially proposed agar method (9). Values obtained for the parameters mentioned above were 0.25 mg per L/>8 mg per L/>32 for ciprofloxacin, 2 mg per L/4 mg per L/2 for linezolid, and 3.12 mg per L/100 mg per L/32 for compound No37. In the case of ciprofloxacin, the SIs reported so far for methicillin-susceptible *Staphylococcus aureus* (MSSA) strains with similar MICs to the strain tested in our study (0.12 to 0.5 mg/L) ranged from 8 to 64 (9, 23, 24). Such significant variations in the SIs of ciprofloxacin (6 to 156) have also been observed among wild-type *Escherichia coli* strains with similar MICs (25). In contrast, the linezolid SIs reported so far for *S. aureus* strains were usually equal to 2 or 4 (26, 39, 40). Likewise, no significant variability in the SIs of vancomycin (32 to 64) and fosfomycin (64 to >256) was observed among methicillin-resistant *Staphylococcus epidermidis* (MRSE) strains (27).

The initially proposed agar-dilution method for the MPC determination was successfully used by many authors, though it implicates several challenges. One is the so-called "inoculum effect" (41, 42). It is known that during MPC determination by agar-dilution assays, "false mutants" (with wild-type MIC) may appear, probably because huge inocula protect them from the drug action. Thus, testing the ability of obtained colonies to regrow on the same drug concentration is necessary (41, 42). Another way to eliminate this effect is to apply fewer cells on a large number of plates (33). This approach is time- and substance-consuming. Thus, it is hard to implement in preclinical screening, where the availability of new substances is frequently limited. In our study, we were also working with novel benzoxaborole No37, available in small amounts, and we had to minimize the plates' usage. That is why we decided to eliminate the inoculum effect by performing MRTests instead of increasing the number of plates.

Obtaining the high-density inoculum is another challenge. Currently, required inocula

are prepared via a one-step concentration of the liquid culture. However, they rarely exceed a density of 10^{11} CFU/mL (9, 36, 43), usually reaching 10^{10} CFU/mL (29, 39, 44 to 48) or 10^{9} CFU/mL (49, 50). The lower the inoculum density, the more plates are needed. Our multi-step concentration of the liquid culture, with many centrifugation-resuspension cycles, increases the chance of an inoculum with a density exceeding 10^{11} CFU/mL. Thus, it gives an advantage in circumstances when a substance is limited.

Finally, it was recently reported that MPC values sometimes show poor experiment-to-experiment repeatability, even within one laboratory. When determining the MPCs of 5 antibiotics from different classes for *S. epidermidis* was repeated 20 times, the results varied significantly for all tested agents (29). This is in contrast with the generally repeatable MIC values. We assume it is connected with the frequency of mutant selection. Mutants selected with low frequency may not always be present in the starting inoculum, as emphasized by Firsov et al. (51). This may make the upper boundary of the MSW changeable. We suggest that the FSMS value should provide a threshold for the MPC. As at least 1×10^{10} CFU must be tested for the MPC determination, we propose an FSMS of $<1 \times 10^{-10}$ (indicating less than 1 mutant per 10^{10} cells) for that. We consider that mutants selected less often are not the dominant mutants due to their rarity. Consequently, we proposed the lowest concentration with an FSMS of $<1 \times 10^{-10}$ as the new MPC-D parameter, defined as the lowest concentration that blocks the selection of dominant mutants. In our study, the MPC-Ds_{10}^{10} of linezolid and No37 were equal to their MPCs. In the case of ciprofloxacin, however, the MPC-D_{10}^{10} was at least 4-fold lower than the MPC_{10}^{10} (16×MIC *versus* >32×MIC, respectively). At the highest concentration tested, mutants were selected with a frequency of 4.5×10^{-11}. Thus, ciprofloxacin MPC determined in our study will not be reproducible in studies where less than 2.2×10^{10} CFU will be examined.

Regardless of the implicated challenges, the existence of the mutant selection window has already been confirmed in *in vitro* dynamic models. These models aim to simulate dosing regimens and cultivate bacteria in circulating broth with the tested agent, whose concentration fluctuates within the defined ranges (44). So far, for many strain–drug combinations, resistant mutants usually emerged when the drug concentrations were kept within the MSW range (39, 44, 46, 52, 53). However, some discrepancies occurred. Allen et al. isolated resistant mutants of *S. aureus* strains from a ciprofloxacin dynamic model, even when fluoroquinolones concentration was 2-fold higher than the designated MPC (23). On the other hand, the heterogeneity of the MSW was reported for the *S. aureus* strain with a broad ciprofloxacin MSW (SI = 16) (44, 53, 54). Authors noticed that its resistant mutants were enriched later and to a lesser extent when the drug concentration was kept in the upper compartment of the window than when it was kept in the lower compartment. Simultaneously, such differences were not observed for a strain with a narrow window. We consider this may be explained by the fact that mutants selected in the upper compartment are not the dominant mutants; in our study, the tested strain had wide ciprofloxacin MSW_{10}^{10} (SI > 32), and its MPC-D_{10}^{10} was at least 4-fold lower than its MPC_{10}^{10}.

It is also apparent that for many drug-strain combinations, the MSWs observed *in vitro* exist *in vivo* as well. This has been proven in the levofloxacin treatment of rabbits infected with *S. aureus* (20), *E. coli* (55), and *Streptococcus pneumoniae* (56), as well as for moxifloxacin tested in a murine model of tuberculosis (57) and for the marbofloxacin treatment of mice infected with *E. coli* (45). In all cases, animals received $\sim 10^{10}$ CFU in 1 mL inoculum, and the treatment began when bacterial counts reached 10^{8} CFU/mL. Resistant mutants were generally recovered, and their numbers were found to increase during the treatment when the drug concentration fluctuated within the MSW. However, while testing fosfomycin against *E. coli*, the MSW was found to exist only *in vitro* (no mutants were recovered in a rabbit tissue cage model) (30), though it was associated with a decreased growth rate of the obtained mutants compared to the paternal strain, which probably made them easy to eradicate by the host's immune system. Simultaneously, the fosfomycin MSWs for *Pseudomonas aeruginosa* were the same *in vitro* and *in vivo*, with no biological fitness costs

of resistance occurred (30). On the other hand, Mei et al. confirmed no *in vivo* selection of the fosfomycin-resistant mutants of *S. aureus* ATCC 29213 within the *in vitro*-determined MSW boundaries, even though there was no decrease in growth rate for the mutants obtained *in vitro* (31). Such a result, however, may be associated with the immune system response and the pleiotropic fosfomycin action *in vivo*, which could not be predicted *in vitro*. Nevertheless, in some cases, *in vitro*-determined MSWs are broader than those observed later *in vivo*. We propose the broth-dilution method for the *in vitro* MPC determination to eliminate these discrepancies. In this method, the 24-h incubation of $\sim 10^{10}$ CFU in a drug-containing broth allows the differentiation of selected mutants into dominant mutants (able to proliferate and establish a resistant population of at least 10 CFU/mL, i.e., able to dominate the population) and inferior mutants (unable to establish a resistant subpopulation due to impaired fitness). This is in contrast to the agar method, where mutants' fitness does not influence the result. It was proven that the host's immune system might successfully overcome mutants with impaired fitness and that they can be easily outcompeted by sensitive bacteria in a non-antibiotic environment (14, 15). In our study, the ciprofloxacin concentration that blocked the selection of dominant mutants was 4-fold lower than the concentration that blocked the selection of inferior mutants (MPC-D = 8×MIC *versus* MPC-F = 32×MIC). We consider inferior mutants unlikely to appear in *in vivo* studies. Thus, utilizing a dominant mutant selection window may increase compatibility with *in vivo* studies.

So far, few attempts have been made to determine the MPC value in a broth medium (42, 58 to 60). Quinn et al. tried to diminish the inoculum effect by increasing the volume of the liquid culture (e.g., introducing 10^{10} CFU into up to 1L of the drug-supplemented broth). However, it turned out that the inoculum effect affected that method too, though to a lesser degree (42). Other authors tested the modified microbroth-dilution method (microtiter assay) to facilitate the introduction of MPC testing into clinical laboratories, exposing up to 10^9 CFU to tested drug concentrations. Obtained results were reproducible and comparable with the agar-dilution method (59, 60). In our study, however, we decided to expose 10^{10} CFU to each drug concentration (exactly as in the agar method), which corresponded to 100 μL of our inoculum. Thus, a microdilution assay was not possible to implement in this study. On the other hand, we also investigated a new compound with limited availability, so we had to minimize its usage. Finally, we decided to conduct our research by inoculating 5 mL of the drug-supplemented broth with 10^{10} CFU, whereas the inoculum effect was eliminated by testing the ability of obtained mutants to regrow on the same drug concentration (bMRTests). In our study, the $MSW_{10}{}^{10}$ ranges of linezolid and novel benzosiloxaborole No37 determined using the broth-dilution method were the same as those determined in the agar-dilution method. In contrast, the $MSWs_{10}{}^{10}$ of ciprofloxacin determined by the broth-dilution method were narrower (SI-D = 8, SI-F = 32) than the $MSWs_{10}{}^{10}$ determined in the agar-dilution method (SI-D = 16, SI $>$ 32). However, the ciprofloxacin $MPC\text{-}D_{10}{}^{10}$ values determined in both methods were comparable (16×MIC in the agar-dilution method *versus* 8×MIC in the broth-dilution method). Thus, our results, like previous reports, indicate that the broth-dilution method may be utilized for MPC determination. It gives results consistent with the established agar-dilution method, and the compatibility is better for the MPC-D determination.

Finally, for the therapeutic application of the MPC values, the MPC-based pharmacodynamic parameter predicting the resistance development must be established (e.g., C_{max}/MPC, AUC/MPC, or $\%T_{MSW}$). There is evidence supporting the hypothesis that MPC-based PK/PD indices may better predict resistance development than the corresponding MIC-based indices (61, 62). It was suggested that the mutants' enrichment of the bacterial cell population depends not only on the total time the drug concentration is in the MSW range but also on its position within the MSW (52, 53). In other words, the time needed inside the MSW range for the mutants' emergence and proliferation is shorter when the drug concentrations fluctuate within the lower compartment of the window (>30% when $C_{max} <$ MPC) and significantly longer when they fluctuate in the upper compartment of the window (>80% when $C_{max} >$ MPC) (20, 45).

For other drug-strain combinations (e.g., marbofloxacin–*K. pneumoniae*), it is the ratio of the time (T) above the MPC value over the time inside the MSW range ($T > MPC/T_{MSW}$) that seems to best predict resistance development (63). As no consensus has been reached, the MPC values are still not used in clinics. Consequently, improvement and standardization of the *in vitro* methods to determine the MPC value is crucial for further research, as it may facilitate establishing novel, MPC-D-related PK/PD indices as a basis for an "anti-mutant" dosing strategy. This, in turn, may prolong the life span of old and new antimicrobial agents.

Conclusions. The MPC is a parameter that was hypothesized to supplement the MIC value in the development of dosing regimens restricting the emergence of resistance. However, switching to high (MPC-based) doses, while those lower (MIC-based) are generally sufficient for a therapeutic success, is cumbersome. Moreover, MPC values show variability among strains with similar MICs, and concerns about their repeatability have been recently raised. Additionally, some discrepancies occurred between the MSW boundaries determined *in vitro* and those observed later *in vivo*. As a result, the MPC-based, "anti-mutant" dosing regimens are yet to be defined. This study proposes a new approach to the *in vitro* determination of MPC values and MSW ranges. It shows that these values may be lower than initially proposed when only related to dominant mutants (MPC-D and MSW-D). In the agar-dilution methodology, we propose determining the upper boundary of the MSW range based on the FSMS value (MPC-D instead of MPC) to increase the repeatability and reproducibility of obtained values. Second, we propose a novel broth-dilution method for determining the MSW range (marked MSW-D), which may eliminate the discrepancies between *in vitro* and *in vivo* values. Additionally, we propose a new method to achieve an inoculum that may exceed 10^{11} CFU/mL for a broader range of strains. Altogether, the proposed new approaches aim to facilitate establishing MPC-D-based, resistance-restricting dosing regimens and their clinical application.

MATERIALS AND METHODS

Antimicrobial agents, bacterial strain, and susceptibility testing. *S. aureus* ATCC 29213 was used in this study. This strain is recommended by EUCAST and CLSI for the routine quality control of methods to determine the activity of antibiotics and chemotherapeutic agents against bacteria (21, 22). Before all experiments, the strain was stored at −80°C and subcultured twice on nutrition agar medium (BioMaxima SA, Lublin, Poland) at 35°C for 24 h to ensure viability. The following antimicrobials were tested: linezolid (Pol-Aura, Warsaw, Poland), ciprofloxacin (Pol-Aura, Warsaw, Poland), and novel benzosiloxaborole compound No37 (synthesized at Warsaw University of Technology, Warsaw, Poland) (64). Powdered forms of linezolid and ciprofloxacin were dissolved according to manufacturers' instructions, while a stock solution of compound No37 was prepared in DMSO (Sigma, St. Louis, MO, USA). All stock solutions were used as fresh preparations. The susceptibility of *S. aureus* ATCC 29213 to the three tested compounds was examined by determining the MIC values according to the CLSI guidance, using the 2-fold broth microdilution method in Mueller-Hinton II broth medium (Becton, Dickinson and Company, Franklin Lakes, NJ, USA) (6). Strain susceptibility results were evaluated after incubation at 35°C for 18 h.

Preparation of the high-density inoculum. The high-density inoculum (above 10^{11} CFU/mL) was obtained by multi-stage, progressive culture concentration by the centrifugation method (Fig. 2). First, three to five colonies of the tested strain from the 24-h culture on nutrition agar medium (BioMaxima SA, Lublin, Poland) were transferred to 15 mL brain heart infusion (BHI) broth (BioMaxima SA, Lublin, Poland) in a glass flask and incubated at 35°C for 6 h with shaking at 140 RPM. The obtained culture was then diluted 1:100 in fresh BHI broth in a glass flask and further incubated at 35°C for 12 h with shaking at 140 RPM. To ensure proper aeration, flasks were filled to a maximum of 50% of the flask volume. Cultures with OD_{600} of >6 were estimated to have a density above 10^9 CFU/mL. If the OD_{600} values were below 6, the next measurement was performed after an additional hour of incubation. The culture with the required OD was centrifuged (2,061 × *g* = 4,000 RPM, 22°C, 15 min), and the obtained bacterial cell pellet was resuspended in sterile 0.9% NaCl to reach half the volume of the initial culture and recentrifuged (2,061 × *g* = 4,000 RPM, 22°C, 15 min). The procedure was repeated until the volume of obtained suspension was equal to 1/100 of the initial volume of the culture. This multi-step approach, with many centrifugation-resuspension cycles, ensured a proper washout of the medium, dead cell elements, and metabolites that might affect the viability of the final inoculum. The final inoculum was estimated to be above 10^{11} CFU/mL. The concentration of the final inoculum was confirmed by serial, 10-fold dilutions in 0.9% NaCl and plating on compound-free agar. After incubation at 35°C for 24 h, the bacterial colonies were counted, and the inoculum concentration was calculated.

FSMS, MPC, MPC-D, MSW, and MSW-D determination by the agar-dilution method (AM). The FSMS, MPC, MPC-D, MSW, and MSW-D parameters were determined simultaneously by the AM (Fig. 3).

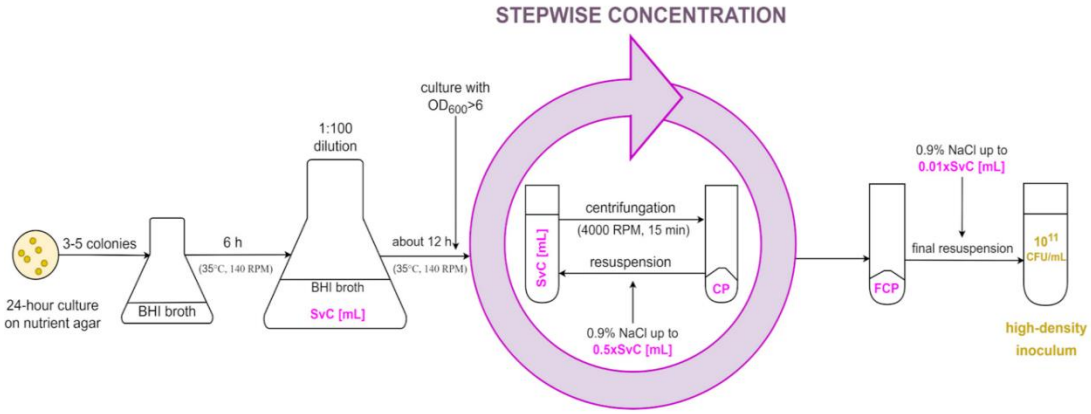

FIG 2 Preparation of the high-density inoculum. SvC, starting volume of bacterial culture; CP, cell pellet; FCP, final cell pellet; BHI, Brain Heart Infusion; 4,000 RPM = 2,061 × *g*.

In the first stage of this study, a single-step resistant-mutant selection was performed. A series of MHII agar plates (Becton, Dickinson and Company, Franklin Lakes, NJ, USA) containing six 2-fold progressively increasing concentrations of the tested compounds (from 1×MIC to 32×MIC) were prepared. Four plates were prepared per concentration, and every plate was inoculated with 25 μL of the high-density inoculum (10^{11} CFU/mL) to ensure a total of 10^{10} CFU were exposed to each concentration. Aliquots were suspended in a 75 μL drop of 0.9% NaCl placed on the plate to facilitate the spreading of the high-density inoculum over the agar surface. All plates were incubated at 35°C for 24 h. They were designated A-series plates in which mutants were selected. After incubation, the plates were screened visually for growth, and colonies were counted. If no growth was visible, plates were reincubated for an additional 24 h under the same conditions. In the second stage of this study, the aMRTests were performed (9, 33). All obtained colonies, as well as the content of the visually clean plates and the content of plates with dense lawn, semi-dense lawn, and colony lawn were transferred to another agar plate with the same compound concentration. Plates were incubated at 35°C and screened for growth after 24 h and 48 h. No growth was confirmed after 72 h. Only colonies that regrew in the aMRTest were considered single-step resistant mutants while determining the FSMS, MPC, MPC-D, MSW, and MSW-D.

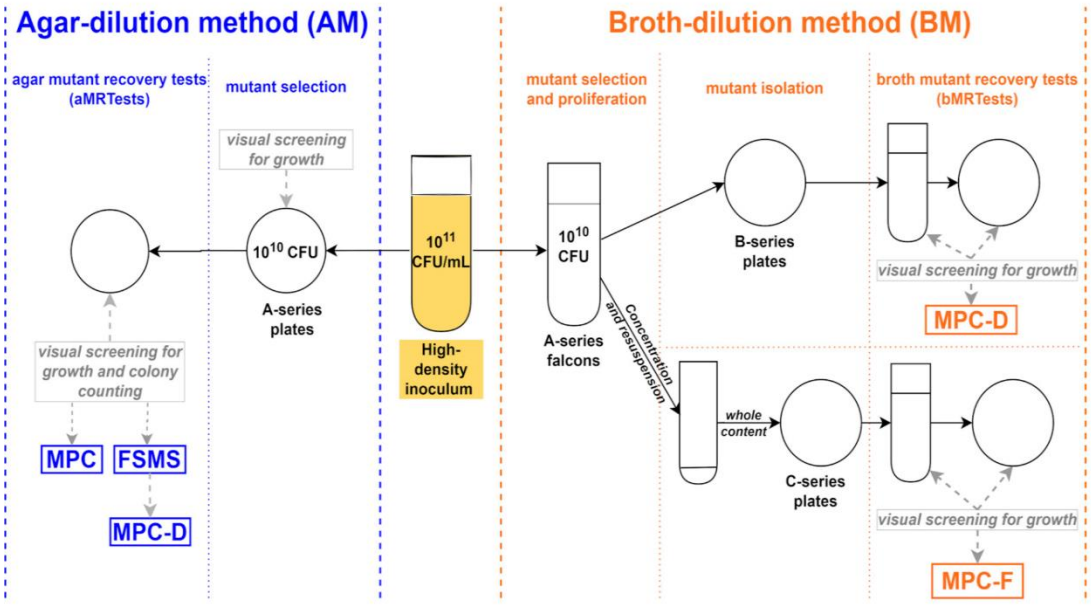

FIG 3 Comparison of the agar-dilution method and the broth-dilution method. MPC, mutant prevention concentration; FSMS, frequency of spontaneous mutant selection; MPC-D, dominant mutant prevention concentration; MPC-F, inferior mutant prevention concentration.

The MPC value was determined according to Dong et al. as the minimal concentration of the agent that causes no mutants to be obtained when a large number of cells ($>10^{10}$ cells) are applied to agar plates containing the agent (9). The FSMS value for each concentration of tested agent was calculated as the ratio of the resistant CFU (mutant colonies grown on 32×MIC agar plates) to a total CFU in 1 mL of the initial inoculum. A frequency below 1×10^{-8} CFU/mL was considered the threshold for reduced mutant selection in the cell population (10, 13), whereas the lowest concentration of the agent with the FSMS value below 1×10^{-10} was taken as the MPC-D value. The lowest concentration that causes no mutant to be obtained on A-series plates was taken as the MPC value.

The MSW parameter was designated the interval of the agent concentration range from the MIC value up to the MPC value, whereas the MSW-D parameter was defined as the interval of the agent concentration range from the MIC value up to the MPC-D value.

Finally, the SI was calculated as the MPC/MIC ratio (10), while the SI-D was calculated as the MPC-D/MIC ratio.

MPC-D, MPC-F, MSW-D, and MSW-F determination by the broth-dilution method (BM). The MPC-D, MPC-F, MSW-D, and MSW-F parameters were determined simultaneously by the BM (Fig. 3).

A series of 2-fold progressively increasing concentrations of the tested compounds (from 1×MIC to 32×MIC) were prepared in MHII broth medium (Becton, Dickinson and Company, Franklin Lakes, NJ, USA). Each plastic laboratory falcon tube with 4.9 mL of MHII broth with the compound was inoculated with 100 μL of the high-density inoculum above 10^{11} CFU/mL. This provided an initial concentration of bacterial cells above 10^{10} CFU/mL in each falcon tube. Falcons were incubated at 35°C for 24 h with shaking at 140 RPM. They were designated A-series falcons, in which mutants were selected and proliferated. The mutants were then isolated by spreading two aliquots of 100 μL of the obtained culture over two MHII agar plates containing the same compound concentration as in the broth culture. These were designated B-series plates and incubated at 35°C for 48 h, then screened visually for growth, and the colonies were counted. To eliminate the inoculum effect, bMRTests were performed, during which the regrowth ability of the obtained resistant mutant colonies in the presence of the same concentration was checked, and the lack of growth on the agar mutant isolation plates was confirmed. Only colonies able to regrow in the bMRTest were taken into account. MPC-D was defined as the lowest drug concentration that, after the 24 h of incubation, prevents mutants selected among 10^{10} CFU from establishing a resistant population of at least 10 CFU/mL in the drug-supplemented broth culture (i.e., mutants are not able to dominate the population). This corresponded to at least 1 colony on each B-series plate. Mutants that established a population of at least 10 CFU/mL were named the dominant mutants.

To establish the MPC-F, the remaining content of the A-series falcons was centrifuged (2,061 × g = 4,000 RPM, 22°C, 15 min) and concentrated to the final culture volume of 100 μL. The entire content of each concentrated culture in the A-series falcons was transferred to MHII agar plates containing the same compound concentration as in the broth cultures. These were designated C-series plates and incubated at 35°C for 48 h, then screened visually for growth, and the colonies were counted. The obtained mutant colonies' ability to regrow at the same concentration in broth, as well as the lack of growth on the agar mutant isolation plates, was examined by the bMRTest. Only colonies able to regrow in the bMRTest were taken into account for the determination of the MPC-F. The MPC-F was the minimal concentration of the agent that allowed no mutant to be obtained on the C-series plates. Mutants isolated on C-series plates that were not able to dominate the population were named the inferior mutants. The detection threshold for the MPC-F parameter determined by the BM is 1 CFU of mutant per 5 mL (the whole volume of the tested culture). This means that we can detect the presence of at least one mutant cell in 5 mL of the broth culture (which corresponds to 1 colony on the tested plates), where an initial concentration of bacterial cells was above 10^{10} CFU/mL in each falcon tube.

The MSW-D parameter was designated the interval of the agent concentration range from the MIC value up to the MPC-D value at which the agent inhibits the emergence of mutants capable of dominating the entire high-density population of the bacterial cells. The MSW-F parameter was defined as the interval of the agent concentration range from the MIC value up to the MPC-F value at which the agent inhibits selection, in a fluid environment, of resistant mutants appearing in the entire population of high-density bacterial cells.

Finally, the SI-D was calculated as the MPC-D/MIC ratio, while the SI-F was calculated as the MPC-F/MIC ratio.

Broth mutant recovery test (bMRTest). The in-broth recovery test was performed for resistant mutants obtained on the B- and C-series plates. The obtained mutant colonies on the plates with compound, the content of the plates on which a dense lawn, a semi-dense lawn, or a colony lawn appeared, and the content of the visually clean plates were transferred to MHII broth with the same compound concentration. falcons were incubated at 35°C with shaking (140 RPM) and were visually screened for growth after 24 h, 48 h, and (if no growth was visible) after 72 h. The observed turbidity of the broth medium indicated the growth of bacteria. To confirm the regrowth ability of the obtained resistant mutants in the presence of the antibacterial compound, a sample of this turbid culture from the falcon tube was plated on agar supplemented with the same compound concentration and incubated at 35°C for up to 72 h. A sample of the culture from the falcon tube that was visually clear after 72 h of incubation was transferred to the MHII agar plate with the same compound concentration and incubated at 35°C for up to 72 h to confirm the lack of growth.

ACKNOWLEDGMENTS

The authors are grateful to Sergiusz Luliński (from the Physical Chemistry Department, Faculty of Chemistry, Warsaw University of Technology, Warsaw, Poland) for providing the new compound No37 for our microbiological studies, and to Jolanta Solecka (from the Department of Environmental Health and Safety, National Institute of Public Health

NIH—National Research Institute, Warsaw, Poland) for the critical review and comments on the manuscript.

This research was funded by the National Science Center (Poland) in the framework of the project UMO-2018/31/B/ST5/00210. The research was carried out with the use of the CePT infrastructure financed by the European Union through the European Regional Development Fund as part of the Operational Program "Innovative Economy" for 2007 to 2013. Moreover, the work was partially supported by the Foundation for the Development of Diagnostics and Therapy, Warsaw, Poland (REGON: 006220910, NIP: 5262173856, KRS: 0000195643).

We declare no conflicts of interest.

REFERENCES

1. WHO. 2022. 2021 Antibacterial agents in clinical and preclinical development: an overview and analysis. World Health Organization, Geneva, Switzerland. https://www.who.int/publications/i/item/9789240047655.
2. FDA. 2022. Antibacterial therapies for patients with an unmet medical need for the treatment of serious bacterial diseases—questions and answers (revision 1): guidance for industry. FDA-2013-D-0744. U.S. Food and Drug Administration, Silver Spring, MD.
3. FDA. 2017. Antibacterial therapies for patients with an unmet medical need for the treatment of serious bacterial diseases. FDA-2013-D-0744. US Food and Drug Administration, Silver Spring, MD.
4. Krajewska J, Laudy AE. 2021. The European Medicines Agency approved the new antibacterial drugs—response to the 2017 WHO report on the global problem of multi-drug resistance. Advancements Microbiol 60:249–264. https://doi.org/10.21307/pm-2021.60.4.20.
5. CLSI. 1999. Methods for determining bactericidal activity of antimicrobial agents. Approved guideline. CLSI guideline M26-A. Clinical and Laboratory Standards Institute, Wayne, PA.
6. CLSI. 2012. Methods for dilution antimicrobial susceptibility tests for bacteria that grow aerobically, 9th ed. CLSI guideline M07-A9. Clinical and Laboratory Standards Institute, Wayne, PA.
7. CLSI. 2008. Reference method for broth dilution antifungal susceptibility testing of yeasts, 3rd ed. CLSI guideline M27-A3. Clinical and Laboratory Standards Institute, Wayne, PA.
8. Cantón E, Pemán J, Viudes A, Quindós G, Gobernado M, Espinel-Ingroff A. 2003. Minimum fungicidal concentrations of amphotericin B for bloodstream *Candida* species. Diagn Microbiol Infect Dis 45:203–206. https://doi.org/10.1016/S0732-8893(02)00525-4.
9. Dong Y, Zhao X, Domagala J, Drlica K. 1999. Effect of fluoroquinolone concentration on selection of resistant mutants of *Mycobacterium bovis* BCG and *Staphylococcus aureus*. Antimicrob Agents Chemother 43:1756–1758. https://doi.org/10.1128/AAC.43.7.1756.
10. Zhao X, Drlica K. 2001. Restricting the selection of antibiotic-resistant mutants: a general strategy derived from fluoroquinolone studies. Clin Infect Dis 33(Suppl 3):S147–S156. https://doi.org/10.1086/321841.
11. Zhao X, Drlica K. 2002. Restricting the selection of antibiotic-resistant mutant bacteria: measurement and potential use of the mutant selection window. J Infect Dis 185:561–565. https://doi.org/10.1086/338571.
12. Martinez JL, Baquero F. 2000. Mutation frequencies and antibiotic resistance. Antimicrob Agents Chemother 44:1771–1777. https://doi.org/10.1128/AAC.44.7.1771-1777.2000.
13. Sun D, Rubio-Aparicio D, Nelson K, Dudley MN, Lomovskaya O. 2017. Meropenem-vaborbactam resistance selection, resistance prevention, and molecular mechanisms in mutants of KPC-producing *Klebsiella pneumoniae*. Antimicrob Agents Chemother 61:e01694-17. https://doi.org/10.1128/AAC.01694-17.
14. Nilsson AI, Berg OG, Aspevall O, Kahlmeter G, Andersson DI. 2003. Biological costs and mechanisms of fosfomycin resistance in *Escherichia coli*. Antimicrob Agents Chemother 47:2850–2858. https://doi.org/10.1128/AAC.47.9.2850-2858.2003.
15. Gustafsson I, Cars O, Andersson DI. 2003. Fitness of antibiotic resistant *Staphylococcus epidermidis* assessed by competition on the skin of human volunteers. J Antimicrob Chemother 52:258–263. https://doi.org/10.1093/jac/dkg331.
16. Sanz-García F, Hernando-Amado S, Martínez JL. 2022. Evolution under low antibiotic concentrations: a risk for the selection of *Pseudomonas aeruginosa* multidrug-resistant mutants in nature. Environ Microbiol 24:1279–1293. https://doi.org/10.1111/1462-2920.15806.
17. Sanz-García F, Sánchez MB, Hernando-Amado S, Martínez JL. 2020. Evolutionary landscapes of *Pseudomonas aeruginosa* towards ribosome-targeting antibiotic resistance depend on selection strength. Int J Antimicrob Agents 55:105965. https://doi.org/10.1016/j.ijantimicag.2020.105965.
18. Gullberg E, Cao S, Berg OG, Ilbäck C, Sandegren L, Hughes D, Andersson DI. 2011. Selection of resistant bacteria at very low antibiotic concentrations. PLoS Pathog 7:e1002158. https://doi.org/10.1371/journal.ppat.1002158.
19. Trampari E, Zhang C, Gotts K, Savva GM, Bavro VN, Webber M. 2022. Cefotaxime exposure selects mutations within the CA-domain of envZ which promote antibiotic resistance but repress biofilm formation in *Salmonella*. Microbiol Spectr 10:e0214521. https://doi.org/10.1128/spectrum.02145-21.
20. Cui J, Liu Y, Wang R, Tong W, Drlica K, Zhao X. 2006. The mutant selection window in rabbits infected with *Staphylococcus aureus*. J Infect Dis 194:1601–1608. https://doi.org/10.1086/508752.
21. EUCAST. 2022. Breakpoint tables for interpretation of MICs and zone diameters. Version 12.0, 2022. http://www.eucast.org. The European Committee on Antimicrobial Susceptibility Testing, Växjö, Sweden.
22. CLSI. 2022. Performance standards for antimicrobial susceptibility testing, 32nd ed. CLSI guideline M100. Clinical and Laboratory Standards Institute, Wayne, PA.
23. Allen GP, Kaatz GW, Rybak MJ. 2004. In vitro activities of mutant prevention concentration-targeted concentrations of fluoroquinolones against *Staphylococcus aureus* in a pharmacodynamic model. Int J Antimicrob Agents 24:150–160. https://doi.org/10.1016/j.ijantimicag.2004.03.011.
24. López Y, Tato M, Gargallo-Viola D, Cantón R, Vila J, Zsolt I. 2019. Mutant prevention concentration of ozenoxacin for quinolone-susceptible or -resistant *Staphylococcus aureus* and *Staphylococcus epidermidis*. PLoS One 14:e0223326. https://doi.org/10.1371/journal.pone.0223326.
25. Marcusson LL, Komp Lindgren P, Olofsson SK, Hughes D, Cars O. 2014. Mutant prevention concentrations of pradofloxacin for susceptible and mutant strains of *Escherichia coli* with reduced fluoroquinolone susceptibility. Int J Antimicrob Agents 44:354–357. https://doi.org/10.1016/j.ijantimicag.2014.06.010.
26. Huang Y, Xu Y, Liu S, Wang H, Xu X, Guo Q, Wu B, Gordeev MF, Wang W, Yuan Z, Wang M. 2014. Selection and characterisation of *Staphylococcus aureus* mutants with reduced susceptibility to the investigational oxazolidinone MRX-I. Int J Antimicrob Agents 43:418–422. https://doi.org/10.1016/j.ijantimicag.2014.02.008.
27. Liu LG, Zhu YL, Hu LF, Cheng J, Ye Y, Li JB. 2013. Comparative study of the mutant prevention concentrations of vancomycin alone and in combination with levofloxacin, rifampicin and fosfomycin against methicillin-resistant *Staphylococcus epidermidis*. J Antibiot (Tokyo) 66:709–712. https://doi.org/10.1038/ja.2013.87.
28. Zhao X, Drlica K. 2008. A unified anti-mutant dosing strategy. J Antimicrob Chemother 62:434–436. https://doi.org/10.1093/jac/dkn229.
29. Gianvecchio C, Lozano NA, Henderson C, Kalhori P, Bullivant A, Valencia A, Su L, Bello G, Wong M, Cook E, Fuller L, Neal JB, III, Yeh PJ. 2019. Variation in mutant prevention concentrations. Front Microbiol 10:42. https://doi.org/10.3389/fmicb.2019.00042.
30. Pan AJ, Mei Q, Ye Y, Li HR, Liu B, Li JB. 2017. Validation of the mutant selection window hypothesis with fosfomycin against *Escherichia coli* and *Pseudomonas aeruginosa*: an *in vitro* and *in vivo* comparative study. J Antibiot (Tokyo) 70:166–173. https://doi.org/10.1038/ja.2016.124.

31. Mei Q, Ye Y, Zhu YL, Cheng J, Chang X, Liu YY, Li HR, Li JB. 2015. Testing the mutant selection window hypothesis in vitro and in vivo with *Staphylococcus aureus* exposed to fosfomycin. Eur J Clin Microbiol Infect Dis 34:737–744. https://doi.org/10.1007/s10096-014-2285-6.
32. Drlica K, Zhao X, Blondeau JM, Hesje C. 2006. Low correlation between MIC and mutant prevention concentration. Antimicrob Agents Chemother 50:403–404. https://doi.org/10.1128/AAC.50.1.403-404.2006.
33. Blondeau JM, Zhao X, Hansen G, Drlica K. 2001. Mutant prevention concentrations of fluoroquinolones for clinical isolates of *Streptococcus pneumoniae*. Antimicrob Agents Chemother 45:433–438. https://doi.org/10.1128/AAC.45.2.433-438.2001.
34. Hansen GT, Blondeau JM. 2005. Comparison of the minimum inhibitory, mutant prevention and minimum bactericidal concentrations of ciprofloxacin, levofloxacin and garenoxacin against enteric Gram-negative urinary tract infection pathogens. J Chemother 17:484–492. https://doi.org/10.1179/joc.2005.17.5.484.
35. Hesje CK, Borsos SD, Blondeau JM. 2009. Benzalkonium chloride enhances antibacterial activity of gatifloxacin and reduces its propensity to select for fluoroquinolone-resistant strains. J Ocul Pharmacol Ther 25:329–334. https://doi.org/10.1089/jop.2009.0031.
36. Metzler K, Hansen GM, Hedlin P, Harding E, Drlica K, Blondeau JM. 2004. Comparison of minimal inhibitory and mutant prevention drug concentrations of 4 fluoroquinolones against clinical isolates of methicillin-susceptible and -resistant *Staphylococcus aureus*. Int J Antimicrob Agents 24:161–167. https://doi.org/10.1016/j.ijantimicag.2004.02.021.
37. Hansen GT, Metzler K, Drlica K, Blondeau JM. 2003. Mutant prevention concentration of gemifloxacin for clinical isolates of *Streptococcus pneumoniae*. Antimicrob Agents Chemother 47:440–441. https://doi.org/10.1128/AAC.47.1.440-441.2003.
38. Hedlin P, Blondeau JM. 2007. Comparative minimal inhibitory and mutant prevention drug concentrations of four fluoroquinolones against ocular isolates of *Haemophilus influenzae*. Eye Contact Lens 33:161–164. https://doi.org/10.1097/01.icl.0000246872.73559.43.
39. Firsov AA, Alieva KN, Strukova EN, Golikova MV, Portnoy YA, Dovzhenko SA, Kobrin MB, Romanov AV, Edelstein MV, Zinner SH. 2017. Testing the mutant selection window hypothesis with *Staphylococcus aureus* exposed to linezolid in an *in vitro* dynamic model. J Antimicrob Chemother 72:3100–3107. https://doi.org/10.1093/jac/dkx249.
40. Allen GP, Deshpande LM. 2010. Determination of the mutant selection window for clindamycin, doxycycline, linezolid, moxifloxacin and trimethoprim/sulfamethoxazole against community-associated methicillin-resistant *Staphylococcus aureus* (MRSA). Int J Antimicrob Agents 35:45–49. https://doi.org/10.1016/j.ijantimicag.2009.09.005.
41. Silverman JA, Oliver N, Andrew T, Li T. 2001. Resistance studies with daptomycin. Antimicrob Agents Chemother 45:1799–1802. https://doi.org/10.1128/AAC.45.6.1799-1802.2001.
42. Quinn B, Hussain S, Malik M, Drlica K, Zhao X. 2007. Daptomycin inoculum effects and mutant prevention concentration with *Staphylococcus aureus*. J Antimicrob Chemother 60:1380–1383. https://doi.org/10.1093/jac/dkm375.
43. Diaz-Diaz S, Recacha E, García-Duque A, Docobo-Pérez F, Blázquez J, Pascual A, Rodríguez-Martínez JM. 2022. Effect of RecA inactivation and detoxification systems on the evolution of ciprofloxacin resistance in *Escherichia coli*. J Antimicrob Chemother 77:641–645. https://doi.org/10.1093/jac/dkab445.
44. Firsov AA, Smirnova MV, Strukova EN, Vostrov SN, Portnoy YA, Zinner SH. 2008. Enrichment of resistant *Staphylococcus aureus* at ciprofloxacin concentrations simulated within the mutant selection window: bolus versus continuous infusion. Int J Antimicrob Agents 32:488–493. https://doi.org/10.1016/j.ijantimicag.2008.06.031.
45. Ferran AA, Kesteman A-S, Toutain P-L, Bousquet-Mélou A. 2009. Pharmacokinetic/pharmacodynamic analysis of the influence of inoculum size on the selection of resistance in *Escherichia coli* by a quinolone in a mouse thigh bacterial infection model. Antimicrob Agents Chemother 53:3384–3390. https://doi.org/10.1128/AAC.01347-08.
46. Homma T, Hori T, Sugimori G, Yamano Y. 2007. Pharmacodynamic assessment based on mutant prevention concentrations of fluoroquinolones to prevent the emergence of resistant mutants of *Streptococcus pneumoniae*. Antimicrob Agents Chemother 51:3810–3815. https://doi.org/10.1128/AAC.01372-06.
47. Park NH, Lee SJ, Lee EB, Birhanu BT, Park SC. 2021. Colistin induces resistance through biofilm formation, via increased phoQ expression, in avian pathogenic *Escherichia coli*. Pathogens 10:1525. https://doi.org/10.3390/pathogens10111525.
48. Jiang L, Xie N, Chen M, Liu Y, Wang S, Mao J, Li J, Huang X. 2020. Synergistic combination of linezolid and fosfomycin closing each other's mutant selection window to prevent enterococcal resistance. Front Microbiol 11:605962.
49. Hovde LB, Rotschafer SE, Ibrahim KH, Gunderson B, Hermsen ED, Rotschafer JC. 2003. Mutation prevention concentration of ceftriaxone, meropenem, imipenem, and ertapenem against three strains of *Streptococcus pneumoniae*. Diagn Microbiol Infect Dis 45:265–267. https://doi.org/10.1016/S0732-8893(02)00546-1.
50. Wentzel JM, Biggs LJ, Van Vuuren M. 2022. Comparing the minimum inhibitory and mutant prevention concentrations of selected antibiotics against animal isolates of *Pasteurella multocida* and *Salmonella typhimurium*. Onderstepoort J Vet Res 89:e1–e7. https://doi.org/10.4102/ojvr.v89i1.1955.
51. Firsov AA, Golikova MV, Strukova EN, Portnoy YA, Romanov AV, Edelstein MV, Zinner SH. 2015. *In vitro* resistance studies with bacteria that exhibit low mutation frequencies: prediction of "antimutant" linezolid concentrations using a mixed inoculum containing both susceptible and resistant *Staphylococcus aureus*. Antimicrob Agents Chemother 59:1014–1019. https://doi.org/10.1128/AAC.04214-14.
52. Alieva KN, Strukova EN, Golikova MV, Portnoy YA, Zinner SH, Firsov AA. 2018. Time inside the mutant selection window as a predictor of staphylococcal resistance to linezolid. J Antibiot 71:514–521. https://doi.org/10.1038/s41429-017-0016-9.
53. Firsov AA, Lubenko IY, Smirnova MV, Strukova EN, Zinner SH. 2008. Enrichment of fluoroquinolone-resistant *Staphylococcus aureus*: oscillating ciprofloxacin concentrations simulated at the upper and lower portions of the mutant selection window. Antimicrob Agents Chemother 52:1924–1928. https://doi.org/10.1128/AAC.01371-07.
54. Firsov A, Lubenko I, Smirnova M, Strukova E, Zinner S. 2008. Heterogeneity of the mutant selection window: selection of resistant *Staphylococcus aureus* at ciprofloxacin constant concentrations simulated close to the MIC or the mutant prevention concentration. Clin Microbiol Infect 14:674.
55. Ni W, Song X, Cui J. 2014. Testing the mutant selection window hypothesis with *Escherichia coli* exposed to levofloxacin in a rabbit tissue cage infection model. Eur J Clin Microbiol Infect Dis 33:385–389. https://doi.org/10.1007/s10096-013-1968-8.
56. Croisier D, Etienne M, Bergoin E, Charles PE, Lequeu C, Piroth L, Portier H, Chavanet P. 2004. Mutant selection window in levofloxacin and moxifloxacin treatments of experimental pneumococcal pneumonia in a rabbit model of human therapy. Antimicrob Agents Chemother 48:1699–1707. https://doi.org/10.1128/AAC.48.5.1699-1707.2004.
57. Almeida D, Nuermberger E, Tyagi S, Bishai WR, Grosset J. 2007. In vivo validation of the mutant selection window hypothesis with moxifloxacin in a murine model of tuberculosis. Antimicrob Agents Chemother 51:4261–4266. https://doi.org/10.1128/AAC.01123-07.
58. Ibrahim KH, Yap LP, Hovde LB, Gunderson BW, Rotschafer JC. 2001. A validation of the mutation prevention concentration (MPC) method using a broth medium, abstr EP1.11. 22nd International Congress of Chemotherapy, Amsterdam, the Netherlands, 30 June to 3 July.
59. Hesje C, Blondeau JM. 2009. Comparison of modified microbroth dilution to agar dilution for determining the mutant prevention concentration of gatifloxacin and moxifloxacin against *Streptococcus pneumoniae* ATCC 49619, abstr P710. 19th European Congress of Clinical Microbiology and Infectious Diseases, Helsinki, Finland, 16 to 19 May.
60. Blondeau JM, Shebelski SD, Vickers R. 2015. Mutant prevention concentration values of SMT19969 against *Clostridium difficile* isolates using a modified microbroth dilution method, abstr D-212. Interscience Conference on Antimicrobial Agents and Chemotherapy, San Diego, California, 17 to 21 September.
61. Liang B, Bai N, Cai Y, Wang R, Drlica K, Zhao X. 2011. Mutant prevention concentration-based pharmacokinetic/pharmacodynamic indices as dosing targets for suppressing the enrichment of levofloxacin-resistant subpopulations of *Staphylococcus aureus*. Antimicrob Agents Chemother 55:2409–2412. https://doi.org/10.1128/AAC.00975-10.
62. Zhang L, Xie H, Wang Y, Wang H, Hu J, Zhang G. 2022. Pharmacodynamic parameters of pharmacokinetic/pharmacodynamic (PK/PD) integration models. Front Vet Sci 9:860472. https://doi.org/10.3389/fvets.2022.860472.
63. Kesteman A-S, Ferran AA, Perrin-Guyomard A, Laurentie M, Sanders P, Toutain P-L, Bousquet-Mélou A. 2009. Influence of inoculum size and marbofloxacin plasma exposure on the amplification of resistant subpopulations of *Klebsiella pneumoniae* in a rat lung infection model. Antimicrob Agents Chemother 53:4740–4748. https://doi.org/10.1128/AAC.00608-09.
64. Brzozowska A, Ćwik P, Durka K, Kliś T, Laudy AE, Luliński S, Serwatowski J, Tyski S, Urban M, Wróblewski W. 2015. Benzosiloxaboroles: silicon benzoxaborole congeners with improved Lewis acidity, high diol affinity, and potent bioactivity. Organometallics 34:2924–2932. https://doi.org/10.1021/acs.organomet.5b00265.

7.5. Publikacja O4

molecules

MDPI

Article

Aromatic Diboronic Acids as Effective KPC/AmpC Inhibitors

Joanna Krajewska [1], Piotr Chyży [2], Krzysztof Durka [3], Patrycja Wińska [3], Krystiana A. Krzyśko [4,*], Sergiusz Luliński [3] and Agnieszka E. Laudy [1,*]

1 Department of Pharmaceutical Microbiology and Bioanalysis, Medical University of Warsaw, 02-097 Warsaw, Poland; joanna.krajewska@ymail.com
2 Centre of New Technologies, University of Warsaw, 02-097 Warsaw, Poland; p.chyzy@cent.uw.edu.pl
3 Faculty of Chemistry, Warsaw University of Technology, 00-664 Warsaw, Poland; kdurka@gmail.com (K.D.); pwinska@ch.pw.edu.pl (P.W.); sergiusz.lulinski@pw.edu.pl (S.L.)
4 Faculty of Physics, University of Warsaw, 02-093 Warsaw, Poland
* Correspondence: krystiana.krzysko@fuw.edu.pl (K.A.K.); alaudy@wp.pl (A.E.L.)

Abstract: Over 30 compounds, including *para*-, *meta*-, and *ortho*-phenylenediboronic acids, *ortho*-substituted phenylboronic acids, benzenetriboronic acids, di- and triboronated thiophenes, and pyridine derivatives were investigated as potential β-lactamase inhibitors. The highest activity against KPC-type carbapenemases was found for *ortho*-phenylenediboronic acid **3a**, which at the concentration of 8/4 mg/L reduced carbapenems' MICs up to 16/8-fold, respectively. Checkerboard assays revealed strong synergy between carbapenems and **3a** with the fractional inhibitory concentrations indices of 0.1–0.32. The nitrocefin hydrolysis test and the whole cell assay with *E. coli* DH5α transformant carrying bla_{KPC-3} proved KPC enzyme being its molecular target. *para*-Phenylenediboronic acids efficiently potentiated carbapenems against KPC-producers and ceftazidime against AmpC-producers, whereas *meta*-phenylenediboronic acids enhanced only ceftazidime activity against the latter ones. Finally, the statistical analysis confirmed that *ortho*-phenylenediboronic acids act synergistically with carbapenems significantly stronger than other groups. Since the obtained phenylenediboronic compounds are not toxic to MRC-5 human fibroblasts at the tested concentrations, they can be considered promising scaffolds for the future development of novel KPC/AmpC inhibitors. The complexation of KPC-2 with the most representative isomeric phenylenediboronic acids **1a**, **2a**, and **3a** was modeled by quantum mechanics/molecular mechanics calculations. Compound **3a** reached the most effective configuration enabling covalent binding to the catalytic Ser70 residue.

Keywords: arylboronic acids; KPC/AmpC β-lactamase inhibitors; molecular docking; time-dependent QM/MM; antibacterial activity

Citation: Krajewska, J.; Chyży, P.; Durka, K.; Wińska, P.; Krzyśko, K.A.; Luliński, S.; Laudy, A.E. Aromatic Diboronic Acids as Effective KPC/AmpC Inhibitors. *Molecules* **2023**, *28*, 7362. https://doi.org/10.3390/molecules28217362

Academic Editor: Jean-Marc Sabatier

Received: 6 October 2023
Revised: 26 October 2023
Accepted: 28 October 2023
Published: 31 October 2023

1. Introduction

Aromatic di- and triboronic acids are popular building blocks used in organic synthesis, for the construction of extended hydrogen-bonded supramolecular assemblies [1] and porous materials with a special emphasis on Boronate Covalent Organic Frameworks [2]. With a few exceptions [3], however, their potential in medicinal chemistry has not been extensively investigated, yet. In this context, it is worth noting that the presence of two or more boronic groups attached to the aromatic backbone results in reduced lipophilicity and increased acidity compared to monoboronic derivatives which are more popular in medicinal chemistry, e.g., they were recognized as potent β-lactamase inhibitors (BLIs) [4]. β-Lactamases, as enzymes hydrolyzing β-lactams, are the main cause of Gram-negative rod resistance to these antibiotics. This mechanism of bacterial resistance has a negative impact on global public health [5–10]. Moreover, from the point of medicinal chemistry, boronic acids and their derivatives have also found other applications, e.g., they have emerged as covalently binding proteasome inhibitors and the most important example is bortezomib used as the anticancer agent for the treatment of multiple myeloma [11].

Among β-lactamases, carbapenemases are the most troublesome as they extend bacterial resistance to the last-resort antibiotics—carbapenems [5]. The most clinically relevant carbapenemases belong mainly to class A according to Ambler classification [6], (e.g., *Klebsiella pneumoniae* carbapenemases—KPCs), class B (the so-called metallo-β-lactamases—MBLs, e.g., New Delhi metallo-β-lactamases—NDMs, Verona integron-encoded metallo-β-lactamases—VIMs), and class D (e.g., carbapenem-hydrolyzing class D β-lactamases—CHDLs and enzyme OXA-48). Class C carbapenemases were rarely described, e.g., ADC-68 in *Acinetobacter baumannii* [5,7]. However, the widespread resistance to third and fourth-generation cephalosporins among bacteria is also worrisome [8]. It results either from the production of the class A extended-spectrum β-lactamases (ESBLs, e.g., CTX-M enzymes) or from the production of class C cephalosporinases (AmpC), both chromosomal (cAmpC) and plasmid-encoded (pAmpC, e.g., CMY-2) [8,9].

Considering the above, in 2017, the World Health Organization (WHO) classified carbapenem-resistant strains of *A. baumannii* (CRAB), *Pseudomonas aeruginosa* (CRPA), and *Enterobacterales* (CRE) as well as third-generation cephalosporin-resistant *Enterobacterales* as the "critical priority pathogens", for which therapeutic options are severely limited [10]. However, the number of new antibacterial agents, both recently approved and under clinical and preclinical development, is still insufficient to address this problem [12,13]. Combining β-lactams with BLIs is a well-known strategy to restore the effectiveness of these antibiotics. BLIs based on the β-lactam scaffold (clavulanic acid, sulbactam, and tazobactam) entered clinics in the 1980s–1990s [14] but they are inactive against carbapenemases. Recently, market authorization gained three non-β-lactam inhibitors of class A carbapenemases (avibactam, relebactam, and vaborbactam) and one potent inhibitor of class A and D carbapenemases (durlobactam) [15,16]. However, class B carbapenemases are still out of the spectrum of clinically available BLIs. Thus, searching for new broad-spectrum inhibitors is urgently needed [13,15].

Boronic acids and their derivatives are well-known groups of competitive, reversible BLIs [4,17]. They react with the nucleophilic serine in the catalytic center of β-lactamases, forming tetrahedral complexes [4]. Vaborbactam (Scheme 1), based on cyclic boronate (boronic acid monoester) pharmacophore, was already marketed in combination with meropenem for the treatment of complicated urinary tract infections. It is a potent inhibitor of class A carbapenemases (KPC, SME) and ESBLs (CTX-M, TEM, and SHV) as well as AmpC enzymes [12]. Three cyclic boronates with the activity extended toward many metallo-β-lactamases and class D enzymes are under clinical trials (taniborbactam, VNRX-7145, and QPX7728) [13] whereas other derivatives are under preclinical development [18]. (2′-*S*)-(1-(3′-Mercapto-2′-methylpropanamido)methyl)boronic acid was recently found to inhibit a broad spectrum of β-lactamases, including some MBLs (VIM-2 and NDM-1) [19]. Various aromatic boronic acids (including phenylboronic acids) also display BLI activity against class A (KPC [20–24] and CTX-M [25,26]) and class C β-lactamases [23,26–30]). Improved affinity toward AmpC enzymes was found for many *meta*-substituted phenylboronic acids, e.g., those bearing amide [27], sulfonamide [27], aza-naphthol [29], and aza-phenol [29] moieties, while carboxyvinyl group in the *ortho* or 1,2,3-triazole in the *meta* position were associated with an increased KPC-2 inhibitory potency [22–24]. Finally, many benzoxaboroles manifest broad-spectrum in vitro inhibition of class A (TEM-1, CTX-M-15, and KPC-2), class C (cAmpC, CMY-2), and class D (OXA-10, OXA-24, and OXA-48) enzymes [17,31,32]. However, some compounds were not able to restore the effectiveness of antibiotics against strains producing particular β-lactamases [19,27,29,32]. This emphasizes the importance of performing microbiological whole-cell assays, to evaluate antibacterial activity. Considering the BLI activity of simple phenylboronic acid (PBA) [33], the major motivation of this work has been the practical evaluation of the effect of the introduction of additional boronic group(s) attached to the aromatic core using appropriate microbiological assays supported by theoretical modeling performed for the most representative systems.

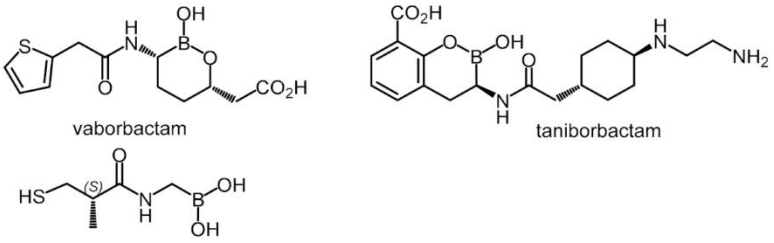

Scheme 1. Examples of boronic acid derivatives showing potent BLI activity.

2. Results and Discussion

2.1. Synthesis

Our study involved over 30 compounds including *para*-(**1a**–**1l**), *meta*-(**2a**–**2g**) and *ortho*-benzenediboronic acids **3a**–**3e** (Scheme 2). In addition, benzenetriboronic acids (**4a**–**4b**) were the subject of our work. Further examples include di- or triboronated thiophene (**5a**–**5c**) and pyridine (**6a**) derivatives. Finally, a few *ortho*-substituted phenylboronic acids (**7a**–**7c**) featuring intramolecular hydrogen-bonding interactions were also investigated. Compounds **1a**, **2a** and **7a** were commercially available. The synthesis of most compounds including **1b**–**1g** [1,34,35], **1j**–**1l** [36,37], **2d**–**2g** [34,35], **3a**–**3d** [38], **4a**–**4b** [35], **5b**–**5c** [39], and **7b** [40] was reported previously. The synthesis of remaining boronic acids **1h**, **1i**, **2b**, **2c**, **3e**, **6a**, **7c** is presented in Scheme 3. In general, they were obtained from appropriate aromatic precursors using the lithiation/boronation reaction sequence with some variations introduced to install the boronic groups effectively. The details of synthetic procedures and compound characterization are given in the Supplementary Materials.

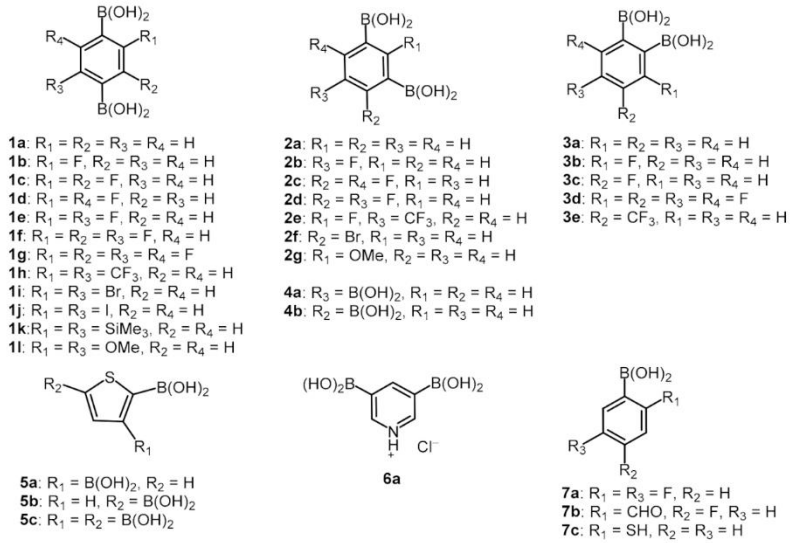

Scheme 2. The structures of studied arylboronic acids.

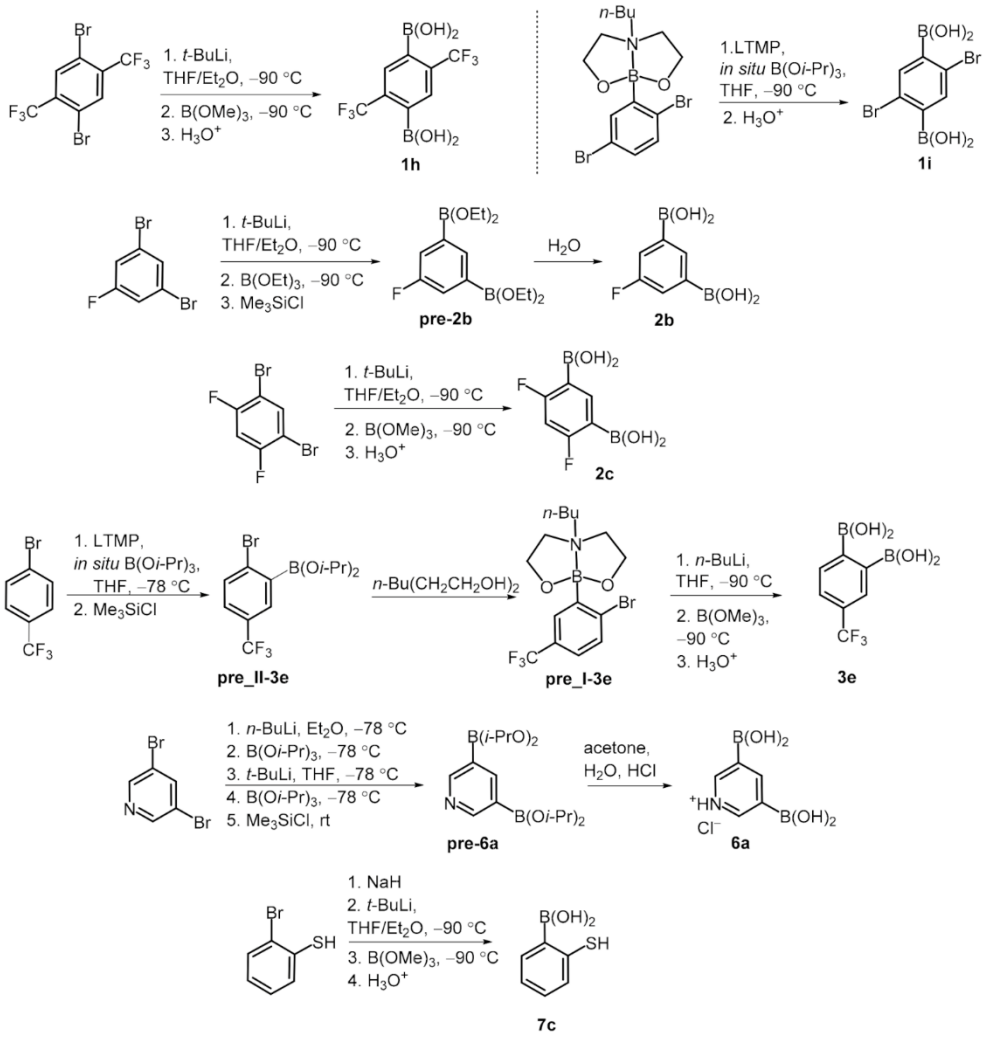

Scheme 3. Synthesis of arylboronic acids **1h**, **1i**, **2b**, **2c**, **3e**, **6a**, **7c**.

2.2. Direct Antimicrobial Activity

It should be emphasized that the main objective of this study was to evaluate the β-lactamase inhibitory capacity of the tested aromatic diboronic acids. However, comprehensive screening of their direct antimicrobial potency was also important. Many BLIs display intrinsic antibacterial activity via inhibiting penicillin-binding proteins (PBPs). It was reported for clavulanic acids [41], sulbactam [42], some diazabicylococtane BLIs [43–46], and recently for boronate BLI xeruborbactam [47]. Though the direct activity of BLIs is usually weak (the minimal inhibitory concentrations—MICs > 64 mg/L) [41,43–45] or moderate (e.g., 16 mg/L for xeruborbactam against CRE strains) [47], it is considered beneficial, as such compounds potentiate β-lactams also against non-β-lactamase-producing organisms. Among various organoboron compounds studied over the past decades [48], benzoxaboroles proved most effective as direct antimicrobials. They usually act as inhibitors of leucyl-tRNA synthetase (leuRS) in fungi [49,50], mycobacteria [51], Gram-positive [52,53], and Gram-negative bacteria [54,55]. Moreover, structurally similar benzosiloxaboroles

displayed high activity against Gram-positive cocci (including methicillin-resistant *Staphylococcus aureus*—MRSA) [56] and yeasts [17]. However, the direct antimicrobial activity of some phenylboronic acids was also reported [57–59]. In this work, we screened the activity of all compounds against six Gram-positive strains, 10 Gram-negative strains, and six yeasts by disc diffusion method followed by the determination of MICs and minimal bactericidal/fungicidal concentrations (MBCs/MFCs). Obtained results are collected in Tables S1–S3 in the Supplementary Materials. A moderate-to-weak activity against Gram-positive strains was found for most tested compounds (Table S1). The lowest MICs were obtained for compound **2e** (0.78–12.5 mg/L for staphylococci, including MRSA; 50–100 mg/L for enterococci) and for compound **7c,** which was equally potent against all tested coccis (MICs 12.5–25 mg/L). These results are comparable with our previous findings for various benzosiloxaboroles [56]. Besides, **1c, 1e**, **1j**, and **7b** displayed moderate activity against staphylococci (MICs 12.5–50 mg/L) and weak against enterococci (MICs 100–400 mg/L), whereas other compounds showed only weak activity regardless of the species. The weak activity (MICs 50–400 mg/L) against Gram-negative rods (except *P. aeruginosa*) was found for some *para-* (**1b**–**1f**, **1i**, and **1j**) and *meta*-phenylenediboronic acids (**2b**–**2e**), as well as for **3a**, **7a**, and **7b** (Table S2). Assuming that multidrug-resistant (MDR) efflux pumps may contribute to Gram-negative rod resistance, the activity of tested agents in the presence of the efflux pumps inhibitor phenylalanine-arginine-β-naphthylamide (PAβN) was also examined [60–62]. Interestingly, only MICs of compounds **2e**, **3e**, and **7b** were significantly reduced in the presence of PAβN (by 4–16-fold). Therefore, it is unlikely that the activity of other compounds is affected by the efflux phenomenon. This is in contrast to benzosiloxaboroles which were actively extruded from bacterial cells [17]. Most tested agents displayed only weak activity against reference yeasts (Table S3). Exceptionally, **3e** was highly active against most *Candida* spp. (MICs 3.12–6.25 mg/L) and moderately active against *Candida krusei* (MIC 25 mg/L) and *Saccharomyces cerevisiae* (MIC 50 mg/L). These values are comparable with those we reported for some benzosiloxaboroles [17,56] and lower than those obtained for various phenylboronic acids [57,58,63]. Moreover, moderate antifungal activity was found for **1i** and **7a**–**7c** (MICs 6.25–50 mg/L). The fungicidal activity was noticed in the case of **3e** (against *Candida albicans*, *Candida tropicalis*, and *Candida guilliermondii* with the MFCs 400 mg/L) and **7c** (against *C. albicans*, *C. tropicalis*, *C. guilliermondii*, and *S. cerevisiae* with the MFCs 25–200 mg/L). To summarize, most of the tested aromatic boronic acids displayed rather weak activity against Gram-positive strains whereas only a few derivatives inhibited the growth of Gram-negative rods and yeasts.

2.3. BLI Activity at High Concentrations

The BLI activity of many boronic acids [4] including some derivatives reported by us recently [17] has prompted us to investigate all of the presented compounds. First, we performed three combination disc tests (CDTs) searching for KPC, AmpC, and ESBL inhibition at high concentrations of tested compounds. PBA was used as the reference inhibitor of both KPC [64] and AmpC [65] enzymes at a concentration of 0.3 mg per disc. Considering that some tested agents inhibited the growth of reference Gram-negative rods, screening tests of direct antimicrobial activity (STDA) against β-lactamase producers were performed using the disc-diffusion method. Discs with 0.3, 0.1, and 0.03 mg of each agent were examined. In the CDTs, concentrations lower than 0.3 mg per disc were used in the case of **1b**–**1f**, **1i**, **1j**, **2c**, **2d**, **7a**, and **7b** (Table S4). A significant difference in the growth inhibition zone diameters around the antibiotic disc with an agent *versus* the same antibiotic disc without an agent was taken as an indicator of BLI activity (Table 1) [64,65]. BLI activity against at least one tested strain was found for the majority (25 out of 33) of tested compounds. Three phenylenediboronic acid regioisomers (**1a, 2a, 3a**), their fluorinated derivatives (**1b**, **1d**, **1e**, **2b**, **3b**, **3c**), benzene-1,2,4-triboronic **4b**, thiophene-2,3-diboronic acid **5a** and 2,5-difluorophenylboronic acid **7a** increased the meropenem activity against the KPC-2-positive strain and ceftazidime activity against both strains producing cephalosporinases (chromosomally encoded cAmpC and plasmid-encoded CMY-2). Some

functionalized phenylenediboronic acids, i.e., those bearing fluorine (**1c**, **1f**, **2c**, **2d**, **3d**), bromine (**1i**, **2f**), CF_3 (**2e**, **3e**), or OMe (**2g**) substituents increased the sensitivity of AmpC-producers only.

Table 1. β-Lactamase inhibitory activity of selected boronic acids.

Disc with Antibiotic ± Tested Agent [a]	Diameter of Inhibition Zone (mm) [b]			
	K. pneumoniae ATCC BAA 1705 KPC-2-Positive	*P. aeruginosa* MUW 700 cAmpC-Positive	*E. coli* 77 CMY-2-Positive	*K. pneumoniae* ATCC 700603 ESBL-Positive
	MEM-10	CAZ-30	CAZ-30	CAZ-30
without agent	6	11	13	14
PBA	**21**	**24**	**24**	14
1a	**19**	**23**	**21**	17
1b	**11** [c]	**20** [c]	**20** [c]	15 [c]
1c	6 [c]	**18** [c]	**20** [c]	14 [c]
1d	**12** [c]	**17** [c]	**20** [c]	14 [c]
1e	**11** [c]	**18** [c]	**20** [c]	15 [c]
1f	6 [c]	**17** [c]	**21** [c]	15 [c]
1i	6 [c]	**16** [c]	16 [c]	14 [c]
2a	**15**	**21**	**22**	16
2b	**19**	**18** [c]	**21** [c]	16
2c	6 [c]	**20** [c]	**19** [c]	13 [c]
2d	6 [c]	**18** [c]	**21** [c]	13 [c]
2e	6	**16**	**19**	16
2f	6	**21**	**19**	15
2g	6	**19**	**20**	13
3a	**17**	**22**	**23**	18
3b	**14**	**22**	**25**	16
3c	**12**	**20**	**20**	16
3d	6	14	**21**	15
3e	6	**17**	17	14
4a	6	**16**	**20**	14
4b	**14**	**21**	**21**	14
5a	**15**	**22**	**20**	16
5c	6	**21**	**22**	16
7a	**13** [d]	**17** [d]	**19** [d]	15 [d]
7c	**13**	11	16	15

MEM-10—A disc with meropenem 10 μg per disc. CAZ-30—A disc with ceftazidime 30 μg per disc. CTX-30—A disc with cefotaxime 30 μg per disc. The diameter of all used antibiotic discs was 6 mm. The amount of reference compound PBA and other agents added onto the antibiotic discs was 0.3 mg per disc; [a] The addition of compounds **1g**, **1h**, **1j**, **1k**, **1l**, **5b**, **6a**, and **7b** onto antibiotic discs did not significantly alter the diameters of the growth inhibition zones in comparison to the results obtained with the antibiotic discs alone; [b] A significant difference in the inhibition zones around the antibiotic disc with an agent versus the same antibiotic disc without an agent is presented in boldface. In the case of meropenem (MEM), a significant difference is at least 4 mm, while for ceftazidime (CAZ) and cefotaxime (CTX), it is at least 5 mm [59,60]; [c] The amount of tested agent added onto the antibiotic discs was 0.1 mg per disc; [d] The amount of tested agent added onto the antibiotic discs was 0.03 mg per disc.

The same activity profile was found for benzene-1,3,5-triboronic acid **4a** and thiophene-2,3,5-triboronic acid **5c**, whereas 2-mercaptophenylboronic acid **7c** increased only the sensitivity of *K. pneumoniae* KPC-2-positive. Lack of BLI activity was observed for phenylene-1,4-diboronic acids including perfluoro derivative **1g**, and compounds bearing bulkier substituents, i.e., CF_3 (**1h)**, I, $SiMe_3$, OMe, (**1j**–**1l**, respectively). Two heteroaromatic compounds, namely thiophene-2,5-(**5b**) and pyridine-3,5-diboronic acid hydrochloride (**6a**) were also inactive. It should be noted that none of the tested boronic acids showed any activity against ESBL-positive *K. pneumoniae*.

2.4. BLI Activity at Low Concentrations

Subsequently, we performed microdilution tests for 25 agents, which displayed BLI activity in the CDTs. They were used at low concentrations (16, 8, and 4 mg/L) as reported previously for known BLIs (vaborbactam, relebactam, and avibactam) [66]. Under these conditions, 18 compounds are inactive against tested Gram-negative bacilli (MICs $\geq$ 400 mg/L), whilst seven present only weak direct activity (MICs ranging from 100–200 mg/L, Table S5). First, we evaluated the capabilities of reducing ceftazidime MICs for two AmpC producers as well as meropenem MICs for four KPC producers and one VIM-positive strain. All KPC- and VIM-positive strains used at this stage were resistant to tested carbapenems, whereas all AmpC-positive strains were resistant to ceftazidime according to EUCAST breakpoints [66] (Table S6). PBA was used as a reference inhibitor of both KPC [64] and AmpC [65] enzymes. At least the 4-fold reduction in a β-lactam MIC was taken as an indicator of BLI activity. Also, the ability of tested agents to restore susceptibility (i.e., to reduce antibiotic MIC to or below EUCAST breakpoint [66]) was examined. Seventeen compounds displayed BLI activity against KPC or AmpC producers. In contrast, none of the tested agents increased the susceptibility of *P. aeruginosa* VIM-positive to meropenem. **1a**, **2a**, **3a**, their fluorinated derivatives (**1b–1f**, **2b–2d**, and **3b**), **4b**, **5a**, **5c**, and **7a** displayed BLI activity towards both cAmpC- and CMY-2-positive strains (Table S6). The strongest ceftazidime MIC reductions were obtained in the presence of *para*-phenylenediboronic acids **1a–1f** and **7a** (up to 32/16/8-fold at 16/8/4 mg/L of a tested agent, respectively), slightly smaller in the presence of *meta*-phenylenediboronic acids **2a–2d** (up to 16/8/4-fold at 16/8/4 mg/L, respectively). All active *para*- and *meta*-phenylenediboronic acids and **7a** reduced ceftazidime MIC of *Escherichia coli* CMY-2-positive to $\leq$8 mg/L, thus reaching EUCAST breakpoint for ceftazidime in the presence of avibactam (at 4 mg/L) [66]. However, only **1a** and **7a** resensitized *P. aeruginosa* cAmpC-positive to ceftazidime (breakpoint in the presence of avibactam at 4 mg/L also equal 8 mg/L [66]). Compounds **3a**, **3b**, **4b**, **5a**, and **5c** were less potent (MIC reductions up to 8/4/2-fold at 16/8/4 mg/L, respectively), and they did not restore sensitivity to ceftazidime of either of the AmpC-positive strains. The potency of *para*- and *meta*-phenylenediboronic acids and **7a** in increasing sensitivity of *E. coli* CMY-2-positive was higher than that for PBA, but weaker in the case of *P. aeruginosa* cAmpC-positive. Compared to unsubstituted acids **1a** and **2a**, their fluoro derivatives were generally more active towards *E. coli* CMY-2-positive (up to 4-fold for **1e**) but less active towards *P. aeruginosa* cAmpC-positive (also up to 4-fold).

BLI activity toward KPC producers was less common than toward AmpC producers. However, significant reductions of meropenem MIC of at least two KPC-positive strains were obtained for 7 compounds: **1a** and its fluorinated derivatives (**1b**, **1d**, **1e**), **3a** and its 4-fluoro derivative **3c**, and **7a** (Table S6). We suppose that the lack of activity of *meta*-phenylenediboronic acids against KPC producers can be ascribed to different structures of binding sites of KPC and AmpC enzymes. Thus, it seems that the mutual *meta* orientation of two boronic groups (the case for **2a** and its derivatives) disfavors binding to KPC. The active agents were subsequently tested with other carbapenems, i.e., with imipenem and ertapenem (Table 2). Among the total of 84 combinations with each carbapenem, significant MIC reductions were obtained 53 times for imipenem, 48 times for meropenem, and 41 times for ertapenem. Each tested agent potentiated all three carbapenems comparably (MIC reductions in most cases differ no more than by 2-fold, rarely by 4-fold).

Table 2. The MIC values of antibiotics alone and in combinations with selected agents (results for other agents are presented in Table S6 in the Supplementary Materials).

Strain		MICs (mg/L) of Antibiotics in the Presence of Tested Agents at the Concentration of 16/8/4 mg per L							
Antibiotic	**MIC (mg/L)**	**+PBA**	**+1a**	**+1b**	**+1d**	**+1e**	**+3a**	**+3c**	**+7a**
***K. pneumoniae* ATCC BAA-1705 KPC-2-positive**									
MEM	32	**8**/16/16	**4**/**8**/16	**8**/16/16	**8**/16/16	**8**/16/16	**4**/**8**/16	16/16/16	**8**/16/16
IMI	16	**4**/8/8	**4**/8/8	**4**/8/8	8/8/16	8/8/16	**2**/**2**/**4**	**4**/**4**/8	**4**/**4**/8
ERT	64	32/64/64	**16**/32/32	32/32/32	32/64/64	32/64/64	**8**/**16**/32	**16**/32/32	32/32/64
***E. coli* 76 KPC-2-positive**									
MEM	64	**16**/**16**/**16**	**8**/**16**/32	**16**/**16**/32	**16**/32/32	**16**/32/32	**4**/**8**/**16**	**16**/32/32	**16**/32/32
IMI	128	**16**/**32**/**32**	**16**/**32**/64	**16**/**32**/64	**32**/64/64	**32**/64/64	**8**/**16**/**16**	**16**/**32**/**32**	**16**/**32**/**32**
ERT	256	**64**/**64**/128	**32**/**64**/**64**	**32**/**64**/128	**64**/**64**/128	**32**/**64**/128	**32**/**64**/**64**	**64**/128/128	**64**/128/128
***K. pneumoniae* 81 KPC-3-positive**									
MEM	16	8/8/8	**1**/**2**/8	**1**/**4**/8	**1**/**4**/8	4/8/8	**0.5**/**1**/**2**	**2**/**2**/**4**	**1**/**4**/**4**
IMI	8	**2**/4/4	**1**/**2**/**2**	**2**/**2**/4	**2**/**2**/4	**2**/**2**/4	**0.5**/**1**/**1**	**1**/**1**/**2**	**1**/**1**/**2**
ERT	32	16/16/16	**2**/**8**/**8**	**8**/16/16	**4**/16/16	16/16/16	**1**/**2**/**8**	**4**/**8**/**8**	**8**/16/16
***K. pneumoniae* 83 KPC-3-positive, CTX-M-3-positive**									
MEM	32	**8**/**8**/16	**4**/16/16	**8**/16/32	**8**/16/32	**8**/16/32	**0.5**/**2**/**8**	**4**/**8**/**8**	**4**/16/16
IMI	8	4/4/8	**2**/**2**/4	**2**/4/4	4/4/4	4/4/4	**0.5**/**1**/**2**	**2**/**2**/4	**1**/**2**/**2**
ERT	64	32/32/32	**16**/**16**/32	**16**/32/32	32/32/64	**16**/32/64	**4**/**8**/**16**	**16**/32/32	**16**/32/32
***E. coli* 77 CMY-2-positive**									
CAZ	64	**8**/**16**/32	**8**/**16**/32	**4**/**8**/**16**	**8**/**16**/**16**	**2**/**4**/**8**	**16**/32/32	32/32/32	**2**/**4**/**8**
***P. aeruginosa* MUW 700 cAmpC-positive**									
CAZ	128	**8**/**8**/**16**	**8**/**16**/**32**	**16**/**16**/**32**	**32**/64/64	**32**/**32**/64	**32**/64/128	128/128/128	**8**/**16**/**32**

MEM—meropenem; IMI—imipenem; ERT—ertapenem; CAZ—ceftazidime; PBA—phenylboronic acid. The significant reductions (at least a 4-fold) in the antibiotic MIC values after the addition of a tested agent are shown in boldface.

The highest activity was found for **3a** (carbapenems' MIC reduction up to 64/16/8-fold at 16/8/4 mg/L of tested agent, respectively). Compounds **1a** and **7a** were less potent (MIC reduction up to 16/8/2-fold at 16/8/4 mg/L, respectively). For comparison, PBA at 16 mg/L reduced carbapenems' MICs only up to 8-fold for KPC-2 producers and up to 4-fold for KPC-3 producers. All seven agents and PBA reduced meropenem MIC of KPC-3-positive strains to ≤8 mg/L—*Enterobacterales* breakpoint for meropenem in the presence of vaborbactam (at 8 mg/L) [66] (Table 2). Six agents (all except **3c**) also resensitized *K. pneumoniae* ATCC BAA-1705 KPC-2-positive, whereas **1a** and **3a** restored the meropenem activity against all studied KPC producers. Moreover, all seven agents reduced imipenem MIC for *K. pneumoniae* 81 KPC-3-positive to ≤2 mg/L (breakpoint in the presence of relebactam at 4 mg/L [66]). Compounds **1a**, **1b**, **3a**, **3c**, and **7a** (unlike PBA) resensitized *K. pneumoniae* 83 KPC-3/CTX-M-3-positive to imipenem, whereas **3a** also resensitized *K. pneumoniae* KPC-2-positive. We did not achieve a reduction of ertapenem MIC to its susceptibility breakpoint (0.5 mg/L, used alone as this antibiotic is not combined with any BLI [66]). However, it is worth noting that **1a** and **3a** potentiated ertapenem better than PBA toward all KPC producers (by up to 8- and 16-fold, respectively). Recently, α-amido-β-triazolylethaneboronic acid at 4 mg/L was found to restore the susceptibility of strains producing various KPC, SHV, TEM, and CTX-M enzymes to ertapenem. However, it should be noted that strains used in our study were much more resistant to this carbapenem (MIC ranges 32–256 mg/L vs. 4–16 mg/L in the previous report [20]).

KPC-2 and KPC-3 enzymes are the most prevalent serine carbapenemases, which differ only in the amino acid at position 272 (histidine in KPC-2, tyrosine in KPC-3) [5]. Interestingly, tested boronic acids potentiated carbapenems better against *K. pneumoniae* 81 KPC-3-positive than against KPC-2 producers (2–4-fold higher MIC reductions). Thus, in order to clearly indicate the molecular target of tested agents, the most representative

derivatives **1a**, **2a**, **3a**, and reference PBA were additionally tested alone and in combination with meropenem against meropenem susceptible *E. coli* DH5α and against *E. coli* 82 TR(pl 81)—the transformant of *E. coli* DH5α carrying a plasmid with bla_{KPC-3} gene from the clinical strain of *K. pneumoniae* 81 KPC-3-positive. Tested agents alone were inactive against both the parent strain and its transformant (MICs of PBA, **1a**, and **2a** > 400 mg/L, MICs of **3a** equal to 400 mg/L). None of them (in concentrations of 4, 8 and 16 mg/L) altered meropenem MIC of *E. coli* DH5α (Table 3). In contrast, significant (at least 4-fold) meropenem MIC reductions were obtained in their presence for *E. coli* 82 TR(pl 81). As expected, **3a** turned out to be the most potent compound, reducing meropenem MIC by 32/16/4-fold at the concentration of 16/8/4 mg/L, respectively. PBA and **1a** were less effective, whereas **2a** reduced meropenem MIC only by 2-fold. Subsequently, total proteins from *E. coli* 82 TR(pl 81) cells were extracted and the nitrocefin hydrolysis test was performed. KPC-3 was the only β-lactamase produced by *E. coli* 82 TR(pl 81). Efficient nitrocefin hydrolysis in the positive control measurement as relative absorbance proved the presence of KPC-3 in the purified protein extract. (Table S7). The reduction in the relative absorbance level by 53/44/42% in the presence of 16 mg/L, and by 43/35/35% in the presence of 8 mg/L of PBA/**3a**/**1a**, respectively, indicated tested agents as effective KPC-3 inhibitors (Tables 3 and S7). Compound **2a** showed only weak BLI activity in concentration 16 mg/L, 29% reduction in relative absorbance. Interestingly, PBA turned out to be the most effective KPC-3 inhibitor in the nitrocefin hydrolysis test, despite its inferiority in potentiating carbapenems against *E. coli* 82 TR(pl 81) as well as clinical KPC producers. Thus, the physicochemical properties of the tested diboronic acids enable their better performance in microbiological whole-cell assays.

Table 3. The effect of agents **1a**, **2a** and **3a** on meropenem MICs against *E. coli* 82 TR(pl 81) KPC-positive and on the activity of KPC-3 in purified protein extract visualized by the nitrocefin hydrolysis test.

Agent Concentration in mg/L	**MICs in mg/L of Meropenem Alone or in Combination with a Tested Agent [Reduction in the Relative Absorbance in the Nitrocefin Hydrolysis Test] ***			
	+PBA	**+1a**	**+2a**	**+3a**
E. coli 82 TR(pl 81)				
0	2	2	2	2
4	**0.50** [44%]	**0.50** [27%]	1 [13%]	**0.50** [30%]
8	**0.25** [43%]	**0.25** [35%]	1 [18%]	**0.125** [35%]
16	**0.25** [53%]	**0.125** [42%]	1 [29%]	**0.062** [44%]
E. coli DH5α **				
0	0.016	0.016	0.016	0.016
16	0.016	0.016	0.016	0.016

PBA—phenylboronic acid as the reference BLI; A significant reduction (at least 4-fold) in the meropenem MIC values after the addition of a tested agent is shown in boldface. * Reduction in the relative absorbance level was calculated as the difference in the relative absorbance between the positive control and the sample of each concentration of tested inhibitor and expressed as a percentage (detailed results of the nitrocefin hydrolysis test are provided in Table S7). ** Meropenem susceptible *E. coli* DH5α, the parent strain of transformant *E. coli* 82 TR(pl 81).

Overall, more agents were active against strains producing cephalosporinases than carbapenemases (16 vs. 7 compounds) (Table S6). However, six compounds (**1a**, **1b**, **1d**, **1e**, **3a** and **7a**) displayed BLI activity toward both KPC and AmpC producers. Interestingly, apart from parent aromatic diboronic acids **1a**, **2a**, and **3a**, only their fluorinated derivatives (except for **1c**) were effective BLIs toward KPC producers. Moreover, 13 compounds restored the sensitivity of at least one strain (Table S6). Notably, **3a** was the most potent agent in resensitizing KPC producers to meropenem (all four strains) and imipenem (3 strains). However, it did not restore the sensitivity of any AmpC producer to ceftazidime. Compound **1a** restored the sensitivity of all KPC producers to meropenem, all KPC-3 producers to imipenem, and two AmpC-positive strains to ceftazidime (Table 2). Fluorinated deriva-

tives **1b**, **1d**, and **1e** proved slightly less successful as the meropenem breakpoint for *E. coli* KPC-2-positive and the ceftazidime breakpoint for *P. aeruginosa* cAmpC-positive were not reached, whereas imipenem breakpoint for *K. pneumoniae* KPC-3/CTX-M-3-positive was not reached with **1d** and **1e**. Compound **7a** was comparably active, as only the meropenem breakpoint for *E. coli* KPC-2-positive was not reached in its presence.

2.5. Synergy Evaluation

To investigate the type of interaction between studied boronic acids and β-lactams, we performed checkerboard assays and calculated fractional inhibitory concentrations indices (FICIs) for compounds that caused at least one significant reduction in any β-lactam MIC. This part of the work included 16 compounds, and PBA as a reference, combined with ceftazidime against two AmpC producers and seven tested agents, and reference PBA, combined with three carbapenems against four KPC producers. Following Bonapace et al., both the lowest and the average FICI were subsequently interpreted [67]. Obtained results are presented in Tables 4 and 5.

Table 4. In vitro interactions between tested agents and ceftazidime, determined by fractional inhibitory concentration index (FICI).

Agent Tested in Combination with CAZ [a]	The Lowest FICI/Interpretation [Average FICI/Interpretation] [b]	
	***E. coli* 77 CMY-2-Positive**	***P. aeruginosa* MUW 700 AmpC-Positive**
PBA	0.15/S [0.30/S]	0.07/S [0.10/S]
1a	0.15/S [0.30/S]	**0.08/S** [0.16/S]
1b	**0.10/S [0.17/S]**	0.14/S [0.18/S]
1c	**0.14/S [0.19/S]**	0.17/S [0.32/S]
1d	0.17/S **[0.23/S]**	0.27/S [0.43/S]
1e	**0.14/S [0.17/S]**	0.29/S [0.38/S]
1f	0.21/S **[0.24/S]**	0.27/S [0.43/S]
2a	0.15/S **[0.22/S]**	0.14/S [0.18/S]
2b	**0.10/S [0.17/S]**	0.26/S [0.35/S]
2c	0.17/S **[0.21/S]**	0.15/S [0.22/S]
2d	**0.14/S [0.19/S]**	0.26/S [0.35/S]
3a	0.29/S [0.44/S]	0.29/S [0.61/I]
3b	0.27/S [0.43/S]	0.27/S [0.60/I]
4b	0.27/S [0.43/S]	0.15/S [0.30/S]
5a	0.27/S [0.43/S]	0.15/S [0.30/S]
5c	0.27/S [0.43/S]	0.27/S [0.43/S]
7a	**0.14/S [0.17/S]**	0.10/S [0.17/S]

CAZ—ceftazidime; S—synergy; I—indifference. FICIs lower than for PBA are shown in boldface. [a] FICIs were calculated only for agents that caused at least one 4-fold ceftazidime MIC reduction; [b] For combinations with at least one MIC value above the highest tested concentration FICIs are equal to or below the presented values.

Table 5. In vitro interactions between tested agents and carbapenems, determined by fractional inhibitory concentration index (FICI).

Strain	Agent Tested	The Lowest FICI/Interpretation [Average FICI/Interpretation] [a]		
		MEM	**IMI**	**ERT**
***K. pneumoniae* ATCC BAA-1705 KPC-2-positive**				
	PBA	0.27/S [0.43/S]	0.27/S [0.43/S]	0.52/I [0.85/I]
	1a	**0.15/S [0.30/S]**	0.27/S [0.43/S]	**0.27/S [0.43/S]**
	1b	0.27/S [0.43/S]	0.27/S [0.43/S]	0.51/I [0.51/I]
	1d	0.29/S [0.44/S]	0.52/I [0.69/I]	0.54/I [0.86/I]
	1e	0.33/S [0.46/S]	0.54/I [0.71/I]	0.58/I [0.88/I]
	3a	**0.17/S [0.32/S]**	**0.15/S [0.19/S]**	**0.17/S [0.32/S]**
	3c	0.51/I [0.51/I]	**0.26/S [0.35/S]**	**0.27/S [0.43/S]**
	7a	0.41/S [0.51/I]	0.33/S [0.43/S]	0.58/I [0.76/I]

Table 5. *Cont.*

Strain	Agent Tested	The Lowest FICI/Interpretation [Average FICI/Interpretation] [a]		
		MEM	IMI	ERT
***E. coli* 76 KPC-2-positive**				
	PBA	0.26/S [0.26/S]	0.15/S [0.22/S]	0.26/S [0.35/S]
	1a	**0.15/S** [0.31/S]	0.15/S [0.30/S]	**0.15/S [0.22/S]**
	1b	0.27/S [0.36/S]	**0.17/S** [0.32/S]	**0.17/S [0.32/S]**
	1d	0.29/S [0.44/S]	0.29/S [0.44/S]	0.27/S [0.36/S]
	1e	0.41/S [0.51/I]	0.41/S [0.51/I]	0.29/S [0.39/S]
	3a	**0.10/S [0.17/S]**	**0.10/S [0.13/S]**	**0.17/S [0.23/S]**
	3c	0.27/S [0.43/S]	0.15/S [0.22/S]	0.27/S [0.43/S]
	7a	0.41/S [0.51/I]	0.29/S [0.30/S]	0.41/S [0.51/I]
***K. pneumoniae* 81 KPC-3-positive**				
	PBA	0.51/I [0.51/I]	0.27/S [0.43/S]	0.51/I [0.51/I]
	1a	**0.08/S [0.24/S]**	**0.15/S [0.22/S]**	**0.08/S [0.20/S]**
	1b	**0.08/S [0.28/S]**	**0.26/S [0.35/S]**	**0.27/S [0.43/S]**
	1d	**0.10/S [0.29/S]**	0.27/S **[0.36/S]**	**0.17/S [0.40/S]**
	1e	**0.33/S [0.46/S]**	0.29/S **[0.38/S]**	0.52/I [0.55/I]
	3a	**0.07/S [0.10/S]**	**0.10/S [0.13/S]**	**0.07/S [0.14/S]**
	3c	**0.14/S [0.18/S]**	**0.14/S [0.18/S]**	**0.15/S [0.22/S]**
	7a	**0.14/S [0.23/S]**	**0.17/S [0.21/S]**	**0.33/S [0.46/S]**
***K. pneumoniae* 83 KPC-3-positive, CTX-M-3-positive**				
	PBA	0.26/S [0.35/S]	0.51/I [0.68/I]	0.51/I [0.51/I]
	1a	**0.15/S** [0.39/S]	**0.26/S [0.35/S]**	**0.26/S [0.35/S]**
	1b	0.27/S [0.60/I]	**0.27/S [0.43/S]**	**0.27/S [0.43/S]**
	1d	0.29/S [0.61/I]	0.51/I **[0.52/I]**	0.52/I [0.69/I]
	1e	0.33/S [0.63/I]	0.52/I **[0.55/I]**	**0.33/S** [0.63/I]
	3a	**0.06/S [0.13/S]**	**0.10/S [0.17/S]**	**0.10/S [0.17/S]**
	3c	**0.15/S [0.22/S]**	**0.26/S [0.35/S]**	**0.27/S [0.43/S]**
	7a	0.29/S [0.47/S]	**0.29/S [0.30/S]**	**0.41/S** [0.51/I]

MEM—meropenem; IMI—imipenem; ERT—ertapenem; PBA—phenylboronic acid; S—synergy; I—indifference; FICIs lower than for PBA are shown in boldface; [a] For combinations with at least one MIC value above the highest tested concentration, FICI is equal to or below the presented value.

Finally, assuming that the lower the average FICI (aFICI) value, the stronger the synergy, we compared aFICIs according to structural classification based on the mutual position and/or the number of boronic functionalities as well as the type of the aromatic ring. Thus, the tested agents were analyzed in the following groups denoted as **G1** (**1a**–**1f**), **G2** (**2a**–**2d**), **G3** (**3a**–**3b**), **G4** (**4b**), **G5** (**5a** and **5c**), and **G7** (PBA and **7a**) in the case of AmpC producers and as **GI** (**1a, 1b, 1d, 1e**), **GIII** (**3a** and **3c**), and **GVII** (PBA and **7a**) in the case of KPC producers. Additionally, we compared unsubstituted boronic acids denoted as **F1** (**1a**, **2a**, **3a**, **4a, 5a, 5c,** and PBA)/**FI** (**1a**, **3a**, PBA) with fluorinated derivatives **F2** (**1b**—**1f**, **2b**—**2d, 3b,** and **7a**)/**FII** (**1b**, **1d**, **1e**, **3c**, and **7a**) for AmpC/KPC producers, respectively. Tested strains were analyzed according to expressed β-lactamases. Due to a lack of normal distribution, the Kruskal–Wallis test was used, followed by Dunn's multiple comparison tests if applicable. The significance level was set at $p < 0.05$. Obtained aFICIs for analyzed groups are presented in Figures 1 and 2.

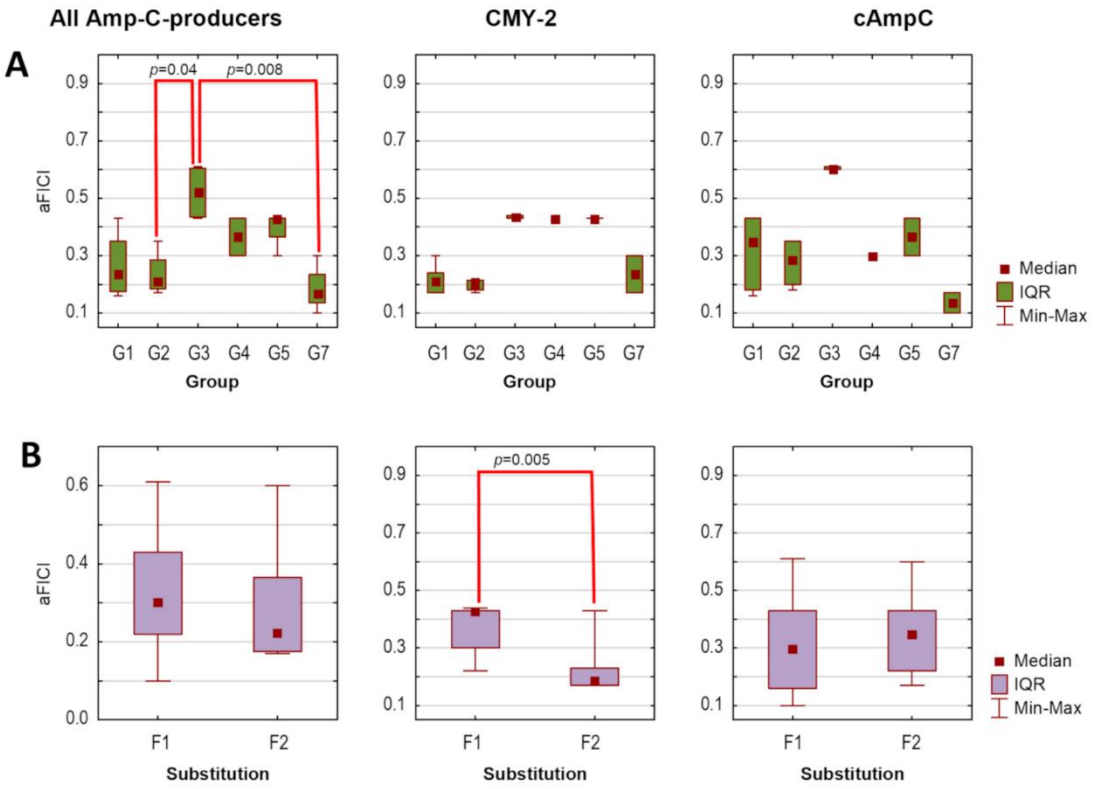

Figure 1. Average fractional inhibitory concentration indices (aFICIs) for ceftazidime combinations with selected boronic acids against AmpC-producing strains (n = 2), according to agents group (**A**) and substitution type (**B**): **G1** (**1a**–**1f**), **G2** (**2a**–**2d**), **G3** (**3a**–**3b**), **G4** (**4b**), **G5** (**5a**, **5c**), **G7** (PBA and **7a**); **F1**—unsubstituted boronic acids (**1a**, **3a**, **4b**, **5a**, **5c**, PBA), **F2**—fluorinated boronic acids (**1b**−**1f**, **2b**−**2d**, **3b**, **7a**). IQR—interquartile range. Significant differences between the groups are marked with red lines ($p < 0.05$).

Synergy with ceftazidime (FICI $\leq$ 0.5) against both AmpC-positive strains was obtained for 14 agents, while synergy against one strain for the remaining two agents (**3a** and **3b**), regardless of whether the lowest or average FICI was interpreted (Table 4). Obtained FICIs are comparable with those recently reported for other phenylboronic acid derivatives combined with ceftazidime against *P. aeruginosa* AmpC-positive [23]. Subsequent statistical analysis revealed that tested combinations are comparably potent against both AmpC producers, as aFICIs did not differ significantly between *E. coli* CMY-2-positive and *P. aeruginosa* cAmpC-positive neither when all agents were analyzed together ($p_{Kruskal–Wallis} = 0.56$), nor within each group separately (all $p_{Kruskal–Wallis}$ values > 0.05). However, the synergy between ceftazidime and **G3** was significantly weaker compared to **G2** ($p_{Dunn} = 0.04$) and **G7** ($p_{Dunn} = 0.008$) when both AmpC producers were analyzed together (Figure 1A). In turn, **F2** acted synergistically with ceftazidime significantly stronger than **F1** toward *E. coli* CMY-2-positive ($p_{Kruskal–Wallis} = 0.005$). In contrast, differences between these groups were non-significant in the case of *P. aeruginosa* cAmpC-positive ($p_{Kruskal–Wallis} = 0.35$) (Figure 1B).

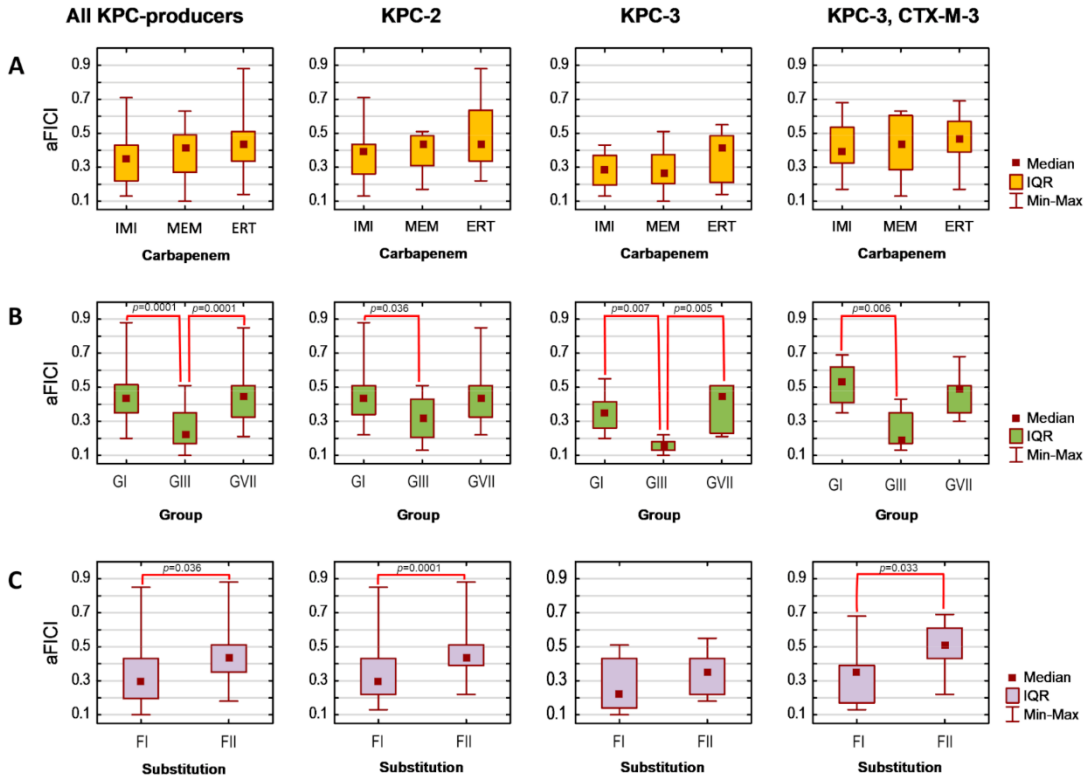

Figure 2. Average fractional inhibitory concentration indices (aFICIs) for carbapenem combinations with selected boronic acids against KPC-producing strains (n = 4), according to carbapenem counterpart (**A**), agents group (**B**), and substitution type (**C**). IQR—interquartile range; IMI—imipenem; MEM—meropenem; ERT—ertapenem; **GI** (**1a, 1b, 1d, 1e**), **GIII** (**3a** and **3c**), **GVII** (PBA and **7a**); **FI**—unsubstituted boronic acids (**1a**, **3a**, PBA); **FII**—fluorinated boronic acids (**1b**, **1d**, **1e**, **3c**, **7a**). Significant differences between the groups are marked with red lines ($p < 0.05$).

Synergy with carbapenems was obtained for 65 per 84 cases, regardless of whether the lowest or average FICI was interpreted (Table 5). Obtained FICIs are comparable with those recently reported for some phenylboronic acids combined with meropenem against *K. pneumoniae* KPC-2-positive [23]. Interestingly, Celenza et al. previously reported that these combinations' FICIs for strains with higher meropenem MICs are even lower [22]. The selected seven boronic acids potentiate each carbapenem comparably as aFICIs for their combination with imipenem, meropenem, and ertapenem did not differ significantly either when all KPC producers were analyzed together ($p_{Kruskal–Wallis} = 0.168$), or within each β-lactamase group (all $p_{Kruskal–Wallis} > 0.05$) (Figure 2B). It was confirmed that they potentiate carbapenems significantly better against the KPC-3-producing strain compared to the KPC-2 producer ($p_{Dunn} = 0.046$) and KPC-3/CTX-M-3-positive one ($p_{Dunn} = 0.026$). Moreover, significant differences in the strength of the synergistic interaction with carbapenems (Figure 2B,C) occurred among both groups ($p_{Kruskal–Wallis} < 0.0001$) and **FI** vs. **FII** ($p_{Kruskal–Wallis} = 0.001$). Regardless of the produced β-lactamase, **GIII** acted synergistically with carbapenems significantly stronger than **GI** (p_{Dunn} values for KPC-2, KPC-3, and KPC-3/CTX-M-3 producers were 0.036, 0.007, and 0.006, respectively). In the case of the KPC-3-positive strain, their aFICIs with carbapenems were also significantly lower than the aFICIs of **GVII** ($p_{Dunn} = 0.005$). Moreover, synergy with carbapenems was significantly

stronger for **FI** than for **FII** in the case of KPC-2 producers ($p_{Kruskal–Wallis}$ = 0.0001) and KPC-3/CTX-M-3-positive strain ($p_{Kruskal–Wallis}$ = 0.033). This is in agreement with the recent findings by Zhou et al. who reported that fluoro derivatives of triazole-substituted phenylboronic acids are weaker KPC-2 inhibitors than unsubstituted compounds, even though fluorine substituents did not significantly alter the docked conformations [24].

Overall, the statistical analysis revealed that 16 arylboronic acids act synergistically with ceftazidime to a similar extent against CMY-2- and cAmpC-positive strains. In contrast, their interaction with carbapenems is significantly stronger against KPC-3- compared to KPC-2- and KPC-3/CTX-M-3-positive strains. The synergy is also comparable regardless of the carbapenem counterpart (imipenem, meropenem, ertapenem). However, synergy strength is influenced by both the structure variation and the presence of fluorine substituent(s). The synergy with carbapenems is the strongest for **GIII**, while synergy with ceftazidime is weaker for **G3** compared to **G2** and **G7**. Moreover, the installation of a fluorine substituent weakens synergy with carbapenems against KPC-2 producers and KPC-3/CTX-M-3 producers, simultaneously increasing the synergy with ceftazidime against CMY-2-positive strain.

2.6. Cytotoxicity Studies

The viability of MRC-5 human fibroblasts was tested after 72 h of treatment with each of the studied compounds used at the following concentrations: 12.5, 25, and 50 mg/L, except for **1a** and **3a** tested at 16, 32, and 64 mg/L. The obtained results are shown in Table S8 in the Supplementary Materials. Monoboronic acids **7b** and **7c** were the most cytotoxic with the viability of MRC-5 in the range of 0–56.4%. Other tested compounds decreased MRC-5 viability by no more than 50% and were less cytotoxic than PBA.

2.7. Molecular Modeling and Hybrid QM/MM Simulations

The crystal structure of a complex of 3-nitrophenylboronic acid (3-NPBA) with KPC-2, deposited in the Protein Data Bank (PDB id 3RXX [68]), was used as a starting point [17] to study the binding diboronic acids **1a**, **2a**, **3a**, and PBA as a reference compound. The active site of KPC-2 was described in the atomistic level of detail (Figure 3) [68,69]. It possesses S1 and S2 cavities (Figure 3A), surrounded by the Ω loop and loop between α3 and α4 helices, that are essential for competitive inhibition and ligand recognition [69,70] starting by anchoring the BLI in the S2 cavity. Critical amino acids (Lys73 and Glu166, see Figure 3B) are responsible for the formation of the protein-ligand dative covalent bond due to the reorganization of protonation states [69]. In turn, the S1 cavity comprises the catalytic serine (Ser70) with the O atom of the side hydroxymethyl group which is potentially able to bind to the sp^2 hybridized boron atom of the BLI. Notably, the other crucial factors for the inhibition mechanism are also preserved, like Ser70 rotamer, the "flipped-out" position of Trp105 and the "in" position of Glu166 [68–70].

Molecular docking was performed for neutral and anionic forms of the chosen arylboronic acids. For **3a**, the structural specificity involving the formation of cyclic oxadiborole forms **3a_III**, **3a_IV**, and **3a_V** (Scheme 4) was considered in accordance with the reported data [38]. For each ligand, we selected modes that fulfilled all criteria established for molecular docking evaluation. In general, most of the modes in the anionic form did not fulfill the distance criterion. The estimated free energies of binding do not significantly differ between ligands ranging from −4.48 ÷ −3.78 kcal/mol (Table 6). The difference of only 0.6 kcal/mol did not allow us to assess the ability of ligands for inhibition properly. For this reason, we performed molecular dynamics (MD) simulations. The selected modes achieved the thermodynamic equilibrium, which allowed us to assess their inhibitory potential.

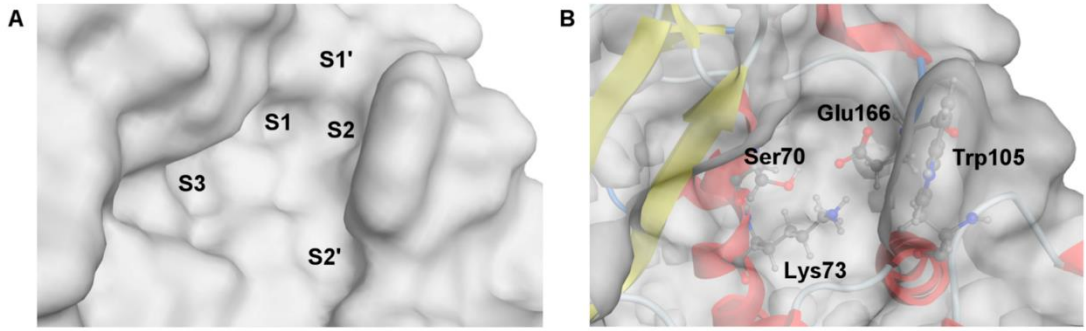

Figure 3. Visualization of the active site structure of KPC-2 carbapenemase, deposited in the Protein Data Bank (ID: 3RXX [68]). (**A**) The molecular surface of the active site is divided into separate cavities, named as S1–S3, S1′ and S2′. (**B**) Location of the critical residues for inhibitory activity of BLI.

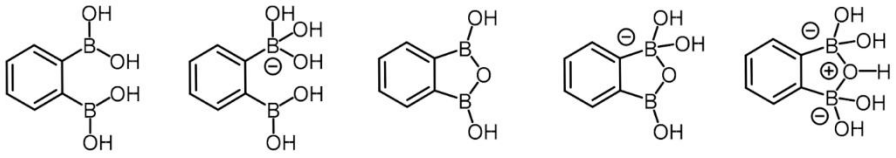

Scheme 4. Possible neutral (**3a_I**, **3a_III**) and anionic (**3a_II**, **3a_IV**, **3a_V**) forms of compound **3a**.

Table 6. The most important data on the computational studies for the selected docking modes. S—the free binding energy, $d_{Ser70(O)–B}$—the distance between the oxygen atom of the serine hydroxyl group and the boron atom of the BLI.

	Molecular Docking			MD		QM/MM	
	S [kcal/mol]	$d_{Ser70(O)–B}$ [Å]	Filling the Active Site	Average for $d_{Ser70(O)–B}$ [Å]	$P_{NECESSARY}$ [%]	$P_{SUFFICIENT}$	$P_{FAVORABLE}$ [%]
PBA	–3.78	3.46	S1, S1′	3.08 ± 0.20	40.4	2/8	10.1
1a	–3.79	3.55	S1, S1′	4.77 ± 0.51	-	-	-
1a	–4.38	3.74	S1, S3	3.52 ± 0.28	2.6	2/8	0.65
1a	–4.18	4.28	S2, S3	3.62 ± 0.32	0.6	-	-
2a	–4.34	3.34	S1, S2, S1′	6.81 ± 0.66	-	-	-
2a	–4.22	3.33	S1, S2	3.57 ± 0.29	1.2	-	-
2a	–4.00	3.45	S1, S2	3.50 ± 0.26	1.2	2/8	0.3
3a_I	–4.36	3.28	S1, S2	3.22 ± 0.19	11	2/8	2.75
3a_I	–4.28	3.10	S1, S2, S1′	5.09 ± 0.93	-	-	-
3a_I	–4.16	3.22	S1, S2	4.21 ± 0.40	-	-	-
3a_III	–4.48	3.08	S1, S3	4.21 ± 0.40	-	-	-
3a_III	–4.26	3.22	S1, S2	3.23 ± 0.28	22.4	4/8	11.2
3a_III	–3.96	3.31	S1, S2	3.30 ± 0.28	14.2	-	-
3a_IV	–4.21	3.30	S1, S2, S3, S1′	3.27 ± 0.18	6.8	6/8	5.1

We analyzed only the results of the stable fragment of the trajectory (time range from 1.8 to 2.0 ns). The most promising arrangement of each compound was selected based on the estimated average distance between the (Ser70)O and B atoms ($d_{Ser70(O)–B}$, Table 6). If we performed MD simulations for various arrangements, we selected only those characterized by the lowest average values. By defining the cutoff set on 3 Å, we determined a set of arrangements able to form a protein-ligand covalent bond (see Section S4.2. Molecular dynamics in the Supplementary Materials).

MD simulations revealed that **2a** and **3a** forms bind to KPC-2 with similar interaction networks (Figure 4), but PBA and **1a** do not. It was caused by the steric clashes for **1a** (see Section S4.1. Molecular docking in the Supplementary Materials) and the lack of the second substituent in PBA, like in the NPBA. The interaction networks, shown in Figure 4, agree with the published experimental and computational studies [68,69].

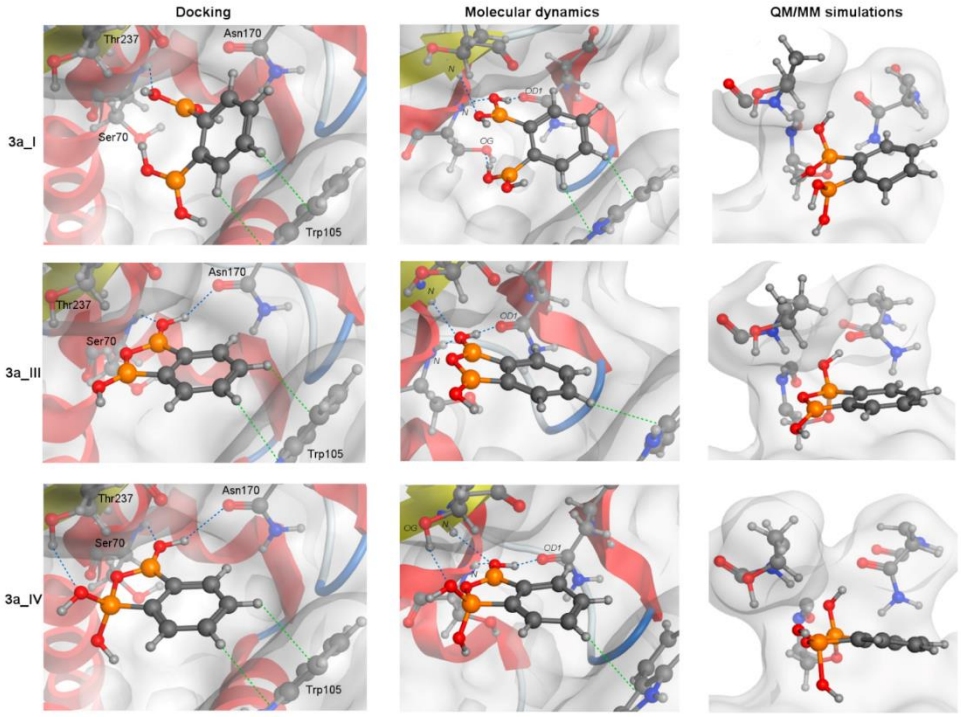

Figure 4. A schematic graphic showing the covalent docking process of three forms of **3a** with the catalytic Ser70 residue. The arrangements obtained from molecular docking (left column), the most frequent structures from MD simulation (middle) and QM/MM simulations (right column, after the formation of protein-ligand covalent bond) are presented. For all structures, the orientation of S1 and S2 cavities are the same. Blue and green dotted lines represent CH-π and hydrogen bond interactions, respectively.

The aromatic rings of **2a** and **3a** compounds occupy the same position as NPBA allowing it to interact with Trp105 via CH-π interactions (green dotted lines, Figure 4). In addition, such compounds form hydrogen bonds (HBs, blue dotted lines, Figure 4) that cover interactions published by Charzewski et al. [69]. The **2a** and all **3a** forms are stabilized by the HBs with the N atom of the Ser70 and Thr237 backbone, and the O atom of the Asn170 side chain (Figure 4), each with high occupancy (≥70%). In addition, the **3a_I** form creates an additional HB with the O atom of the Ser70 OH group. On the other hand, only in the MD simulations of **3a_IV** form, we detected a characteristic HB with the O atom of the Th237 OH group, observed in 99% of all analyzed simulation frames. It is worth noting that despite the same interaction network, the distance between the (Ser70) O and B atoms is significantly larger for the **2a** compound than for the **3a** (Table 6). The aromatic rings of PBA and **1a** are slightly shifted (compared to NPBA), limiting the hydrogen bonding to only the N atoms of the Ser70 and Thr237 backbone.

Finally, from the analyzed part of the trajectory, we extracted an arrangement with a minimal $d_{\mathrm{Ser70(O)–B}}$ value. We treated this arrangement as the most promising binding

mode of each ligand. For such an arrangement (and a corresponding docking mode), we performed hybrid QM/MM simulations with eight repetitions (4 repetitions for each starting structure). For each diboronic acid, the formation of a protein-ligand covalent bond was observed, in agreement with the mechanism published by Charzewski et al. (Scheme 5, Table S9) [69]. The minimal time to form a protein-ligand covalent bond was estimated. PBA required 10.59 ps, 1a—8.49 ps, 2a—17.56 ps, **3a_I**—27.31 ps, **3a_III**—10.63 ps, and **3a_IV**—1.46 ps (Table S9). Such a covalent bond was observed up to 150 ps, after which the simulations were stopped. It is qualitatively consistent with the reported experimental data (Table 2). The results indicate that all analyzed boronic acids can form a covalent bond with KPC-2 (Tables 6 and S9), and therefore, can be qualified as BLIs [69].

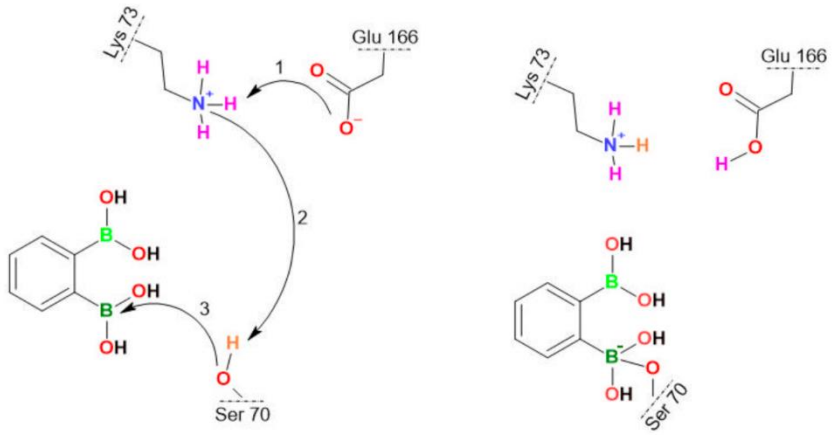

Scheme 5. The covalent bond formation between the Ser70 OH group of KPC-2 and the boron atom of **3a_I**. The stepwise proton transfer is highlighted with the curved arrows: the proton transfer from Lys70 to Glu166 occurs (Step 1), inducing the Glu166 rearrangement followed by the rapprochement of BLI towards Ser70, the proton transfer from Ser70 to Lys73 (Step 2), and finally the nucleophilic addition between Ser70 and BLI (Step 3), as reported previously [69].

Based on the MD simulations of the most promising modes, the probability of favorable conditions for the formation of a covalent bond ($P_{NECESSARY}$) was estimated. It can be quantified using the $d_{Ser70(O)–B}$ value as a criterion. We concluded that such a rapprochement differs depending on the ligand. For PBA, $P_{NECESSARY}$ was estimated as 40.4% of arrangements that are close enough which is the highest value among all analyzed ligands. The rest of the compounds have the following $P_{NECESSARY}$: **1a**—2.6%, **2a**—1.2%, **3a_I**—11%, **3a_III**—22.4%, **3a_IV**—6.8%. This indicates that the mutual *ortho* location of boronic groups favors binding confirming the high potential of **3a**. However, apart from $d_{Ser70(O)–B}$ value, other parameters such as the distance, angle, and active site amino acid conformations must also be optimal. Unfortunately, the impact of all these parameters cannot be predicted. We are able to find the correct distance and angle to form a covalent bond, but the random and unpredictable changes in the amino acid position do not allow us to determine the ideal conditions for nucleophilic addition. In our study, the use of crystallographic structure (with already defined Ser70, Glu166 and loops conformations enabling covalent binding) let us estimate the probabilities of covalent bond formation ($P_{SUFFICIENT}$). This information we obtained from QM/MM simulations. Knowing the $P_{SUFFICIENT}$, we can also estimate the probability of forming a covalent bond under favorable conditions ($P_{FAVORABLE}$). Assuming that $P_{NECESSARY}$ and $P_{SUFFICIENT}$ are independent, $P_{FAVORABLE} = P_{NECESSARY} \times P_{SUFFICIENT}$. For PBA, $P_{FAVORABLE}$ is 10.1%, for **1a**—0.65%, for **2a**—0.3%, for all forms **3a**—19.05% (**3a_I**—2.75%, **3a_III**—11.2%, **3a_IV**—5.1%). These

results correspond to the experiments (Table 2) that allow us to relate higher $P_{FAVORABLE}$ with lower MIC values, pointing out that the **3a** is the most active BLI.

It should be noted that the cyclic anionic form **3a_V** lacks the sp^2-hybridized B atom needed to form a dative bond with Ser70 whilst simulations indicate that events involving the transformation of **3a_I** and **3a_III** into **3a_V** can occur (Figure S16). Interestingly, the transformation of **3a_III** required the participation of additional water molecules and Glu166 (Figure S17). Simulations also showed that the covalent docking process depends on the type of diboronic acid isomer. The binding mechanisms of **2a** and **3a** with the catalytic Ser70 residue start identically by filling the active site with an aromatic ring in the S2 cavity and forming the CH-π interaction with Trp105 (Figure 4). Next, the binding pose is relaxed, resulting in the stabilization via the HBs with the N atom of the Ser70 and Thr237 backbone, and the O atom of the Asn170 sidechain (Figure 4). Such an arrangement is waiting for a proton transfer from Lys73 to Glu166 and nucleophilic addition by the oxygen atom of the Ser70 OH group, leading to form a protein-ligand covalent bond. However, the larger average distance $d_{Ser70(O)–B}$ for **2a**, suggests that the covalent bonding efficiency of BLI in *meta* substitution is lower than for *ortho*. For the **1a**, its *para* substitution prevents filling the narrow S1 and S2 cavities simultaneously forcing it to adopt a different docking process.

Notably, each form of **3a** differs in the stabilization process of an arrangement waiting for proton transfer. The **3a_I** creates a unique HB with the O atom of the Ser70 OH group. We speculate that this HB is unfavorable for the competitive inhibition mechanism. In **3a_I**, it reduces the number of beneficial arrangements of the catalytic Ser70 residue, ready for forming a protein-ligand covalent bond. In the case of the **3a_III**, the lack of the HB with the O atom of the Ser70 OH group enlarges the probability of favorable conditions for the formation of a covalent bond (Table 6). The most interesting is the **3a_IV** form, where the presence of an anionic form allows it to create the HB with the side chain of Thr237, which is an additional element in the stabilization process. Considering that the *ortho* substitution allows for cyclization, as well as that the anionic form creates an HB with the oxygen atom of the Thr237 OH group, we hypothesize that these factors allow the **3a** to be the most promising BLI.

3. Materials and Methods

3.1. Antimicrobial Activity

3.1.1. Bacterial and Fungal Strains and Their Growth Conditions

Direct antimicrobial activity was determined in this study for the following strains: (1) Gram-negative bacteria from *Enterobacteriales* order: *Escherichia coli* ATCC 25922, *Klebsiella pneumoniae* ATCC 13883, *Proteus mirabilis* ATCC 12453, *Enterobacter cloacae* DSM 6234, *Serratia marcescens* ATCC 13880; (2) Gram-negative non-fermentative rods: *Pseudomonas aeruginosa* ATCC 27853, *Acinetobacter baumannii* ATCC 19606, *Stenotrophomonas maltophilia* ATCC 13637, *Burkholderia cepacia* ATCC 25416, *Bordetella bronchiseptica* ATCC 4617; (3) Gram-positive cocci: methicillin-sensitive *Staphylococcus aureus* ATCC 6538P (MSSA), methicillin-resistant *S. aureus* subsp. *aureus* ATCC 43300 (MRSA), *S. epidermidis* ATCC 12228, *Enterococcus faecalis* ATCC 29212, *E. faecium* ATCC 6057, *Bacillus subtilis* ATCC 6633; (4) yeasts: *Candida albicans* ATCC 90028, *C. parapsilosis* ATCC 22019, *C. tropicalis* IBA 171, *C. tropicalis* (Castellani) Berkhout ATCC 750, *C. guilliermondii* IBA 155, *C. krusei* ATCC 6258, and *Saccharomyces cerevisiae* ATCC 9763. The following strains were used for evaluating the BLI activity of tested agents: (1) two standard strains: *K. pneumoniae* ATCC BAA-1705 (with carbapenemase KPC-2) and *K. pneumoniae* ATCC 700603 (with extended-spectrum β-lactamase, ESBL, SHV-12); (2) six clinical isolates producing various classes of β-lactamases: carbapenemases KPC-2 (*E. coli* 76) and KPC-3 (*K. pneumoniae* 81 and 83), metallo-β-lactamase from VIM family (*P. aeruginosa* 1204), plasmid-acquired AmpC cephalosporinase CMY-2 (*E. coli* 77), and with overexpression of chromosomally encoded cephalosporinase AmpC (*P. aeruginosa* MUW 700); (3) *E. coli* DH5α and *E. coli* 82 TR(pl 81)—the transformant of *E. coli* DH5α with a plasmid from the clinical strain of *K. pneumoniae* 81 carrying the bla_{KPC-3} gene. All strains were stored at −80 °C. Prior to

testing, each bacterial strain was subcultured twice on tryptic soy agar TSA (Biomaxima, Lublin, Poland) medium and yeast strains on Sabouraud dextrose agar (Biomaxima, Lublin, Poland) for 24–48 h at 30 °C to ensure viability.

3.1.2. Determination of Direct Antimicrobial Activity

Direct antimicrobial activity against Gram-negative and Gram-positive bacterial strains, as well as against yeast, was examined as previously described [56] by the disc-diffusion test, the MIC determination assay, the MBC (for bacteria), and the MFC (for yeasts) determination tests. All the above-mentioned tests were performed according to EUCAST [71,72] and CLSI [73–77] recommendations. The following reference agents were used: nitrofurantoin (for Gram-negative rods), linezolid (for Gram-positive bacteria), and fluconazole (in the case of fungi). The new aromatic diboronic acids were dissolved in DMSO (Sigma, St. Louis, MO, USA). In the disc-diffusion test, the concentration of new agents was 0.4 mg per disc [17]. Depending on the solubility, the MIC and MBC/MFC values were determined up to 100 mg/L for **1k**, up to 200 mg/L for **7c**, and up to 400 mg/L for the remaining compounds: **1a**–**1j**, **2a**–**2g**, **3a**–**3f**, **4a**–**4b**, **5a**–**5c**, **6a** and **7a**–**7b**.

3.1.3. Determination of MICs in the Presence of PAβN

To investigate the contribution of the MDR efflux pumps to the resistance of Gram-negative rods to the newly synthesized compounds, the MIC values of studied agents, with or without the pump inhibitor, PAβN (20 mg/L) (Sigma, St. Louis, MO, USA), were evaluated [78]. The MIC determination was performed in Mueller–Hinton II broth medium (MHB) (Becton, Dickinson and Company, Franklin Lakes, NJ, USA) using 2-fold serial dilutions of tested agents, according to the CLSI guidelines [75]. To minimize the influence of PAβN on the destabilization of bacterial cell covers, the tests were conducted in the presence of 1 mM $MgSO_4$ (Sigma, St. Louis, MO, USA) [79]. At least a 4-fold reduction in the MIC value after the addition of PAβN was considered significant [80].

3.1.4. Determination of BLI Activity

A two-stage approach was implemented for detecting the BLI activity of the tested agents. Initially, all compounds were subjected to combination disc tests (CDTs). For agents expressing BLI activity in the CDTs, microdilution tests were performed, and their synergy with antibiotics was evaluated.

Combination Disc Tests for Detection of BLI Activity

Prior to combination disc tests, screening tests of direct antimicrobial activity (STDA) of the tested agent against β-lactamase-producing strains were performed by the disc-diffusion method [72]. Discs with 0.3 mg, 0.1 mg, and 0.03 mg of each agent were examined. The highest amount of an agent that caused no effect on bacterial growth was used in further experiments. Concentrations that partially inhibited bacterial growth (isolated colonies or faint growth within the zone) were excluded from further experiments.

The three following CDTs were performed on Mueller–Hinton II agar (MHA) plates (Becton, Dickinson and Company, Franklin Lakes, NJ, USA) as described previously [17], according to the general EUCAST recommendations [64] and methodology described by Yagi et al. [65]. Briefly:

1. CDT-KPC test for detection of KPC-type carbapenemase-producing strain was performed on the recommended strain *K. pneumoniae* ATCC BAA-1705. Discs with meropenem (MEM-10) (Becton, Dickinson and Company, Franklin Lakes, NJ, USA) alone and supplemented with one of the tested agents (TA) at the concentration consistent with the STDA result (0.3 mg or 0.1 mg or 0.03 mg per disc) were utilized. As the reference, the standard KPC inhibitor PBA (Sigma) at the concentration of 0.3 mg per disc was used. In this study, we considered the new compound has KPC-inhibitory activity when the increase in the diameter of the inhibition zone around MEM-TA vs. MEM-10 is at least 4 mm [64].

2. CDT-AmpC test for detection class C β-lactamase-producing strain was performed on two clinical isolates: *P. aeruginosa* MUW 700 overexpressing chromosomally encoded cephalosporinase AmpC and *E. coli* 77 with plasmid-acquired AmpC cephalosporinase CMY-2. Discs with ceftazidime (CAZ-30) (Becton, Dickinson and Company, Franklin Lakes, NJ, USA), ceftazidime with a tested agent (CAZ-TA) at the concentration consistent with the STDA result, and ceftazidime with 0.3 mg of PBA (CAZ-PBA) as the reference AmpC inhibitor were utilized. We assumed the tested agent inhibits AmpC cephalosporinases when the diameter of the inhibition zone around CAZ-TA was at least 5 mm larger than that around CAZ-30 for both tested strains, considering that the same increase should be obtained for CAZ-PBA discs.
3. CDT-ESBL EUCAST test for detection of ESBL-producing strain was performed on the recommended strain *K. pneumoniae* ATCC 700603, utilizing discs with ceftazidime (CAZ-30) (Becton, Dickinson and Company, Franklin Lakes, NJ, USA), ceftazidime with a tested agent (CAZ-TA) at the concentration consistent with the STDA result, and ceftazidime with 0.01 mg of clavulanic acid (CAZ-CL) (Becton, Dickinson and Company, Franklin Lakes, NJ, USA) as the reference ESBL inhibitor. In the case of clavulanic acid, the diameter of the inhibition zone around CAZ-CL should be at least 5 mm larger than that around CAZ-30 [64]. We consider the tested agent inhibits ESBL when the diameter of the inhibition zone around CAZ-TA is also at least 5 mm larger than that around CAZ-30.

Microdilution Tests for BLI Activity Detection and Synergy Evaluation

To examine the ability of tested agents to inhibit various carbapenemases and AmpC-enzymes, their synergy with antibiotics against β-lactamase-producing strains was assessed by checkerboard microdilution assay [67], with slight modification. Checkerboards were prepared in microtiter plates, with seven two-fold dilutions of β-lactams (1–64 mg/L) in the rows and three two-fold dilutions of tested agents and PBA (4–16 mg/L) in the columns. Tested agents' concentrations were limited to the concentrations at which the newest commercially available BLIs (vaborbactam, relebactam, and avibactam) are used in susceptibility testing [66]. Plates were inoculated and incubated as in the MIC microdilution assay [75]. Parallel, MICs of tested agents and PBA alone were determined by the microdilution assay [75]. Following the incubation, antibiotic MICs in the presence of each agent's concentration were determined. Moreover, for the first well without growth found in each checkerboard row and column along the growth/non-growth interface, the fractional inhibitory concentration index (FICI) was calculated using the formula below [67]:

$$\text{FICI} = [(\text{MIC of antibiotic in combination})/(\text{MIC of antibiotic alone})] + [(\text{MIC of the tested agent in combination})/(\text{MIC of tested agent alone})].$$

For calculations, all off-scale MICs were converted to the next-highest doubling concentration. Subsequently, both the average and the lowest FICI were interpreted [67]. The interpretation was as follows: FICI $\leq$ 0.5, synergy; 0.5 < FICI $\leq$ 4, indifference and FICI > 4, antagonism [81]. Primarily, examined combinations consisted of meropenem (Pol-Aura, Morag, Poland) plus tested agents against carbapenemases-producing strains and ceftazidime (Pol-Aura, Morag, Poland) plus tested agents against AmpC-producing strains. For agents that reduced meropenem MIC at least 4-fold for at least two tested strains, similar assays were performed with imipenem (Pol-Aura, Morag, Poland) and ertapenem (Pol-Aura, Morag, Poland).

3.1.5. Statistical Analysis

We analyzed aFICIs of compounds that caused at least one significant antibiotic MIC reduction. Owing to a lack of normal distribution, which was tested using the Shapiro–Wilk test, the analysis of variance (ANOVA) Kruskal–Wallis test was used to compare tested combinations' average FICIs according to agents' structural classification (6 groups of agents), agents' substitution type (unsubstituted boronic acids vs. fluorinated derivatives),

and carbapenem partner (for KPC producers). Post hoc analysis for Kruskal–Wallis ANOVA was conducted using a multiple comparison test (Dunn's test). All statistical calculations were performed using STATISTICA version 13.3 PL (StatSoft, Cracow, Poland) software. The significance level was set at $p < 0.05$.

3.1.6. Nitrocefin Hydrolysis Test

Overnight culture of *E. coli* 82 TR(pl 81) in MHB was diluted 1:100 into fresh MHB and incubated with shaking at 37 °C until an OD_{600} of 1 was attained. For the induction of the KPC-3 production meropenem was added to reach the concentration of 0.25 mg/L (0.125 × MIC). Further incubation was performed under the same conditions until an OD_{600} of 3 was reached. The culture with the required OD_{600} was centrifuged (6700× *g*, 10 min) and the supernatant was discarded. From the obtained bacterial cell pellet total proteins were extracted with the ReadyPreps™ Protein Preparation Kit (Epicentre Biotechnologies, Madison, WI, USA) and used in the subsequent nitrocefin hydrolysis test, performed in a 96-well microplate. Nitrocefin is a chromogenic cephalosporin substrate routinely used to detect the presence of β-lactamases. First, 20 µL of the protein extract was mixed with 80 µL of tested agents (**1a**, **2a**, **3a** and PBA as a reference BLI, each examined at concentrations: 4, 8 and 16 mg/L) or with 80 µL of the phosphate buffer (positive control—corresponding to KPC enzyme activity in the purified total proteins extracted from *E. coli* 82 TR(pl 81) cells). After 10 min of incubation at the room temperature 100 µL of the nitrocefin (Oxoid, Basingstoke, Hampshire, England) was added to reach its final concentration of 150 µM. β-lactamases hydrolyze the β-lactam ring of nitrocefin, causing its degradation and color change. Nitrocefin hydrolysis was evaluated after 3 min of the incubation at room temperature.

As in our previous publication [60] the presence of β-lactamases in the purified protein extract with and without tested agents was assessed by the spectrophotometric measurement of the rates of nitrocefin hydrolysis as relative absorbance at 486 nm. The level of the measured absorbance indicated β-lactamase activity. Finally, the difference in the relative absorbance between the positive control and the sample concentration of the tested inhibitors was calculated and expressed as a percentage. A reduction in the relative absorbance level in the presence of a tested agent was taken as an indicator of the BLI activity of a used aromatic diboronic acid. The experiment was performed in triplicate.

3.2. Cytotoxicity Studies

MRC-5 human fibroblasts (ECACC) were cultured in MEME, Minimum Essential Medium Eagle (Merck) supplemented with 10% fetal bovine serum (Merck), 2 mM l-glutamine, antibiotics (100 U/mL penicillin, 100 µg/mL streptomycin, Merck) and 1% non-essential amino acids (Merck). Cells were grown in 75 cm^2 cell culture flasks (Sarstedt) in a humidified atmosphere of CO_2/air (5/95%) at 37 °C. MTT-based viability assay was conducted as described previously [56]. Optical densities were measured at 570 nm using a BioTek microplate reader. All measurements were carried out in three replicates, and the results were expressed as a percent of viable cells versus control cells.

3.3. Docking and Time-Dependent Quantum Mechanics/Molecular Mechanics

3.3.1. Structure Preparation and Molecular Docking

Computational studies were carried out to confirm the inhibitory properties of most representative derivatives of aromatic diboronic acids. As a reference system, the structure of carbapenemase KPC-2 (PDB ID: 3RXX [68]) was chosen, which proved the competitive inhibition mechanism of the BLI [17,25,69]. At first, the active site protonated at pH 7.0 was optimized [82] and minimized in the AMBER10 force field [83] using the Molecular Operating Environment (MOE, 2019) [84]. The semi-flexible docking protocol in the MOE was applied to predict the binding mode of each ligand (in the neutral and anionic form) [84]. As a result, ten modes of each ligand based on the lowest free energy of binding, estimated by the GBVI/WSA Δ*G* scoring function, were obtained [85]. A geometric analysis was

made to distinguish the potential BLI by checking the distance between the oxygen atom of the serine hydroxyl group and the boron atom. The analysis involved only ligands with the above-mentioned distance below 4.5 Å, which allows the formation of the protein-ligand covalent bond. For the ligands with such ability, molecular dynamics calculations were performed to verify the binding stability.

3.3.2. Molecular Dynamics Simulations

Each system was put in the rectangular simulation box, solvated with a 6Å water shell of TIP3P water molecules, and neutralized with NaCl ions. Then, we run the 2 ns molecular dynamics at the 310 K in the AMBER10:EHT force field [83] using the Molecular Operating Environment (MOE, 2019) [83]. The Nosé–Poincaré Andersen integrating algorithm was applied [85,86] with a 1.0 fs time step. The results of the most stable fragment of the entire trajectory (time range from 1.8 to 2.0 ns) were analyzed. Only arrangements that adopted the oxygen atom of the serine hydroxyl group-boron atom distance lower than 3 Å were selected. Based on them, the probability of favorable conditions ($P_{NECESSARY}$) for the formation of a covalent bond was determined as $P_{NECESSARY}$ = the number of frames with $d_{Ser70(O)\text{-}B} \leq 3$Å divided by the number of frames in all the analyzed fragments of trajectory $\times$ 100%). If the multiple systems of the same ligand were obtained, the one with the best average estimation of the oxygen atom of the serine hydroxyl group-boron atom distance was picked. Finally, the arrangements with the lowest distance allowing for the formation of a protein-ligand covalent bond were determined. For these arrangements, QM/MM simulations were performed to validate the mechanism of the formation of protein-ligand covalent bonds.

3.3.3. Quantum Mechanics/Molecular Mechanics

The performed hybrid approach employed a quantum mechanics component [69,87,88]. The MOPAC environment [89], integrated with NAMD software (version 2.12) [90] was used. The complexes were parameterized, prepared, and optimized in the CHARMM36 force field with the CGENFF parameters [91,92] using the NAMD/2.12 [90]. The published parameters and the simulation protocol [69]. Ligand atoms, selected amino acids of the active site (Ser70, Lys73, Ser130, Asn132, Glu166, Asn170, Lys234, Thr237), and the water molecules within 5 Å of any ligand atom were considered chemically important. Eight repetitions of the QM/MM, each including the 0.25 ps energy minimization and 50 ps simulation, were conducted. For the most promising arrangements, the simulation time was extended to 150 ps. VMD was used to detect the proton transfers and the formation of a protein-ligand covalent bond [93]. The probabilities of covalent bond formation ($P_{SUFFICIENT}$) were estimated as a measure of sufficient conditions for forming a dative covalent bond ($P_{SUFFICIENT}$ = number of the QM/MM repetitions with detected protein-ligand covalent bond divided by the number of all performed repetitions). The probability of the formation of a covalent bond under favorable conditions ($P_{FAVORABLE}$), was estimated using the formula $P_{FAVORABLE} = P_{NECESSARY} \times P_{SUFFICIENT}$.

4. Conclusions

In conclusion, we found that many studied aromatic diboronic acids and their derivatives display potent BLI activity at low, clinically achievable concentrations. Respective SAR analysis for three series of diboronic acids **1a**–**1l**, **2a**–**2g**, **3a**–**3e** indicates that most of the fluorinated derivatives maintain activity comparable to respective parent compounds. In turn, the introduction of bulkier, lipophilic groups (I, CF_3, $SiMe_3$, OMe) has adverse effects and in general such compounds are not effective BLIs. Notably, selected agents are active against both KPC and AmpC enzymes responsible for the critical priority pathogen resistance. Moreover, they can restore the sensitivity of clinical strains to the last resort antibiotics (carbapenems, 3rd generation cephalosporins) at similar concentrations as inhibitors currently used in clinics. Among them, phenylene-1,2-diboronic acid **3a** was the most effective in potentiating carbapenems against KPC producers. This was con-

firmed by QM/MM simulations and the observed mechanism of the KPC-BLI covalent bond. Phenylene-1,3-diboronic acids potentiated ceftazidime against AmpC producers best, whereas phenylene-1,4-diboronic acids were highly effective in potentiating both carbapenems against KPC producers and ceftazidime against AmpC producers. Moreover, fluoro-substitution increased CMY-2 inhibitory activity, slightly reducing KPC/cAmpC inhibitory potency. Benzene-1,2,4-triboronic and boronated thiophenes increased only ceftazidime activity against AmpC producers to a moderate degree. Importantly, phenylenediboronic acids overcome simple PBA in KPC/AmpC inhibitory potency and, gratifyingly, display significantly reduced toxicity. Thus, it seems that the concept involving the introduction of the second boronic group to the structure can be considered a promising tool for the development of effective KPC/AmpC inhibitors. Since the functionalization with lipophilic groups seems to be ineffective, future work could involve the installation of substituents possessing a distinctive hydrophilic character, e.g., amide, amino acid, and peptide residues. We are planning to test this concept and the obtained results will be reported in due course.

Supplementary Materials: The following supporting information can be downloaded at: https://www.mdpi.com/article/10.3390/molecules28217362/s1, Synthetic procedures; Molecular modeling and hybrid QM/MM simulations; Figures S1–S14: NMR spectra of synthesized compounds; Figure S15: Two types of the binding modes of 1a: A) The perpendicular configuration of ligand to Trp105, B) The parallel configuration of ligand to Trp105; Figure S16: Transformation of **3a_I** to **3a_V**; Figure S17: Transformation of **3a_III** to **3a_V**; Table S1: The antibacterial activity of tested agents against standard Gram-positive strains; Table S2: The antibacterial activity of tested agents against standard Gram-negative strains; Table S3: The antifungal activity of tested agents against yeast strains; Table S4: The antibacterial activity of studied compounds against β-lactamase-producing Gram-negative strains; Table S5: The antibacterial activity of tested agents against β-lactamase-producing Gram-negative strains; Table S6: The MIC values of antibiotics alone and in combination with studied compounds against standard and clinical strains of Gram-negative rods producing various classes of β-lactamases; Table S7: The effect of agents **1a**, **2a** and **3a** on the activity of KPC-3 in the purified protein extract from *E. coli* 82 TR(pl 81) cells, visualized by the nitrocefin hydrolysis test; Table S8: Viability of MRC-5 cells (% of viable cells ± SD) after 72 h-treatment with the studied compounds; Table S9: The simulation times to reach the most important steps in mechanism of protein-ligand covalent bond formation in the most promising BLIs, calculated from the beginning of the process. References [69,75,84,94–98] are cited in the Supplementary Materials.

Author Contributions: Conceptualization, J.K., K.A.K., S.L. and A.E.L.; methodology, J.K., P.C., K.D., P.W., K.A.K., S.L. and A.E.L.; software, J.K., P.C., K.D., P.W., K.A.K., S.L. and A.E.L.; validation, J.K., P.C., K.D. and P.W.; formal analysis, K.A.K., S.L. and A.E.L.; investigation, J.K., P.C., K.D., P.W., K.A.K., S.L. and A.E.L.; resources, K.A.K., S.L. and A.E.L.; data curation, J.K., P.C., K.D. and P.W.; writing—original draft preparation, J.K., P.C., K.D., P.W., K.A.K., S.L. and A.E.L.; writing—review and editing, J.K., K.A.K., S.L. and A.E.L.; visualization, J.K., P.C., K.D., P.W., K.A.K., S.L. and A.E.L.; supervision, K.A.K., S.L. and A.E.L.; project administration, S.L. and A.E.L.; funding acquisition, K.A.K., S.L. and A.E.L. All authors have read and agreed to the published version of the manuscript.

Funding: This research was funded by the National Science Centre (Poland) in the framework of the project UMO-2018/31/B/ST5/00210. Moreover, the microbiological studies were partially supported by the Foundation for the Development of Diagnostics and Therapy, Warsaw, Poland (REGON: 006220910, NIP: 5262173856, KRS: 0000195643). Molecular modelling studies were supported by Faculty of Physics, University of Warsaw, 501-D111-01-1110102 (PP/BF). Computations were carried out using infrastructure financed by POIG. 02.01.00-14-122/09.

Institutional Review Board Statement: Not applicable.

Informed Consent Statement: Not applicable.

Data Availability Statement: All obtained data in this work are included in the submitted manuscript.

Acknowledgments: The research on antimicrobial activity was carried out with the use of the CePT infrastructure financed by the European Union through the European Regional Development Fund as part of the Operational Program "Innovative Economy" for 2007–2013.

Conflicts of Interest: The authors declare no conflict of interest.

References

1. Durka, K.; Jarzembska, K.N.; Kamiński, R.; Luliński, S.; Serwatowski, J.; Woźniak, K. Structural and energetic landscape of fluorinated 1,4-phenylenediboronic acids. *Cryst. Growth Des.* **2012**, *12*, 3720–3734. [CrossRef]
2. Waller, P.J.; Gándara, F.; Yaghi, O.M. Chemistry of covalent organic frameworks. *Acc. Chem. Res.* **2015**, *48*, 3053–3063. [CrossRef]
3. Larcher, A.; Nocentini, A.; Supuran, C.T.; Winum, J.Y.; van der Lee, A.; Vasseur, J.J.; Laurencin, D.; Smietana, M. Bis-benzoxaboroles: Design, synthesis, and biological evaluation as carbonic anhydrase inhibitors. *ACS Med. Chem. Lett.* **2019**, *10*, 1205–1210. [CrossRef]
4. Krajnc, A.; Lang, P.A.; Panduwawala, T.D.; Brem, J.; Schofield, C.J. Will morphing boron-based inhibitors beat the β-lactamases? *Curr. Opin. Chem. Biol.* **2019**, *50*, 101–110. [CrossRef]
5. Hammoudi Halat, D.; Ayoub Moubareck, C. The current burden of carbapenemases: Review of significant properties and dissemination among Gram-negative bacteria. *Antibiotics* **2020**, *9*, 186. [CrossRef]
6. Ambler, R.P. The structure of beta-lactamases. *Philos. Trans. R. Soc. Lond. B Biol. Sci.* **1980**, *289*, 321–331. [CrossRef]
7. Słoczyńska, A.; Wand, M.E.; Tyski, S.; Laudy, A.E. Analysis of bla_{CHDL} genes and insertion sequences related to carbapenem resistance in *Acinetobacter baumannii* clinical strains isolated in Warsaw, Poland. *Int. J. Mol. Sci.* **2021**, *22*, 2486. [CrossRef]
8. Burillo, A.; Bouza, E. Controversies over the management of infections caused by Amp-C- and ESBL-producing *Enterobacterales*: What questions remain for future studies? *Curr. Opin. Infect. Dis.* **2022**, *35*, 575–582. [CrossRef]
9. Jackson, N.; Belmont, C.R.; Tarlton, N.J.; Allegretti, Y.H.; Adams-Sapper, S.; Huang, Y.Y.; Borges, C.A.; Frazee, B.W.; Florence-Petrovic, D.; Hufana, C.; et al. Genetic predictive factors for nonsusceptible phenotypes and multidrug resistance in expanded-spectrum cephalosporin-resistant uropathogenic *Escherichia coli* from a multicenter cohort: Insights into the phenotypic and genetic basis of coresistance. *mSphere* **2022**, *7*, e0047122. [CrossRef]
10. World Health Organization. Prioritization of Pathogens to Guide Discovery, Research and Development of New Antibiotics for Drug-Resistant Bacterial Infections, Including Tuberculosis. Available online: https://apps.who.int/iris/handle/10665/311820 (accessed on 1 October 2023).
11. Adams, J.; Kauffman, M. Development of the proteasome inhibitor Velcade (Bortezomib). *Cancer Investig.* **2004**, *22*, 304–311. [CrossRef]
12. Krajewska, J.; Laudy, A.E. The European Medicines Agency approved the new antibacterial drugs—response to the 2017 WHO report on the global problem of multi-drug resistance. *Adv. Microbiol.-N. Y.* **2021**, *60*, 249–264. [CrossRef]
13. World Health Organization. 2021 Antibacterial Agents in Clinical and Preclinical Development: An overview and analysis. Available online: https://www.who.int/publications/i/item/9789240047655 (accessed on 1 October 2023).
14. Bush, K.; Bradford, P.A. β-Lactams and β-lactamase inhibitors: An overview. *Cold Spring Harb. Perspect. Med.* **2016**, *6*, a025247. [CrossRef]
15. Papp-Wallace, K.M. The latest advances in β-lactam/β-lactamase inhibitor combinations for the treatment of Gram-negative bacterial infections. *Expert Opin. Pharmacother.* **2019**, *20*, 2169–2184. [CrossRef]
16. U.S. Food and Drug Administration. FDA Approves New Treatment for Pneumonia Caused by Certain Difficult-to-Treat Bacteria. Available online: https://www.fda.gov/news-events/press-announcements/fda-approves-new-treatment-pneumonia-caused-certain-difficult-treat-bacteria (accessed on 1 October 2023).
17. Durka, K.; Laudy, A.E.; Charzewski, Ł.; Urban, M.; Stępień, K.; Tyski, S.; Krzyśko, K.A.; Luliński, S. Antimicrobial and KPC/AmpC inhibitory activity of functionalized benzosiloxaboroles. *Eur. J. Med. Chem.* **2019**, *171*, 11–24. [CrossRef]
18. Lang, P.A.; Parkova, A.; Leissing, T.M.; Calvopiña, K.; Cain, R.; Krajnc, A.; Panduwawala, T.D.; Philippe, J.; Fishwick, C.W.G.; Trapencieris, P.; et al. Bicyclic boronates as potent inhibitors of AmpC, the class C β-lactamase from *Escherichia coli*. *Biomolecules* **2020**, *10*, 899. [CrossRef]
19. Wang, Y.L.; Liu, S.; Yu, Z.J.; Lei, Y.; Huang, M.Y.; Yan, Y.H.; Ma, Q.; Zheng, Y.; Deng, H.; Sun, Y.; et al. Structure-based development of (1-(3′-mercaptopropanamido)methyl)boronic acid derived broad-spectrum, dual-action inhibitors of metallo- and serine-β-lactamases. *J. Med. Chem.* **2019**, *62*, 7160–7184. [CrossRef]
20. Rojas, L.J.; Taracila, M.A.; Papp-Wallace, K.M.; Bethel, C.R.; Caselli, E.; Romagnoli, C.; Winkler, M.L.; Spellberg, B.; Prati, F.; Bonomo, R.A. Boronic acid transition state inhibitors active against KPC and other class A β-lactamases: Structure-activity relationships as a guide to inhibitor design. *Antimicrob. Agents Chemother.* **2016**, *60*, 1751–1759. [CrossRef]
21. Zhou, J.; Stapleton, P.; Haider, S.; Healy, J. Boronic acid inhibitors of the class A β-lactamase KPC-2. *Bioorganic Med. Chem.* **2018**, *26*, 2921–2927. [CrossRef]
22. Celenza, G.; Vicario, M.; Bellio, P.; Linciano, P.; Perilli, M.; Oliver, A.; Blazquez, J.; Cendron, L.; Tondi, D. Phenylboronic acid derivatives as validated leads active in clinical strains overexpressing KPC-2: A step against bacterial resistance. *ChemMedChem* **2018**, *13*, 713–724. [CrossRef]
23. Linciano, P.; Vicario, M.; Kekez, I.; Bellio, P.; Celenza, G.; Martín-Blecua, I.; Blázquez, J.; Cendron, L.; Tondi, D. Phenylboronic acids probing molecular recognition against class A and class C β-lactamases. *Antibiotics* **2019**, *8*, 171. [CrossRef]

24. Zhou, J.; Stapleton, P.; Xavier-Junior, F.H.; Schatzlein, A.; Haider, S.; Healy, J.; Wells, G. Triazole-substituted phenylboronic acids as tunable lead inhibitors of KPC-2 antibiotic resistance. *Eur. J. Med. Chem.* **2022**, *240*, 114571. [CrossRef] [PubMed]
25. Alsenani, T.A.; Rodríguez, M.M.; Ghiglione, B.; Taracila, M.A.; Mojica, M.F.; Rojas, L.J.; Hujer, A.M.; Gutkind, G.; Bethel, C.R.; Rather, P.N.; et al. Boronic acid transition state inhibitors as potent inactivators of KPC and CTX-M β-lactamases: Biochemical and structural snalyses. *Antimicrob. Agents Chemother.* **2023**, *67*, e0093022. [CrossRef]
26. Tondi, D.; Venturelli, A.; Bonnet, R.; Pozzi, C.; Shoichet, B.K.; Costi, M.P. Targeting class A and C serine β-lactamases with a broad-spectrum boronic acid derivative. *J. Med. Chem.* **2014**, *57*, 5449–5458. [CrossRef] [PubMed]
27. Tondi, D.; Powers, R.A.; Caselli, E.; Negri, M.C.; Blázquez, J.; Costi, M.P.; Shoichet, B.K. Structure-based design and in-parallel synthesis of inhibitors of AmpC beta-lactamase. *Chem. Biol.* **2001**, *8*, 593–611. [CrossRef]
28. Eidam, O.; Romagnoli, C.; Caselli, E.; Babaoglu, K.; Pohlhaus, D.T.; Karpiak, J.; Bonnet, R.; Shoichet, B.K.; Prati, F. Design, synthesis, crystal structures, and antimicrobial activity of sulfonamide boronic acids as β-lactamase inhibitors. *J. Med. Chem.* **2010**, *53*, 7852–7863. [CrossRef]
29. Buzzoni, V.; Blazquez, J.; Ferrari, S.; Calò, S.; Venturelli, A.; Costi, M.P. Aza-boronic acids as non-beta-lactam inhibitors of AmpC-β-lactamase. *Bioorganic Med. Chem. Lett.* **2004**, *14*, 3979–3983. [CrossRef] [PubMed]
30. Caselli, E.; Romagnoli, C.; Vahabi, R.; Taracila, M.A.; Bonomo, R.A.; Prati, F. Click chemistry in lead optimization of boronic acids as β-lactamase inhibitors. *J. Med. Chem.* **2015**, *58*, 5445–5458. [CrossRef]
31. Xia, Y.; Cao, K.; Zhou, Y.; Alley, M.R.; Rock, F.; Mohan, M.; Meewan, M.; Baker, S.J.; Lux, S.; Ding, C.Z.; et al. Synthesis and SAR of novel benzoxaboroles as a new class of β-lactamase inhibitors. *Bioorganic Med. Chem. Lett.* **2011**, *21*, 2533–2536. [CrossRef]
32. McKinney, D.C.; Zhou, F.; Eyermann, C.J.; Ferguson, A.D.; Prince, D.B.; Breen, J.; Giacobbe, R.A.; Lahiri, S.; Verheijen, J.C. 4,5-Disubstituted 6-aryloxy-1,3-dihydrobenzo[c][1,2]oxaboroles are broad-spectrum serine β-lactamase inhibitors. *ACS Infect. Dis.* **2015**, *1*, 310–316. [CrossRef]
33. Kiener, P.A.; Waley, S.G. Reversible inhibitors of penicillinases. *Biochem. J.* **1978**, *169*, 197–204. [CrossRef]
34. Durka, K.; Kurach, P.; Luliński, S.; Serwatowski, J. Functionalization of dihalophenylboronic acids by deprotonation of their N-butyldiethanolamine esters. *Eur. J. Org. Chem.* **2009**, *2009*, 4325–4332. [CrossRef]
35. Durka, K.; Luliński, S.; Smętek, J.; Dąbrowski, M.; Serwatowski, J.; Woźniak, K. The influence of boronate groups on the selectivity of the Br–Li exchange in model dibromoaryl boronates. *Eur. J. Org. Chem.* **2013**, *2013*, 3023–3032. [CrossRef]
36. Durka, K.; Górka, J.; Kurach, P.; Luliński, S.; Serwatowski, J. Electrophilic ipso-iodination of silylated arylboronic acids. *J. Organomet. Chem.* **2010**, *695*, 2635–2643. [CrossRef]
37. Faury, T.; Dumur, F.; Clair, S.; Abel, M.; Porte, L.; Gigmes, D. Side functionalization of diboronic acid precursors for covalent organic frameworks. *CrystEngComm* **2013**, *15*, 2067–2075. [CrossRef]
38. Durka, K.; Luliński, S.; Serwatowski, J.; Woźniak, K. Influence of fluorination and boronic group synergy on the acidity and structural behavior of o-phenylenediboronic acids. *Organometallics* **2014**, *33*, 1608–1616. [CrossRef]
39. Borowska, E.; Durka, K.; Luliński, S.; Serwatowski, J.; Woźniak, K. On the directing effect of boronate groups in the lithiation of boronated thiophenes. *Eur. J. Org. Chem.* **2012**, *2012*, 2208–2218. [CrossRef]
40. Singh, A.; Kumar, R. Sustainable Passerini-tetrazole three component reaction (PT-3CR): Selective synthesis of oxaborol-tetrazoles. *Chem. Commun.* **2021**, *57*, 9708–9711. [CrossRef]
41. Finlay, J.; Miller, L.; Poupard, J.A. A review of the antimicrobial activity of clavulanate. *J. Antimicrob. Chemother.* **2003**, *52*, 18–23. [CrossRef]
42. Penwell, W.F.; Shapiro, A.B.; Giacobbe, R.A.; Gu, R.F.; Gao, N.; Thresher, J.; McLaughlin, R.E.; Huband, M.D.; DeJonge, B.L.; Ehmann, D.E.; et al. Molecular mechanisms of sulbactam antibacterial activity and resistance determinants in *Acinetobacter baumannii*. *Antimicrob. Agents Chemother.* **2015**, *59*, 1680–1689. [CrossRef]
43. Morinaka, A.; Tsutsumi, Y.; Yamada, M.; Suzuki, K.; Watanabe, T.; Abe, T.; Furuuchi, T.; Inamura, S.; Sakamaki, Y.; Mitsuhashi, N.; et al. OP0595, a new diazabicyclooctane: Mode of action as a serine β-lactamase inhibitor, antibiotic and β-lactam 'enhancer'. *J. Antimicrob. Chemother.* **2015**, *70*, 2779–2786. [CrossRef]
44. Asli, A.; Brouillette, E.; Krause, K.M.; Nichols, W.W.; Malouin, F. Distinctive binding of avibactam to penicillin-binding proteins of Gram-negative and Gram-positive bacteria. *Antimicrob. Agents Chemother.* **2016**, *60*, 752–756. [CrossRef] [PubMed]
45. Moya, B.; Barcelo, I.M.; Bhagwat, S.; Patel, M.; Bou, G.; Papp-Wallace, K.M.; Bonomo, R.A.; Oliver, A. WCK 5107 (Zidebactam) and WCK 5153 are novel inhibitors of PBP2 showing potent "β-lactam enhancer" activity against *Pseudomonas aeruginosa*, including multidrug-resistant metallo-β-lactamase-producing high-risk clones. *Antimicrob. Agents Chemother.* **2017**, *61*, e02529-16. [CrossRef]
46. Durand-Réville, T.F.; Guler, S.; Comita-Prevoir, J.; Chen, B.; Bifulco, N.; Huynh, H.; Lahiri, S.; Shapiro, A.B.; McLeod, S.M.; Carter, N.M.; et al. ETX2514 is a broad-spectrum β-lactamase inhibitor for the treatment of drug-resistant Gram-negative bacteria including *Acinetobacter baumannii*. *Nat. Microbiol.* **2017**, *2*, 17104. [CrossRef]
47. Sun, D.; Tsivkovski, R.; Pogliano, J.; Tsunemoto, H.; Nelson, K.; Rubio-Aparicio, D.; Lomovskaya, O. Intrinsic antibacterial activity of xeruborbactam *in vitro*: Assessing spectrum and mode of action. *Antimicrob. Agents Chemother.* **2022**, *66*, e0087922. [CrossRef] [PubMed]

48. Coghi, P.S.; Zhu, Y.; Xie, H.; Hosmane, N.S.; Zhang, Y. Organoboron compounds: Effective antibacterial and antiparasitic agents. *Molecules* **2021**, *26*, 3309. [CrossRef] [PubMed]
49. Mazzantini, D.; Celandroni, F.; Calvigioni, M.; Lupetti, A.; Ghelardi, E. In vitro resistance and evolution of resistance to tavaborole in *Trichophyton rubrum*. *Antimicrob. Agents Chemother.* **2021**, *65*, e02324-20. [CrossRef] [PubMed]
50. Rock, F.L.; Mao, W.; Yaremchuk, A.; Tukalo, M.; Crépin, T.; Zhou, H.; Zhang, Y.K.; Hernandez, V.; Akama, T.; Baker, S.J.; et al. An antifungal agent inhibits an aminoacyl-tRNA synthetase by trapping tRNA in the editing site. *Science* **2007**, *316*, 1759–1761. [CrossRef]
51. Ganapathy, U.S.; Del Rio, R.G.; Cacho-Izquierdo, M.; Ortega, F.; Lelièvre, J.; Barros-Aguirre, D.; Lindman, M.; Dartois, V.; Gengenbacher, M.; Dick, T. A leucyl-tRNA synthetase inhibitor with broad-spectrum antimycobacterial activity. *Antimicrob. Agents Chemother.* **2021**, *65*, e02420-20. [CrossRef]
52. Hu, Q.H.; Liu, R.J.; Fang, Z.P.; Zhang, J.; Ding, Y.Y.; Tan, M.; Wang, M.; Pan, W.; Zhou, H.C.; Wang, E.D. Discovery of a potent benzoxaborole-based anti-pneumococcal agent targeting leucyl-tRNA synthetase. *Sci. Rep.* **2013**, *3*, 2475. [CrossRef]
53. Si, Y.; Basak, S.; Li, Y.; Merino, J.; Iuliano, J.N.; Walker, S.G.; Tonge, P.J. Antibacterial activity and mode of action of a sulfonamide-based class of oxaborole leucyl-tRNA-synthetase inhibitors. *ACS Infect. Dis.* **2019**, *5*, 1231–1238. [CrossRef]
54. Purnapatre, K.P.; Rao, M.; Pandya, M.; Khanna, A.; Chaira, T.; Bambal, R.; Upadhyay, D.J.; Masuda, N. In vitro and in vivo activities of DS86760016, a novel leucyl-tRNA synthetase inhibitor for Gram-negative pathogens. *Antimicrob. Agents Chemother.* **2018**, *62*, e01987-17. [CrossRef]
55. Hernandez, V.; Crépin, T.; Palencia, A.; Cusack, S.; Akama, T.; Baker, S.J.; Bu, W.; Feng, L.; Freund, Y.R.; Liu, L.; et al. Discovery of a novel class of boron-based antibacterials with activity against Gram-negative bacteria. *Antimicrob. Agents Chemother.* **2013**, *57*, 1394–1403. [CrossRef] [PubMed]
56. Pacholak, P.; Krajewska, J.; Wińska, P.; Dunikowska, J.; Gogowska, U.; Mierzejewska, J.; Durka, K.; Woźniak, K.; Laudy, A.E.; Luliński, S. Development of structurally extended benzosiloxaboroles—synthesis and in vitro biological evaluation. *RSC Adv.* **2021**, *11*, 25104–25121. [CrossRef]
57. Borys, K.M.; Wieczorek, D.; Pecura, K.; Lipok, J.; Adamczyk-Woźniak, A. Antifungal activity and tautomeric cyclization equilibria of formylphenylboronic acids. *Bioorganic Chem.* **2019**, *91*, 103081. [CrossRef]
58. Adamczyk-Woźniak, A.; Gozdalik, J.T.; Wieczorek, D.; Madura, I.D.; Kaczorowska, E.; Brzezińska, E.; Sporzyński, A.; Lipok, J. Synthesis, properties and antimicrobial activity of 5-trifluoromethyl-2-formylphenylboronic acid. *Molecules* **2020**, *25*, 799. [CrossRef] [PubMed]
59. Adamczyk-Woźniak, A.; Gozdalik, J.T.; Kaczorowska, E.; Durka, K.; Wieczorek, D.; Zarzeczańska, D.; Sporzyński, A. (Trifluoromethoxy)phenylboronic acids: Structures, properties, and antibacterial activity. *Molecules* **2021**, *26*, 2007. [CrossRef] [PubMed]
60. Laudy, A.E.; Osińska, P.; Namysłowska, A.; Hare, O.; Tyski, S. Modification of the susceptibility of Gram-negative rods producing ESβLS to β-lactams by the efflux phenomenon. *PLoS ONE* **2015**, *10*, e0119997. [CrossRef]
61. Colclough, A.L.; Alav, I.; Whittle, E.E.; Pugh, H.L.; Darby, E.M.; Legood, S.W.; McNeil, H.E.; Blair, J.M. RND efflux pumps in Gram-negative bacteria; regulation, structure and role in antibiotic resistance. *Future Microbiol.* **2020**, *15*, 143–157. [CrossRef]
62. Zając, O.M.; Tyski, S.; Laudy, A.E. The contribution of efflux systems to levofloxacin resistance in *Stenotrophomonas maltophilia* clinical strains isolated in Warsaw, Poland. *Biology* **2022**, *11*, 1044. [CrossRef]
63. Adamczyk-Woźniak, A.; Tarkowska, M.; Lazar, Z.; Kaczorowska, E.; Madura, I.D.; Maria Dąbrowska, A.; Lipok, J.; Wieczorek, D. Synthesis, structure, properties and antimicrobial activity of para trifluoromethyl phenylboronic derivatives. *Bioorganic Chem.* **2022**, *119*, 105560. [CrossRef]
64. European Committee on Antimicrobial Susceptibility Testing. Guidelines for detection of resistance mechanisms and specific resistance of clinical and/or epidemiological importance. Document version 2.0. 2017. Available online: https://www.eucast.org/resistance_mechanisms (accessed on 1 October 2023).
65. Yagi, T.; Wachino, J.; Kurokawa, H.; Suzuki, S.; Yamane, K.; Doi, Y.; Shibata, N.; Kato, H.; Shibayama, K.; Arakawa, Y. Practical methods using boronic acid compounds for identification of class C beta-lactamase-producing *Klebsiella pneumoniae* and *Escherichia coli*. *J. Clin. Microbiol.* **2005**, *43*, 2551–2558. [CrossRef] [PubMed]
66. European Committee on Antimicrobial Susceptibility Testing (EUCAST). Breakpoint Tables for Interpretation of MICs and Zone Diameters. Version 13.0. 2023. Available online: https://www.eucast.org/clinical_breakpoints (accessed on 1 October 2023).
67. Bonapace, C.R.; Bosso, J.A.; Friedrich, L.V.; White, R.L. Comparison of methods of interpretation of checkerboard synergy testing. *Diagn. Microbiol. Infect. Dis.* **2002**, *44*, 363–366. [CrossRef]
68. Ke, W.; Bethel, C.R.; Papp-Wallace, K.M.; Pagadala, S.R.; Nottingham, M.; Fernandez, D.; Buynak, J.D.; Bonomo, R.A.; van den Akker, F. Crystal structures of KPC-2 β-lactamase in complex with 3-nitrophenyl boronic acid and the penam sulfone PSR-3-226. *Antimicrob. Agents Chemother.* **2012**, *56*, 2713–2718. [CrossRef]
69. Charzewski, Ł.; Krzyśko, K.A.; Lesyng, B. Exploring covalent docking mechanisms of boron-based inhibitors to class A, C and D β-lactamases using time-dependent hybrid QM/MM simulations. *Front. Mol. Biosci.* **2021**, *8*, 633181. [CrossRef] [PubMed]

70. Tooke, C.L.; Hinchliffe, P.; Bonomo, R.A.; Schofield, C.J.; Mulholland, A.J.; Spencer, J. Natural variants modify *Klebsiella pneumoniae* carbapenemase (KPC) acyl-enzyme conformational dynamics to extend antibiotic resistance. *J. Biol. Chem.* **2021**, *296*, 100126. [CrossRef] [PubMed]
71. European Committee on Antimicrobial Susceptibility Testing (EUCAST). Method for the Determination of Broth Dilution MIC of Antifungal Agents for Yeasts. Document E.DEF 7.3.2. 2020. Available online: https://www.eucast.org/fileadmin/src/media/PDFs/EUCAST_files/AFST/Files/EUCAST_E_Def_7.3.2_Yeast_testing_definitive_revised_2020.pdf (accessed on 1 October 2023).
72. European Committee on Antimicrobial Susceptibility Testing. EUCAST Disk Diffusion Method for Antimicrobial Susceptibility Testing. Document version 11.0. 2023. Available online: https://www.eucast.org/fileadmin/src/media/PDFs/EUCAST_files/Disk_test_documents/2023_manuals/Manual_v_11.0_EUCAST_Disk_Test_2023.pdf (accessed on 1 October 2023).
73. Clinical and Laboratory Standards Institute (CLSI). *Method for Antifungal Disk Diffusion Susceptibility Testing of Yeasts*, 2nd ed.; Approved Standard, CLSI Dokument M44-A2; CLSI: Wayne, PA, USA, 2009.
74. Clinical and Laboratory Standards Institute (CLSI). *Reference Method for Broth Dilution Antifungal Susceptibility Testing of Yeasts*, 3rd ed.; CLSI Dokument M27-A3; CLSI: Wayne, PA, USA, 2008.
75. Clinical and Laboratory Standards Institute (CLSI). *Methods for Dilution Antimicrobial Susceptibility Tests for Bacteria that Grow Aerobically*, 9th ed.; Approved Standard, CLSI Dokument M07-A9; CLSI: Wayne, PA, USA, 2012.
76. Clinical and Laboratory Standards Institute (CLSI). *Methods for Determining Bactericidal Activity of Antimicrobial Agents. CLSI Dokument M26-A*; CLSI: Wayne, PA, USA, 1999.
77. Cantón, E.; Pemán, J.; Viudes, A.; Quindós, G.; Gobernado, M.; Espinel-Ingroff, A. Minimum fungicidal concentrations of amphotericin B for bloodstream *Candida species*. *Diagn. Microbiol. Infect. Dis.* **2003**, *45*, 203–206. [CrossRef] [PubMed]
78. Misra, R.; Morrison, K.D.; Cho, H.J.; Khuu, T. Importance of real-time assays to distinguish multidrug efflux pump-inhibiting and outer membrane-destabilizing activities in *Escherichia coli*. *J. Bacteriol.* **2015**, *197*, 2479–2488. [CrossRef]
79. Lamers, R.P.; Cavallari, J.F.; Burrows, L.L. The efflux inhibitor phenylalanine-arginine beta-naphthylamide (PAβN) permeabilizes the outer membrane of gram-negative bacteria. *PLoS ONE* **2013**, *8*, e60666. [CrossRef]
80. Laudy, A.E.; Kulińska, E.; Tyski, S. The impact of efflux pump inhibitors on the activity of selected non-antibiotic medicinal products against Gram-negative bacteria. *Molecules* **2017**, *22*, 114. [CrossRef]
81. Odds, F.C. Synergy, antagonism, and what the chequerboard puts between them. *J. Antimicrob. Chemother.* **2003**, *52*, 1. [CrossRef]
82. Labute, P. Protonate3D: Assignment of ionization states and hydrogen coordinates to macromolecular structures. *Proteins* **2009**, *75*, 187–205. [CrossRef]
83. Case, D.A.; Darden, T.A.; Cheatham III, T.E.; Simmerling, C.L.; Wang, J.; Duke, R.E.; Luo, R.; Crowley, M.; Walker, R.C.; Zhang, W.; et al. AMBER 10. University of California, San Francisco, 2008. Available online: https://infoscience.epfl.ch/record/121435 (accessed on 1 October 2023).
84. Chemical Computing Group ULC, Molecular Operating Environment (MOE). 1010 Sherbrooke St.West 910, Montreal, QC, Canada, 2018. Available online: https://www.chemcomp.com/Products.htm (accessed on 1 October 2023).
85. Labute, P. The generalized Born/volume integral implicit solvent model: Estimation of the free energy of hydration using London dispersion instead of atomic surface area. *J. Comput. Chem.* **2008**, *29*, 1693–1698. [CrossRef]
86. Bond, S.D.; Leimkuhler, B.J.; Laird, B.B. The Nosé–Poincaré method for constant temperature molecular dynamics. *J. Comp. Phys.* **1999**, *151*, 114–134. [CrossRef]
87. Meroueh, S.O.; Fisher, J.F.; Schlegel, H.B.; Mobashery, S. Ab initio QM/MM study of class A β-lactamase acylation: Dual participation of Glu166 and Lys73 in a concerted base promotion of Ser70. *J. Am. Chem. Soc.* **2005**, *127*, 15397–15407. [CrossRef] [PubMed]
88. Chudyk, E.I.; Limb, M.A.; Jones, C.; Spencer, J.; van der Kamp, M.W.; Mulholland, A.J. QM/MM simulations as an assay for carbapenemase activity in class A β-lactamases. *Chem. Commun.* **2014**, *50*, 14736–14739. [CrossRef]
89. Stewart, J.J.P. *MOPAC 2016*; Stewart Computational Chemistry: Colorado Springs, CO, USA, 2016.
90. Phillips, J.C.; Hardy, D.J.; Maia, J.D.C.; Stone, J.E.; Ribeiro, J.V.; Bernardi, R.C.; Buch, R.; Fiorin, G.; Hénin, J.; Jiang, W.; et al. Scalable molecular dynamics on CPU and GPU architectures with NAMD. *J. Chem. Phys.* **2020**, *153*, 044130. [CrossRef]
91. Brooks, B.R.; Brooks, C.L., 3rd; Mackerell, A.D., Jr.; Nilsson, L.; Petrella, R.J.; Roux, B.; Won, Y.; Archontis, G.; Bartels, C.; Boresch, S.; et al. CHARMM: The biomolecular simulation program. *J. Comput. Chem.* **2009**, *30*, 1545–1614. [CrossRef]
92. Vanommeslaeghe, K.; Hatcher, E.; Acharya, C.; Kundu, S.; Zhong, S.; Shim, J.; Darian, E.; Guvench, O.; Lopes, P.; Vorobyov, I.; et al. CHARMM general force field: A force field for drug-like molecules compatible with the CHARMM all-atom additive biological force fields. *J. Comput. Chem.* **2010**, *31*, 671–690. [CrossRef] [PubMed]
93. Humphrey, W.; Dalke, A.; Schulten, K. VMD: Visual Molecular Dynamics. *J. Mol. Graph.* **1996**, *14*, 33–38. [CrossRef] [PubMed]
94. Ren, Y.; Bazan, G.C. Trifluoromethyl-substituted conjugated oligoelectrolytes. *Chemistry* **2010**, *16*, 11028–11036. [CrossRef]
95. ETEST. Application Guide. Available online: https://www.biomerieux-usa.com/sites/subsidiary_us/files/supplementary_inserts_-_16273_-_b_-_en_-_eag_-_etest_application_guide-3.pdf (accessed on 1 October 2023).
96. Espinel-Ingroff, A. Etest for antifungal susceptibility testing of yeasts. *Diagn. Microbiol. Infect. Dis.* **1994**, *19*, 217–220. [CrossRef] [PubMed]

97. Pfaller, M.A.; Bale, M.; Buschelman, B.; Lancaster, M.; Espinel-Ingroff, A.; Rex, J.H.; Rinaldi, M.G. Selection of candidate quality control isolates and tentative quality control ranges for in vitro susceptibility testing of yeast isolates by National Committee for Clinical Laboratory Standards proposed standard methods. *J. Clin. Microbiol.* **1994**, *32*, 1650–1653. [CrossRef] [PubMed]
98. European Committee on Antimicrobial Susceptibility Testing. Reading guide. EUCAST disk diffusion method for antimicrobial susceptibility testing. Document version 9.0. Available online: https://www.eucast.org/fileadmin/src/media/PDFs/EUCAST_files/Disk_test_documents/2022_manuals/Reading_guide_v_9.0_EUCAST_Disk_Test_2022.pdf (accessed on 1 October 2023).

Supplementary Materials

Aromatic Diboronic Acids as Effective KPC/AmpC Inhibitors

Joanna Krajewska [1], Piotr Chyży [2], Krzysztof Durka [3], Patrycja Wińska [3], Krystiana A. Krzyśko [4,*], Sergiusz Luliński [3] and Agnieszka E. Laudy [1,*]

[1] Department of Pharmaceutical Microbiology and Bioanalysis, Medical University of Warsaw, 02-097 Warsaw, Poland; joanna.krajewska@ymail.com (J.K.); alaudy@wp.pl A.E.L.)
[2] Centre of New Technologies, University of Warsaw, 02-097 Warsaw, Poland; p.chyzy@cent.uw.edu.pl (P.C.)
[3] Faculty of Chemistry, Warsaw University of Technology, 00-664 Warsaw, Poland; kdurka@gmail.com (K.D.); pwinska@ch.pw.edu.pl (P.W.); sergiusz.lulinski@pw.edu.pl (S.L.)
[4] Faculty of Physics, University of Warsaw, 02-093 Warsaw, Poland krystiana.krzysko@fuw.edu.pl (K.A.K.)
* Correspondence: krystiana.krzysko@fuw.edu.pl (K.A.K.); alaudy@wp.pl (A.E.L.)

List of contents

1. Synthetic procedures S2
1. NMR spectra of synthesized compounds S8
2. Antimicrobial activity S15
3. Cytotoxic activity S23
4. Molecular modeling and hybrid QM/MM simulations S24
5. References S31

2. Antimicrobial activity

Table S1. The antibacterial activity of tested agents against standard Gram-positive strains.

Agent tested	MIC in mg/L [MBC in mg/L][a] (Diameter of inhibition zone in mm)					
	S. aureus ATCC 6538P	*S. aureus* ATCC 43300 MRSA	*S. epidermidis* ATCC 12228	*E. faecalis* ATCC 29212	*E. faecium* ATCC 6057	*B. subtilis* ATCC 6633[b]
1a	200 (-)	400 (-)	400 (14)	200 (-)	400 (-)	NT (17)
1b	25 (14)	100 (13)	100 (17)	200 (-)	200 (-)	NT (23)
1c	25 (22)	50 (22)	50 (28)	200 (16)	200 (15)	NT (28)
1d	25 (-)	200 (-)	25 (21)	>400 (-)	>400 (-)	NT (15)
1e	**12.5** (20)	25 (26)	25 (21)	200 (15)	100 (14)	NT (28)
1f	50 (17)	200 (16)	50 (17)	400 (-)	200 (-)	NT (13)
1g	>400 (-)	>400 (-)	>400 (-)	>400 (-)	>400 (-)	NT (-)
1h	400 (13)	400 (14)	200 (-)	400 (-)	400 (-)	NT (12)
1i	25 (14)	100 (11)	50 (21)	200 (14)	200 (11)	NT (18)
1j	50 (19)	50 (21)	50 (25)	400 (-)	400 (-)	NT (20)
1k[c]	100 (-)	100 (-)	100 (-)	>100 (-)	100 (-)	NT (11)
1l	NT (-)	NT (-)	NT (-)	NT (-)	NT (-)	NT (-)
2a	100 (20)	400 (-)	200 (21)	200 (-)	>400 (-)	NT (18)
2b	100 (14)	400 (15)	50 (19)	400 (-)	400 (14)	NT (17)
2c	50 (20)	100 (19)	50 (-)	400 (-)	400 (-)	NT (-)
2d	50 (22)	100 (19)	50 (12)	200 (14)	200 (14)	NT (15)
2e	**6.25** (29)	**12.5** (25)	**0.78** (35)	50 (21)	100 (18)	NT (20)
2f	50 [400] (14)	200 (13)	100 (25)	>400 (-)	200 (-)	NT (22)
2g	>400 (-)	>400 (-)	>400 (-)	>400 (-)	400 (-)	NT (-)
3a	200 (-)	400 (-)	200 (20)	400 (-)	50 (16)	NT (24)
3b	>400 (-)	>400 (-)	400 (21)	>400 (-)	>400 (-)	NT (-)
3c	200 (13)	400 (11)	100 (24)	400 (-)	400 (12)	NT (18)
3d	200 (20)	400 (18)	200 (21)	200 (12)	200 (16)	NT (12)
3e	100 (17)	400 (15)	200 (21)	200 (14)	200 (13)	NT (22)
4a	>400 (-)	>400 (-)	>400 (-)	>400 (-)	400 (-)	NT (-)
4b	25 (20)	200 (-)	200 (20)	200 (-)	200 (-)	NT (18)
5a	100 (-)	400 (-)	400 (13)	100 (-)	>400 (-)	NT (15)
5b	>400 (-)	>400 (-)	>400 (-)	200 (-)	>400 (-)	NT (-)
5c	400 (-)	>400 (-)	>400 (-)	200 (-)	>400 (-)	NT (-)
6a	50 (-)	400 (-)	400 (-)	>400 (-)	400 (-)	NT (-)
7a	50 (-)	100 (-)	100 (-)	400 (-)	400 (-)	NT (-)
7b	50 [100] (19)	50 (20)	50 [100] (30)	200 (14)	200 (14)	NT (22)
7c[d]	**12.5** (23)	25 (22)	**12.5** (30)	25 (23)	**12.5** (25)	NT (26)
LIN[e]	1 [>128] (25)	2 [>128] (25)	1 [>128] (26)	2 [>128] (15)	2 [>128] (14)	NT (30)

The highest activity against Gram-positive bacteria indicated by the low MIC values (≤**12.5** mg/L) is shown in boldface.

(-) – The inhibition zone was not observed in the disc-diffusion method. The diameter of paper discs was 9 mm; NT – not tested.

[a] Only the MBC values ≤400 mg/L are presented.

[b] The growth type of *B. subtilis* in the MHB medium prevented reading the MIC values of tested substances.

[c] The MIC and MBC values of the substance were determined up to 100 mg/L. In the table, only the MBC values ≤100 mg/L are presented. The tested substance dissolved in DMSO precipitated after implementation into the MHB medium at a concentration above 100 mg/L.

[d] The MIC and MBC values of the substance were determined up to 200 mg/L. In the table, only the MBC values ≤200 mg/L are presented. The tested substance dissolved in DMSO precipitated after implementation into the MHB medium at a concentration above 200 mg/L.

[e] LIN, linezolid was used as a reference agent active against Gram-positive bacteria. The diameter of the commercial disc containing 0.03 mg of linezolid was 6 mm; the MIC of linezolid was determined according to the CLSI recommendations [75].

Table S2. The antibacterial activity of tested agents against standard Gram-negative strains.

	MIC in mg/L [MBC in mg/L][a] / x-fold reduction of MIC in the presence of PAßN[b] (Diameter of inhibition zone in mm)									
Agent tested	*E. coli* **ATCC 25922**	*K. pneumoniae* **ATCC 13883**	*P. mirabilis* **ATCC 12453**	*E. cloacae* **DSM 6234**	*S. marcescens* **ATCC 13880**	*P. aeruginosa* **ATCC 27853**	*S. maltophilia* **ATCC 13637**	*A. baumannii* **ATCC 19606**	*B. cepacia* **ATCC 25416[c]**	*B. bronchiseptica* **ATCC 4617[c]**
1a	>400 (-)	>400 (-)	>400 (-)	>400 (-)	>400 (-)	>400 (-)	>400 (-)	>400 (-)	>400 (11)	400 [400] (13)
1b	400 (19)	400 (-)	400/2 (17)	400/2 (-)	400/2 (-)	>400/≥2 (-)	400/2 (18)	400 (-)	400 (15)	100 (21)
1c	200 (20)	200 (-)	200 (16)	200 (-)	200/2 (-)	400/2 (-)	100 (21)	400/2 (12)	200 (20)	50 (24)
1d	200 (-)	400 (-)	200 (-)	200 (-)	400 (18)	>400 (-)	200 (12)	200 (-)	400 (14)	100 (15)
1e	100 [200] (-)	200 [400]/2 (16)	100 (-)	100 (18)	100 (18)	400/2 (-)	50 [400] (20)	200/2 (14)	200 (18)	50 [200] (23)
1f	100 [100] (17)	100 [100] (21)	100 (17)	100 [100] (17)	100 (21)	>400 (-)	200/2 (14)	100 (16)	50 (20)	50 (20)
1g	>400 (-)	>400 (-)	>400 (-)	>400 (-)	>400 (-)	>400 (-)	>400 (-)	>400 (-)	>400 (-)	>400 (-)
1h	>400/≥2 (-)	>400 (-)	>400 (-)	>400 (-)	>400 (-)	>400 (-)	>400/≥2 (-)	>400 (-)	>400 (-)	>400 (-)
1i	100/**4** (17)	200/2 (13)	100/2 (21)	100/2 (19)	200/**4** (21)	>400/≥2 (-)	50 (17)	100/2 (17)	400 (16)	100 (14)
1j	100/4 (14)	400/2 (14)	200/2 (17)	200/2 (17)	200/2 (18)	>400 (-)	50 [400](15)	50 (15)	200 (17)	100 (20)
1k[d]	>100 (-)	>100 (-)	>100 (-)	>100 (-)	>100 (-)	>100 (-)	>100 (-)	>100 (-)	>100 (-)	>100 (-)
1l	NT (-)	NT (-)	NT (-)	NT (-)	NT (-)	NT (-)	NT (-)	NT (-)	NT (-)	NT (-)
2a	>400 (-)	>400 (-)	>400 (-)	>400 (-)	>400 (-)	>400 (-)	400 (-)	>400 (-)	>400 (15)	200 (12)
2b	400 (-)	400 (17)	400 (-)	400 (-)	400 (-)	>400 (-)	100 (19)	>400/≥2 (-)	400 (12)	100 (18)
2c	200 (12)	200 (12)	400 (12)	200 (12)	200 (11)	>400 (-)	50 (21)	400 (13)	200 (13)	50 (22)
2d	200 (12)	400 (12)	400 (11)	400 (11)	100 (11)	>400 (-)	50 (29)	400/2 (11)	400 (-)	50 (20)
2e	400/2 (-)	400/**4** (-)	>400/**≥4** (-)	>400/**≥4** (-)	400/2 (-)	>400/**≥4** (-)	25 (15)	400/2 (-)	400 (14)	100 (14)
2f	>400 (13)	>400 (11)	>400 (-)	>400/≥2 (-)	>400/≥2 (-)	>400 (-)	100 (18)	>400/≥2 (-)	>400 (-)	200 (13)
2g	>400 (-)	>400 (-)	>400 (-)	>400 (-)	>400 (-)	>400 (-)	>400 (-)	>400 (-)	>400 (-)	>400 (-)
3a	400/2 (-)	400 (-)	400 (-)	400/2 (-)	400 (-)	400/2 (-)	400/2 (-)	400 (-)	400 (-)	400 (-)
3b	>400 (-)	>400 (-)	>400 (-)	>400/≥2 (-)	>400 (-)	>400/≥2 (-)	>400/≥2 (13)	>400 (-)	>400 (-)	>400 (-)
3c	>400/≥2 (-)	>400/≥2 (-)	>400/≥2 (-)	>400/≥2 (-)	>400/≥2 (-)	>400/≥2 (11)	>400 (12)	>400 (-)	>400 (-)	400 (12)
3d	>400/≥2 (-)	>400/≥2 (-)	>400/≥2 (-)	>400/≥2 (-)	>400 (-)	>400/≥2 (11)	200/2 (12)	400/2 (-)	>400 (-)	>400 (-)
3e	>400/**≥8** (13)	>400/**≥4** (12)	>400/≥2 (13)	>400/**≥8** (-)	>400/**≥16** (9)	>400/**≥16** (-)	200 [400]/**4** (14)	400/**4** (-)	>400 (10)	400 (-)
4a	>400 (-)	>400 (-)	>400 (-)	>400 (-)	>400 (-)	>400 (-)	>400 (-)	>400 (-)	>400 (-)	>400 (-)
4b	>400 (-)	>400 (-)	>400 (-)	>400 (-)	>400 (-)	>400 (-)	>400/≥2 (-)	>400 (-)	>400 (11)	400 (-)
5a	>400 (-)	>400 (-)	>400 (-)	400 (-)	>400 (-)	>400/**≥4** (-)	400 (-)	>400 (-)	400 (-)	200 (20)
5b	>400 (-)	>400 (-)	>400 (-)	>400 (-)	>400 (-)	>400 (-)	>400 (-)	>400 (-)	>400 (-)	>400 (-)
5c	>400 (-)	>400 (-)	>400 (-)	>400 (-)	>400 (-)	>400 (-)	>400 (-)	>400 (-)	>400 (-)	400 (-)

6a	>400 (-)	>400 (-)	>400 (-)	>400 (-)	>400 (-)	>400 (-)	>400 (-)	>400/≥2 (-)	>400 (-)	>400 (-)
7a	50 (20)	100 (22)	100 (22)	100/2 (22)	50 (25)	400 (-)	100 (19)	100/2 (18)	50 (23)	50 (22)
7b	100/2 (18)	400/8 (13)	400/4 (11)	400/8 (14)	400/8 (15)	>400/≥16 (11)	12,5 [400]/4 (17)	100/2 (20)	400 (16)	50 (20)
7c[e]	>200/**≥8** (15)	>200/≥2 (-)	>200/**≥4** (-)	>200/**≥4** (-)	>200/≥2 (-)	>200 (-)	50 [100]/2 (15)	>200/**≥16** (13)	>200 (15)	50 (19)
Nf[f]	**8 [8] (24)**	**32 [32] (23)**	**128 [>128]**	**32 [32] (17)**	**128 [>128] (12)**	**>128 [>128] (-**	**128 [>128] (-)**	**64 [128] (9)**	**32 [32] (12)**	**64 [128] (-)**

The significant decreases (at least a 4-fold) in the MIC values of tested compounds after the addition of PAβN are shown in boldface. The test was performed in the MHB medium supplemented with 1 mM $MgSO_4$.

PAβN – efflux pump inhibitor; (-) – The inhibition zone was not observed in the disc-diffusion method. The diameter of the paper discs was 9 mm; NT – not tested. The MIC determination could not be performed, because the tested substance dissolved in DMSO precipitated after implementation into the MHB (Mueller-Hinton II broth) medium.

[a] Only the MBC values ≤400 mg/L are presented.

[b] In the table, only at least 2-fold decreases in the MIC values of tested compounds after the addition of PAβN are presented.

[c] The growth of *B. cepacia* ATCC 25416 and *B. bronchiseptica* ATCC 4617 strains was inhibited in the MHB medium supplemented with 1 mM $MgSO_4$ and 20 mg/L PAβN.

[d] The MIC and MBC values of the substance were determined up to 100 mg/L. In the table, only the MBC values ≤100 mg/L are presented. The tested substance dissolved in DMSO precipitated after implementation into the MHB medium at a concentration above 100 mg/L.

[e] The MIC and MBC values of the substance were determined up to 200 mg/L. In the table, only the MBC values ≤200 mg/L are presented. The tested substance dissolved in DMSO precipitated after implementation into the MHB medium at a concentration above 200 mg/L.

[f] Nf, nitrofurantoin was used as a reference agent active against Gram-negative bacteria. The diameter of a commercial disc containing 0.3 mg of nitrofurantoin was 6 mm; the MIC of nitrofurantoin was determined according to the CLSI recommendations [75].

Table S3. The antifungal activity of tested agents against yeast strains.

	MIC in mg/L [MFC in mg/L][a] (Diameter of inhibition zone in mm)						
Agent tested	***C. albicans* ATCC 90028**	***C. parapsilosis* ATCC 22019**	***C. tropicalis* IBA 171**	***C. tropicalis* ATCC 750**	***C. guilliermondii* IBA 155**	***C. krusei* ATCC 6258**	***S. cerevisiae* ATCC 9763**
1a	>400 (-)	>400 (-)	>400 (-)	>400 (-)	>400 (-)	>400 (-)	400 (-)
1b	>400 (-)	100 (12)	400 (-)	>400 (-)	400 (24)	100 (22)	25 (14)
1c	>400 (-)	>400 (-)	>400 (-)	>400 (-)	>400 (-)	400 (-)	200 (-)
1d	200 (-)	200 (14)	200 (-)	400 (-)	200 (16)	200 (-)	200 (13)
1e	>400 (-)	>400 (15)	>400 (-)	>400 (-)	>400 (16)	>400 (16)	400 (13)
1f	50 (24)	100 (20)	50 (20)	100 (18)	50 (29)	100 (19)	50 (20)
1g	>400 (-)	>400 (-)	>400 (-)	>400 (-)	>400 (-)	400 (-)	>400 (-)
1h	>400 (-)	>400 (-)	>400 (-)	>400 (-)	>400 (-)	>400 (-)	>400 (-)
1i	**12.5 (31)**	50 (24)	25 (29)	50 (25)	25 (34)	50 (22)	50 (24)
1j	200 (24)	>400 (15)	>400 (15)	>400 (17)	400 (30)	400 (23)	>400 (20)
1k[b]	>100 (-)	>100 (-)	>100 (-)	>100 (-)	>100 (-)	>100 (-)	>100 (-)
1l	NT (-)	NT (-)	NT (-)	NT (-)	NT (-)	NT (-)	NT (-)
2a	400 (-)	>400 (-)	400 (-)	>400 (-)	>400 (14)	>400 (-)	>400 (-)
2b	>400 (-)	>400 (-)	>400 (-)	>400 (-)	>400 (-)	>400 (-)	>400 (-)
2c	>400 (-)	>400 (-)	>400 (-)	>400 (-)	>400 (-)	>400 (-)	>400 (-)
2d	400 (-)	>400 (-)	>400 (-)	>400 (-)	400 (-)	400 (-)	>400 (-)
2e	400 (-)	400 (-)	400 (-)	>400 (-)	>400 (14)	>400 (-)	>400 (-)
2f	>400 (-)	>400 (-)	>400 (-)	>400 (-)	>400 (-)	400 (-)	200 (-)
2g	>400 (-)	>400 (-)	>400 (-)	>400 (-)	>400 (-)	>400 (-)	>400 (-)
3a	>400 (-)	25 (-)	>400 (-)	>400 (-)	>400 (-)	400 (-)	25 (-)
3b	400 (-)	200 (-)	200 (-)	200 (-)	400 (-)	100 (-)	100 (13)
3c	100 (-)	100 (-)	50 (-)	50 (-)	>400 (-)	200 (-)	100 (-)
3d	100 (-)	>400 (-)	>400 (-)	>400 (-)	200 (-)	50 (-)	200 (-)
3e	**6.25** [400]	**12.5** (30)	**6.25** [400]	**12.5** (28)	**3.12** [400] (40)	25 (23)	50 (23)
4a	>400 (-)	>400 (-)	>400 (-)	>400 (-)	>400 (-)	>400 (-)	>400 (-)
4b	>400 (-)	>400 (-)	>400 (-)	>400 (-)	>400 (-)	>400 (-)	>400 (-)
5a	400 (-)	>400 (-)	>400 (-)	>400 (-)	>400 (-)	>400 (-)	>400 (-)
5b	400 (-)	>400 (-)	>400 (-)	>400 (-)	>400 (-)	400 (-)	>400 (-)
5c	400 (-)	>400 (-)	>400 (-)	>400 (-)	>400 (-)	>400 (-)	>400 (-)
6a	>400 (-)	>400 (-)	>400 (-)	>400 (-)	>400 (-)	>400 (-)	>400 (-)
7a	25 (29)	25 (21)	25 (25)	50 (21)	25 (33)	50 (15)	50 (18)
7b	**6.25** (31)	**12.5** (17)	50 (22)	50 (21)	25 (27)	25 (28)	**6.25** (35)
7c[c]	50 [200] (33)	50 (29)	**12.5** [100]	50 [200] (20)	25 [200] (40)	50 (16)	**12.5** [25] (34)
F][d]	1 (43)	2 (32)	0.38 (39)	0.38 (40)	0.75 (40)	64[e] (16)	16[f] (12)

The highest activity against yeasts indicated by the low MIC values (≤12.5 mg/L) is shown in boldface.

(-) – The inhibition zone was not observed in the disc-diffusion method. The diameter of paper discs was 9 mm; NT – not tested. The MIC determination could not be performed, because the tested substance dissolved in DMSO precipitated after implementation into the RPMI medium.

[a] Only the MFC values ≤400 mg/L are presented.

[b] The MIC and MFC values of the substance were determined up to 100 mg/L. In the table, only the MFC values ≤100 mg/L are presented. The tested substance dissolved in DMSO precipitated after implementation into the RPMI medium at a concentration above 100 mg/L.

[c] The MIC and MFC values of the substance were determined up to 200 mg/L. In the table, only the MFC values ≤200 mg/L are presented. The tested substance dissolved in DMSO precipitated after implementation into the RPMI medium at a concentration above 200 mg/L.

[d] FL, fluconazole was used as a reference antifungal agent; the diameter of the commercial disc containing 0.025 mg of fluconazole was 6 mm; the MIC value of fluconazole was determined by the Etest method 95].

[e] The ellipse was visible pointing the MIC value 64 mg/L, however, with macro-colonies up to concentration ≥256 mg/L. In accordance with the recommendations for Etest method, the MIC value of fluconazole against *C. krusei* can be also interpreted as ≥256 mg/L [95,96]. *C. krusei* is intrinsically resistant to fluconazole.

[f] The ellipse was visible pointing the MIC value 16 mg/L, with colonies up to concentration ≥256 mg/L. There are no recommendations for Etest method interpretation of the MIC value of fluconazole against *S. cerevisiae*. The obtained MIC 16 mg/L is in line with the published results [97].

Table S4. The antibacterial activity of studied compounds against β-lactamase-producing Gram-negative strains.

Agent tested	Diameter of inhibition zone (mm) around discs with 0.03/0.1/0.3 mg of a tested agent			
	***K. pneumoniae* ATCC BAA 1705 KPC(+)**	***P. aeruginosa* MUW 700 AmpC(+)**	***E. coli* 77 CMY-2(+)**	***K. pneumoniae* ATCC 700603 ESBL(+)**
PBA	-/-/-	-/-/-	-/-/-	-/-/-
1a	-/-/-	-/-/-	-/-/-	-/-/-
1b	-/-/13*	-/-/12*	-/-/12*	-/-/12*
1c	-/-/12*	-/-/13	-/-/17*	-/-/14*
1d	-/-/15*	-/-/12*	-/-/13*	-/-/14*
1e	-/-/15*	-/-/14	-/-/18*	-/-/14*
1f	-/-/16	-/-/12*	-/-/15*	-/-/18*
1g	-/-/-	-/-/-	-/-/-	-/-/-
1h	-/-/-	-/-/-	-/-/-	-/-/-
1i	-/-/15*	-/-/12*	-/-/16*	-/-/13*
1j	-/-/-	-/-/14*	-/-/-	-/-/11*
1k	-/-/-	-/-/-	-/-/-	-/-/-
1l	-/-/-	-/-/-	-/-/-	-/-/-
2a	-/-/-	-/-/-	-/-/-	-/-/-
2b	-/-/-	-/-/11*	-/-/13	-/-/-
2c	-/-/14*	-/-/11*	-/-/15*	-/-/13*
2d	-/-/11*	-/-/12*	-/-/15*	-/-/11*
2e	-/-/-	-/-/-	-/-/-	-/-/-
2f	-/-/-	-/-/-	-/-/-	-/-/-
2g	-/-/-	-/-/-	-/-/-	-/-/-
3a	-/-/-	-/-/-	-/-/-	-/-/-
3b	-/-/-	-/-/-	-/-/-	-/-/-
3c	-/-/-	-/-/-	-/-/-	-/-/-
3d	-/-/-	-/-/-	-/-/-	-/-/-
3e	-/-/-	-/-/-	-/-/-	-/-/-
4a	-/-/-	-/-/-	-/-/-	-/-/-
4b	-/-/-	-/-/-	-/-/-	-/-/-
5a	-/-/-	-/-/-	-/-/-	-/-/-
5b	-/-/-	-/-/-	-/-/-	-/-/-
5c	-/-/-	-/-/-	-/-/-	-/-/-
6a	-/-/-	-/-/-	-/-/-	-/-/-
7a	-/12*/17	-/11*/12	-/13*/18	-/18*/18
7b	-/-/14	-/-/-	-/12*/14	-/-/13*
7c	-/-/-	-/-/-	-/-/-	-/-/-

(-) – indicates no inhibition zone; PBA – phenylboronic acid.

* colonies within the inhibition zone. The diameter of the outer zone edge is presented, according to EUCAST recommendations for the fosfomycin testing against *E. coli* [98].

Table S5. The antibacterial activity of tested agents against β-lactamase-producing Gram-negative strains.

	MIC in mg/L					
Agent tested*	***E. coli* 76 KPC-2(+)**	***E. coli* 77 CMY-2(+)**	***K. pneumoniae* ATCC BAA-1705 KPC-2(+)**	***K. pneumoniae* 81 KPC-3(+)**	***K. pneumoniae* 83 KPC-3(+), CTX-M-3(+)**	***P. aeruginosa* MUW 700 AmpC(+)**
PBA	>400	>400	>400	>400	>400	>400
1a	>400	>400	>400	>400	>400	>400
1b	400	400	>400	>400	>400	>400
1c	200	200	200	200	200	400
1d	400	400	400	400	400	>400
1e	100	100	200	200	200	200
1f	100	100	100	100	100	>400
1i	100	100	200	200	200	>400
2a	>400	>400	>400	>400	>400	>400
2b	400	400	>400	>400	>400	>400
2c	200	200	400	200	200	>400
2d	200	200	400	400	400	>400
2e	>400	>400	>400	>400	>400	>400
2f	>400	>400	>400	>400	>400	>400
2g	>400	>400	>400	>400	>400	>400
3a	400	400	400	400	400	400
3b	>400	>400	>400	>400	>400	>400
3c	>400	>400	>400	>400	>400	>400
3d	>400	>400	>400	>400	>400	>400
3e	>400	>400	>400	>400	>400	>400
4a	>400	>400	>400	>400	>400	>400
4b	>400	>400	>400	>400	>400	>400
5a	>400	>400	>400	>400	>400	>400
5c	>400	>400	>400	>400	>400	>400
7a	100	100	100	200	100	400
7c	>200	>200	>200	>200	>200	>200

PBA – phenylboronic acid.

* MICs of agents **1g**, **1h**, **1j**, **1k**, **1l**, **5b**, **6a**, and **7b** for β-lactamase-producing Gram-negative strains were not determined since those compounds did not show any β-lactamase inhibitory activity at high concentration, according to the results of the CDTs test presented in Table 1. Thus, they were not qualified for β-lactamase inhibitory activity testing at low concentrations.

Table S6. The MIC values of antibiotics alone and in combination with studied compounds against standard and clinical strains of Gram-negative rods producing various classes of β-lactamases.

Agent tested*	MICs (mg/L) of antibiotics alone or in combination with 16/8/4 mg per L of the tested agent						
	K. pneumoniae ATCC BAA-1705 KPC-2(+)	*E. coli 76* KPC-2(+)	*K. pneumoniae* 81 KPC-3(+)	*K. pneumoniae* 83 KPC-3(+), CTX-M-3(+)	*E. coli* 77 CMY-2(+)	*P. aeruginosa* MUW 700 AmpC(+)	*P. aeruginosa* 1204 VIM(+)
	MEM	MEM	MEM	MEM	CAZ	CAZ	MEM
without agent	32	64	16	32	64	128	64
PBA	**8**/16/16	**16/16/16**	8/8/8	**8/8**/16	**8/16**/32	**8/8/16**	64/64/64
1a	**4/8**/16	**8/16**/32	**1/2**/8	**4**/16/16	**8/16**/32	**8/16/32**	64/64/64
1b	**8**/16/16	**16/16**/32	**1/4**/8	**8**/16/32	**4/8/16**	**16/16/32**	64/64/64
1c	16/32/32	32/32/64	8/16/16	32/32/32	**4/8/16**	**16/32**/64	64/64/64
1d	**8**/16/16	**16**/32/32	**1/4**/8	**8**/16/32	**8/16/16**	**32**/64/64	64/64/64
1e	**8**/16/16	**16**/32/32	**4**/8/8	**8**/16/32	**2/4/8**	**32/32**/64	64/64/64
1f	16/32/32	32/64/64	8/16/16	16/32/32	**4/8/16**	**32**/64/64	64/64/64
1i	32/32/32	64/64/64	16/16/16	32/32/32	32/32/32	64/64/64	64/64/64
2a	16/16/16	32/32/64	8/8/16	**4**/16/16	**8/16/16**	**16/16/32**	64/64/64
2b	16/16/16	32/32/32	8/8/16	**8**/16/16	**4/8/16**	**32/32**/64	64/64/64
2c	32/32/32	64/64/64	16/16/16	16/16/32	**8/8/16**	**16/32/32**	64/64/64
2d	32/32/32	64/64/64	16/16/16	16/16/16	**4/8/16**	**32/32**/64	64/64/64
2e	32/32/32	64/64/64	16/16/16	32/32/32	32/32/32	128/128/128	64/64/64
2f	32/32/32	64/64/64	8/16/16	16/16/16	32/64/64	64/64/128	64/64/64
2g	32/32/32	64/64/64	16/16/16	32/32/32	32/64/64	64/64/128	64/64/64
3a	**4/8**/16	**4/8/16**	**0.5/1/2**	**0.5/2/8**	**16**/32/32	**32**/64/128	64/64/64
3b	16/32/32	32/64/64	8/8/16	16/16/16	**16**/32/32	**32**/64/128	64/64/64
3c	16/16/16	**16**/32/32	**2/2/4**	**4/8/8**	32/32/32	128/128/128	64/64/64
3d	32/32/32	64/64/64	16/16/16	32/32/32	32/32/64	128/128/128	64/64/64
3e	32/32/32	64/64/64	8/16/16	16/16/16	64/64/64	128/128/128	64/64/64
4a	16/32/32	64/64/64	8/8/8	16/16/32	64/64/64	128/128/128	64/64/64
4b	16/16/32	32/32/64	**4**/8/8	16/16/32	**16**/32/32	**16/32**/64	64/64/64
5a	32/32/32	64/64/64	16/16/16	16/16/16	**16**/32/32	**16/32**/64	64/64/64
5c	32/32/32	64/64/64	16/16/16	16/16/16	**16**/32/32	**32**/64/64	64/64/64
7a	**8**/16/16	**16**/32/32	**1/4/4**	**4**/16/16	**2/4/8**	**8/16/32**	64/64/64
7c	16/32/32	64/64/64	8/16/16	32/32/32	64/64/64	128/128/128	64/64/64

MEM - meropenem; CAZ- ceftazidime; PBA - phenylboronic acid; The significant decreases (at least a 4-fold) in the antibiotic MIC values after the addition of a tested agent are shown in boldface.

* Agents **1g**, **1h**, **1j**, **1k**, **1l**, **5b**, **6a**, and **7b** were not tested in combinations with antibiotics against β-lactamase-producing Gram-negative strains due to negative results in the combination disc tests.

Table S7. The effect of agents **1a**, **2a** and **3a** on the activity of KPC-3 in the purified protein extract from *E. coli* 82 TR(pl 81) cells, visualized by the nitrocefin hydrolysis test.

Agent concentration in mg/L	Relative absorbance[1] (% Relative absorbance)[2] [Reduction of relative absorbance in %][3]			
	PBA[4]	**1a**	**2a**	**3a**
1st repetition				
0	1.986 (100%)	1.832 (100%)	1.866 (100%)	1.912 (100%)
4	1.093 (55%) [45%]	1.348 (74%) [26%]	1.605 (86%) [14%]	1.451 (76%) [24%]
8	1.117 (56%) [44%]	1.201 (66%) [34%]	1.528 (82%) [18%]	1.249 (65%) [35%]
16	0.957 (48%) [52%]	1.076 (59%) [41%]	1.280 (69%) [31%]	1.077 (56%) [44%]
2nd repetition				
0	2.007 (100%)	1.762 (100%)	1.823 (100%)	1.973 (100%)
4	1.087 (54%) [46%]	1.320 (75%) [25%]	1.649 (90%) [10%]	1.436 (73%) [27%]
8	1.183 (59%) [41%]	1.214 (69%) [31%]	1.520 (83%) [17%]	1.305 (66%) [34%]
16	0.975 (49%) [51%]	0.998 (57%) [43%]	1.377 (76%) [24%]	1.090 (55%) [45%]
3rd repetition				
0	2.07 (100%)	1.826 (100%)	1.851 (100%)	1.968 (100%)
4	1.232 (60%) [40%]	1.308 (72%) [28%]	1.595 (86%) [14%]	1.174 (60%) [40%]
8	1.165 (56%) [44%]	1.079 (59%) [41%]	1.499 (81%) [19%]	1.279 (65%) [35%]
16	0.933 (45%) [55%]	1.066 (58%) [42%]	1.274 (69%) [31%]	1.114 (57%) [43%]

[1] The presence of β-lactamases in the purified protein extract with and without tested agents was assessed by measurement of the rates of nitrocefin hydrolysis as relative absorbance at 486 nm. The level of measured absorbance indicating β-lactamase activity.

[2] Percentage of the relative absorbance measured for the purified protein extract with tested agent in comparison to the absorbance determination without this agent.

[3] Reduction of the relative absorbance level was calculated as the difference in the relative absorbance between the positive control and the sample each concentration of tested inhibitor and expressed as a percentage.

[4] PBA (phenylboronic acid) was used as the reference β-lactamase inhibitor.

3. Cytotoxic activity

Table S8. Viability of MRC-5 cells (% of viable cells ± SD) after 72 h-treatment with the studied compounds. The results were calculated from the MTT-based assay data.

Compound	Concentration of compound [mg/L]		
	12.5	**25**	**50**
1a*	112.8±12.5	103.2±11.8	89.9±11.4
1b	140.4±6.7	140.1±8.3	117.0±1.3
1c	111.5±3.8	102.8±3.0	96.7±3.3
1d	111.6±1.1	104.1±8.9	83.3±1.2
1e	107.1± 3.3	105.0±10.0	116.6±4.6
1f	97.4±2.2	89.9±1.9	78.1±0.9
1g	104.2±8.2	107.4±9.2	98.7±5.8
1h	101.3±4.3	104.1±5.0	98.8±3.2
1i	122.3±0.0	113.9±4.8	101.4±0.9
1j	125.3±2.8	117.4±1.2	88.6±3.5
1k	84.3±0.9	74.2±3.5	28.9±1.0
1l	109.5±1.6	114.4±1.8	105.1±7.8
2a	94.4±2.2	75.2±10.3	73.1±13.6
2b	108.0±1.1	87.9±1.7	73.8±1.9
2c	89.1±0.5	83.6±2.7	63.8±2.5
2d	107.1±7.6	88.0±4.3	75.2±9.4
2e	96.6±6.4	84.4±4.8	63.1±1.4
2f	103.3±8.8	92.1±0.9	76.2±0.7
2g	111.3±9.7	117.3±3.7	103.4±5.1
3a*	109.6±9.3	106.3±10.6	76.2±4.2
3b	98.1±6.1	91.2 ± 13.5	87.1 ± 8.0
3c	97.1±6.9	105.5±4.5	82.3±12.9
3d	91.3±7.4	100.0 ±7.7	77.7±15.5
3e	98.8±25.6	92.9±2.7	64.4±0.4
4a	101.9±6.9	84.4±6.4	87.9±8.5
4b	114.0±1.8	106.4±0.1	97.3±13.6
5a	88.6±9.2	87.1±1.6	79.2±5.1
5b	101.1±7.7	110.3±2.7	87.3±13.6
5c	102.5±3.4	97.9±1.4	85.6±0.7
6a	138.3±3.6	133.5±0.7	127.2±2.6
7a	83±2.9	79.9±3.7	67.3±3.1
7b	48.9±3.8	6.4±1.4	0.9±0.7
7c	56.4±3.0	6.6±5.1	0±0.1
PBA	81.5 ± 3.7	79.1 ± 4.4	58.7 ± 4.3

* the data were obtained for the following concentrations of compound: 16, 32 and 64 mg/L. PBA (phenylboronic acid) was used as the reference β-lactamase inhibitor.

5. References

69. Charzewski, Ł.; Krzyśko, K.A.; Lesyng, B. Exploring covalent docking mechanisms of boron-based inhibitors to class A, C and D β-lactamases using time-dependent hybrid QM/MM simulations. Front. Mol. Biosci. 2021, 8, 633181, DOI:https://doi.org/10.3389/fmolb.2021.63318175.
75. Clinical and Laboratory Standards Institute (CLSI). Methods for dilution antimicrobial susceptibility tests for bacteria that grow aerobically. Approved Standard, CLSI Dokument M07-A9. 9th ed. CLSI: Wayne, PA, USA 2012.
84. Chemical Computing Group ULC, Molecular Operating Environment (MOE). 1010 Sherbrooke St.West 910, Montreal, QC, Canada, 2018. Available online: https://www.chemcomp.com/Products.htm (accessed on 1 October 2023).
94. Ren, Y.; Bazan, G.C. Trifluoromethyl-substituted conjugated oligoelectrolytes. Chemistry 2010, 16, 11028-11036, doi:https://doi.org/10.1002/chem.201000885.
95. ETEST. Application guide. Available online: https://www.biomerieux-usa.com/sites/subsidiary_us/files/supplementary_inserts_-_16273_-_b_-_en_-_eag_-_etest_application_guide-3.pdf (accessed on 1 October 2023)
96. Espinel-Ingroff, A. Etest for antifungal susceptibility testing of yeasts. Diagn. Microbiol. Infect. Dis. 1994, 19, 217-220, doi:10.1016/0732-8893(94)90034-5.
97. Pfaller, M.A.; Bale, M.; Buschelman, B.; Lancaster, M.; Espinel-Ingroff, A.; Rex, J.H.; Rinaldi, M.G. Selection of candidate quality control isolates and tentative quality control ranges for in vitro susceptibility testing of yeast isolates by National Committee for Clinical Laboratory Standards proposed standard methods. J. Clin. Microbiol. 1994, 32, 1650-1653, doi:10.1128/jcm.32.7.1650-1653.1994.
98. European Committee on Antimicrobial Susceptibility Testing. Reading guide. EUCAST disk diffusion method for antimicrobial susceptibility testing. Document version 9.0. Available online: https://www.eucast.org/fileadmin/src/media/PDFs/EUCAST_files/Disk_test_documents/2022_manuals/Reading_guide_v_9.0_EUCAST_Disk_Test_2022.pdf (accessed on 1 October 2023)

Kompletne *Supplementary Materials* do **Publikacji O4** dostępne są pod adresem:
https://www.mdpi.com/article/10.3390/molecules28217362/s1

8. Podsumowanie

Narastająca w ostatnich latach oporność drobnoustrojów i postępująca utrata skuteczności znanych antybiotyków, której towarzyszy niedostateczna liczba nowych leków przeciwdrobnoustrojowych wprowadzanych do obrotu oraz przechodzących badania kliniczne stanowi poważne zagrożenie dla zdrowia publicznego. Konieczne są zarówno działania prowadzące do spowolnienia zjawiska narastania oporności na znane antybiotyki (m. in. opracowanie schematów dawkowania ograniczających selekcję lekoopornych mutantów) jak i poszukiwanie nowych, najlepiej innowacyjnych substancji aktywnych wobec wielolekoopornych drobnoustrojów, zwłaszcza tych ujętych na listach patogenów priorytetowych WHO. W badaniach przedklinicznych niezbędne jest także zwiększenie precyzji metod *in vitro* charakteryzujących potencjał związków do selekcjonowania oporności *in vivo*, w celu typowania do dalszych prac kandydata na potencjalny lek w jak najmniejszym stopniu narażonego w przyszłości na szybką utratę skuteczności klinicznej.

W niniejszej pracy poszukiwano substancji o aktywności przeciwdrobnoustrojowej wśród nowo otrzymanych benzosiloksaboroli i pokrewnych heterocykli o rozszerzonym pierścieniu (44 związki) oraz kwasów aryloboronowych (33 związki), głównie di- oraz triboronowych. Opracowano także nowe podejście do oceny potencjału selekcjonowania oporności przez związki przeciwbakteryjne.

I. <u>Podsumowanie poszukiwań nowych związków o aktywności przeciwdrobnoustrojowej</u>

1. Wykazano wysoką, porównywalną z linezolidem bezpośrednią aktywność przeciwgronkowcową 18 z 44 badanych benzosiloksaboroli, w tym: 16 pochodnych benzenosulfonianowych (zakres wartości MIC 0,39–3,12 mg/l) oraz 2 pochodnych sulfonamidowych (zakres wartości MIC 3,12– 6,25 mg/l). Wysoką aktywność benzosiloksaboroli sulfonamidowych potwierdzono także wobec pięciu klinicznych szczepów MRSA (zakres wartości MIC 3,12–6,25 mg/l). Ponadto wykazano wysoką aktywność przeciwenterokokową 3 benzosiloksaboroli benzenosulfonianowych (MIC 6,25 mg/l) oraz aktywność od umiarkowanej po niską wobec ziarenkowców Gram-dodatnich kolejnych 10 benzosiloksaboroli (zakres wartości MIC 12,5–>400 mg/l). Jednocześnie stwierdzono, że badane beznzosiloksaborole nie wykazują istotnej aktywności

bezpośredniej wobec grzybów drożdżopodobnych ani bakterii Gram-ujemnych oraz w większości (31 z 44 badanych związków) nie są substratami dla pomp błonowych bakterii Gram-ujemnych.

2. Zaobserwowano, że aktywność benzosiloksaboroli benzenosulfonianowych wobec ziarenkowców Gram-dodatnich nasila się w obecności w pierścieniu benzenowym atomu chloru lub grupy trifluorometylowej w pozycji *para*, obu tych podstawników lub dwóch atomów chloru w pozycji *para* i *meta* lub trzech grup metylowych w pozycji 2, 4 i 6. Pochodne takie wykazywały wyższą niż linezolid aktywność wobec szczepów *S. aureus* - wartości MIC dla MSSA w zakresie 0,39–0,78 mg/l (MIC linezolidu 1 mg/l), a dla MRSA w zakresie 0,39–1,56 mg/l (MIC linezolidu 2 mg/l). Były one również wysoce aktywne wobec enterokoków (MIC 6,25 mg/l). Z kolei benzosiloksaborole benzenosulfonianowe niepodstawione przy pierścieniu beznenowym lub podstawione fluorem, bromem, jodem, jedną grupą metylową, nitrową, metoksylową, acetylową lub tert-butylową wykazywały aktywność wobec szczepów *S. aureus* porównywalną lub mniejszą niż linezolid (zakres wartości MIC 1,56–3,12 mg/l) oraz umiarkowaną wobec enterokoków (wartości MIC 12,5–50 mg/l).
3. Na podstawie dokonanego przeglądu piśmiennictwa dotyczącego właściwości przeciwdrobnoustrojowych benzoksaboroli wskazano syntetazę leucylo-tRNA (LeuRS) jako prawdopodobny punkt uchwytu otrzymanych benzosiloksaboroli. Analiza wyników badań mikrobiologicznych pozwoliła na wytypowanie najbardziej aktywnych związków do dalszych badań *in silico*. Były to dwa benzosiloksaborole sulfonamidowe (**3e** i **3f**) o wysokiej bezpośredniej aktywności przeciwgronkowcowej (MIC 3,12–6,25 mg/l) i dwa benzosiloksaborole (**3a** i **3d**) o niskiej aktywności wobec gronkowców (MIC 50–200 mg/l). Wykonane przez zewnętrzną jednostkę dokowanie molekularne potwierdziło, że najbardziej aktywne związki mogą tworzyć stabilne addukty z LeuRS i wiązać się do jej miejsca aktywnego. Zatem bezpośrednia aktywność wobec ziarenkowców Gram-dodatnich wykazana w niniejszej pracy wynika najprawdopodobniej z wiązania się badanych benzosiloksaboroli z enzymem LeuRS.
4. Wykazano wysoką bezpośrednią aktywność przeciwgronkowcową kwasu 2-fluoro-5-trifluorometylo-1,3-fenylenodiboronowego (zakres wartości MIC

0,78–12,5 mg/l) oraz aktywność przeciwgrzybiczą od wysokiej po umiarkowaną wobec szczepów *Candida* spp. kwasu 4-trifluorometylo-1,2-fenylenodiboronowego (zakres wartości MIC 3,12–25 mg/l). Ponadto stwierdzono, że wśród 33 badanych kwasów aryloboronowych bezpośrednią aktywność przeciwdrobnoustrojową od umiarkowanej po niską (zakres wartości MIC 12,5–>400 mg/l) wobec bakterii Gram-dodatnich wykazuje 25 pochodnych, wobec bakterii Gram-ujemnych 19 pochodnych, a wobec grzybów drożdżopodobnych 21 pochodnych. Badane kwasy aryloboronowe w większości (29 z 33 związków) nie są substratami dla błonowych pomp MDR bakterii Gram-ujemnych.

5. Stwierdzono, że wśród 33 badanych kwasów aryloboronowych 25 pochodnych wykazuje aktywność BLI w wysokich stężeniach (30–300 μg/krążek). Spośród nich 17 związków wykazuje aktywność BLI także w niskich stężeniach (4–16 mg/l), porównywalnych ze stężeniami, w których stosowane są najnowsze inhibitory β-laktamaz (waborbaktam, awibaktam oraz relebaktam). Spośród 17 związków, które w niskich stężeniach miały aktywność BLI, 16 pochodnych zwiększało wrażliwość na ceftazydym AmpC-dodatnich szczepów *E. coli* i *P. aeruginosa,* a 7 związków zwiększało wrażliwość na karbapenemy KPC-dodatnich szczepów *K. pneumoniae* oraz *E. coli.* W szczególności stwierdzono, że:
    a. Aktywność BLI w niskich stężeniach wykazują wyłącznie niepodstawione kwasy aryloboronowe oraz ich fluorowe pochodne.
    b. Kwas *orto*-fenylenodiboronowy wśród badanych związków wykazuje najwyższą aktywność BLI wobec szczepów KPC-dodatnich – osiągnięto nawet 64/16/8-krotne redukcje wartości MIC karbapenemów dla tych szczepów odpowiednio przy jego stężeniach 16/8/4 mg/l. Przywrócił on wrażliwość na meropenem wszystkim czterem badanym szczepom KPC-dodatnim, a na imipenem 3 z 4 badanych szczepów. Związek ten wykazywał także aktywność BLI w niskich stężeniach wobec szczepów AmpC-dodatnich (osiągnięto maksymalnie 4/2/2-krotne redukcje wartości MIC ceftazydymu odpowiednio przy jego stężeniach 16/8/4 mg/l), nie przywrócił on jednak wrażliwości tych szczepów na ceftazydym.

c. Kwas *para*-fenylenodiboronowy w niskich stężeniach wykazuje zarówno aktywność BLI wobec szczepów KPC-dodatnich (przywrócił wrażliwość na meropenem wszystkim czterem badanym szczepom, a na imipenem 3 z 4 badanych szczepów) jak i wobec szczepów AmpC-dodatnich (przywrócił wrażliwość na ceftazydym obu badanym szczepom).
d. Kwasy *meta*-fenylenodiboronowe w niskich stężeniach wykazują aktywność BLI jedynie wobec szczepów AmpC-dodatnich – przywracają wrażliwość na ceftazydym szczepowi *E. coli* CMY-2-dodatniemu oraz zwiększają wrażliwość szczepu *P. aeruginosa* cAmpC-dodatniego na ceftazydym (nawet 8/8/4-krotnie odpowiednio przy ich stężeniach 16/8/4 mg/l), nie przywracając jednak jego wrażliwości na ten antybiotyk.
e. Kwasy tiofenoboronowe oraz kwas fenyleno-1,2,4-triboronowy w niskich stężeniach wykazują aktywność BLI jedynie wobec szczepów AmpC-dodatnich – powodują maksymalnie 4/2/2-krotne redukcje wartości MIC ceftazydymu odpowiednio przy ich stężeniach 16/8/4 mg/l, nie przywracając jednak wrażliwości na ceftazydym żadnemu z badanych szczepów AmpC-dodatnich.

6. W badaniach z wykorzystaniem całych komórek oraz wyizolowanych białek całkowitych transformanta *E. coli* DH5α niosącego gen bla_{KPC-3} potwierdzono, że enzymy typu KPC są celem molekularnym dla kwasów *orto*- i *para*- ale nie *meta*-fenyleonodiboronowych. Kwasy *orto*- i *para*-fenylenodiboronowe w stężeniach 16/8/4 mg/l redukowały wartości MIC meropenemu badanego transformanta odpowiednio 32/16/4-krotnie oraz 16/8/4-krotnie, a kwas *meta*-fenylenodiboronowy maksymalnie 2-krotnie. Ponadto w teście hydrolizy nitrocefiny uzyskano redukcje absorbancji dla białek całkowitych transformanta w obecności kwasów *orto*-, *para*- i *meta*-fenylenodiboronowych w porównaniu do kontroli pozytywnej. Redukcja absorbancji wynosiła przy obecności w/w kwasów fenylenodiboronowych odpowiednio 44/42/29% przy stężeniu 16 mg/l oraz 35/35/18% przy stężeniu 8 mg/l. Symulacje QM/MM przeprowadzone następnie przez zespoły z Uniwersytetu Warszawskiego i Politechniki Warszawskiej wykazały, że kwas *orto*-fenylenodiboronowy najczęściej i najszybciej spośród badanych związków osiągał konfigurację pozwalającą na przeprowadzenie addycji nukleofilowej w sprzyjających warunkach do KPC-2.

7. Metodą szachownicy wyznaczono w sumie 34 wartości FICI dla kombinacji z ceftazydymem 17 aromatycznych kwasów boronowych (i PBA) o aktywności BLI w niskich stężeniach wobec szczepów AmpC-dodatnich oraz 96 wartości FICI dla kombinacji z 3 karbapenemami (meropenem, imipenem oraz ertapenem) 7 kwasów fenyloboronowych o aktywności BLI w niskich stężeniach wobec szczepów KPC-dodatnich. Następnie przeprowadzono analizę statystyczną, która pozwoliła na udowodnienie, że:
    a. synergia z karbapenemami jest istotnie silniejsza w przypadku kwasów *orto*-fenylenodiboronowych niż w przypadku kwasów *para*-fenylenodiboronowych i fenyloboronowych (w obu przypadkach p=0,0001);
    b. synergia kwasów fenyloboronowych z karbapenemami jest istotnie silniejsza wobec szczepów KPC-3-dodatnich niż wobec szczepów KPC-2-dodatnich (p=0,046);
    c. synergia z ceftazydymem jest istotnie słabsza w przypadku kwasów *orto*-fenylenodiboronowych niż kwasów *meta*-fenylenodiboronowych (p=0,04) oraz fenyloboronowych (p=0,008);
    d. wprowadzenie podstawnika fluorowego nasila synergię działania kwasów aryloboronowych z ceftazydymem wobec szczepów CMY-2-dodatnich (p=0,005) oraz osłabia synergię kwasów fenyloboronowych z karbapenemami wobec szczepów KPC-dodatnich (p=0,036).

II. Podsumowanie prac nad nowym podejściem do oceny potencjału do selekcjonowania oporności bakterii przez związki przeciwbakteryjne

1. Opracowano nowe parametry *in vitro* charakteryzujące potencjał związków do selekcjonowania oporności:
    a. parametry MPC-D i MSW-D odnoszące się do tzw. dominujących mutantów (selekcjonowanych z dużą częstością, bez znaczących zmian w sprawności w porównaniu do komórek typu dzikiego, co do których istnieje wysokie prawdopodobieństwo, że będą one w stanie ustanowić oporną populację *in vivo*);
    b. parametry MPC-F i MSW-F odnoszące się do mutantów o obniżonej sprawności, które mogą powstać *in vitro,* ale jest mało prawdopodobne by były selekcjonowane *in vivo*.

2. Nowością pracy jest także powiązanie wartości klasycznego MPC z częstością selekcji opornych mutantów w metodzie rozcieńczeń w agarze co ma miejsce w opracowanej metodyce wyznaczania wartości nowego parametru MPC-D. Zaproponowano by w metodzie rozcieńczeń w agarze wartość MPC-D wyznaczać jako najmniejsze stężenie, dla którego wartość FSMS wynosi $<10^{-10}$, co jest kluczowe dla zwiększenia powtarzalności tego parametru (MPC-D) w porównaniu do oryginalnej wartości MPC (bowiem mutanty rzadziej powstające, nie zawsze mogą być wykryte w trakcie badań *in vitro*).
3. Aby zwiększyć zgodność zakresów MSW wyznaczanych *in vitro* z zakresami obserwowanymi później *in vivo*, zaproponowano wyznaczanie wartości MPC-D oraz MPC-F nową metodą rozcieńczeń związku w bulionie. W tej metodzie MPC-D zdefiniowano jako najniższe stężenie leku, które uniemożliwia lekoopornym mutantom selekcjonowanych spośród 10^{10} CFU ustanowienie opornej populacji o gęstości co najmniej 10 CFU/ml w trakcie 24-godzinnej inkubacji w podłożu płynnym ze związkiem. Natomiast MPC-F zdefiniowano jako najniższe stężenie leku całkowicie hamujące selekcję opornych mutantów po 24-godzinnej inkubacji w podłożu płynnym ze związkiem.
4. Wyznaczono parametry MPC i MPC-D cyprofloksacyny, linezolidu i nowego benzosiloksaborolu No37 dla szczepu *S. aureus* ATCC 29213 metodą rozcieńczeń w agarze oraz parametry MPC-D i MPC-F metodą rozcieńczeń w bulionie. Wykazano, że w przypadku niektórych antybiotyków (np. cyprofloksacyna) wartości MPC-D mogą być niższe niż wartości MPC, przez co bardziej akceptowalne klinicznie jako podstawa schematów dawkowania. Natomiast w przypadku innych związków (np. linezolid, benzosiloksaborol No37) wartości MPC-D są równe wartościom MPC.
5. Opracowano nową metodę otrzymywania inokulum bakteryjnego o wysokiej gęstości ($>10^{11}$ CFU/ml), polegającą na wielostopniowym zagęszczaniu hodowli płynnej. Wyjściowe inokula szczepu *S. aureus* ATCC 29213, uzyskane nową metodą, miały gęstości $5–7{,}5 \times 10^{11}$ CFU/ml, co jest kluczowe przy wyznaczaniu parametrów MPCs.

9. Wnioski

1. Uzyskane wyniki bezpośredniej aktywności przeciwgronkowcowej i przeciwenterokokowej benzosiloksaboroli benzenosulfonianowych oraz sulfonamidowych, które są porównywalne lub wyższe niż aktywność linezolidu (także wobec klinicznych szczepów MRSA) wskazują, iż benzosiloksaborole są innowacyjną grupą związków o obiecującej, bezpośredniej aktywności wobec ziarenkowców Gram-dodatnich. Ich prawdopodobnym punktem uchwytu jest syntetaza leucylo-tRNA.

2. Na podstawie uzyskanych wyników badań mikrobiologicznych wysnuto wnioski dotyczące korelacji struktura-aktywność bezpośrednia benzosiloksaboroli. Kluczowe znaczenie dla uzyskania wysokiej aktywności benzosiloksaboroli wobec ziarenkowców Gram-dodatnich ma obecność w cząsteczce ugrupowania benzenosulfonianowego lub sulfonamidowego. Aktywność benzosiloksaboroli benzenosulfonianowych nasila obecność w pierścieniu benzenowym podstawnika chloru lub grupy trifluorometylowej w pozycji *para*, obu tych podstawników lub dwóch atomów chloru w pozycji *para* i *meta* lub trzech grup metylowych w pozycji 2, 4 i 6. Uzyskane analizy wskazują na celowość prowadzenia w przyszłości dalszych ukierunkowanych już syntez związków o określonych strukturach, tak aby uzyskać najwyższą aktywność przeciwdrobnoustrojową.

3. Wyniki szerokospektralnych i pogłębionych badań mikrobiologicznych, wskazują iż kwasy fenylenodiboronowe są obiecującymi strukturami wyjściowymi do projektowania pochodnych o aktywności inhibitorów β-laktamaz typu KPC/AmpC. Wprowadzenie do cząsteczki kwasu fenyloboronowego dodatkowej grupy boronowej w pozycji *orto* istotnie zwiększa siłę synergistycznego oddziaływania tego związku z karbapenemami wobec szczepów KPC-dodatnich choć osłabia synergię z ceftazydymem wobec szczepów AmpC-dodatnich. Z kolei obecność fluoru w cząsteczce kwasów aryloboronowych osłabia synergię działania tych kwasów z karbapenemami, ale nasila synergię z ceftazydymem.

4. Wykazana w pracy wysoką aktywność kwasów fenylenodiboronowych jako inhibitorów enzymów typu KPC/AmpC, w połączeniu z ich brakiem

cytotoksyczności w aktywnym zakresie stężeń oraz cytotoksycznością PBA w tym samym zakresie stężeń, pozwala stwierdzić iż kwasy fenylenodiboronowe mogą być postrzegane jako lepsze niż PBA struktury wyjściowe do syntezy nowych, innowacyjnych inhibitorów β-laktamaz bakterii Gram-ujemnych, zwłaszcza enzymów typu KPC.

5. Zaproponowany w niniejszej pracy, nowy parametr MPC-D, dzięki swojemu powiązaniu z częstością selekcji opornych mutantów *in vitro,* powinien charakteryzować się lepszą powtarzalnością niż parametr MPC. Ma również szansę być bardziej akceptowalny klinicznie jako podstawa schematów dawkowania, bowiem dla niektórych kombinacji antybiotyk-szczep wartość MPC-D jest niższa niż wartość MPC. Wyznaczanie wartości MPC-D za pomocą nowej metody rozcieńczeń w bulionie może zwiększyć zgodność zakresów MSW wyznaczanych *in vitro* z tymi obserwowanymi *in vivo*, dzięki możliwości zróżnicowania lekoopornych mutantów otrzymywanych *in vitro* na mutanty zdolne do dominowania w populacji i te zdolne jedynie do przeżycia w obecności związku.

10. Bibliografia

1. Chew, M.; Sharrock, K. Medical milestones: celebrating key advances since 1840. *BMJ* **2007**, *334 (suppl)*, 1-22.
2. Kardos, N.; Demain, A.L. Penicillin: the medicine with the greatest impact on therapeutic outcomes. *Appl. Microbiol. Biotechnol.* **2011**, *92*, 677-687, doi:10.1007/s00253-011-3587-6.
3. Walesch, S.; Birkelbach, J.; Jézéquel, G.; Haeckl, F.P.J.; Hegemann, J.D.; Hesterkamp, T.; Hirsch, A.K.H.; Hammann, P.; Müller, R. Fighting antibiotic resistance-strategies and (pre)clinical developments to find new antibacterials. *EMBO Rep.* **2023**, *24*, e56033, doi:10.15252/embr.202256033.
4. Antimicrobial Resistance Collaborators. Global burden of bacterial antimicrobial resistance in 2019: a systematic analysis. *Lancet* **2022**, *399*, 629-655, doi:10.1016/s0140-6736(21)02724-0.
5. Banerjee, S.; Denning, D.W.; Chakrabarti, A. One Health aspects & priority roadmap for fungal diseases : A mini-review. *Indian. J. Med. Res.* **2021**, *153*, 311-319, doi:10.4103/ijmr.IJMR_768_21.
6. O'Neill, J. Tackling drug-resistant infections globally: final report and recommendations. Government of the United Kingdom Report **2016.** Dostępne online: https://apo.org.au/node/63983 (16-11-2023)
7. World Health Organization. Antimicrobial resistance: global report on surveillance. Dostępne online: https://apps.who.int/iris/handle/10665/112642 (16-11-2023).
8. World Health Organization. Global action plan on antimicrobial resistance. Dostępne online: http://www.wpro.who.int/entity/drug_resistance/resources/global_action_plan_eng.pdf (16-11-2023).
9. Martínez, J.L.; Coque, T.M.; Baquero, F. What is a resistance gene? Ranking risk in resistomes. *Nat. Rev. Microbiol.* **2015**, *13*, 116-123, doi:10.1038/nrmicro3399.
10. Clinical and Laboratory Standards Institute (CLSI). Methods for dilution antimicrobial susceptibility tests for bacteria that grow aerobically. Approved Standard, 9th ed., CLSI guideline M07-A9, CLSI: Wayne, PA, USA, **2012**.
11. European Committee on Antimicrobial Susceptibility Testing. Method for the determination of broth dilution MIC of antifungal agents for yeasts. Document E.DEF 7.3.2. **2020**.
12. European Committee on Antimicrobial Susceptibility Testing. Breakpoint tables for interpretation of MICs and zone diameters. Version 13.0. **2023**.
13. European Committee on Antimicrobial Susceptibility Testing. Breakpoint tables for interpretation of MICs for antifungal agents. Version 10.0. **2020**.
14. Clinical and Laboratory Standards Institute. Performance standards for antimicrobial susceptibility testing. 33rd edition. CLSI guideline M100-ED33. CLSI: Wayne, PA, USA, **2023**.
15. Clinical and Laboratory Standards Institute. Performance standards for antifungal susceptibility testing of yeasts, 3rd edition. CLSI guideline M27M44S-ED3. CLSI: Wayne, PA, USA, **2022**.

16. Baker, S.; Thomson, N.; Weill, F.X.; Holt, K.E. Genomic insights into the emergence and spread of antimicrobial-resistant bacterial pathogens. *Science (New York, N.Y.)* **2018**, *360*, 733-738, doi:10.1126/science.aar3777.

17. Liu, G.; Thomsen, L.E.; Olsen, J.E. Antimicrobial-induced horizontal transfer of antimicrobial resistance genes in bacteria: a mini-review. *J. Antimicrob. Chemother.* **2022**, *77*, 556-567, doi:10.1093/jac/dkab450.

18. Martinez, J.L.; Baquero, F. Mutation frequencies and antibiotic resistance. *Antimicrob. Agents. Chemother.* **2000**, *44*, 1771-1777, doi:10.1128/aac.44.7.1771-1777.2000.

19. Schroeder, J.W.; Yeesin, P.; Simmons, L.A.; Wang, J.D. Sources of spontaneous mutagenesis in bacteria. *Crit. Rev. Biochem. Mol. Biol.* **2018**, *53*, 29-48, doi:10.1080/10409238.2017.1394262.

20. Kivisaar, M. Mutation and recombination rates vary across bacterial chromosome. *Microorganisms* **2019**, *8*, doi:10.3390/microorganisms8010025.

21. Drlica, K. The mutant selection window and antimicrobial resistance. *J. Antimicrob. Chemother.* **2003**, *52*, 11-17, doi:10.1093/jac/dkg269.

22. Igler, C.; Rolff, J.; Regoes, R. Multi-step vs. single-step resistance evolution under different drugs, pharmacokinetics, and treatment regimens. *Elife* **2021**, *10*, doi:10.7554/eLife.64116.

23. Magiorakos, A.P.; Srinivasan, A.; Carey, R.B.; Carmeli, Y.; Falagas, M.E.; Giske, C.G.; Harbarth, S.; Hindler, J.F.; Kahlmeter, G.; Olsson-Liljequist, B.; et al. Multidrug-resistant, extensively drug-resistant and pandrug-resistant bacteria: an international expert proposal for interim standard definitions for acquired resistance. *Clin. Microbiol. Infect.* **2012**, *18*, 268-281, doi:10.1111/j.1469-0691.2011.03570.x.

24. Denning, D.W. Antifungal drug resistance: an update. *Eur. J. Hosp. Pharm.* **2022**, *29*, 109-112, doi:10.1136/ejhpharm-2020-002604.

25. Nesme, J.; Simonet, P. The soil resistome: a critical review on antibiotic resistance origins, ecology and dissemination potential in telluric bacteria. *Environ. Microbiol.* **2015**, *17*, 913-930, doi:10.1111/1462-2920.12631.

26. Revitt-Mills, S.A.; Robinson, A. Antibiotic-induced mutagenesis: under the microscope. *Front. Microbiol.* **2020**, *11*, 585175, doi:10.3389/fmicb.2020.585175.

27. Stennett, H.L.; Back, C.R.; Race, P.R. Derivation of a precise and consistent timeline for antibiotic development. *Antibiotics (Basel)* **2022**, *11*, doi:10.3390/antibiotics11091237.

28. Hutchings, M.I.; Truman, A.W.; Wilkinson, B. Antibiotics: past, present and future. *Curr. Opin. Microbiol.***2019**, *51*, 72-80,

    doi: 10.1016/j.mib.2019.10.008.

29. Abraham, E.P.; Chain, E. An enzyme from bacteria able to destroy penicillin. 1940. *Rev. Infect. Dis.* **1988**, *10*, 677-678.

30. Mendes, R.E.; Paukner, S.; Doyle, T.B.; Gelone, S.P.; Flamm, R.K.; Sader, H.S. Low prevalence of Gram-positive isolates showing elevated lefamulin MIC results during the SENTRY Surveillance Program for 2015-2016 and characterization of

resistance mechanisms. *Antimicrob. Agents. Chemother.* **2019**, *63*, doi: 10.1128/aac.02158-18.

31. Chavers, L.S.; Moser, S.A.; Benjamin, W.H.; Banks, S.E.; Steinhauer, J.R.; Smith, A.M.; Johnson, C.N.; Funkhouser, E.; Chavers, L.P.; Stamm, A.M.; et al. Vancomycin-resistant enterococci: 15 years and counting. *J. Hosp. Infect.* **2003**, *53*, 159-171, doi:10.1053/jhin.2002.1375.
32. Hammoudi Halat, D.; Ayoub Moubareck, C. The current burden of carbapenemases: review of significant properties and dissemination among Gram-negative bacteria. *Antibiotics (Basel)* **2020**, *9*, 186, doi: 10.3390/antibiotics9040186.
33. Quinn, J.P.; Dudek, E.J.; DiVincenzo, C.A.; Lucks, D.A.; Lerner, S.A. Emergence of resistance to imipenem during therapy for *Pseudomonas aeruginosa* infections. *J. Infect. Dis.* **1986**, *154*, 289-294, doi:10.1093/infdis/154.2.289.
34. Klemm, E.J.; Wong, V.K.; Dougan, G. Emergence of dominant multidrug-resistant bacterial clades: lessons from history and whole-genome sequencing. *Proc. Natl. Acad. Sci. U. S. A.* **2018**, *115*, 12872-12877, doi:10.1073/pnas.1717162115.
35. Miller, R.A. A Case for antifungal stewardship. *Curr. Fungal. Infect. Rep.* **2018**, *12*, 33-43, doi:10.1007/s12281-018-0307-z.
36. Vanreppelen, G.; Wuyts, J.; Van Dijck, P.; Vandecruys, P. Sources of antifungal drugs. *J. Fungi (Basel)***2023**, *9*, 171.
37. Bush, K.; Bradford, P.A. β-Lactams and β-lactamase inhibitors: an overview. *Cold Spring Harb. Perspect. Med.* **2016**, *6*, a025247, doi: 10.1101/cshperspect.a025247.
38. World Health Organization. 2021 Antibacterial agents in clinical and preclinical development: an overview and analysis. Dostępne online: https://www.who.int/publications/i/item/9789240047655 (16-11-2023).
39. Centers for Disease Control and Prevention. Germs develop antibiotic resistance. Dostępne online: https://www.cdc.gov/drugresistance/pdf/threats-report/Select-Germs-Develop-Resistance-Over-Time.pdf (16-11-2023).
40. Maertens, J.A. History of the development of azole derivatives. *Clin. Microbiol. Infect.* **2004**, *10 Suppl 1*, 1-10, doi: 10.1111/j.1470-9465.2004.00841.x.
41. Holt, R.J.; Azmi, A. Miconazole-resistant *Candida*. *Lancet* **1978**, *1*, 50-51, doi:10.1016/s0140-6736(78)90403-8.
42. Speller, D.C.; Fakunle, F.; Cairns, S.A.; Stephens, M. Cryptococcal meningitis complicating systemic lupus erythematosus: two patients treated with flucytosine and amphotericin B. *J. Clin. Pathol.* **1977**, *30*, 254-261, doi: 10.1136/jcp.30.3.254.
43. Thomson, C.J.; Amyes, S.G. TRC-1: emergence of a clavulanic acid-resistant TEM beta-lactamase in a clinical strain. *FEMS Microbiol. Lett.* **1992**, *70*, 113-117, doi:10.1016/0378-1097(92)90669-f.
44. Castanheira, M.; Rhomberg, P.R.; Flamm, R.K.; Jones, R.N. Effect of the β-lactamase inhibitor vaborbactam combined with meropenem against serine carbapenemase-producing *Enterobacteriaceae*. *Antimicrob. Agents. Chemother.* **2016**, *60*, 5454-5458, doi:c.
45. Ito, A.; Sato, T.; Ota, M.; Takemura, M.; Nishikawa, T.; Toba, S.; Kohira, N.; Miyagawa, S.; Ishibashi, N.; Matsumoto, S.; et al. *In vitro* antibacterial properties

of cefiderocol, a novel siderophore cephalosporin, against Gram-negative bacteria. *Antimicrob. Agents. Chemother.* **2018**, *62*, doi:10.1128/aac.01454-17.

46. Zhao, X.; Drlica, K. Restricting the selection of antibiotic-resistant mutants: a general strategy derived from fluoroquinolone studies. *Clin. Infect. Dis.* **2001**, *33 Suppl 3*, S147-156, doi: 10.1086/321841.

47. Gullberg, E.; Cao, S.; Berg, O.G.; Ilbäck, C.; Sandegren, L.; Hughes, D.; Andersson, D.I. Selection of resistant bacteria at very low antibiotic concentrations. *PLoS Pathog.* **2011**, *7*, e1002158, doi: 10.1371/journal.ppat.1002158.

48. Hernando-Amado, S.; Sanz-García, F.; Blanco, P.; Martínez, J.L. Fitness costs associated with the acquisition of antibiotic resistance. *Essays Biochem.* **2017**, *61*, 37-48, doi:10.1042/ebc20160057.

49. Nilsson, A.I.; Berg, O.G.; Aspevall, O.; Kahlmeter, G.; Andersson, D.I. Biological costs and mechanisms of fosfomycin resistance in *Escherichia coli*. *Antimicrob. Agents. Chemother.* **2003**, *47*, 2850-2858, doi:10.1128/aac.47.9.2850-2858.2003.

50. Gustafsson, I.; Cars, O.; Andersson, D.I. Fitness of antibiotic resistant *Staphylococcus epidermidis* assessed by competition on the skin of human volunteers. *J. Antimicrob. Chemother.* **2003**, *52*, 258-263, doi: 10.1093/jac/dkg331.

51. Hughes, D. Selection and evolution of resistance to antimicrobial drugs. *IUBMB Life* **2014**, *66*, 521-529, doi: 10.1002/iub.1278.

52. Sanz-García, F.; Hernando-Amado, S.; Martínez, J.L. Evolution under low antibiotic concentrations: a risk for the selection of *Pseudomonas aeruginosa* multidrug-resistant mutants in nature. *Environ. Microbiol.* **2022**, *24*, 1279-1293, doi:10.1111/1462-2920.15806.

53. Sanz-García, F.; Sánchez, M.B.; Hernando-Amado, S.; Martínez, J.L. Evolutionary landscapes of *Pseudomonas aeruginosa* towards ribosome-targeting antibiotic resistance depend on selection strength. *Int. J. Antimicrob. Agents* **2020**, *55*, 105965, doi:10.1016/j.ijantimicag.2020.105965.

54. Sanz-García, F.; Hernando-Amado, S.; López-Causapé, C.; Oliver, A.; Martínez, J.L. Low ciprofloxacin concentrations select multidrug-resistant mutants overproducing efflux pumps in clinical isolates of *Pseudomonas aeruginosa*. *Microbiol. Spectr.* **2022**, *10*, e0072322, doi:10.1128/spectrum.00723-22.

55. Anderson, J.R.; Lam, N.B.; Jackson, J.L.; Dorenkott, S.M.; Ticer, T.; Maldosevic, E.; Velez, A.; Camden, M.R.; Ellis, T.N. Progressive sub-MIC exposure of *Klebsiella pneumoniae* 43816 to cephalothin induces the evolution of beta-lactam resistance without acquisition of beta-lactamase genes. *Antibiotics (Basel)* **2023**, *12*, doi:10.3390/antibiotics12050887.

56. Bengtsson-Palme, J.; Kristiansson, E.; Larsson, D.G.J. Environmental factors influencing the development and spread of antibiotic resistance. *FEMS Microbiol. Rev.* **2018**, *42*, doi:10.1093/femsre/fux053.

57. World Health Organization. WHO global strategy for containment of antimicrobial resistance. WHO/CDS/CSR/DRS/2001.2. Dostępne online: https://apps.who.int/iris/handle/10665/66860 (16-11-2023)

58. Dong, Y.; Zhao, X.; Domagala, J.; Drlica, K. Effect of fluoroquinolone concentration on selection of resistant mutants of *Mycobacterium bovis* BCG and

Staphylococcus aureus. *Antimicrob. Agents. Chemother.* **1999**, *43*, 1756-1758, doi:10.1128/aac.43.7.1756.

59. Zhao, X.; Drlica, K. Restricting the selection of antibiotic-resistant mutant bacteria: measurement and potential use of the mutant selection window. *J. Infect. Dis.* **2002**, *185*, 561-565, doi:10.1086/338571.

60. Zhao, X. Clarification of MPC and the mutant selection window concept. *J. Antimicrob. Chemother.* **2003**, *52*, 731; author reply 732-733, doi:10.1093/jac/dkg376.

61. Blondeau, J.M.; Zhao, X.; Hansen, G.; Drlica, K. Mutant prevention concentrations of fluoroquinolones for clinical isolates of *Streptococcus pneumoniae*. *Antimicrob. Agents. Chemother.* **2001**, *45*, 433-438, doi:10.1128/aac.45.2.433-438.2001.

62. Hansen, G.T.; Blondeau, J.M. Comparison of the minimum inhibitory, mutant prevention and minimum bactericidal concentrations of ciprofloxacin, levofloxacin and garenoxacin against enteric Gram-negative urinary tract infection pathogens. *J. Chemother.* **2005**, *17*, 484-492, doi: 10.1179/joc.2005.17.5.484.

63. Alieva, K.N.; Strukova, E.N.; Golikova, M.V.; Portnoy, Y.A.; Zinner, S.H.; Firsov, A.A. Time inside the mutant selection window as a predictor of staphylococcal resistance to linezolid. *J. Antibiot. (Tokyo)* **2018**, *71*, 514-521, doi: http://dx.doi.org/10.1038/s41429-017-0016-9.

64. Firsov, A.A.; Alieva, K.N.; Strukova, E.N.; Golikova, M.V.; Portnoy, Y.A.; Dovzhenko, S.A.; Kobrin, M.B.; Romanov, A.V.; Edelstein, M.V.; Zinner, S.H. Testing the mutant selection window hypothesis with *Staphylococcus aureus* exposed to linezolid in an *in vitro* dynamic model. *J. Antimicrob. Chemother.* **2017**, *72*, 3100-3107, doi:10.1093/jac/dkx249.

65. Firsov, A.A.; Lubenko, I.Y.; Smirnova, M.V.; Strukova, E.N.; Zinner, S.H. Enrichment of fluoroquinolone-resistant *Staphylococcus aureus:* oscillating ciprofloxacin concentrations simulated at the upper and lower portions of the mutant selection window. *Antimicrob. Agents. Chemother.* **2008**, *52*, 1924-1928, doi:10.1128/aac.01371-07.

66. Firsov, A.A.; Smirnova, M.V.; Strukova, E.N.; Vostrov, S.N.; Portnoy, Y.A.; Zinner, S.H. Enrichment of resistant *Staphylococcus aureus* at ciprofloxacin concentrations simulated within the mutant selection window: bolus *versus* continuous infusion. *Int. J. Antimicrob. Agents* **2008**, *32*, 488-493, doi:10.1016/j.ijantimicag.2008.06.031.

67. Homma, T.; Hori, T.; Sugimori, G.; Yamano, Y. Pharmacodynamic assessment based on mutant prevention concentrations of fluoroquinolones to prevent the emergence of resistant mutants of *Streptococcus pneumoniae*. *Antimicrob. Agents. Chemother.* **2007**, *51*, 3810-3815, doi:10.1128/aac.01372-06.

68. Cui, J.; Liu, Y.; Wang, R.; Tong, W.; Drlica, K.; Zhao, X. The mutant selection window in rabbits infected with *Staphylococcus aureus*. *J. Infect. Dis.* **2006**, *194*, 1601-1608, doi:10.1086/508752.

69. Ni, W.; Song, X.; Cui, J. Testing the mutant selection window hypothesis with *Escherichia coli* exposed to levofloxacin in a rabbit tissue cage infection model. *Eur. J. Clin. Microbiol. Infect. Dis.* **2014**, *33*, 385-389, doi:10.1007/s10096-013-1968-8.

70. Croisier, D.; Etienne, M.; Bergoin, E.; Charles, P.E.; Lequeu, C.; Piroth, L.; Portier, H.; Chavanet, P. Mutant selection window in levofloxacin and moxifloxacin treatments of experimental pneumococcal pneumonia in a rabbit model of human therapy. *Antimicrob. Agents. Chemother.* **2004**, *48*, 1699-1707, doi:10.1128/aac.48.5.1699-1707.2004.

71. Almeida, D.; Nuermberger, E.; Tyagi, S.; Bishai, W.R.; Grosset, J. *In vivo* validation of the mutant selection window hypothesis with moxifloxacin in a murine model of tuberculosis. *Antimicrob. Agents. Chemother.* **2007**, *51*, 4261-4266, doi:10.1128/AAC.01123-07.

72. Ferran, A.A.; Kesteman, A.S.; Toutain, P.L.; Bousquet-Mélou, A. Pharmacokinetic/pharmacodynamic analysis of the influence of inoculum size on the selection of resistance in *Escherichia coli* by a quinolone in a mouse thigh bacterial infection model. *Antimicrob. Agents. Chemother.* **2009**, *53*, 3384-3390, doi:10.1128/aac.01347-08.

73. Zhao, X.; Drlica, K. A unified anti-mutant dosing strategy. *J. Antimicrob. Chemother.* **2008**, *62*, 434-436, doi:10.1093/jac/dkn229.

74. Metzler, K.; Hansen, G.M.; Hedlin, P.; Harding, E.; Drlica, K.; Blondeau, J.M. Comparison of minimal inhibitory and mutant prevention drug concentrations of 4 fluoroquinolones against clinical isolates of methicillin-susceptible and -resistant *Staphylococcus aureus*. *Int. J. Antimicrob. Agents* **2004**, *24*, 161-167, doi:10.1016/j.ijantimicag.2004.02.021.

75. Hansen, G.T.; Metzler, K.; Drlica, K.; Blondeau, J.M. Mutant prevention concentration of gemifloxacin for clinical isolates of *Streptococcus pneumoniae*. *Antimicrob. Agents. Chemother.* **2003**, *47*, 440-441, doi:10.1128/aac.47.1.440-441.2003.

76. Hedlin, P.; Blondeau, J.M. Comparative minimal inhibitory and mutant prevention drug concentrations of four fluoroquinolones against ocular isolates of *Haemophilus influenzae*. *Eye Contact Lens* **2007**, *33*, 161-164, doi:10.1097/01.icl.0000246872.73559.43.

77. Sun, D.; Rubio-Aparicio, D.; Nelson, K.; Dudley, M.N.; Lomovskaya, O. Meropenem-vaborbactam resistance selection, resistance prevention, and molecular mechanisms in mutants of KPC-producing *Klebsiella pneumoniae*. *Antimicrob. Agents. Chemother.* **2017**, *61*, doi:10.1128/aac.01694-17.

78. Krajewska, J.; Tyski, S.; Laudy, A.E. Mutant prevention concentration, frequency of spontaneous mutant selection, and mutant selection window-a new approach to the *in vitro* determination of the antimicrobial potency of compounds. *Antimicrob. Agents. Chemother.* **2023**, *67*, e0137322, doi:10.1128/aac.01373-22.

79. Blondeau, J.M.; Hansen, G.; Metzler, K.; Hedlin, P. The role of PK/PD parameters to avoid selection and increase of resistance: mutant prevention concentration. *J. Chemother.* **2004**, *16 Suppl 3*, 1-19, doi:10.1080/1120009x.2004.11782371.

80. Diaz-Diaz, S.; Recacha, E.; García-Duque, A.; Docobo-Pérez, F.; Blázquez, J.; Pascual, A.; Rodríguez-Martínez, J.M. Effect of RecA inactivation and detoxification systems on the evolution of ciprofloxacin resistance in *Escherichia coli*. *J. Antimicrob. Chemother.***2022**, *77*, 641-645, doi:10.1093/jac/dkab445.

81. Park, N.H.; Lee, S.J.; Lee, E.B.; Birhanu, B.T.; Park, S.C. Colistin induces resistance through biofilm vormation, *via* increased *phoQ* expression, in avian pathogenic *Escherichia coli*. *Pathogens* **2021**, *10*, doi: 10.3390/pathogens10111525.

82. Jiang, L.; Xie, N.; Chen, M.; Liu, Y.; Wang, S.; Mao, J.; Li, J.; Huang, X. Synergistic combination of linezolid and fosfomycin closing each other's mutant eelection window to prevent enterococcal resistance. *Front. Microbiol.* **2020**, *11*, 605962, doi: 10.3389/fmicb.2020.605962.

83. Gianvecchio, C.; Lozano, N.A.; Henderson, C.; Kalhori, P.; Bullivant, A.; Valencia, A.; Su, L.; Bello, G.; Wong, M.; Cook, E.; et al. Variation in mutant prevention concentrations. *Front. Microbiol.* **2019**, *10*, doi:10.3389/fmicb.2019.00042.

84. Hovde, L.B.; Rotschafer, S.E.; Ibrahim, K.H.; Gunderson, B.; Hermsen, E.D.; Rotschafer, J.C. Mutation prevention concentration of ceftriaxone, meropenem, imipenem, and ertapenem against three strains of *Streptococcus pneumoniae*. *Diagn. Microbiol. Infect. Dis.* **2003**, *45*, 265-267, doi:10.1016/s0732-8893(02)00546-1.

85. Wentzel, J.M.; Biggs, L.J.; Van Vuuren, M. Comparing the minimum inhibitory and mutant prevention concentrations of selected antibiotics against animal isolates of *Pasteurella multocida* and *Salmonella typhimurium*. *Onderstepoort. J. Vet. Res.* **2022**, *89*, e1-e7, doi:10.4102/ojvr.v89i1.1955.

86. Pan, A.J.; Mei, Q.; Ye, Y.; Li, H.R.; Liu, B.; Li, J.B. Validation of the mutant selection window hypothesis with fosfomycin against E*scherichia coli* and *Pseudomonas aeruginosa*: an *in vitro* and *in vivo* comparative study. *J. Antibiot. (Tokyo)* **2017**, *70*, 166-173, doi:10.1038/ja.2016.124.

87. Mei, Q.; Ye, Y.; Zhu, Y.L.; Cheng, J.; Chang, X.; Liu, Y.Y.; Li, H.R.; Li, J.B. Testing the mutant selection window hypothesis *in vitro* and *in vivo* with *Staphylococcus aureus* exposed to fosfomycin. *Eur. J. Clin. Microbiol. Infect. Dis.* **2015**, *34*, 737-744, doi:10.1007/s10096-014-2285-6.

88. European Commission. Communication from the Commission on a community strategy against antimicrobial resistance, Brussels, 20.06.2001, COM(2001) 333 final, Volume 1. Dostępne online: https://eur-lex.europa.eu/legal-content/EN/TXT/PDF/?uri=CELEX:52001DC0333&from=EL (16.11.2023).

89. World Health Organization. Fifty-eighth World Health Assembly, Geneva, 16-25 May 2005: resolutions and decisions: annex. WHA58.27: Improving the containment of antimicrobial resistance. Dostępne online: https://apps.who.int/gb/ebwha/pdf_files/WHA58/WHA58_27-en.pdf (16-11-2023).

90. European Commission. EU One Health Action Plan against Antimicrobial Resistance (AMR). Dostępne online: https://health.ec.europa.eu/system/files/2020-01/amr_2017_action-plan_0.pdf (16.11.2023).

91. World Health Organization. Prioritization of pathogens to guide discovery, research and development of new antibiotics for drug-resistant bacterial infections, including tuberculosis. Dostępne online: https://apps.who.int/iris/handle/10665/311820 (16.11.2023).

92. World Health Organization. WHO fungal priority pathogens list to guide research, development and public health action. Dostępne online: https://www.who.int/publications/i/item/9789240060241 (16-11-2023)

93. World Health Organization. Five key points to consider for the development and optimal use of new antibiotics. Dostępne online: https://cdn.who.int/media/docs/default-source/antimicrobial-resistance/amr-gcp-irc/five-key-points-to-consider-for-the-development-and-optimal-use-of-new-antibiotics.pdf?sfvrsn=c4a77671_5 (16-11-2023)

94. Krajewska, J.; Laudy, A.E. The European Medicines Agency approved the new antibacterial drugs – response to the 2017 WHO report on the global problem of multi-drug resistance. *Advancements Microbiol.* **2021**, *60*, 249-264, doi: https://doi.org/10.21307/PM-2021.60.4.20.

95. U.S. Food and Drug Administration. Xacduro. Highlights of prescribing information. Dostępne online:

https://www.accessdata.fda.gov/drugsatfda_docs/label/2023/216974Orig1s000Correctedlbl.pdf (16-11-2023).

96. U.S. Food and Drug Administration. Rezzayo. Highlights of prescribing information. Dostępne online:

https://www.accessdata.fda.gov/drugsatfda_docs/label/2023/217417s000lbl.pdf (16-11-2023).

97. European Medicines Agency. Cresemba Dostępne online: https://www.ema.europa.eu/en/medicines/human/EPAR/cresemba (16-11-2023).

98. U.S. Food and Drug Administration. Cresemba. Highlights of prescribing information. Dostępne online:

https://www.accessdata.fda.gov/drugsatfda_docs/label/2021/207500s008,207501s007lbl.pdf (16-11-2023).

99. de Oliveira, H.C.; Bezerra, B.T.; Rodrigues, M.L. Antifungal development and the urgency of minimizing the impact of fungal diseases on public health. *ACS Bio. Med. Chem. Au.* **2023**, *3*, 137-146, doi:10.1021/acsbiomedchemau.2c00055.

100. Bouz, G.; Doležal, M. Advances in antifungal drug development: an up-to-date mini review. *Pharmaceuticals (Basel)* **2021**, *14*, doi:10.3390/ph14121312.

101. Shaw, K.J. GR-2397: review of the novel siderophore-like antifungal agent for the treatment of invasive aspergillosis. *J. Fungi (Basel)* **2022**, *8*, doi:10.3390/jof8090909.

102. Uluisik, I.; Karakaya, H.C.; Koc, A. The importance of boron in biological systems. *J. Trace Elem. Med. Biol.* **2018**, *45*, 156-162, doi:10.1016/j.jtemb.2017.10.008.

103. World Health Organization. Trace elements in human nutrition and health. Dostępne online: https://apps.who.int/iris/handle/10665/37931 (16.11.2023).

104. Fernandes, G.F.S.; Denny, W.A.; Dos Santos, J.L. Boron in drug design: Recent advances in the development of new therapeutic agents. *Eur. J. Med. Chem.* **2019**, *179*, 791-804, doi:10.1016/j.ejmech.2019.06.092.

105. Baker, S.J.; Ding, C.Z.; Akama, T.; Zhang, Y.K.; Hernandez, V.; Xia, Y. Therapeutic potential of boron-containing compounds. *Future Med. Chem.* **2009**, *1*, 1275-1288, doi:10.4155/fmc.09.71.

106. Plescia, J.; Moitessier, N. Design and discovery of boronic acid drugs. *Eur. J. Med. Chem.* **2020**, *195*, 112270, doi:10.1016/j.ejmech.2020.112270.

107. Das, B.C.; Adil Shareef, M.; Das, S.; Nandwana, N.K.; Das, Y.; Saito, M.; Weiss, L.M. Boron-containing heterocycles as promising pharmacological agents. *Bioorg. Med. Chem.* **2022**, *63*, 116748, doi:10.1016/j.bmc.2022.116748.

108. Torssell, K. Arylboronic acids. III. Bromination of tolylboronic acids according to Wohl-Ziegler. *Ark. Kemi.* **1957**, *10*, 507-511.

109. Brzozowska, A.; Ćwik, P.; Durka, K.; Kliś, T.; Laudy, A.E.; Luliński, S.; Serwatowski, J.; Tyski, S.; Urban, M.; Wróblewski, W. Benzosiloxaboroles: silicon benzoxaborole congeners with improved Lewis acidity, high diol affinity, and potent bioactivity. *Organometallics* **2015**, *34*, 2924-2932, doi: 10.1021/acs.organomet.5b00265.

110. Durka, K.; Laudy, A.E.; Charzewski, Ł.; Urban, M.; Stępień, K.; Tyski, S.; Krzyśko, K.A.; Luliński, S. Antimicrobial and KPC/AmpC inhibitory activity of functionalized benzosiloxaboroles. *Eur. J. Med. Chem.* **2019**, *171*, 11-24, doi: 10.1016/j.ejmech.2019.03.028.

111. Adamczyk-Woźniak, A.; Borys, K.M.; Sporzyński, A. Recent developments in the chemistry and biological applications of benzoxaboroles. *Chem. Rev.* **2015**, *115*, 5224-5247, doi: 10.1021/cr500642d.

112. Nowicki, K.; Pacholak, P.; Luliński, S. Heteroelement analogues of benzoxaborole and related ring expanded systems. *Molecules* **2021**, *26*, 5464, doi: 10.3390/molecules26185464.

113. Silva, M.P.; Saraiva, L.; Pinto, M.; Sousa, M.E. Boronic acids and their derivatives in medicinal chemistry: synthesis and biological applications. *Molecules* **2020**, *25*, doi: 10.3390/molecules25184323.

114. Ambler, R.P. The structure of beta-lactamases. *Philos. Trans. R. Soc. Lond. B. Biol. Sci.* **1980**, *289*, 321-331, doi: 10.1098/rstb.1980.0049.

115. Słoczyńska, A.; Wand, M.E.; Tyski, S.; Laudy, A.E. Analysis of bla_{CHDL} genes and insertion sequences related to carbapenem resistance in *Acinetobacter baumannii* clinical strains isolated in Warsaw, Poland. *Int. J. Mol. Sci.* **2021**, *22*, 2486, doi: 10.3390/ijms22052486.

116. Namysłowska, A.; Laudy, A.E.; Tyski, S. Mechanizmy oporności *Acinetobacter baumannii* na związki przeciwbakteryjne. *Postępy Mikrobiologii* **2015**, *54*, 392-406.

117. Burillo, A.; Bouza, E. Controversies over the management of infections caused by Amp-C- and ESBL-producing *Enterobacterales*: what questions remain for future studies? *Curr. Opin. Infect. Dis.* **2022**, *35*, 575-582, doi: 10.1097/qco.0000000000000863.

118. Jackson, N.; Belmont, C.R.; Tarlton, N.J.; Allegretti, Y.H.; Adams-Sapper, S.; Huang, Y.Y.; Borges, C.A.; Frazee, B.W.; Florence-Petrovic, D.; Hufana, C.; et al. Genetic predictive factors for nonsusceptible phenotypes and multidrug resistance in expanded-spectrum cephalosporin-resistant uropathogenic *Escherichia coli* from

a multicenter cohort: insights into the phenotypic and genetic basis of coresistance. *mSphere* **2022**, *7*, e0047122, doi: 10.1128/msphere.00471-22.

119. Papp-Wallace, K.M. The latest advances in β-lactam/β-lactamase inhibitor combinations for the treatment of Gram-negative bacterial infections. *Expert Opin. Pharmacother.* **2019**, *20*, 2169-2184, doi:10.1080/14656566.2019.1660772.
120. Kiener, P.A.; Waley, S.G. Reversible inhibitors of penicillinases. *Biochem. J.* **1978**, *169*, 197-204, doi:10.1042/bj1690197.
121. European Committee on Antimicrobial Susceptibility Testing. Guidelines for detection of resistance mechanisms and specific resistance of clinical and/or epidemiological importance. Document version 2.0. **2017**.
122. Alsenani, T.A.; Rodríguez, M.M.; Ghiglione, B.; Taracila, M.A.; Mojica, M.F.; Rojas, L.J.; Hujer, A.M.; Gutkind, G.; Bethel, C.R.; Rather, P.N.; et al. Boronic acid transition state inhibitors as potent inactivators of KPC and CTX-M β-lactamases: biochemical and structural snalyses. *Antimicrob. Agents. Chemother.* **2023**, *67*, e0093022, doi:10.1128/aac.00930-22.
123. Krajnc, A.; Lang, P.A.; Panduwawala, T.D.; Brem, J.; Schofield, C.J. Will morphing boron-based inhibitors beat the β-lactamases? *Curr. Opin. Chem. Biol.* **2019**, *50*, 101-110, doi:10.1016/j.cbpa.2019.03.001.
124. McKinney, D.C.; Zhou, F.; Eyermann, C.J.; Ferguson, A.D.; Prince, D.B.; Breen, J.; Giacobbe, R.A.; Lahiri, S.; Verheijen, J.C. 4,5-Disubstituted 6-aryloxy-1,3-dihydrobenzo[c][1,2]oxaboroles are broad-spectrum serine β-lactamase inhibitors. *ACS Infect. Dis.* **2015**, *1*, 310-316, doi:10.1021/acsinfecdis.5b00031.
125. Xia, Y.; Cao, K.; Zhou, Y.; Alley, M.R.; Rock, F.; Mohan, M.; Meewan, M.; Baker, S.J.; Lux, S.; Ding, C.Z.; et al. Synthesis and SAR of novel benzoxaboroles as a new class of β-lactamase inhibitors. *Bioorg. Med. Chem. Lett.* **2011**, *21*, 2533-2536, doi:10.1016/j.bmcl.2011.02.024.
126. Yan, Y.H.; Li, Z.F.; Ning, X.L.; Deng, J.; Yu, J.L.; Luo, Y.; Wang, Z.; Li, G.; Li, G.B.; Xiao, Y.C. Discovery of 3-aryl substituted benzoxaboroles as broad-spectrum inhibitors of serine- and metallo-β-lactamases. *Bioorg. Med. Chem. Lett.* **2021**, *41*, 127956, doi:10.1016/j.bmcl.2021.127956.
127. Hecker, S.J.; Reddy, K.R.; Lomovskaya, O.; Griffith, D.C.; Rubio-Aparicio, D.; Nelson, K.; Tsivkovski, R.; Sun, D.; Sabet, M.; Tarazi, Z.; et al. Discovery of cyclic boronic acid QPX7728, an ultrabroad-spectrum inhibitor of serine and metallo-β-lactamases. *J. Med. Chem.* **2020**, *63*, 7491-7507, doi: 10.1021/acs.jmedchem.9b01976.
128. Findlay, J.; Poirel, L.; Nordmann, P. *In vitro*-obtained meropenem-vaborbactam resistance mechanisms among clinical *Klebsiella pneumoniae* carbapenemase-producing *K. pneumoniae* isolates. *J. Glob. Antimicrob. Resist.* **2023**, *32*, 66-71, doi:10.1016/j.jgar.2022.12.009.
129. FDA. Advancing health through innovation: 2017 new drug therapy approvals report. Dostępne online: https://www.fda.gov/media/110526/download (16-11-2023).
130. European Medicines Agency. Vaborem Dostępne online: https://www.ema.europa.eu/en/medicines/human/EPAR/vaborem (16-11-2023).

131. European Medicines Agency. Vaborem: EPAR - Product information. Dostępne online: https://www.ema.europa.eu/en/documents/product-information/vaborem-epar-product-information_en.pdf (16-11-2023).

132. Tiseo, G.; Suardi, L.R.; Leonildi, A.; Giordano, C.; Barnini, S.; Falcone, M. Meropenem/vaborbactam plus aztreonam for the treatment of New Delhi metallo-β-lactamase-producing *Klebsiella pneumoniae* infections. *J. Antimicrob. Chemother.* **2023**, dkad206, doi:10.1093/jac/dkad206.

133. Belati, A.; Bavaro, D.F.; Diella, L.; De Gennaro, N.; Di Gennaro, F.; Saracino, A. Meropenem/vaborbactam plus aztreonam as a possible treatment strategy for bloodstream infections caused by ceftazidime/avibactam-resistant *Klebsiella pneumoniae*: a retrospective case series and literature review. *Antibiotics (Basel)* **2022**, *11*, doi:10.3390/antibiotics11030373.

134. Karlowsky, J.A.; Wise, M.G.; Hackel, M.A.; Pevear, D.C.; Moeck, G.; Sahm, D.F. Ceftibuten-ledaborbactam activity against multidrug-resistant and extended-spectrum-β-lactamase-positive clinical isolates of *Enterobacterales* from a 2018-2020 Global Surveillance Collection. *Antimicrob. Agents. Chemother.* **2022**, *66*, e0093422, doi:10.1128/aac.00934-22.

135. Sun, D.; Tsivkovski, R.; Pogliano, J.; Tsunemoto, H.; Nelson, K.; Rubio-Aparicio, D.; Lomovskaya, O. Intrinsic antibacterial activity of xeruborbactam *in vitro*: assessing spectrum and mode of action. *Antimicrob. Agents. Chemother.* **2022**, *66*, e0087922, doi:10.1128/aac.00879-22.

136. Karlowsky, J.A.; Hackel, M.A.; Wise, M.G.; Six, D.A.; Uehara, T.; Daigle, D.M.; Cusick, S.M.; Pevear, D.C.; Moeck, G.; Sahm, D.F. *In vitro* activity of cefepime-taniborbactam and comparators against clinical isolates of Gram-negative bacilli from 2018 to 2020: results from the Global Evaluation of Antimicrobial Resistance via Surveillance (GEARS) Program. *Antimicrob. Agents. Chemother.* **2023**, *67*, e0128122, doi:10.1128/aac.01281-22.

137. Hernández-García, M.; García-Castillo, M.; Ruiz-Garbajosa, P.; Bou, G.; Siller-Ruiz, M.; Pitart, C.; Gracia-Ahufinger, I.; Mulet, X.; Pascual, Á.; Tormo, N.; et al. *In vitro* activity of cefepime-taniborbactam against carbapenemase-producing *Enterobacterales* and *Pseudomonas aeruginosa* isolates recovered in Spain. *Antimicrob. Agents. Chemother.* **2022**, *66*, e0216121, doi:10.1128/aac.02161-21.

138. Liu, B.; Trout, R.E.L.; Chu, G.H.; McGarry, D.; Jackson, R.W.; Hamrick, J.C.; Daigle, D.M.; Cusick, S.M.; Pozzi, C.; De Luca, F.; et al. Discovery of taniborbactam (VNRX-5133): a broad-spectrum serine- and metallo-β-lactamase inhibitor for carbapenem-resistant bacterial infections. *J. Med. Chem.* **2020**, *63*, 2789-2801, doi:10.1021/acs.jmedchem.9b01518.

139. Le Terrier, C.; Gruenig, V.; Fournier, C.; Nordmann, P.; Poirel, L. NDM-9 resistance to taniborbactam. *Lancet Infect. Dis.* **2023**, *23*, 401-402, doi:10.1016/s1473-3099(23)00069-5.

140. Le Terrier, C.; Nordmann, P.; Buchs, C.; Di, D.Y.W.; Rossolini, G.M.; Stephan, R.; Castanheira, M.; Poirel, L. Wide dissemination of Gram-negative bacteria producing the taniborbactam-resistant NDM-9 variant: a One Health concern. *J. Antimicrob. Chemother.* **2023**, doi:10.1093/jac/dkad210.

141. Abbott, C.; Satola, S.W.; Weiss, D.S. Heteroresistance to cefepime-taniborbactam in metallo-β-lactamase-encoding *Enterobacterales*. *Lancet Infect. Dis.* **2023**, doi:10.1016/s1473-3099(23)00426-7.

142. Trout, R.E.; Zulli, A.; Mesaros, E.; Jackson, R.W.; Boyd, S.; Liu, B.; Hamrick, J.; Daigle, D.; Chatwin, C.L.; John, K.; et al. Discovery of VNRX-7145 (VNRX-5236 Etzadroxil): an orally bioavailable β-lactamase inhibitor for *Enterobacterales* expressing Ambler class A, C, and D enzymes. *J. Med. Chem.* **2021**, *64*, 10155-10166, doi:10.1021/acs.jmedchem.1c00437.

143. Chatwin, C.L.; Hamrick, J.C.; Trout, R.E.L.; Myers, C.L.; Cusick, S.M.; Weiss, W.J.; Pulse, M.E.; Xerri, L.; Burns, C.J.; Moeck, G.; et al. Microbiological characterization of VNRX-5236, a broad-spectrum β-lactamase inhibitor for rescue of the orally bioavailable cephalosporin ceftibuten as a carbapenem-sparing agent against strains of *Enterobacterales* expressing extended-spectrum β-lactamases and serine carbapenemases. *Antimicrob. Agents. Chemother.* **2021**, *65*, e0055221, doi:10.1128/aac.00552-21.

144. Mendes, R.E.; Rhomberg, P.R.; Watters, A.A.; Castanheira, M. *In vitro* activity of the orally bioavailable ceftibuten/VNRX-7145 (VNRX-5236 etzadroxil) combination against a challenge set of *Enterobacterales* pathogens carrying molecularly characterized β-lactamase genes. *J. Antimicrob. Chemother.* **2022**, *77*, 689-694, doi:10.1093/jac/dkab425.

145. Lomovskaya, O.; Tsivkovski, R.; Sun, D.; Reddy, R.; Totrov, M.; Hecker, S.; Griffith, D.; Loutit, J.; Dudley, M. QPX7728, an ultra-broad-spectrum β-lactamase inhibitor for intravenous and oral therapy: overview of biochemical and microbiological characteristics. *Front. Microbiol.* **2021**, *12*, 697180, doi:10.3389/fmicb.2021.697180.

146. Lomovskaya, O.; Tsivkovski, R.; Nelson, K.; Rubio-Aparicio, D.; Sun, D.; Totrov, M.; Dudley, M.N. Spectrum of beta-lactamase inhibition by the cyclic boronate QPX7728, an ultrabroad-spectrum beta-lactamase inhibitor of serine and metallo-beta-lactamases: enhancement of activity of multiple antibiotics against isogenic strains expressing single beta-lactamases. *Antimicrob. Agents. Chemother.* **2020**, *64*, doi:10.1128/aac.00212-20.

147. Lomovskaya, O.; Nelson, K.; Rubio-Aparicio, D.; Tsivkovski, R.; Sun, D.; Dudley, M.N. Impact of intrinsic resistance mechanisms on potency of QPX7728, a new ultrabroad-spectrum beta-lactamase inhibitor of serine and metallo-beta-lactamases in *Enterobacteriaceae*, *Pseudomonas aeruginosa*, and *Acinetobacter baumannii*. *Antimicrob. Agents. Chemother.* **2020**, *64*, doi:10.1128/aac.00552-20.

148. Lang, P.A.; Parkova, A.; Leissing, T.M.; Calvopiña, K.; Cain, R.; Krajnc, A.; Panduwawala, T.D.; Philippe, J.; Fishwick, C.W.G.; Trapencieris, P.; et al. Bicyclic boronates as potent inhibitors of AmpC, the class C β-lactamase from *Escherichia coli*. *Biomolecules* **2020**, *10*, 899, doi:10.3390/biom10060899.

149. Cahill, S.T.; Tyrrell, J.M.; Navratilova, I.H.; Calvopiña, K.; Robinson, S.W.; Lohans, C.T.; McDonough, M.A.; Cain, R.; Fishwick, C.W.G.; Avison, M.B.; et al. Studies on the inhibition of AmpC and other β-lactamases by cyclic boronates. *Biochim. Biophys. Acta Gen. Subj.* **2019**, *1863*, 742-748, doi:10.1016/j.bbagen.2019.02.004.

150. Cahill, S.T.; Cain, R.; Wang, D.Y.; Lohans, C.T.; Wareham, D.W.; Oswin, H.P.; Mohammed, J.; Spencer, J.; Fishwick, C.W.; McDonough, M.A.; et al. Cyclic boronates inhibit all classes of β-lactamases. *Antimicrob. Agents. Chemother.* **2017**, *61*, doi:10.1128/aac.02260-16.

151. Tooke, C.L.; Hinchliffe, P.; Krajnc, A.; Mulholland, A.J.; Brem, J.; Schofield, C.J.; Spencer, J. Cyclic boronates as versatile scaffolds for KPC-2 β-lactamase inhibition. *RSC Med. Chem.* **2020**, *11*, 491-496, doi:10.1039/c9md00557a.

152. Tondi, D.; Powers, R.A.; Caselli, E.; Negri, M.C.; Blázquez, J.; Costi, M.P.; Shoichet, B.K. Structure-based design and in-parallel synthesis of inhibitors of AmpC beta-lactamase. *Chem. Biol.* **2001**, *8*, 593-611, doi:10.1016/s1074-5521(01)00034-5.

153. Tondi, D.; Venturelli, A.; Bonnet, R.; Pozzi, C.; Shoichet, B.K.; Costi, M.P. Targeting class A and C serine β-lactamases with a broad-spectrum boronic acid derivative. *J. Med. Chem.* **2014**, *57*, 5449-5458, doi:10.1021/jm5006572.

154. Rojas, L.J.; Taracila, M.A.; Papp-Wallace, K.M.; Bethel, C.R.; Caselli, E.; Romagnoli, C.; Winkler, M.L.; Spellberg, B.; Prati, F.; Bonomo, R.A. Boronic acid transition state inhibitors active against KPC and other class A β-lactamases: structure-activity relationships as a guide to inhibitor design. *Antimicrob. Agents. Chemother.* **2016**, *60*, 1751-1759, doi:10.1128/aac.02641-15.

155. Linciano, P.; Vicario, M.; Kekez, I.; Bellio, P.; Celenza, G.; Martín-Blecua, I.; Blázquez, J.; Cendron, L.; Tondi, D. Phenylboronic acids probing molecular recognition against class A and class C β-lactamases. *Antibiotics (Basel)* **2019**, *8*, 171, doi:10.3390/antibiotics8040171.

156. Zhou, J.; Stapleton, P.; Haider, S.; Healy, J. Boronic acid inhibitors of the class A β-lactamase KPC-2. *Bioorg. Med. Chem.* **2018**, *26*, 2921-2927, doi:10.1016/j.bmc.2018.04.055.

157. Zhou, J.; Stapleton, P.; Xavier-Junior, F.H.; Schatzlein, A.; Haider, S.; Healy, J.; Wells, G. Triazole-substituted phenylboronic acids as tunable lead inhibitors of KPC-2 antibiotic resistance. *Eur. J. Med. Chem.* **2022**, *240*, 114571, doi:10.1016/j.ejmech.2022.114571.

158. Santucci, M.; Spyrakis, F.; Cross, S.; Quotadamo, A.; Farina, D.; Tondi, D.; De Luca, F.; Docquier, J.D.; Prieto, A.I.; Ibacache, C.; et al. Computational and biological profile of boronic acids for the detection of bacterial serine- and metallo-β-lactamases. *Sci. Rep.* **2017**, *7*, 17716, doi:10.1038/s41598-017-17399-7.

159. Eidam, O.; Romagnoli, C.; Caselli, E.; Babaoglu, K.; Pohlhaus, D.T.; Karpiak, J.; Bonnet, R.; Shoichet, B.K.; Prati, F. Design, synthesis, crystal structures, and antimicrobial activity of sulfonamide boronic acids as β-lactamase inhibitors. *J. Med. Chem.* **2010**, *53*, 7852-7863, doi:10.1021/jm101015z.

160. Morandi, S.; Morandi, F.; Caselli, E.; Shoichet, B.K.; Prati, F. Structure-based optimization of cephalothin-analogue boronic acids as beta-lactamase inhibitors. *Bioorg. Med. Chem.* **2008**, *16*, 1195-1205, doi:10.1016/j.bmc.2007.10.075.

161. Buzzoni, V.; Blazquez, J.; Ferrari, S.; Calò, S.; Venturelli, A.; Costi, M.P. Aza-boronic acids as non-beta-lactam inhibitors of AmpC-beta-lactamase. *Bioorg. Med. Chem. Lett.* **2004**, *14*, 3979-3983, doi:10.1016/j.bmcl.2004.05.054.

162. Caselli, E.; Romagnoli, C.; Vahabi, R.; Taracila, M.A.; Bonomo, R.A.; Prati, F. Click chemistry in lead optimization of boronic acids as β-lactamase inhibitors. *J. Med. Chem.* **2015**, *58*, 5445-5458, doi:10.1021/acs.jmedchem.5b00341.

163. Bouza, A.A.; Swanson, H.C.; Smolen, K.A.; VanDine, A.L.; Taracila, M.A.; Romagnoli, C.; Caselli, E.; Prati, F.; Bonomo, R.A.; Powers, R.A.; et al. Structure-based analysis of boronic acids as inhibitors of *Acinetobacter*-derived cephalosporinase-7, a unique class C β-lactamase. *ACS Infect. Dis.* **2018**, *4*, 325-336, doi:10.1021/acsinfecdis.7b00152.

164. Introvigne, M.L.; Beardsley, T.J.; Fernando, M.C.; Leonard, D.A.; Wallar, B.J.; Rudin, S.D.; Taracila, M.A.; Rather, P.N.; Colquhoun, J.M.; Song, S.; et al. Sulfonamidoboronic acids as "cross-class" inhibitors of an expanded-spectrum class C cephalosporinase, ADC-33, and a class D carbapenemase, OXA-24/40: strategic compound design to combat resistance in *Acinetobacter baumannii*. *Antibiotics (Basel)* **2023**, *12*, doi:10.3390/antibiotics12040644.

165. Werner, J.P.; Mitchell, J.M.; Taracila, M.A.; Bonomo, R.A.; Powers, R.A. Exploring the potential of boronic acids as inhibitors of OXA-24/40 β-lactamase. *Protein Sci.* **2017**, *26*, 515-526, doi:10.1002/pro.3100.

166. Wang, Y.L.; Liu, S.; Yu, Z.J.; Lei, Y.; Huang, M.Y.; Yan, Y.H.; Ma, Q.; Zheng, Y.; Deng, H.; Sun, Y.; et al. Structure-based development of (1-(3'-mercaptopropanamido)methyl)boronic acid derived broad-spectrum, dual-action inhibitors of metallo- and serine-β-lactamases. *J. Med. Chem.* **2019**, *62*, 7160-7184, doi: 10.1021/acs.jmedchem.9b00735.

167. Durka, K.; Jarzembska, K.N.; Kamiński, R.; Luliński, S.; Serwatowski, J.; Woźniak, K. Structural and energetic landscape of fluorinated 1,4-phenylenediboronic acids. *Cryst. Growth Des.* **2012**, *12*, 3720-3734, doi:10.1021/cg3005272.

168. Waller, P.J.; Gándara, F.; Yaghi, O.M. Chemistry of covalent organic frameworks. *Acc. Chem. Res.* **2015**, *48*, 3053-3063, doi:10.1021/acs.accounts.5b00369.

169. Larcher, A.; Nocentini, A.; Supuran, C.T.; Winum, J.Y.; van der Lee, A.; Vasseur, J.J.; Laurencin, D.; Smietana, M. Bis-benzoxaboroles: design, synthesis, and biological evaluation as carbonic anhydrase inhibitors. *ACS Med. Chem. Lett.* **2019**, *10*, 1205-1210, doi:https://10.1021/acsmedchemlett.9b00252.

170. Zhang, P.; Ma, S. Recent development of leucyl-tRNA synthetase inhibitors as antimicrobial agents. *MedChemComm.* **2019**, *10*, 1329-1341, doi:10.1039/c9md00139e.

171. Rock, F.L.; Mao, W.; Yaremchuk, A.; Tukalo, M.; Crépin, T.; Zhou, H.; Zhang, Y.K.; Hernandez, V.; Akama, T.; Baker, S.J.; et al. An antifungal agent inhibits an aminoacyl-tRNA synthetase by trapping tRNA in the editing site. *Science (New York, N.Y.)* **2007**, *316*, 1759-1761, doi:10.1126/science.1142189.

172. Korkegian, A.; O'Malley, T.; Xia, Y.; Zhou, Y.; Carter, D.S.; Sunde, B.; Flint, L.; Thompson, D.; Ioerger, T.R.; Sacchettini, J.; et al. The 7-phenyl benzoxaborole series is active against *Mycobacterium tuberculosis*. *Tuberculosis (Edinb.)* **2018**, *108*, 96-98, doi:10.1016/j.tube.2017.11.003.

173. Mandal, S.; Parish, T. A novel benzoxaborole is active against *Escherichia coli* and binds to FabI. *Antimicrob. Agents. Chemother*. **2021**, *65*, e0262220, doi:10.1128/aac.02622-20.

174. Bonardi, A.; Nocentini, A.; Cadoni, R.; Del Prete, S.; Dumy, P.; Capasso, C.; Gratteri, P.; Supuran, C.T.; Winum, J.Y. Benzoxaboroles: new potent inhibitors of the carbonic anhydrases of the pathogenic bacterium *Vibrio cholerae*. *ACS Med. Chem. Lett.* **2020**, *11*, 2277-2284, doi: 10.1021/acsmedchemlett.0c00403.

175. U.S. Food and Drug Administration. Center for Drug Evaluation and Research. APPLICATION NUMBER: 204427Orig1s000. Clinical Microbiology Review - Tavaborole. Dostępne online:

https://www.accessdata.fda.gov/drugsatfda_docs/nda/2014/204427Orig1s000ODMemo.pdf (16-11-2023).

176. Baker, S.J.; Zhang, Y.K.; Akama, T.; Lau, A.; Zhou, H.; Hernandez, V.; Mao, W.; Alley, M.R.; Sanders, V.; Plattner, J.J. Discovery of a new boron-containing antifungal agent, 5-fluoro-1,3-dihydro-1-hydroxy-2,1- benzoxaborole (AN2690), for the potential treatment of onychomycosis. *J. Med. Chem.* **2006**, *49*, 4447-4450, doi:10.1021/jm0603724.

177. Krajewska, J.; Nowicki, K.; Durka, K.; Marek-Urban, P.H.; Wińska, P.; Stępniewski, T.; Woźniak, K.; Laudy, A.E.; Luliński, S. Oxazoline scaffold in synthesis of benzosiloxaboroles and related ring-expanded heterocycles: diverse reactivity, structural peculiarities and antimicrobial activity. *RSC Adv.* **2022**, *12*, 23099-23117, doi:10.1039/d2ra03910a.

178. Mazzantini, D.; Celandroni, F.; Calvigioni, M.; Lupetti, A.; Ghelardi, E. *In vitro* resistance and evolution of resistance to tavaborole in *Trichophyton rubrum*. *Antimicrob. Agents. Chemother.* **2021**, *65*, e02324-02320, doi:10.1128/aac.02324-20.

179. Liu, S.; She, P.; Li, Z.; Li, Y.; Li, L.; Yang, Y.; Zhou, L.; Wu, Y. Drug synergy discovery of tavaborole and aminoglycosides against *Escherichia coli* using high throughput screening. *AMB Express* **2022**, *12*, 151, doi:10.1186/s13568-022-01488-6.

180. Dong, W.; Li, S.; Wen, S.; Jing, W.; Shi, J.; Ma, Y.; Huo, F.; Gao, F.; Pang, Y.; Lu, J. *In vitro* susceptibility testing of GSK656 against *Mycobacterium* species. *Antimicrob. Agents. Chemother.* **2020**, *64*, doi:10.1128/aac.01577-19.

181. Li, X.; Hernandez, V.; Rock, F.L.; Choi, W.; Mak, Y.S.L.; Mohan, M.; Mao, W.; Zhou, Y.; Easom, E.E.; Plattner, J.J.; et al. Discovery of a potent and specific *M. tuberculosis* leucyl-tRNA synthetase inhibitor: (S)-3-(aminomethyl)-4-chloro-7-(2-hydroxyethoxy)benzo[c][1,2]oxaborol-1(3H)-ol (GSK656). *J. Med. Chem.* **2017**, *60*, 8011-8026, doi:10.1021/acs.jmedchem.7b00631.

182. Kim, T.; Hanh, B.T.; Heo, B.; Quang, N.; Park, Y.; Shin, J.; Jeon, S.; Park, J.W.; Samby, K.; Jang, J. A screening of the MMV pandemic response box reveals epetraborole as a new potent inhibitor against *Mycobacterium abscessus*. *Int. J. Mol. Sci.* **2021**, *22*, doi:10.3390/ijms22115936.

183. Ganapathy, U.S.; Gengenbacher, M.; Dick, T. Epetraborole Is active against *Mycobacterium abscessus*. *Antimicrob. Agents. Chemother.* **2021**, *65*, e0115621, doi:10.1128/aac.01156-21.

184. Sullivan, J.R.; Lupien, A.; Kalthoff, E.; Hamela, C.; Taylor, L.; Munro, K.A.; Schmeing, T.M.; Kremer, L.; Behr, M.A. Efficacy of epetraborole against *Mycobacterium abscessus* is increased with norvaline. *PLoS Pathog.* **2021**, *17*, e1009965, doi:10.1371/journal.ppat.1009965.

185. Palencia, A.; Li, X.; Bu, W.; Choi, W.; Ding, C.Z.; Easom, E.E.; Feng, L.; Hernandez, V.; Houston, P.; Liu, L.; et al. Discovery of novel oral protein synthesis inhibitors of *Mycobacterium tuberculosis* that target leucyl-tRNA synthetase. *Antimicrob. Agents. Chemother.* **2016**, *60*, 6271-6280, doi:10.1128/aac.01339-16.

186. Ganapathy, U.S.; Del Rio, R.G.; Cacho-Izquierdo, M.; Ortega, F.; Lelièvre, J.; Barros-Aguirre, D.; Lindman, M.; Dartois, V.; Gengenbacher, M.; Dick, T. A leucyl-tRNA synthetase inhibitor with broad-spectrum antimycobacterial activity. *Antimicrob. Agents. Chemother.* **2021**, *65*, e02420-02420, doi:10.1128/aac.02420-20.

187. O'Dwyer, K.; Spivak, A.T.; Ingraham, K.; Min, S.; Holmes, D.J.; Jakielaszek, C.; Rittenhouse, S.; Kwan, A.L.; Livi, G.P.; Sathe, G.; et al. Bacterial resistance to leucyl-tRNA synthetase inhibitor GSK2251052 develops during treatment of complicated urinary tract infections. *Antimicrob. Agents. Chemother.* **2015**, *59*, 289-298, doi:10.1128/aac.03774-14.

188. Mendes, R.E.; Alley, M.R.; Sader, H.S.; Biedenbach, D.J.; Jones, R.N. Potency and spectrum of activity of AN3365, a novel boron-containing protein synthesis inhibitor, tested against clinical isolates of *Enterobacteriaceae* and nonfermentative Gram-negative bacilli. *Antimicrob. Agents. Chemother.* **2013**, *57*, 2849-2857, doi:10.1128/aac.00160-13.

189. Purnapatre, K.P.; Rao, M.; Pandya, M.; Khanna, A.; Chaira, T.; Bambal, R.; Upadhyay, D.J.; Masuda, N. *In vitro* and *in vivo* activities of DS86760016, a novel leucyl-tRNA synthetase inhibitor for Gram-negative pathogens. *Antimicrob. Agents. Chemother.* **2018**, *62*, e01987-01917, doi:10.1128/aac.01987-17.

190. Kumar, M.; Rao, M.; Purnapatre, K.P.; Barman, T.K.; Joshi, V.; Kashyap, A.; Chaira, T.; Bambal, R.B.; Pandya, M.; Khodor, S.A.; et al. DS86760016, a leucyl-tRNA synthetase Inhibitor with activity against *Pseudomonas aeruginosa*. *Antimicrob. Agents. Chemother.* **2019**, *63*, doi:10.1128/aac.02122-18.

191. Nguyen, T.Q.; Heo, B.E.; Hanh, B.T.B.; Jeon, S.; Park, Y.; Choudhary, A.; Lee, S.; Kim, T.H.; Moon, C.; Min, S.J.; et al. DS86760016, a leucyl-tRNA synthetase inhibitor, is active against *Mycobacterium abscessus*. *Antimicrob. Agents. Chemother.* **2023**, *67*, e0156722, doi:10.1128/aac.01567-22.

192. Hu, Q.H.; Liu, R.J.; Fang, Z.P.; Zhang, J.; Ding, Y.Y.; Tan, M.; Wang, M.; Pan, W.; Zhou, H.C.; Wang, E.D. Discovery of a potent benzoxaborole-based anti-pneumococcal agent targeting leucyl-tRNA synthetase. *Sci. Rep.* **2013**, *3*, 2475, doi:10.1038/srep02475.

193. Hao, G.; Li, H.; Yang, F.; Dong, D.; Li, Z.; Ding, Y.; Pan, W.; Wang, E.; Liu, R.; Zhou, H. Discovery of benzhydrol-oxaborole derivatives as *Streptococcus pneumoniae* leucyl-tRNA synthetase inhibitors. *Bioorg. Med. Chem.* **2021**, *29*, 115871, doi: 10.1016/j.bmc.2020.115871.

194. Si, Y.; Basak, S.; Li, Y.; Merino, J.; Iuliano, J.N.; Walker, S.G.; Tonge, P.J. Antibacterial activity and mode of action of a sulfonamide-based class of oxaborole

leucyl-tRNA-synthetase inhibitors. *ACS Infect. Dis.* **2019**, *5*, 1231-1238, doi: 10.1021/acsinfecdis.9b00071.

195. Borys, K.M.; Wieczorek, D.; Pecura, K.; Lipok, J.; Adamczyk-Woźniak, A. Antifungal activity and tautomeric cyclization equilibria of formylphenylboronic acids. *Bioorg. Chem.* **2019**, *91*, 103081, doi: 10.1016/j.bioorg.2019.103081.
196. Mandal, S.M.; Pegu, R.; Porto, W.F.; Franco, O.L.; Pratihar, S. Novel boronic acid derivatives of bis(indolyl) methane as anti-MRSA agents. *Bioorg. Med. Chem. Lett.* **2017**, *27*, 2135-2138, doi:10.1016/j.bmcl.2017.03.070.
197. Adamczyk-Woźniak, A.; Gozdalik, J.T.; Kaczorowska, E.; Durka, K.; Wieczorek, D.; Zarzeczańska, D.; Sporzyński, A. (Trifluoromethoxy)phenylboronic acids: structures, properties, and antibacterial activity. *Molecules* **2021**, *26*, 2007, doi: 10.3390/molecules26072007.
198. Adamczyk-Woźniak, A.; Gozdalik, J.T.; Wieczorek, D.; Madura, I.D.; Kaczorowska, E.; Brzezińska, E.; Sporzyński, A.; Lipok, J. Synthesis, properties and antimicrobial activity of 5-trifluoromethyl-2-formylphenylboronic acid. *Molecules* **2020**, *25*, 799, doi: 10.3390/molecules25040799.
199. Fontaine, F.; Héquet, A.; Voisin-Chiret, A.S.; Bouillon, A.; Lesnard, A.; Cresteil, T.; Jolivalt, C.; Rault, S. Boronic species as promising inhibitors of the *Staphylococcus aureus* NorA efflux pump: study of 6-substituted pyridine-3-boronic acid derivatives. *Eur. J. Med. Chem.* **2015**, *95*, 185-198, doi: 10.1016/j.ejmech.2015.02.056.
200. Fontaine, F.; Hequet, A.; Voisin-Chiret, A.S.; Bouillon, A.; Lesnard, A.; Cresteil, T.; Jolivalt, C.; Rault, S. First identification of boronic species as novel potential inhibitors of the *Staphylococcus aureus* NorA efflux pump. *J. Med. Chem.* **2014**, *57*, 2536-2548, doi: 10.1021/jm401808n.
201. European Committee on Antimicrobial Susceptibility Testing. EUCAST disk diffusion method for antimicrobial susceptibility testing. Document version 11.0. **2023**.
202. Clinical and Laboratory Standards Institute (CLSI). Method for antifungal disk diffusion susceptibility testing of yeasts. Approved Standard, 2nd edition. CLSI guideline M44-A2. CLSI: Wayne, PA, USA, **2009**
203. Clinical and Laboratory Standards Institute. Methods for determining bactericidal activity of antimicrobial agents. Approved guideline. CLSI gudeline M26-A. CLSI: Wayne, PA, USA, **1999**
204. Cantón, E.; Pemán, J.; Viudes, A.; Quindós, G.; Gobernado, M.; Espinel-Ingroff, A. Minimum fungicidal concentrations of amphotericin B for bloodstream *Candida species*. *Diagn. Microbiol. Infect. Dis.* **2003**, *45*, 203-206, doi:10.1016/s0732-8893(02)00525-4.
205. Sy, C.L.; Chen, P.Y.; Cheng, C.W.; Huang, L.J.; Wang, C.H.; Chang, T.H.; Chang, Y.C.; Chang, C.J.; Hii, I.M.; Hsu, Y.L.; et al. Recommendations and guidelines for the treatment of infections due to multidrug resistant organisms. *J. Microbiol. Immunol. Infect.* **2022**, *55*, 359-386, doi:10.1016/j.jmii.2022.02.001.
206. Guo, Y.; Song, G.; Sun, M.; Wang, J.; Wang, Y. Prevalence and therapies of antibiotic-resistance in *Staphylococcus aureus*. *Front. Cell. Infect. Microbiol.* **2020**, *10*, doi:10.3389/fcimb.2020.00107.

207. Prasetyoputri, A.; Jarrad, A.M.; Cooper, M.A.; Blaskovich, M.A.T. The Eagle effect and antibiotic-induced persistence: two sides of the same coin? *Trends Microbiol.* **2019**, *27*, 339-354, doi:10.1016/j.tim.2018.10.007.

208. Laudy, A.E. Non-antibiotics, efflux pumps and drug resistance of Gram-negative rods. *Pol. J. Microbiol.* **2018**, *67*, 129-135, doi:10.21307/pjm-2018-017.

209. Laudy, A.E.; Mrowka, A.; Krajewska, J.; Tyski, S. The influence of efflux pump inhibitors on the activity of non-antibiotic NSAIDS against Gram-negative rods. *PLoS One* **2016**, *11*, e0147131, doi:10.1371/journal.pone.0147131.

210. Zając, O.M.; Tyski, S.; Laudy, A.E. The contribution of efflux systems to levofloxacin resistance in *Stenotrophomonas maltophilia* clinical strains isolated in Warsaw, Poland. *Biology (Basel)* **2022**, *11*, 1044, doi:10.3390/biology11071044.

211. Nikaido, H.; Pagès, J.M. Broad-specificity efflux pumps and their role in multidrug resistance of Gram-negative bacteria. *FEMS Microbiol. Rev.* **2012**, *36*, 340-363, doi:10.1111/j.1574-6976.2011.00290.x.

212. Opperman, T.J.; Nguyen, S.T. Recent advances toward a molecular mechanism of efflux pump inhibition. *Front. Microbiol.* **2015**, *6*, 421, doi:10.3389/fmicb.2015.00421.

213. Lamers, R.P.; Cavallari, J.F.; Burrows, L.L. The efflux inhibitor phenylalanine-arginine beta-naphthylamide (PAβN) permeabilizes the outer membrane of gram-negative bacteria. *PLoS One* **2013**, *8*, e60666, doi:10.1371/journal.pone.0060666.

214. Misra, R.; Morrison, K.D.; Cho, H.J.; Khuu, T. Importance of real-time assays to distinguish multidrug efflux pump-inhibiting and outer membrane-destabilizing activities in *Escherichia coli*. *J. Bacteriol.* **2015**, *197*, 2479-2488, doi:10.1128/jb.02456-14.

215. Schuster, S.; Bohnert, J.A.; Vavra, M.; Rossen, J.W.; Kern, W.V. Proof of an outer membrane target of the efflux inhibitor Phe-Arg-β-Naphthylamide from random mutagenesis. *Molecules* **2019**, *24*, 470, doi: https://.doi.org/10.3390/molecules24030470.

216. Bonapace, C.R.; Bosso, J.A.; Friedrich, L.V.; White, R.L. Comparison of methods of interpretation of checkerboard synergy testing. *Diagn. Microbiol. Infect. Dis.* **2002**, *44*, 363-366, doi: 10.1016/s0732-8893(02)00473-x.

11. Opinie Komisji Bioetycznej

Komisja Bioetyczna
przy Warszawskim Uniwersytecie Medycznym

Tel.: 022/ 57 - 20 -303
Fax: 022/ 57 - 20 -165

ul. Żwirki i Wigury nr 61
02-091 Warszawa

e-mail: komisja.bioetyczna@wum.edu.pl
www.komisja-bioetyczna.wum.edu.pl

Warszawa, dnia 21 lutego 2022r.

AKBE/ 72 / 2022

Dr hab. Agnieszka E. Laudy
Zakład Mikrobiologii Farmaceutycznej,
ul. Banacha 1b, 02-097 Warszawa

OŚWIADCZENIE

Niniejszym oświadczam, że Komisja Bioetyczna przy Warszawskim Uniwersytecie Medycznym w dniu 21 lutego 2022r. przyjęła do wiadomości informację na temat badania pt:" Badanie aktywności związków przeciwdrobnoustrojowych, syntetycznych jak i pochodzenia naturalnego, a także środków dezynfekcyjnych wobec szczepów klinicznych ziarenkowców Gram-dodatnich i szczepów klinicznych grzybów." Przedstawione badanie nie stanowi eksperymentu medycznego w rozumieniu art. 21 ust. 1 ustawy z dnia 5 grudnia 1996 r. o zawodach lekarza i lekarza dentysty(Dz.U. z 2018 r. poz. 617) i nie wymaga uzyskania opinii Komisji Bioetycznej przy Warszawskim Uniwersytecie Medycznym, o której mowa w art. 29 ust.1 ww. ustawy.

Przewodnicząca Komisji Bioetycznej

Prof. dr hab. n. med. Magdalena Kuźma –Kozakiewicz

Komisja Bioetyczna
przy Warszawskim Uniwersytecie Medycznym

Tel.: 022/ 57 - 20 -303
Fax: 022/ 57 - 20 -165

ul. Żwirki i Wigury nr 61
02-091 Warszawa

e-mail: komisja.bioetyczna@wum.edu.pl
www.komisja-bioetyczna.wum.edu.pl

Warszawa, dnia 17 stycznia 2022r.

AKBE/ 3 / 2022

Dr hab. Agnieszka E. Laudy
Zakład Mikrobiologii Farmaceutycznej,
ul. Banacha 1b, 02-097 Warszawa

OŚWIADCZENIE

Niniejszym oświadczam, że Komisja Bioetyczna przy Warszawskim Uniwersytecie Medycznym w dniu 17 stycznia 2022r. przyjęła do wiadomości informację na temat badania pt„ Charakterystyka fenotypowa i genotypowa oraz badanie mechanizmów oporności na związki przeciwdrobnoustrojowe szczepów klinicznych Gram-ujemnych pałeczek niefermentujących oraz rzędu Enterobacterales."Przedstawione badanie nie stanowi eksperymentu medycznego w rozumieniu art. 21 ust. 1 ustawy z dnia 5 grudnia 1996 r. o zawodach lekarza i lekarza dentysty(Dz.U. z 2018 r. poz. 617) i nie wymaga uzyskania opinii Komisji Bioetycznej przy Warszawskim Uniwersytecie Medycznym, o której mowa w art. 29 ust.1 ww. ustawy.

Przewodnicząca Komisji Bioetycznej

Prof. dr hab. n. med. Magdalena Kuźma –Kozakiewicz

12. Oświadczenia współautorów publikacji

Warszawa, 20.12.2023

mgr farm. Joanna Krajewska

Oświadczenie

Jako współautor pracy przeglądowej pt. **„The European Medicines Agency approved the new antibacterial drugs – response to the 2017 WHO report on the global problem of multi-drug resistance"** Postępy Mikrobiologii – Advancements of Microbiology 2021, 60:249-264, doi: 10.21307/pm-2021.60.4.20, oświadczam, że mój wkład merytoryczny w przygotowanie, przeprowadzenie i opracowanie badań oraz przedstawienie pracy w formie publikacji polegał na:

współautorstwie koncepcji pracy, wykonaniu przeglądu piśmiennictwa i zebraniu materiałów, przygotowaniu i edycji pierwszej wersji manuskryptu, współudziale w opracowaniu ostatecznej wersji manuskryptu.

Mój udział procentowy w przygotowaniu publikacji określam na 80%.

Jako współautor interdyscyplinarnej pracy oryginalnej pt. **„Development of structurally extended benzosiloxaboroles – synthesis and in vitro biological evaluation"** RSC Advances 2021, 11:25104-25121, doi: 10.1039/d1ra04127d oświadczam, że mój wkład merytoryczny w przygotowanie, przeprowadzenie i opracowanie badań oraz przedstawienie pracy w formie publikacji polegał na:

współuczestniczeniu w projektowaniu eksperymentów mikrobiologicznych, byłam głównym wykonawcą zadań badawczych z zakresu mikrobiologii, współudziale w opracowaniu i interpretacji wyników mikrobiologicznych, współudziale w przygotowaniu i edycji pierwszej oraz ostatecznej wersji manuskryptu.

Publikacja jest interdyscyplinarna, a część mikrobiologiczna stanowi 30% tego artykułu. Mój udział procentowy w części mikrobiologicznej określam na 64%.

Jako współautor interdyscyplinarnej pracy oryginalnej pt. "**Oxazoline scaffold in synthesis of benzosiloxaboroles and related ring-expanded heterocycles: diverse reactivity, structural peculiarities and antimicrobial activity**", RSC Advances 2022, 12:23099-23117, doi: 10.1039/d2ra03910a oświadczam, że mój wkład merytoryczny w przygotowanie, przeprowadzenie i opracowanie badań oraz przedstawienie pracy w formie publikacji polegał na:

współuczestniczeniu w tworzeniu koncepcji badań i projektowaniu eksperymentów mikrobiologicznych, byłam głównym wykonawcą zadań badawczych z zakresu mikrobiologii, współudziale w opracowaniu i interpretacji wyników mikrobiologicznych, współudziale w przygotowaniu i edycji pierwszej oraz ostatecznej wersji manuskryptu.
Publikacja jest interdyscyplinarna, a część mikrobiologiczna stanowi 20% tego artykułu. Mój udział procentowy w części mikrobiologicznej określam na 65%.

Jako współautor pracy oryginalnej pt. "**Mutant prevention concentration, frequency of spontaneous mutant selection, and mutant selection window — a new approach to the *in vitro* determination of the antimicrobial potency of compounds**" Antimicrobial Agents and Chemotherapy 2023, 67(5):e0137322, doi: 10.1128/aac.01373-22, oświadczam, że mój wkład merytoryczny w przygotowanie, przeprowadzenie i opracowanie badań oraz przedstawienie pracy w formie publikacji polegał na:

współuczestniczeniu w tworzeniu koncepcji badań i projektowaniu eksperymentów, byłam głównym wykonawcą zadań badawczych, współudziale w opracowaniu i interpretacji wyników, współudziale w przygotowaniu i edycji pierwszej oraz ostatecznej wersji manuskryptu.
Mój udział procentowy w przygotowaniu publikacji określam na 60%.

Jako współautor interdyscyplinarnej pracy oryginalnej pt. **"Aromatic diboronic acids as effective KPC/AmpC inhibitors"** Molecules 2023, 28:7362, doi: 10.3390/molecules28217362 oświadczam, że mój wkład merytoryczny w przygotowanie, przeprowadzenie i opracowanie badań oraz przedstawienie pracy w formie publikacji polegał na:

współuczestniczeniu w tworzeniu koncepcji badań i projektowaniu eksperymentów mikrobiologicznych, byłam głównym wykonawcą zadań badawczych z zakresu mikrobiologii i związanej z nią analizy statystycznej, współudziale w opracowaniu i interpretacji wyników mikrobiologicznych, współudziale w przygotowaniu i edycji pierwszej oraz ostatecznej wersji manuskryptu.
Publikacja jest interdyscyplinarna, a część mikrobiologiczna stanowi 65% tego artykułu. Mój udział procentowy w części mikrobiologicznej określam na 65%.

A. Lewicki
.....
(podpis promotora)

Joanna Krzyżewska
.....
(podpis autora rozprawy doktorskiej)

dr hab. n. farm. Agnieszka E. Laudy Warszawa, 20.12.2023

Oświadczenie

Jako współautor pracy przeglądowej pt. **„The European Medicines Agency approved the new antibacterial drugs – response to the 2017 WHO report on the global problem of multi-drug resistance"** Postępy Mikrobiologii – Advancements of Microbiology 2021, 60:249-264, doi: 10.21307/pm-2021.60.4.20, oświadczam, że mój wkład merytoryczny w przygotowanie, przeprowadzenie i opracowanie badań oraz przedstawienie pracy w formie publikacji polegał na:

wyborze tematyki manuskryptu, analizie i korekcie koncepcji pracy, współudziale w opracowaniu pierwotniej i ostatecznej wersji manuskryptu. Pełniłam funkcję autora korespondencyjnego i odpowiadałam za pozyskanie funduszy.

Mój udział procentowy w przygotowaniu publikacji określam na 20%.

Jako współautor pracy oryginalnej pt. **„Development of structurally extended benzosiloxaboroles – synthesis and in vitro biological evaluation"** RSC Advances 2021, 11:25104-25121, doi: 10.1039/d1ra04127d oświadczam, że mój wkład merytoryczny w przygotowanie, przeprowadzenie i opracowanie badań oraz przedstawienie pracy w formie publikacji polegał na:

współudziale w tworzeniu koncepcji badań i projektowaniu eksperymentów mikrobiologicznych, współudziale w opracowaniu i interpretacji wyników mikrobiologicznych, współudziale w przygotowaniu pierwszej oraz ostatecznej wersji manuskryptu. Pełniłam funkcję autora korespondencyjnego i koordynatora projektu badawczego w części dotyczącej mikrobiologii.

Publikacja jest interdyscyplinarna, a część mikrobiologiczna stanowi 30% tego artykułu. Mój udział procentowy w części mikrobiologicznej określam na 34%.

Jako współautor pracy oryginalnej pt. **"Oxazoline scaffold in synthesis of benzosiloxaboroles and related ring-expanded heterocycles: diverse reactivity, structural peculiarities and antimicrobial activity"**, RSC Advances 2022, 12:23099-23117, doi: 10.1039/d2ra03910a oświadczam, że mój wkład merytoryczny w przygotowanie, przeprowadzenie i opracowanie badań oraz przedstawienie pracy w formie publikacji polegał na:

współuczestniczeniu w tworzeniu koncepcji badań i projektowaniu eksperymentów mikrobiologicznych, współudziale w opracowaniu i interpretacji wyników mikrobiologicznych, współudziale w przygotowaniu pierwszej oraz ostatecznej wersji

manuskryptu. Pełniłam funkcję autora korespondencyjnego i koordynatora projektu badawczego w części dotyczącej mikrobiologii. Współodpowiadałam za pozyskanie funduszy. Publikacja jest interdyscyplinarna, a część mikrobiologiczna stanowi 20% tego artykułu. Mój udział procentowy w części mikrobiologicznej określam na 35%.

Jako współautor pracy oryginalnej pt. "**Mutant prevention concentration, frequency of spontaneous mutant selection, and mutant selection window — a new approach to the *in vitro* determination of the antimicrobial potency of compounds**" Antimicrobial Agents and Chemotherapy 2023, 67(5):e0137322, doi: 10.1128/aac.01373-22, oświadczam, że mój wkład merytoryczny w przygotowanie, przeprowadzenie i opracowanie badań oraz przedstawienie pracy w formie publikacji polegał na:

wyborze tematyki badawczej, współuczestniczeniu w tworzeniu koncepcji pracy i projektowaniu eksperymentów, współudziale w analizie i interpretacji wyników, współudziale w przygotowaniu pierwszej wersji manuskryptu, w poprawie tekstu i opracowaniu ostatecznej wersji manuskryptu. Pełniłam funkcję autora korespondencyjnego, koordynatora projektu badawczego i odpowiadałam za pozyskanie funduszy.

Mój udział procentowy w przygotowaniu publikacji określam na 35%.

Jako współautor pracy oryginalnej pt. **"Aromatic diboronic acids as effective KPC/AmpC inhibitors"** Molecules 2023, 28:7362, doi: 10.3390/molecules28217362 oświadczam, że mój wkład merytoryczny w przygotowanie, przeprowadzenie i opracowanie badań oraz przedstawienie pracy w formie publikacji polegał na:

współuczestniczeniu w tworzeniu koncepcji całej pracy, współudziale w projektowaniu eksperymentów mikrobiologicznych, w opracowaniu i interpretacji wyników mikrobiologicznych, współudziale w przygotowaniu pierwszej wersji manuskryptu, w poprawie tekstu i opracowaniu ostatecznej wersji manuskryptu. Pełniłam funkcję koordynatora pracy i autora korespondencyjnego manuskryptu. Byłam współodpowiedzialna za pozyskanie funduszy.

Publikacja jest interdyscyplinarna, a część mikrobiologiczna stanowi 65% tego artykułu. Mój udział procentowy w części mikrobiologicznej określam na 35%.

Jednocześnie wyrażam zgodę na wykorzystanie w/w prac jako części rozprawy doktorskiej mgr farm. Joanny Krajewskiej.

A. Landy

.....

(podpis oświadczającego)

Warszawa, 18.12.2023

prof. dr hab. inż. Sergiusz Luliński

Oświadczenie

Jako współautor pracy oryginalnej pt. **„Development of structurally extended benzosiloxaboroles – synthesis and in vitro biological evaluation"** *RSC Advances* 2021, *11*, 25104-25121, doi: 10.1039/d1ra04127d oświadczam, że mój wkład merytoryczny w przygotowanie, przeprowadzenie i opracowanie badań oraz przedstawienie pracy w formie publikacji polegał na:

współudziale w tworzeniu koncepcji badań, syntezie badanych związków, opracowaniu i interpretacji wyników chemicznych, przygotowaniu pierwszej oraz ostatecznej wersji manuskryptu. Pełniłem funkcję autora korespondencyjnego z zakresu syntezy chemicznej. Byłem koordynatorem projektu i współodpowiedzialnym za pozyskanie funduszy.

Publikacja jest interdyscyplinarna, a część dotycząca syntezy chemicznej stanowi 65% tego artykułu. Mój udział procentowy w części syntezy i analizy chemicznej określam na 20%.

Jako współautor pracy oryginalnej pt. "**Oxazoline scaffold in synthesis of benzosiloxaboroles and related ring-expanded heterocycles: diverse reactivity, structural peculiarities and antimicrobial activity**", *RSC Advances* 2022, *12*, 23099-23117, doi: 10.1039/d2ra03910a oświadczam, że mój wkład merytoryczny w przygotowanie, przeprowadzenie i opracowanie badań oraz przedstawienie pracy w formie publikacji polegał na:

współudziale w tworzeniu koncepcji badań, syntezie badanych związków, opracowaniu i interpretacji wyników chemicznych, przygotowaniu pierwszej i ostatecznej wersji manuskryptu. Pełniłem funkcję autora korespondencyjnego z zakresu syntezy chemicznej. Byłem koordynatorem projektu i współodpowiedzialnym za pozyskanie funduszy.

Publikacja jest interdyscyplinarna, a część dotycząca syntezy chemicznej stanowi 65% tego artykułu. Mój udział procentowy w części syntezy i analizy chemicznej określam na 60%.

Jako współautor pracy oryginalnej pt. **"Aromatic diboronic acids as effective KPC/AmpC inhibitors"** Molecules 2023, 28:7362, doi: 10.3390/molecules28217362 oświadczam, że mój wkład merytoryczny w przygotowanie, przeprowadzenie i opracowanie badań oraz przedstawienie pracy w formie publikacji polegał na:

współudziale w tworzeniu koncepcji badań, syntezie badanych związków, opracowaniu i interpretacji wyników chemicznych, przygotowaniu pierwszej i ostatecznej wersji manuskryptu. Pełniłem funkcję koordynatora projektu badawczego w części synteza chemiczna. Byłem współodpowiedzialny za pozyskanie funduszy.

Publikacja jest interdyscyplinarna, a część dotycząca syntezy chemicznej stanowi 10% tego artykułu. Mój udział procentowy w części syntezy i analizy chemicznej określam na 60%.

Jednocześnie wyrażam zgodę na wykorzystanie w/w prac jako części rozprawy doktorskiej mgr farm. Joanny Krajewskiej.

S. Lulińska

.....
(podpis oświadczającego)

dr hab. inż. Krzysztof Durka

Warszawa, 18.12.2023

Oświadczenie

Jako współautor pracy oryginalnej pt. **„Development of structurally extended benzosiloxaboroles – synthesis and in vitro biological evaluation"** RSC Advances 2021, 11:25104-25121, doi: 10.1039/d1ra04127d oświadczam, że mój wkład merytoryczny w przygotowanie, przeprowadzenie i opracowanie badań oraz przedstawienie pracy w formie publikacji polegał na:

Wykonaniu pomiarów rentgenostrukturalnych, rozwiązaniu oraz udokładnieniu struktur krystalicznych wybranych związków prezentowanych w pracy. Wykonałem również odpowiednie rysunki struktur molekularnych oraz opisałem sposób wykonania pomiarów rentgenowskich. Publikacja jest interdyscyplinarna, a część dotycząca syntezy chemicznej stanowi 65% tego artykułu. Mój udział procentowy w części syntezy i analizy chemicznej określam na 10%.

Jako współautor pracy oryginalnej pt. "**Oxazoline scaffold in synthesis of benzosiloxaboroles and related ring-expanded heterocycles: diverse reactivity, structural peculiarities and antimicrobial activity**", RSC Advances 2022, 12:23099-23117, doi: 10.1039/d2ra03910a oświadczam, że mój wkład merytoryczny w przygotowanie, przeprowadzenie i opracowanie badań oraz przedstawienie pracy w formie publikacji polegał na:

Wykonaniu pomiarów rentgenostrukturalnych, rozwiązaniu oraz udokładnieniu struktur krystalicznych wybranych związków prezentowanych w pracy. Wykonałem odpowiednie rysunki struktur molekularnych oraz opisałem sposób wykonania pomiarów rentgenowskich. Wykonałem obliczenia DFT. Publikacja jest interdyscyplinarna, a część dotycząca syntezy chemicznej stanowi 65% tego artykułu. Mój udział procentowy w części syntezy i analizy chemicznej określam na 20%.

Jako współautor pracy oryginalnej pt. **"Aromatic diboronic acids as effective KPC/AmpC inhibitors"** Molecules 2023, 28:7362, doi: 10.3390/molecules28217362 oświadczam, że mój wkład merytoryczny w przygotowanie, przeprowadzenie i opracowanie badań oraz przedstawienie pracy w formie publikacji polegał na:

Współudziale w opracowaniu badań eksperymentalnych i współwykonaniu syntez badanych związków, opracowaniu i interpretacji wyników chemicznych. Publikacja jest interdyscyplinarna, a część dotycząca syntezy chemicznej stanowi 10% tego artykułu. Mój udział procentowy w części syntezy i analizy chemicznej określam na 40%.

Jednocześnie wyrażam zgodę na wykorzystanie w/w prac jako części rozprawy doktorskiej mgr farm. Joanny Krajewskiej.

Krzysztof Durka

.....

(podpis oświadczającego)

dr hab. Patrycja Wińska

Warszawa, 19.12.2023

Oświadczenie

Jako współautor pracy oryginalnej pt. **„Development of structurally extended benzosiloxaboroles – synthesis and in vitro biological evaluation"** RSC Advances 2021, 11:25104-25121, doi: 10.1039/d1ra04127d oświadczam, że mój wkład merytoryczny w przygotowanie, przeprowadzenie i opracowanie badań oraz przedstawienie pracy w formie publikacji polegał na:

współudziale w wykonaniu badań cytotoksyczności i interpretacji wyników, przygotowaniu pierwszej wersji manuskryptu zgłoszonego do czasopisma.

Publikacja jest interdyscyplinarna, a część dotycząca badań cytotoksyczności stanowi 5% tego artykułu. Mój udział procentowy w części badań cytotoksyczności określam na 100%.

Jako współautor pracy oryginalnej pt. **"Oxazoline scaffold in synthesis of benzosiloxaboroles and related ring-expanded heterocycles: diverse reactivity, structural peculiarities and antimicrobial activity"**, RSC Advances 2022, 12:23099-23117, doi: 10.1039/d2ra03910a oświadczam, że mój wkład merytoryczny w przygotowanie, przeprowadzenie i opracowanie badań oraz przedstawienie pracy w formie publikacji polegał na:

wykonaniu badań cytotoksyczności i interpretacji wyników, przygotowaniu pierwszej i ostatecznej wersji manuskryptu.

Publikacja jest interdyscyplinarna, a część dotycząca badań cytotoksyczności stanowi 5% tego artykułu. Mój udział procentowy w części badań cytotoksyczności określam na 100%.

Jako współautor pracy oryginalnej pt. **"Aromatic diboronic acids as effective KPC/AmpC inhibitors"** Molecules 2023, 28:7362, doi: 10.3390/molecules28217362 oświadczam, że mój wkład merytoryczny w przygotowanie, przeprowadzenie i opracowanie badań oraz przedstawienie pracy w formie publikacji polegał na:

wykonaniu badań cytotoksyczności i interpretacji wyników, przygotowaniu pierwszej wersji manuskryptu.

Publikacja jest interdyscyplinarna, a część dotycząca badań cytotoksyczności stanowi 5% tego artykułu. Mój udział procentowy w części badań cytotoksyczności określam na 100%.

Jednocześnie wyrażam zgodę na wykorzystanie w/w prac jako części rozprawy doktorskiej mgr farm. Joanny Krajewskiej.

P. Wińska

(podpis oświadczającego)

Warszawa, 19.12.2023 r.

Prof. dr hab. Krzysztof Woźniak
Wydział Chemii UW
Uniwersytet Warszawski

Oświadczenie

Jako współautor pracy oryginalnej pt. **„Development of structurally extended benzosiloxaboroles – synthesis and in vitro biological evaluation”** RSC Advances 2021, 11:25104-25121, doi: 10.1039/d1ra04127d oświadczam, że mój wkład merytoryczny w przygotowanie, przeprowadzenie i opracowanie badań oraz przedstawienie pracy w formie publikacji polegał na:

współudziale w charakterystyce strukturalnej otrzymanych związków.

Publikacja jest interdyscyplinarna, a część dotycząca syntezy chemicznej stanowi 65% tego artykułu. Mój udział procentowy w części syntezy i analizy chemicznej określam na 5%.

Jako współautor pracy oryginalnej pt. “**Oxazoline scaffold in synthesis of benzosiloxaboroles and related ring-expanded heterocycles: diverse reactivity, structural peculiarities and antimicrobial activity**”, RSC Advances 2022, 12:23099-23117, doi: 10.1039/d2ra03910a oświadczam, że mój wkład merytoryczny w przygotowanie, przeprowadzenie i opracowanie badań oraz przedstawienie pracy w formie publikacji polegał na:

współudziale w charakterystyce strukturalnej otrzymanych związków.

Publikacja jest interdyscyplinarna, a część dotycząca syntezy chemicznej stanowi 65% tego artykułu. Mój udział procentowy w części syntezy i analizy chemicznej określam na 5%.

Jednocześnie wyrażam zgodę na wykorzystanie w/w prac jako części rozprawy doktorskiej mgr farm. Joanny Krajewskiej.

Krzysztof Woźniak; Uniwersytet Warszawski
Elektronicznie podpisany przez Krzysztof Woźniak; Uniwersytet Warszawski
Data: 2023.12.19 13:45:11 +01'00'

.....
(podpis oświadczającego)

Warszawa, 19.12.2023 r.

dr inż. Paulina H. Marek-Urban

Oświadczenie

Jako współautor pracy oryginalnej pt. "**Oxazoline scaffold in synthesis of benzosiloxaboroles and related ring-expanded heterocycles: diverse reactivity, structural peculiarities and antimicrobial activity**", RSC Advances 2022, 12:23099-23117, doi: 10.1039/d2ra03910a oświadczam, że mój wkład merytoryczny w przygotowanie, przeprowadzenie i opracowanie badań oraz przedstawienie pracy w formie publikacji polegał na:

współudziale w analizach strukturalnych otrzymanych związków.

Publikacja jest interdyscyplinarna, a część dotycząca syntezy chemicznej stanowi 65% tego artykułu. Mój udział procentowy w części syntezy i analizy chemicznej określam na 10%.

Jednocześnie wyrażam zgodę na wykorzystanie powyższej pracy jako części rozprawy doktorskiej mgr farm. Joanny Krajewskiej.

Paulina H. Marek-Urban

(podpis oświadczającego)

Warszawa, 19.12.2023 r.

mgr inż. Piotr Pacholak

Oświadczenie

Jako współautor pracy oryginalnej pt. **„Development of structurally extended benzosiloxaboroles – synthesis and in vitro biological evaluation”** RSC Advances 2021, 11:25104-25121, doi: 10.1039/d1ra04127d oświadczam, że mój wkład merytoryczny w przygotowanie, przeprowadzenie i opracowanie badań oraz przedstawienie pracy w formie publikacji polegał na:

projektowaniu i wykonaniu syntez badanych związków, współudziale w opracowaniu i interpretacji wyników syntez chemicznych, współudziale w przygotowaniu pierwszej i ostatecznej wersji manuskryptu.

Publikacja jest interdyscyplinarna, a część dotycząca syntezy chemicznej stanowi 65% tego artykułu. Mój udział procentowy w części syntezy i analizy chemicznej określam na 30%.

Jednocześnie wyrażam zgodę na wykorzystanie powyższej pracy jako części rozprawy doktorskiej mgr farm. Joanny Krajewskiej.

.....
(podpis oświadczającego)

Warszawa, 20.12.2023 r..

mgr inż. Urszula Gogowska

Oświadczenie

Jako współautor pracy oryginalnej pt. **„Development of structurally extended benzosiloxaboroles – synthesis and in vitro biological evaluation"** RSC Advances 2021, 11:25104-25121, doi: 10.1039/d1ra04127d oświadczam, że mój wkład merytoryczny w przygotowanie, przeprowadzenie i opracowanie badań oraz przedstawienie pracy w formie publikacji polegał na:

współudziale w syntezie badanych związków. Badania te stanowiły część mojej pracy magisterskiej wykonanej w Katedrze Chemii Fizycznej Wydziału Chemicznego Politechniki Warszawskiej, której promotorem był prof. dr hab. inż. Sergiusz Luliński.

Publikacja jest interdyscyplinarna, a część dotycząca syntezy chemicznej stanowi 65% tego artykułu. Mój udział procentowy w części syntezy i analizy chemicznej określam na 15%.

Jednocześnie wyrażam zgodę na wykorzystanie powyższej pracy jako części rozprawy doktorskiej mgr farm. Joanny Krajewskiej.

Prof. dr hab. Sergiusz Luliński
Promotor pracy magisterskiej Pani mgr inż. Jolanty Dunikowskiej – S. Luliński

Dr. hab. Agnieszka E. Laudy
Promotor rozprawy doktorskiej Pani mgr. Joanny Krajewskiej – A. Laudy

Mgr. Joanna Krajewska – Joanna Krajewska

.....
(podpis oświadczającego)

Warszawa, 20.12.2023 r.

mgr inż. Jolanta Dunikowska

Oświadczenie

Jako współautor pracy oryginalnej pt. **„Development of structurally extended benzosiloxaboroles – synthesis and in vitro biological evaluation"** *RSC Advances* **2021**, *11*, 25104-25121, doi: 10.1039/d1ra04127d oświadczam, że mój wkład merytoryczny w przygotowanie, przeprowadzenie i opracowanie badań oraz przedstawienie pracy w formie publikacji polegał na:

współudziale w syntezie badanych związków. Badania te stanowiły część mojej pracy magisterskiej wykonanej w Katedrze Chemii Fizycznej Wydziału Chemicznego Politechniki Warszawskiej, której promotorem był prof. dr hab. inż. Sergiusz Luliński.

Publikacja jest interdyscyplinarna, a część dotycząca syntezy chemicznej stanowi 65% tego artykułu. Mój udział procentowy w części syntezy i analizy chemicznej określam na 20%.

Jednocześnie wyrażam zgodę na wykorzystanie powyższej pracy jako części rozprawy doktorskiej mgr farm. Joanny Krajewskiej.

Prof. dr hab. Sergiusz Luliński
Promotor pracy magisterskiej Pani mgr inż. Jolanty Dunikowskiej – S. Luliński

Dr. hab. Agnieszka E. Laudy
Promotor rozprawy doktorskiej Pani mgr. Joanny Krajewskiej – A. Laudy

Mgr. Joanna Krajewska – Joanna Krajewska

.....
(podpis oświadczającego)

Warszawa, 19.12.2023 r.

dr hab. Jolanta Mierzejewska

Katedra Biotechnologii Środków Leczniczych i Kosmetyków
Wydział Chemiczny Politechniki Warszawskiej
jolanta.mierzejewska@pw.edu.pl

Oświadczenie

Jako współautor pracy oryginalnej pt. **„Development of structurally extended benzosiloxaboroles – synthesis and in vitro biological evaluation"** RSC Advances 2021, 11:25104-25121, doi: 10.1039/d1ra04127d oświadczam, że mój wkład merytoryczny w powstanie tej publikacji polegał na przeprowadzeniu wstępnych przesiewowych badań przeciwdrobnoustrojowych na nowo-zsyntezowanych związkach.
Mój udział w publikacji określam na 2%.

Jednocześnie wyrażam zgodę na wykorzystanie powyższej pracy jako części rozprawy doktorskiej mgr farm. Joanny Krajewskiej.

Jolanta Mierzejewska
.....
(podpis oświadczającego)

Barcelona, 21.12.2023 r.

dr inż. Tomasz Stępniewski

Oświadczenie

Jako współautor pracy oryginalnej pt. "**Oxazoline scaffold in synthesis of benzosiloxaboroles and related ring-expanded heterocycles: diverse reactivity, structural peculiarities and antimicrobial activity**", RSC Advances 2022, 12:23099-23117, doi: 10.1039/d2ra03910a oświadczam, że mój wkład merytoryczny w przygotowanie, przeprowadzenie i opracowanie badań oraz przedstawienie pracy w formie publikacji polegał na:

współudziale w badaniach dokowania molekularnego.

Publikacja jest interdyscyplinarna, a część dotycząca dokowania molekularnego stanowi 10% tego artykułu. Mój udział procentowy w części dotyczącej dokowania molekularnego określam na 40%.

Jednocześnie wyrażam zgodę na wykorzystanie powyższej pracy jako części rozprawy doktorskiej mgr farm. Joanny Krajewskiej.

.....
(podpis oświadczającego)

STEPNIEWSKI TOMASZ MACIEJ - Y4627893P

Digitally signed by STEPNIEWSKI TOMASZ MACIEJ - Y4627893P
Date: 2023.12.21 14:53:42 +01'00'

Warszawa, 19.12.2023 r.

mgr inż. Krzysztof Nowicki

Oświadczenie

Jako współautor pracy oryginalnej pt. "**Oxazoline scaffold in synthesis of benzosiloxaboroles and related ring-expanded heterocycles: diverse reactivity, structural peculiarities and antimicrobial activity**", RSC Advances 2022, 12:23099-23117, doi: 10.1039/d2ra03910a oświadczam, że mój wkład merytoryczny w przygotowanie, przeprowadzenie i opracowanie badań oraz przedstawienie pracy w formie publikacji polegał na:

współudziale w tworzeniu koncepcji badań, współudziale w badaniach dokowania molekularnego oraz współudziale w przygotowaniu pierwszej i ostatecznej wersji manuskryptu.

Publikacja jest interdyscyplinarna, w której część dotycząca syntezy chemicznej stanowi 65% a część dotycząca dokowania molekularnego 10% tego artykułu. Mój udział procentowy w części syntezy i analizy chemicznej określam na 5%, a w części dotyczącej dokowania molekularnego na 60%.

Jednocześnie wyrażam zgodę na wykorzystanie powyższej pracy jako części rozprawy doktorskiej mgr farm. Joanny Krajewskiej.

Krzysztof Nowicki
(podpis oświadczającego)

Warszawa, 20.12.2023 r.

prof. dr hab. Stefan Tyski

Oświadczenie

Jako współautor pracy oryginalnej pt. "**Mutant prevention concentration, frequency of spontaneous mutant selection, and mutant selection window — a new approach to the *in vitro* determination of the antimicrobial potency of compounds**" Antimicrobial Agents and Chemotherapy 2023, 67(5):e0137322, doi:10.1128/aac.01373-22 oświadczam, że mój wkład merytoryczny w przygotowanie, przeprowadzenie i opracowanie badań oraz przedstawienie pracy w formie publikacji polegał na:

konsultacji koncepcji badań, współudziale w analizie i interpretacji wyników, współudziale w przygotowaniu pierwszej oraz ostatecznej wersji manuskryptu.

Mój udział procentowy w przygotowaniu publikacji określam na 5%.

Jednocześnie wyrażam zgodę na wykorzystanie powyższej pracy jako części rozprawy doktorskiej mgr farm. Joanny Krajewskiej.

.....
(podpis oświadczającego)

Warszawa, 22.12.2023

dr Krystiana A. Krzyśko

Oświadczenie

Jako współautor pracy pt. **"Aromatic diboronic acids as effective KPC/AmpC inhibitors"** Molecules 2023, 28:7362, doi: 10.3390/molecules28217362 oświadczam, że mój wkład merytoryczny w przygotowanie, przeprowadzenie i opracowanie badań oraz przedstawienie pracy w formie publikacji polegał na:

współudziale w tworzeniu koncepcji i w wykonaniu badań dokowania oraz dynamiki molekularnej, opracowaniu i interpretacji uzyskanych wyników, przygotowaniu pierwszej i ostatecznej wersji manuskryptu. Byłam autorem korespondencyjnym z zakresu dokowania i dynamiki molekularnej. Koordynowałam prace z zakresu dokowania i dynamiki molekularnej.

Publikacja jest interdyscyplinarna, a część dotycząca dokowania i dynamiki molekularnej stanowi 20% tego artykułu. Mój udział procentowy w części dotyczącej dokowania i dynamiki molekularnej określam na 50%.

Jednocześnie wyrażam zgodę na wykorzystanie powyższej pracy jako części rozprawy doktorskiej mgr farm. Joanny Krajewskiej.

Krzyśko
.....
(podpis oświadczającego)

Warszawa,…….

mgr Piotr Chyży

Oświadczenie

Jako współautor pracy pt. **"Aromatic diboronic acids as effective KPC/AmpC inhibitors"** Molecules 2023, 28:7362, doi: 10.3390/molecules28217362 oświadczam, że mój wkład merytoryczny w przygotowanie, przeprowadzenie i opracowanie badań oraz przedstawienie pracy w formie publikacji polegał na:

współudziale w projektowaniu i w wykonaniu badań dokowania oraz dynamiki molekularnej, opracowaniu i interpretacji uzyskanych wyników, przygotowaniu pierwszej wersji manuskryptu.

Publikacja jest interdyscyplinarna, a część dotycząca dokowania i dynamiki molekularnej stanowi 20% tego artykułu. Mój udział procentowy w części dotyczącej dokowania i dynamiki molekularnej określam na 50%.

Jednocześnie wyrażam zgodę na wykorzystanie powyższej pracy jako części rozprawy doktorskiej mgr farm. Joanny Krajewskiej.

Chyży Piotr. Podpisany elektronicznie przez Piotr Chyży; Uniwersytet Warszawsk 22.12.2023 12:57:34 +01'00'

……
(podpis oświadczającego)